

**METABOLOMICS AS A TOOL IN THE IDENTIFICATION AND
PRODUCTION OF NEW MARINE-DERIVED ANTIBIOTICS
FROM SPONGES AND ENDOSYMBIOTIC BACTERIA**

A THESIS PRESENTED FOR THE DEGREE OF DOCTOR OF

PHILOSOPHY IN

THE FACULTY OF SCIENCE

THE UNIVERSITY OF STRATHCLYDE

BY

CHRISTINA VICTORIA VIEGELMANN

B.Sc., R.Ph., M.Sc.

Strathclyde Institute of Pharmacy and Biomedical Sciences

University of Strathclyde

161 Cathedral Street

Glasgow

G4 0RE

United Kingdom

May 2014

This thesis is the result of the author's original research. It has been composed by the author and has not been previously submitted for examination which has led to the award of a degree.

The copyright of this thesis belongs to the author under the terms of the United Kingdom Copyright Acts as qualified by University of Strathclyde Regulation 3.50. Due acknowledgement must always be made of the use of any material contained in, or derived from, this thesis.

Signed:

Date:

Acknowledgements

I would like to extend my deepest gratitude to my supervisor, Dr. RuAn Edrada-Ebel, for giving me the opportunity to undertake this PhD, for teaching, supporting and helping me grow. I have learned so much. This whole endeavour would not have been possible without her. My heartfelt thanks are also due to my second supervisor, Prof. Brian McNeil, for his guidance, assistance and encouragement.

Many thanks to Ms. Carol Clements for the antimicrobial assays, Dr. Tong Zhang for his help with the NMR and mass spectrometers, Mr. Walter McEwan for his assistance with the bioreactor, Dr. Roth Tate for the lessons on molecular biology techniques, Mrs. Louise Young and Miss Grainne Abbott for the cytotoxicity assays, Ms. Patricia Keating from the Department of Pure and Applied Chemistry for teaching me MALDI and helping me with my GC samples, Mr. Craig Irving for running my NMR samples in the Department of Pure and Applied Chemistry, and Dr. Mike Winson for his assistance with the quorum sampling assay and teaching me many new microbiology techniques.

I would like to thank my collaborators in Würzburg and Cork, particularly Dr. Usama Abdelmohsen, Prof. Ute Hentschel, Dr. Lekha Menon, Dr. Jonathan Kennedy, and Prof. Alan Dobson. I would also like to thank the Scottish Overseas Research Student Award Scheme (SORSAS) from the Scottish Research Council and the Beaufort Marine Biodiscovery Research award from the Irish government (under the National Development Plan (2007-2013)) for funding my PhD, as well as the University of Strathclyde for the University Scholarship.

I am extremely grateful to my students who have done some work for this project: Alex Leong, Rebecca Thomson, Dominick Perrocco, Jennifer Parker, and Sean Haughey. My thanks are also due to Dr. Mariana Fazenda, Dr. Pete Gardner, and Ivo Kretzers and the others from the Fermentation group for all of their assistance and support. I would also like to thank Jeehan Alestad for her invaluable friendship through these years, as well as for her guidance in bioinformatics and for lending me various reagents and standards throughout the years. To Fr. Brendan Slevin, Catholic

chaplain of the university, and the other members of the Strathclyde Catholic Society, I owe my thanks for helping me grow spiritually as I grew academically, and for providing me with a life outside the laboratory.

I have been truly blessed to have such wonderful labmates, my dear friends: Enitome Bafor, Nurkhalida Kamal, Ahmed Tawfike, Noor Wini Binti Mazlan, Dr. Lynsey McIntyre, Weqas Alotaibi, Cheng Cheng, Daniela de Paula, Bela Sanchez, Catherine Dowdells and Dr. Tantima Kumlung, and also to have the best flatmate I could ever have asked for, Taposhri Ganguly. Their help, support, and encouragement have ensured that I thoroughly enjoyed the last three years. There are so many more friends I have made, and I cannot name them all here, but I hope they know that I am extremely grateful to them for coming into and brightening up my life.

And last but definitely not least- to my entire family, most especially Pippa, Bish, Mummy, Daddy, Ninang Ba, Atchi Con, and Nana Arlene, thank you so much for absolutely everything. I have run out of words and cannot tell you enough how much I love you. I am truly the most blessed girl alive to have such a family.

Table of Contents

ACKNOWLEDGEMENTS	III
TABLE OF CONTENTS	V
PUBLICATIONS	X
ABSTRACT	XI
CHAPTER 1 : GENERAL INTRODUCTION	1
1.1 Sponges	3
1.1.1 Physiology of Sponges	3
1.1.2 Sponges as Sources of Bioactive Metabolites	5
1.1.3 Sponges and Microbial Symbionts	7
1.1.4 <i>Haliclona simulans</i>	10
1.2 Actinomycetes	16
1.2.1 The Genus <i>Streptomyces</i>	17
1.2.2 The Genus <i>Microbacterium</i>	17
1.3 Convention on Biological Diversity	18
1.4 Trypanosomiasis	19
1.4.1 Human African Trypanosomiasis	19
1.4.2 Human American Trypanosomiasis	20
1.4.3. Current Drugs for Trypanosomiasis	21
1.5 <i>Mycobacterium marinum</i> and <i>Mycobacterium tuberculosis</i>	21
1.6 Metabolomics	24
1.6.1 Applications of Metabolomics	25
1.6.2 Mass Spectrometry	27
1.6.3 Nuclear Magnetic Resonance Spectroscopy	28
1.6.4 Multivariate Analysis	29
1.7 Fermentation	31
1.8 Summary and Conclusion	35
1.9 Hypothesis and Aims of the Study	35
CHAPTER 2 MATERIALS AND GENERAL METHODS	37
2.1 Reagents	38
2.2 Equipment	38
2.2.1 General Equipment	38
2.2.2 Microbiology Equipment	39
2.2.3 Liquid Chromatography – Mass Spectrometry Instruments	39
2.2.4 Gas Chromatography- Mass Spectrometry Instruments	39
2.2.5 Nuclear Magnetic Resonance Instruments	40
2.2.6 Flash Chromatography Equipment	40
2.2.7 TLC Plates	41
2.3 Software	41
2.4 General Methods	42
2.4.1 Liquid Chromatography-High Resolution Fourier Transform Mass Spectrometry	42
2.4.2 Data Mining Using MZmine 2.10	44
2.4.3 Gas Chromatography-Mass Spectrometry	45

2.4.4 Nuclear Magnetic Resonance Spectroscopy	45
2.4.5 Measurement of Optical Rotation	45
2.4.6 Bioassays	46
2.4.6.1 Anti-trypanosomal Assay	46
2.4.6.2 Anti-mycobacterium Assay	47
2.4.6.3 Anti-nocardia Assay	48
2.4.6.4 Antifungal Assays	49
2.4.6.5 Antibacterial Assays	49
2.4.6.6 Anti-calcineurin Assay	49
2.4.6.7 Cytotoxicity Assay	49
2.4.7 Column Chromatography	50
2.4.7.1 Diaion® HP20 Chromatography	50
2.4.7.2 Sephadex® LH-20 Chromatography	51
2.4.7.3 Adsorption Chromatography using Silica Gel	52
2.4.8 Thin Layer Chromatography	52
2.4.9 Bioinformatics Analysis	54

CHAPTER 3 EXTRACTION AND ANALYSIS OF ANTIBIOTICS FROM THE SPONGE *HALICLONA SIMULANS* **55**

3.1 Introduction	56
3.2 Methodology	57
3.2.1 Acquisition of Sponge Sample	57
3.2.2 Extraction of Sponge Metabolites	57
3.2.3 Removal of Salt using HP20 Chromatography	57
3.2.3.1 Preparation of Sample for HP20 Chromatography	57
3.2.3.2 Fractionation of Sponge Extract	57
3.2.4 Medium-Pressure Liquid Chromatography of Pooled HP20 Fractions	58
3.2.4.1 Pooling of Fractions	58
3.2.4.2 Fractionation of Pooled Fractions	59
3.2.4.3 Pooling of MPLC Fractions	60
3.2.5 Normal Phase Chromatography of B-5	60
3.2.6 Isolation of Bioactive Metabolites from a Second Batch of <i>H. simulans</i>	60
3.2.7 Derivatisation of B-3 for GCMS	63
3.3 Results	63
3.3.1 Extraction of Sponge Metabolites and Fractionation with HP20	63
3.3.2 MPLC of Non-polar HP20 Fractions	65
3.3.3 Identification and Structure Elucidation of Purified Compounds	71
3.3.3.1 24-Methylenecholesterol	71
3.3.3.2 24-Vinyl-cholest-9-ene-3 β ,24-diol	79
3.3.3.3 20-Methyl-pregn-6-en-3 β -ol, 5 α ,8 α -epidioxy	88
3.3.3.4 Antimicrobial Activities and Cytotoxicity of the <i>H. simulans</i> Sterols	95
3.3.3.5 Identification of Compounds from Active Fractions Using the AntiMarin Database	97
3.4 Discussion	101

CHAPTER 4 METABOLOMIC PROFILING OF *STREPTOMYCES* SP. SM8 ISOLATED FROM *H. SIMULANS* **112**

4.1 Introduction	113
4.2 Methodology	114
4.2.1 Acquisition of the Sample	114
4.2.2 Dereplication of Small-scale and Up-scale Samples	114

4.2.3 Medium-Pressure Liquid Chromatography of Pooled SM8 Samples	115
4.2.4 Pooling of Fractions for Antimicrobial Assays	115
4.2.5 Preparation of Fractions for Low Resolution LC-MS	116
4.2.6 Analysis of the SM8 Fractions with MZmine 2.10 and Comparison with the DNP	116
4.2.7 Identification of Antimycins in SM8 Extracts	116
4.2.8 Isolation of Compounds from SM8 Extract	116
4.2.9 Quorum Signalling Assay Using TLC Overlay Technique	118
4.2.10 Comparison of <i>H. simulans</i> Extracts and SM8 Extracts	118
4.3 Results	119
4.3.1 Dereplication of Small-Scale and Up-scale SM8 Extracts	119
4.3.2 Medium Pressure Liquid Chromatography of Up-scale SM8 Extracts	123
4.3.3 Confirmation of Antimycin A Production using Gene Knock-out Studies and LC-HRFTMS	134
4.3.4 Isolation of Compounds from SM8 Extract	138
4.3.5 Comparison of Endosymbiont and Host Sponge Metabolic Profiles	161
4.4 Discussion	176

CHAPTER 5 DEREPLICATION, METABOLIC PROFILING AND ANALYSIS OF COMPOUNDS FROM BACTERIA ISOLATED FROM MARINE SPONGES **190**

5.1 Introduction	191
5.2 Methodology	192
5.2.1 Screening and Dereplication of Bacterial Isolates	192
5.2.1.1 Acquisition of Bacterial Extracts	192
5.2.1.2 Screening of Samples with LC-HRFTMS and NMR	192
5.2.2 Isolation and Analysis of Antibiotic Compounds from EG4	193
5.2.2.1 Small-scale Growth of EG4 on Agar Plates	193
5.2.2.1.1 Preparation of M1 Agar	193
5.2.2.1.2 Inoculation of EG4	194
5.2.2.1.3 Preparation of EG4 Stock	194
5.2.2.1.4 Extraction and Analysis of EG4 Metabolites	195
5.2.2.2 Up-scaling of EG4 Culture	195
5.2.2.3 MPLC Fractionation of EG4 Extracts	196
5.2.3 Chemical Profiling of EG4 in Shake Flask Cultures Over the Course of Seven Days	197
5.2.4 Isolation of Bioactive Compounds from EG4 Extract	197
5.2.4.1 MPLC Fractionation of EG4 Extract Using BÜCHI Flash Chromatography System	197
5.2.4.2 Fractionation of EG4_569-573 Using Conventional Chromatography	198
5.2.4.3 MPLC Fractionation of EG4_215-392 using Biotage® Flash Chromatography System	198
5.2.4.4 Preparative TLC of EG4_215-392_wash and EG4_615-626	199
5.2.5 Metabolic Profiling of EG4 Under Different Media Conditions	199
5.2.5.1 Cultivation of EG4 on Variations of M1 Agar	199
5.2.5.2 Shake Cultures of EG4 Comparing Artificial Seawater and Royal Nature	200
5.2.5.3 Shake Cultures of EG4 using Variations of M1 Broth	200
5.2.6 Fermentation of EG4	201
5.2.6.1 Parameters	201
5.2.6.2 Cell Count	201
5.2.6.2.1 Cell Count Using Haemocytometer	201
5.2.6.2.2 Viable Cell Count Using Spread Plate Technique	202
5.2.6.3 Metabolic Profiling of EG4 Bioreactor Extracts	202

5.3 Results	202
5.3.1 Dereplication of Marine Actinomycetes	202
5.3.2 Optimisation of Extraction Method	206
5.3.3 Up-scaling of EG4 Cultures	207
5.3.4 Medium Pressure Liquid Chromatography of Up-scaled EG4 Extracts	209
5.3.5 Metabolic Profiling of EG4 Over Time	212
5.3.6 Isolation of Compounds from EG4	226
5.3.6.1 Normal Phase MPLC of EG4 Up-scaled Extract	227
5.3.6.2 Conventional Silica Chromatography of EG4_569-573	234
5.3.6.3 Biotage® Flash Chromatography and Preparative TLC of EG4_215-392	248
5.3.6.3.1 215-392_B	251
5.3.6.3.2 Indole-3-Carboxaldehyde and Octadecanoic Acid, 2,3-Dihydroxypropyl Ester	257
5.3.6.3.3 3,4-Dihydroxy-5,6-bis(1 <i>H</i> -indol-3-yl)-3,5-cyclohexadiene	266
5.3.6.4 Preparative TLC of EG4_615-626	272
5.3.6.4.1 1-Methyl-β-Carboline	273
5.3.6.4.2 Uracil	277
5.3.6.4.3 615-626_6	281
5.3.6.4.4 1,4-Dibenzylimidazolidine	287
5.3.7 Metabolic Profiling of EG4 on Variations of M1 Agar	291
5.3.7.1 PCA of EG4 and M1 Agar Extracts	299
5.3.7.2 PCA of EG4 Extracts After Exclusion of Media Peaks	302
5.3.7.3 OPLS-DA of EG4 Extracts Classified According to Anti-trypanosomal Activity	305
5.3.7.4 OPLS-DA of EG4 Extracts Classified According to Anti-mycobacterium Activity	311
5.3.8 Comparison of EG4 Extracts when Grown on M1 Containing Artificial Seawater or Royal Nature Pre-formulated Salt	313
5.3.9 Metabolic Profiling of EG4 Cultured in Variations of M1 Broth	315
5.3.9.1 PCA of EG4 M1 Broth Extracts after Exclusion of Media Peaks	320
5.3.9.2 OPLS-DA of Blank M1 Broth Extracts According to Anti-trypanosomal Activity	321
5.3.10 Fermentation of EG4	324
5.4 Discussion	336
CHAPTER 6 CONCLUSIONS AND FUTURE WORK	355
6.1 Conclusions	356
6.1.1 Isolation of Bioactive Steroids from <i>H. simulans</i>	356
6.1.2 Identification of Bioactive Compounds from SM8	357
6.1.3 Comparison of the Metabolomes of SM8 and <i>H. simulans</i>	358
6.1.4 Dereplication of Marine Actinomycetes	358
6.1.5 Culture and Extraction of EG4	359
6.1.6 Isolation and Identification of Compounds from EG4	359
6.1.7 Optimisation of Culture Conditions of EG4 to Enhance the Production of Anti-trypanosomal and Anti-mycobacterial Metabolites	360
6.1.8 Fermentation of EG4	362
6.2 Future Work	362
REFERENCES	364
APPENDICES	407
Appendix I NMR Spectra of Novel Steroids Isolated from <i>Haliclona simulans</i>	408

IA B-4/R-13 (24-vinyl-cholest-9-ene-3 β ,24-diol)	408
IB R-17 (20-methyl-pregn-6-en-3 β -ol, 5 α ,8 α -epidioxy)	411
Appendix II NMR Spectra of the Butenolides from SM8 (<i>Streptomyces</i> sp.) (JEOL 400MHz, DMSO)	415
Appendix III NMR Spectra of Novel Compounds Isolated from EG4 (<i>Microbacterium</i> sp.)	419
IIIA Fraction EG4_215-392_B3 (3,4-dihydroxy-5,6-bis(1H-indol-3-yl)-3,5-cyclohexadiene)	419
IIIB EG4_615-626_6 (Dianiline compound)	423
IIIC EG4_615-626_10 (1,4-dibenzylimidazolidine)	425
Appendix IV Antimicrobial Activities of Active SM8 Fractions Following Sephadex[®] LH-20 Chromatography	428
Appendix V BLAST Search of Nystatin Biosynthetic Clusters within <i>Streptomyces</i> sp. SM8 Genome	431
VA Alignment of the NysA and <i>Streptomyces</i> sp. SM8 PKS sequence	431
VB Alignment of the NysB and <i>Streptomyces</i> sp. SM8 PKS sequence	432
VC Alignment of the NysC and <i>Streptomyces</i> sp. SM8 PKS sequence	434
VD Alignment of the NysI and <i>Streptomyces</i> sp. SM8 PKS sequence	436
VE Alignment of the NysJ and <i>Streptomyces</i> sp. SM8 PKS sequence	439
Appendix VI BLAST Search for Thaxtomin Biosynthetic Clusters within the <i>Microbacterium testaceum</i> StLB037 Genome	440
VIA Alignment of the TxtA and <i>M. testaceum</i> StLB037 NRPS module sequence	440
VIB Alignment of the TxtB and <i>M. testaceum</i> StLB037 NRPS module sequence	441
Appendix VII BLAST Search for DasR within the <i>Microbacterium testaceum</i> StLB037 Genome.	442
Appendix VII BLAST Search of Surfactin Biosynthetic Clusters within the <i>Microbacterium testaceum</i> StLB037 Genome	443
VIIA Alignment of surfactin synthetase srfAA and NRPS modules from <i>Microbacterium testaceum</i> StLB037	443
VIIIB Alignment of surfactin synthetase srfAB and NRPS modules from <i>Microbacterium testaceum</i> StLB037	444
VIIC Alignment of surfactin synthetase srfAC and NRPS modules from <i>Microbacterium testaceum</i> StLB037	445
Appendix VIII Posters and Publications from This Thesis	446

Publications

Viegelmann, C., Margassery, L.M., Kennedy, J., Zhang, T., O'Brien, C., O'Gara, F., Morrissey, J.P., Dobson, A.D.W., Edrada-Ebel, R. (2014) Metabolomic Profiling and Genomic Study of a Marine Sponge-Associated *Streptomyces* sp. *Marine Drugs* (Under revision)

MacIntyre, L., Zhang, T., Viegelmann, C., Martinez, I.J., Cheng, C., Dowdells, C., Gernert, C., Abdelmohsen, U., Hentschel, U., Edrada-Ebel, R. (2014) Metabolomic Tools for Secondary Metabolite Discovery from Marine Microbial Endosymbionts. *Marine Drugs* (Accepted for publication)

Viegelmann, C., Parker, J., Ooi, T.T., Clements, C., Abbott, G., Young, L., Kennedy, J., Dobson, A.D.W., Edrada-Ebel, R. (2014) Isolation and Identification of Antitrypanosomal and Antimycobacterial Steroids from the Sponge *Haliclona simulans*. *Marine Drugs* 12(5): 2937-2952

Abdelmohsen, U., Cheng, C., Viegelmann, C., Zhang, T., Grkovic, T., Ahmed, S., Quinn, R., Hentschel, U., Edrada-Ebel, R. (2014) Dereplication Strategies for Targeted Isolation of New Anti-trypanosomal Actinosporins A and B from a Marine Sponge-Associated *Actinokineospora* sp. EG49. *Marine Drugs* 12(3): 1220-1244

Tawfike, A., Viegelmann, C., Edrada-Ebel, R. (2013) Metabolomics and Dereplication Strategies in Natural Products. *Methods Mol. Biol.*, 1055: 227-244

Abstract

Metabolomic methods can be utilised to screen diverse biological systems for potentially novel and sustainable sources of antibiotics and pharmacologically-active drugs. Marine sponges and their endosymbionts have proven to be abundant sources of bioactive compounds. HR-LCFTMS and NMR were used in the identification of compounds isolated from a marine bacterium and its host sponge, as well as in the dereplication and metabolic profiling of other sponge-associated bacteria.

24-Methylenecholesterol and two novel steroids, 24-vinyl-cholest-9-ene-3 β ,24-diol and 20-methyl-pregn-6-en-3 β -ol, 5 α ,8 α -epidioxy, all significantly active against *Trypanosoma brucei* and moderately active against *Mycobacterium marinum* were isolated from the Irish Sea sponge *Haliclona simulans*. Extracts from SM8, the *Streptomyces* sp. isolated from *H. simulans* demonstrated antibacterial and antifungal activities. NMR spectroscopy identified the major components of the antibacterial fractions as polyhydroxylated saturated fatty acids. HR-LCFTMS assisted in identifying members of the antimycin A family in the antifungal fractions. This was further confirmed using gene knockout studies. Three butenolides were also isolated from the SM8 extracts.

HR-LCFTMS was applied to the dereplication of extracts from bacteria from marine sponges. EG4, a *Microbacterium* sp. isolated from *Callyspongia* aff. *implexa*, was selected and its cultivation optimised from small scale to larger scale production, under different media conditions, with the aid of metabolomic methods and multivariate analysis to identify and trace biomarkers. In addition, several compounds that were active against *T. brucei* and *M. marinum* and *Nocardia farcinica* were isolated and identified.

Metabolomics has become a powerful tool in systems biology which allows us to gain insights into the potential of natural marine isolates for synthesis of significant quantities of promising new agents, and allows us to manipulate the environment within fermentation systems in a rational manner to select the desired bioactive metabolome.

Chapter 1 : General Introduction

1. General Introduction

Since the discovery of penicillin and its widespread use during World War II, many have become complacent about infectious diseases, believing that with antibiotics, death due to infection has become a thing of the past. However, in 2004, infectious and parasitic diseases ranked as the second leading cause of death in the world, after cardiovascular diseases, with respiratory infections considered as the fourth and fifth most common cause of death in women and men respectively, worldwide (WHO, 2008). The World Health Organization has also estimated that lower respiratory tract infections and diarrhoeal diseases were the greatest contributors to the burden of disease as quantified by the disability-adjusted life year (DALY) (WHO, 2008).

The evolutionary capabilities of microorganisms are at the root of antibiotic resistance. As the microorganisms adapt to survive, the current antibiotics used against them become less and less effective. This, coupled with the misuse of antibiotics and the lack of new antibiotics being introduced to the market, has led to drug resistance becoming a major health threat. The lack of effective antibiotics also leaves mankind susceptible to possible bioterrorism attacks using multidrug resistant microorganisms; a very real and dangerous threat (Gilligan, 2002).

Natural products have traditionally been good sources of new drug compounds, including antibiotics. Despite this, it was only in the 1950s that discovery from natural products began to include marine sources, and it was not until the late 1960s that interest in marine natural products really began to grow (Proksch et al., 2006).

Sponges are sessile marine invertebrates that rely mainly on chemical means of defence. Metabolites discovered from sponges that play a role in their survival include antimicrobial agents, anti-fouling compounds, ichthyotoxic substances and fish deterrents (Braekman and Daloze, 1986, Clark et al., 2001, Dobretsov et al., 2004, Hertiani et al., 2010). However, it is often unclear whether the metabolites are produced directly by the sponge or whether they are accumulated from food particles or excreted by endosymbiotic bacteria (Kobayashi and Ishibashi, 1993, Proksch, 1994). An advantage of compounds produced by sponge-associated bacteria as

opposed to compounds secreted by the sponges themselves is that sponges are non-sustainable sources of drugs, whereas bacteria can be more readily cultured.

Metabolomics is an emerging field that encompasses the study of the metabolome, which is the collection of all the metabolites of an organism. Commonly used techniques include mass spectrometry (MS) and nuclear magnetic resonance (NMR) spectroscopy, which allow metabolic profiling and identification of metabolites. It is hoped that by using these techniques, new lead compounds can be discovered from sponge endosymbionts.

This review includes a brief discussion on sponges, particularly *Haliclona simulans*, but does not include specific sponge-related bacteria. However, two genera, *Streptomyces* and *Microbacterium*, are mentioned as they are included in the study. Trypanosomiasis is also discussed as a disease requiring novel drugs, the lead compounds for which may be discovered in the project. The review also focuses on applications of metabolomics and multivariate data analysis, including recent examples of marine metabolomics.

1.1 Sponges

Sponges belong to the Phylum *Porifera*. *Porifera* comes from the Latin words *porus*, meaning “pore”, and *ferre*, meaning “to bear”. They can be classified into three classes, *Calcarea*, *Hexactinellida*, and *Demospongiae*. *Demospongiae* is the largest class with approximately 95% of sponges belonging to it (Brusca and Brusca, 1990).

1.1.1 Physiology of Sponges

Sponges are sessile animals that feed by filtering large amounts of water through their systems. Their bodies are composed of several different types of cells; however, many of these cells are undifferentiated and may change into other types of cells (Bergquist, 1978).

A book, *Sponges*, describes the physiology of poriferans (Bergquist, 1978). Water enters the sponge via small holes called ostia and flows through a series of channels that make up the aquiferous system before exiting from the larger osculum.

Choanocytes are flagellated cells that are responsible for the flow of water through the sponge. Choanocytes also capture particles from 0.1-1.5 μm , such as bacteria. In this way bacteria enter the sponge. The pinacoderm is the epithelium of the sponge. It is one cell thick and is composed of pinacocytes. In between the pinacoderm and choanoderm lies the mesohyl (Bergquist, 1978). The mesohyl is a matrix, and in it are various cells that have different functions. The most common cells in the mesohyl are archaeocytes, which can differentiate into other cells (Osinga et al., 1999, Taylor et al., 2007). These amoeboid cells are mobile and play an important role in the digestion of food particles (Brusca and Brusca, 1990). The physiology of sponges can be seen in Figure 1-1.

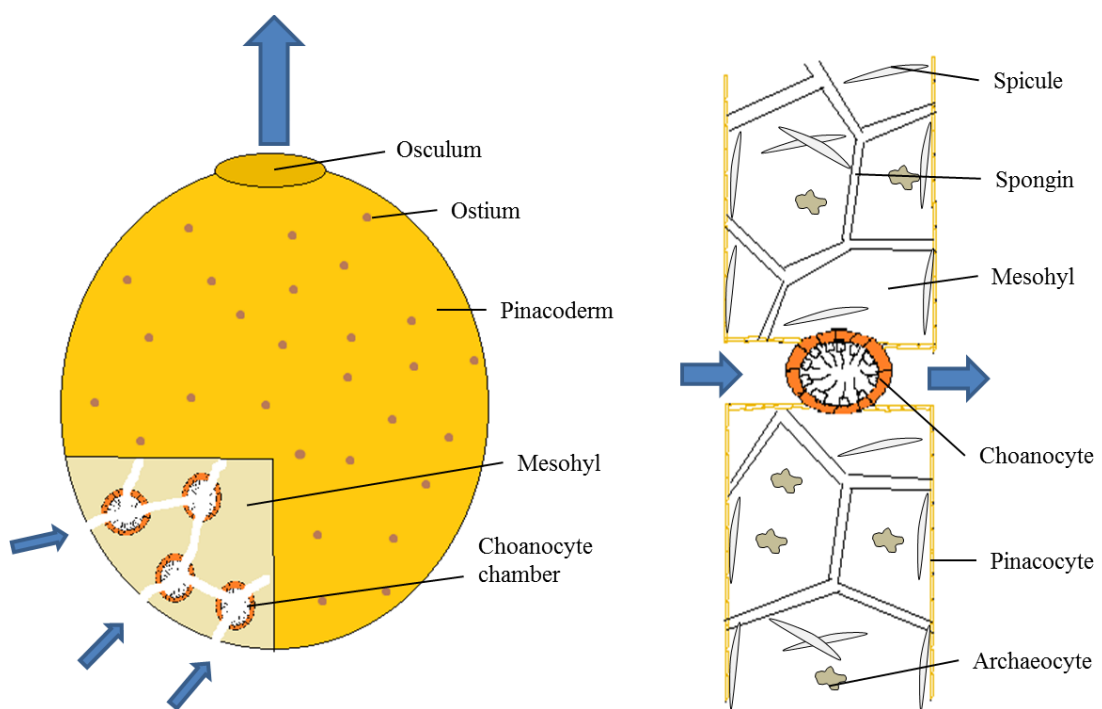


Figure 1-1: Diagram of sponge physiology (adapted from (Osinga et al., 1999)). The left side of the diagram depicts the exterior of a sponge with a cross-section showing the canals through which the water current passes. The blue arrows indicate the flow of water. The water enters the sponge through small pores called ostia and exits through the larger pore, the osculum. The pinacoderm is the epithelium of the sponge. The mesohyl is the matrix that lies in between the pinacoderm and the choanoderm. The right side of the figure shows the interior of the sponge in more detail. The yellow cells are the pinacocytes. The orange cells are choanocytes that form a choanocyte chamber. The flagella of these cells are responsible for the flow of water throughout the sponge. Each flagellum has a collar of microvilli that assists in the capture of food particles. The mesohyl contains spongin (collagenous fibers), spicules (composed of silica or calcium carbonate), and archaeocytes which can digest food and differentiate into other types of cells. (Osinga et al., 1999)

1.1.2 Sponges as Sources of Bioactive Metabolites

Being sessile animals, sponges rely heavily on chemical means of defence against predators and even fouling organisms. These chemicals must be potent in order to still have an effect even after immediate dilution upon secretion into the surrounding seawater (Haefner, 2003). For example, a study of *Latrunculia magnifica*, a sponge that lives in exposed conditions in the Red Sea, indicated that it has an anti-cholinesterase component that is highly toxic to fish, with a lethal dose of 0.4 mg/L (Neeman et al., 1975). The ichthyotoxic and anti-feeding effects of three sponges, *Petrosia seriata*, *Carteriospongia foliascens* and *Axinella damiconis*, were tested. It was discovered that the first two produced ichthyotoxic compounds whereas the latter had only deterrent properties (Braekman and Dalozé, 1986).

Sponges were the first marine invertebrates to be extensively studied by researchers looking for novel compounds (Bergquist, 1978). Interest in sponge metabolites began in the 1950s when Bergmann and Feeney first reported the isolation of two sponge nucleosides, spongouridine (**1**) and spongothymidine (**2**) (Bergmann and Feeney, 1950, Bergmann and Feeney, 1951, Bergmann and Burke, 1955). The knowledge gained from this discovery eventually led to the development of several FDA- and EMEA- approved drugs: cytarabine arabinoside (Ara-C) (**3**), an anti-leukaemic agent, adenine arabinoside (Vidarabine or Ara-A) (**4**), an antiviral agent, and even azidothymidine (AZT) (**5**) which is used in the treatment of HIV (Newman and Cragg, 2004). A recent review names several other drug candidates from sponges that have reached clinical testing. Eribulin mesylate (E7389) (**6**) is a potential anti-cancer macrolide currently in Phase III testing. Hemiasterlin (E7974) (**7**) is a tripeptide that is also a potential anti-cancer agent. It is now undergoing Phase I clinical studies (Mayer et al., 2010).

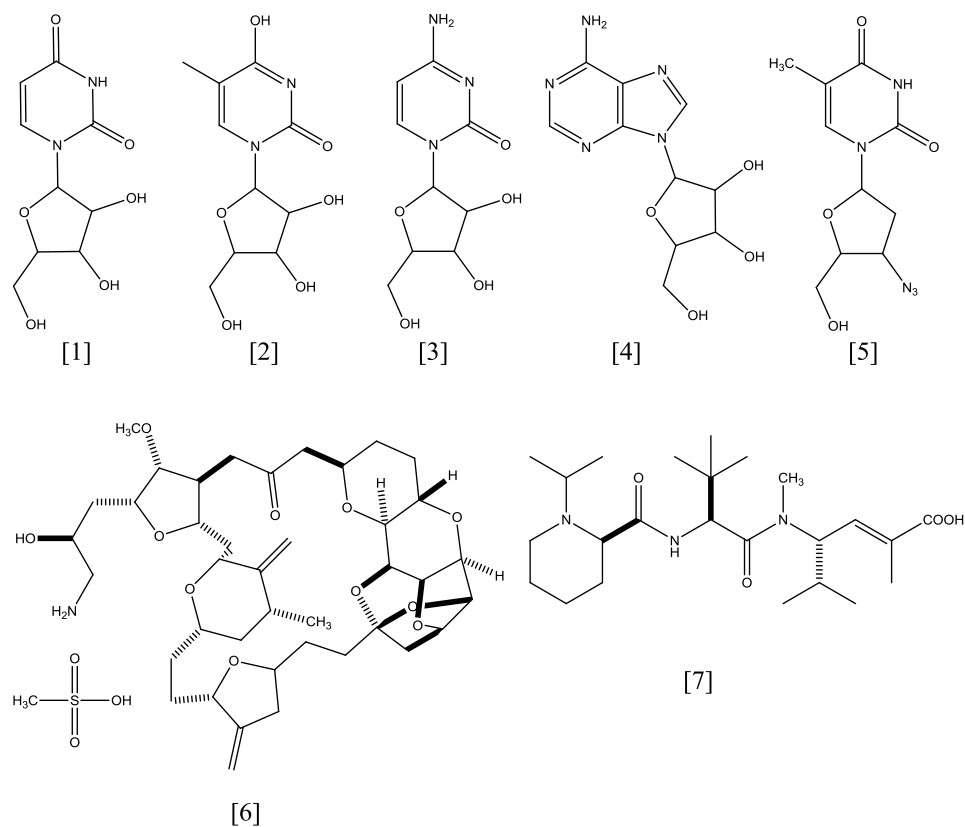


Figure 1-2: Compounds isolated from sponges that are precursors to or are drugs on the market or undergoing clinical trials. The sponge nucleosides (1) and (2) led to the development of other nucleosides that are currently on the market as anti-cancer (3) and anti-viral (4 and 5) agents. Eribulin mesylate (6) and hemiasterlin (7), also sponge-derived drugs, are currently undergoing clinical testing.

Sponges remain at the forefront of marine natural product discovery. Figure 1-3, adapted from the latest review by Blunt in 2014, shows that sponges produced 28% of all novel marine natural products discovered in 2012. This number does not include compounds from microorganisms isolated from sponges.

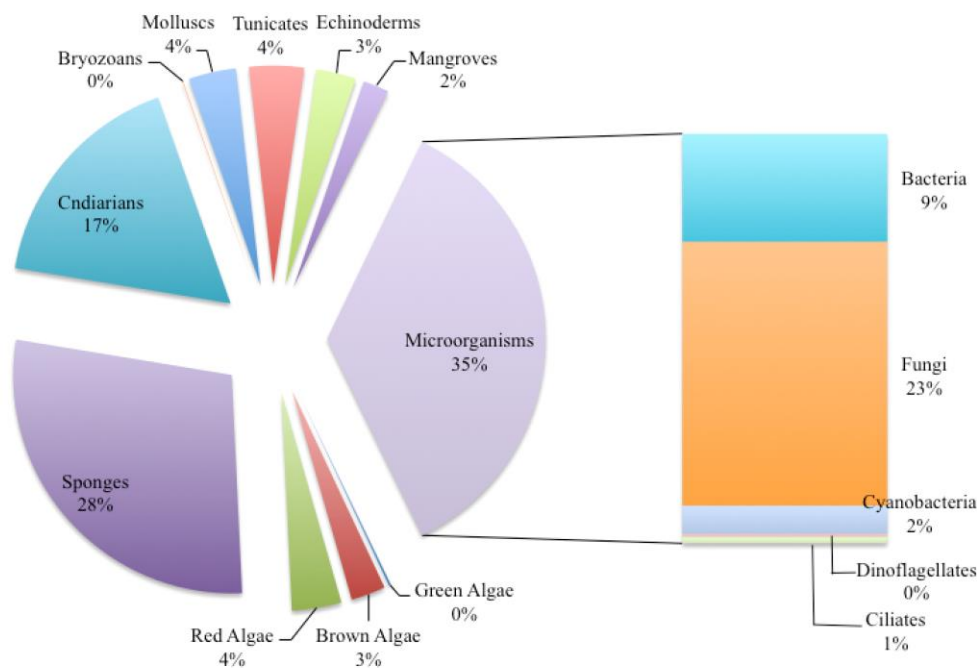


Figure 1-3: Percentages of novel marine compounds discovered in 2012 (Blunt et al., 2014). Of the marine invertebrates and plants considered, sponges were the most prolific source of natural products, being responsible for 28% of novel compounds. This does not include products of microorganisms isolated from sponges. Marine microorganisms were the source of 35% of novel marine compounds in 2012.

One major challenge when dealing with sponge metabolites is the difficulty in procuring the desired compounds in sufficient quantities both for research and commercialisation. The current solutions include the complete synthesis of the compound, sponge cultivation, culturing of the sponge-associated microorganisms that are suspected to produce the desired metabolite, and the use of metagenomics to produce metabolites using cloned biosynthesis genes (Taylor et al., 2007).

1.1.3 Sponges and Microbial Symbionts

Sponges play host to a range of microorganisms such as bacteria, fungi, yeast, dinoflagellates, diatoms and microalgae (Taylor et al., 2007). Bacteria are typically found in the mesohyl of the metazoans, although photosynthetic bacteria such as cyanobacteria also inhabit the surface of sponges, contributing to their colour (Hentschel et al., 2006, Usher et al., 2004). Studies have shown that microorganisms in sponges can account for as much as 38% of the sponge biomass (Vacelet and

Donadey, 1977). The concentration of bacteria in “high bacterial abundance sponges” is as much as two to four orders of magnitude greater than the concentration of bacteria in the surrounding seawater, indicating that these sponges are excellent hosts for their associated bacteria (Friedrich et al., 2001, Scheuermayer et al., 2006).

Not all sponges have high concentrations of bacteria. “Low bacterial abundance sponges” are those species whose bacterial numbers are similar to those of seawater and whose mesohyl appears free from bacteria (Scheuermayer et al., 2006). This indicates that the presence of bacteria in sponges is a selective rather than general occurrence. The bacteria associated with sponges are also different from the bacteria commonly found in natural seawater, suggesting the existence of sponge-specific bacteria (Hentschel et al., 2002, Taylor et al., 2005). Contrasting evidence has been found regarding the diversity of microbiological communities in sponges. It has been reported that common bacteria existed in different sponge species collected from different areas, including France, Palau, Japan, Australia, Croatia and California (Hentschel et al., 2002). On the other hand, other research has shown that the microbial community of *Cymbastela concentrica* remained the same over eight collection points across 500 km of temperate ocean, but differed from the community of the same species grown in tropical water (Taylor et al., 2005). However, different approaches were used for these two studies (16S-RNA sequencing and 16S rDNA-DGGE respectively) and further studies on a greater number or variety of samples are needed to reconcile the current findings.

The bacteria living in sponges also compete with each other. Several strains of *Mycobacterium* spp. were found from the sponge *Amphimedon queenslandica*, alongside a novel *Salinospora* species that produced rifampicin to which two of the three classes of *Mycobacterium* sp. were susceptible. It is likely that the third class of *Mycobacterium* sp. adapted to become resistant to rifampicin (Izumi et al., 2010).

The close association between microorganisms and sponges has resulted in the theory that many of the metabolites thought to be from sponges actually belong to the sponge-associated microorganisms. Indeed, various studies have shown that

some compounds obtained from bacterial cultures were identical to those found in sponge extracts.

In 1983, Schmitz and colleagues elucidated the structure of three diketopiperazines (**8**, **9**, **10**) from extracts from the sponge *Tedania ignis* (Schmitz et al., 1983). Five years later, Stierle and his team proved that the same diketopiperazines were actually produced by *Micrococcus* bacteria isolated from the same sponge species (Stierle et al., 1988). Another example is discoderamide (**11**), first isolated from the sponge *Discodermia dissoluta* (Gunasekera et al., 1991), which is very similar in structure to ikarugamycin (**12**), an antibiotic produced by *Streptomyces phaeochromogenes* var. *ikaruganensis* (Ito and Hirata, 1977). This suggests that discoderamide might be of bacterial origin (Kobayashi and Ishibashi, 1993). 3-Methyl-2'-deoxyuridine (**13**) was first isolated from a Swedish sponge, *Geodia baretii* (Lidgren et al., 1988), and subsequently from *Streptomyces microflavus*, which was taken from the sponge *Hymeniacion perlevis* from China (Li et al., 2011).

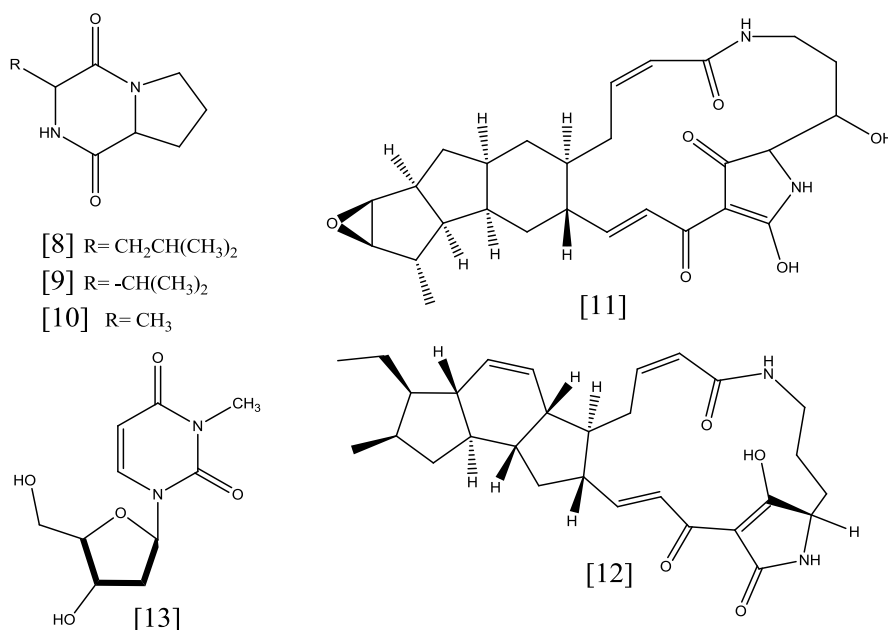


Figure 1-4: Compounds isolated from both sponges and bacteria. The diketopiperazines (**8-10**) and 3-methyl-2'-deoxyuridine (**13**), first isolated from sponges, were subsequently proven to be bacterial products. Discoderamide (**11**) is also postulated to be a bacterial product due to its structural similarity to ikarugamycin (**12**).

According to the ‘great plate count anomaly’, less than 1% of the bacteria that grow on sponges can be cultured in the laboratory (Scheuermayer et al., 2006). The unique environmental conditions created by sponges results in a challenge that has, so far, been insurmountable. Nevertheless, the production of active metabolites by sponge-associated bacteria, and not the sponges themselves, is a distinct advantage. Metabolites from microorganisms are much more sustainable than those obtained directly from sponges. It is easier to control the growth conditions of microorganisms as opposed to those of sponges, particularly if the sponges are cultured in the ocean. Genetic engineering may also be used to regulate genes of microorganisms and thereby activate certain pathways (Peric-Concha and Long, 2003). In addition, as metabolites are generally found in low quantities in sponges, a large amount of sponge biomass is necessary.

An example of the difficulty in the production of sponge metabolites is the case of halichondrin B. It is an antimetabolic compound produced by *Halichondria okadai* and *Lissodendoryx* sp. (Osinga et al., 1999). Although promising as an anti-cancer agent, its development had to be suspended temporarily due to supply problems. It was only when a procedure allowing the complete synthesis of Halichondrin B (Aicher et al., 1992) was developed that analogues such as E7389 were created. This compound, otherwise known as eribulin mesylate (**6**), is currently undergoing phase III clinical trials (Mayer et al., 2010) and has completed phase II trials on non-small cell lung carcinoma (NSCLC) (Gitlitz et al., 2009).

1.1.4 *Haliclona simulans*

The sponge studied in this project is *Haliclona simulans*. This sponge belongs to the family *Chalinidae* of the order *Haplosclerida* and the class *Demospongiae* (Kennedy et al., 2009).

The genus *Haliclona* has already given rise to many interesting metabolites, with as many as 190 compounds of various chemical classes and functions having been reported (Yu et al., 2006). Yu’s group, for instance, elucidated the structures of some cholesterol-type steroids and A-nor-steroids from *H. oculata*, a sponge taken from the South China Sea (Yu et al., 2006). Clark and colleagues found several alkyl

amino alcohols with antifungal properties from a *Haliclona* sponge from the Great Barrier Reef (Clark et al., 2001). Erickson and her team isolated the salicylihalamides, macrolides with potent cytotoxic activity, from a *Haliclona* sponge in Australia. However, the authors did note that these compounds were structurally more related to fungal compounds than those typically isolated from sponges (Erickson et al., 1997). It is therefore possible that the salicylihalamides were produced by symbiotic fungi and not by the sponges themselves.

(+)-Helianane (**14**) is a heterocyclic sesquiterpene isolated from an Indo-Pacific *Haliclona fascigera*. It is similar in structure to (-)-heliannuol from sunflowers (Harrison and Crews, 1997). More recently a meroditerpene, halioxepine (**15**), possessing cytotoxic and anti-oxidant activity, was isolated from an Indonesian *Haliclona* sp. (Trianto et al., 2011). Haliclostanone sulphate (**16**) is a sterol with a rare cis-junction between the C and D rings. It was isolated from *Haliclona* sp. together with halistanol sulphate (**17**) (Sperry and Crews, 1997).

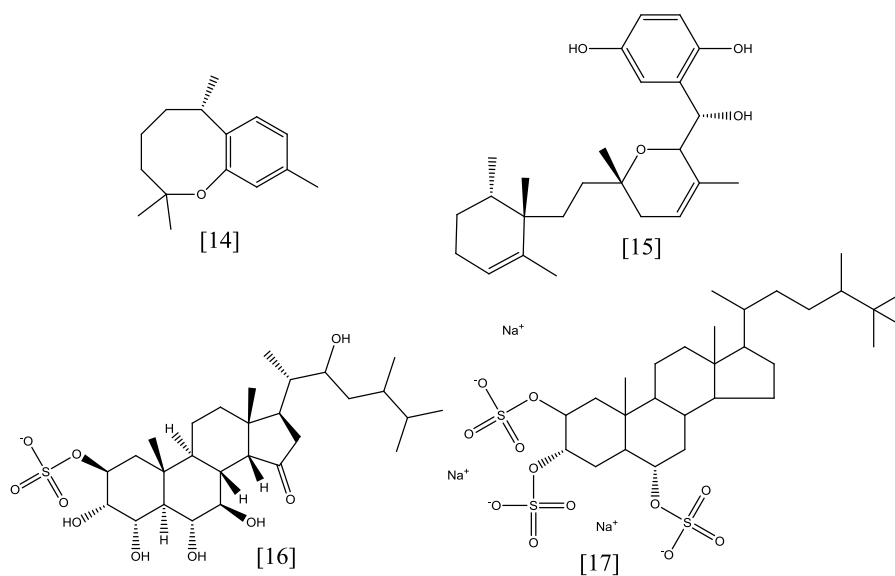
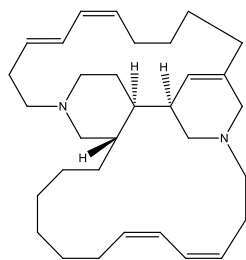


Figure 1-5: Terpenes isolated from *Haliclona* sponges.

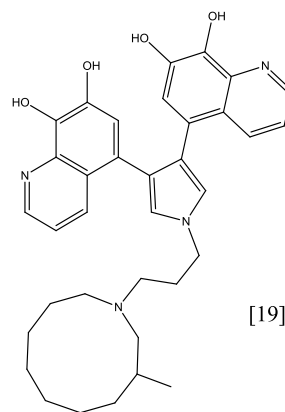
The alkaloids are another class that have been represented by metabolites from the *Haliclona* genus. Halicyclamine A (**18**), for example, is a tetracyclic diamine alkaloid from an Indonesian *Haliclona* sponge (Jaspars et al., 1994). Halitulins (**19**) are cytotoxic alkaloids from a South African sample of *H. tulearensis*. This compound resembles the structures of other compounds isolated from other sponges and some ascidians (Kashman et al., 1999). Haliclonadiamine (**20**) is an alkaloid from a *Haliclona* sponge from Palau. It was proven to have antimicrobial properties (Fahy et al., 1988). Papuamine (**21**), its unsymmetrical diastereoisomer, was isolated from *Haliclona* sp. from Papua New Guinea. It has antifungal activity (Baker et al., 1988).

An important group of alkaloids are the cytotoxic manzamines. Manzamine A, B, C and Y (**22, 23, 24, 25**) were isolated from *Haliclona* sp. from Japan (Kobayashi et al., 1995b, Sakai and Higa, 1986, Sakai et al., 1987). It has recently been proven, however, that manzamines are produced by sponge-associated actinomycetes (Peraud, 2006). Haliclamine C, D, E and F (**26, 27, 28, 29**) are alkaloids isolated from the arctic sponge *H. viscosa* and are possible biosynthetic precursors of the manzamines. Haliclamine C and D have antibacterial activity but haliclamine E and F were not tested (Schmidt et al., 2009, Volk et al., 2004).

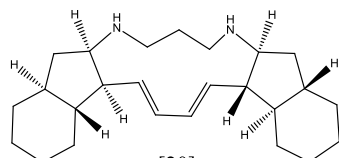
The saraine alkaloids from *Reniera (Haliclona) sarai* have unusual structures and a broad range of bioactivity (Cimino et al., 1990). The biological activity of the saraines includes antibacterial activity against Gram-positive bacteria, haemolytic activity, insecticidal and ascaricidal activity, anti-fouling activity, and inhibition of acetylcholinesterase and of the development of fertilised sea urchin eggs (Defant et al., 2011). Another macrocyclic diamine alkaloid, haliclonin A (**30**), was isolated from a Korean *Haliclona* sp. and possessed antibacterial and cytotoxic activity (Jang et al., 2009). Haliclonacyclamine A and B (**31, 32**) are cytotoxic alkaloids isolated from *Haliclona* sp. from the Great Barrier Reef (Charan et al., 1996). A novel ceramide, N-docosanoyl-D-erythro-(2*S*,3*R*)-16-methyl-heptadecasphing-4(E)-enine (**33**), from *H. koremella* was also proven to have anti-fouling activity against macroalgae (Hattori et al., 1998).



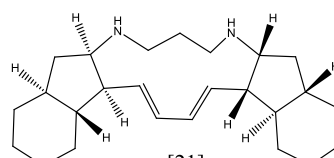
[18]



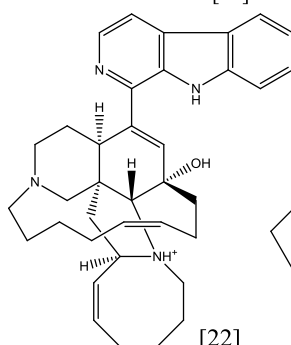
[19]



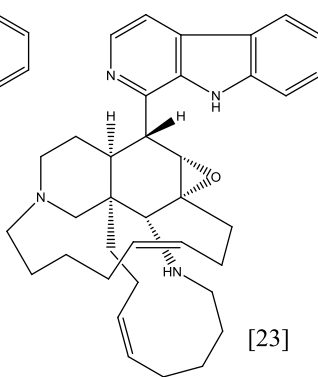
[20]



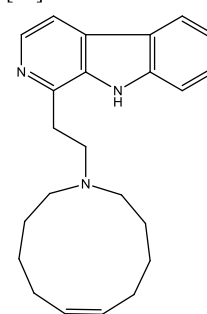
[21]



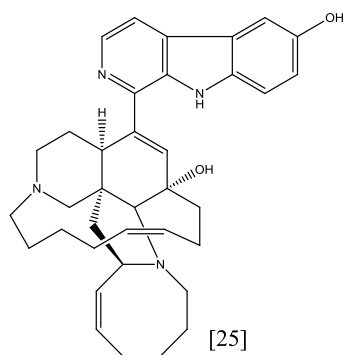
[22]



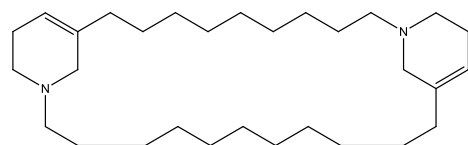
[23]



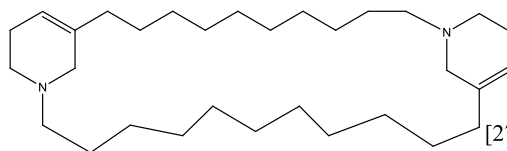
[24]



[25]



[26]



[27]

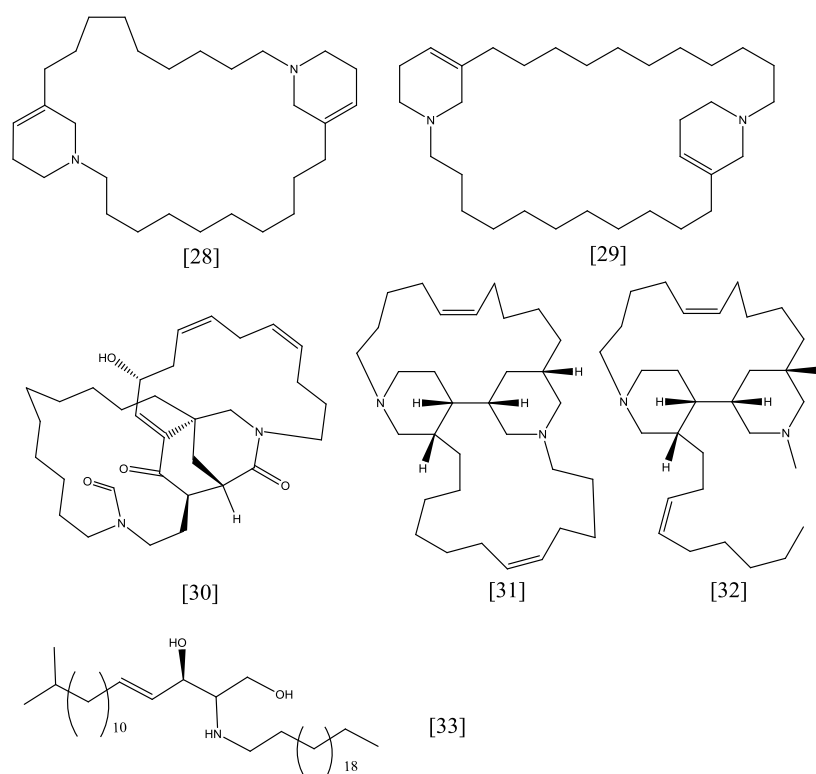


Figure 1-6: Alkaloids isolated from *Haliclona* sponges.

Hexapeptides such as waiakeamide (**34**) and haligramide A and B (**35**, **36**) have been isolated from a *Haliclona* sp. from Palau (Sera et al., 2003) and *H. nigra* from Papua New Guinea (Rashid et al., 2000). Haliclonamides A and B (**37**, **38**) are cyclic peptides, also isolated from a Palau *Haliclona* sp., that have the ability to bind iron and may be involved in iron uptake by the sponge (Guan et al., 2001). Haliclonamide C-E (**39-41**) were also isolated from a *Haliclona* sp. sponge from Palau and these, together with haliclonamide A and B, were discovered to have anti-fouling activity (Sera et al., 2002). Halipeptins A-C (**42-44**) are cyclic depsipeptides that have anti-inflammatory activity. They were isolated from a Vanuatu *Haliclona* sp. (Della Monica et al., 2002, Randazzo et al., 2001). Kendarimide A (**45**), a novel peptide that reverses multidrug resistance in cancer cells, was isolated from an Indonesian *Haliclona* sp. (Aoki et al., 2004).

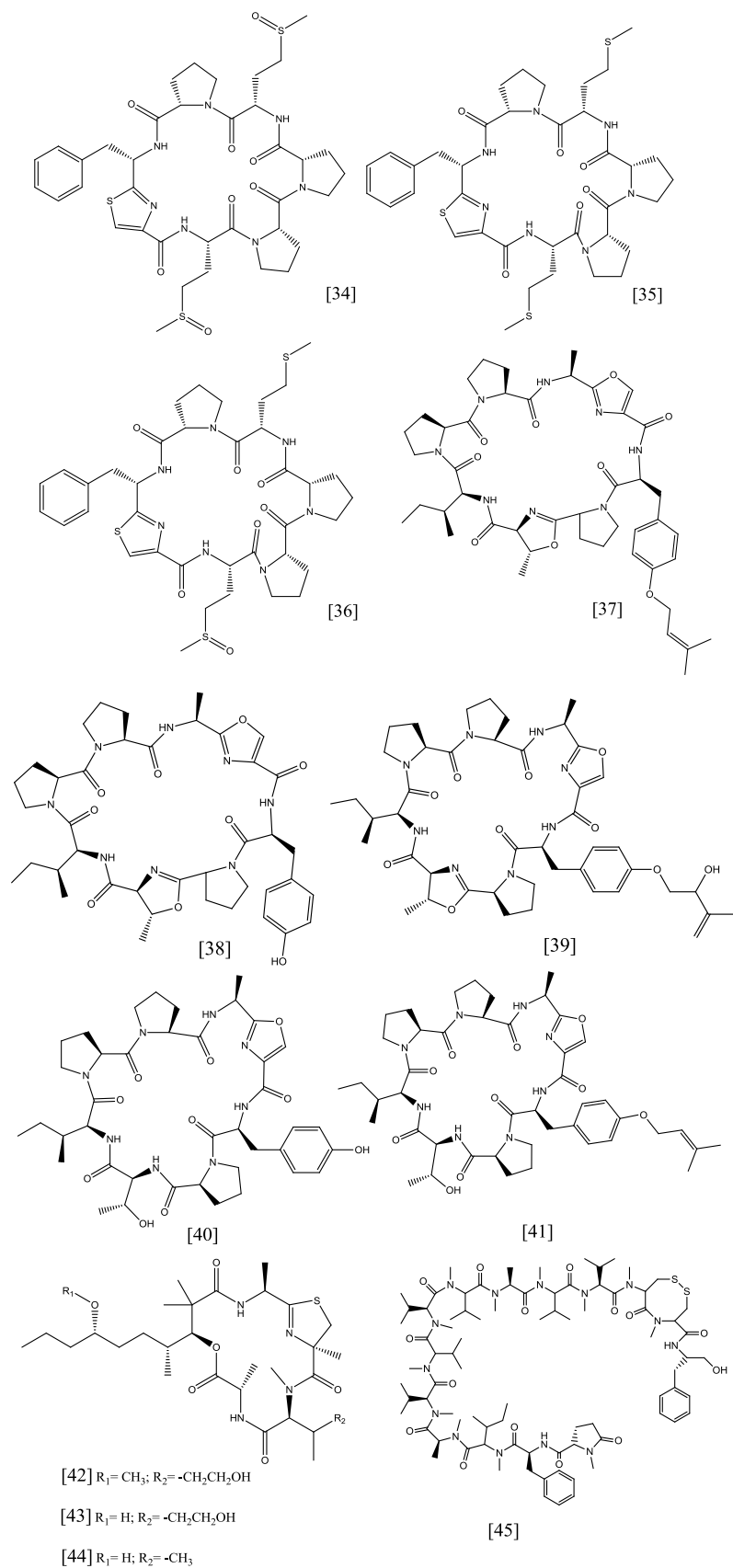


Figure 1-7: Peptides isolated from *Halicona* sponges.

Baker and his colleagues have studied the fungal community of *H. simulans*. Eighty fungi from a sponge sample from Ireland were cultured and assayed for antimicrobial activity. They found that several of the fungal isolates were active against *Escherichia coli*, *Bacillus sp.*, *Staphylococcus aureus*, and *Candida glabrata* (Baker et al., 2009).

Kennedy and his team started studying the bacterial symbionts of *H. simulans* collected from Ireland. They cultured the microorganisms and tested the antibiotic properties of the bacterial extracts. Of the 52 strains that they tested, only 15 of them did not possess antibacterial activity against the nine target bacteria (Kennedy et al., 2009). A comparison of this study with a metagenomic analysis of the bacterial community of the same sponge species (Kennedy et al., 2008) revealed that most of the bacteria detected by the metagenomic analysis were unable to be cultured in the laboratory.

Haliclona simulans, by virtue of its genus, which has already produced a large quantity of active metabolites, and its bacterial community, therefore appears to be a very promising source of lead compounds.

1.2 Actinomycetes

Actinomycetes are Gram-positive bacteria belonging to the order Actinomycetales. They are well known for being abundant producers of bioactive secondary metabolites. Two-thirds of all naturally-derived antibiotics are produced by actinomycetes (Okami and Hotta, 1988). Belonging to this order is the *Streptomyces* genus, which is well-known for producing a variety of antibiotics.

Although traditionally associated with soil, actinomycetes have more recently been found in the marine environment. The first marine actinomycete, *Rhodococcus marinonascens*, was characterised in 1984 (Helmke and Weyland, 1984). Other recently discovered genera include *Salinospora* and *Marinophilus*, both of which produce bioactive compounds (Jensen and Fenical, 2005).

1.2.1 The Genus *Streptomyces*

The genus *Streptomyces* belongs to the family Streptomycetaceae. They are Gram-positive, aerobic and produce mycelium and long branching filaments (Dietz, 1986). Streptomycetes are well-known for producing a vast and diverse amount of antibiotics. Streptomycin was the first aminoglycoside antibiotic that was discovered and used clinically. Rifamycins, anthracyclines, β -lactams, macrolides, nucleosides, polyenes, tetracyclines and polyether antibiotics are also produced by streptomycetes (Crandall and Hamill, 1986).

Novel compounds recently isolated from sponge-associated *Streptomyces* sp. include tetra- and hexapeptides, anthracyclines (Kozone et al., 2011, Motohashi et al., 2010a, Motohashi et al., 2010b), phenazines (Izumikawa et al., 2010, Mitova et al., 2008), trichostatin analogues (Hosoya et al., 2012), trisubstituted 2(1*H*)-pyrazinones (Motohashi et al., 2011), an anthracene derivative (Schneemann et al., 2010), a chitinase (Han et al., 2009), a new deoxyuridine 3-acetyl-5-methyl-2'-deoxyuridine (Li et al., 2011), and an indole alkaloid called streptomycindole (Huang et al., 2011).

Extracts of sponge-associated *Streptomyces* sp. have activity against a wide variety of human-pathogenic fungi and bacteria (Dharmaraj and Sumantha, 2009), as well as fish-pathogenic bacteria (Selvan et al., 2012).

1.2.2 The Genus *Microbacterium*

The genus *Microbacterium* belongs to the *Microbacteriaceae* family of the suborder *Micrococcineae* under the order *Actinomycetales* and class *Actinobacteria* (Zhi et al., 2009). The genus was first described by Orla-Jensen in 1919. Members of this genus were characterized by Speck as being “*short, Gram-positive, non-motile, non-sporulating, diptheroid-like rods which form catalase, produce predominantly lactic acid in milk, fail to liquefy gelatine, usually fail to produce nitrite from nitrate, and are very thermoduric*” (Speck, 1943). The optimum temperature for the growth of *Microbacteria* sp. is 30°C (Doetsch and Pelczar, 1948).

Microbacterium sp. are widely distributed in the marine environment and have been isolated from sources such as hydroids, ascidians, deep-sea sediment, and puffer fish

(Kageyama et al., 2007a, Kageyama et al., 2007b, Wu et al., 2008, Yu et al., 2004). Culture-independent techniques have shown that bacteria from the genus *Microbacterium* can be found in sponges (Xin et al., 2008). A *Microbacterium* sp. has been isolated from a Hawaiian sponge *Suberites zeteki* (Zhu et al., 2008). Another sponge-associated *Microbacterium* sp. was isolated from *Halichondria panicea* from Croatia and was found to produce four new glycolipids and one diphosphatidylglycerol (Wicke et al., 2000).

A novel species of *Microbacterium* has recently been cultured from a *Callyspongia* sp. sponge from the Red Sea in Egypt (Abdelmohsen et al., 2010). It is this novel species that was studied in this dissertation.

1.3 Convention on Biological Diversity

In 1988, the United Nations Environment Programme (UNEP) gathered a group of experts to assess the need for an international convention to protect biodiversity. The Convention on Biological Diversity was opened for signature at the United Nations Conference on Environment and Development (UNCED) in Rio de Janeiro, Brazil from the 5th of June, 1992 until the 4th of June, 1993 and was implemented on the 29th of December 1993 (SCBD, 2014). The primary aims of the convention are as follows: “*the conservation of biological diversity, the sustainable use of its components, and the fair and equitable sharing of the benefits from the use of genetic resources.*” (UNEP, 1992). The convention recognised that the protection of biological diversity is a global issue, but it required that countries act on a national level by the establishment of strategic plans and targets as well as regulatory bodies to facilitate the sharing of both resources and benefits.

The Cartagena Protocol on Biosafety to the Convention on Biological Diversity is a supplementary agreement to the Convention on Biological Diversity. It was finalised on the 29th of January, 2000 in Montreal, Canada. The Cartagena Protocol is focused on the protection of biological diversity from the effects of biotechnology and, in particular, living modified organisms resulting from biotechnology, which are recognised as being important for advances in healthcare, agriculture and nutrition (UNEP, 2000).

To address the third aim of the Convention on Biological Diversity, the Nagoya Protocol on Access to Genetic Resources and the Fair and Equitable Sharing of Benefits Arising from their Utilization to the Convention on Biological Diversity was adopted on the 29th of October, 2010 in Nagoya, Japan. The Nagoya Protocol is concerned with the exchange of genetic resources and traditional knowledge, subject to prior informed consent of the relevant parties, and the sharing of the benefits that arise from the use of these resources and knowledge (UNEP, 2010).

Pursuant to its aims, the Convention on Biological Diversity both protects the biological resources and facilitates the sharing of these resources and the subsequent benefits obtained from them. To the best of this author's knowledge, the collection of the sponge, *H. simulans*, and its endosymbiont, *Streptomyces* sp. SM8, from the Irish Sea as well as the isolation of the *Microbacterium* sp. from a sponge from the Red Sea in Egypt were performed in accordance to the guidelines set out by the Convention and with prior informed consent of the countries involved.

1.4 Trypanosomiasis

Trypanosomiasis is a vector-transmitted disease caused by parasitic protozoa called trypanosomes. Human African trypanosomiasis is also known as the sleeping sickness and is caused by *Trypanosoma brucei rhodesiense* and *T. b. gambiense* transmitted by the tsetse fly. Human American trypanosomiasis is caused by *T. cruzi* transmitted by the reduviid bug (Pereira, 1990). It is also called Chagas disease and is predominantly found in Latin America. Both are included in the list of the WHO's neglected tropical diseases. *Trypanosoma brucei brucei*, *T. congolense* and *T. vivax* infect livestock such as cattle, sheep and goats (Hoet et al., 2004).

1.4.1 Human African Trypanosomiasis

Infection with human African trypanosomiasis occurs when the bite of a tsetse fly (*Glossina* spp.) transmits metacyclic trypomastigotes into the host. The protozoa then grow and replicate extracellularly in the skin, usually leading to the development of a chancre. The trypanosomes then travel through the lymphatic system to reach the blood stream. *T. b. gambiense* causes a chronic type of trypanosomiasis with the

death of the host occurring, if left untreated, after a year. *T. b. rhodesiense*, on the other hand, causes a more acute type of trypanosomiasis with the death of the host occurring within weeks or months (Mansfield, 1990).

1.4.2 Human American Trypanosomiasis

Human American trypanosomiasis is transmitted to humans by the reduviid bug, also known as the assassin bug. The metacyclic trypomastigotes come from the urine or faeces of the insect and enter the human host through dermal abrasions or mucous membranes. The trypomastigotes enter host cells and transform into amastigotes, which replicate inside the host cells to form other amastigotes or form new trypomastigotes. These trypomastigotes can enter other cells or enter the bloodstream. They can be taken up by a reduviid bug, becoming epimastigotes in the insect before becoming metacyclic trypomastigotes once attached to the rectal gland of the insect (Pereira, 1990).

Human American trypanosomiasis, or Chagas Disease, affects the CNS and the heart. It has two stages – the acute stage, which occurs first and lasts for one to two months, and the chronic stage. Symptoms in the acute phase include fever, oedema, lymphadenopathy, electrocardiographic changes and enlargement of the heart. The chronic phase can occur as the cardiac form, the gastrointestinal form, or the indeterminate form, which is the most common (Brener and Krettli, 1990).

1.4.3. Current Drugs for Trypanosomiasis

The treatment for human African trypanosomiasis depends on the stage of the disease. The various medications are listed in Table 1-1.

Table 1-1: Current drugs for human African trypanosomiasis (Legros et al., 2002)

Drug	Organism	Stage
Pentamidine	<i>T. b. gambiense</i>	1
Suramin	<i>T. b. gambiense</i> <i>T. b. rhodesiense</i>	1
Melarsoprol	<i>T. b. gambiense</i> <i>T. b. rhodesiense</i>	2
Eflornithine	<i>T. b. gambiense</i>	2
Nifurtimox	<i>T. b. gambiense</i> <i>T. b. rhodesiense</i>	2

Eflornithine is better tolerated than melarsoprol, although it is more difficult to administer. Nifurtimox is more commonly used to treat Chagas' Disease but, in certain cases, can treat human African trypanosomiasis as well (Legros et al., 2002). There has been an initiative to reduce the use of melarsoprol in the treatment of human African trypanosomiasis. By 2010, 88% of cases were treated without melarsoprol. However, this has resulted in the increase of the cost of treatment for one patient with second-stage *T. b. gambiense* infection from US\$30 in 2001 to US\$440 in 2010. Hence, it is imperative that cheaper and less toxic drugs are brought to the market (WHO, 2013). There are fewer drugs for Chagas' Disease. Benznidazole is the drug of choice with nifurtimox being second in line (Bern et al., 2007).

With only a few drugs registered for trypanosomiasis and many of them having serious adverse effects, it is clear that newer, more effective, better-tolerated and preferably cheaper drugs are needed to fight trypanosomiasis.

1.5 *Mycobacterium marinum* and *Mycobacterium tuberculosis*

Tuberculosis (TB) is a disease caused by *Mycobacterium tuberculosis*, a Gram-positive, acid-fast bacillus. The most common form of tuberculosis is pulmonary; however, extrapulmonary TB can also occur. TB, if left untreated, is an often-fatal

disease with up to 70% of HIV negative patients dying within 10 years. The mortality rate is higher for HIV positive patients with untreated TB as the average survival rate becomes less than 6 months (Tiemersma et al., 2011). Although treatment is available, TB remains the second leading cause of death from infectious disease in the world, after HIV (WHO, 2012).

Despite the consistent decrease in incidence and mortality of TB cases globally since 2006 and probability that the Millennium Development Goal of 2015 will be achieved, the global burden of TB is still high. Approximately 8.7 million new cases of TB and 1.4 million deaths due to TB were reported in 2011 (WHO, 2012). In addition, there is insufficient data to determine the global trend of multidrug-resistant TB (MDR-TB), largely due to lack of testing for resistance in many countries. However, surveillance of TB drug resistance is on-going in many countries and the data was expected by the WHO at the end of 2012. In 2011 the estimated number of MDR-TB cases was 310,000. At least one case of extensively drug-resistant TB (XDR-TB) has been reported in 84 countries (WHO, 2012).

It has been approximately half a century since the first-line TB drugs were first used. New medicines are necessary in order to combat MDR-TB and XDR-TB, shorten the current treatment regimens, treat latent TB in patients that are infected with the bacteria but have not developed the disease, and to improve the prognosis of patients with both TB and HIV. Eleven prospective TB drugs are undergoing clinical trials. The pipeline depicting the journey of development of these drugs is shown in Figure 1-8. Research is also underway on TB vaccines, with 12 in clinical trials (WHO, 2012). While this is encouraging, it is still important to continue the search for lead compounds from environmentally-friendly sources, such as bacteria that can be easily cultured in the laboratory.

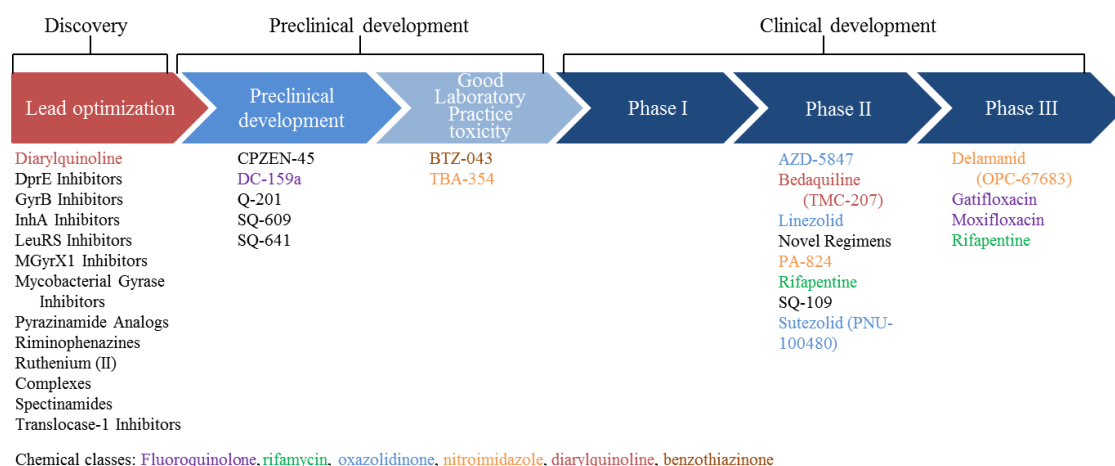


Figure 1-8: Pipeline for new TB drugs (adapted from WHO, 2012). Many classes of compounds are being tested in the drug discovery phase as potential lead compounds against *M. tuberculosis*. As of 2012, seven were undergoing preclinical development whereas eleven had reached phases II and III of clinical testing (WHO, 2012).

Mycobacterium marinum is a nontuberculous mycobacterium found in aquatic environments. It is a common pathogen of fish and amphibians, but it can also infect humans through abraded or damaged skin if the person comes into contact with an infected fish or contaminated water (Aubry et al., 2002, Petrini, 2006). Antibiotics such as clarithromycin, the cyclines, ethambutol, rifampicin and rifamycin are the first-line treatment for *M. marinum*, although no treatment regimen has yet been established. Surgery may also need to be performed in some cases (Aubry et al., 2002, Petrini, 2006).

M. marinum is closely related to *M. tuberculosis*, having < 85% nucleotide identity and sharing 3000 orthologs that have an average of 85% amino acid identity (Stinear et al., 2008). Cutaneous lesions caused by *M. marinum* are indistinguishable from cutaneous tuberculosis, caused by *M. tuberculosis*, and it is only through culture of the bacteria that the pathogen can be identified (MacGregor, 1995). As such, *M. marinum* is often utilized as a model for tuberculosis (Stinear et al., 2008).

1.6 Metabolomics

Metabolomics is, as mentioned previously, a new field of science that deals with the study of the metabolites of an organism. As new as it is, various definitions have been given for this field by various authors. Fiehn described four approaches to metabolomics. These include *target analysis*, in which a specific substrate is studied to determine the effect of gene mutagenesis; *metabolite profiling*, which is the analysis of a pre-determined class or group of compounds; *metabolomics*, or the study of all of the metabolites of a biological system; and lastly, *metabolite fingerprinting* which involves the grouping of compounds according to their source or class, without identifying each individual metabolite (Fiehn, 2002). Griffiths and his colleagues, on the other hand, defined only two branches of metabolomics: global and targeted. They stated that global metabolomics is “*the dynamic, qualitative and quantitative analysis of all small molecules (<1000 Da) in a cell-type, tissue, body fluid or organism.*” Targeted metabolomics, on the other hand, limits its focus to a certain class of compound (Griffiths et al., 2007). These are similar to Fiehn’s *metabolomics* and *metabolite profiling*, respectively. Another term commonly encountered is *metabonomics*. The difference between metabolomics and metabonomics is indistinct, with the two being used interchangeably. However, metabonomics has been defined as “*the quantitative measurement of the dynamic multiparametric metabolic response of living systems to pathophysiological stimuli or genetic modification.*” (Nicholson et al., 1999). Because Nicholson worked primarily with nuclear magnetic resonance (NMR), many associate metabonomics with the analysis of a system using NMR while considering metabolomics as a mass spectrometry (MS)-dominated field.

A major challenge of metabolomics is that there is a large amount of data generated, and not all of it is useful. The deconvolution of metabolomic data includes at least three aspects: distinguishing the metabolite signals from the noise, determining the chemical identity and, if possible, elucidating the chemical structure of the metabolite of interest, and determining the pathways in which the metabolite is involved (Kell, 2004). Several mathematical approaches, such as Principal component analysis and independent components analysis, are used to cluster the

data points and thus make data interpretation simpler. Additionally, improvements need to be made on the amount of metabolites that can be detected in a sample, as NMR and MS are estimated to measure only a hundred and a thousand metabolites respectively out of several thousand cellular metabolites, as well as on the identification and quantification of the metabolites (Viant, 2007a).

Two of the most common techniques used in metabolomics are MS and NMR. MS has the advantage of a lower limit of detection; it is more sensitive than NMR (Viant, 2007b). However, structures are easier to elucidate using NMR spectra. This technique also allows the differentiation of isomers.

1.6.1 Applications of Metabolomics

Metabolic profiling has been used in plants in order to identify the compounds they contain and screen them for possible activity. Studies of tomatoes using NMR and liquid chromatography-mass spectrometry (LC-MS), for instance, have profiled the metabolites present in the fruit, including the pharmacologically active lycopene and carotenoids (Moco et al., 2006, Tiziani et al., 2006). The field of medicine also used metabolomics to diagnose disease states such as cancer and diabetes (Madsen et al., 2010, Trethewey et al., 1999). It was postulated that by studying the changes in the metabolome of *Escherichia coli* grown in varying conditions, a clearer picture of the metabolism of *E. coli* could be generated (Tweeddale et al., 1998). In their study, they also tested the effect of a gene regulator, RpoS, by measuring the metabolic changes that the cells without RpoS underwent. Although limited in the methodology that they used, the group proved that metabolome study is useful in studying cell responses to various conditions.

Metabolomics has also been applied, though to a lesser extent, in environmental marine studies. These generally involve the study of the changes in the metabolome of aquatic organisms caused by stressors such as toxicants and diseases (Tjeerdema, 2008, Viant, 2007a). It has also been involved in the study of symbiotic relationships, such as between dinoflagellates and corals, and also in the identification of corals based on their chemical profiles (Gordon and Leggat, 2010). NMR has been used to study the effect of temperature on the metabolome of a coral

pathogen, *Vibrio coralliilyticus*, which varies its pathogenicity depending on the temperature (Boroujerdi et al., 2009). NMR was also used to study the metabolite profiles of the different organs of oysters (Tikunov et al., 2010).

The advantage of metabolomics is that it allows the classification of the phenotype of the organism or cell involved. Changes in the genotype of an organism do not always lead to the expected, equivalent result, making the functional effects of genotypic changes incredibly difficult to determine without phenotypic studies (Trethewey et al., 1999). In addition, more than one pathway can be affected by a single mutation. This might not be predictable with traditional genetics, but a global metabolomic analysis would indicate which metabolites are up- or down-regulated. Compared to the other members of the “omics cascade”, metabolomics provides an overview of what is happening in the system, rather than what could happen (Figure 1-9), and as such provides better functional information (Bedair and Sumner, 2008, Dettmer et al., 2007). Another advantage is the conservation of metabolites across various species. As the field is still developing and new methods are discovered, one technique developed on a certain organism can generally be applied to other species (Viant, 2007a).

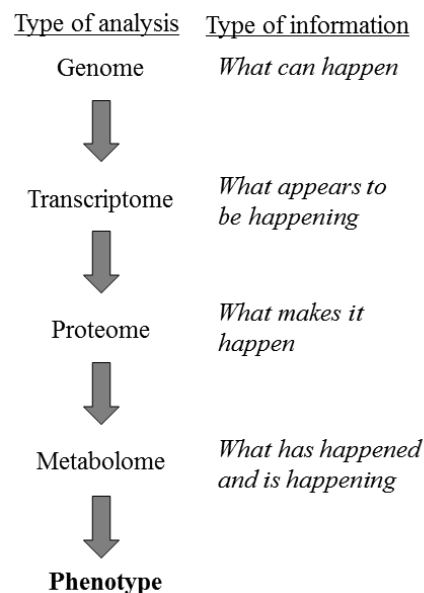


Figure 1-9: The "Omics" cascade (adapted from Dettmer et al., 2007). The “Omics” cascade shows the information that can be obtained from each type of analysis. The metabolome is the closest to the phenotype and as such is the best indicator of the metabolic processes of the organism (Dettmer et al., 2007).

The following steps are generally applied in metabolomic analyses:

- 1) Experiment design- the experiment must be designed in such a way that the results obtained are statistically valid and contain the maximum amount of information from the appropriate number of samples (Trygg et al., 2007).
- 2) Sampling – this includes obtaining samples from biological sources, such as from test animals, humans, cells or microorganisms. The samples must be treated properly to minimise degradation or production of new metabolites after sampling (Dettmer et al., 2007).
- 3) Sample preparation- this step involves extracting the relevant metabolites from the biological matrix; for example, from blood serum or microbiological media (Dettmer et al., 2007).
- 4) Sample analysis – using analytical techniques such as MS and NMR.
- 5) Data export – this step includes the processing of the data to remove noise and background effects (Dettmer et al., 2007). Examples of processes are apodisation and baseline normalisation in NMR spectra and chromatogram deconvolution, retention time and baseline normalisation and peak alignment for MS data.
- 6) Data analysis – using MS and NMR processing software as well as tools designed to perform multivariate analysis.

1.6.2 Mass Spectrometry

MS is a detection method. It is most often coupled to a separation technique such as gas chromatography (GC) or liquid chromatography (LC). High-Performance Liquid Chromatography (HPLC) is preferred for non-volatile polar compounds and labile, high molecular weight compounds (Tolstikov et al., 2007). As it is more sensitive, MS can complement NMR spectroscopy, which can be used to quickly and economically provide a general idea of the metabolites present in a sample (Viant, 2007b). As mentioned above, MS is coupled with separation techniques allowing the simplification of the spectra obtained. The metabolites in a mixture can be separated from each other using chromatography and their mass spectra can be viewed

individually, unlike when NMR is used, as NMR only shows an overview of all of the metabolites present in the mixture. However, depending on the ionisation technique used, certain classes of metabolites may not ionise, hence not all metabolites will be detected. Another disadvantage of MS is that it is a destructive method of analysis compared to NMR, which is non-destructive.

A recent example of the use of LC-MS in metabolomics is the analysis of the response of *Streptomyces coelicolor* to salt stress. This actinomycete is well-known to be highly adaptive to various environmental conditions, and using LC-MS Kol and his group were able to identify the compounds that are up-regulated by the bacteria when they are exposed to salt (Kol et al., 2010). MS and NMR can also be used to determine whether metabolites from sponges are identical to those from microorganisms, as in the case of the brominated diphenyl ethers from the *Dysidea* sp. sponge (Elyakov et al., 1991) and diketopiperazines from *Tedania ignis* (Stierle et al., 1988).

1.6.3 Nuclear Magnetic Resonance Spectroscopy

NMR spectroscopy is a non-destructive analytical technique that measures the resonance of atomic nuclei upon the application of a magnetic field. It is useful in metabolomics as it is non-discriminating and provides a fingerprint of all of the compounds present in the mixture, providing they possess the atom being studied (e.g. ^1H , ^{13}C , ^{15}N , ^{19}F , ^{23}Na , ^{31}P). In addition, it is more reproducible than MS (Madsen et al., 2010). However, it is less sensitive than MS and, as it does not involve a separation method, the major metabolites in the mixture may mask the less abundant ones.

NMR can be used both to identify metabolites in extracts as well as to detect differences or the occurrence of unknown metabolites in extracts. For example, ^1H NMR spectroscopy was used to identify and quantify the metabolites present in extracts of the malarial parasite *Plasmodium falciparum* as well as to compare the different extraction techniques used in the study (Teng et al., 2009). It has also been used to study metabolic changes that occurred in oxytetracycline-treated red abalone infected with a Rickettsiales-like prokaryote. NMR was used to complement

histological examinations of the treated and untreated infected red abalone and it allowed the detection of metabolic changes prior to and after histological manifestations of the Withering Syndrome, allowing for the possibility of earlier detection of diseases as well as the ability to track the recovery of abalones after infection (Rosenblum et al., 2006). ^1H NMR and ^1H HRMAS (high-resolution magic angle spinning) of *Pseudomonas aeruginosa* cultures and subsequent PCA proved that these techniques could distinguish between planktonic and biofilm cultures of *P. aeruginosa* (Gjersing et al., 2007). Another application of ^1H NMR is the identification of different genera and species of common human pathogens and of different strains of MRSA by ^1H NMR analysis of bacterial suspensions. This can be used in the rapid diagnosis of patients with bacterial infection and subsequent prescription of appropriate antibiotics (Bourne et al., 2001, Delpassand et al., 1995, Garg et al., 2004, Ohara et al., 2001). ^1H NMR was also successfully used to distinguish between virulent and non-virulent strains of *Bacillus cereus*, whereas in the same study no genetic difference could be determined (Bundy et al., 2005).

1.6.4 Multivariate Analysis

Multivariate data analysis involves the simultaneous analysis of all variables to obtain information from a data set (Wiklund, 2008). This is advantageous in that all variables are considered, thereby minimising data loss. The different approaches in multivariate analysis and their primary uses are summarised in Table 1-2. These can be unsupervised, in which the groupings of the samples are initially unknown, or supervised, in which the groups of samples are known and taken into account during analysis.

Table 1-2: Summary of methods used in multivariate analysis (adapted from Wiklund, 2008)

Overview	Classification	Discrimination	Regression
Trends Outliers Quality control Biological diversity Patient monitoring	Pattern recognition Diagnostics Healthy/diseased Toxicity mechanisms Disease progression	Discriminating between groups Biomarker candidates Comparing studies or instrumentation	Comparing blocks of omics data Metab vs proteomic vs genomic Correlation spectroscopy
PCA	SIMCA	PLS-DA OPLS-DA	O2-PLS

Factor analysis is a statistical approach that determines correlations between many variables by summarising the information into a smaller number of highly interrelated variables, known as factors (Hair et al., 2010). PCA, or principal component analysis, is a type of factor analysis that provides a graphical overview of the data and simplifies the data to a form more easily understandable. The objective of PCA is primarily, as mentioned above, to determine relationships between objects. PCA can aid in differentiating between classes of samples as well as in the detection of trends or outlying observations in the data. Data reduction is another common goal of PCA (Wiklund, 2008).

In PCA, the data is defined by a set of variables (principal components), each being a linear combination of the original variables. The first principal component has the largest sample variance. The second principal component has the next largest sample variance that is uncorrelated with the first component (Everitt and Dunn, 2001). PCA essentially simplifies a data matrix, X , into smaller matrices T , which shows the dominant “object patterns” of X , and P' , which shows the “variable patterns”. X possesses N objects and K variables that can be plotted as N points in K -space (alternatively called M -space for measurement space or multivariate space). This is difficult to visualise but it can be imagined that this “point swarm” can be projected onto a plane (Wold et al., 1987). Two plots can be used for PCA – the score scatter plot, which summarises the samples or observations (T), and the loading scatter plot which summarises the variables (P').

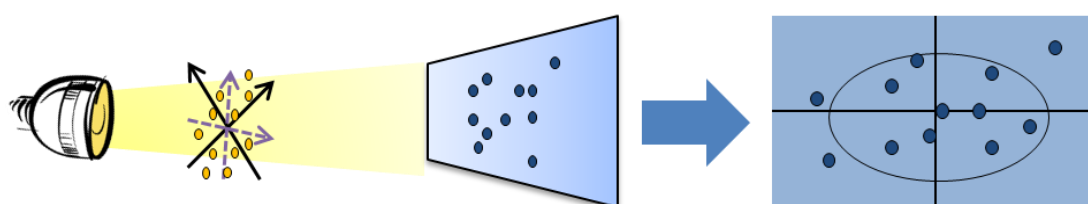


Figure 1-10: Diagram depicting the principle behind PCA (adapted from Wiklund, 2008). N objects are plotted in K space. The first principal component defines the largest variance between the objects. The second principal component is orthogonal to the first and defines the next largest variance. A projection simplifies the complex model onto a plane.

Another technique commonly used in metabolomics is OPLS-DA (orthogonal partial least squares – discriminant analysis or orthogonal projection of latent structures – discriminant analysis). Partial least squares (PLS) is a method of studying the

correlation between a descriptor matrix X and a response matrix Y . OPLS includes an orthogonal signal correction (OSC) filter, which allows systemic variation in X that is orthogonal or uncorrelated to Y to be studied (Bylesjo et al., 2006). Discriminant analysis allows the separation of classes. In contrast to PCA, OPLS-DA identifies the variables responsible for class separation; hence it can be used in the identification of biomarkers (Wiklund, 2008). Pareto scaling is recommended for metabolomic analysis as it renders PCA insensitive to artefacts such as baseline changes (Aranibar et al., 2006).

1.7 Fermentation

Fermentation comes from the Latin word *fervere*, which means to boil. For biochemists the process of fermentation is merely the catabolism of organic substrates to produce energy, whereas for industrial microbiologists it is “*any process for the production of product by the mass culture of a microorganism*” (Stanbury et al., 1995). Fermentation involves inducing the overproduction of certain metabolites by the microorganism by exploiting the regulatory mechanisms that the microorganism uses. Examples of these regulatory mechanisms are substrate induction, feedback control, and regulation based on the nutritional sources (carbon, nitrogen and phosphorous) available. Genetic and nutritional manipulation can be performed to overcome these mechanisms and thereby increase the production of the desired compounds (Sanchez and Demain, 2002).

There are five reasons why industrial fermentation is important (Demain, 2007):

- 1) Microorganisms have a high surface-to-volume ratio, allowing for the efficient uptake of nutrients necessary for production of large quantities of metabolites,
- 2) microorganisms can perform a wide range of metabolic reactions on various substrates,
- 3) the culture can be upscaled relatively easily from shake flasks to industrial scale fermenters,

4) the microorganisms can be genetically modified to optimise production of the desired compound, modify existing compounds or produce new compounds, and

5) microorganisms have the ability to produce specific enantiomers, as opposed to the mixtures of enantiomers generally obtained during chemical synthesis.

Interestingly, fermentation was already widely used in ancient history. Various microorganisms such as yeast, lactic acid bacteria and algae were utilized, quite unknowingly, by humans to make food and drinks. Indeed, fermentation was being performed about 10,000 years before microorganisms were even discovered (Ward, 1995). Louis Pasteur was the first person, in 1857, to suggest that yeast cells were living entities and that they were responsible for fermentation, marking the beginning of the field of fermentation microbiology (El-Mansi et al., 2007). Today, fermentation is not only applied to food and beverages but can be used in the production of microbial biomass, such as baking yeast, microbial enzymes, microbial metabolites, recombinant products and in the transformation or structural modification of a compound (Stanbury et al., 1995). Examples of compounds produced by fermentation are in Table 1-3 below. Aside from the vitamins and amino acids mentioned, other pharmaceutical products from microorganisms include antibiotics, immunosuppressants, enzymes, anti-cancer drugs, and the cholesterol-lowering statins (Demain, 2007).

Table 1-3: Examples of compounds produced by fermentation and other processes (Demain, 2007). Methods are chemical synthesis (C), extraction (E), enzymatic processes (En), fermentation (F) and bioconversion (B).

Compound	Method	Tons/Year	Market \$Million	Organism
Biotin (Vitamin H)	C	88	64	
β-Carotene (provitamin A)	C, E, F	100	-	<i>Blakeslea trispora</i> , <i>Dunaliella salina</i> , <i>D. bardawil</i>
Folic Acid	C	534	17	
γ-Linoleic acid	F	1000	-	<i>Mortierella isabellina</i>
Niacin	C	28,000	133	
Orotic acid (vitamin B ₁₃)	F	100	-	<i>Corynebacterium glutamicum</i>
Pantothenate	C, F	10,000	156	
Provitamin D3	C, E	3,800	70	
Pyridoxine (vitamin B ₆)	C	3,800	70	
Riboflavin (vitamin B ₂)	F	4,600	134	<i>Ashbya gossypii</i> , <i>Bacillus subtilis</i>
Thiamine (vitamin B ₁)	C, F	3,700	67	
Tocopherol	C, E	10,000	-	
Vitamin A (retinol)	C	2,800	308	
Vitamin B ₁₂ (cyanocobalamin)	F	25	105	<i>Propionibacterium shermanii</i> , <i>Pseudomonas dentrificans</i>
Vitamin C (ascorbic acid)	C + B	107,000	486	<i>Gluconobacter oxydans</i>
Vitamin E	C, E	30,000	89	
Vitamin F (polyunsat. fatty acids)	E, F	1,000	-	Fungi
Vitamin K ₂	C	2	-	
Amino Acids				
L-Alanine	En	500	-	
L-Arginine	F	1,200	150	
L-Aspartic acid	En	10,000	43	
L-Cysteine	En	3,000	4.6	
L-Glutamic acid	F	1,600,000	1,500	
L-Glutamine	F	1,300	-	
Glycine	C	22,000	-	
L-Histidine	F	400	-	
L-Isoleucine	F	400	-	
L-Leucine	F	500	-	
L-Lysine-HCl	F	850,000	1,500	
DL-Methionine	C	400,000	2,300	
L-Phenylalanine	F	12,650	198	
L-Proline	F	350	-	
L-Serine	F	300	-	
L-Threonine	F	70,000	270	
L-Tryptophan	En	3,000	150	
L-Tyrosine	F	165	50	
L-Valine	F	500	-	

Fermentation today has indeed become a science with many different facets, including the selection and sterilization of the media, the preparation of and aseptic introduction of the inoculum into the fermenter, the actual growth of the cells in such an environment so as to promote the production of the desired product, and finally the extraction and purification of the product (Stanbury et al., 1995). This process is depicted in Figure 1-11.

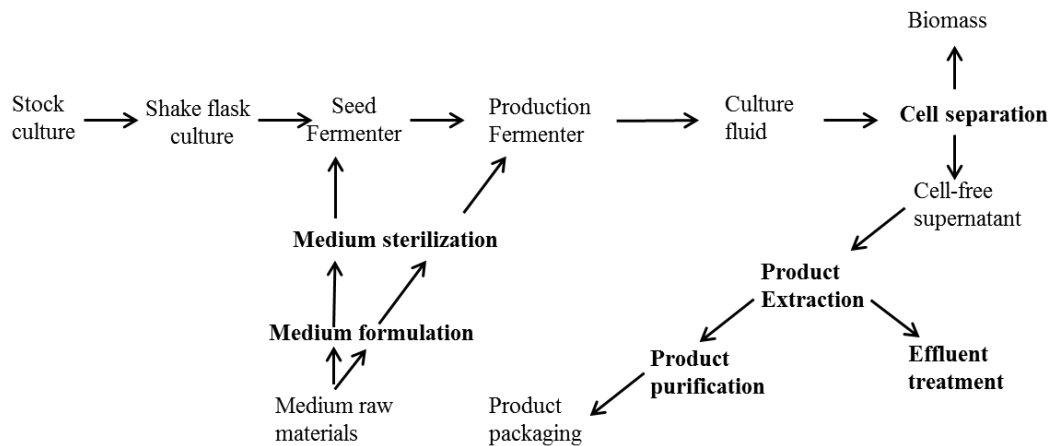


Figure 1-11: Schematic diagram of the fermentation process (adapted from Stanbury et al., 1995). The microorganism is grown from a stock culture in a shake flask prior to being cultured in a seed fermenter, after which it is grown in the production fermenter. After the cultivation of the microorganisms the cells are separated from the broth and the product is extracted. Processes are labelled in bold text. (Stanbury et al., 1995)

As the microorganism is cultured with a specific target in mind, the environment in which the microorganism is grown is optimised to promote the production of that target. The media is carefully selected, as is the type of fermentation. Batch fermentations are ‘closed systems’ wherein the amount of media is finite and all of the media is added to the vessel at the beginning of the fermentation. In fed-batch fermentations the substrate is added incrementally. This method is preferred in cases where the media might otherwise be too viscous or the substrate used too rapidly by the microorganisms. Continuous fermentations are ‘open’ systems in which new media is pumped into the system as older media is being pumped out (Ward, 1995). Certain parameters, such as pH and dissolved oxygen tension, are usually monitored and controlled to facilitate the intended reactions and transformations.

1.8 Summary and Conclusion

In light of the threat of man-caused bioterrorism and increasing bacterial and protozoal resistance to antibiotics, it is imperative that new antibiotics are discovered from sustainable sources. The marine environment has served as a rich source of previously unknown compounds, and of the marine creatures studied, sponges have proven to be the most fruitful in terms of the number of active metabolites discovered (Faulkner, 2002). However, as it has been shown that sponges play host to a wide variety of microorganisms, it is unclear whether sponge-associated bacteria and fungi in fact produce the metabolites formerly believed to have come from the sponges. The genus *Haliclona* has been well studied. Over 190 bioactive metabolites have been isolated from this genus alone (Yu et al., 2006). Research has been conducted on the microbial community of *Haliclona simulans* and evidence has been found for the production of antibiotics by some of the bacterial and fungal strains (Baker et al., 2009, Kennedy et al., 2009).

Metabolomics is a new field dedicated to analysing the complete set of metabolites of an organism, cell, or body fluid. It can be used to detect changes in a metabolome or to identify the metabolites present in the sample, as has already been demonstrated in studies of bacteria and plants. Metabolomics can be used to facilitate the search for active metabolites amongst the many compounds produced by sponges and their bacteria.

1.9 Hypothesis and Aims of the Study

Hypothesis: The application of metabolomics to marine natural products research enhances the discovery of novel bioactive compounds from sponges and endosymbiotic bacteria by allowing early-stage dereplication and targeted isolation through multivariate analysis, thereby reducing the chances of re-isolating known compounds.

The aim of this study is to ultimately discover antibiotic compounds from sponges and sponge-associated bacteria using metabolomic techniques, mainly liquid chromatography- high resolution Fourier transform mass spectrometry (LC-HRFTMS) and NMR. The following objectives will be accomplished:

1. Isolation of pure compounds from the sponge *Haliclona simulans*
2. The use of LC-HRFTMS and NMR to analyse extracts and compounds from *H. simulans*
3. The use of bioassays to determine the activity, if any, of compounds isolated from *H. simulans*
4. The use of LC-HRFTMS and NMR to identify and isolate compounds from *Streptomyces* sp. cultured from *H. simulans*
5. Dereplication of bacterial extracts from Mediterranean and Caribbean sponge bacteria using LC-HRFTMS and NMR
6. Extraction and isolation of bioactive compounds from the selected bacteria
7. Up-scaling of the bacterial culture to optimise production of the desired bioactive compounds

Chapter 2 Materials and General Methods

2. Materials and General Methods

2.1 Reagents

Acetone (HPLC grade), acetonitrile (HPLC grade), dichloromethane (HPLC grade), ethyl acetate (HPLC and Analytical Reagent grade), hexane (HPLC grade), methanol (HPLC and Analytical Reagent grade) were all purchased from Fisher Scientific, UK.

Celite[®] 545AW-Reagent Grade and Diaion[®] HP20 were both obtained from Supelco, USA. Celite[®] S from Sigma-Aldrich Co., Missouri, USA was also used. Sephadex[®] LH-20 was procured from Fluka Chemie AG Buchs, Switzerland. Silica gel 60 0.035-0.070 mm (220-440 mesh) from Alfa Aesar, Heysham, England was used for conventional column chromatography.

The deuterated solvents used for NMR were deuterated dimethyl sulfoxide (DMSO) or deuterated chloroform (CDCl₃) from Euriso-Top, France or from Sigma-Aldrich Co., Missouri, USA. The reagent used for steroid derivatisation, N-methyl-N-(trimethylsilyl)trifluoroacetamide (MSTFA) was also purchased from Sigma-Aldrich Co., Missouri, USA.

Royal Nature Advanced Pro Formula Salt by Royal Nature, Israel, was used to make up the artificial seawater for some of the bacterial experiments. Polypropylene glycol (M.W. average 2025) was used as an antifoaming agent during the fermentation of EG4. It was purchased from BDH, VWR International Ltd, England.

2.2 Equipment

2.2.1 General Equipment

The analytical miller (model: IKA A11 Basic) was purchased from IKA, Germany. Two rotary evaporators (model no: R-110 and R-3) were from BÜCHI, Switzerland. The centrifuge used was Force 7 from Fisher Scientific. The Ultrawave sonicator was from Scientific Laboratory Supplies, Ltd. The UV lamp (UVGL-55 Handheld UV Lamp) was purchased from UVP, Cambridge, UK. The heat gun HL 2010 E Type 3482 was the product of Steinel, USA. The Stuart[®] block heater SBH 130D/3

was from Bibby Scientific Ltd., Staffordshire, UK. The freeze dryer (model: Christ Alpha 2-4) was from Martin Christ Gefriertrocknungsanlagen GmbH, Germany. The optical rotations of the compounds were measured on a 341 Polarimeter from PerkinElmer, Inc., USA.

2.2.2 Microbiology Equipment

The laminar flow hood (BioMAT²) was purchased from Medical Air Technology, UK. The stand incubator (Incu-160S) used for agar plates was from SciQuip Ltd., Shropshire, UK. The rotary shaker used was from Gallenkamp, UK. The homogenizer (IKA T18 Basic Ultra-Turrax) and handheld homogenizer (Ultra-Turrax T8) came from IKA Labortechnik, Germany. A Biostat Q Fermenter (B. Braun Biotech International, Switzerland) was used for the fermentation set up. The cell disruptor (Model 4000) was from Constant Systems Ltd., Warwick, UK.

2.2.3 Liquid Chromatography – Mass Spectrometry Instruments

The High Pressure Liquid Chromatography (UltiMate-3000)-Mass Spectrometry (Exactive) instrument was from Thermo Scientific, Germany. Another HPLC-MS system was used for some of the later analyses was the Accela HPLC system coupled to an Exactive mass spectrometer (Thermo Scientific, Germany). The low-resolution mass spectrometry system was a Finnigan LCQ-Deca coupled to an HPLC (series 1100) from Hewlett Packard. Fragmentation was performed on a Finnigan Surveyor system coupled to a Thermo-Finnigan LTQ Orbitrap (Thermo Scientific, Germany).

2.2.4 Gas Chromatography- Mass Spectrometry Instruments

The high-resolution GC-MS at SIPBS is a Focus GC coupled to a DSQ II from Thermo Scientific, Germany. The column, InertCap 1MS (ID: 0.25 mm, length: 30 m, df: 0.25 μ m) was purchased from GL Sciences Inc., Japan. The low-resolution GC-MS used at the Department of Pure and Applied Chemistry is a Thermo Finnigan Polaris Q with Trace GC. The column used was an Agilent DB5-ms UI (ID: 0.25 mm, length: 30 m, df: 0.25 μ m).

2.2.5 Nuclear Magnetic Resonance Instruments

The Nuclear Magnetic Resonance spectroscopy machine JNM-LA400 model was from JEOL, Japan and the magnet NMR AS400 model EUR0034 came from Oxford Instruments, England. The NMR has a Pulse-Field Gradient “Autotune”TM probe 40TH5AT/FG broadband high sensitivity probe for 5mm tubes. It has FG coils, 2H lock channel and can operate at various temperatures.

An AVANCE-III 600 instrument with a 14.1 T Bruker UltraShield magnet from the Department of Pure and Applied Chemistry was also used. It has a 24 position autosampler, 3 channel console, is DQD and Waveform-equipped and can use either a BBO-z-ATMA-[³¹P-¹⁸³W/¹H] probe or a TBI-z-[¹H, ¹³C, ³¹P-¹⁵N] probe.

DMSO and CDCl₃ Shigemi[®] tubes and Wilmad[®] NMR capillary tubes were purchased from Sigma-Aldrich Inc., USA.

2.2.6 Flash Chromatography Equipment

Flash chromatography or medium pressure liquid chromatography (MPLC) is a separation technique that is similar in principle to conventional column chromatography. In flash chromatography, however, pressure is applied to elute the sample through the column at a faster rate and to obtain higher resolution (Still et al., 1978). The solvent system and the column to be used were selected following thin layer chromatography so the uppermost band or the compound of interest had an R_f value of 0.3 on the TLC plate.

The BÜCHI MPLC instrument was the Sepacore <<Easy Synthesis>> Purification System, consisting of two C-601 pump modules and the C-615 pump manager (BÜCHI, Switzerland). This allowed binary solvent gradients with flow rates of 2.5 to 250 mL/min. The columns and the column stand were purchased from VersaFlash/Supelco, Sigma-Aldrich, Germany. The fraction collector (CF2) was from Spectrum Labs. The Reveleris[®] Flash Forward system of Grace Davison Discovery Sciences (Illinois, United States) was also used for flash chromatography. This system had the advantage of having two detectors, an evaporative light scattering detector (ELSD) and a UV detector (wavelength range: 200-500 nm). This

ensured greater sensitivity and the detection of all peaks and not just the UV-active compounds. The system also allowed for a binary solvent gradient; however, there were four independent channels so up to four solvents can be used in a single run. The flow rate could range from 4 to 200 mL/min and was automatically adjusted if the pressure became too high. The fraction collector was built into the system and the trays recognised by the software, thus reducing errors. In addition, the chromatogram could be saved and printed. Another system, the Biotage[®] Isolera[™] Spektra One Flash Purification System ISO-1SV, a product of Biotage, Uppsala, Sweden, was also used. This had a UV detector (wavelength range: 200-400 nm) but did not have an ELSD. Again, the Biotage had four solvent channels allowing four solvents to be used in a binary gradient during a single run. Biotage[®] SNAP cartridges were used which permitted the loading of samples onto frits before being placed into the column. This minimised problems with the solubility of the samples.

2.2.7 TLC Plates

The normal phase thin layer chromatography plates (TLC silica gel 60 F₂₅₄), reverse phase TLC plates (TLC silica gel 60 RP-18 F₂₅₄S) and preparative TLC plates (TLC silica gel 60 F₂₅₄ on 20x20 cm aluminium sheets) were from Merck KGaA, Germany.

2.3 Software

LC-MS and GC-MS spectra were viewed using Thermo Xcalibur 2.1 (Thermo Scientific, Germany). To convert the raw data into separate positive and negative ionisation files, a program called msconvert from ProteoWizard (pwiz) was used. The files were then imported to the data mining software, MZmine 2.10.

The databases used for the identification of compounds were the Dictionary of Natural Products (DNP) 2012 and AntiMarin 2012, a combination of Antibase and MarinLit. MestReNova (MNova) 2.8 by Mestrelab Research, S.L, (Santiago de Compostela, Spain) was used to process all NMR data. SIMCA 13 (Umetrics AB, Umeå, Sweden) was used for multivariate data analysis.

2.4 General Methods

2.4.1 Liquid Chromatography-High Resolution Fourier Transform Mass Spectrometry

The following method was used on both of the LC-HRFTMS systems, the UltiMate 3000-Exactive Orbitrap and Accela-Exactive Orbitrap from Thermo Scientific, Germany:

Column: ACE 5 C18 75x3.0 mm (Hichrom Ltd, UK)

Mobile Phase: 0.1% formic acid in water (A)

0.1% formic acid in acetonitrile (B)

Injection volume: 10 μ L

Flow rate: 300 μ L/min

Gradient: 0-30 min	10-100% B
30-35 min	100% B
35-36 min	100%-10% B
36-40 min	10% B (equilibration)

High resolution mass spectrometry analysis was performed in both positive and negative mode with a spray voltage of 4.5 kV and a capillary temperature of 320°C. The mass range varied from m/z 150-1500 or 75-1500.

The Finnigan Surveyor – Thermo Finnigan LTQ Orbitrap was used when the fragmentation of a compound was required. It could only be operated at one ionisation mode at one time. The positive ionisation mode was used in all experiments in this project. The method used is outlined below:

Column: ACE 5 C18 75x3.0 mm (Hichrom Ltd., UK)

Mobile Phase: 0.1% formic acid in water (A)

0.1% formic acid in acetonitrile (B)

Injection volume: 10 μ l

Flow rate: 300 μ l/min

Gradient: 0-30 min	10%-100% B
30-35 min	100% B
35-36 min	100%-10% B
36-45 min	10% B (equilibration)

There were two scan events. For scan event 1 the scan range was 75.0000-1200.0000. For scan event 2 the activation type used was CID with an isotope width (m/z) of 0.9. The normalized collision energy was 35.0 kv. Activation Q was set at 0.250 ms and the activation time was 30.00 ms. Wideband activation was switched on.

For the low-resolution LC-MS (HP 1100-Finnigan LCQ Deca) the following method was used:

Column: ACE 5 C18 75x3.0 mm (Hichrom Ltd., UK)

Mobile Phase: 0.1% formic acid in water (A)

0.1% formic acid in acetonitrile (B)

Flow rate: 400 μ l/min

Gradient: 0-30 min	10%-100% B
30-35 min	100% B
35-36 min	100%-10% B
36-40 min	10% B (equilibration)

2.4.2 Data Mining Using MZmine 2.10

The LC-MS chromatograms and spectra were viewed using Thermo Xcalibur 2.1 or MZmine 2.10. The files were sliced into positive or negative ionisation modes using the msconvert file slicer from ProteoWizard, after which the files were imported for processing into MZmine 2.10.

The chromatograms were first cropped to 0.5-38.0 minutes using the crop filter under the dataset filtering function. The centroid mass detector was used for peak detection with the noise level set to 1.0E4 and the MS level set to 1. The chromatogram builder function was set to a minimum time span of 0.2 min, minimum height of 1.0E4 and m/z tolerance of 0.001 m/z or 5.0 ppm. For chromatogram deconvolution the algorithm used was the local minimum search. The chromatographic threshold was set to 90.0%. The search minimum in RT range was 0.4 minutes, minimum relative height was 5.0%, minimum absolute height was 3.0E4, minimum ratio of peak top/edge was 2 and the peak duration range was 0.3-5.0 min. Isotopes were detected using the isotopic peaks grouper. The m/z tolerance was 0.001 m/z or 5.0 ppm, RT tolerance was 0.2 absolute (minutes), the maximum charge was 2 and the representative isotope used was the most intense. Retention time normalization was performed using the RT normalizer. Again, m/z tolerance was 0.001 m/z or 5.0 ppm while the RT tolerance and the minimum standard intensity were set to 5% (relative) and 5.0E3 respectively. The peak lists were all aligned using the join aligner (m/z tolerance 0.001 m/z or 5.0 ppm, weight for m/z : 20, RT tolerance: 5.0% relative, weight for RT: 20). The aligned peak list was gap-filled using the peak finder function (intensity tolerance: 1%, m/z tolerance: 0.001 m/z or 5.0 ppm, RT tolerance: 0.5 min). An adduct search was performed with the RT tolerance set at 0.2 absolute (min), the m/z tolerance at 0.001 m/z or 5.0 ppm and the maximum relative adduct peak height at 30%. The adducts searched for were Na, K, NH₄ and ACN+H. A complex search was also performed using [M+H]⁺ for the positive ionisation mode and [M-H]⁻ for the negative ionisation mode. The RT tolerance was set at 0.2 absolute (min), m/z tolerance was kept at 0.001 m/z or 5.0 ppm, and the maximum complex peak height was set at 50%. A custom database search was then performed using either the DNP or AntiMarin databases. Alternatively, for the comparison of

the different EG4 extracts, the positive and negative peak lists were exported to MS-Excel where they were compared to the AntiMarin 2012 database using an in-house macro. This enabled the removal of blank media peaks using the macro, as well as allowing the preparation of the data for SIMCA 13 analysis by combining the positive and negative peak lists into one MS-Excel file.

2.4.3 Gas Chromatography-Mass Spectrometry

One microliter of sample was injected into the column. The oven temperature began at 80°C for 1 minute after which the temperature was increased at a rate of 15 deg/min until a temperature of 200°C. This temperature was maintained for 15 minutes. The temperature was then again increased at a rate of 5 deg/min until the final temperature of 320°C. This was held for 10 minutes until the end of the run. The base temperature of the SSL was 250°C. The mode was splitless. The split flow was on at 15 mL/min. The splitless time was 1 minute. The carrier method was set to constant flow. The initial value was 1.50 mL/min and the initial time was 1 minute. The MS transfer line was maintained at a temperature of 320°C. The source temperature of the DSQ II mass spectrometer was set to 250°C. The mass range used was 50.0-800.0.

2.4.4 Nuclear Magnetic Resonance Spectroscopy

Samples were dissolved in 600 µL of a suitable deuterated solvent and transferred to an NMR tube. For small quantities of samples Shigemi® tubes or Wilmad® NMR capillary tubes were used to improve the resolution of the spectra. The volume of solvents used for these tubes was 180 µL. Samples were then processed using MNova 2.8.

2.4.5 Measurement of Optical Rotation

The optical rotation or specific rotation of some isolated compounds was measured using a 341 polarimeter (PerkinElmer Inc., USA). The compounds were dissolved in a suitable solvent (chloroform) to a concentration of 1 mg/mL. Ten readings from the

machine were averaged and the optical rotation was calculated using the following equation:

$$[\alpha]_D^{20} = \frac{\alpha}{l + c}$$

where α is the average of the measured rotation ($^{\circ}$), l is the path length in decimetres, and c is the concentration of the solution in g/mL.

2.4.6 Bioassays

The crude extracts and fractions of *H. simulans* and *Microbacterium* sp. (EG4) were tested for activity against *Trypanosoma brucei brucei*, *Mycobacterium marinum*, and, for some EG4 fractions, *Nocardia farcinica*. These assays were performed by Ms. Carol Clements at the Strathclyde Institute for Drug Research (SIDR). The cytotoxicity assays performed on the sterols isolated from *H. simulans* were also carried out at the SIDR by Mrs. Louise Young and Mrs. Grainne Abbott. The crude extracts and fractions of the *Streptomyces* SM8 strain were assayed for antimicrobial and anti-calcineurin activity by Dr. Lekha Menon Margassery at the Environmental Research Institute (ERI), University College Cork (UCC).

2.4.6.1 Anti-trypanosomal Assay

The samples were dissolved in a sufficient quantity of DMSO to reach a concentration of 10 mg/mL or 1 mg/100 μ L. The samples were initially screened at one concentration (20 μ g/mL) to determine their *in vitro* activity. The 10 mg/mL stock solutions of the samples were diluted 1 in 10 with HMI-9 and 4 μ L was pipetted into 96 μ L HMI-9 in the 96-well plate. One hundred microliters of trypanosome suspension (containing *Trypanosoma brucei* S427 blood stream form at 3×10^4 trypanosomes/ml) were added to make the final concentration of the extracts 20 μ g/ml. DMSO was used as the negative control at a concentration of 1 to 0.002% and suramin was used as the positive control at a concentration range of 1 to 0.008 μ M. The plate was incubated at 37 $^{\circ}$ C, 5% CO₂ with a humidified atmosphere for 48 hours, after which 20 μ L of Alamar blue was added. The plate was incubated under the same conditions for another 24 hours and the fluorescence read using the Wallac

Victor microplate reader with excitation at 530 nm and emission at 590 nm. The results were calculated as percentages of control values.

The minimum inhibitory concentration (MIC) for the active compounds were then determined. Four microliters of the 10 mg/mL stock solutions were pipetted into one column of the transparent flat-bottomed 96-well plates after which 196 μ L of HMI-9 was added, resulting in a concentration of 200 μ g/mL. One-to-one serial dilutions with HMI-9 were carried out in the other columns of the plate. One hundred microliters of trypanosome suspension (containing *Trypanosoma brucei* S427 blood stream form at 3×10^4 trypanosomes/mL) were added so that the final concentration of the compounds ranged from 100 μ g/mL to 0.17 μ g/mL. DMSO and suramin were used as the negative and positive controls respectively, at the same concentrations used in the initial screen. The plate was incubated, Alamar blue added, and the fluorescence was read in the same manner as the initial screen. The results were calculated as percentages of control values and the MICs were determined.

MIC assays were only performed on samples having sufficient activity (>90% inhibition); thus, where no MIC was available the % inhibition was reported.

2.4.6.2 Anti-mycobacterium Assay

M. marinum resembles *M. tuberculosis*; however, it is less dangerous to humans and is faster-growing, hence it is the model used in screening for anti-mycobacterial activity. *Mycobacterium marinum* ATCC.BAA535 from the thawed stock cryoculture was streaked onto Columbia (5% horse blood) agar slopes and incubated at 31°C for 5 days. A loopful of the culture was then transferred into 10 mL of sterile 0.9% NaCl containing glass beads. The suspension was mixed and allowed to settle. 1 mL of the supernatant was added to 10 mL sterile MHB saline that had been used to zero the turbidity meter. The turbidity of the solution was adjusted to be the same as a 0.5 McFarland standard. A few drops of Tween 80 0.02% were filter sterilized and added to homogenise the suspension. This was then shaken and the inoculum diluted 1 in 10 with cation adjusted Mueller Hinton Broth for use in the assay.

Samples were dissolved in a sufficient quantity of DMSO to reach a concentration of 10 mg/mL or 1 mg/100 μ L. For the initial screen, the 10 mg/mL stock solutions of the samples were diluted ten times to 1000 μ g/mL using MHB. Twenty microlitres of each extract were placed in each well and 80 μ L of MHB was added to each. DMSO was included as the negative control at a concentration range of 1 to 0.002% and gentamycin was included as the positive control at a range of 100 to 0.78 μ g/mL. One hundred microlitres of the bacterial suspension were added to the wells. The plates were sealed and incubated at 31°C for 5 days before the addition of 10 μ L of Alamar blue. The plates were again sealed and incubated at the same temperature for 24 hours after which fluorescence was determined using the Wallac Victor microplate reader. The results were calculated as percentages of control values.

The MICs of the active samples were determined following the same procedure; however, the final concentrations of the test solutions in the 96-well plate ranged from 100 to 0.17 μ g/mL.

MIC assays were only performed on samples having sufficient activity (>90% inhibition); thus, where no MIC was available the % inhibition was reported.

2.4.6.3 Anti-nocardia Assay

The assay against *N. farcinica* followed the same procedure as *M. marinum*. The difference was in the incubation periods as *N. farcinica* grows faster than *M. marinum*. *N. farcinica* was incubated on Columbia agar slopes for 4 days as opposed to 5 days for *M. marinum*. Prior to the addition of Alamar blue, the assay plate was incubated for 3 days for *N. farcinica* rather than the 5 days required for *M. marinum*. Finally, following the addition of Alamar blue, the plate was incubated for 20 hours rather than 24 hours before the fluorescence was determined. The same concentrations of the test solutions and controls were used.

2.4.6.4 Antifungal Assays

The SM8 crude extracts and fractions were assayed for activity against *Candida albicans* SC5314, *C. glabrata* CBS138, *Saccharomyces cerevisiae* BY4741, *Kluyveromyces marxianus* CBS6556, and *Aspergillus fumigatus* Af293 by following a resazurin-based method previously reported for yeast (Liu et al., 2007).

2.4.6.5 Antibacterial Assays

The strains used for the antibacterial activity of the SM8 crude extracts and fractions were *Bacillus subtilis* IE32, *Escherichia coli* 12210, *Staphylococcus aureus* NC000949 and *Pseudomonas aeruginosa* PA01. The assays were also performed in 96-well microtitre plates using resazurin dye as an indicator (Sarker et al., 2007).

2.4.6.6 Anti-calcineurin Assay

The high-throughput anti-calcineurin assay (Margassery et al., 2012) that was performed on the SM8 crude extracts and fractions was developed by Dr. Lekha Menon Margassery at the ERI, UCC. The calcineurin pathway in *S. cerevisiae* BY4741 *CDRE::lacA* reporter strain was triggered by the alkaline stress. This would normally result in the translocation of the Crz1p transcription factor which would bind to the CDRE element in the nucleus, activating expression of the *CDRE::lacZ* gene on the reporter strain. The inhibition of the calcineurin signalling pathway would prevent the expression of this gene. This extent of gene expression would then be detected using a modified β -galactosidase activity assay (Margassery et al., 2012).

2.4.6.7 Cytotoxicity Assay

The three sterols isolated from *H. simulans* were tested for cytotoxicity against normal fibroblasts from human foreskin (Hs27 cells) derived from ECACC (Sigma-Aldrich, Dorset, UK). The cells were cultured in DMEM media supplemented with 10% (v/v) foetal bovine serum, 2 mM glutamine and 50 μ g/mL penicillin/streptomycin solution (all from Invitrogen, Paisley, UK) in a humidified incubator at 37°C in the presence of 5% CO₂. Cells were routinely passaged at 90-95% confluence.

The cells were then seeded at a concentration of 7500 cells/well in black 96-well flat-bottomed plates and allowed to adhere overnight. The three sterols were then added at a concentration range of 0.1 nM to 100 µM (in half log units) and incubated for 48 hours. Viability was assessed using a CellTiter-Glo[®] (Promega, Southampton, UK) kit according to the manufacturer's instructions. The luminescence was then measured using a Wallac Victor 2 (Perkin Elmer, Cambridge, UK). The IC₅₀ values of the sterols were determined and all results confirmed microscopically.

2.4.7 Column Chromatography

Column chromatography was performed using three types of stationary phase – Diaion[®] HP20, Sephadex[®] LH-20 and silica gel.

2.4.7.1 Diaion[®] HP20 Chromatography

Diaion[®] HP20 is a highly porous styrenic adsorption resin. It therefore uses both selective adsorption and molecular sieving mechanisms. In this project it was used to de-salt the sponge extracts and to remove the salt and sugar from the bacterial extracts. The column was prepared by suspending a sufficient quantity of Diaion[®] HP20 (so that the column was half-filled) in analytical reagent-grade methanol. This suspension was poured into the column, which had been plugged with cotton that had previously been soaked in methanol. This was to prevent bubbles from rising and disturbing the packing of the column. More methanol was added and the HP20 was activated for three hours. The methanol was then drained from the column. A cotton pledget was placed above the HP20. Fresh methanol was passed through the column to wash it. The washing was collected and passed through the column a second time. The column was then washed with pure-grade water twice. The column was equilibrated overnight in fresh pure-grade water. The preparation of the sponge and bacterial extracts for dry-loading onto the column is described in Chapter 3 and Chapter 5 respectively. The sample was placed on top of the column and covered once more with cotton (Figure 2-1):

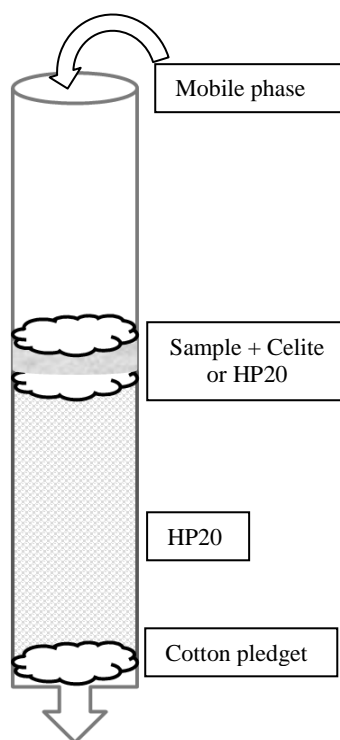


Figure 2-1: Setup of the HP20 column. The cotton pledget at the bottom prevents the HP20 from escaping the column. The sample may be mixed with Celite or more HP20 and dry-loaded onto the column. Another piece of cotton is placed above the sample and this is usually weighed down by a stirring rod to prevent the HP20 from floating when the mobile phase is added.

2.4.7.2 Sephadex[®] LH-20 Chromatography

Sephadex[®] LH-20 is a hydroxypropylated dextran that has both hydrophilic and lipophilic properties. It makes use of molecular sieving to separate the analytes. It is useful in separating lipids, steroids, and low molecular weight peptides. In this project it was used to separate the crude extracts of *Streptomyces* sp. which were found to contain a high quantity of lipids. Sephadex[®] LH-20 was suspended in methanol and poured into the column. It was then allowed to settle overnight. The sample was carefully pipetted onto the top of the Sephadex[®] and small amounts of mobile phase were added until the sample had been adsorbed into the Sephadex[®]. A larger volume of solvent was then poured into the column. Once all the bands had been eluted and the column washed, the fractions collected were analysed and pooled using TLC. The pooled fractions were submitted for NMR, LC-HRFTMS and antimicrobial assays.

2.4.7.3 Adsorption Chromatography using Silica Gel

Silica gel is a common stationary phase for adsorption chromatography. The surface of the silica gel has silanol groups which interact with the compounds. The less polar compounds have fewer interactions with these hydroxyl groups and thus elute much faster from the column (Braithwaite and Smith, 1996). Silica columns were prepared by suspending the silica gel in the most non-polar component of the mobile phase. The slurry was then poured into the column and the silica was left to settle. The column was then equilibrated with the desired mobile phase. As with the Sephadex column, the sample was gently pipetted along the inside of the column so that it would flow down the glass and would not disturb the settled silica. Small amounts of the mobile phase were added until the mobile phase above the silica was colourless, indicating that the sample had been adsorbed into the silica. A larger quantity of mobile phase was poured into the column. After the collection of all the bands and the washing of the column, the fractions were pooled according to their TLC chromatograms and submitted for NMR and LC-HRFTMS analysis as well as for antimicrobial assays.

2.4.8 Thin Layer Chromatography

Thin layer chromatography (TLC) can be used as an analytical technique for the identification of a compound based on its R_f value. It is also used to determine the purity of a sample and to estimate the number of compounds present in an extract, and even to decide on a suitable solvent system for flash chromatography. It can also be used as a preparative technique to purify compounds.

For normal phase TLC, the fractions were all dissolved in suitable nonpolar solvents and spotted 1 cm above the bottom edge of TLC silica gel 60 F₂₅₄ plates (Merck KGaA, Germany). The mobile phases used were varying proportions of hexane and ethyl acetate, and dichloromethane and methanol. For reverse phase TLC the fractions were dissolved in water or methanol and spotted 1 cm above the bottom edge of TLC silica gel 60 RP-18 F₂₅₄S plates. These were eluted with water and methanol as the mobile phase. The run of the plates was generally 5 cm.

The spots were detected using the UVGL-55 Handheld UV Lamp (UVP, Cambridge, UK) under short wavelength UV light (254 nm) and long wavelength UV light (365 nm). Compounds that quenched fluorescence or phosphorescence could be seen as dark spots on a green background at 254 nm as silica gel F₂₅₄ contained a phosphorescent indicator. Other analytes that fluoresced at 365 or 366 nm could be seen under long wavelength radiation as coloured bands (Wall, 2005). Conjugated double bond systems, such as aromatic systems, could be seen under short wavelength UV radiation. Alkaloids and flavonoids could be seen under long wavelength UV radiation. The plates were then sprayed with p-anisaldehyde-sulphuric acid spray reagent and heated to 170°C. This spray reagent was used to see many natural products such as essential oil components, steroids, terpenes, sugars, phenolic compounds, and sapogenins (Wall, 2005).

For preparative TLC the samples were spotted in a band 2 cm above the bottom edge of the plate. The TLC chamber contained 400 mL of the mobile phase. Prior to the elution of the plates, tissue paper was placed inside the chamber to allow the mobile phase to run up the tissue, thus making the equilibration of the chamber faster. It is important to use a saturated or equilibrated chamber because if the vapour phase is not saturated the solvent front will begin to evaporate from the plate as it rises. The velocity of the solvent front decreases and the solvent front will be concave in shape. The spots near the solvent front having a high R_f value will be compressed into bands. In addition, the plates can be developed several times to improve resolution (Wall, 2005). The bands were viewed under UV light and marked with pencil. Unlike analytical TLC, the plates were not sprayed with p-anisaldehyde reagent. The bands were cut out of the plates and the compounds were recovered with acetone.

2.4.9 Bioinformatics Analysis

The National Center for Biotechnology Information (NCBI) website (<http://www.ncbi.nlm.nih.gov/>) was used to obtain the gene sequences for *Streptomyces* sp. SM8 (accession no. PRJNA180938) and *Microbacterium testaceum* StLB037 (accession no. NC_015125) as well as enzymes and regulatory proteins for Basic Local Alignment Search Tool (BLAST) analysis. The sequences obtained from the BLAST analysis were aligned using the MultAlin website (<http://multalin.toulouse.inra.fr/multalin/multalin.html>) (Corpet, 1988).

**Chapter 3 Extraction and Analysis of Antibiotics from the
Sponge *Haliclona simulans***

3. Extraction and Analysis of Antibiotics from the Sponge *Haliclona simulans*

3.1 Introduction

Annually, compounds isolated from sponges make up 25-37% of the new natural products discovered from the marine environment (Blunt et al., 2004, Blunt et al., 2013). Many of these metabolites are biologically active and possess fish deterrent, anti-cancer, anti-viral, anti-fouling and antibiotic properties. Although the degree to which sponges can perform *de novo* synthesis is still being debated, it is important to isolate and identify metabolites present in the sponge extract as these can be compounds originally produced by endosymbionts and/or further modified by the host sponge. These endosymbionts are, however, sometimes difficult to culture in a laboratory. Metabolites produced directly by the sponge as opposed to microorganisms are subject to sustainability problems since it is more difficult to culture sufficient quantities of sponges than to culture microorganisms. Nevertheless, these natural products can serve as lead compounds or targets for synthesis.

Haliclona simulans (class *Demospongiae*, order *Haplosclerida*, family *Chalinidae*) is an orange or light brown sponge that is characteristically hard and brittle. The spicules are described as “short, fat oxea 120-150 x 5-12 μm ”. The repent-branching and the distribution of the oscules along the branches also assist in the identification of the sponge (Ackers et al., 2007). The fungal and bacterial communities living within *H. simulans* have been studied by the group at the Environmental Research Institute, University College Cork (Baker et al., 2009, Kennedy et al., 2008), but the metabolic analysis of the whole sponge itself has not yet been performed. This chapter details the extraction, fractionation, isolation and identification of bioactive compounds from *H. simulans*.

3.2 Methodology

3.2.1 Acquisition of Sponge Sample

A sponge, *Haliclona simulans*, was collected from Kilkieran Bay, Galway, Northern Ireland by the Environmental Research Institute, University College Cork. It was freeze-dried, sealed under vacuum and sent to the Strathclyde Institute of Pharmacy and Biomedical Science, University of Strathclyde where it was stored at -20°C until the extraction of its metabolites.

3.2.2 Extraction of Sponge Metabolites

One bag of freeze-dried *H. simulans*, weighing 73.96 g, was finely ground using an analytical mill (IKA, Germany). The powder was then macerated in HPLC-grade acetone at room temperature with constant stirring for three hours. This was repeated three times. The acetone was pooled and evaporated under vacuum using a rotary evaporator. The cold extraction process was repeated by soaking the marc in HPLC-grade methanol three times. The methanol was also evaporated under vacuum. The combined extract weight was 13.8821 g.

3.2.3 Removal of Salt using HP20 Chromatography

3.2.3.1 Preparation of Sample for HP20 Chromatography

The dried sponge extract was reconstituted in 20 mL methanol and 20 mL acetone. The flasks were sonicated to aid in the dissolution of the sample. The sample was mixed thoroughly with sufficient Celite[®] and placed in the fume hood for two nights to dry.

3.2.3.2 Fractionation of Sponge Extract

The HP20 column was prepared according to the procedure in **2.4.7.1**. The Celite[®] containing the adsorbed extract was loaded at the top of the column. Purified sand was added to reduce the caking of the Celite[®]. The compounds were eluted using a gradient of 100% pure-grade water to 100% methanol (HPLC grade) in 10% increments. The volume for each eluant was 250 mL. Each eluant was allowed to

pass through the column completely to dryness before the next solvent was added. 250 mL of 50:50 acetone:methanol (HPLC grade), followed by two additional elutions with 100% methanol, were used to wash the column.

Two millilitres of each fraction were collected for LC-HRFTMS analysis. This was performed using UltiMate3000-Exactive Orbitrap following the method in 2.4.1. The rest of the fractions were dried under vacuum using a rotary evaporator and placed in the desiccator prior to weighing.

3.2.4 Medium-Pressure Liquid Chromatography of Pooled HP20 Fractions

3.2.4.1 Pooling of Fractions

The collected fractions starting with 30:70 pure-grade water:methanol (HPLC grade) to the 2nd washing with 100% methanol were subjected to thin layer chromatography (TLC). These fractions were analysed along with fractions collected by a previous student who had also performed the same extraction and HP20 chromatographic procedure on another sample of *H. simulans*.

Fractions eluted with 50:50 acetone:methanol, 1st methanol wash, and 2nd methanol wash were pooled together with the methanol wash from the previous sponge sample. The total weight of the pooled fractions was 1.3966 g. The pooled fractions were dissolved in 200 μ L of ethyl acetate and 800 μ L of hexane. Upon addition of hexane, a white precipitate formed. This was collected by centrifugation at 10,000 rpm for 5 minutes and subjected to NMR.

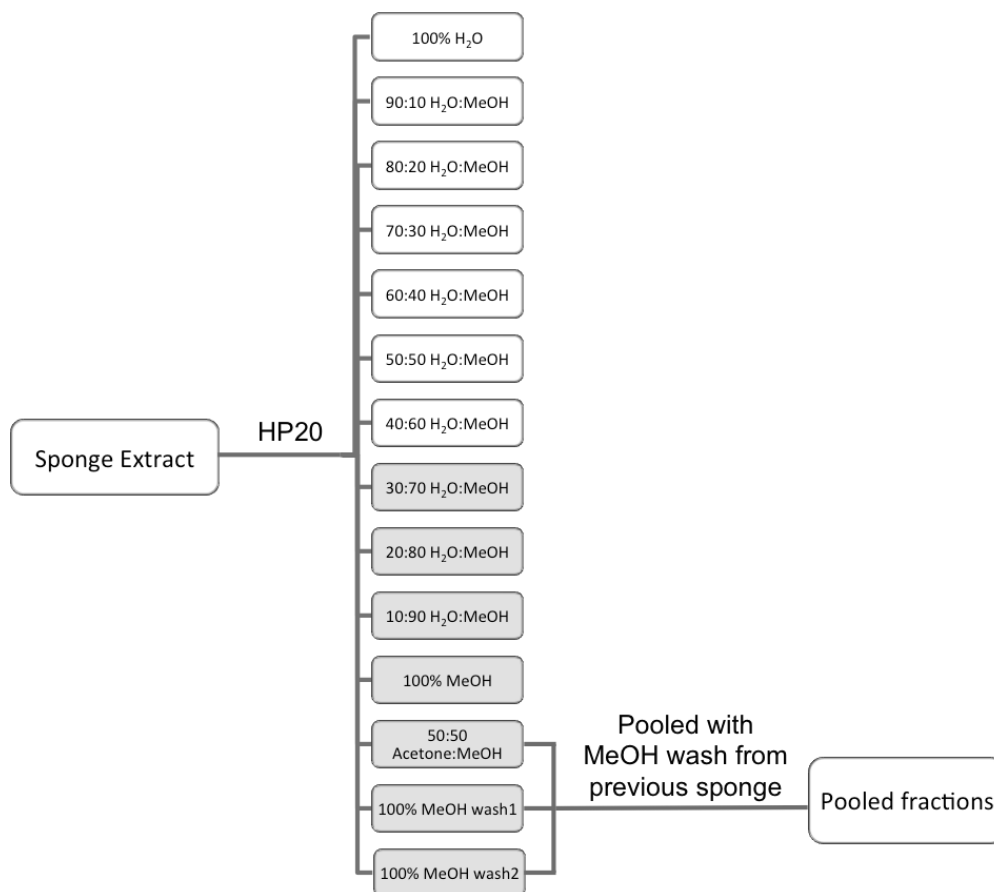


Figure 3-1: Flowchart of HP20 chromatography. The flowchart depicts the fractions collected following HP20 chromatography and the subsequent pooling of non-polar fractions with similar fractions obtained from a previous extraction of an *H. simulans* sponge. Cells in grey were analysed using TLC.

3.2.4.2 Fractionation of Pooled Fractions

The pooled fractions were loaded into a column and fractionated with the BÜCHI flash chromatography system (BÜCHI, Switzerland) using the following method:

Column: VersaPak Silica (Spherical) 23 x 110 mm (23g)

Mobile Phase: Hexane (A) , ethyl acetate (B)

Flow rate: 10 mL/min

Gradient: 0-5 min	0% B
5-35 min	0-100% B
35-40 min	100% B

The fractions were collected every 15 seconds. In total, 168 test tubes were collected. The column was inverted and washed with 250 mL of 70:30 dichloromethane:methanol.

3.2.4.3 Pooling of MPLC Fractions

The 168 fractions collected were analysed by TLC using mobile phase combinations of hexane:ethyl acetate and dichloromethane:methanol. From test tubes 85 until 168 the fractions were pooled by colour as no differences could be seen on the TLC plates in terms of R_f values. Tubes 85-106 were yellow whereas tubes 107-155 were pink. Tubes 156-167 were colourless. Twelve fractions (B-1 to B-12) were obtained in total. These were then dried, weighed and submitted for NMR, LC-HRFTMS and antimicrobial assays.

3.2.5 Normal Phase Chromatography of B-5

Fraction B-5 was subjected to further purification using a conventional column in which silica was used as the stationary phase. The silica was suspended in dichloromethane to form a slurry then poured into the column and allowed to settle. The column was then equilibrated with 95:5 dichloromethane:methanol and the sample was carefully loaded on top of the silica. The sample was eluted at a flow rate of approximately 1mL/5min. The fraction collector (CF2) was set to move at a rate of 1 tube/5min.

3.2.6 Isolation of Bioactive Metabolites from a Second Batch of *H. simulans*

Two more samples of freeze-dried *H. simulans* (designated A and B), weighing 47.12 g and 60.48 g respectively after grinding were extracted and fractionated following the same procedure as 3.2.2 and 3.2.3. The combined acetone and methanol extracts weighed 10.91 g and 14.22 g respectively. The samples were dry-loaded onto the column by first mixing them with HP20 and allowing the solvents to evaporate before transferring the sample-loaded HP20 to the column. The gradient used for elution was the same as in the previous fractionation (3.2.3.2); however, for

this elution the column was washed three times with 50:50 methanol:acetone followed by three washes with 100% acetone. 1.5 mL aliquots of each fraction were taken for LC-MS analysis. The rest of the fractions were dried under vacuum using a rotary evaporator. The fractions from extracts A and B were also compared using TLC and were found to be the same. Fractions A5-A9 and Fractions B5-B9 eluting with 50:50 methanol:acetone (fractions 5-7) and with 100% methanol (fractions 8-9) were all pooled together to give a total weight of 2.7898 g.

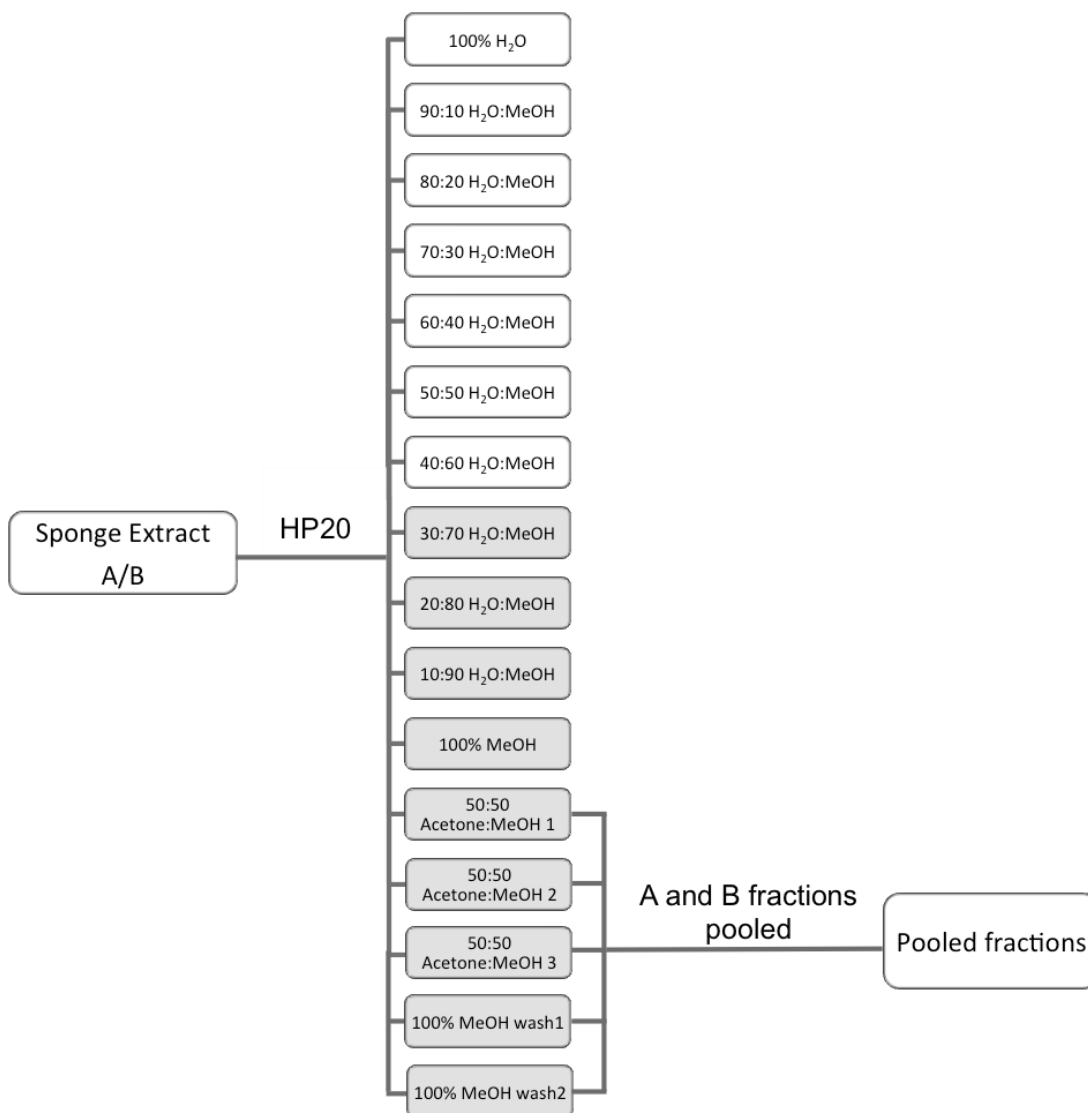


Figure 3-2: Flowchart of the HP20 chromatography, TLC and pooling after the extraction of the second batch of *H. simulans*. The grey cells were subjected to TLC with 30:70 H₂O:MeOH designated as fraction 1 and 100%MeOH wash 2 as fraction 9.

The pooled fractions were mixed with Celite[®] in preparation for fractionation with the Reveleris[®] flash chromatography system (Grace Davison Discovery Sciences, USA). The solid loader was too small to accommodate all of the Celite[®] mixture so the sample was divided into approximately half and two separate fractionations were performed. The first fractionation had the following conditions:

Column: Generic Silica 24g/32 mL (20x130 mm)

Mobile Phase: Hexane, ethyl acetate

Flow rate: 10 mL/min

Gradient: 0-5 min	0% ethyl acetate
5-50 min	0-100% ethyl acetate
50-60 min	100% ethyl acetate

ELSD threshold: 5 mV

UV threshold: 0.05 AU

UV wavelengths: 254 and 280 nm

The column was then washed with 80:20 acetone:methanol (HPLC grade). All peaks were collected into test tubes and TLC was performed to pool the similar fractions. Thirty-one fractions were obtained in the first fractionation.

The second fractionation followed the same method; however, the pressure exceeded the limits, possibly due to precipitation of some compounds in 100% hexane. The machine accordingly adjusted the flow rate to 2 mL/min. This led to a much slower elution and, as a result, not all compounds had eluted at the end of the method. The column was then washed with 60:40 dichloromethane:methanol followed by 50:50 dichloromethane:methanol until most of the compounds had eluted from the column. The separation of this fractionation was not as good as that of the first, therefore only the compounds obtained from the first separation were chosen for further analysis.

Pooled fractions from the first fractionation on the Reveleris[®] system were submitted for LC-HRFTMS, NMR and anti-trypanosomal and anti-mycobacterial assays. Identification of compounds from the active fractions, aside from those predominantly containing sterols, was performed using MZmine 2.10 and the AntiMarin 2012 database using the same parameters as in **2.4.2**.

3.2.7 Derivatisation of B-3 for GCMS

One milligram of B-3 was dried under nitrogen at 50°C. 500 µL of acetonitrile was added and the sample was dried once again under the same conditions. 200 µL of N-methyl-N-(trimethylsilyl)-trifluoroacetamide (MSTFA) (Sigma-Aldrich, USA) was added and the vial was closed tightly prior to heating at 80°C for 30 minutes. The sample was then submitted to Ms. Patricia Keating at the Department of Pure and Applied Chemistry for GCMS analysis.

3.3 Results

3.3.1 Extraction of Sponge Metabolites and Fractionation with HP20

The extraction of freeze-dried *H. simulans* with acetone and methanol was performed three times. The metabolites were separated according to polarity using normal phase chromatography with HP20 as the stationary phase. An aliquot of each fraction was taken and the metabolites present in each were identified from the high-resolution mass spectrometry data using the AntiMarin 2012 database in order to determine the potential compounds and classes of compounds within the sponge. Microorganisms such as bacteria and fungi as well as marine invertebrates such as sponges produce many of the identified compounds. Those previously isolated from *Haliclona* sp. are shown in Table 3-1 and Figure 3-3. These compounds were putatively identified based on their mass-to-charge ratios (m/z) but their presence in the extract remains to be confirmed by isolation, as it is possible that the compounds in the extract are molecular isomers of those in the database.

Table 3-1: Compounds identified in the *H. simulans* HP20 fractions that have previously been isolated from *Haliclona* sp.

Name	Formula	Exact Mass	RT	Eluting Solvent	Reference
[1] Palmitamidoethanesulfonic acid	C ₁₈ H ₃₇ NO ₄ S	363.2442	20.56 21.07	80:20W:M 70:30W:M 60:40W:M 30:70W:M 20:80W:M 10:90W:M 100%MeOH 50:50A:M 100%MeOHw1	(Wang et al., 2009)
[2] 5-(Nonadecapentaenyl)-benzene-1,3-diol	C ₂₅ H ₃₄ O ₂	366.2550	18.63	80:20W:M 60:40W:M 40:60W:M 30:70W:M 20:80W:M 10:90W:M 100%MeOH 50:50A:M 100%MeOHw1	(Barrow and Capon, 1991)
[3] 24-Ketocholest-5,25-dien-3 β -ol	C ₂₇ H ₄₂ O ₂	398.3184	27.71 27.13	70:30W:M, 100%MeOH 50:50 A:M	(Seldes et al., 1985)
[4] 43 β -Hydroxycholest-5,25-dien-24-one				100%MeOHw1 100%MeOHw2	(Findlay and Patil, 1985)
[5] (E)-Stigmast-4,24(24)-dien-3-one	C ₂₉ H ₄₆ O	410.3550	32.24	100% Water 50:50A:M 100%MeOHw1 100%MeOHw2	(Sheikh and Djerassi, 1974)
[6] Haliclamine E	C ₂₉ H ₅₂ N ₂	428.4132	12.83	50:50A:M 100%MeOHw1 100%MeOHw2	(Schmidt et al., 2009)

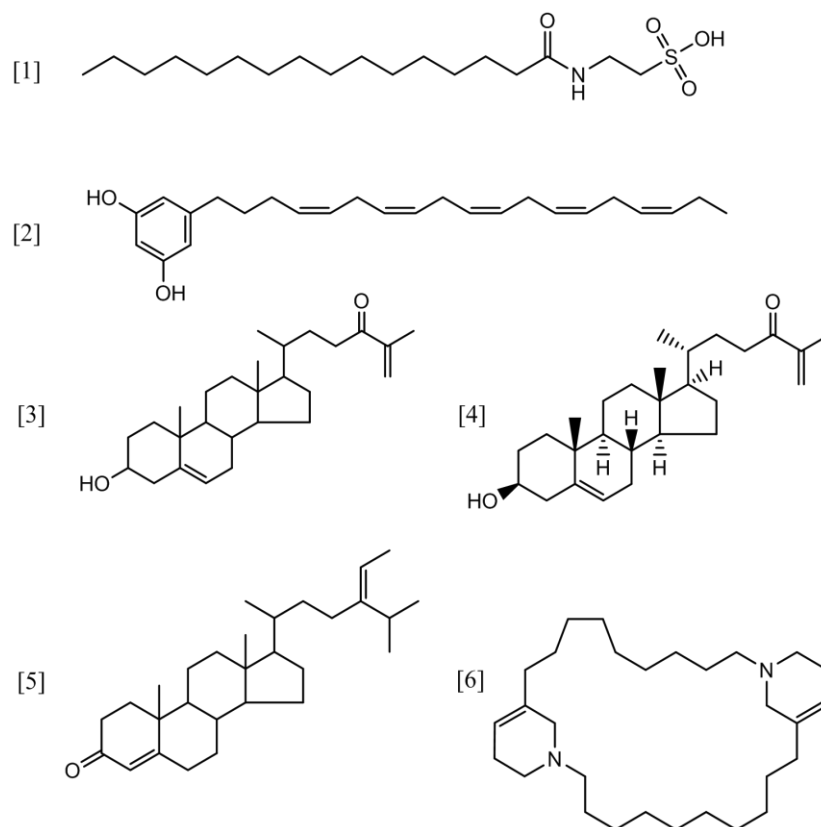


Figure 3-3: Compounds identified using HR-FTLCMS that have previously been isolated from *Haliclona* sp. The compounds include a taurine derivative (1), an alkenyl resorcinol (2), steroids (3-5), and an alkaloid (6).

3.3.2 MPLC of Non-polar HP20 Fractions

TLC was performed for a qualitative comparison of the non-polar fractions to those obtained by a previous MPharm student, Theng Theng Ooi, who had performed the same extraction procedure on a different batch of *H. simulans* during her final year project. Samples of the TLC plates are shown in Figure 3-4. Ooi had obtained anti-trypanosomal activity in her non-polar fractions (Ooi, 2010); hence, the non-polar fractions, beginning from 50:50 acetone:MeOH were pooled and re-fractionated using MPLC on the BÜCHI instrument.

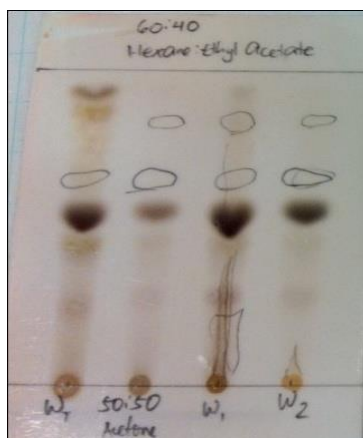


Figure 3-4: TLC plate showing a comparison between the different fractions collected after HP20 chromatography. The mobile phase system used was 60:40 hexane:ethyl acetate. The samples analysed were W_T (Ooi's wash), 50:50 acetone (50:50 acetone: methanol), W_1 (first wash with 100% methanol), and W_2 (second wash with 100% methanol). The samples were all similar, hence they were pooled together for further work.

Twelve fractions of *H. simulans* extract were obtained after pooling the fractions collected during MPLC. A TLC summary plate was prepared which is depicted in Figure 3-5. The fractions were tested for anti-trypanosomal and anti-mycobacterium activity. The results are shown together with the weight of the fractions in Table 3-2.

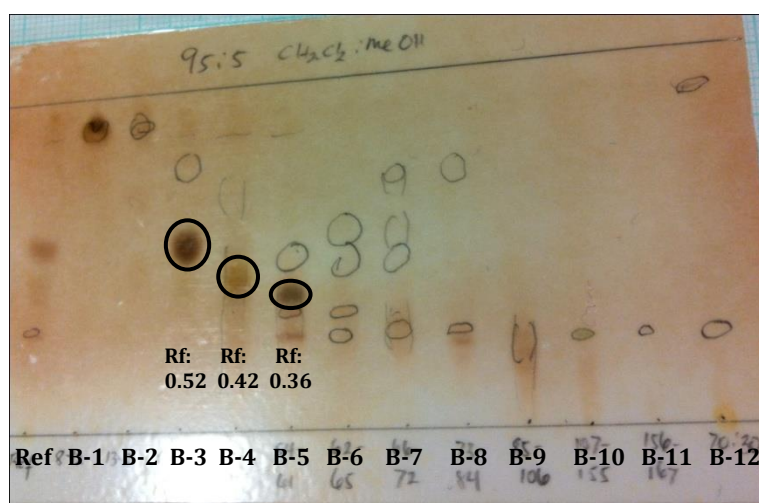


Figure 3-5: TLC summary plate of the fractions of *H. simulans* extract obtained after MPLC. The mobile phase used was 95:5 dichloromethane:methanol. The encircled spots and corresponding Rf values show the isolated compounds.

Table 3-2: Summary of the weights and antimicrobial activities obtained for *H. simulans* BÜCHI fractions after pooling. Cells highlighted in yellow indicate the isolated pure compounds. Cells in grey indicate the highest activity. MIC values were not obtained for the *M. marinum* assay.

Fraction number	Test tube numbers	Yield (mg)	Anti-Trypanosomal activity MIC (µg/mL)	% Inhibition of <i>M. marinum</i> (100 µg/mL)
B-1	8-12	39.1	Not significantly active	73.0
B-2	13-21	29.6	Not significantly active	96.2
B-3	22-42	239.2	12.5	79.0
B-4	43-53	45.8	1.6	97.2
B-5	54-61	27.8	3.12	78.2
B-6	62-65	5.6	3.12	85.8
B-7	66-72	7.3	3.12	96.0
B-8	73-84	15.2	6.25	77.1
B-9	85-106	12	6.25	61.2
B-10	107-155	7.8	25	32.5
B11	156-168	0.3	Not tested	Not tested
B-12	70:30 DCM:MeOH washing	190.9	12.5	63.9
Suramin	Control	-	0.16	-
Gentamycin	Control	-	-	100

B-4 had the lowest MIC, indicating that, out of the fractions tested, it was the most potent inhibitor of *T. b. brucei*. It also was the strongest inhibitor of *M. marinum* growth. B-2 was also a strong inhibitor of *M. marinum*. The major component of B-2 appeared to be fatty acids (Figure 3-6). B-5, B-6 and B-7 were the next most potent fractions against *T. brucei* and all had activity against *M. marinum*; however, the TLC plate revealed that these fractions were still a mixture of four or more compounds. Analysis of the ¹H NMR spectra of the active fractions showed that B-5 was not pure but was not identical to the previous fraction, indicating that it contained a different major component. The succeeding fractions, likewise, were still mixtures of several compounds and the limited quantity of each fraction precluded further purification. The precipitate which was obtained upon dissolution of the extract in ethyl acetate and hexane prior to flash chromatography was proven by NMR to be a mixture of B-3 and B-4 (Figure 3-6).

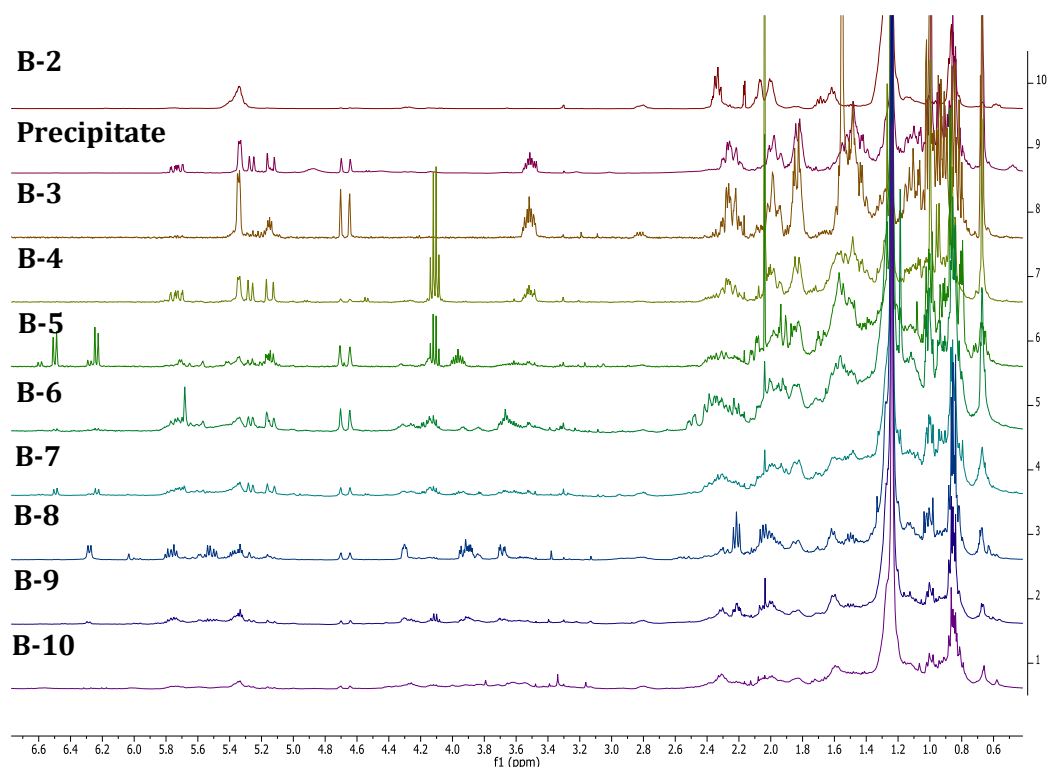


Figure 3-6: ^1H NMR spectra of active *H. simulans* fractions following flash chromatography with the BÜCHI system (400 MHz, CDCl_3). The major component of B-2 appeared to be fatty acids. The precipitate was evidently a mixture of B-3 and B-4. B-5, B-6, B-7 and B-8 also contained steroids as their major components; however, these fractions were not as pure as B-3 and B-4.

The next two batches of *H. simulans*, designated A and B, were extracted and fractionated simultaneously. A TLC summary plate (Figure 3-7) of the fractions obtained from the HP20 separation showed that the major components of the extracts were identical. Fractions A5-A9 and B5-B9 were pooled together and re-fractionated using the Flash Reveleris[®] system. Thirty-one fractions were obtained. The TLC summary plate is shown in Figure 3-8 and the weights and activities are presented in Table 3-3. These fractions were tested against both *T. b. brucei* and *M. marinum*.

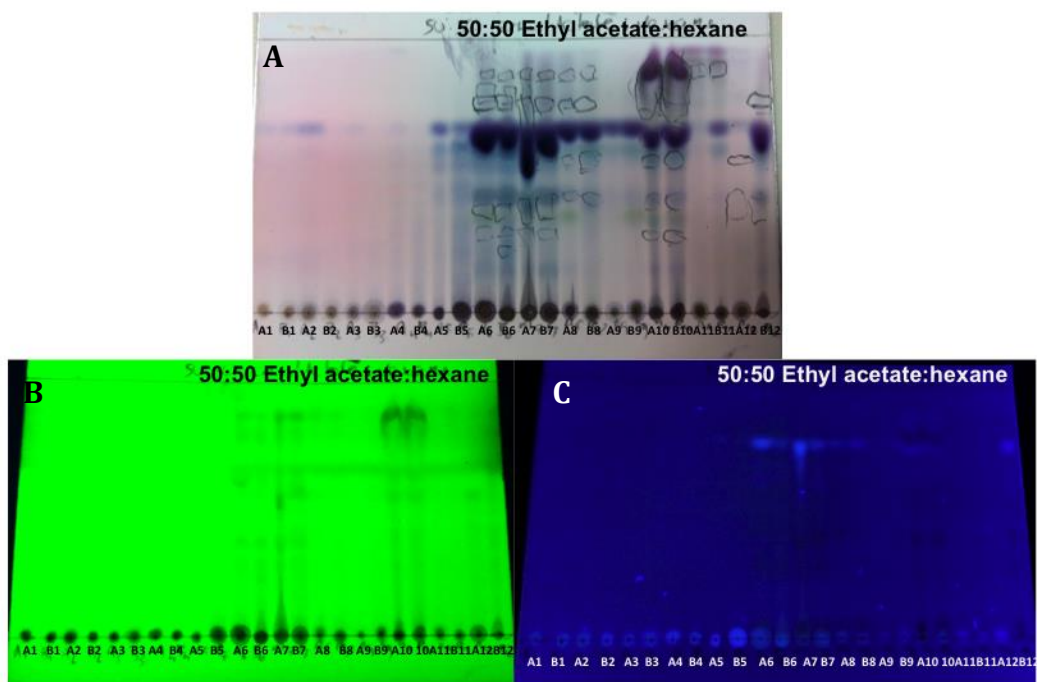


Figure 3-7: TLC summary plate of HP20 fractions. The plate was (A) sprayed with p-anisaldehyde sulphuric acid spray reagent, (B) visualised under short UV wavelength, and (C) visualised under long UV wavelength.

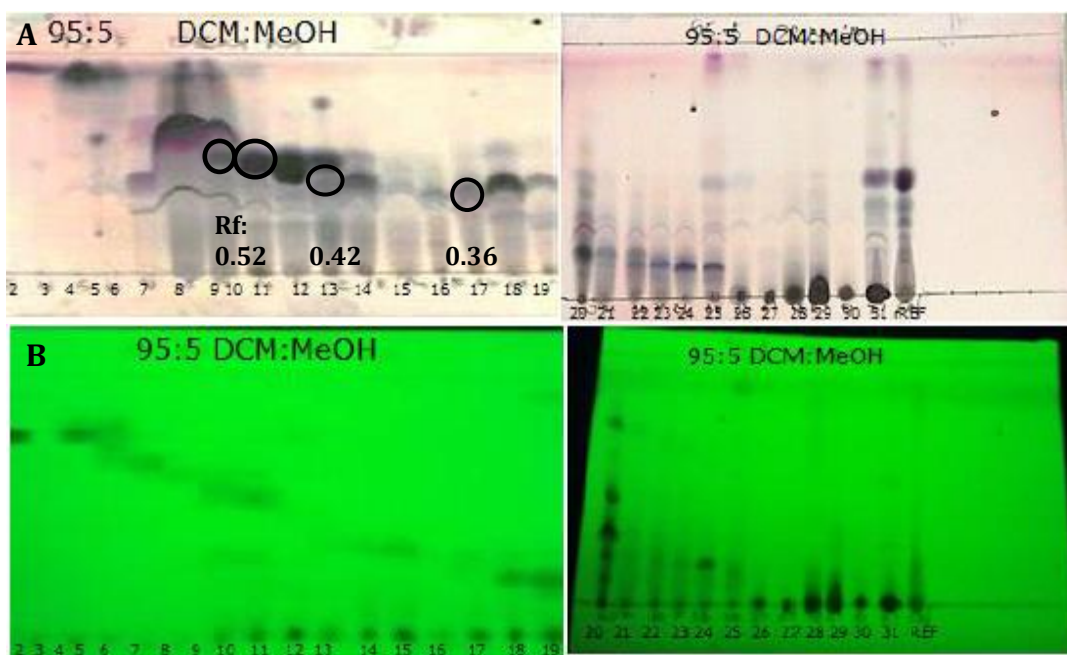


Figure 3-8: TLC summary plates of *H. simulans* fractions following Reveleris® MPLC. The plates were (A) sprayed with p-anisaldehyde sulphuric acid spray reagent, and (B) visualised under short UV wavelength. Encircled spots and corresponding Rf values indicate isolated steroids.

Table 3-3: Summary for the weights and anti-trypanosomal and -mycobacterium activities obtained for *H. simulans* Reveleris® fractions after pooling. The grey cells indicate the highest activity. Fractions in yellow have been isolated and identified.

Fraction number	Test tube numbers	Yield (mg)	% Inhibition of <i>T.b.brucei</i> (20 µg/mL)	% Inhibition of <i>M. marinum</i> (100 µg/mL)
R-1	2	1.5	-	-
R-2	3-15	0.3	-	-
R-3	16-17	0.9	-	-
R-4	18-28	5.8	77.6	73.5
R-5	29-36	2.2	-	-
R-6	37-39	1.5	-	-
R-7	40-44	7.5	4.0	12.6
R-8	45-47	9.7	19.0	57.4
R-9	48-52	12.8	97.4	77.9
R-10	53-56	2.0	100.2	76.3
R-11	57-60	332.8	102.4	99.3
R-12	62-65	12.9	98.9	95.7
R-13	66	11.5	99.0	76.4
R-14	67-69	2.3	-	-
R-15	70-71	2.9	-	-
R-16	72	4.7	18.4	17.3
R-17	73	6.7	99.8	96.8
R-18	74-75	1.6	-	-
R-19	76	0.4	-	-
R-20	77	4.6	99.6	50.0
R-21	78-79	2.1	-	-
R-22	80	3.2	-	-
R-23	81	2.6	-	-
R-24	82	4.7	86.3	12.2
R-25	83-89	16.4	100.6	33.1
R-26	90-97	2.7	-	-
R-27	98	0.6	-	-
R-28	99-100	2.5	-	-
R-29	101-113	44.2	5.5	13.5
R-30	114-120	9.0	4.8	42.8
R-31	Wash	19.6	51.2	-16

The majority of fractions that were tested possessed anti-trypanosomal activity. Although activity against *M. marinum* was less prevalent, some fractions still possessed significant *M. marinum* inhibitory activity, with R-11, R-13 and R-17 having nearly 100% inhibition. These fractions were active against both *T. b. brucei* and *M. marinum*, as opposed to R-20, -24 and -25 which were more selective against *T. b. brucei*.

3.3.3 Identification and Structure Elucidation of Purified Compounds

Three sterols were isolated from the sponge extracts. Two of them were isolated from both the BÜCHI and the Reveleris[®] fractionations (B-3 and R-10 and -11, B-4 and R-13) whereas the third was obtained as a pure compound using the Reveleris[®] system (R-17).

3.3.3.1 24-Methylenecholesterol

B-3, R-10 and R-11 appeared as white needle-like crystals. It was suspected that these compounds were identical to that obtained by Ooi, who isolated anti-trypanosomal agents from *H. simulans*. This was confirmed by a comparison of the ¹H NMR spectra of the four fractions. The spectra are shown in Figure 3-9. In addition, B-3, R-10 and R-11 all have an R_f value of 0.52 when eluted using 95:5 dichloromethane:methanol.

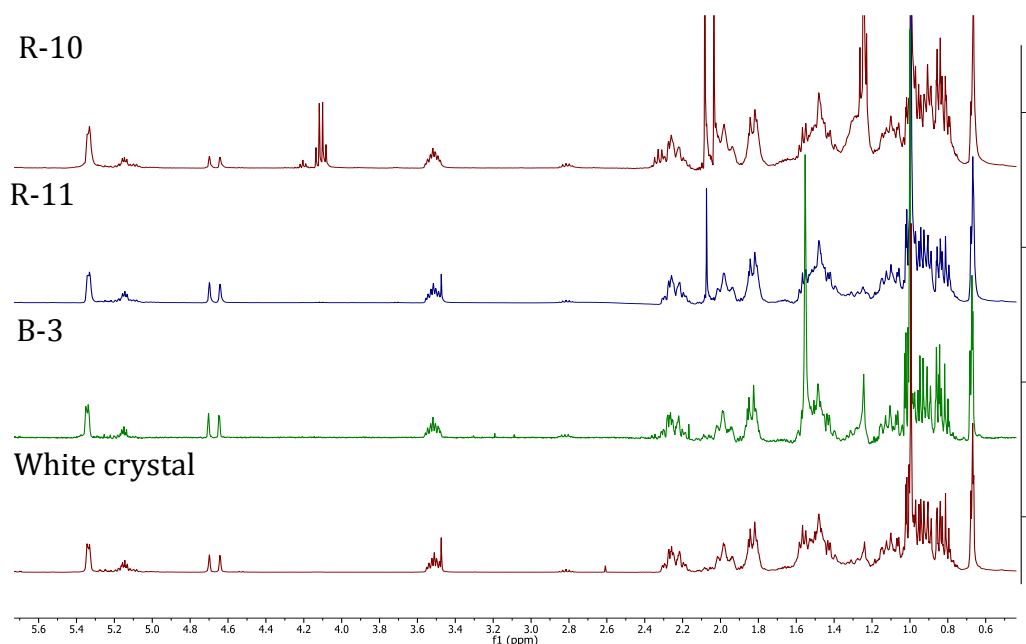


Figure 3-9: Stacked ^1H -NMR spectra of R-10 (top red), R-11 (blue), B-3 (green) and the white crystals obtained by Ooi (bottom red) (400 MHz, CDCl_3). The spectra are identical, save for the ethyl acetate peaks in R-10. This confirmed that the four samples contained the same sterol.

The white crystal was identified as 24-methylenecholesterol (Ooi, 2010). 24-Methylenecholesterol was isolated in the largest quantity during all three extractions of *H. simulans*, suggesting that it is the major non-polar compound present in the sponge. The white crystals obtained by Ooi had an MIC of 25 $\mu\text{g}/\text{mL}$ (62.81 μM) against *T. b. brucei* whereas those obtained in this study had MIC values of 12.5 $\mu\text{g}/\text{mL}$ (B-3) and 6.25 $\mu\text{g}/\text{mL}$ (R-11), which are equivalent to 31.41 μM and 15.70 μM , respectively. B-3 and R-11 had anti-mycobacterial MIC values of 50 $\mu\text{g}/\text{mL}$ (125.63 μM) and 100 $\mu\text{g}/\text{mL}$ (251.27 μM) respectively. These differences in MIC values can be attributed to differences in the purity of the crystals obtained. 24-Methylenecholesterol has also been reported to have a minimum effective concentration (MEC) of 50 μM against *T. brucei* (Bazin et al., 2006). Tables 3-5 and -6 display the comparison of ^{13}C and ^1H NMR data for 24-methylenecholesterol and the compounds obtained in this study.

Table 3-4: 24-Methylenecholesterol

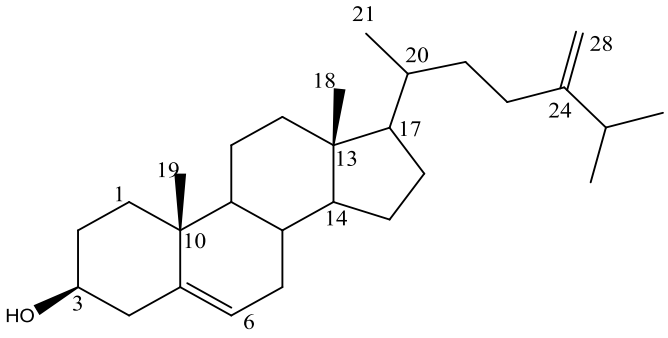
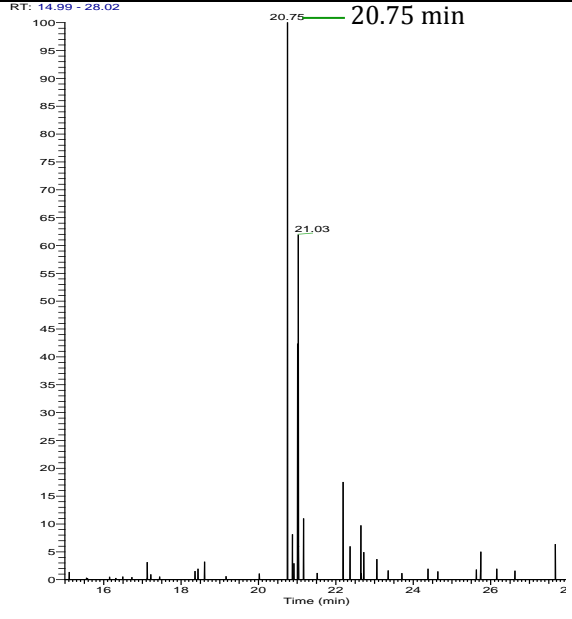
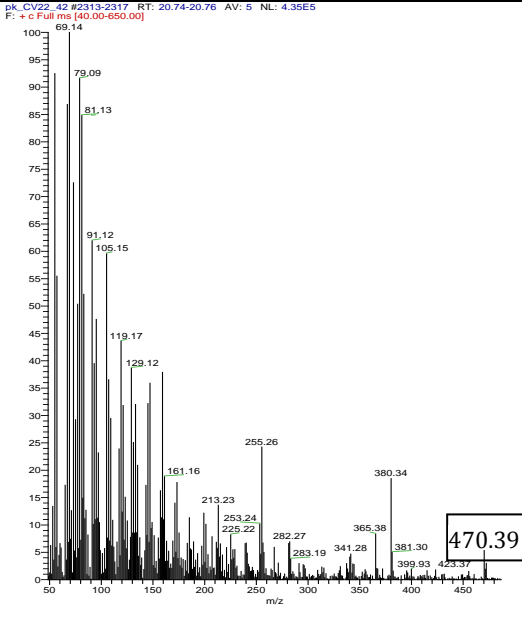
24-Methylenecholesterol	
<p>Synonyms</p> <p>Sample Codes</p> <p>Sample Amount</p> <p>Physical Description</p> <p>Molecular Formula</p> <p>Molecular Weight</p> <p>Optical Rotation $[\alpha]_D^{20}$</p> <p>Retention time (GC-MS)</p>	<p>Chalinasterol</p> <p>Ostreasterol</p> <p>Ergosta-5,24(28)-dien-3β-ol</p> <p>B-3, R-10, R-11</p> <p>239.2mg, 2.0 mg, 32.8 mg</p> <p>White needle-like crystals</p> <p>$C_{28}H_{46}O$</p> <p>398 g/mol</p> <p>-23 ($c=0.1, CHCl_3$)</p> <p>20.75 min (derivatised steroid)</p>
	
EI-GCMS spectra of derivatised 24-methylenecholesterol $[M+CH_3Si]^+$	
<p>RT: 14.99 - 28.02</p> <p style="text-align: center;">20.75 min</p> 	<p>pk_CV22_42 #2313-2317 RT: 20.74-20.76 AV: 5 NL: 4.35E5</p> <p>F: +c Full ms (40.00-650.00)</p> 

Table 3-5: ^{13}C NMR comparison of the isolated steroids with values for 24-methylenecholesterol found in literature (400 MHz, CDCl_3).

Position	24-Methylene cholesterol (Bazin et al., 2006) δ_{C} ppm	White crystals (Ooi, 2010) δ_{C} ppm	R-11 δ_{C} ppm (multiplicity as seen from DEPT-135)
1	37.2	37.3	37.3 (CH_2)
2	31.6	31.7	31.7 (CH_2)
3	71.8	71.9	71.9 (CH)
4	42.2	42.4	42.3 (CH_2)
5	140.7	140.8	140.8 (C)
6	121.7	121.8	121.8 (CH)
7	31.0	31.1	31.0 (CH_2)
8	31.9	32.0	32.0 (CH)
9	50.1	50.2	50.2 (CH)
10	36.5	36.6	36.6 (C)
11	21.8	21.2	21.2 (CH_2)
12	39.8	39.8	39.8 (CH_2)
13	42.3	43.2	42.4 (C)
14	56.7	56.8	56.8 (CH)
15	24.3	24.4	24.4 (CH_2)
16	28.2	28.3	28.3 (CH_2)
17	56.0	56.1	56.1 (CH)
18	11.8	12.0	11.9 (CH_3)
19	19.4	19.5	19.5 (CH_3)
20	35.7	35.8	35.9 (CH)
21	18.7	18.8	18.8 (CH_3)
22	22.7	22.1	23.9 (CH_2)
23	34.7	34.8	34.8 (CH_2)
24	156.8	156.8	157.0 (C)
25	33.8	33.9	33.9 (CH)
26	22.0	22.0	22.1 (CH_3)
27	29.7	29.8	28.1 (CH_3)
28	105.9	106.0	106.0 (CH_2)

Table 3-6: ¹H NMR comparison of isolated steroids with values for 24-methylenecholesterol found in literature (400MHz, CDCl₃).

Position	24-Methylene cholesterol (Bazin et al., 2006) δ ppm, (multiplicity, <i>J</i>)	White crystals (Ooi, 2010) δ ppm, (multiplicity, <i>J</i>)	B-3 δ ppm, (multiplicity, <i>J</i>)	R-11 δ ppm, (multiplicity, <i>J</i>)
1-CH ₂			1.81 (d, 5.9 Hz)	1.81 (d, 5.1 Hz)
2-CH ₂			1.50 (m)	1.50 (m)
3-CH	3.52 (m)	3.52 (m)	3.51 (m)	3.52 (td, 5.3, 11.0 Hz)
4-CH ₂			2.27 (m)	2.27 (m)
6-CH	5.34 (d, 5.1 Hz)	5.34 (d, 5.6 Hz)	5.34 (d, 5.1 Hz)	5.34 (d, 5.9 Hz)
7-CH ₂			1.95 (m)	1.95 (m)
18-CH ₃	0.68 (d, 3 Hz)	0.67 (t, 3.1 Hz)	0.68 (dd, 2.1 and 4.0 Hz)	0.67 (t, 3.1 Hz)
19-CH ₃	1.01 (s)	0.99 (s)	1.00 (s)	0.99 (s)
21-CH ₃	0.94 (d, 6.6 Hz)	0.93 (d, 6.5 Hz)	0.94 (d, 6.6 Hz)	0.93 (d, 6.7 Hz)
26-CH ₃ and 27-CH ₃	1.02 (d, 6.5 Hz)	1.02 (d, 2.2 Hz)	1.02 (d, 2.2 Hz)	1.02 (d, 2.3 Hz)
28-CH ₂	4.65 and 4.71 (d, 1.28 Hz)	4.64 (s) and 4.70 (d, 1.6 Hz)	4.65 (d, 1.8 Hz) and 4.70 (s)	4.64 (s) and 4.70 (s)

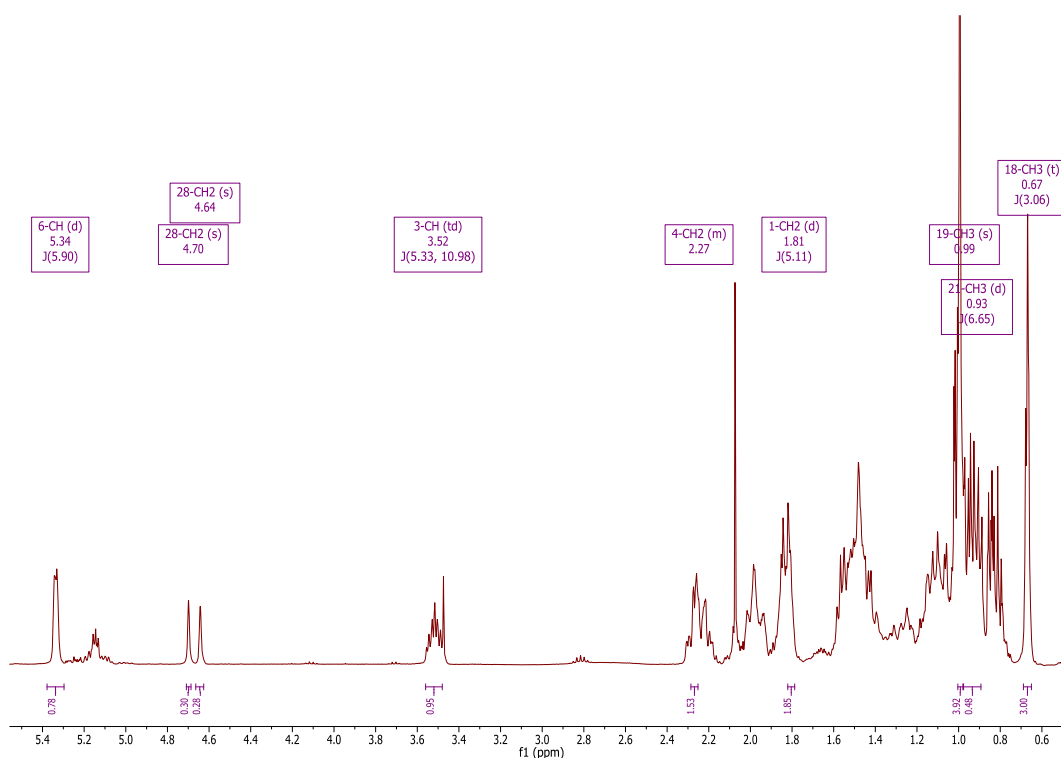


Figure 3-10: ^1H NMR of R-11 (400 MHz, CDCl_3). Although the aliphatic region possessed many overlapping peaks, the two methyl groups (18- and 19- CH_3) that are characteristic of sterols were evident. Peaks in the olefinic region showed the presence of double bonds.

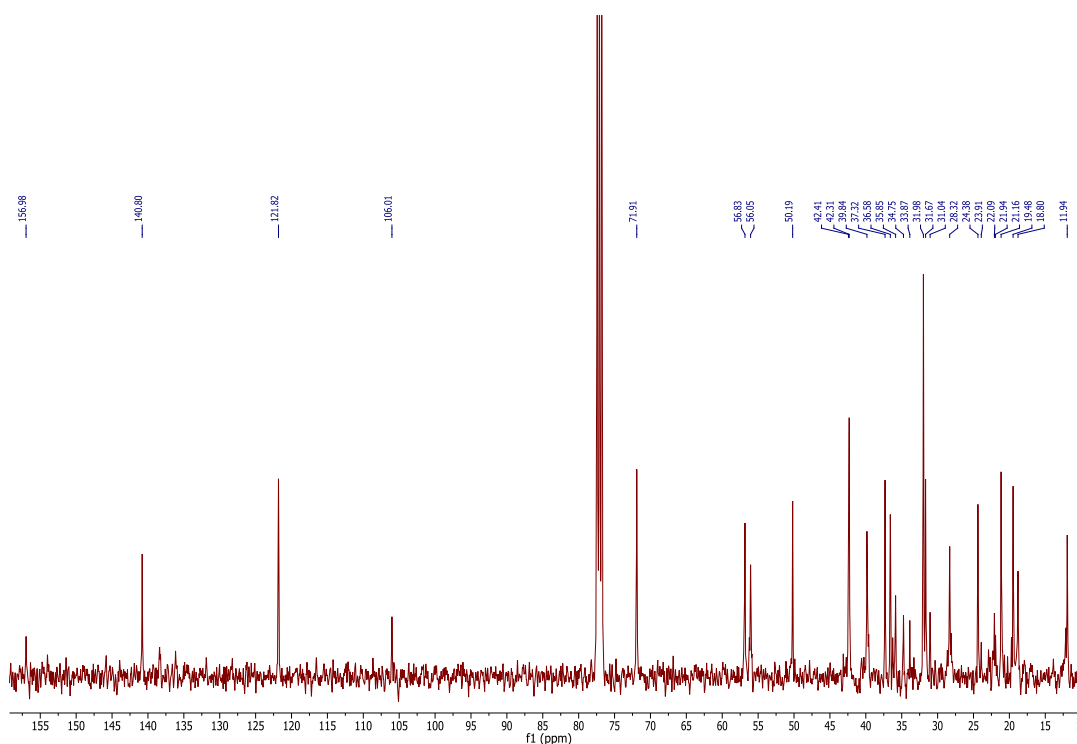


Figure 3-11: ^{13}C NMR spectrum of R-11 (100 MHz, CDCl_3). Many peaks were seen in the upfield region indicating an aliphatic system. The presence of deshielded peaks signified oxygenated as well as olefinic carbons.

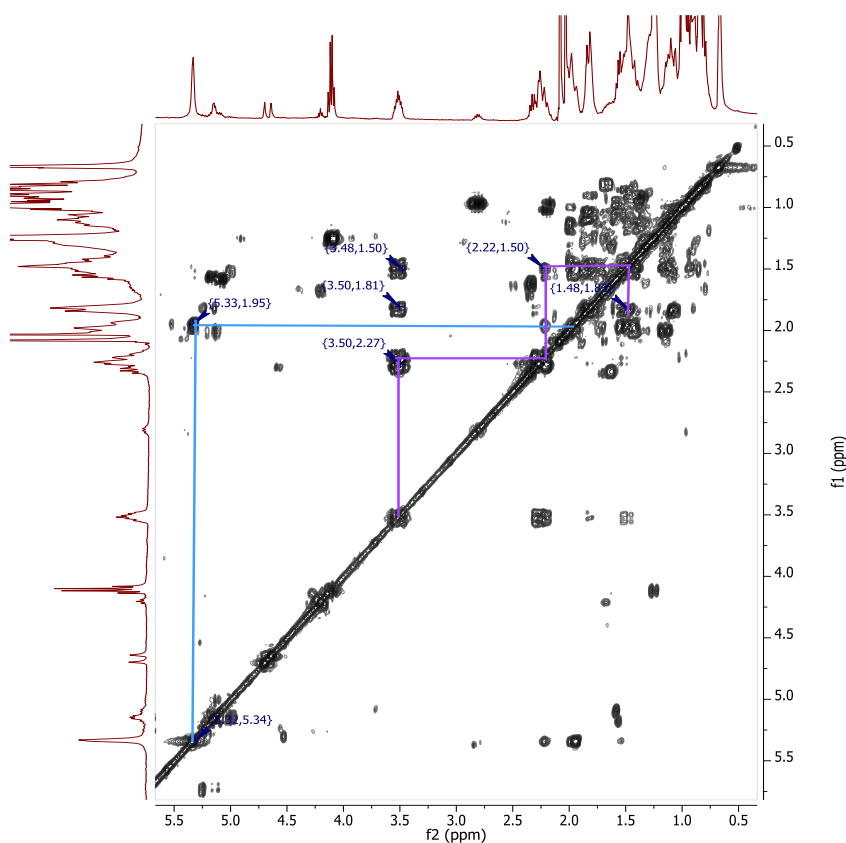


Figure 3-12: COSY of R-10 (400 MHz, CDCl₃). Spin systems are marked in blue (the olefinic system on the B-ring) and purple (correlations on the A-ring) as shown on the structure in Figure 3-13.

The triplet of doublet at δ_{H} 3.52 corresponded to the hydrogen attached to the hydroxyl-bearing carbon, C-3. The correlation spectroscopy (COSY) spectrum allowed the assignment of the other protons in the spin system. H-3 correlated to a peak at δ_{H} 2.27. This was relatively downfield for an aliphatic signal and corresponded to H-4 as it is adjacent to the olefinic system of C-5 and C-6. H-4 did not couple with any other proton indicating the end of the spin system. H-3 also coupled with peaks at δ_{H} 1.50 and δ_{H} 1.81 which corresponded to H-2 and H-1 respectively. These correlations were also seen in the rotating frame nuclear overhauser effect spectroscopy (ROESY) spectrum. No correlation was seen between H-3 and CH₃-19, indicating that H-3 is oriented below the plane of the nucleus; therefore it has an α orientation. This was corroborated by the coupling constants of 5.3 and 11.0, which imply axial-axial and axial-equatorial coupling. H-3 is therefore in the α , axial position whereas the OH-3 group is in the β , equatorial position. Also

displayed in the COSY was the correlation between the doublet at δ_{H} 5.34 (H-6) and a peak at δ_{H} 1.95 (H-7). The two singlets at δ_{H} 4.64 and 4.70 were deshielded and were not coupling with any other proton indicating that these were the geminal protons of the exomethylene group (H-28). The peaks at δ_{H} 0.67 and 0.99 did not couple with other protons in the COSY, thus they were assigned as the methyl groups of H-18 and H-19 respectively. The COSY correlations can be seen in Figure 3-13. The colours of the arrows match the lines depicting the spin systems in Figure 3-12.

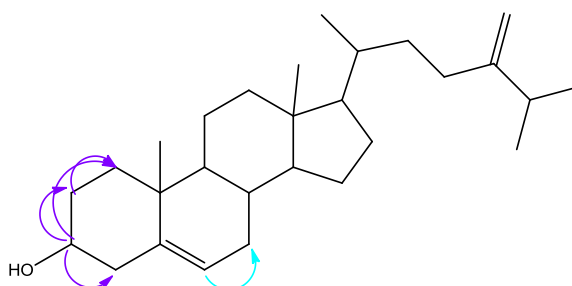


Figure 3-13: COSY correlations of R-10. The blue and purple arrows show the corresponding correlations detected in the COSY spectrum in Figure 3-12.

The steroid was derivatised using MSTFA (Sigma-Aldrich, USA) to facilitate ionisation on the GC-MS. Electron impact (EI)-GCMS was used to confirm the structure of the compound. The derivatisation process involves the attachment of trimethylsilyl groups to the any oxygen present in the compound, rendering the compound less polar and more volatile.

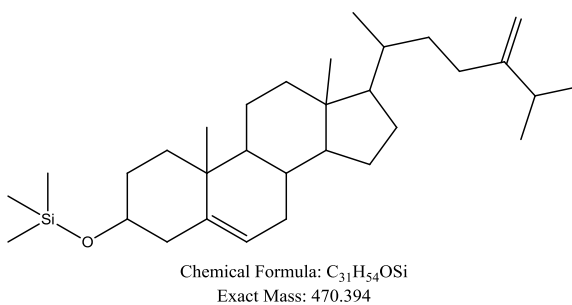


Figure 3-14: 24-Methylenecholesterol after derivatisation. The silanol group attached to the oxygen decreased the polarity of the compound and enhanced its ionisation and volatility in the GC-MS.

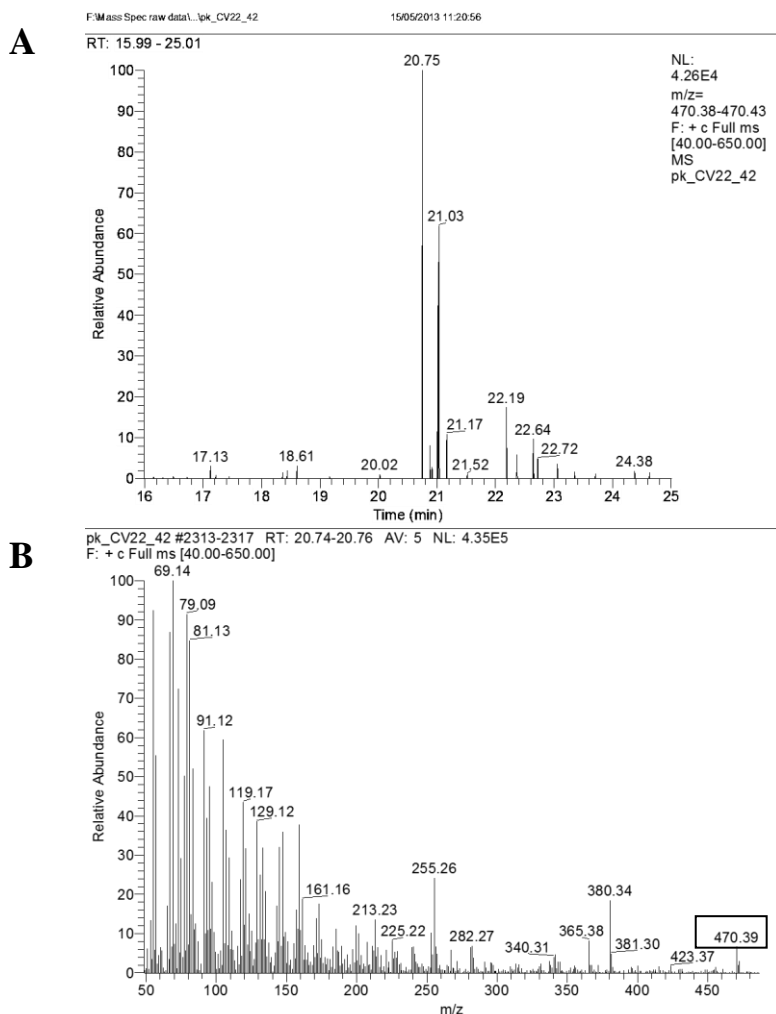


Figure 3-15: EI-GCMS spectra for the derivatised B-3. (A) Extracted ion chromatogram of m/z 470.39, and (B) corresponding mass spectrum. The peak showing m/z 470.39 $[M+CH_3Si]^+$ corresponds to derivatised 24-methylenecholesterol.

3.3.3.2 24-Vinyl-cholest-9-ene-3 β ,24-diol

B-4 and R-13 exhibited greater anti-trypanosomal activity than 24-methylenecholesterol (B-3/R-10, 11). The mean MICs of B-4/R-13 against *T. b. brucei* and *M. marinum* were 1.96 ± 0.77 $\mu\text{g/mL}$ (4.58 ± 1.80 μM) and 100 $\mu\text{g/mL}$ (233.64 μM) respectively. Comparison of 1D and 2D NMR spectra indicated that these steroids, B-4 and R-13, were identical (Figure 3-16). In addition, the R_f value of both spots on the TLC was 0.42 when eluted with 95:5 dichloromethane:methanol. The proposed structure was not found in any databases, although it is closely related to saringosterol. It is therefore a novel steroid. NMR analyses were performed to

elucidate the structure of the steroid. The NMR spectral data are shown below in Table 3-8, while the spectra are shown in Figure 3-17 to Figure 3-20.

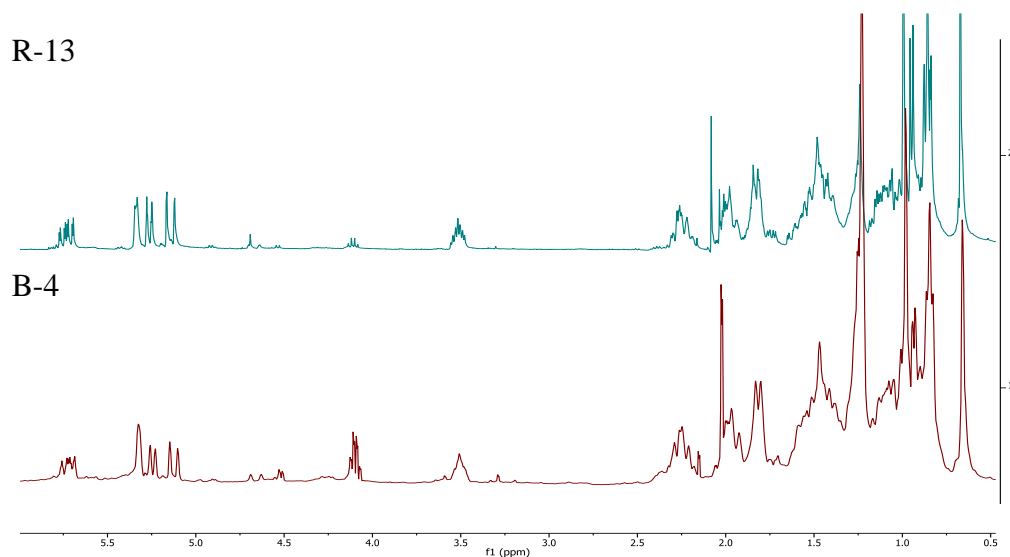


Figure 3-16: ¹H NMR spectra of R-13 (top) and B-4 (bottom) (400 MHz, CDCl₃). The spectra were similar, indicating that the compounds they contained were identical; however, B-4 possessed more impurities than R-14.

Table 3-7: 24-Vinyl-cholest-9-ene-3 β ,24-diol

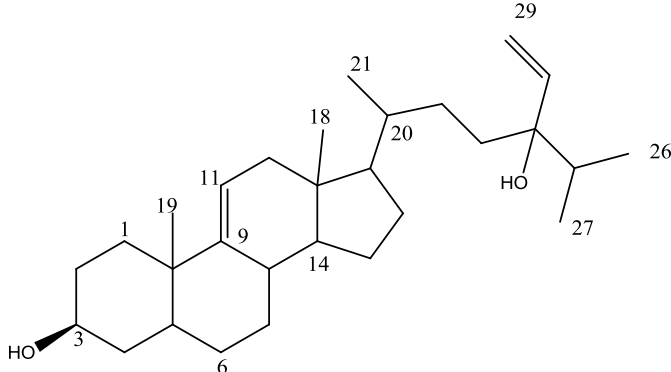
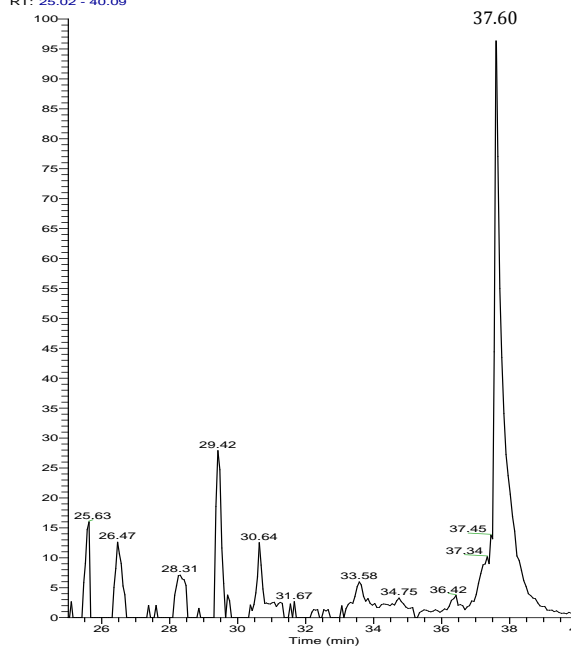
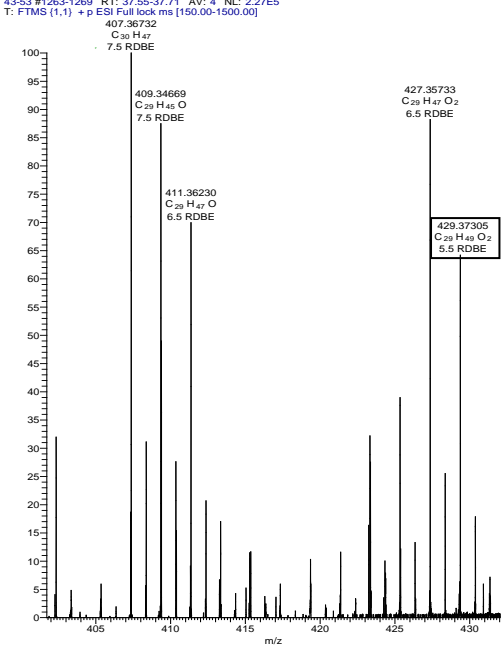
24-Vinyl-cholest-9-ene-3β,24-diol (NOVEL)	
Synonyms	-
Sample Codes	B-4, R-13
Sample Amount	45.8 mg and 11.5 mg
Physical Description	Very fine, colourless or pale yellow crystals
Molecular Formula	C ₂₉ H ₄₈ O ₂
Molecular Weight	428 g/mol
Optical Rotation [α]_D²⁰	-4.5 (c=0.1, CHCl ₃)
Retention time (LC-MS)	37.60 min
	
LC-HRFTMS spectra [M+H]⁺	
<p>RT: 25.02 - 40.09</p> 	<p>43-53 #1263-1269 RT: 37.55-37.71 AV: 4 NL: 2.27E5 T: FTMS (1,1) + p ESI Full lock ms [150.00-1500.00] 407.36732 C₂₉H₄₇ 7.5 RDBE</p> 

Table 3-8: ^{13}C and ^1H chemical shifts for saringosterol and B-4 (400MHz, CDCl_3). Highlighted rows indicate where the chemical shifts differ from that of saringosterol.

Position	Saringosterol (Ayyad et al., 2003) δ_{C} ppm	B-4 δ_{C} ppm (multiplicity)	B-4 δ_{H} ppm (multiplicity, J)
1	37.15	37.3 (CH_2)	1.82 (d, 9.9 Hz)
2	32.55	31.6 (CH_2)	1.45 (d, 12.9 Hz)
3	72.47	71.9 (CH)	3.51 (tt, 4.7, 10.6 Hz)
4	37.91	42.3 (CH_2)	2.24 (m)
5	141.41	50.2 (CH)	0.90 (d, 4.0 Hz)
6	122.38	34.8 (CH_2)	
7	32.33	22.01 (CH_2)	
8	36.86	21.1 (CH)	
9	50.76	140.8 (C)	-
10	37.91	36.6 (C)	-
11	21.73	121.8 (CH)	5.32 (d, 5.0 Hz)
12	40.40	39.8 (CH_2)	1.14 (d, 4.7 Hz) and 1.94 (m)
13	42.99	42.4 (C)	-
14	57.40	56.0 (CH)	1.06 (m)
15	24.96	24.4 (CH_2)	1.01 (d, 2.6 Hz) and 1.55 (dd, 3.4 and 7.8 Hz)
16	29.04	29.8 (CH_2)	
17	56.54	56.8 (CH)	
18	12.51	11.9 (CH_3)	0.66 (s)
19	17.33	19.5 (CH_3)	0.98 (s)
20	36.51	36.3 (CH)	1.41 (d, 3.9 Hz)
21	18.37	19.0 (CH_3)	0.93 (d, 6.4 Hz)
22	32.32	28.3 (CH_2)	1.85
23	28.92	28.5 (CH_2)	1.11, 1.99
24	89.83	89.2 (C)	-
25	29.16	32.0 (CH)	1.99
26	20.05	17.8 (CH)	0.98
27	19.54	16.7 (CH_3)	0.87
28	137.84	137.2 (CH)	5.72 (ddd, 3.3, 11.3, 18.0 Hz)
29	117.00	116.3 (CH_2)	5.12 (d, 17.9 Hz), 5.25 (d, 11.4 Hz)

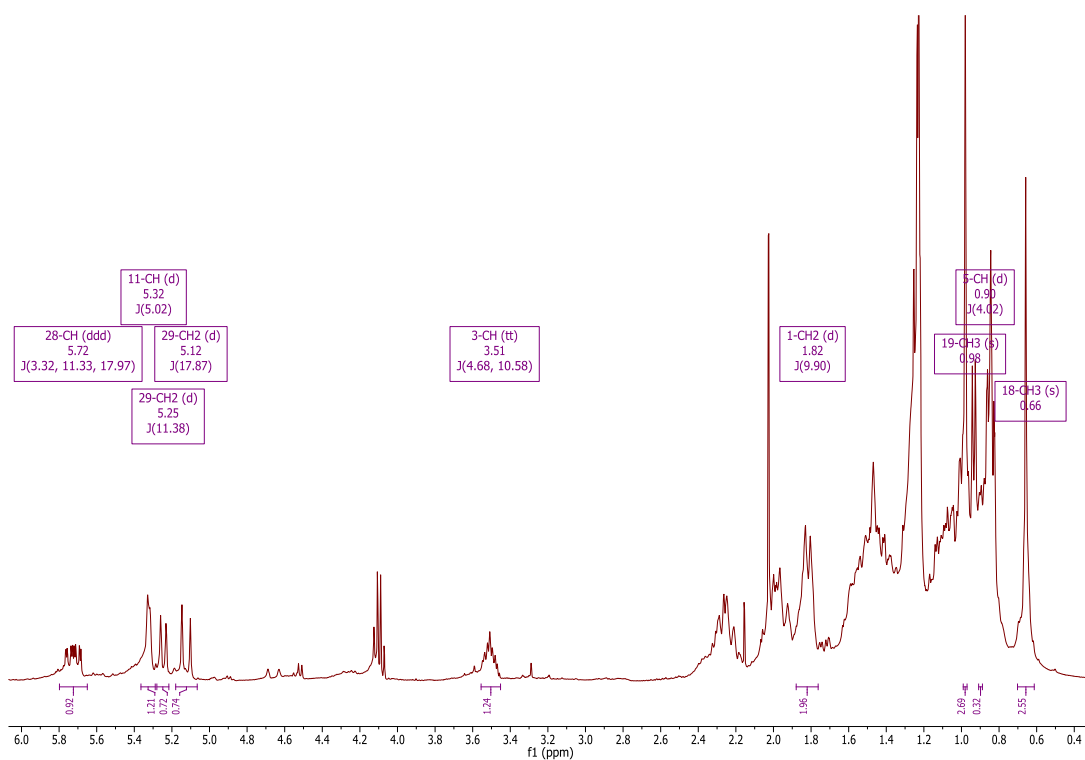


Figure 3-17: ^1H NMR of B-4 (400 MHz, CDCl_3). The chemical shifts, multiplicity and integration of some peaks are shown. The characteristic sterol peaks are present, as well as peaks in the olefinic region that correspond to the presence of double bonds in the structure.

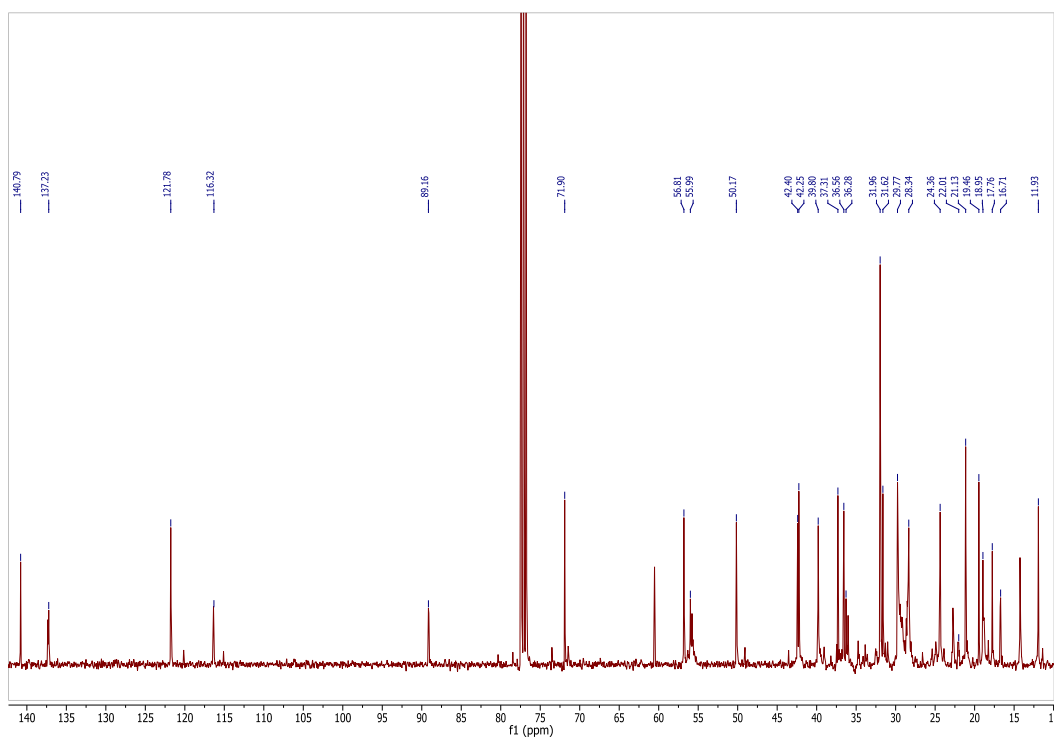


Figure 3-18: ^{13}C NMR spectrum of B-4 (100 MHz, CDCl_3).

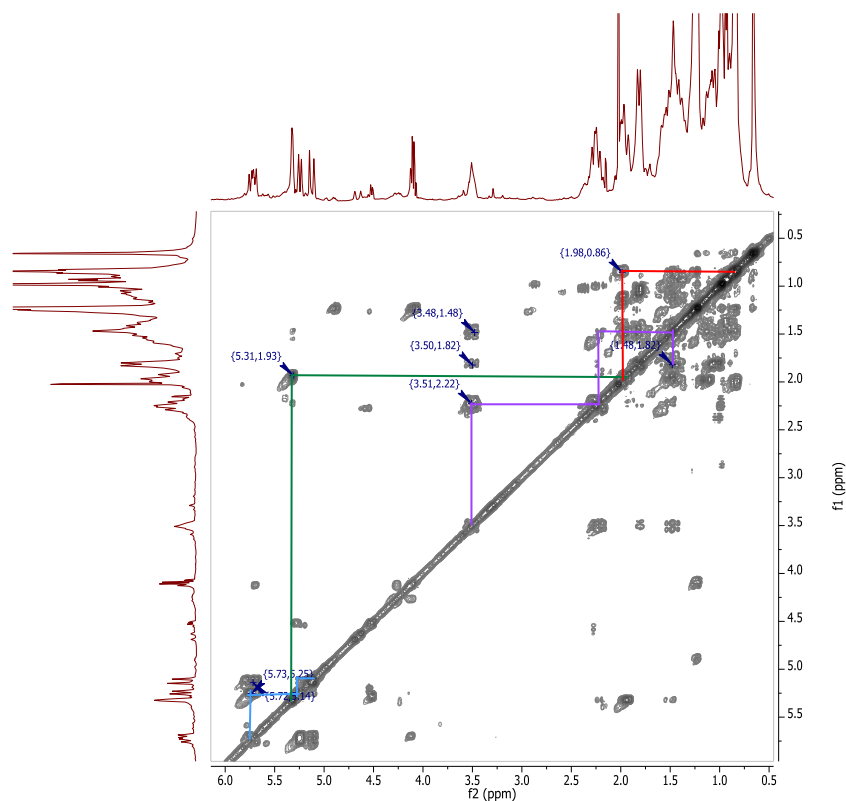


Figure 3-19: COSY spectrum of B-4 (400 MHz, CDCl₃). Spin systems are marked with different colours. The blue spin system indicated the presence of an exomethylene group in the side chain. The red spin system was the aliphatic part of the side chain. The green and purple lines marked spin systems in the C and A rings respectively.

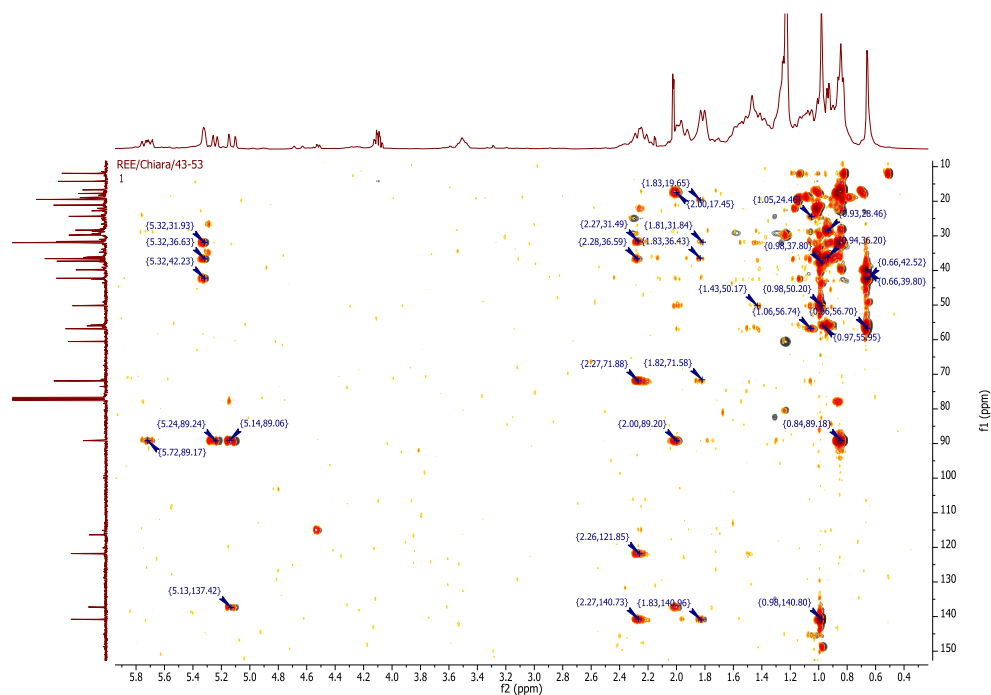


Figure 3-20: HMBC of B-4 (black) and R-13 (orange) (400 MHz and 100 MHz, CDCl₃). The spectra were the same, confirming that the two fractions contained the same steroid. The x-axis is the ¹H spectrum whereas the y-axis is the ¹³C spectrum of B-4.

From the COSY, the exomethylene group was clearly visible by the coupling of the doublet of doublet of doublets (ddd) at δ_{H} 5.72 (H-28) to the two doublets at δ_{H} 5.25 and 5.12 that belonged to the geminal protons of H-29, forming an ABX system. The distortionless enhancement by polarization transfer (DEPT135) spectrum confirmed this, showing that C-29 (δ_{C} 116.3) was a CH_2 group. The downfield chemical shift of C-29 indicated that it was attached to a double bond as aliphatic CH_2 groups generally have chemical shifts of up to 60 ppm, whereas aromatic or olefinic carbons have chemical shifts ranging from 100-160 ppm. The coupling constants for H-28 were 3.3, 11.3 and 18.0 Hz. These indicated cis/trans coupling as H-28 was cis-oriented towards one of the protons of H-29 and was trans-oriented towards the other. The spin system was further corroborated by the ^2J and ^3J coupling shown in the heteronuclear multiple bond connectivity (HMBC) spectrum in which the quaternary carbon of C-24 at δ_{C} 89.2 was correlating with the protons of the exomethylene group at δ_{H} 5.72, 5.25 and 5.12 (H-28 and H-29 respectively). Also visible were the couplings of C-24 with H-25 (δ_{H} 1.99) and the hydrogens on the methyl group of C-27 (δ_{H} 0.87). The coupling of H-25 to H-27 can be seen in the COSY (marked in red) and the coupling of H-25 (δ_{H} 1.99) to C-26 (δ_{C} 17.8) can be ascertained in the HMBC. The methyl group of H-21 (δ_{H} 0.93) correlated with C-20 (δ_{C} 36.3) and C-22 (δ_{C} 28.3).

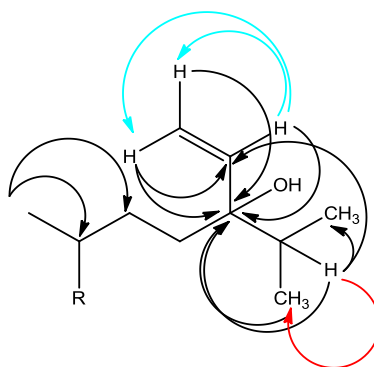


Figure 3-21: Substructure of B-4 and R-13. The black arrows indicate the coupling observed between the hydrogens and carbons in the HMBC whereas the light blue and red arrows indicate the coupling observed between neighbouring hydrogens in the COSY.

The second spin system clearly evident in the COSY (marked in Figure 3-19 in green) was assigned to the olefinic region of the steroid nucleus. The doublet at δ_{H} 5.32 assigned to H-11 showed coupling of the olefinic hydrogen with one of the two

protons at H-12 (δ_{H} 1.99). The HMBC also confirmed the position of C-12 as it was one of the three carbons correlating with the methyl group on C-18. Crosspeaks were observed from CH_3 -18 (δ_{H} 0.66) to C-12 (δ_{C} 39.8), C-13 (δ_{C} 42.4) and C-17 (δ_{C} 56.8). HMBC correlations of H-14 (δ_{H} 1.06) with C-15 (δ_{C} 24.4), and of H-14 with C-17 were also visible. The doublet for H-11 at δ_{H} 5.32 correlated with C-10 (δ_{C} 36.6) and C-13 (δ_{C} 42.4).

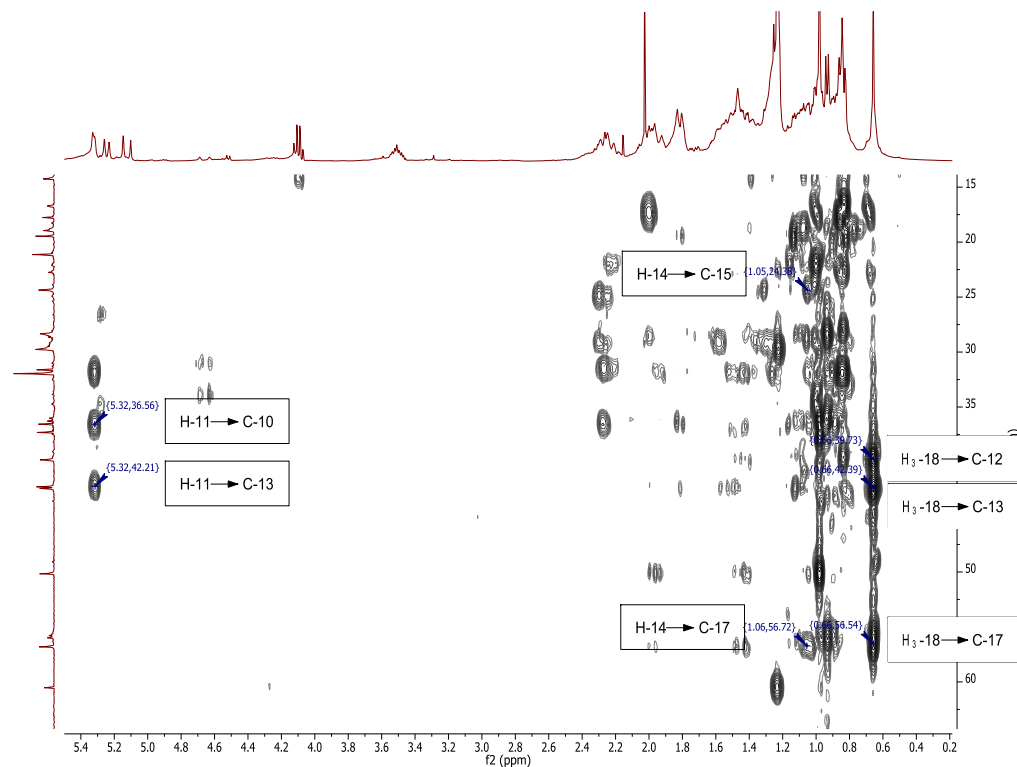


Figure 3-22: Expansion of the HMBC of B-4 highlighting the correlations between H-11 and C-10 and -13. This shows how the location of the double bond differs from that of saringosterol. Other relevant correlations are also labelled.

The third spin system seen in the COSY (marked in purple in Figure 3-19 and Figure 3-23) showed coupling of H-3 to H-4, H-2 and H-1. The downfield shift of C-3 to δ_{C} 71.9 indicated that it was oxygen-bound. H-3 is a triplet of triplet at δ_{H} 3.51 and coupled to a multiplet at δ_{H} 2.24 (H-4). It also coupled to a doublet at δ_{H} 1.45 (H-2) and δ_{H} 1.82 (H-1). This was confirmed in the HMBC as the long-range correlation of H-1, H-2 and H-4 to C-3 was observed. H-1 also correlated with C-19 (δ_{C} 19.5), C-2 (δ_{C} 31.6), and C-9 (δ_{C} 140.8). H-4 correlated with C-1, C-2 as well as C-3. H-2 coupled with C-5 (δ_{C} 50.2). The methyl group on C-19 (δ_{H} 0.98) correlated with C-1 (δ_{C} 37.3), C-5 (δ_{C} 50.2), C-8 (δ_{C} 21.1) and C-9 (δ_{C} 140.8). The coupling constants of

H-3, 4.7 and 10.6 Hz, proved that the hydrogen is axial and therefore that the hydroxyl group attached to C-3 is β -oriented.

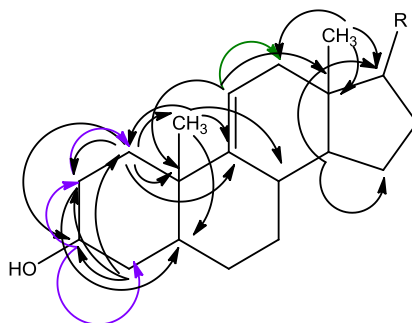


Figure 3-23: Substructure of B-4 and R-13. The arrows indicate the carbons seen by the hydrogens in the HMBC. The purple and green arrows show the ¹H-¹H coupling as seen in the COSY and are coloured by spin system.

The whole structure is depicted in Table 3-7. B-4/R-13 appears to be novel as searches of databases have not found an exact match. The compound is similar to saringosterol, except for the position of the double bond in the nucleus (Figure 3-24). Saringosterol is a sterol previously isolated from the algae *Sargassum asperifolium* (Ayyad et al., 2003).

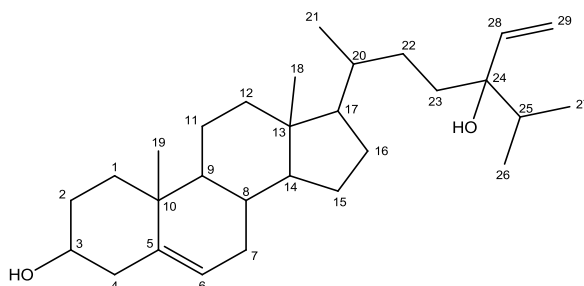


Figure 3-24: Saringosterol. The structure of saringosterol is similar to that proposed for B-4/R-13. The only difference is that saringosterol has a double bond at C-5 whereas B-4/R-13 has a double bond at C-9.

The compound has a chemical formula of C₂₉H₄₈O₂ and an exact mass of 428.37. Using the Exactive Orbitrap high-resolution mass spectrometer, an *m/z* of 429.37305 [M+H]⁺ was detected (Figure 3-25).

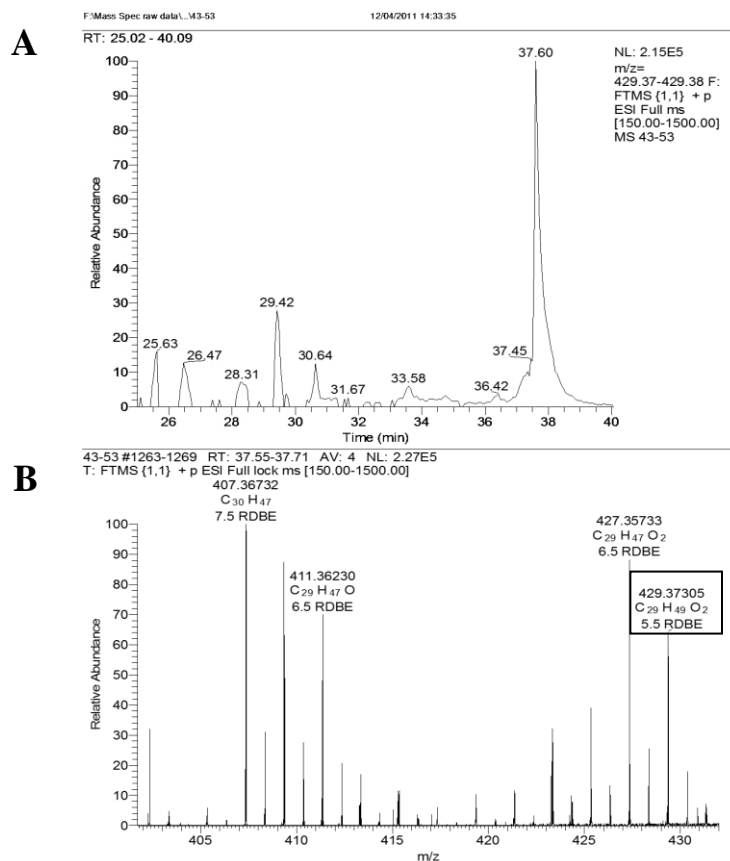


Figure 3-25: (A) Extracted ion chromatogram and (B) mass spectrum of B-4.

3.3.3.3 20-Methyl-pregn-6-en-3 β -ol, 5 α ,8 α -epidioxy

Another new steroid, R-17, was isolated. It had an R_f value of 0.36 on the TLC plate when eluted with 95:5 dichloromethane:methanol. B-5 was found to have the same R_f value but NMR spectroscopy, and indeed, the TLC summary plates showed that R-17 was purer. The subsequent attempt to purify B-5 using conventional normal phase chromatography did not result in a steroid with greater purity than R-17. The Reveleris[®] flash chromatography system was therefore more efficient and provided better separation of compounds than the BÜCHI system. Both R-17 and B-5 were active against *T. brucei* and *M. marinum*, although R-17 had greater inhibitory activity against *M. marinum*, perhaps because of its higher purity.

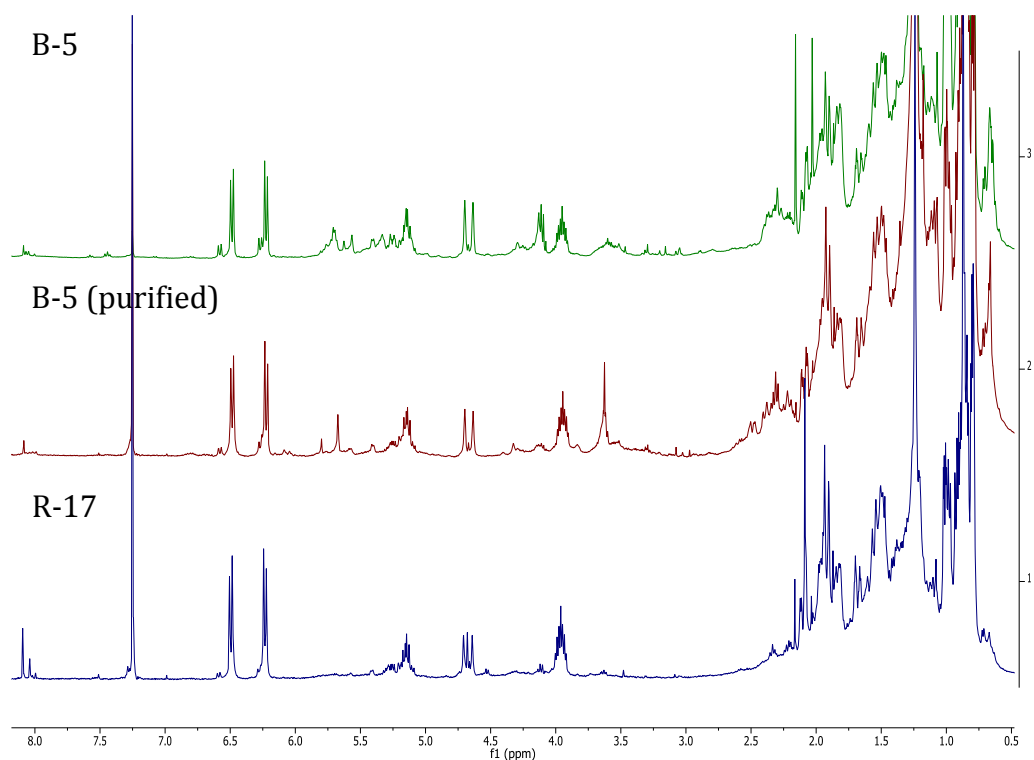


Figure 3-26: ^1H NMR spectra comparison of B-5 (top), B-5 purified (middle) and R-17 (bottom). The different degrees of purity are evident with R-17 being the purest. B-5 was purified using a conventional silica column; however, the fraction obtained still possessed more impurities than R-17.

R-17 was elucidated as a sterol peroxide with a shortened side chain. The NMR spectral data are shown in Table 3-10 and the 1D and 2D NMR spectra are shown in Figure 3-27 to Figure 3-29. The NMR data, particularly of the steroid nucleus, were compared to that of ergosterol peroxide.

Table 3-9: 20-Methyl-pregn-6-en-3 β -ol, 5 α ,8 α -epidioxy

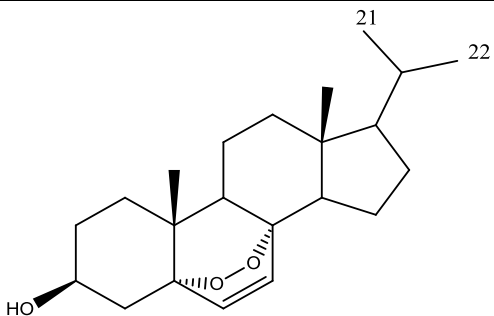
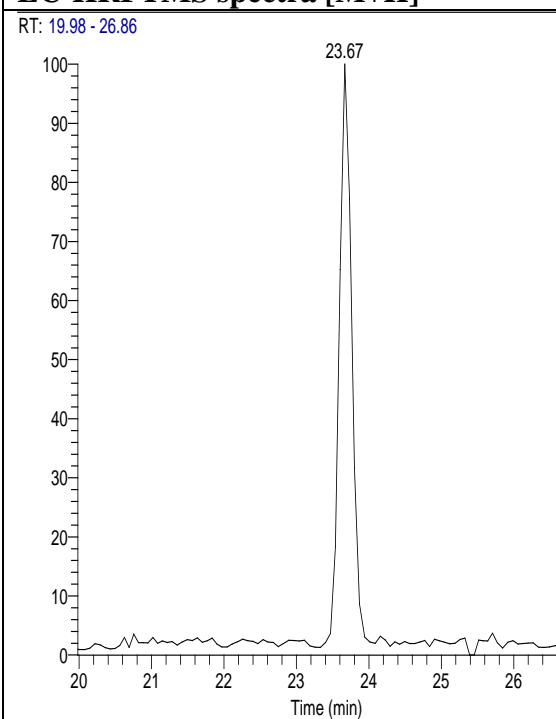
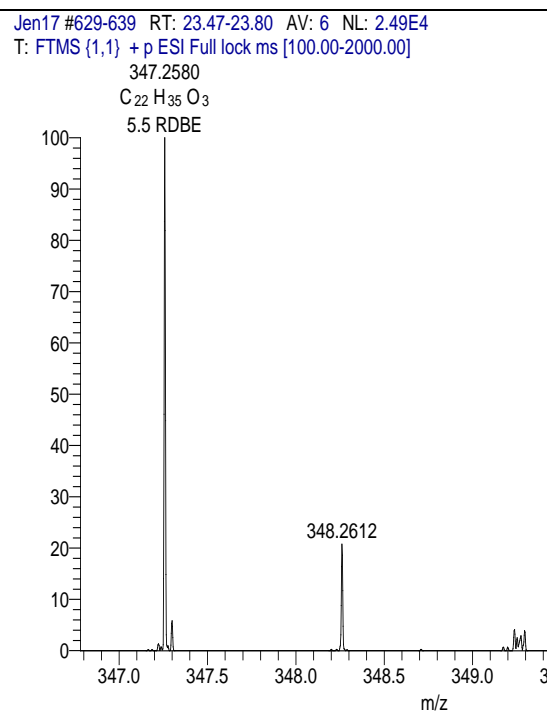
20-Methyl-pregn-6-en-3β-ol, 5α,8α-epidioxy (NOVEL)	
Synonyms	-
Sample Codes	B-5, R-17
Sample Amount	27.8 mg, 6.7 mg
Physical Description	Small, white needle-like crystals
Molecular Formula	C ₂₂ H ₃₄ O ₃
Molecular Weight	346 g/mol
Optical Rotation [α]_D²⁰	+5 (c=0.1, CHCl ₃)
Retention time (LC-MS)	23.67 min
	
LC-HRFTMS spectra [M+H]⁺	
<p>RT: 19.98 - 26.86</p> 	<p>Jen17 #629-639 RT: 23.47-23.80 AV: 6 NL: 2.49E4 T: FTMS {1,1} + p ESI Full lock ms [100.00-2000.00]</p> <p>347.2580 C₂₂H₃₅O₃ 5.5 RDBE</p> 

Table 3-10: Comparison of ¹³C and ¹H NMR data of R-17 to ergosterol peroxide (Kim et al., 1997).

Position	Ergosterol peroxide (Kim et al., 1997) δ_C ppm	R-17 δ_C ppm (multiplicity)	Ergosterol peroxide (Kim et al., 1997) δ_H ppm (multiplicity, <i>J</i>)	R-17 δ_H ppm (multiplicity, <i>J</i>)
1	35.06	34.8 (CH ₂)	1.71 (dd, 13.5, 3.1 Hz), 1.98 (dd, 13.5, 3.1 Hz)	1.68, 1.94 (d, 4.6 Hz)
2	30.47	30.2 (CH ₂)	1.55 (dd-like), 1.85 (dd-like)	1.52, 1.83
3	66.84	66.6 (CH)	3.98 (m)	3.96 (tt, 5.1, 11.1 Hz)
4	37.29	37.0 (CH ₂)	1.94 (dd-like), 2.11 (dd-like)	1.90 (s), 2.12 (d, 4.8 Hz)
5	83.10	82.2 (C)	-	-
6	135.80	135.5 (CH)	6.51 (d, 8.6 Hz)	6.23 (d, 8.5 Hz)
7	131.12	130.8 (CH)	6.25 (d, 8.6 Hz)	6.49 (d, 8.5 Hz)
8	79.82	79.5 (C)	-	-
9	51.43	51.1 (CH)	1.50 (dd-like)	1.50 (m)
10	37.33	36.0 (C)	-	-
11	23.77	23.5 (CH ₂)	1.22 (m), 1.53 (m)	1.20, 1.49
12	39.70	39.5 (CH ₂)	1.25 (m), 1.96 (m)	1.21, 1.97
13	44.93	44.8 (C)	-	-
14	52.05	51.7 (CH)	1.57 (m)	1.57 (d, 3.6 Hz)
15	21.01	20.7 (CH ₂)	1.40 (m), 1.65 (m)	0.99
16	29.05	29.8 (CH ₂)	1.35 (m), 1.80 (m)	1.24 (s)
17	56.55	56.2 (CH)	1.24 (m)	1.20
18	13.25	12.7 (CH ₃)	0.83 (s)	0.80 (s)
19	18.57	18.3 (CH ₃)	0.89 (s)	0.87 (s)
20	40.14	33.9 (CH)	2.03 (m)	1.98 (m)
21	21.26	22.1 (CH ₃)	1.00 (d, 6.6 Hz)	0.98 (d, 7.0 Hz)
22	135.58	28.4 (CH ₂)	5.15 (dd, 15.2, 7.7 Hz)	1.02 (d, 7.0 Hz)
23	132.40	-	5.22 (dd, 15.2, 8.2 Hz)	-
24	43.14	-	1.85 (m)	-
25	33.44	-	1.50 (m)	-
26	20.03	-	0.82 (d, 6.7 Hz)	-
27	20.34	-	0.84 (d, 6.7 Hz)	-
28	17.95	-	0.91 (d, 6.7 Hz)	-

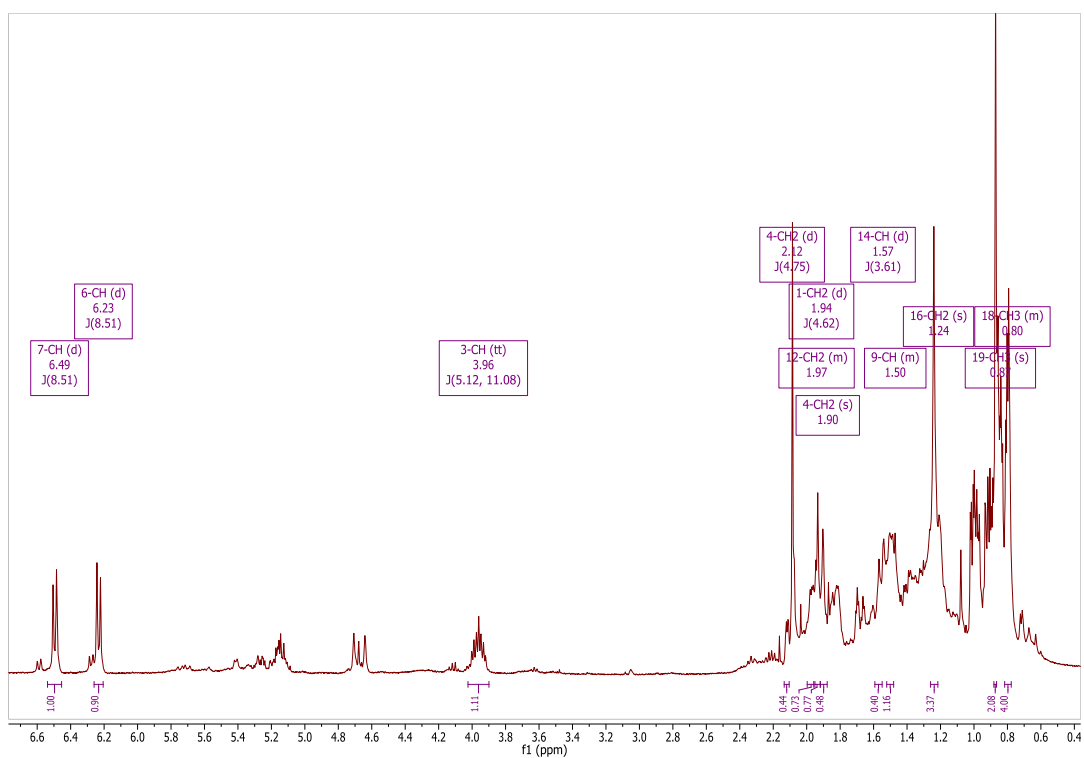


Figure 3-27: ^1H NMR of R-17 (400 MHz, CDCl_3). The chemical shifts, multiplicity, and coupling constants of selected peaks are labelled.

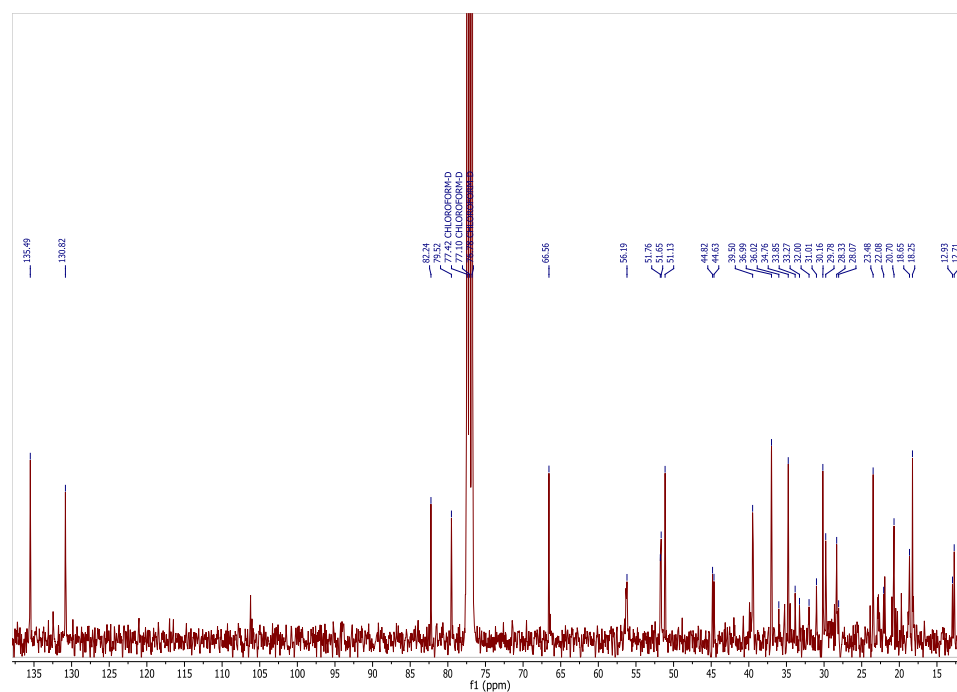


Figure 3-28: ^{13}C NMR spectrum of R-17 (100 MHz, CDCl_3).

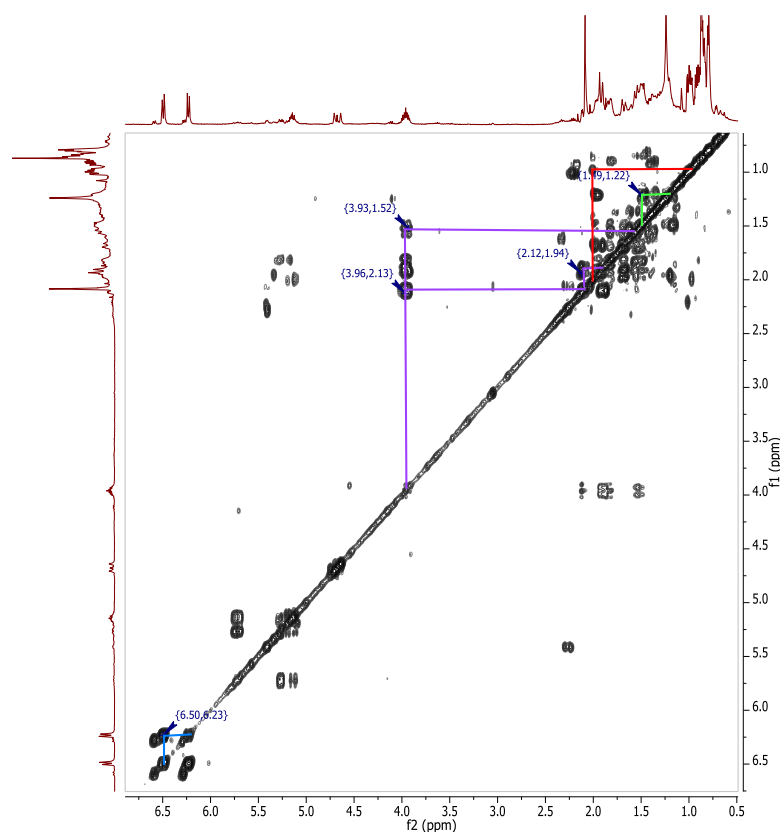


Figure 3-29: COSY spectrum of R-17 (400 MHz, CDCl₃). Different spin systems are marked in different colours. The blue spin system was indicative of the olefinic bond near the peroxide functional group. The purple spin system shows the correlations on the A-ring whereas the green and red spin systems are on the C-ring and side chain respectively.

R-17 differed from the previous two steroids in the presence of the peroxide functional group as well as the shortened side chain. The peaks belonging to the steroid nucleus were assigned using the COSY and HMBC. The methyl group of C-19 had a chemical shift of δ_{H} 0.87 and δ_{C} 18.3. It had long-range interactions with C-6, C-9 (δ_{C} 51.1), C-1 and C-4, thus confirming the carbon and proton assignments of rings A and B. The methyl group of C-18 assisted in confirming the assignments of rings C and D. H-18 (δ_{H} 0.80) correlated with C-17 (δ_{C} 56.2), C-14 (δ_{C} 51.7), C-13 (δ_{C} 44.8), C-12 (δ_{C} 39.5) and C-15 (δ_{C} 20.7).

The two doublets at δ_{H} 6.23 and 6.49 (H-6 and H-7 respectively) were shown on the COSY to form an isolated spin system (marked in blue). The HMBC spectrum confirmed that H-6 and H-7 correlated with oxygenated carbons (δ_{C} 82.2 and 79.5, C-5 and C-8 respectively). The orientation of the 5,8-epidioxy peroxide group was confirmed by comparing the chemical shifts and coupling patterns of H-6 and H-7 to

the values found in literature. A $5\alpha,8\alpha$ -epidioxy group results in chemical shifts of 6.5 and 6.3 ppm for H-6 and H-7 whereas a $5\beta,8\beta$ -epidioxy group would result in chemical shifts of 5.9 and 5.6 respectively (Gauvin et al., 2000).

The assignment of the side chain proved challenging as there were many overlaps in the aliphatic region. The chemical shifts of the methyl group at C-21 were assigned based on the COSY and J-resolved spectra. The J-resolved showed that the peak at δ_{H} 0.98 (H-21) was a doublet, therefore it must have been attached to the $-\text{CH}$ of C-20 rather than the $-\text{CH}_2$ of C-22. It had a correlation in the COSY with a peak at δ_{H} 1.98, which was assigned to H-20. It was also correlating on the HMBC with C-17. The heteronuclear multiple quantum coherence (HMQC) spectrum showed that C-21 had a chemical shift of δ_{C} 22.1. A peak at δ_{H} 1.02 correlated with both C-21 and C-20 (δ_{C} 33.9) on the HMBC, although correlation with C-20 cannot be seen on the COSY. This was then assigned as H-22.

The proposed structure for R-17 can be seen in Table 3-9. The predicted chemical formula and mass matched the LC-HRFTMS data (Figure 3-31).

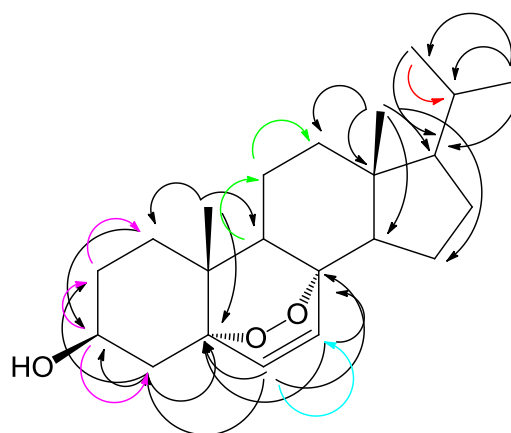


Figure 3-30: Proposed structure of R-17. The black arrows show the HMBC correlations whereas the coloured ones correspond to the correlations seen in the COSY spectrum.

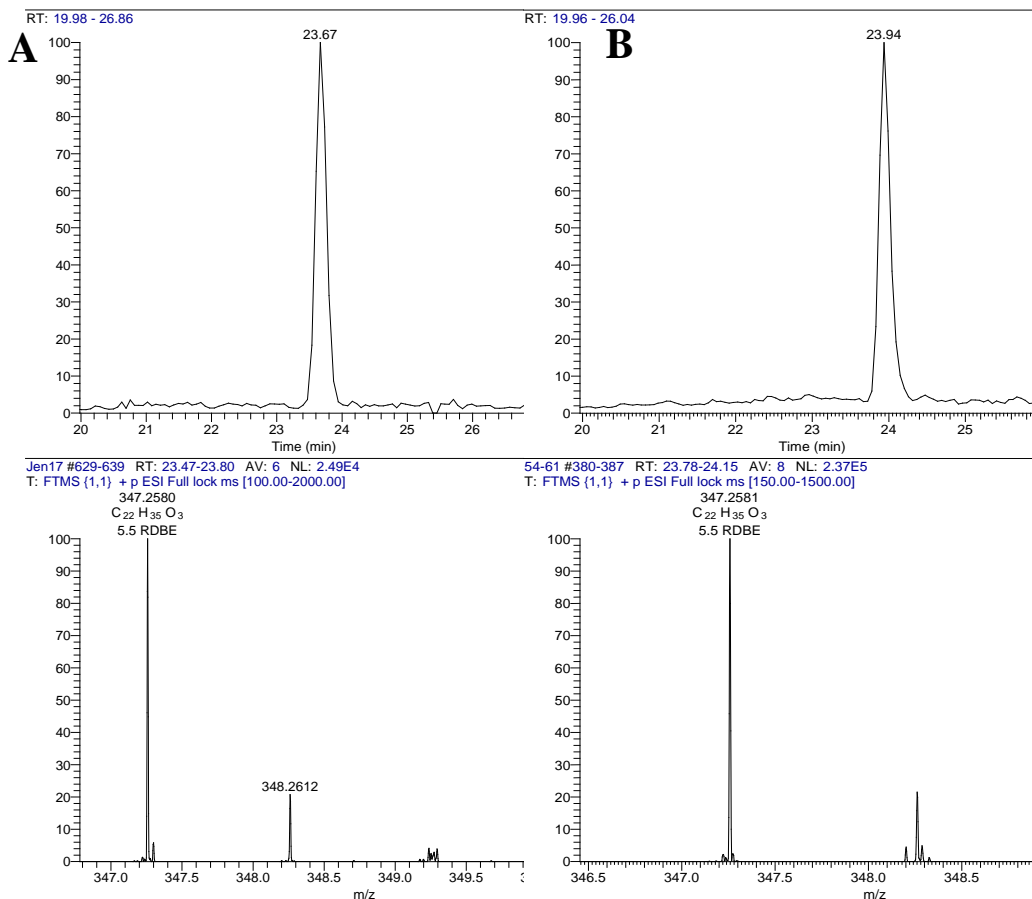


Figure 3-31: Extracted ion chromatogram of (A) R-17 and (B) B-5. The m/z 347.258 $[M+H]^+$ and a predicted formula $C_{22}H_{35}O_3$ matching that of the predicted structure are seen.

3.3.3.4 Antimicrobial Activities and Cytotoxicity of the *H. simulans* Sterols

The MIC values of the three sterols against *T. b. brucei* and *M. marinum* were determined by averaging the results of four independent assays. The assays were performed by testing various concentrations of the sterols (in $\mu\text{g/mL}$) against the test organisms (Figure 3-32). The concentrations at which cell viability became less than 10% were averaged and converted to μM (Table 3-11). The IC_{50} of the sterols against Hs27 cells were determined by averaging the results of three independent assays. The results are shown in Table 3-11 and the changes in cell morphology depicted in Figure 3-33.

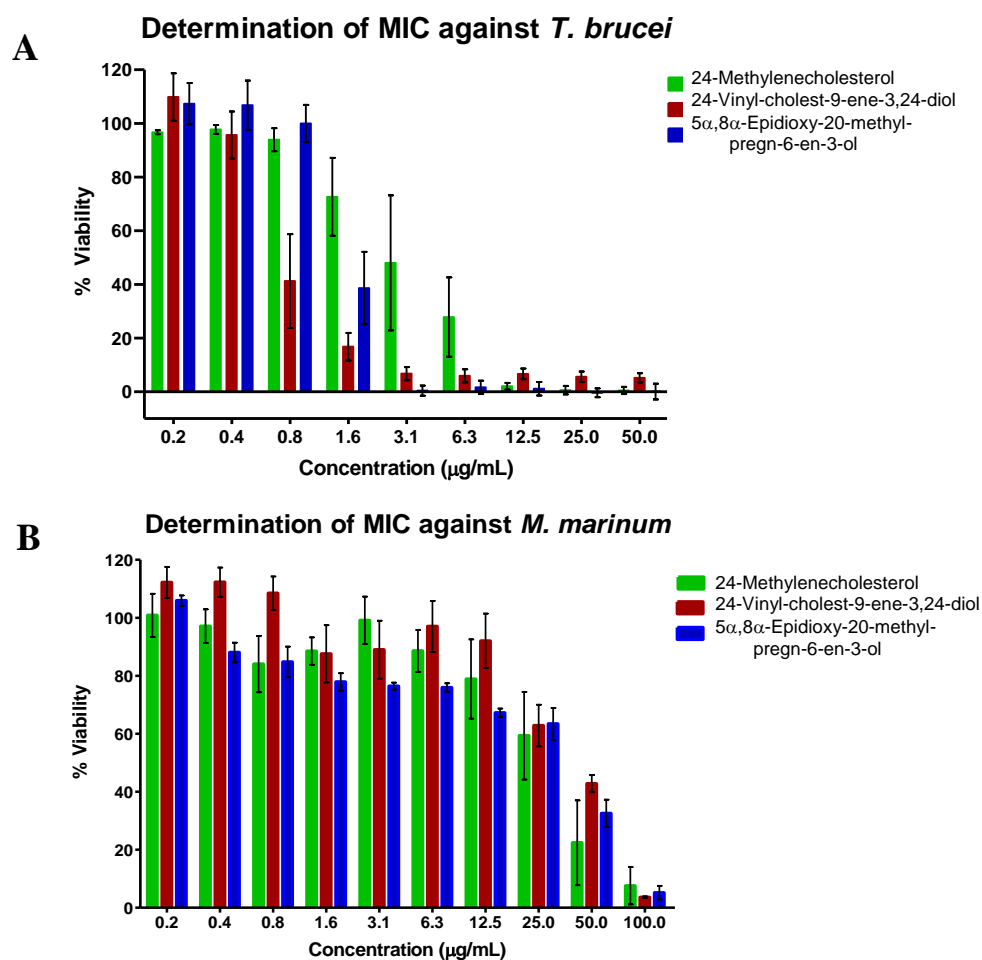


Figure 3-32: Determination of the MIC of the sterols against (A) *T. b. brucei* and (B) *M. marinum*. The assays were performed using various concentrations of the sterols in $\mu\text{g/mL}$. The mean values were then converted to μM . The saringosterol derivative was the most potent against *T. b. brucei*, followed by the sterol peroxide. 24-Methylenecholesterol was the most potent against *M. marinum*.

Table 3-11: MICs of sterols and control drugs against *T. b. brucei* and *M. marinum* and cytotoxicity against Hs27 cells. The sterols are labelled as follows: (1) 24-methylenecholesterol, (2) 24-vinyl-cholest-9-ene- $3\beta,24$ -diol, (3) 5 $\alpha,8\alpha$ -epidioxy-20-methyl-pregn-6-en- 3β -ol

Sterol	MIC Average \pm Std Dev (n=4)		Cytotoxicity on Hs27 cells IC ₅₀ (μM) \pm Std Dev (n=3)
	<i>T. brucei</i> (μM)	<i>M. marinum</i> (μM)	
1	21.56 \pm 11.80	156.90 \pm 54.35	58 \pm 3.53
2	4.58 \pm 1.80	233.44 \pm 0	>100 \pm 4.03
3	9.01 \pm 0	288.81 \pm 0	100 \pm 2.95
Suramin	0.11 \pm 0	-	
Gentamycin	-	13.48 \pm 0	

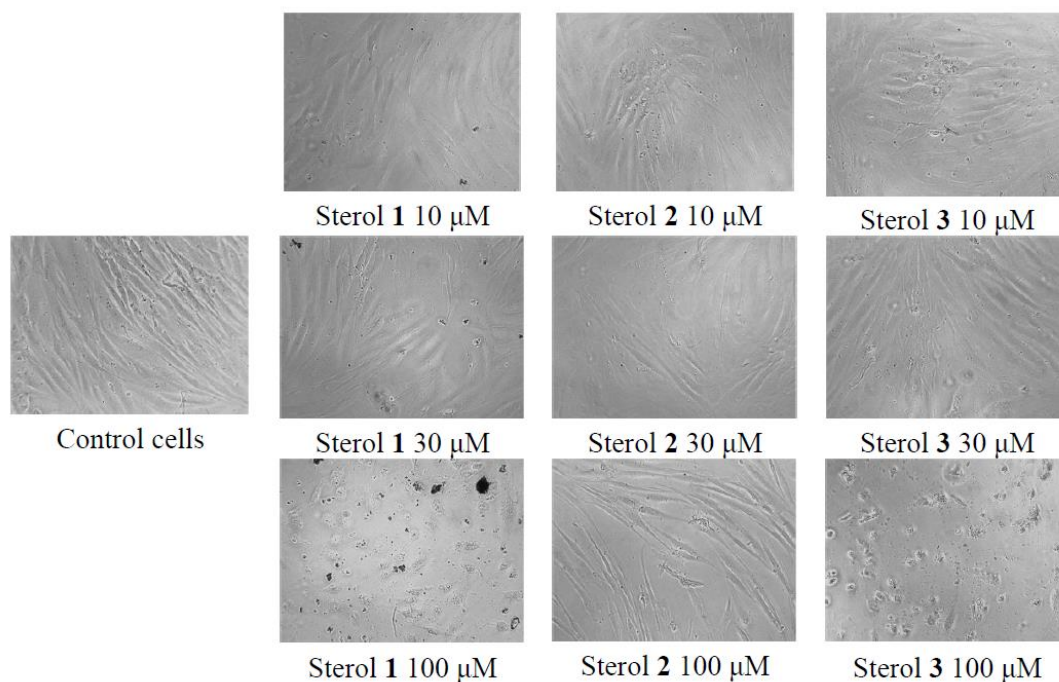


Figure 3-33: Cell cytotoxicity assay of sterols on normal human fibroblasts Hs27. Sterol 1: 24-methylenecholesterol; sterol 2: 24-vinyl-cholest-9-ene-3-diol; sterol 3: 5 α ,8 α -epidioxy-20-methyl-pregn-6-en-3-ol. Assays were performed in triplicate. The saringosterol derivative (2) showed no cytotoxicity and no change in cell morphology. At 100 μ M of 24-methylenecholesterol (1) and the sterol peroxide (3), the Hs27 cells shrunk 10x to irregularly shaped cells.

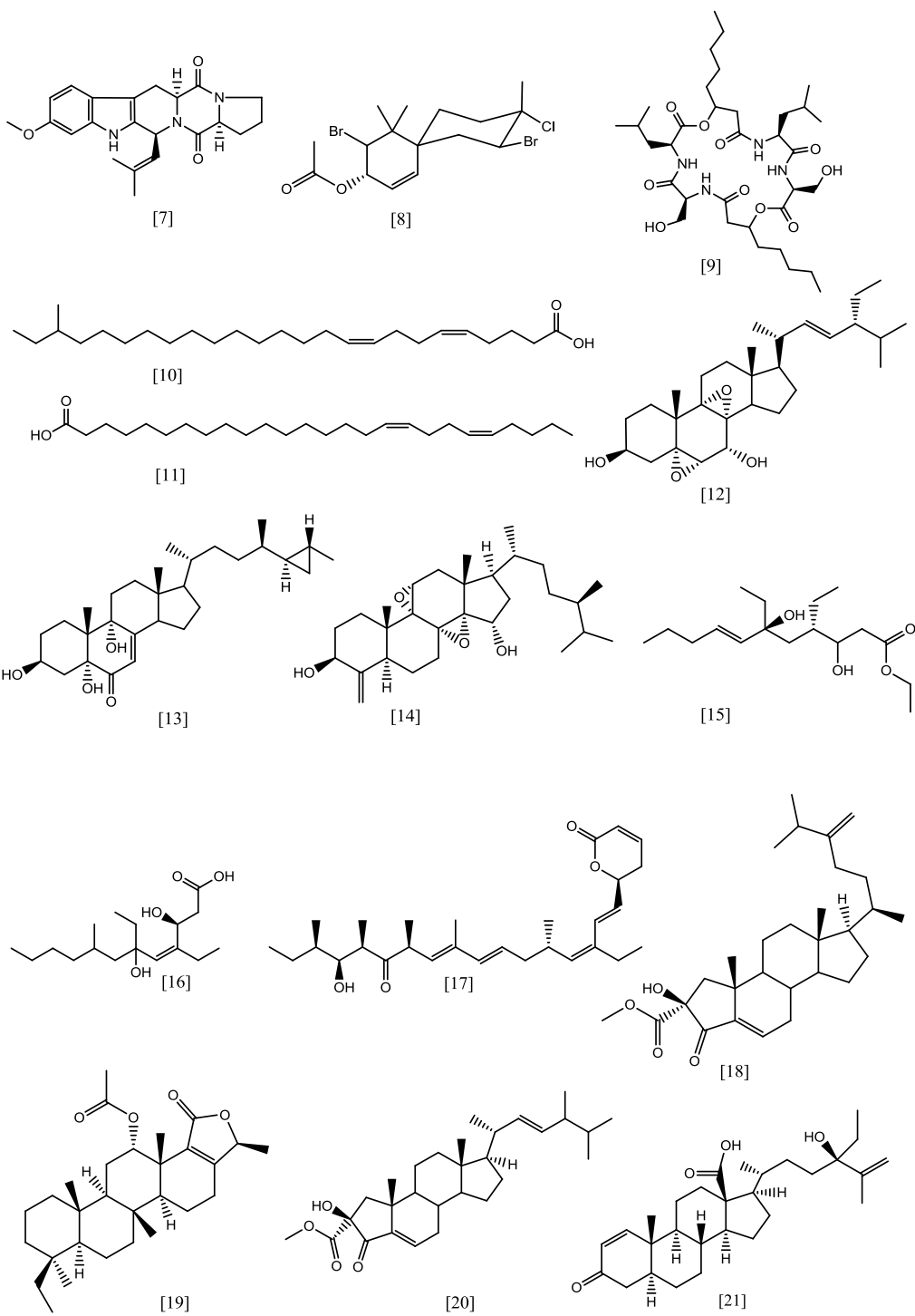
24-Methylenecholesterol was the most cytotoxic sterol, causing cell death at 58 μ M. This is still above its MIC against *T. brucei* (21.56 μ M), thus it may still be considered as a lead compound against trypanosomiasis.

3.3.3.5 Identification of Compounds from Active Fractions Using the AntiMarin Database

The other active fractions obtained following the Reveleris[®] fractionation were not pure and not of sufficient quantities to allow further purification. The possible active constituents of these fractions were therefore examined by comparing the HR-LCFTMS data to the AntiMarin 2012 database to identify known compounds. Compound hits of peaks with the largest peak area are enumerated in Table 3-12. Where there was more than one hit, only those metabolites previously isolated from sponges were considered. If there was more than one hit but none from a sponge, as in the case of R-24, the compound from a bacterium was given. The structures are shown in Figure 3-34.

Table 3-12: Compounds identified using the AntiMarin 2012 database from the active fractions of *H. simulans* after MPLC fractionation with the Reveleris®

Fraction		Name	Formula (MW)	RT	Source	Reference
R-4	[M+H] ⁺	[7] Fumitremorgin C	C ₂₂ H ₂₅ N ₃ O ₃ (379.1896)	25.91	<i>Aspergillus fumigatus</i> , <i>Neosartorya fischeri</i> (<i>Aspergillus fischerianus</i>)	(Beuchat et al., 1989)
	[M-H] ⁻	[8] Hydroxy-dibromo-chloro-chamigren acetate	C ₁₆ H ₂₃ Br ₂ Cl O ₂ (439.9753)	28.15	Mollusca, Rhodophyta	(Rovirosa et al., 1991)
R-9	[M+H] ⁺	[9] Icosalide B	C ₃₄ H ₆₀ N ₄ O ₁₀ (684.4309)	33.27	Fungi	(Boros et al., 2006)
	[M-H] ⁻	[10] 23-Methyl-5,9-pentacosadienoic acid	C ₂₆ H ₄₈ O ₂ (392.3654)	36.05	Porifera <i>Cribochalina vasculum</i> , Porifera <i>Ircinia strobilina</i>	(Carballeria and Reyes, 1990)
		[11] 17,21-Hexacosadienoic acid pyrrolidide			Porifera <i>Pseudaxinella</i> cf. <i>lunaecharta</i> , Porifera <i>Trikentrion loeve</i>	(Barnathan et al., 1996)
R-20	[M+H] ⁺	[12] Homaxisterol B2	C ₂₉ H ₄₆ O ₄ (548.3396)	24.87	Porifera <i>Homaxinella</i> sp.	(Mansoor et al., 2006)
		[13] Topsentisterol C1			Porifera <i>Topsentia</i> sp.	(Luo et al., 2006b)
		[14] Conicasterol F			Porifera <i>Theonella swinhoei</i>	
	[M-H] ⁻	[15]	C ₁₇ H ₃₂ O ₄ (300.2301)	23.17	Porifera <i>Chondrosia collectrix</i>	(Stierle and Faulkner, 1979)
		[16] Woodylide C			Porifera <i>Plakortis simplex</i>	
R-24	[M+H] ⁺	[17] Callystatin A	C ₂₉ H ₄₄ O ₄ (456.3240)	22.26	Porifera <i>Callyspongia truncata</i>	(Kobayashi and Kitagawa, 1999)
		[18] Anthosterone B			Porifera <i>Anthoarcuata graceae</i>	(Tischler et al., 1988)
		[19] 12a-Acetoxy-dimethylscler-17-enolactone			Porifera <i>Carteriospongia foliascens</i>	(Barron et al., 1991)
		[20] Phorbasterone A			Porifera <i>Phorbasteron amaranthus</i>	(Masuno et al., 2004)
		[21] Norselic Acid B				
		[22] Norselic Acid D			Porifera <i>Crella</i> sp.	(Ma et al., 2009)
	[M-H] ⁻	[23] 3-Anteisoheptadecanoyl-5-hydroxymethyl tetronic acid	C ₂₂ H ₃₈ O ₅ (382.2719)	22.54	Actinomycete strain DSM 7357	(Roggo et al., 1994a, Roggo et al., 1994b)
R-25	[M+H] ⁺	[24] (Z)-9-Octadecenamide	C ₁₈ H ₃₅ NO (281.2719)	29.02	Cyanobacterium	(Dembitsky et al., 2000)
	[M-H] ⁻	[25] Strongyloidiol E	C ₃₁ H ₄₈ O ₂ (452.3654)	35.64	Porifera <i>Strongylophora</i> sp.	(Watanabe et al., 2005)
		[26] Acetyldehydroconicasterol			Porifera <i>Theonella swinhoei</i>	



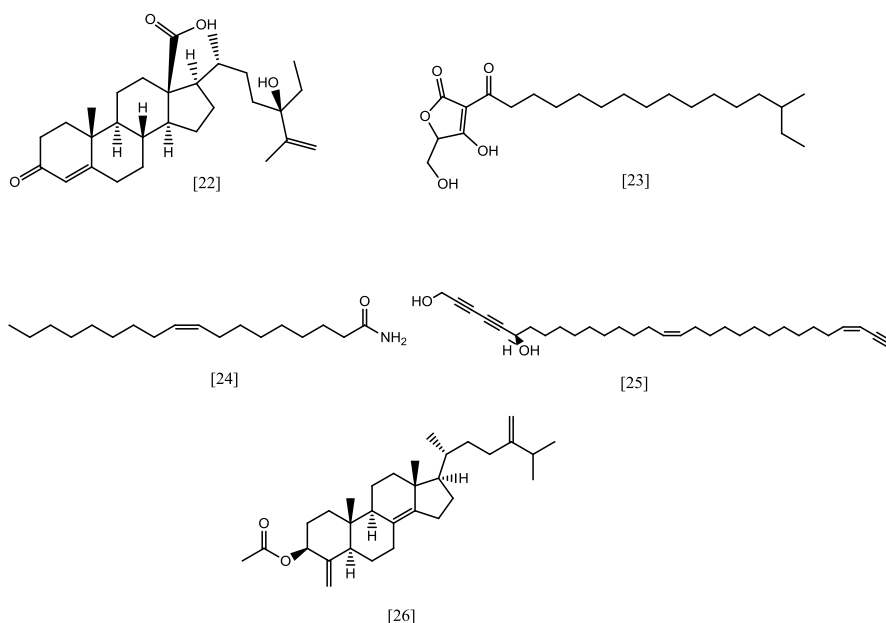


Figure 3-34: Structures of major compounds identified using the AntiMarin 2012 database from the remaining active fractions of *H. simulans*.

Although the presence of the compounds must be verified by isolation or comparison with a standard, the isotopic pattern of the peak putatively identified as hydroxy-dibromo-chloro-chamigren acetate (**8**) confirmed the presence of halogen atoms. The $[M-H]^-$, $[M-H+2]^-$, $[M-H+4]^-$ and $[M-H+6]^-$ ions were seen in a ratio of approximately 100:95:50:15 (Figure 3-35). This did not match the predicted isotope pattern of hydroxyl-dibromo-chloro-chamigren which should have resulted in a ratio of 51:100:48:15. Other predicted formulae for m/z 438.96771 $[M-H]^-$ are $C_{18}H_8O_5N_4Br$ which would have an $[M-H]^-:[M-H+2]^-$ ratio of 100:97, and $C_6H_{14}O_{12}N_4Cl_3$ for which the ratio would be 100:95:30:3. These compounds were not identified in the database, however.

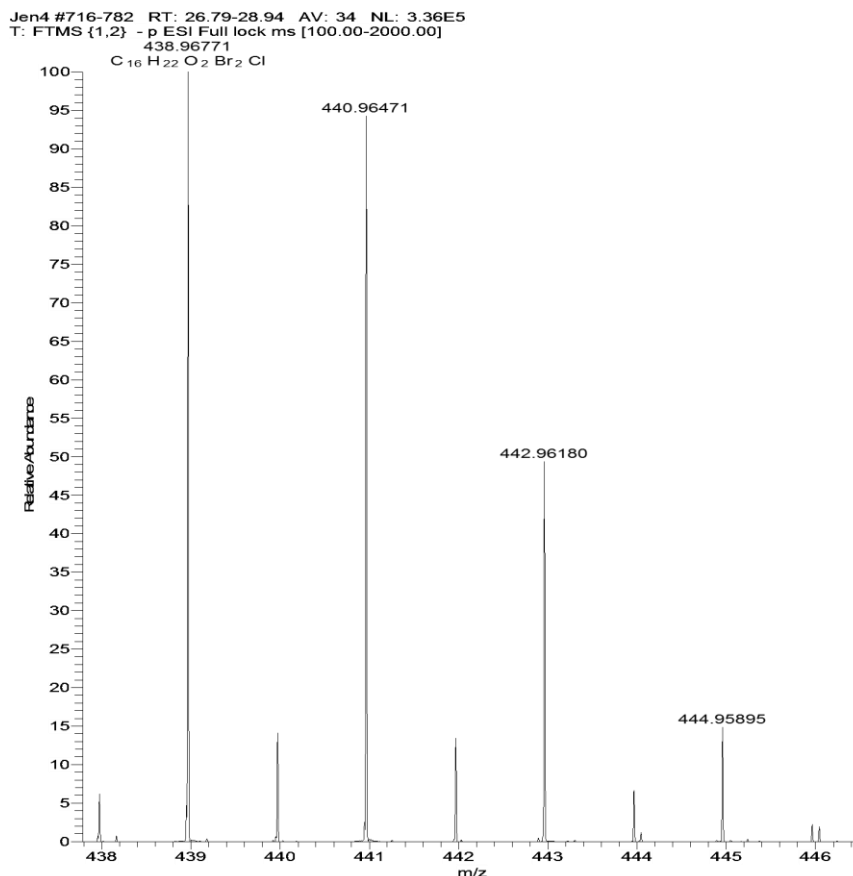


Figure 3-35: Isotopic pattern seen for m/z 438.96771 [M-H]. The peaks have a ratio of 100:95:50:15, which does not match any of the patterns that were expected for the predicted compounds.

3.4 Discussion

The non-polar metabolites of *H. simulans* possessed inhibitory activity against *Trypanosoma brucei brucei* and *Mycobacterium marinum*. Three relatively pure sterols were isolated from the sponge. All three showed varying degrees of anti-trypanosomal and anti-mycobacterial activity. Cytotoxicity was evident in 24-methylenecholesterol at concentrations greater than the MIC for anti-trypanosomal activity.

Two flash chromatography systems were compared: the BÜCHI and the Reveleris[®]. The fractions from the BÜCHI were collected by time; that is, each test tube corresponded to 15 seconds or 2.5 mL. The contents of each test tube were then qualitatively determined using TLC and similar fractions were pooled. In this manner, two pure steroids, B-3 and B-4, were isolated. A third fraction, B-5,

contained a steroid as a major compound but possessed many impurities, and a subsequent purification step was insufficient. In contrast, the Reveleris[®] used both a UV detector as well as an evaporative light scattering detector (ELSD). The fractions were therefore collected based on the peaks seen by the two detectors. The resulting test tubes were still assayed using TLC and pooled in a similar manner, but this was facilitated by following the chromatogram obtained from the Reveleris[®]. Three pure steroids, R-11, R-13 and R-17, were obtained following fractionation. The Reveleris[®] is therefore superior to the BÜCHI in the separation of compounds.

B-3 and R-11 appeared as white needle-like crystals. The same compound had previously been isolated from *H. simulans* by Ms. Theng Theng Ooi, who identified the crystals as 24-methylenecholesterol. The average MIC of the 24-methylenecholesterol samples against *T. brucei* was $8.59 \pm 4.69 \mu\text{g/mL}$ ($21.56 \pm 11.80 \mu\text{M}$). The variations in the assay results could have been due to differences in the purity of the isolated compounds, as well as the difficulty in dissolving the crystals in DMSO. In literature, 24-methylenecholesterol had a minimum effective concentration (MEC) of 50 μM (Bazin et al., 2006). The procedures of the assays were slightly different as the concentration of the bloodstream forms was 3×10^4 trypanosomes/mL for the assay performed in this study and 2×10^5 trypanosomes/mL in the assay performed by Bazin and colleagues. In addition, in the latter assay the MEC was assessed visually using a microscope to count viable cells, whereas for the former assay the fluorescence is measured after incubation of the cells with Alamar Blue. Different strains of *T. b. brucei* were used in the assays, as *T. b. brucei* CMP (Chatenay-Malabry Parasitologie) was used by Bazin et al. and *T. b. brucei* S427 was used in this study. These variations may also account for the difference in the MIC values obtained.

24-Methylenecholesterol was first isolated in 1945 from the sponge *Chalina arbuscula* Verill (Bergmann et al., 1945). It was initially called chalinasterol; however, the structure was erroneously elucidated. The structure of chalinasterol has since been corrected to be 24-methylenecholesterol. This steroid was then isolated in 1972 from sponges *Cliona celata* and *Hymeniacidon perleve* (Erdman and Thomson, 1972). It has since been isolated from algae (Xiao et al., 2013), crustaceans such as

crab, lobsters and shrimp, molluscs such as oysters, clams and scallops (Phillips et al., 2012), herring (Mika et al., 2012), limpets (Kawashima et al., 2011) and diatoms (Giner and Wikfors, 2011). Another study of four marine sponges, two of which were *Haliclona* sponges, *Haliclona* sp. and *H. permollis*, found 24-methylenecholesterol in all four sponges (Sheikh and Djerassi, 1974). It was also found to be the major component of two other sponges, *Geodia megastrella* and *Orina arcoferus* (Kingston et al., 1979). 24-Methylenecholesterol appears to be a precursor to many other sponge sterols (Giner, 1993). It has likewise been isolated from a soft coral, *Sinularia dura* (Radwan et al., 2008) and tested against a range of microorganisms including *Mycobacterium intracellulare*. A concentration of 50 µg/mL was inactive against *M. intracellulare*. In this study a concentration of 100 µg/mL caused an inhibition of approximately 79-99% in the growth of *M. marinum* compared to the control. The MIC was determined to be 62.50 ± 21.65 µg/mL (156.90 ± 54.35 µM). 24-Methylenecholesterol was the most cytotoxic of the three sterols isolated, having an IC₅₀ of 58 ± 3.53 µM against Hs27 cells.

B-4/R-13 was a yellow compound. It was the most active of all fractions tested against *T. b. brucei*, having an average MIC of 1.96 ± 0.77 µg/mL (4.58 ± 1.80 µM). NMR analysis proved that the compound was similar in structure to the steroid saringosterol, which was first isolated from a brown alga (Ikekawa et al., 1966). Saringosterol has been shown to be active against trypanosomes with an IC₅₀ of 3.3 ± 0.5 µg/mL (Hoet et al., 2007). It was also active against *M. tuberculosis* (MIC: 0.25 µg/mL) and was not harmful to mammalian cells (Wachter et al., 2001). The stereochemistry of the methylene group at C-28 of the saringosterols isolated from nature tends to be a 1:1 mixture of 24*S* and 24*R* epimers (Wachter et al., 2001, Hoet et al., 2007). The 24*R* epimer is more active than the 24*S* epimer (MIC: 0.125 and 1 µg/mL respectively), however (Wachter et al., 2001). 100 µg/mL of B-4 inhibited the growth of 97.2% of *M. marinum* compared to the control, whereas R-13 inhibited 76.4%. The MIC of B-4 was determined to be 100 µg/mL (233.44 µM). It is possible that the position of the double bond has an effect on the activity of the sterol. The assays were also different, as in literature the activity of saringosterol against *M. tuberculosis*, not *M. marinum*, is reported. In addition, the stereochemistry of the saringosterol derivative isolated in this study was unable to be determined by

comparison of the NMR data to that in the literature (Catalan et al., 1983); therefore it is not known whether the isolated derivative is the more or less active epimer or a mixture of both. However, the optical activity ($[\alpha]_D^{20}$ -4.5) was quite low indicating that the fraction could be a mixture of epimers.

Although it is uncommon for the double bond to be at the $\Delta^{9(11)}$ position, as in B-4/R-13, other steroids with this nucleus have previously been isolated from marine sources. Starfish, such as *Acanthaster planci* L., have been good sources of such steroids, generally in the form of saponenols; that is, the steroidal aglycone portion of saponins. For example, thornasterol A and B were isolated from *A. planci* (Kitagawa et al., 1975, Kitagawa et al., 1978). A dihydroxypregnane derivative, asterone (3 β ,6 α -dihydroxy-5 α -pregn-9(11)-en-20-one), was isolated from the starfish *Asterias forbesi* (ApSimon et al., 1973). It was also isolated from a *Haliclona* sponge, *H. rubens*, although at the time of publication the authors had not identified it as asterone (Ballantine et al., 1977). *H. rubens* has since been renamed to *Amphimedon compressa*. Another dihydroxypregnane derivative, (20*R*)-5 α -pregn-9(11)-ene-3 β ,6 α ,20-triol, was isolated as a minor constituent of the saponin hydrolysate of *A. forbesi* and *A. vulgaris* (ApSimon et al., 1980). Some $\Delta^{9(11)}$ steroids were also found in sea cucumbers (Goad et al., 1985). $\Delta^{9(11)}$ Sterols have found applications as lead compounds for anti-inflammatory drugs as they possess fewer side effects than the conventional corticosteroids (Reeves et al., 2013). It is therefore interesting to note that 24-vinyl-cholest-9-ene-3 β ,24-diol was the least cytotoxic of the three *H. simulans* sterols isolated.

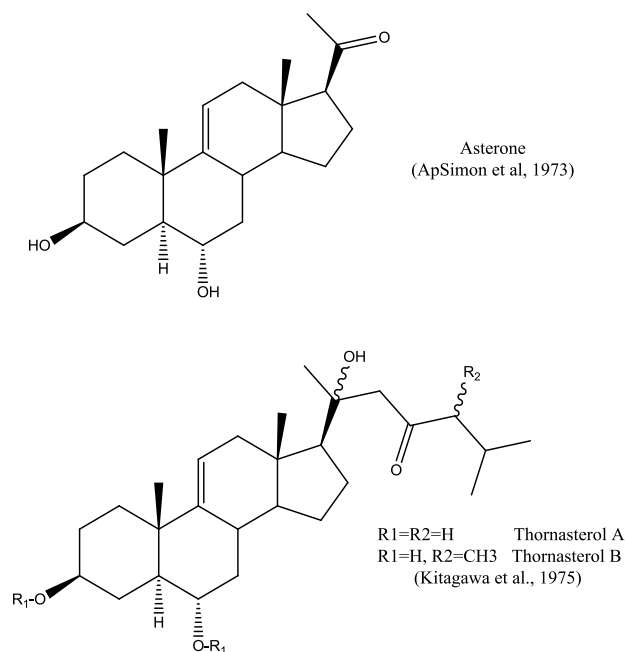


Figure 3-36: Examples of $\Delta^{9(11)}$ steroids from marine sources.

The third sterol isolated, B-5/R-17, was a $5\alpha,8\alpha$ -epidioxy sterol with a shortened side chain. Aside from the side chain, B-5/R-17 bears similarity to ergosterol peroxide, a common fungal metabolite that has previously been isolated from sponges (Mansoor et al., 2005, Luo et al., 2006b, Prawat et al., 2011) and marine fungi alike. Pinheiro et al. reported the isolation of ergosterol peroxide from a marine fungus obtained from a sponge (Pinheiro et al., 2012). It is possible that B-5/R-17 is a fungal metabolite in its own right or one that has been metabolised by the host sponge into a more useful compound. Some earlier studies do assert that sponges are capable of *de novo* sterol biosynthesis (Walton and Pennock, 1972, Kerr et al., 1989, Silva et al., 1991); indeed, cell-free assays have served to confirm this claim (Giner and Djerassi, 1990, Kerr et al., 1990). Some scientists, however, still believe that most of the sterols found in sponges are obtained from their diet or endosymbionts due to the slow rate or nonexistence of sterol biosynthesis in sponges (Kanazawa, 2001). It has been proven that sponges can modify exogenous sterols, both by oxidising or reducing the ring system and by developing the side chain. *Tethya aurantia*, for example, aside from synthesising its own sterols, can perform both alkylation and dealkylation at C-24 (Malik et al., 1988). An example of modifications to the ring system involves the 7-dehydrogenation of dietary sterols by

Fasciospongia cavernosa. This transforms the dietary sterols to $\Delta^{5,7}$ -sterols and maintains a constant cell membrane composition (De Rosa et al., 1999). While it is possible, and perhaps even likely, in most sponges, that *de novo* steroid synthesis, dietary steroid modification and direct incorporation of dietary sterols all occur, the extent of each and the contribution of each to the total sterol composition of the sponges is unknown. It is also not clear what role the endosymbiotic microorganisms play as it is possible that they are responsible not just for supplying exogenous sterols, but also for the metabolism of the dietary sterols (Goad, 1981). Indeed, bacteria such as *Mycobacterium* sp. possess the ability to transform and degrade sterols (Wang et al., 1990). Not many bacteria, however, are capable of *de novo* sterol synthesis. This is more common in fungi (Volkman, 2003).

Alternatively, the $5\alpha,8\alpha$ -epidioxy sterols could be artefacts, a result of the oxidation of a $\Delta^{5,7}$ -sterol, as has been observed in *Dysidea* sp. (Elenkov et al., 1994). However, $5\alpha,8\alpha$ -epidioxy sterols have also been isolated from a sponge, *Luffariella cf. variabilis* and these sterols are believed by the researchers to be natural products and not artefacts as the isolation was done rapidly and no precursors were found (Gauvin et al., 2000). In addition, as previously mentioned, some fungi produce these epidioxy sterols and so it cannot be ruled out that B-5/R-17 is a natural product of *H. simulans* or an endosymbiont. Another well-known anti-protozoal agent possessing an endoperoxide moiety is artemisinin, an anti-malarial compound derived from plants.

Short side chain sterols, such as B-5/R-17, are uncommon but have previously been isolated from the marine environment, including from tunicates, gorgonians and sponges (Palermo et al., 1996, Carlson et al., 1978). These sterols may be *in vivo* autoxidative products from sterols with unsaturated side chains and are not degradation products obtained during laboratory work-up. Alternatively, 20-hydroxy sterols could be converted, by the removal of water, to a 3β -hydroxy C_{21} -sterol with an olefinic 2-carbon side chain. This subsequently may be transmethylated by S-adenosylmethionine (SAM). Examples of side chains that may be generated by this mechanism are depicted in the figure below.

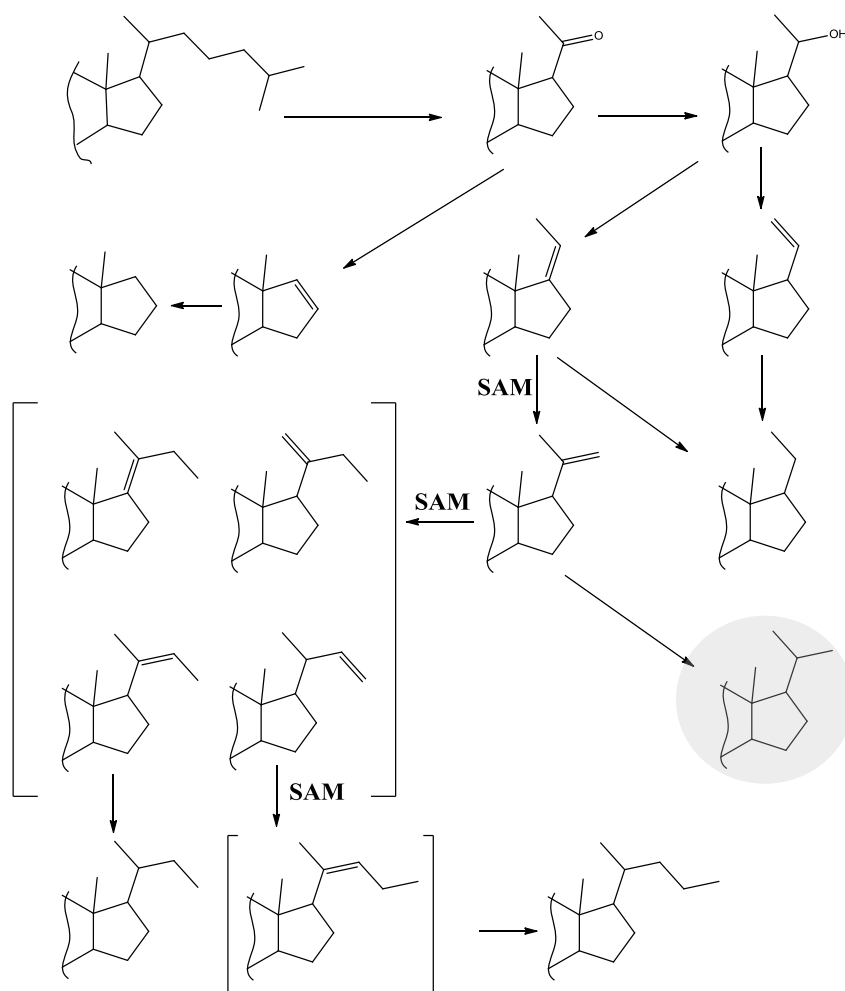


Figure 3-37: Possible mechanism of the formation of short side chain sterols by transmethylation from SAM (adapted from Goad, 1981). The structures in brackets are those that had not been isolated at the time that this scheme was written (Goad, 1981). The short side chain of R-17 is encircled.

Several 20-hydroxy and 20-keto pregnane derivatives have been isolated from *A. compressa* (*H. rubens*) from Jamaica. These include 3 β -hydroxy-17 β -pregn-5-ene-20-one, 3 β ,20 β -dihydroxy-17 β -pregn-5-ene, 3 β ,20 α -dihydroxy-17 β -pren-5-ene and other unidentified keto sterols including asterone (Ballantine et al., 1977). Sterols such as these could be precursors for short side chain synthesis using the transmethylation mechanism described above.

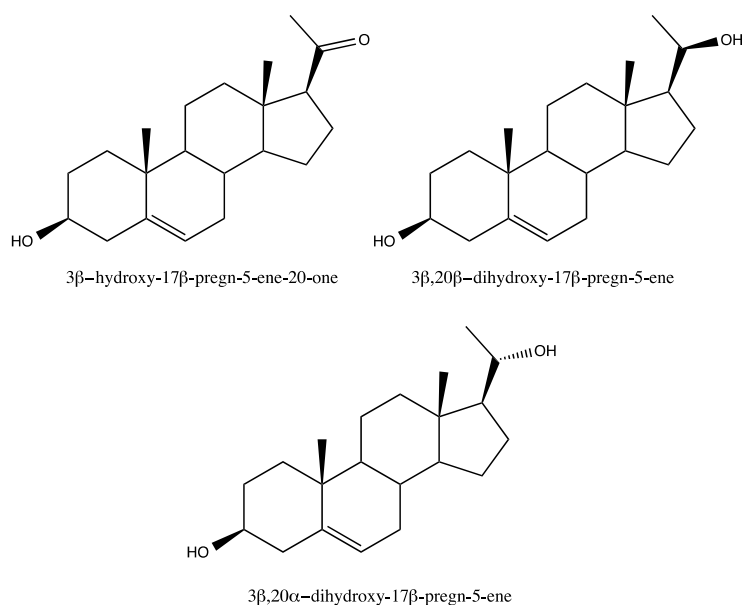


Figure 3-38: Examples of pregnane precursors from *A. compressa* (*H. rubens*) (Ballantine et al., 1977). These could potentially act as precursors for short side chain sterols through the mechanisms illustrated in Figure 3-37.

Sterols and steroids have previously been isolated from a sponge of the same genus, *Haliclona oculata* (Findlay and Patil, 1985, Yu et al., 2006). These compounds were not tested for trypanocidal activity, however. Other steroids have been studied and structure-activity relationships have been drawn. It is believed that the steroids affect the sterol biosynthetic pathway of the parasites (Figure 3-39). The sterol biosynthetic pathway in trypanosomatids is similar to that in fungi in that the major sterol synthesised is ergosterol, as opposed to cholesterol for mammals. The disruption of this pathway results in the loss of integrity of the mitochondrial membrane as well as the membrane surrounding the protozoal body. The structural features of ergosterol that make it necessary for the growth of trypanosomes are a 3β-hydroxy group, a 24β-methyl group, a double bond at C22 and the absence of methyl groups at C4 and C14 (de Souza and Rodrigues, 2009).

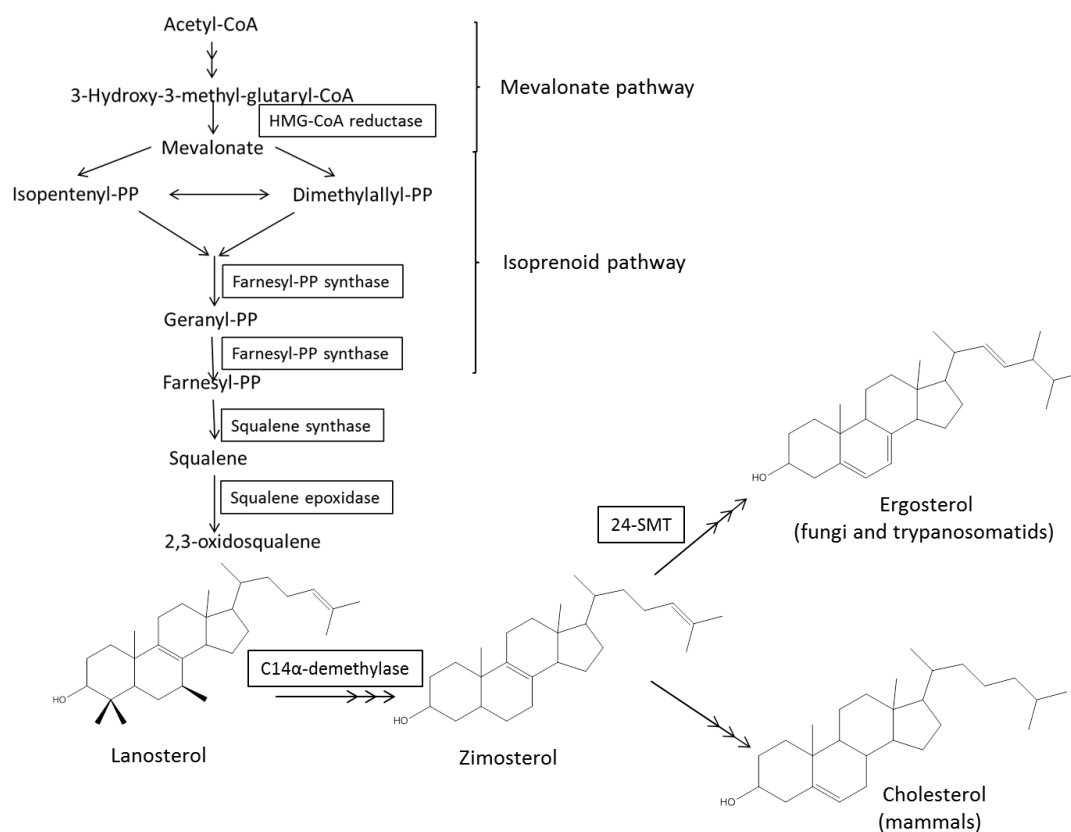


Figure 3-39: Sterol biosynthesis pathway. The enzyme involved in each step is boxed. The production of squalene is the first committed step in the biosynthesis of sterols. The methylation of the C-24 group by 24-sterol methyltransferase (24-SMT) is one of the most important steps in the biosynthesis of ergosterol. The 24-SMT is found in plants, fungi and trypanosomatids but not in mammals (de Souza and Rodrigues, 2009).

24-Sterol methyltransferase (24-SMT) is the enzyme required for the methylation of C-24 in the production of ergosterol. It is not present in animal cells; hence compounds that target this enzyme may have fewer adverse effects than drugs that target other enzymes in the pathway (de Souza and Rodrigues, 2009). The 3 β -hydroxy group is required for the inhibition of the 24-SMT of *Leishmania major* by azasterols (Lorente et al., 2004) as well as for the binding of sterols to plant yeast SMT (Song and Nes, 2007). Although the mechanism of action of the sponge sterols in this study is not known, it is possible that they act by inhibiting 24-SMT thereby disrupting the sterol biosynthetic pathway in *T. b. brucei*.

Aside from the 3 β -hydroxy group, other functional groups that contribute to anti-trypanosomal activity are hydroxylated side chains, such as the one proposed for B-4/R-13, and peroxide groups, such as on R-17. Saringosterol, which possesses a

hydroxylated side chain, had an IC₅₀ value of 7.8 μM against *T. brucei*. β-Sitosterol, stigmasterol and clerosterol, all with the same nucleus as saringosterol but without a hydroxyl group on their side chain, had IC₅₀ values of >240, 134.6, and 129.8 μM, respectively. The addition of a peroxide group to saringosterol, as in the case of 24-hydroperoxy-24-vinylcholesterol further improved the IC₅₀ to 3.2 μM (Hoet et al., 2007). The same compound was found to be toxic to KB tumour cells, however, so it is possible that sterols possessing this functional group are also more dangerous to mammalian cells than the sterols without peroxide functional groups (Ktari and Guyot, 1999). In this study, 24-viny-cholest-9-ene-3,24-dienol (B-4/R-11) was the most active against *T. b. brucei*, perhaps due to the hydroxylated side chain. The potency of the sterol peroxide may have been reduced by the shortened side chain. The latter also caused morphological changes in the normal fibroblast cells at concentrations of 100 μM, perhaps due to the presence of the peroxide group.

Recent research has shown that human steroids such as dehydroepiandrosterone and epiandrosterone may be used to treat trypanosomiasis by inhibiting the glucose-6-phosphate dehydrogenase (G6PD) enzyme in trypanosomes (Cordeiro et al., 2009, Gupta et al., 2011) which is the enzyme involved in the first committed step of the pentose-phosphate pathway. This prevents the formation of NADPH, increasing the susceptibility of the trypanosomes to oxidative stress (Gupta et al., 2011). Further research is now being conducted to find analogues of the human steroids that would selectively inhibit trypanosomal G6PD without causing adverse effects in humans. This is another potential mechanism of action of the three sterols isolated in this study.

The genus *Mycobacterium* has also been reported to possess a sterol biosynthetic pathway that is homologous to the pathway of *S. cerevisiae* (Lamb et al., 1998). One of the genes discovered in *Mycobacterium* encoded for a sterol 14α-demethylase (MT 14-DM) (Bellamine et al., 1999). The functional groups that are required for substrates to bind to MT 14-DM in *M. tuberculosis* have already been determined (Bellamine et al., 2001). The 3β-hydroxy functional group is necessary for binding, as well as a 14α-methyl group. The absence of the 4β-methyl group favoured the binding of the sterols to the enzyme, as did the presence of the double bond on C-8

rather than C-5, C-7 or C-9. Although the three sterols isolated in this project all contain the 3 β -hydroxy moiety, none possess the 14 α -methyl group required to bind to this enzyme. It is possible that they act upon another enzyme in the pathway or by a different mechanism altogether. The sterol pathway in *Mycobacterium* has not been fully elucidated, and although the role of sterol metabolism in the pathogenesis of *Mycobacterium* has been postulated (Gamielien et al., 2002), the function of sterols in cell growth and viability is unknown. Nevertheless, it has already been proven that some sterols, such as cholesterol, ergosterol and ergosterol peroxide (Rugutt and Rugutt, 2002) and the 5(6 \rightarrow 7) abeosterols (Wei et al., 2008) possess strong anti-mycobacterial activity.

The three sterols isolated from *H. simulans* all possessed activity against *T. b. brucei* and *M. marinum*. Sponges are well-known for possessing a diverse range of steroids that have both conventional and unconventional side chains and nuclei. This is confirmed by the diversity of nuclei and side chains isolated from *H. simulans* in this study. Steroids are essential in regulating membrane fluidity of eukaryotic cells. Indeed, in sponges, even unconventional steroids are found in the cellular membranes (Lawson et al., 1988). However, the bioactive sterols isolated from *H. simulans* in this study may be products of the sponge-associated microorganisms, rather than the host sponge itself, as at this point their true source cannot be confirmed. They may nonetheless serve as useful lead compounds in the search for new drugs and they add weight to the theory that there remain to be discovered a large number of novel compounds from marine sponges.

**Chapter 4 Metabolomic Profiling of *Streptomyces* sp. SM8
Isolated from *H. simulans***

4. Metabolomic Profiling of *Streptomyces* sp. SM8 Isolated from *H. simulans*

4.1 Introduction

As mentioned in Chapter 1, sponges play host to a wide variety of marine bacteria. The bacterial communities of *Haliclona* sponges from across the globe have been studied (Kennedy et al., 2009, Khan et al., 2010, Khan et al., 2011, Jiang et al., 2007) and these show a diverse range of endosymbionts, many of which produce bioactive metabolites. Of the 52 bacteria isolated from *H. simulans* from the Irish Sea, 29 possessed antibiotic activity against at least one of the bacterial or fungal test strains (Kennedy et al., 2009).

In two studies of *Haliclona* sp., one from the South China Sea (Jiang et al., 2007) and the other from Japanese Coastal waters (Khan et al., 2011), *Streptomyces* sp. were the dominant cultivable bacterial genus. Moreover, there was a definite overlap in the bacterial species identified in both sponges. In another species, *H. gellidus* from Monterey Bay, California, the most abundant bacterial phyla were the γ - and the β -*Proteobacteria* whereas *Actinobacteria* was only found in low quantities in one sponge sample. An extract of *H. gellidus* showed no cytotoxicity activity and only weak antibacterial activity, corroborating the absence of the *Actinobacteria*, which are known for producing bioactive metabolites. It was postulated that because *H. gellidus* grows under rocks, it has less need for chemical defence compared to other *Haliclona* sp. that grow in more open waters (Sipkema et al., 2009).

A *Streptomyces* sp., SM8, was isolated from *H. simulans* collected from the Irish Sea. Partial 16S rRNA sequencing indicated that this strain bore 100% similarity to *Streptomyces violascens* XSD-115 (Kennedy et al., 2009). SM8 produced white spores, whereas another strain, *S. violascens* NBRC 12920^T/AB184246 was described as having violet and spiny spores, with the spores being produced in spiral chains (Labeda et al., 2012). Other strains of *S. violascens* have been reported to produce antibiotics such as actinomycin D and actinomycin X₂ (V) (El-Tarabily et al., 1996), protease inhibitors such as trypsin and chymotrypsin inhibitors (Jonsson and Torstensson, 1972), and 3 β -hydroxysteroid oxidase (Tomioka et al., 1976). It has been questioned whether or not it is possible to find new metabolites from

Streptomyces sp., as this genus is one of the most widely studied. Recently, several new species of *Streptomyces* have been isolated from a *Haliclona* sp. sponge from Japan. Seven novel compounds from three novel strains of *Streptomyces* sp. were isolated (Khan et al., 2011, Motohashi et al., 2010a, Motohashi et al., 2010b, Kozone et al., 2011), proving that marine *Streptomyces* sp. are still valuable sources of potential novel natural products.

This chapter describes the dereplication of SM8 and the isolation of compounds from the bacterial extract. In addition, the metabolome of SM8 is compared with that of its host sponge, *H. simulans*.

4.2 Methodology

4.2.1 Acquisition of the Sample

Extracts from the *Streptomyces* sp. SM8 isolated from *H. simulans*, were obtained from the Environmental Research Institute (ERI), University College Cork (UCC). The initial samples consisted of nine small-scale and seven up-scale extracts. The small-scale samples were grown in 50-400 mL of broth whereas the up-scaled ones were grown in 16-20 L. Additional extracts were subsequently received for isolation work.

4.2.2 Dereplication of Small-scale and Up-scale Samples

The samples were dissolved in deuterated DMSO and subjected to ¹H NMR analysis. They were subsequently lyophilized and redissolved in 50:50 methanol (HPLC):pure water to give a final concentration of 1 mg/mL. These samples were then analysed on the Exactive-Orbitrap using the same method as described in **2.4.1**. The data mining parameters used were the same as in **2.4.2**; however, the noise level for the centroid mass detector and the minimum height for the chromatogram builder were set at 1.0E5, while the minimum absolute height for chromatogram deconvolution was at 3.0E5. The databases used were AntiMarin 2012 and DNP 2012, although the latter database was filtered to only include natural products from *Streptomyces* sp. This was to give an indication of the compounds that were potentially produced by SM8.

Multivariate analysis was performed on the data using SIMCA 13. All variables were scaled using pareto scaling.

4.2.3 Medium-Pressure Liquid Chromatography of Pooled SM8 Samples

The up-scaled SM8 samples were pooled together to give a combined weight of 343.7 mg. The pooled samples were then fractionated using the following MPLC method:

Column: VersaPak C-18 (Spherical) 23 x 53 mm (15g)

Mobile Phase: Pure-grade water (A), methanol (HPLC-grade) (B)

Gradient: 0-5 min	1% B
5-35 min	1-50% B
35-40 min	50% B
40-65 min	50-100% B

The flow rate used was 10 mL/min. The fractions were collected every 15 seconds in a test tube. A total of 264 fractions were collected. The column was then washed three times with 100% methanol, each wash performed for five minutes and collected in a conical flask.

4.2.4 Pooling of Fractions for Antimicrobial Assays

Four fractions representing a minute were pooled for the antimicrobial assays by taking a 400 μ L aliquot from each of the four test tubes. The 66 pooled fractions were then dried and weighed, after which they were sent to the ERI, UCC for the *Bacillus subtilis* and *Candida albicans* assays.

4.2.5 Preparation of Fractions for Low Resolution LC-MS

A 600 µL aliquot from every even-numbered test tube was collected and subjected to LCQ-Deca analysis (2.4.1). The fractions were then pooled based on the similarities of their chromatograms.

4.2.6 Analysis of the SM8 Fractions with MZmine 2.10 and Comparison with the DNP

The active fractions of the SM8 extract were subjected to high resolution LC-MS with the Exactive-Orbitrap. The MZmine 2.10 parameters were the same as section 4.2.2. The peaks were compared to the DNP database with the biological source limited to *Streptomyces* sp.

4.2.7 Identification of Antimycins in SM8 Extracts

A gene knockout study was performed on SM8 by ERI at UCC. The *antC* gene was deleted, resulting in the formation of $\Delta antC$ mutants. The extracts of the wild-type and mutant SM8 were then received for high resolution LC-MS and these were compared to an Antimycin A standard (Antimycin A, from *Streptomyces* sp.) purchased from Sigma-Aldrich Co. MO, USA using the LTQ-Orbitrap.

4.2.8 Isolation of Compounds from SM8 Extract

A larger quantity of SM8 extract (SM8-1 and SM8-4), weighing 810.3 mg, was obtained from ERI, UCC, Ireland. It was initially analysed using NMR to ensure that it was identical to the previous extract. The extract was then fractionated using Sephadex[®] LH20 with methanol as the mobile phase at a flow rate of approximately 1 mL/15 minutes (0.067 mL/min) and a collection volume of 1 mL/test tube. An aliquot of each tube was sent to ERI for activity assays. The active fractions were subsequently pooled based on their activity and similarities in the TLC. The pooled fraction 110-126, which predominantly exhibited antibacterial and some antifungal and anti-calcineurin activity, was further chromatographed with a BÜCHI MPLC using a C-18 column (VersaPak C-18 (spherical) 23x53mm (15g)) and a flow rate of

15 mL/min. The sample was eluted with 60:40 H₂O:MeOH for an hour followed by 50:50 H₂O:MeOH. The column was washed with 100% MeOH. The fractions were again pooled by TLC and sent to ERI for bioassay. The active fractions were reconstituted in deuterated DMSO or CDCl₃ and structures of the compounds were elucidated.

Fraction 127-156, also obtained from the Sephadex[®] separation, displayed antifungal activity. This fraction was subjected to purification on a conventional silica column with the following solvent systems: 95:5 hexane:ethyl acetate, 90:10 hexane:ethyl acetate, 80:20 hexane:ethyl acetate, and 50:50 hexane:ethyl acetate, followed by washing of the column with 70:30 dichloromethane:methanol, 50:50 acetone:methanol and 100% methanol. The collected fractions were pooled following TLC and aliquots sent to ERI for activity testing.

Fraction 127-156U1 was further fractionated using the Biotage[®] Isolera[™] Spektra One Flash Purification System (ISO-1SV). The method is outlined below.

Column: 25g SNAP cartridge (silica) 30x72 mm

Mobile phase: Hexane (A), ethyl acetate (B)

Flow rate: 25 mL/min

Gradient:	0-55 min	25% B
	55-70 min	25-50% B
	70-80 min	50% B
	80-95 min	50-90% B
	95-100 min	90-100% B

Detection mode: UV1 (235nm); UV2 (365nm)

Start threshold: 20mAU

4.2.9 Quorum Signalling Assay Using TLC Overlay Technique

The method used was adapted from the method developed by McClean and colleagues (McClean et al., 1997). 6.3 mg of SM8_110-126D and 6.8 mg of SM8_127-156S1 were each dissolved in 300 μ L of acetonitrile. Ten microlitres of each fraction was spotted three times on the same spot of a C18 TLC plate in order to increase the concentration of butenolides on that spot. Two stimulatory control mixtures were prepared. These were the ‘H-standard’, which consisted of homoserine lactones with a single ketone functional group in their side chain, and the ‘O-standard’, in which the homoserine lactones had two ketone groups in their side chain. They were spotted so that the H-standard consisted of 2.52 mmol BHL (butyryl homoserine lactone), 0.25 μ mol HHL (hexanoyl homoserine lactone), 1.00 mmol OHL (octanoyl homoserine lactone) and the O-standard consisted of 1.00 μ mol OHHL (oxo-hexanoyl homoserine lactone) and 5.00 μ mol OOHL (oxo-octanoyl homoserine lactone). The plate was eluted in 60:40 MeOH:H₂O and allowed to dry. Once dry, luria agar seeded with *Chromobacterium violaceum* CV026 was poured over the TLC plate. The plate was left at room temperature and examined the next day for the development of purple spots indicating the presence of compounds able to stimulate the production of violacein.

4.2.10 Comparison of *H. simulans* Extracts and SM8 Extracts

The extract of the host sponge, *H. simulans* and the endosymbiont, SM8, were compared using LC-HRFTMS. The aliquots taken for LC-MS from each *H. simulans* fraction after HP-20 chromatography were pooled (100 μ L from each aliquot), dried and re-suspended in 10:90 H₂O:MeOH to a final concentration of 1 mg/mL. This was performed for the two *H. simulans* samples extracted in **Chapter 3**, HSA and HSB. However, the 100% water aliquot from the sponge extracts was not included because of high salt concentration. The 90:10 H₂O:MeOH aliquot for HSA was also not included as there appeared to be some contamination of the sample. The pooled extracts were then analysed with the Exactive-Orbitrap using the same method as **2.4.1**.

The results were compared with those of the SM8-1 and -4 extracts using MZmine 2.10 and SIMCA 13. The MZmine 2.10 parameters used were similar to those used in 2.4.2. Once the samples had been processed with MZmine 2.10 the data was exported to MS-Excel where the positive and negative peak lists were combined and the data further analysed using SIMCA 13. Pareto scaling was applied on all variables.

GC-MS was another technique used to compare the SM8 and *H. simulans* extracts. The ethyl acetate-soluble portions of the extracts of HSA and of SM8 grown on oatmeal media were analysed on the Focus GC-DSQ II from Thermo Scientific using the method outlined in 2.4.3. The peaks were putatively identified using the NIST 2011 and MAINLIB libraries.

4.3 Results

4.3.1 Dereplication of Small-Scale and Up-scale SM8 Extracts

The small-scale and up-scaled extracts of SM8 were compared using NMR and high resolution LC-MS. The results are shown in Figure 4-1 and Figure 4-2 below:

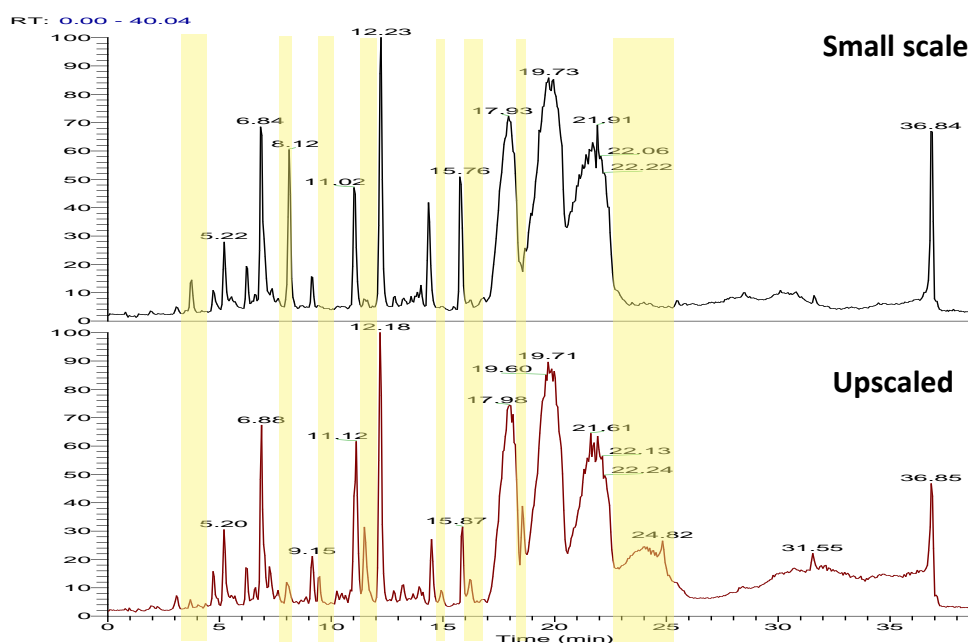


Figure 4-1: Comparison of the chromatograms of the small-scale and up-scale extracts of SM8. The differences between the two chromatograms are highlighted. The first two highlighted peaks, which were relatively polar, were present in the small scale but not the up-scaled samples, whereas the remaining peaks were found solely in the up-scaled samples.

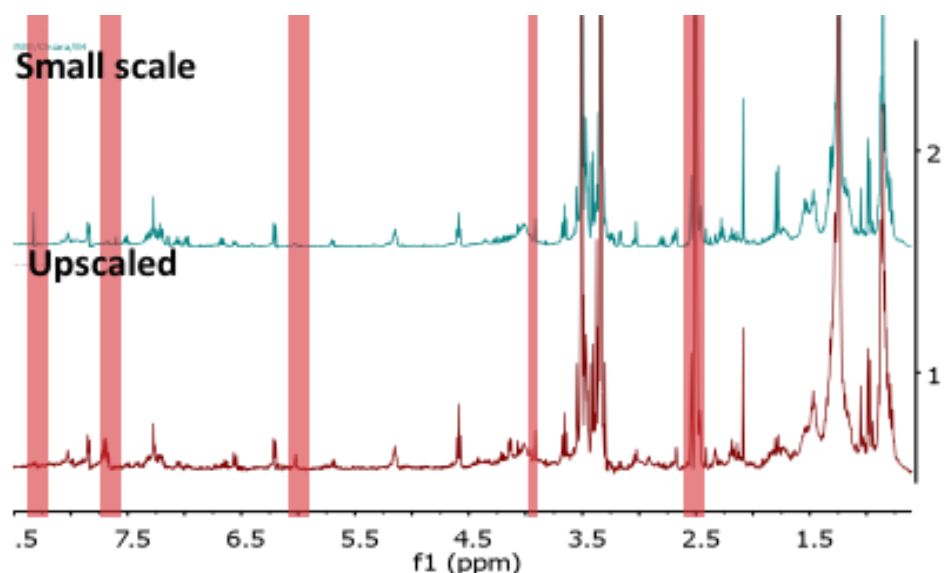


Figure 4-2: Comparison of ^1H NMR spectra of extracts from small-scale and up-scale SM8 cultures (400 MHz, DMSO). The differences between the two spectra are highlighted. There were fewer differences that were seen compared to the LC-MS data, as NMR is less sensitive than LC-MS. The major compounds produced by the two cultures were therefore similar.

As evidenced in Figure 4-1 and Figure 4-2, there were slight differences between the small-scale and up-scaled extracts. Analysis of the LC-HRFTMS data with MZmine 2.10 and the AntiMarin database (November 2012) showed that there were more compounds being produced in the up-scaled culture. While there were many compounds that were produced in both the small-scale and up-scale cultures (Table 4-1), it was also evident that there were more compounds being produced solely in the samples obtained from the up-scaled culture. Both the extracts from small-scale and the up-scaled cultures possessed antimicrobial activity. However, the newly detected compounds that were produced solely in the up-scale cultures do not necessarily correlate with bioactivity. The analysis of the LC-HRFTMS data was repeated using the DNP 2012 database while limiting the search with *Streptomyces* sp. as the biological source. The results are in Table 4-2. The putative identification of metabolites giving the largest peak area is shown in Table 4-3.

Table 4-1: Summary of the total number of peaks and compounds identified using AntiMarin from the small-scale and up-scaled SM8 cultures

Criteria	Pos		Neg	
	Total	Identified	Total	Identified
All samples considered	1044	301	88	47
Present in all small-scale samples	806	254	85	44
Present in all up-scale samples	1004	292	88	47
Present in all small- and all up-scale samples	789	248	85	44
Present in all small-scale but not in any up-scale samples	6	1	0	0
Present in all up-scale but not in any small-scale samples	77	20	0	0

Table 4-2: Summary of the total number of peaks and compounds identified from the small-scale and up-scaled cultures of SM8 using the DNP with the biological source limited to *Streptomyces* sp.

Criteria	Pos		Neg	
	Total	Identified	Total	Identified
All samples considered	1044	122	88	23
Present in all small-scale samples	806	104	85	21
Present in all up-scale samples	1004	118	88	23
Present in all small- and all up-scale samples	789	101	85	21
Present in all small-scale but not in any up-scale samples	6	1	0	0
Present in all up-scale but not in any small-scale samples	77	8	0	0

Table 4-3: Major peaks from the small-scale and up-scaled cultures of SM8 which were identified from DNP 2012 with the biological source limited to *Streptomyces* sp.

Sample		<i>m/z</i>	RT	Name	Formula	Reference
Only in small-scale	[M+H] ⁺	577.3717	21.35	[1] PD118576	C ₃₃ H ₅₂ O ₈	(Wilton et al., 1985)
Only in up-scale	[M+H] ⁺	723.4663	23.64	[2] Dianemycin	C ₄₇ H ₇₈ O ₁₄	(Hamill et al., 1969)
Both	[M+H] ⁺	228.2685	15.83	[3] Medelamine B	C ₁₅ H ₃₃ N	(Morino et al., 1995)
	[M+H] ⁺	460.2697	11.14	[4] Isomigrastatin	C ₂₇ H ₃₉ NO ₇	(Woo et al., 2002)
	[M-H] ⁻	458.2565				
	[M-H] ⁻	533.2522	19.16	[5] Antimycin A2a	C ₂₇ H ₃₈ N ₂ O ₉	(Liu and Strong, 1959)

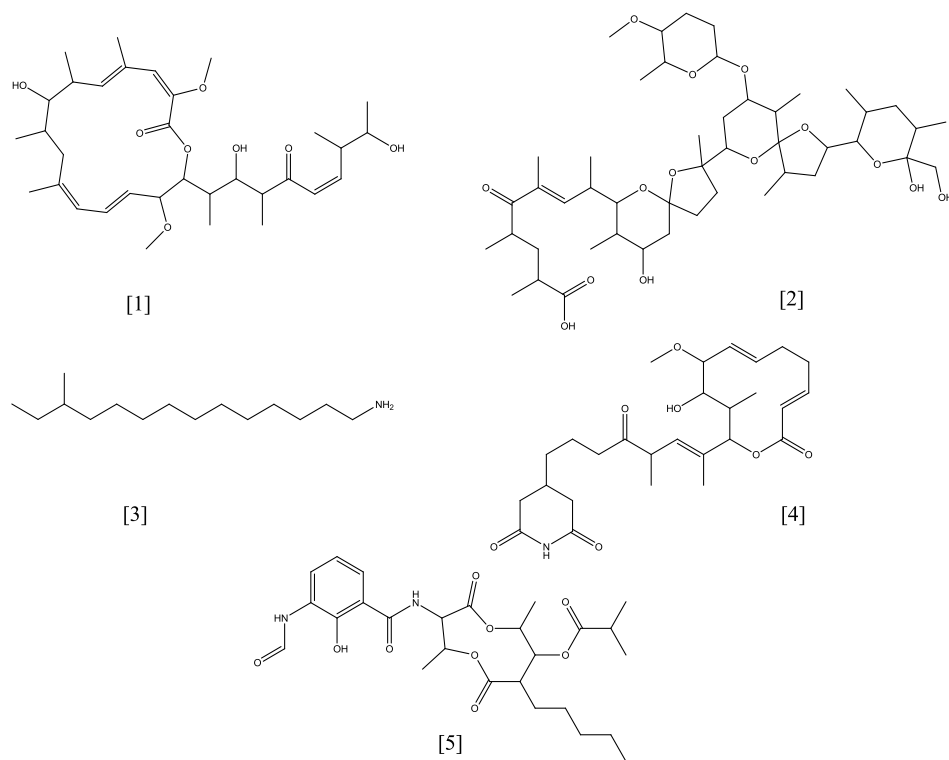


Figure 4-3: Structures of compounds with greatest peak areas identified from SM8 small scale and up-scale extracts.

Table 4-3 above showed examples of compounds previously isolated from *Streptomyces* sp. that have been identified in the extracts of SM8. No compounds that ionise in the negative mode were found solely in the small-scale or solely in the up-scale cultures. Antibiotic PD 118576 (**1**) is known to have antibacterial, antifungal and anti-tumour activity (Hatfield et al., 1992). Dianemycin (**2**) possessed antibacterial, antifungal and anti-inflammatory activity (Hamill et al., 1969, Lee et al., 1997). Medelamine B (**3**) and isomigrastatin (**4**) were described as anti-cancer compounds (Ju et al., 2009). The antimycin group of compounds (**5**) are well-known antifungal metabolites produced by *Streptomyces* sp. The presence of these antimycin compounds that were identified using high resolution LC-MS was confirmed by comparison with a standard. Applying these techniques allows insight into the types of compounds being produced by the strain.

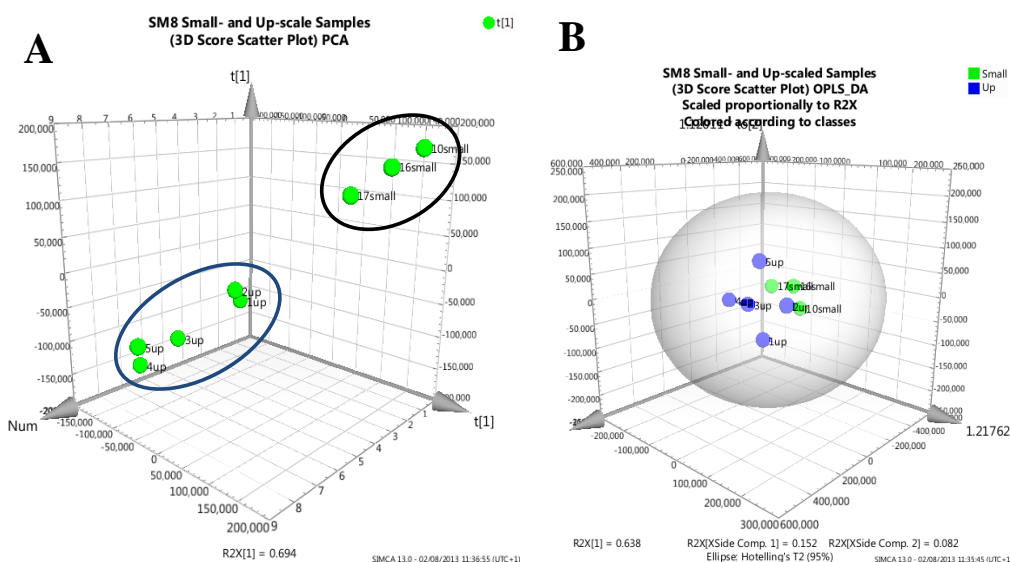


Figure 4-4: Score scatter plot of small scale vs up-scale SM8 extracts using (A) PCA and (B) OPLS-DA. The PCA score plot showed separation of the small scale from the up-scaled samples; however, all of the samples clustered together in the OPLS-DA plot, indicating that there were only minor differences between the two cultures.

In Figure 4-4, it can be seen that, using Principal Component Analysis (PCA), a type of unsupervised multivariate analysis, the small-scale samples and the up-scale samples formed separate clusters, indicating that there were differences in the metabolites produced between the two groups. Using the supervised method of multivariate analysis, the orthogonal partial least squares – discriminant analysis (OPLS-DA), the small-scale and up-scale samples clustered together indicating only minor differences between the two types of cultures. Nonetheless, only the up-scaled extracts were pooled for further work, giving a total amount of 343.7 mg.

4.3.2 Medium Pressure Liquid Chromatography of Up-scale SM8 Extracts

After normal phase MPLC, 264 fractions were collected, in addition to three washings of the column. The fractions were pooled using two different methods: by retention time and by the similarities of their mass spectra. The samples that were pooled by retention time (per minute) were sent to UCC for antimicrobial assays. The MICs of the fractions showing activity and the corresponding fractions after pooling based on the mass spectra are shown in Table 4-4.

Table 4-4: Active fractions from the SM8 extract

Minute	Yield (mg)	Activity	MIC ($\mu\text{g/mL}$)	Pooled fraction
55	6.5	<i>B. subtilis</i>	7.42	221-226
56	4.4 5.1	<i>B. subtilis</i>	9.4	227-228 229-230
59	9.1	<i>C. albicans</i>	80	239-242
60	13.0	<i>C. albicans</i>	90	243-248

The active fractions were subjected to NMR and LC-HRFTMS. The spectra are shown in Figure 4-6 and Figure 4-7. The most prominent known compound putatively identified from each fraction is stated in Table 4-5 and the structures are in Figure 4-5. In some cases, isomers were identified, such as kitamycin A (**6**) and B (**7**), antimycins A3 (**8**) and A7 (**9**), and antimycin A2, A8, A11, and A17 (**10**, **11**, **12**, **13** respectively).

Table 4-5: Compounds with the largest peak area that were identified from the active SM8 fractions using the DNP 2012 database with the biological source limited to *Streptomyces* sp.

Fraction		<i>m/z</i>	RT	Name	Formula	Reference
221-226	[M+H] ⁺	465.2235	19.53	[6] Kitamycin A or [7] B	C ₂₃ H ₃₂ N ₂ O ₈	(Hayashi and Nozaki, 1999)
	[M-H] ⁻	519.2353	19.43	[8] Antimycin A3 or [9] A7	C ₂₆ H ₃₆ N ₂ O ₉	(Liu and Strong, 1959)
227-228, 229-230	[M+H] ⁺	535.2652	20.70	[10] Antimycin A2, [11] A8, [12] A11 or [13] A17	C ₂₇ H ₃₈ N ₂ O ₉	(Liu and Strong, 1959, Hosotani et al., 2005)
	[M-H] ⁻	533.2512	20.67			
239-242	[M+H] ⁺	521.2493	24.34	[8] Antimycin A3 or [9] A7	C ₂₆ H ₃₆ N ₂ O ₉	(Liu and Strong, 1959)
	[M-H] ⁻	519.2352	24.25			
243-248	[M+H] ⁺	535.2650	25.63	[10] Antimycin A2, [11] A8, [12] A11 or [13] A17	C ₂₇ H ₃₈ N ₂ O ₉	(Liu and Strong, 1959, Hosotani et al., 2005)
	[M-H] ⁻	519.2352	24.25			

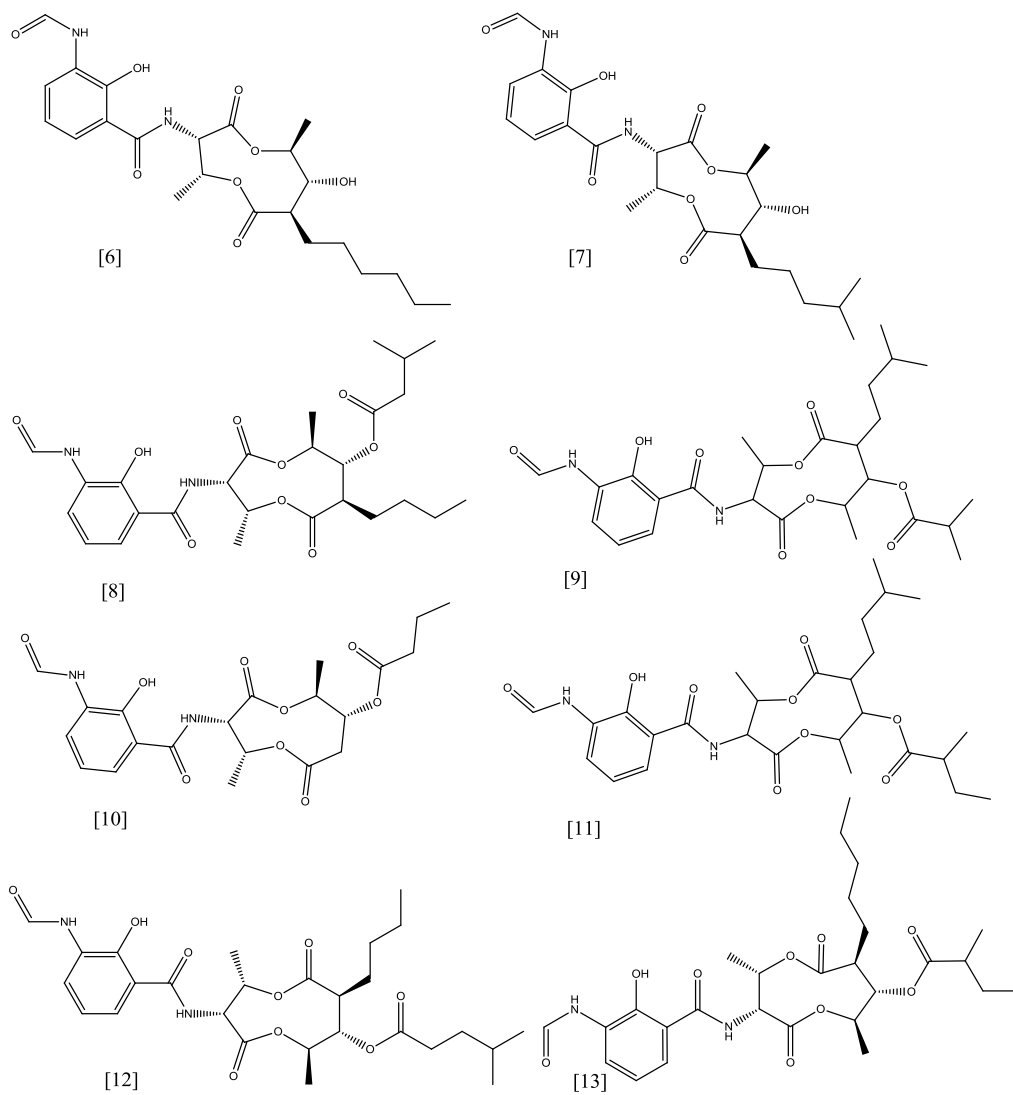


Figure 4-5: Structures of compounds identified from active SM8 fractions. All of the identified compounds belonged to the antimycin class of compounds.

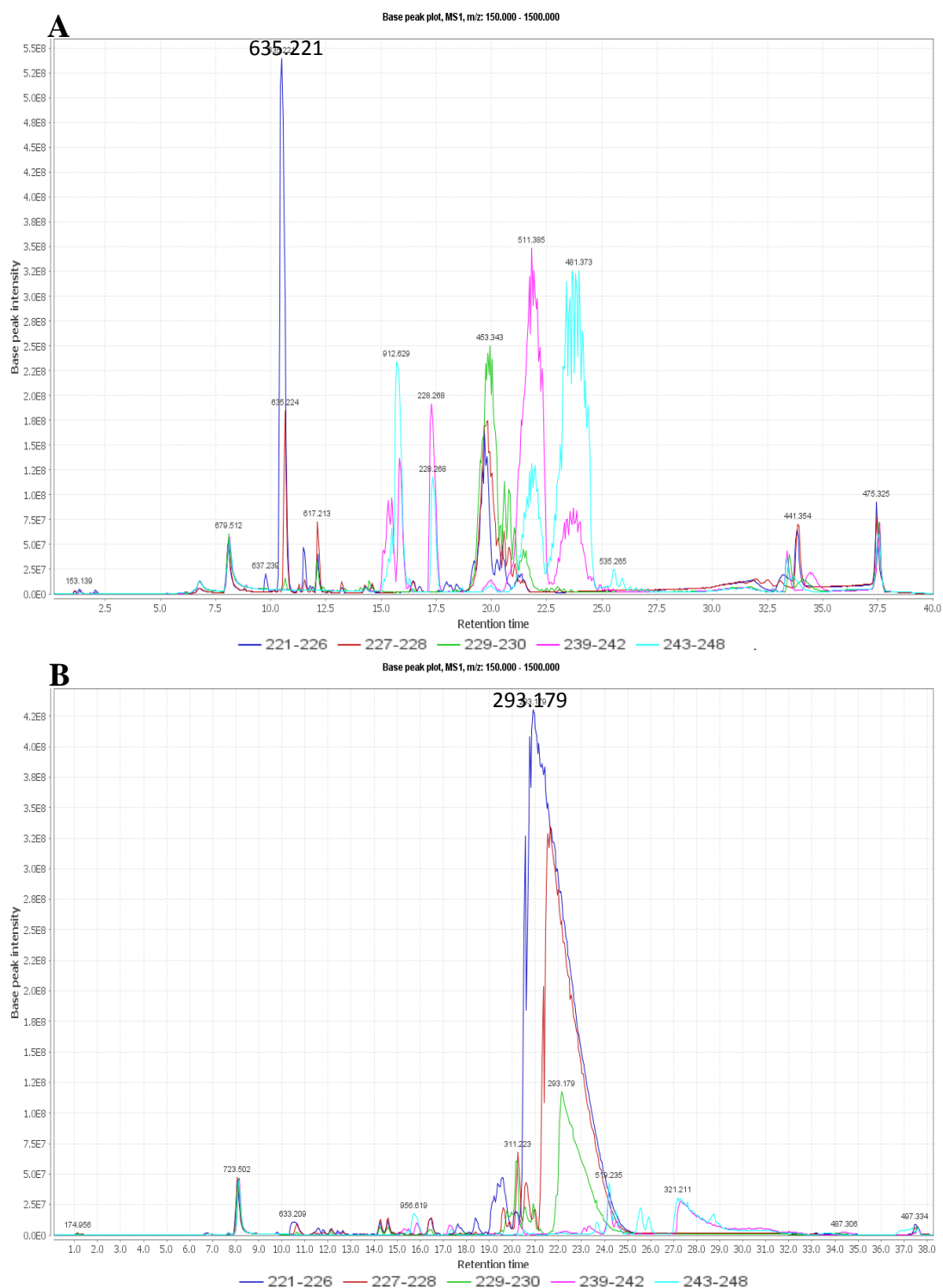


Figure 4-6: Total ion chromatograms of the most active fractions of SM8 showing both (A) positive ionisation and (B) negative ionisation. The chromatograms are coloured as follows: 221-226 (dark blue), 227-228 (red), 239-242 (pink), 243-248 (light blue). The two most intense peaks in each chromatogram are labelled: 635.221 $[M+H]^+$ and 293.179 $[M-H]^-$ for the positive and negative ionisation modes, respectively. Both were not identified in the database.

The most intense peaks in both spectra ($635.221 [M+H]^+$ and $293.179 [M-H]^-$) were both not identified by the database. The AntiMarin 2012 database was also searched for these compounds but no hits were found.

Presaturation was performed to suppress the water peak in the ^1H NMR spectra of the active antibacterial and antifungal fractions (Figure 4-7). The peaks in the aliphatic region indicated that the major compounds in these fractions were fatty acids. Some fatty acids have been known to have antibacterial activity; it is thought that they affect cell membrane permeability and cell metabolism (Kabara et al., 1972). Smaller peaks in the downfield regions, particularly the aromatic peaks at δ_{H} 7.5-8.5, are visible in Figure 4-7. These indicated the presence of compounds other than fatty acids. However, due to the small quantities of the fractions no further purification work could be performed until larger quantities of SM8 extract were procured.

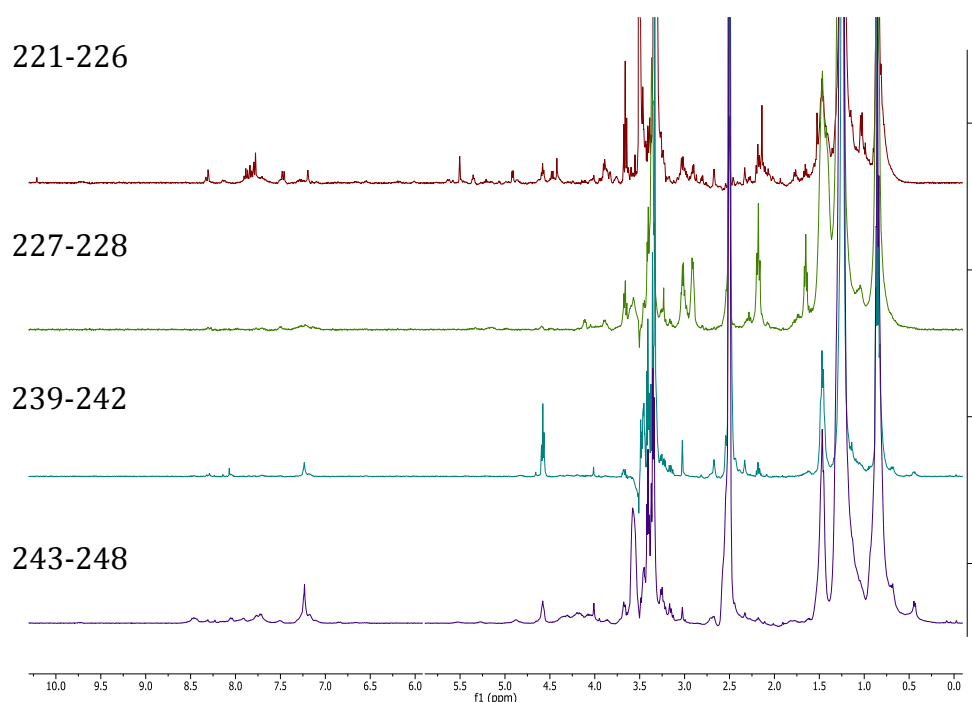


Figure 4-7: ^1H spectra of active SM8 fractions after presaturation (400 MHz, DMSO). The major components of the fractions were fatty acids; however, peaks in the aromatic region indicated the presence of other compounds within the fractions.

The high resolution LC-MS spectra of fractions 221-226 and 227-230 indicated the presence of two inseparable components having m/z 375.2757 and 417.3228 $[M-H]^-$ in the negative mode and m/z 377.2898 and 419.3668 $[M+H]^+$ in the positive mode with molecular formulas of $C_{20}H_{40}O_6$ and $C_{23}H_{46}O_6$, respectively (Figure 4-9). Both ion peaks had ring double bond equivalents (RDBE) of 1.0, which signified the aliphatic and polyhydroxylated nature of the compounds. Further analysis of the 1H NMR spectra of the fractions confirmed that the major components were polyhydroxylated saturated fatty acids. The peaks corresponded to the terminal methyl groups (δ_H 0.80 to 1.00), aliphatic CH_2 groups (δ_H 1.24 to 1.30), hydroxyl-bound CH (δ_H 3.00-4.50), and the CH_2 group attached to the acid terminus (δ_H 2.19-2.80). The oxymethine protons also corresponded to peaks at 60-70 ppm in the ^{13}C NMR spectrum. The positions of the hydroxyl groups were determined using MS^n fragmentation in the positive mode (Figure 4-10). This was further validated by the COSY data. The two polyhydroxylated saturated fatty acids were therefore elucidated as 3,6,8,11-tetrahydroxy-16,17-dimethyloctadecanoic acid and 2,8,10,10-tetrahydroxy-18-methyldocosanoic acid (Figure 4-8).

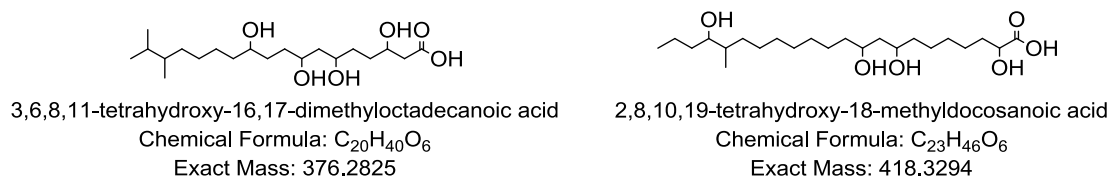


Figure 4-8: Proposed structures of polyhydroxylated fatty acids found in fractions 221-230.

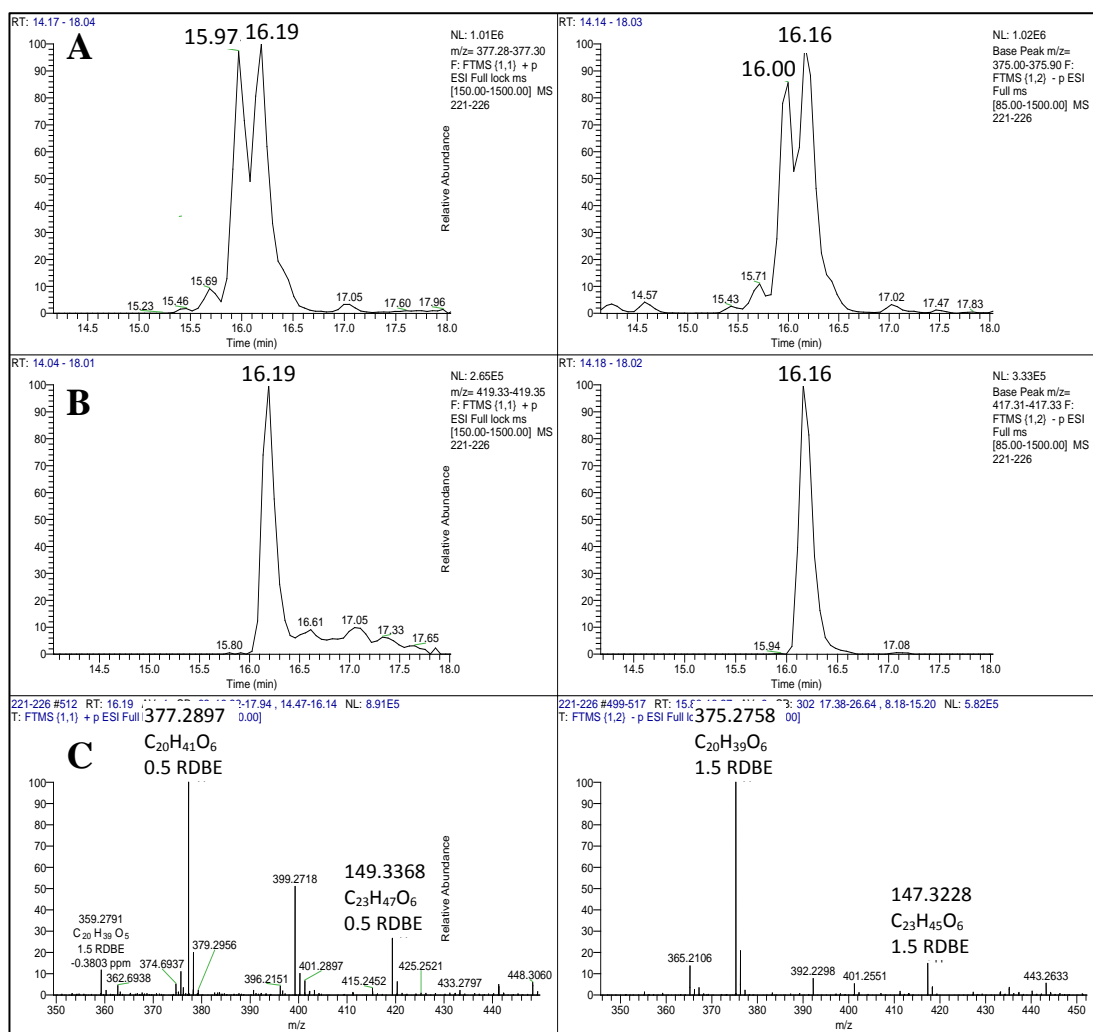
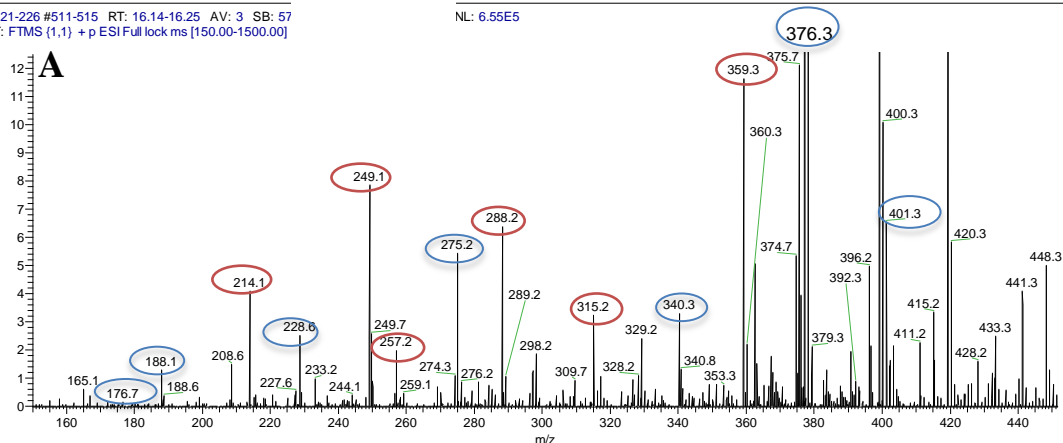


Figure 4-9: Extracted ion chromatograms and mass spectra of fractions 221-230. The positive ionisation mode is on the left side of the graph whereas the negative ionisation mode is depicted on the right. Extracted ion chromatogram for (A) m/z 377.2897 $[M+H]^+$ and 375.2758 $[M-H]^-$, and (B) m/z 419.3368 $[M+H]^+$ and 417.3228 $[M-H]^-$, respectively. (C) Mass spectra.



B

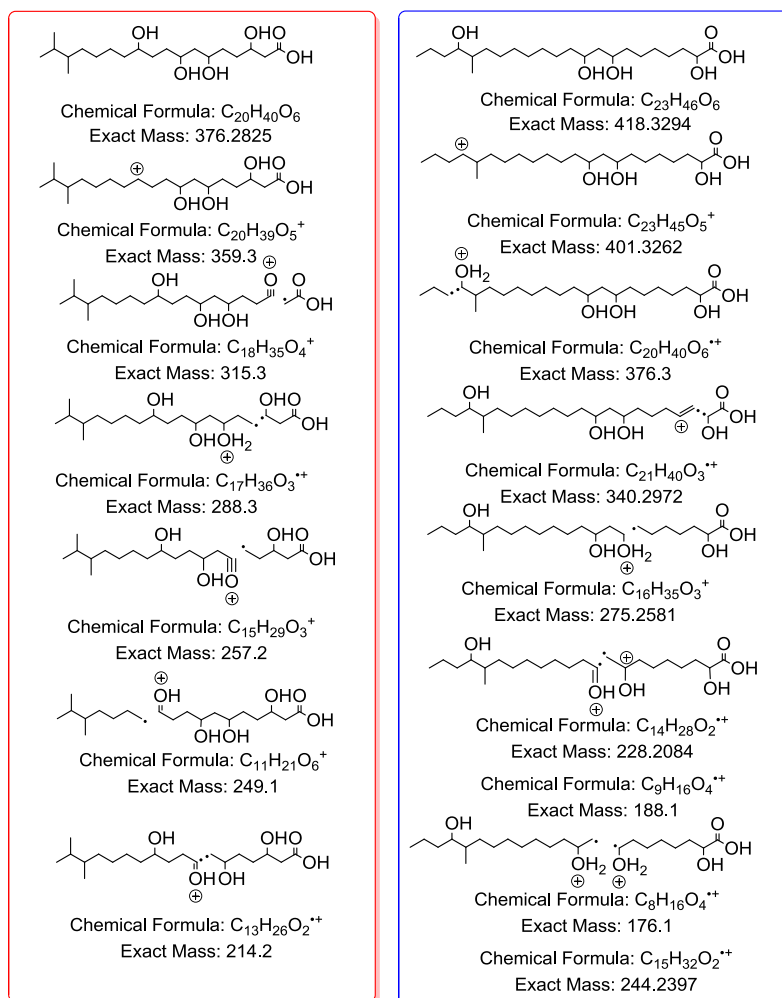


Figure 4-10: Fragmentation of polyhydroxylated saturated fatty acids. (A) Source fragmentation of fraction 221-226 in the positive ionisation mode showing the MS^n ion peaks for m/z 377.2898 (red) and 419.3668 (blue). (B) Proposed fragmentation for 3,6,8,11-tetrahydroxy-16,17-dimethyloctadecanoic acid (red) and 2,8,10,19-tetrahydroxy-18-methyldocosanoic acid (blue).

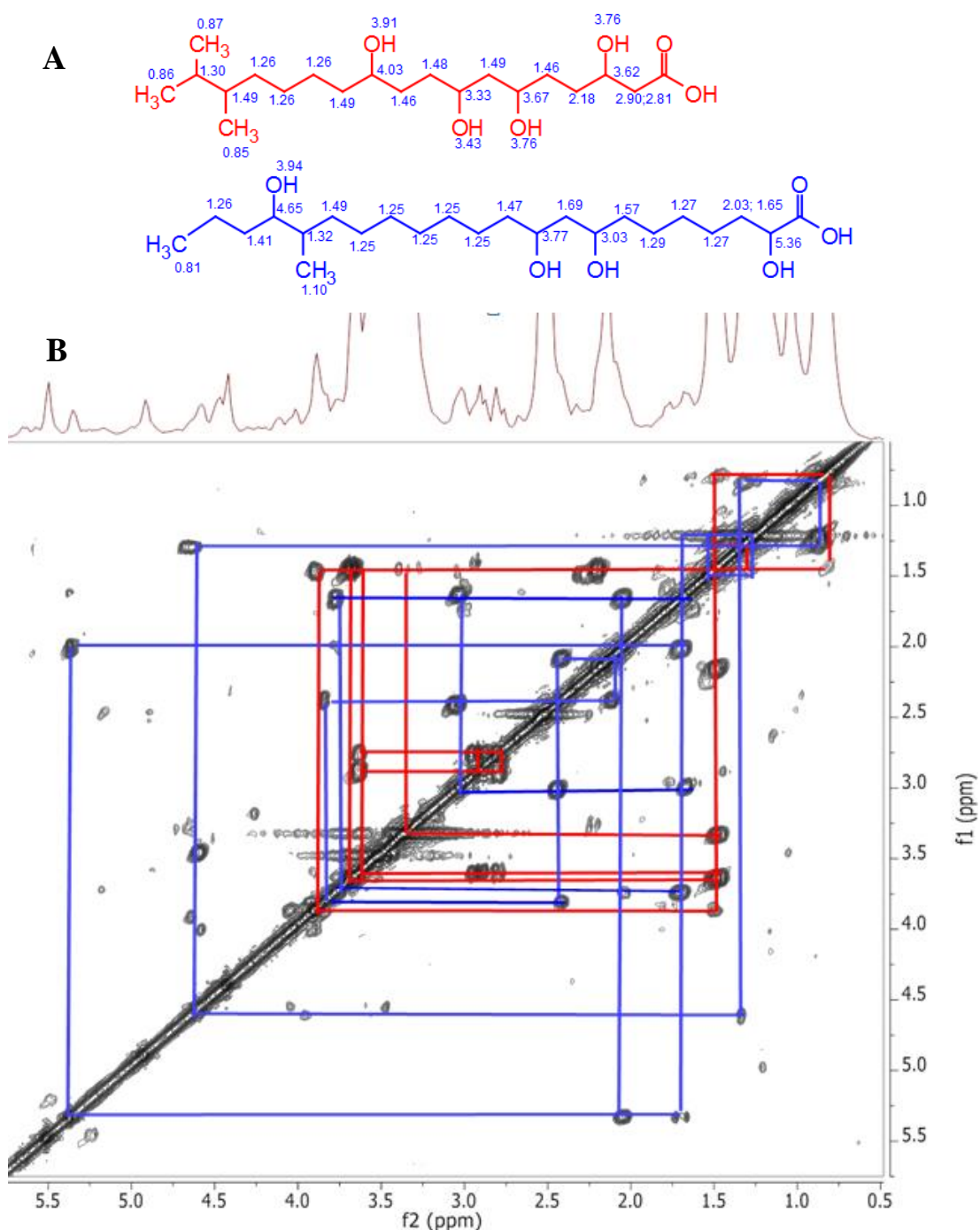


Figure 4-11: ^1H - ^1H COSY spectrum of fractions 221-226 and 227-230. (A) Proposed structures of the polyhydroxylated saturated fatty acids showing the predicted chemical shifts. (B) COSY spectrum showing the correlations that correspond to each fatty acid.

These fatty acids were similar to tetrahydroxy saturated fatty acids previously isolated from fungi (Girisham et al., 1986, Turner and Aldridge, 1983). They have also been found as degradation products of guanidylfungin A and B (Takesako and Beppu, 1984a, Takesako and Beppu, 1984b), which are similar in structure to

nystatin, a polyene antibiotic. The biosynthetic pathway of nystatin has been established, and it is thus known that the proteins NysA, NysB, NysC, NysI and NysJ are involved in the elongation of the polyketide chain (Brautaset et al., 2000). A BLAST search was performed to detect the presence of the conserved domains of these proteins within the SM8 sequence. The homology results are shown in Table 4-6 below. The alignments can be seen in Appendix V.

Table 4-6: Homology results of nystatin biosynthetic clusters in the SM8 genome

Protein	Accession number	Function	SM8 protein accession number	Identity	E-value
NysA	AAF71774	PKS (Loading molecule)	WP_008414592.1	57%	0.0
NysB	AAF71775	PKS (elongation)	WP_008409601.1	53%	0.0
NysC	AAF71776	PKS (elongation)	WP_008414556.1	61%	0.0
NysI	AAF71766	PKS (elongation)	WP_008409601.1	65%	0.0
NysJ	AAF71767	PKS (elongation)	WP_008413985.1	59%	0.0

The conserved domains in the nystatin proteins included polyketide synthases (PKS), acetyltransferase domains in the PKS, PKS dehydratase, ketoreductases (KR), Rossmann-fold NAD(P) (+) binding proteins, enoylreductase domains of PKS, and phosphopantetheine attachment sites. As the SM8 sequences are similar to the conserved domains of the nystatin biosynthetic proteins, it is possible that the proteins of SM8 produce compounds similar to nystatin. The fatty acids that were isolated from the SM8 cultures could either be precursors to or degradation products of polyene antibiotics. Nystatin was not detected in any of the SM8 cultures.

Figure 4-12 shows the extracted ion chromatogram of the active fractions and the antimycin A standard, highlighting m/z 535.2-535.5 $[M+H]^+$ which was identified to be antimycin A2. As seen in the chromatogram, the antimycin A2 peak in the standard had a retention time of 25 minutes. Therefore the peak of 243-248 (yellow) that had the same retention time can be confirmed as antimycin A2. However, the peaks of 227-228 and 229-230 (green and pink respectively) had an earlier retention

time and could therefore belong to another antimycin isomer. Likewise, the presence of antimycin A3 in fraction 239-242 could be confirmed by the extracted ion chromatogram of m/z 521.2-521.5 $[M+H]^+$ in Figure 4-13 below. There was a slight shift in retention time, most likely because the standard was analysed using a different instrument from the samples, but following the same method.

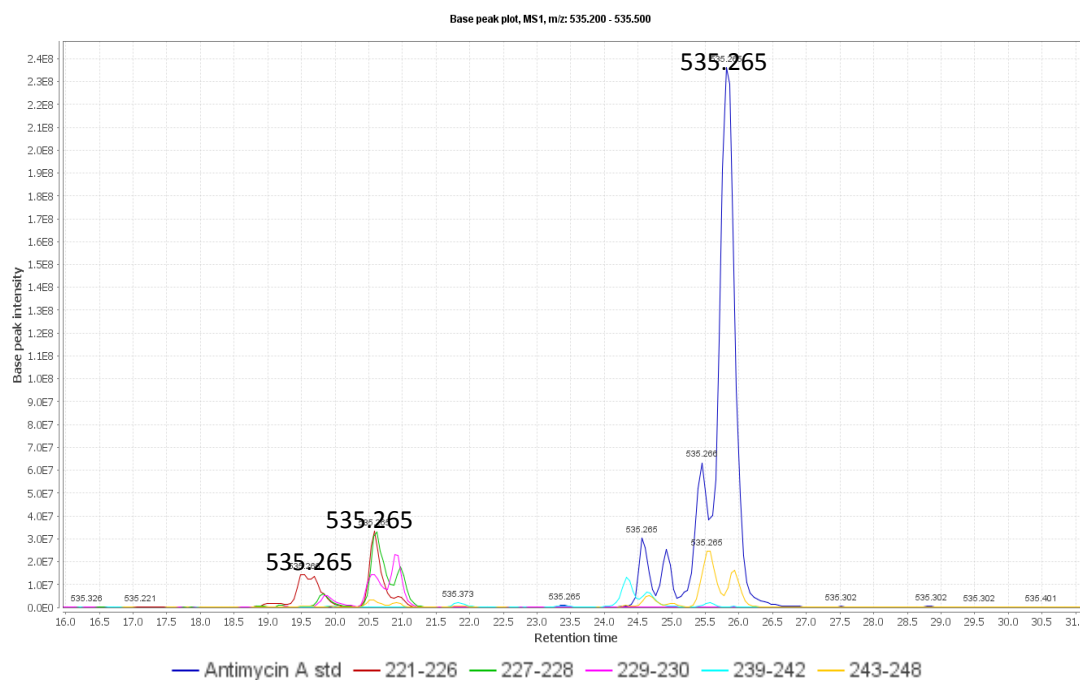


Figure 4-12: Extracted ion chromatogram of m/z 535.2-535.5 $[M+H]^+$ of the active fractions and the antimycin A standard in positive ionisation mode. The chromatograms are coloured as follows: antimycin A standard (dark blue), 221-226 (red), 227-228 (green), 229-230 (pink), 239-242 (light blue), 243-248 (yellow). A peak corresponding to m/z 535.265 $[M+H]^+$ that matched that of the antimycin A standard was seen in fraction 243-248. Other peaks having the same m/z and a retention time of 19-21 minutes were visible in the fractions but not in the standard.

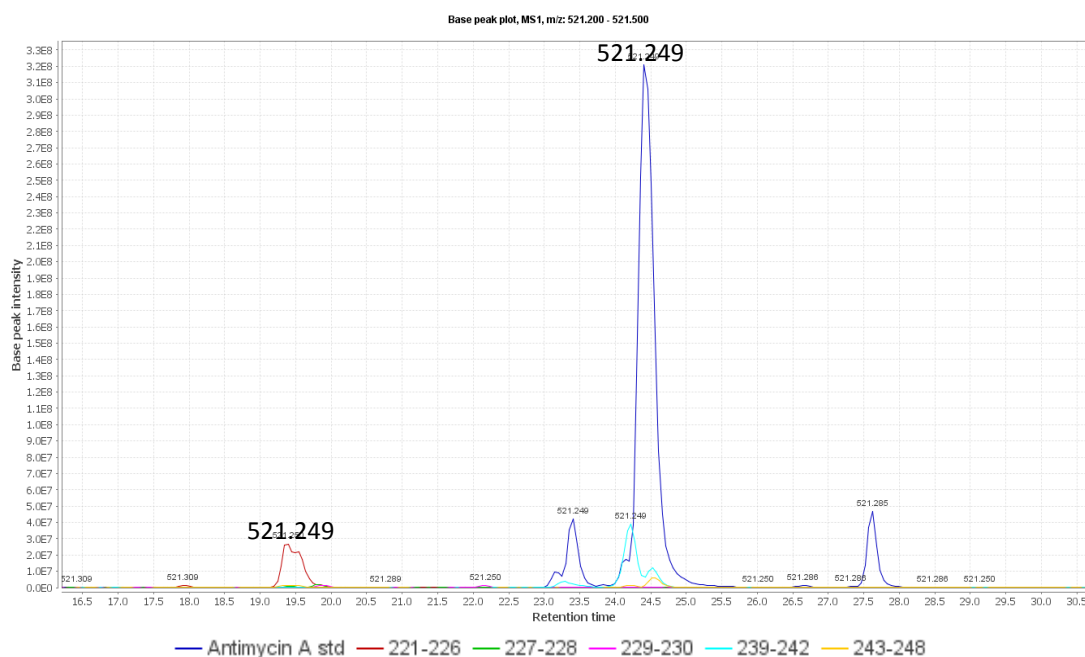


Figure 4-13: Extracted ion chromatogram of the antimycin A standard and the active fractions, highlighting m/z 521.2-521.5 $[M+H]^+$. The chromatograms are coloured as follows: antimycin A standard (dark blue), 221-226 (red), 227-228 (green), 229-230 (pink), 239-242 (light blue), 243-248 (yellow). A peak corresponding to m/z 521.249 $[M+H]^+$ that matched that of the antimycin A standard was seen in fraction 239-242. Another peak having the same m/z and a retention time of 19.5 minutes was visible in the fraction 221-226 but not in the standard.

4.3.3 Confirmation of Antimycin A Production using Gene Knock-out Studies and LC-HRFTMS

Another experiment was performed to confirm the production of antimycins by SM8. The antimycin gene cluster was detected in the SM8 genome by the group at ERI and, as antimycins have antifungal properties, a knock-out study was performed by deleting the *antC* gene cluster to determine if these are the compounds responsible for the antifungal activity of the SM8 extract. The antimycin gene cluster is depicted in Figure 4-14 below. The *antC* gene, which encodes a non-ribosomal peptide synthetase (NRPS) that is essential for antimycin production, was disrupted and a 3kb part of the gene was deleted.

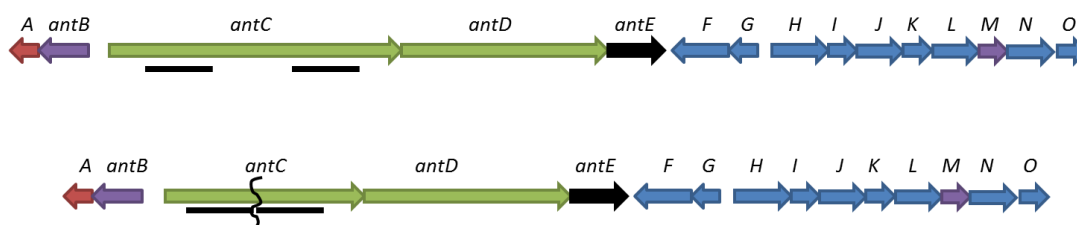


Figure 4-14: Antimycin gene cluster. The antimycin gene cluster of SM8 was identified by group of Kennedy at the ERI, UCC. Genes are colour coded according to their roles in the pathway: regulation (red), NRPS and PKS scaffold biosynthesis (green), 3-formamidosalicylic acid starter unit biosynthesis (blue), post-PKS/NRPS tailoring (purple), PKS extender unit supply (black). The black lines under *antC* represent the regions that were PCR amplified and cloned to produce a plasmid that was used to delete part of the *antC* gene. The lower gene cluster is the antimycin gene cluster after deletion of part of the *antC* gene.

Wild-type (WT) SM8 and mutant (MUT) SM8, lacking the antimycin gene cluster, were cultured on two types of media, OM (oatmeal medium) and SYP (starch-yeast extract-peptone medium). The extracts were assayed at the ERI for antifungal activity and were then sent to SIPBS for the mass spectrometry analysis.

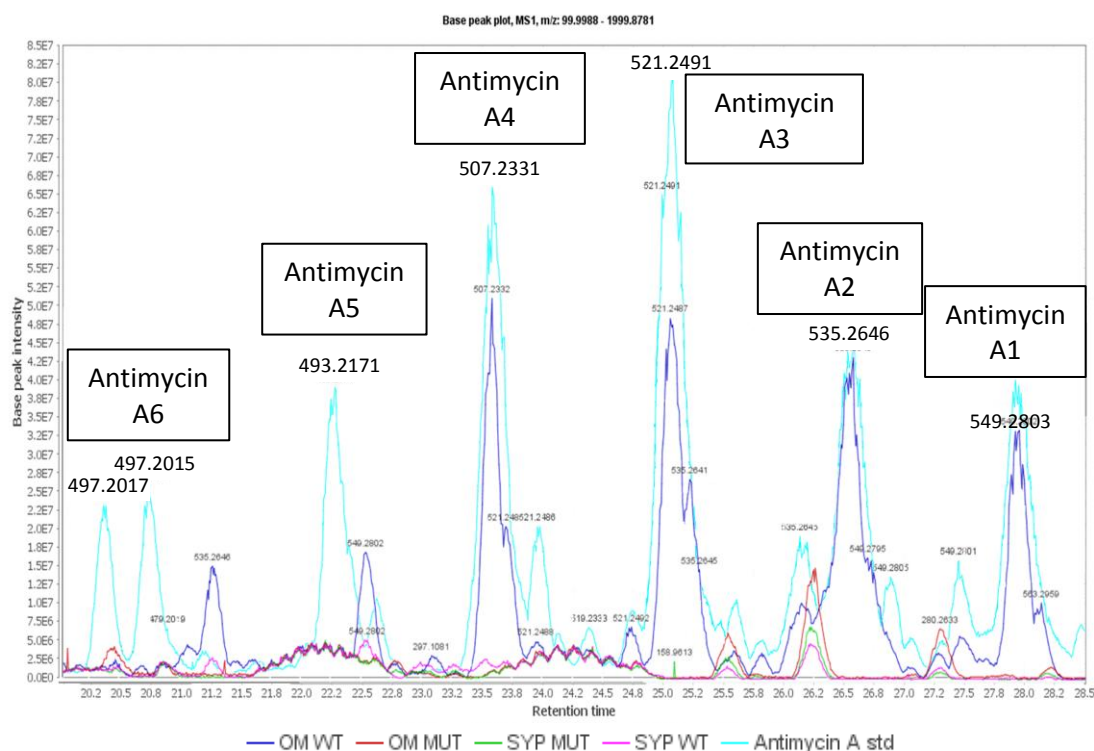
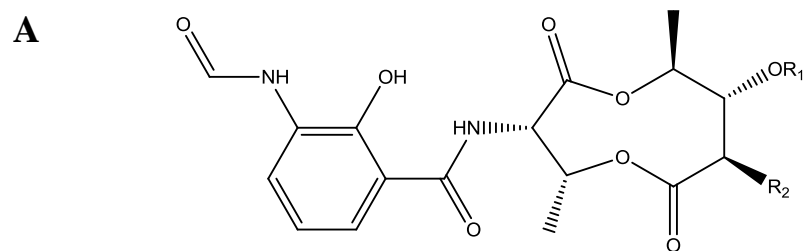


Figure 4-15: Total ion chromatogram of SM8 extracts compared to the antimycin A standard. The chromatograms are coloured as follows: OM-WT (dark blue), OM-MUT (red), SYP-WT (pink), SYP-MUT (green), antimycin A standard (light blue). The intensity of the samples was increased compared to the standard to enable the viewing of the smaller peaks. OM-WT clearly possessed antimycins A1-A4; however, the presence of these antimycins was not evident in the SYP –WT sample.

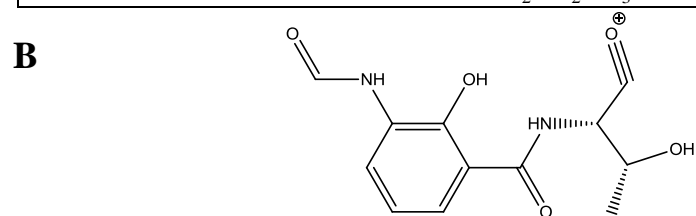
Figure 4-15 shows the comparisons of the SM8 extracts with the antimycin A standard using LC-HRFTMS. The light blue peaks belong to the standard. The dark blue peaks are those from the OM-WT and clearly showed the presence of antimycins. The SYP-WT possessed compounds of the same m/z but different retention times, and at lower concentrations than the OM-WT. It is possible that these are isomers of antimycin other than those present in the standard. The findings reflect the antifungal activity of the extracts, as the OM-WT extract had more potent antifungal activity compared to the SYP-WT. The mutants did not contain antimycins. The fragment ion at 265.081 $[M+H]^+$ is indicative of antimycins so this was searched for in the mass spectra. The structures of antimycins A1-A4 are shown in Figure 4-16, along with the fragmentation of the dilactone ring of antimycin A1a to generate the fragment ion with an m/z of 265.081 $[M+H]^+$. A summary of the findings is displayed in Table 4-7 below.

Table 4-7: Presence of antimycins in SM8 extracts. As peaks with the same m/z but different retention times were sometimes found, the peaks with the largest peak area are highlighted.

Anti-mycin A	m/z	Formula	STD		OM WT		OM MUT		SYPWT		SYP MUT	
			RT	265	RT	265	RT	265	RT	265	RT	265
1	549.280	$C_{28}H_{41}O_9N_2$			22.54	✓			22.56	✓		
			27.92	✓	27.95	✓						
2	535.264	$C_{27}H_{39}O_9N_2$			19.97	✓			20.90	✓		
					21.26	✓			21.27	✓		
			25.61	✓	25.23	✓						
			26.58	✓	26.58	✓						
3	521.249	$C_{26}H_{37}O_9N_2$			19.77	✓			19.65	✓		
			23.95	✓	23.68	✓						
			25.08	✓	25.07	✓						
4	507.233	$C_{25}H_{35}O_9N_2$	23.58	✓	23.59	✓			18.53			
5	493.217	$C_{24}H_{33}O_9N_2$	22.27	✓								
6	479.202	$C_{23}H_{31}O_9N_2$	20.35	✓								
			20.72	✓								



Antimycin	R ₁	R ₂
A1a	C=OCH(CH ₃)CH ₂ CH ₃	(CH ₂) ₅ CH ₃
A1b	C=OCH ₂ CH(CH ₃) ₂	(CH ₂) ₅ CH ₃
A2a	C=OCH(CH ₃) ₂	(CH ₂) ₅ CH ₃
A2b	C=OCH ₂ CH ₂ CH ₃	(CH ₂) ₅ CH ₃
A3a	C=OCH(CH ₃)CH ₂ CH ₃	(CH ₂) ₃ CH ₃
A3b	C=OCH ₂ CH(CH ₃) ₂	(CH ₂) ₃ CH ₃
A4a	C=OCH(CH ₃) ₂	(CH ₂) ₃ CH ₃
A4b	C=OCH ₂ CH ₂ CH ₃	(CH ₂) ₃ CH ₃
Deisovaleryl antimycin A3	H	(CH ₂) ₃ CH ₃
A5	C=OCH ₂ CH(CH ₃) ₂	CH ₂ CH ₃
A6	C=OCH ₂ CH ₂ CH ₃	CH ₂ CH ₃



Chemical Formula: C₁₂H₁₃N₂O₅⁺

Exact Mass: 265.0819

Figure 4-16: Antimycins A1 to A6. (A) Antimycin nucleus. The various side chains are listed. (B) The structure of the 265 [M+H]⁺ ion formed during fragmentation of antimycin compounds.

4.3.4 Isolation of Compounds from SM8 Extract

A new batch of SM8 extracts was received from the ERI. This amounted to 810.3 mg. Following the Sephadex[®] fractionation of these extracts, the samples were assayed for activity at the ERI. The activities are seen in Figure 4-17 and Appendix IV.

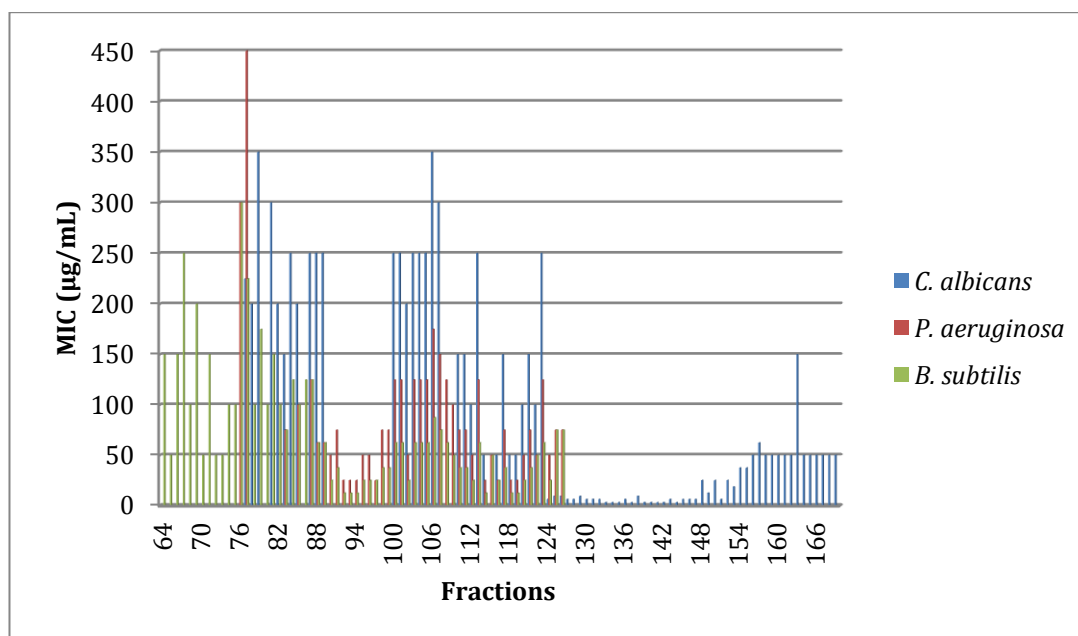


Figure 4-17: Graphical representation of the specific activity of the SM8 Sephadex[®] fractions against *C. albicans*, *P. aeruginosa* and *B. subtilis*. A smaller MIC value signified more potent activity. Activity against *B. subtilis* appeared in the earlier fractions. The activity against *P. aeruginosa* occurred from fractions 76-126 and overlapped with the activity against the other two test organisms. The antifungal activity appeared from fraction 77 until the last fraction, 169. It was most potent from fraction 124 to 147.

Figure 4-17 shows the activities of the fractions when tested against *C. albicans*, *P. aeruginosa* and *B. subtilis*. Lower MIC values indicate greater potency. Activity against *B. subtilis* appeared in the earlier fractions, whereas activity against *C. albicans* occurred in the later fractions. The active fractions were then pooled together based on their similarity on the TLC plates. The plates are shown in Figure 4-18. The resulting weights of the pooled active fractions are listed in Table 4-8.

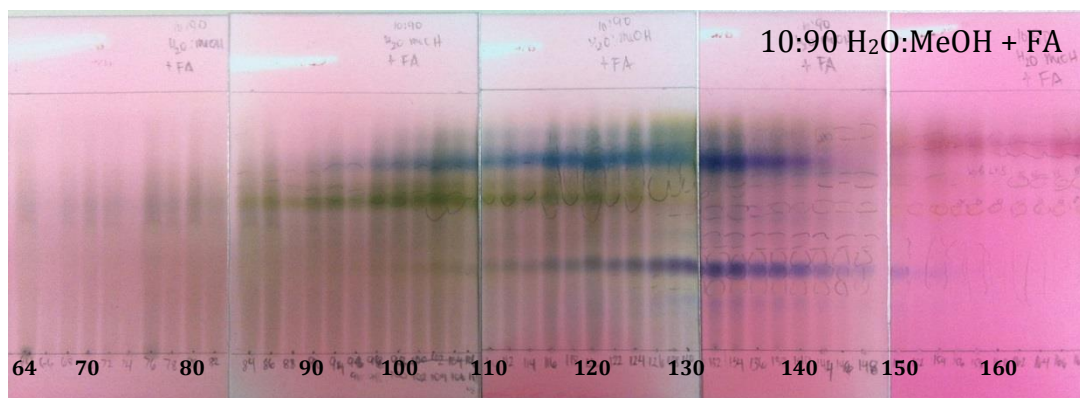


Figure 4-18: Reverse-phase TLC of active SM8 fractions that were obtained after separation through Sephadex® LH-20. The mobile phase used was 10:90 water:methanol with a drop of formic acid.

Table 4-8: Yields of the pooled active fractions.

Pooled Fractions	Yield (mg)
64-75	39.2
76-89	94.9
90-99	53.0
100-109	81.3
110-126	170.9
127-156	158.5
157-169	16.7

Sample 110-126 was selected for purification as it had the greatest quantity and possessed all three types of activity; however, it was primarily antibacterial. Following reversed phase MPLC and subsequent pooling using TLC, an aliquot of each pooled fraction was assayed by the ERI. The TLC summary plates are in Figure 4-19 and the resulting weights of the active fractions are shown in Table 4-9. The AntiMarin database was used to identify compounds from the LC-MS data. These can be seen in Table 4-10 and Figure 4-20.

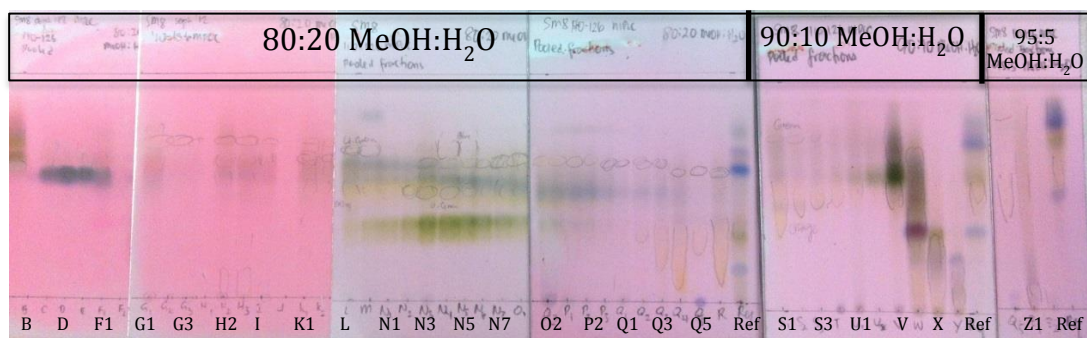


Figure 4-19: TLC summary plate of the pooled fractions following MPLC of 110-126. The mobile phases used were 80:20 methanol:water, 90:10 methanol:water, and 95:5 methanol:water.

Table 4-9: Yields and activity of the active fractions following MPLC of 110-126.

Fraction	Yield (mg)	Antibacterial activity against <i>B. subtilis</i>	
		MIC ($\mu\text{g/mL}$)	Number of wells
N5	1.0	12.5	3
P3	0.5	50	1 (mild)
Q1	0.7	50	1(mild)
R	2.6	25	2
S1	1.1	25	2
S3	1.2	12.5	3
T	0.5	12.5	3
U1	1.1	12.5	3
V	20.8	6.25	4/ (5th is mild)
W	34.2	12.5	3
X	7.5	12.5	3
Y	3.2	12.5	3
Z1	16.2	50	1 (mild)
Z2	0.7	50	1 (mild)

Table 4-10: Compounds putatively identified from the antibacterial SM8_110-126 fractions using the AntiMarin 2012 database.

Fraction		m/z	RT	Formula	Name	Source	Reference
N5	[M+H] ⁺	451.2083	15.72	C ₂₂ H ₃₀ N ₂ O ₈	[14] Urauchimycin-A	[B] (marine) <i>Streptomyces</i> sp. Ni-80 (FERM P-12392)	(Imamura et al., 1993)
	[M-H] ⁻	449.1933	15.71		[15] Urauchimycin-B		
P3	[M+H] ⁺	507.2270	17.28	C ₃₂ H ₃₀ N ₂ O ₄	[16] Cochliodinol	[F] <i>Chaetomium globosum</i> , <i>Chaetomium cochlioides</i>	(Saito et al., 1988, Jerram et al., 1975, Brewer et al., 1968, Brewer et al., 1970)
	[M-H] ⁻	519.2348	17.53	C ₂₆ H ₃₆ N ₂ O ₉	[17] Antimycin A7a	[B] <i>Streptomyces</i> sp.	(Barrow et al., 1997)
Q1	[M+H] ⁺	521.2501	17.49	C ₂₆ H ₃₆ N ₂ O ₉	[17] Antimycin A7a	[B] <i>Streptomyces</i> sp.	(Barrow et al., 1997)
	[M-H] ⁻	519.2348	17.53				
R	[M+H] ⁺	521.2501	18.51	C ₂₆ H ₃₆ N ₂ O ₉	[18] Antimycin A3b; Blastmycin	[B] <i>Streptomyces kitazawaensis</i> , <i>S. blastomyceticus</i>	(Kinoshita et al., 1969, Kinoshita et al., 1971, Aburaki and Kinoshita, 1979, Liu and Strong, 1959, Wasserman and Gambale, 1985)
	[M-H] ⁻	651.3756	19.22	C ₃₅ H ₅₆ O ₁₁	[19] Testosterone 5α-reductase inhibitor II	[F] <i>Gliocladium</i> ATCC no. 20826	(Borris et al., 1989)
S1	[M+H] ⁺	535.2657	18.71	C ₂₇ H ₃₈ N ₂ O ₉	[20] Antimycin A2b	[B] <i>Streptomyces kitazawaensis</i> , <i>S. griseus</i>	(Barrow et al., 1997)
	[M-H] ⁻	519.2348	17.53	C ₂₆ H ₃₆ N ₂ O ₉	[17] Antimycin A7a	[B] <i>Streptomyces</i> sp.	(Barrow et al., 1997)
S3	[M+H] ⁺	535.2657	18.71	C ₂₇ H ₃₈ N ₂ O ₉	[20] Antimycin A2b	[B] <i>Streptomyces kitazawaensis</i> , <i>S. griseus</i>	(Barrow et al., 1997)
	[M-H] ⁻	707.4378	21.60		[21] Kaimonolide A dehydration product	[B] <i>Streptomyces</i> no. 4155	(Hirota et al., 1989)
T	[M+H] ⁺	535.2657	18.71	C ₂₇ H ₃₈ N ₂ O ₉	[20] Antimycin A2b	[B] <i>Streptomyces kitazawaensis</i> , <i>S. griseus</i>	(Barrow et al., 1997)
	[M-H] ⁻	707.4378	21.60		[21] Kaimonolide A dehydration product	[B] <i>Streptomyces</i> no. 4155	(Hirota et al., 1989)
U1	[M+H] ⁺	535.2657	18.71	C ₂₇ H ₃₈ N ₂ O ₉	[20] Antimycin A2b	[B] <i>Streptomyces kitazawaensis</i> , <i>S. griseus</i>	(Barrow et al., 1997)
	[M-H] ⁻	515.3226	15.73	C ₂₇ H ₄₈ O ₉	[22] 21-O-a-L-Rhamnopyranosyl-18R-hydroxydihydroalloprotolichesterinate	[L] lichens <i>Acarospora gobiensis</i> , <i>Lecanora fructulosa</i> , <i>Leptogium saturninum</i> , <i>Peltigera canina</i> , <i>Rhizoplaca peltata</i> , <i>Xanthoparmelia camtschadalis</i> ,	(Rezanka and Guschina, 2001)
V	[M+H] ⁺	549.2813	21.27	C ₂₈ H ₄₀ N ₂ O ₉	[23] Antimycin A1b	[B] <i>S.kitazawaensis</i> , <i>S. griseus</i> , [B] <i>Streptomyces</i> sp. HKI 111-L, [B] marine <i>Streptomyces</i> sp. B 3497	(Abidi and Adams, 1987, Haegele and Desiderio, 1973, Kluepfel et al., 1970, Schilling et al., 1970, Endo and Yonehara, 1970, Sehgal et al., 1976, Singh et al., 1972)
W	[M-H] ⁻	547.2664	20.09				
X	[M+H] ⁺	549.2811	25.28				
	[M-H] ⁻	483.3329	20.42	C ₂₇ H ₄₈ O ₇	[24] Euryspongiol A2	Porifera <i>Euryspongia</i> sp	(Dopeso et al., 1994)
Y and Z1	[M+H] ⁺	577.3122	28.04	C ₃₀ H ₄₄ N ₂ O ₄	[25] Antimycin A16	[B] <i>Streptomyces</i> sp. SPA-10191, <i>S.sp.</i> SPA-8893	(Hosotani et al., 2005)
	[M-H] ⁻	721.4171	18.86	C ₄₀ H ₅₈ N ₄ O ₈	[26] Antanapeptin D	[C] Madagascan <i>Lyngbya majuscula</i>	(Nogle and Gerwick, 2002)
Y and Z1	[M+H] ⁺	549.2813	21.27	C ₂₈ H ₄₀ N ₂ O ₉	[23] Antimycin A1b	[B] <i>S.kitazawaensis</i> , <i>S.griseus</i> , [B] <i>Streptomyces</i> sp. HKI 111-L, [B] marine <i>Streptomyces</i> sp. B 3497	(Abidi and Adams, 1987, Haegele and Desiderio, 1973, Kluepfel et al., 1970, Schilling et al., 1970, Endo and Yonehara, 1970, Sehgal et al., 1976, Singh et al., 1972)
	[M-H] ⁻	547.2664	20.09				

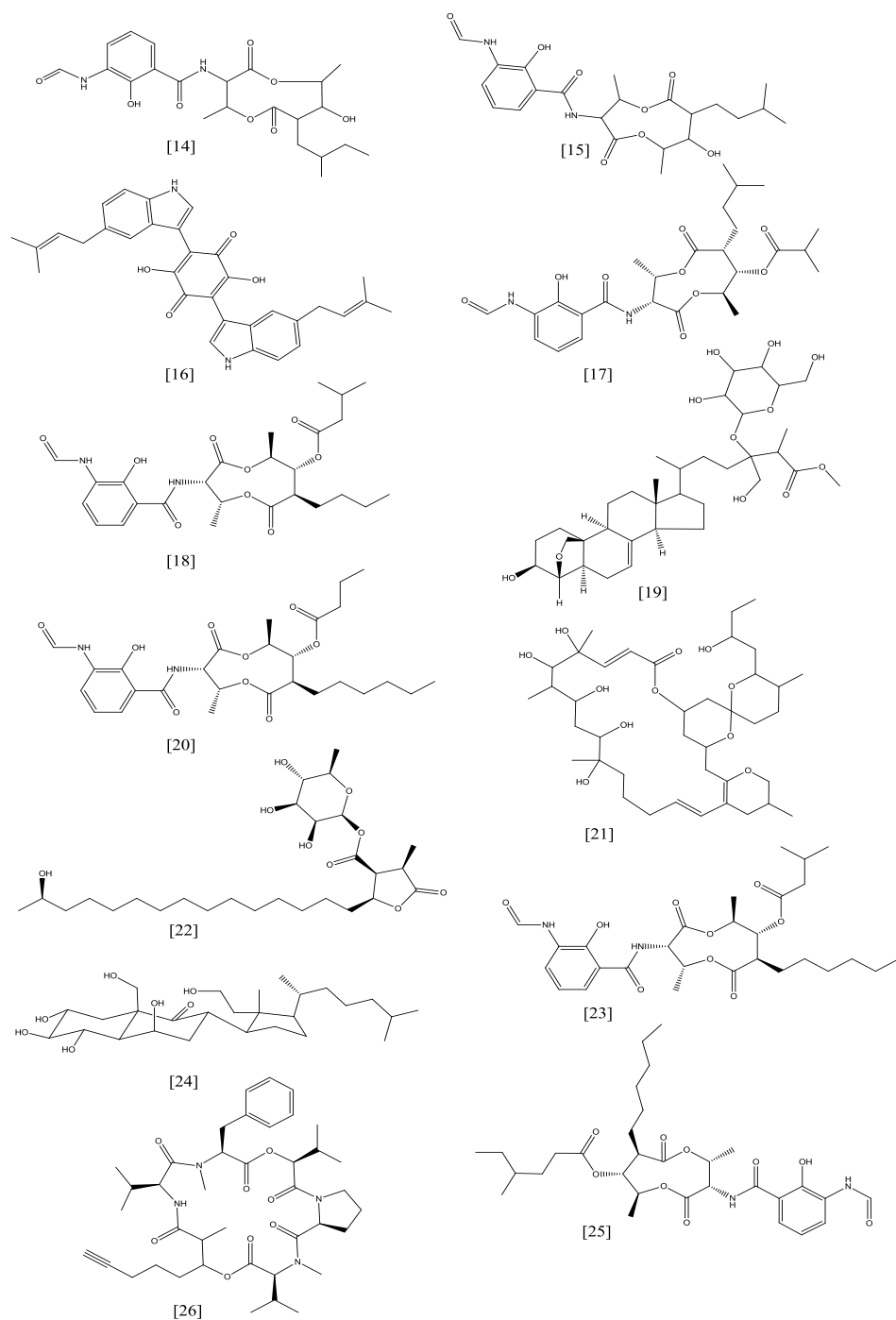


Figure 4-20: Structures of compounds putatively identified from the active SM8_110-126 fractions using the AntiMarin 2012 database. Once again, many of the compounds belonged to the antimycin family.

Only the later and more non-polar fractions showed any activity, as seen in Table 4-9. These fractions were active against *B. subtilis*. No antifungal or anti-calcineurin activity was found. Members of the antimycin family were prevalent in the active fractions, as seen in Table 4-10. Urauchimycin A (**14**) and B (**15**) are also antimycins

(Imamura et al., 1993). These are known antifungal agents. However, once again, the antibacterial activity could have been due to the presence of fatty acids in the later fractions (Figure 4-21).

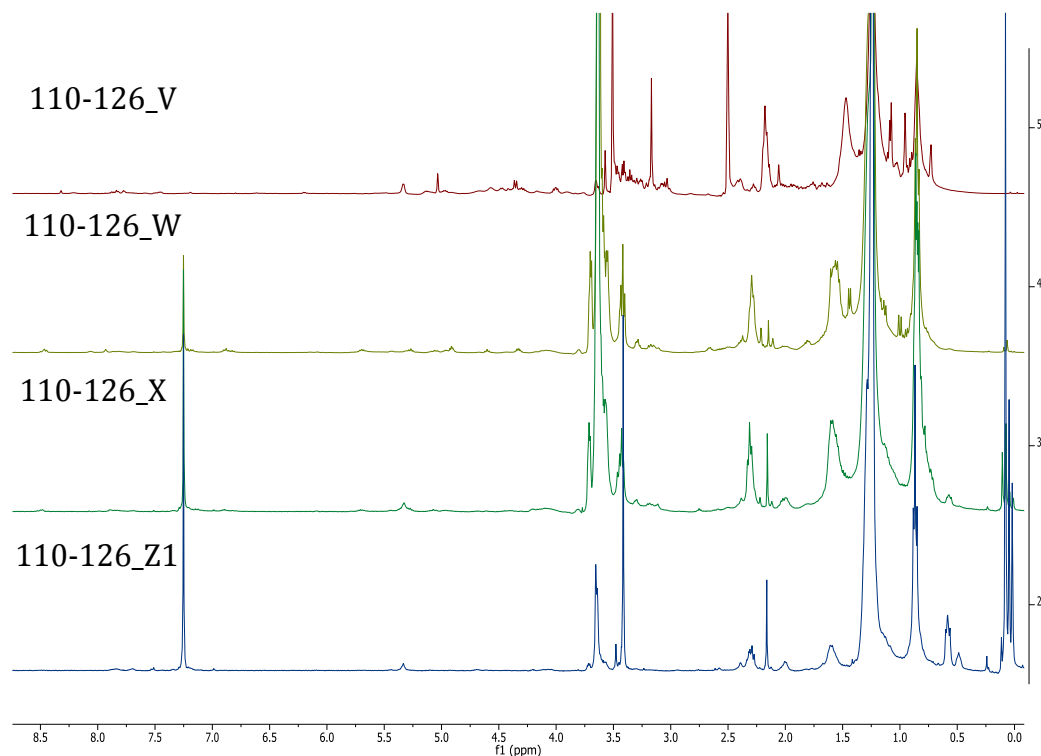
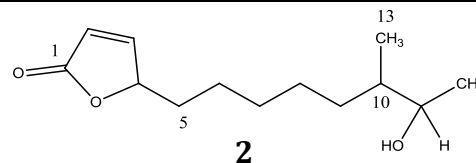
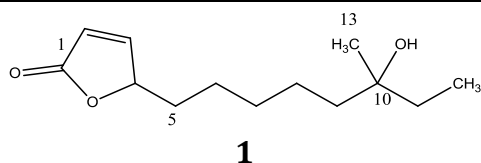


Figure 4-21: ^1H NMR spectra of some antibacterial SM8_110-126 fractions. SM8_110-126_V was dissolved in DMSO whereas the others were dissolved in CDCl_3 . All measurements were taken at 400 MHz. The major compounds in the fractions are fatty acids. Impurities can be seen as small peaks in the downfield region of the spectra.

Fraction 110-126D was inactive in all of the assays performed. However, it was determined through NMR and LC-MS to be a mixture of two furanone isomers. The ^{13}C chemical shifts of the two compounds were compared to the values found in literature. These can be seen in Table 4-12. Mukku et al. referred to these compounds as butenolides 1 and 2 respectively, and that nomenclature shall be followed here to prevent confusion between the two isomers (Mukku et al., 2000).

Table 4-11: Butenolides 1 and 2.

	Butenolide 1	Butenolide 2
Synonyms	4,10-Dihydroxy-10-methyl-dodec-2-en-1,4-olide	4,11-Dihydroxy-10-methyl-dodec-2-en-1,4-olide
Sample Codes	110-126D, 127-156S1, S2, U1_320-349	110-126D, 127-156S1, S2, U1_320-349
Sample Amount	5.5 mg, 6.5 mg, 2.0 mg, 2.0 mg	5.5 mg, 6.5 mg, 2.0 mg, 2.0 mg
Physical Description	-	-
Molecular Formula	C ₁₃ H ₂₃ O ₃	C ₁₃ H ₂₃ O ₃
Molecular Weight	226 g/mol	226 g/mol
Retention time (LC-MS)	13.15 min	14.62 min



LC-HRFTMS Spectra of Butenolides 1 and 2 ([M+H]⁺)

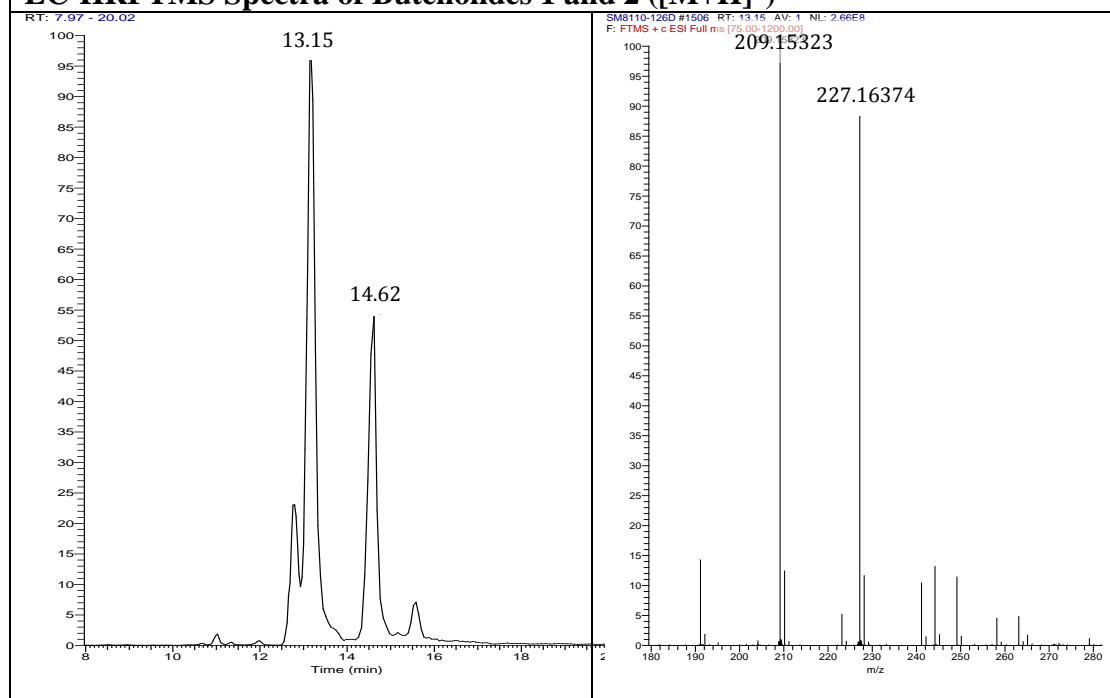


Table 4-12: Comparison of ^{13}C and ^1H NMR data of purified furanones to butenolide 1 and 2 (Mukku et al., 2000).

	Butenolide 1	Compound D (major component: 71.43%)		Butenolide 2	Compound D (minor component: 28.57%)	
	δ_{C}	δ_{C}	δ_{H} ppm (multiplicity, J)	δ_{C}	δ_{C}	δ_{H} ppm (multiplicity, J)
1 CO	173.2	173.6	-	173.2	173.6	-
2 CH	121.6	120.8	6.20 (dd, 1.8, 5.7 Hz)	121.6	120.8	6.20 (dd, 1.8, 5.7 Hz)
3 CH	156.2	159.3	7.84 (dd, 1.4, 5.7 Hz)	156.3	159.3	7.84 (dd, 1.4, 5.7 Hz)
4 CH	83.4	83.7	5.15 (m)	83.4	83.7	5.15 (m)
5 CH ₂	33.1	34.4	1.71, 1.55 (dd, 6.9, 14.3 Hz))	32.4	34.4	1.71, 1.55 (dd, 6.9, 14.3 Hz))
6 CH ₂	25.0	25.0	1.33	25.0	25.0	1.33
7 CH ₂	29.9	30.1	1.28	29.6	30.1	1.28
8 CH ₂	23.6	23.8	1.28	27.0	27.2	1.28
9 CH ₂	41.1	41.5	1.28	32.4	32.8	1.28
10 Cq/ CH	72.9	71.2	-	39.6	41.0	1.28
11 CH ₂	34.3	34.4	1.33	71.3	70.0	3.42 (m)
12 CH ₃	8.2	8.8	0.79 (t, 7.5 Hz)	19.5	19.9	0.96 (d, 6.3 Hz)
13 CH ₃	26.4	26.9	0.98 (s)	14.2	15.1	0.77 (d, 6.6 Hz)

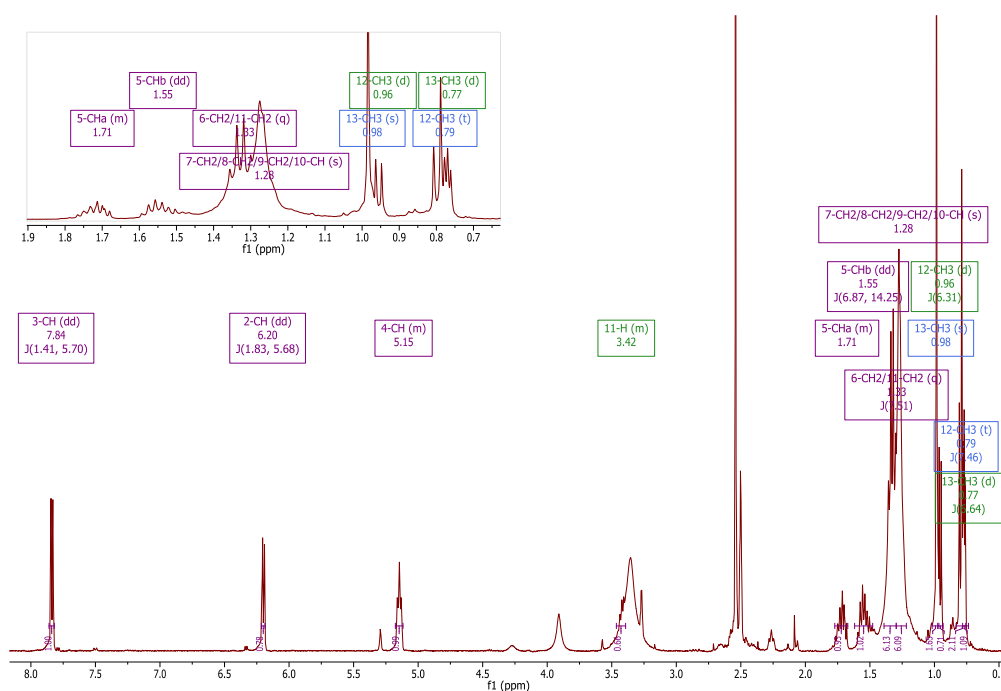


Figure 4-22: ^1H NMR of Fraction 110-126D (400 MHz, DMSO). The chemical shifts, multiplicities and coupling constants of the peaks are labelled. The labels in purple indicate peaks common to both butenolides. Labels in blue indicate peaks specifically for butenolide 1 and those in green indicate peaks specifically for butenolide 2.

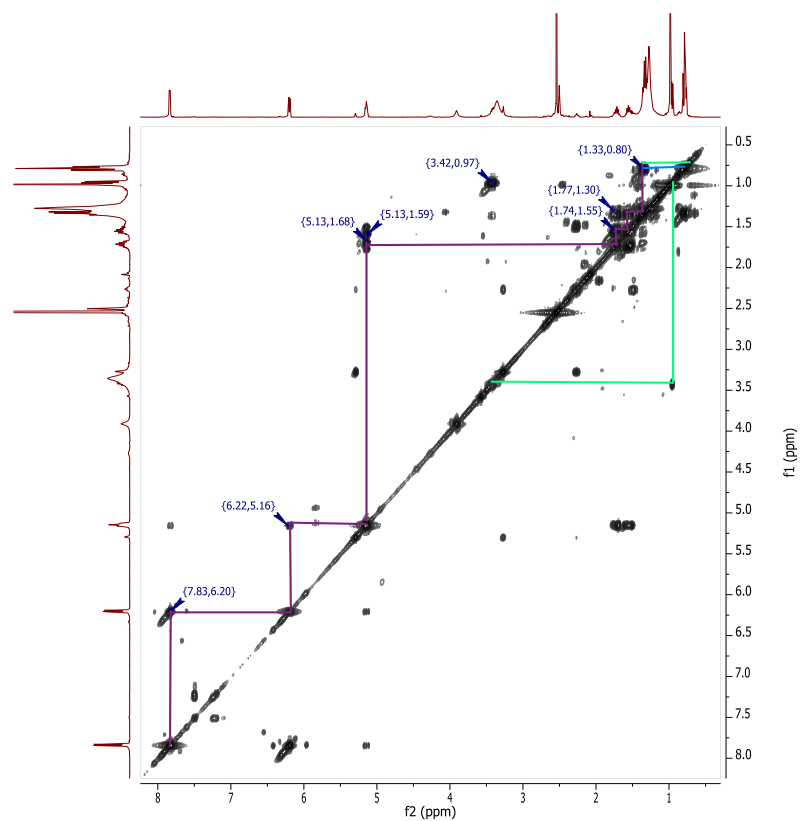


Figure 4-23: ^1H - ^1H COSY spectrum of Fraction 110-126D (400 MHz, DMSO). The purple lines indicate the spin systems belonging to both compounds whereas the blue and green lines indicate spin systems specific to butenolide 1 and 2 respectively.

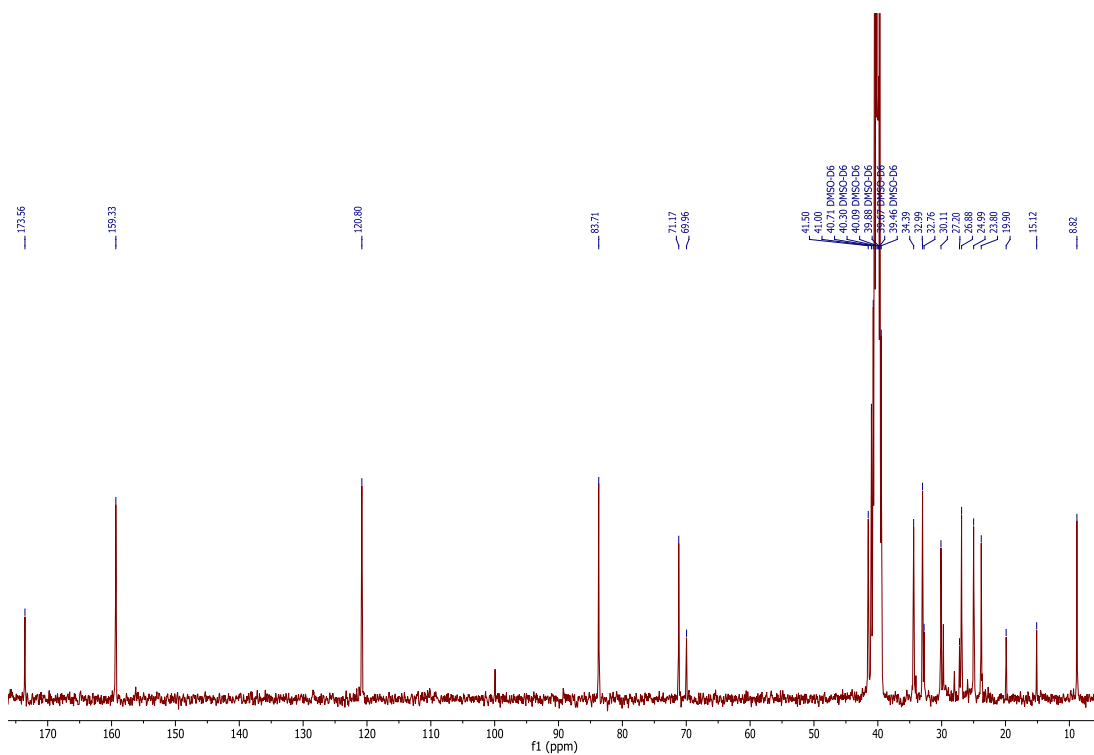


Figure 4-24: ^{13}C NMR spectrum of Fraction 110-126D (100 MHz, DMSO).

The two doublet of doublets at δ_{H} 6.20 and 7.84 (2-CH and 3-CH respectively) coupled to each other in the COSY (Figure 4-23). Their coupling could also be seen in the HMBC together with coupling to a quaternary carbon (1-CO) at δ_{C} 173.6, indicating that they were beside a ketone group. The coupling constant of 5.7 Hz was indicative of a 5-membered ring. Following the spin system on the COSY, the multiplet at δ_{H} 5.15 belonged to 4-CH. This was attached to a chiral carbon and as such caused the geminal protons of 5-CH₂ to appear at different chemical shifts (δ_{H} 1.71 and 1.55). These two coupled with the aliphatic system at δ_{H} 1.33 and 1.28.

Several 1D total correlation spectroscopy (TOCSY) experiments were performed to assist in assigning the overlapping peaks to the proper isomer. These can be seen in Appendix II. The ¹H spectrum portrayed the methyl group at δ_{H} 0.98 as a singlet, indicating that it was attached to a quaternary carbon. The COSY corroborated this as the peak did not couple with any other peak in the spectrum. In the HMBC spectrum it was seen that the protons of this group of butenolide 1 were associating with C-9, C-10, and C-11 (δ_{C} 41.5, 71.2 and 34.4 respectively). C-10 was an oxygenated quaternary carbon. All of this resulted in the assignment of the methyl group at δ_{H} 0.98 as 13-CH₃ of the first butenolide. The triplet at δ_{H} 0.77 belonged therefore to the terminal 12-CH₃ as it was split into a triplet by the two protons of the neighbouring 11-CH₂ group at δ_{H} 1.33. These interactions were confirmed in the COSY as well as in the HMBC where it was seen that the protons of 12-CH₃ were correlating with C-11 and C-10, and the protons of 11-CH₂ were likewise correlating with C-12 (δ_{C} 8.8).

The conformation of the alkyl chain of the second butenolide was elucidated in the same manner. The 12-CH₃ occurred in the ¹H spectrum as a doublet at δ_{H} 0.96 that was split by the proton on 11-CH at δ_{H} 3.42 which was attached to the hydroxylated C-11 (δ_{C} 70.0). The coupling of 12-CH₃ to 11-CH was evident on the COSY as well as the HMBC. It also correlated with C-9, C-10 and C-13 at δ_{C} 32.8, 41.0, and 15.1 respectively. The HMBC also showed correlations between 11-CH and C-9 and C-13, as well as between 13-CH₃ and C-9 and C-11.

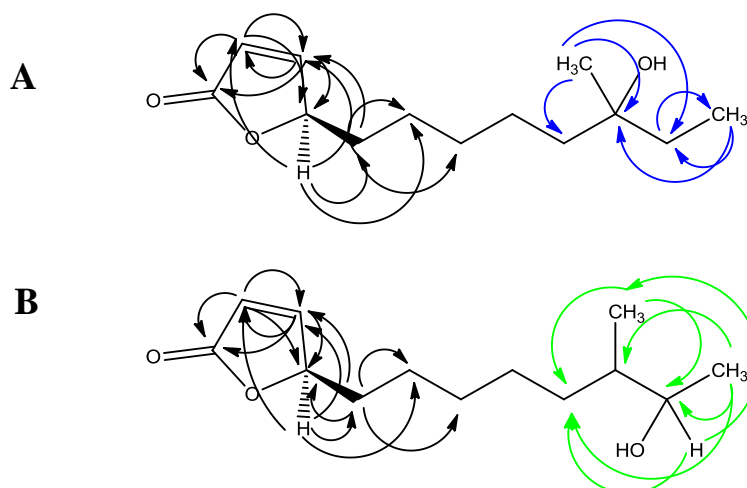


Figure 4-25: HMBC correlations of the butenolides of Fraction 110-126D. Black arrows indicate correlations common to both butenolide 1 and 2 whereas the blue and green arrows depict correlations specific to (A) butenolide 1 and (B) butenolide 2 respectively.

Fraction D produced a blue-violet spot on the TLC plate after spraying with anisaldehyde, as previously reported (Mukku et al., 2000). The extracted ion chromatogram and the corresponding mass spectra can be seen in Figure 4-26 below. The peak corresponding to $227.1368 [M+H]^+$ matched that predicted for the butenolides. The peak at $209.1532 [M+H]^+$ is likely the butenolide with the removal of H_2O .

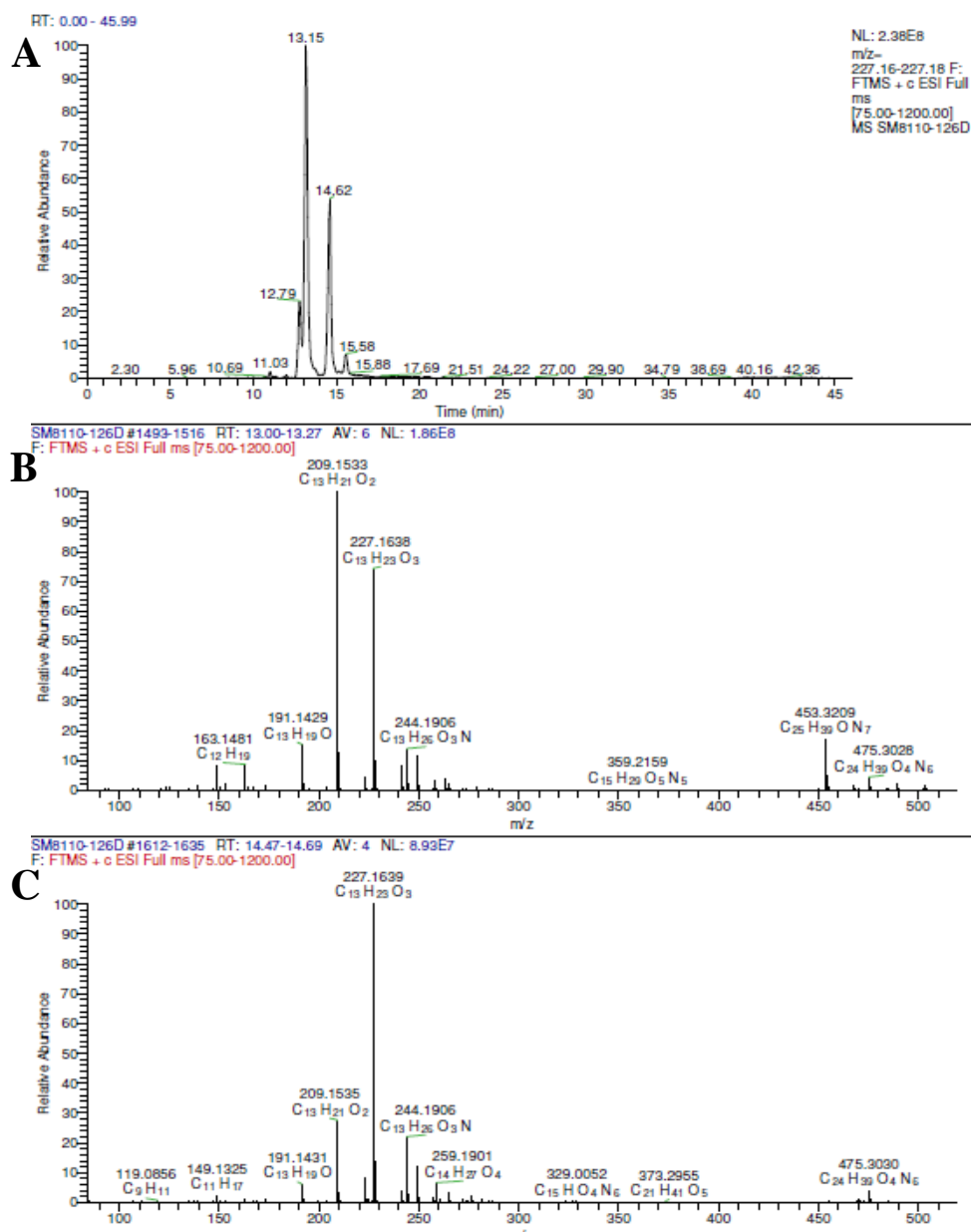


Figure 4-26: The extracted ion chromatogram of m/z 227.16-227.18 of Fraction 110-126D. (A) Extracted ion chromatogram, (B) mass spectrum corresponding to the peak at RT 13.00-13.27 min and (C) mass spectrum corresponding to the peak at RT 14.47-14.69 min. The predicted formula of $C_{13}H_{23}O_3$ $[M+H]^+$ matched the proposed molecular formula of the butenolides.

The fractions obtained from the Sephadex[®] separation that possessed solely antifungal activity (fractions 127-156) were purified using a conventional silica column. The TLC summary plates are shown in Figure 4-27 and the active fractions and their corresponding weights are in Table 4-13.

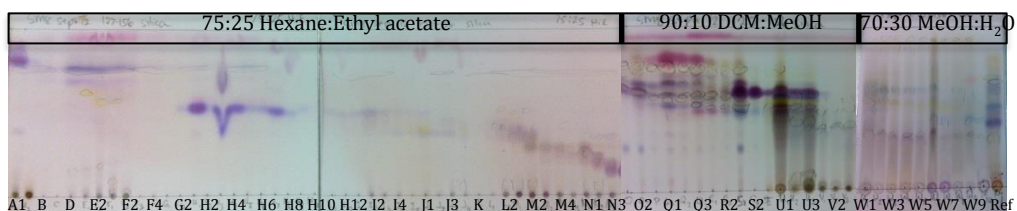


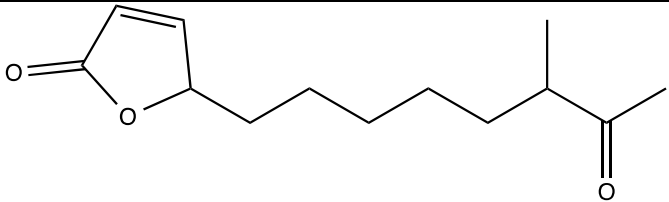
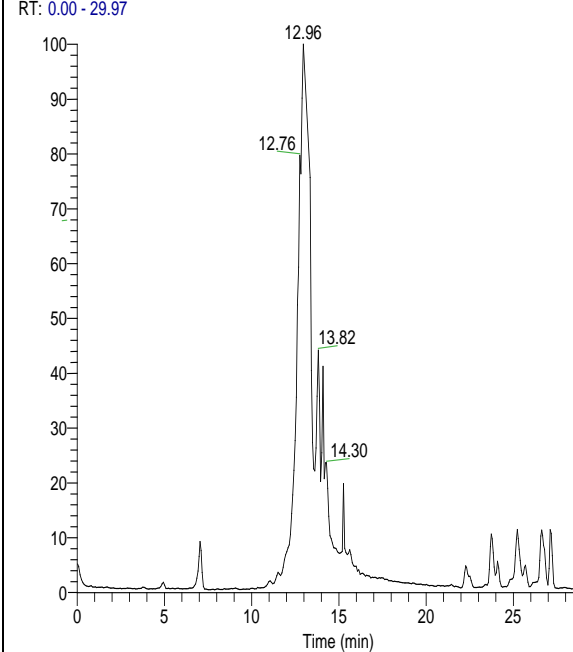
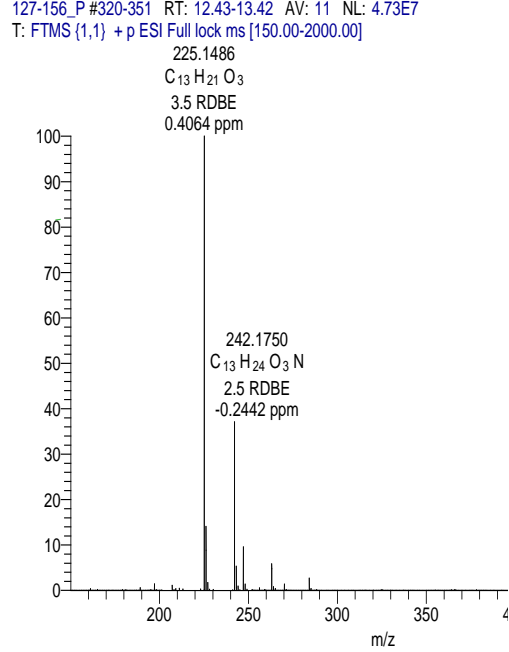
Figure 4-27: TLC summary plate of fractions after silica chromatography of 127-156. The first two plates were eluted with 75:25 hexane:ethyl acetate, the third with 90:10 DCM:MeOH, and the last plate was a C18 plate with 70:30 methanol:water.

Table 4-13: Yields and activities of active fractions following silica chromatography of 127-156.

Fraction	Yield (mg)	Antifungal activity (<i>C. albicans</i>)		Anti-calcineurin activity
		MIC $\mu\text{g/mL}$	Number of wells	
A1	2.0	-	-	+
D	2.0	-	-	+
E2	3.6	-	-	+
H1	1.8	-	-	+
M1	0.6	-	-	++
M2	1.7	-	-	+
M3	1.9	-	-	++
M4	2.7	-	-	+
N1	7.0	-	-	+
N3	3.0	-	-	++
O1	2.2	6.25	4	+++
P	2.6	3.125	5	++
Q3	6.2	6.25	4	+
R1	3.5	6.25	4	+
S1	6.5	12.5	3	++
S2	2.0	25	2	+
T	2.2	12.5	3	+
U1	46.2	25	2	+
U3	10.7	25	2	+
V1	2.3	25	2	+
V3	3.5	50	1	+
W1	12.4	50	1	+
W2	6.6	-	-	+
W10	3.3	-	-	+

Fraction P was the most potent antifungal fraction. It also had some anti-calcineurin activity. NMR analysis indicated that although the major component of this fraction was a butenolide, it was different to the two butenolides previously identified. Figure 4-28 showed that the peak for 13-CH₃ was also a doublet but it was at a more downfield chemical shift than that of butenolide 2. In addition, analysis of the COSY spectrum (Figure 4-29) indicated that 13-CH₃ was correlating with a peak at δ_{H} 2.49 ppm as opposed to a peak at 3.42 ppm, unlike butenolide 2. The major ion seen in the LC-HRFTMS spectrum (Table 4-14) had an m/z of 225.1486 [M+H]⁺. The compound therefore had a formula of C₁₃H₂₀O₃. It was thus determined that the butenolide in Fraction P corresponded to 'butenolide 4' that was also previously isolated from a *Streptomyces* strain (Mukku et al., 2000).

Table 4-14: Butenolide 4

Butenolide 4	
Synonyms	4-Hydroxy-10-methyl-11-oxo-dodec-2-en-1,4-olide
Sample Codes	127-156P
Sample Amount	2.6 mg
Physical Description	-
Molecular Formula	C ₁₃ H ₂₀ O ₃
Molecular Weight	224 g/mol
Retention time (LC-MS)	12.96 min
	
LC-HRFTMS Spectrum of Butenolide 4 ([M+H]⁺)	
<p>RT: 0.00 - 29.97</p>  <p style="text-align: center;">Time (min)</p>	<p>127-156_P #320-351 RT: 12.43-13.42 AV: 11 NL: 4.73E7 T: FTMS (1,1) + p ESI Full lock ms [150.00-2000.00]</p> <p>225.1486 C₁₃H₂₁O₃ 3.5 RDBE 0.4064 ppm</p>  <p style="text-align: center;">m/z</p>

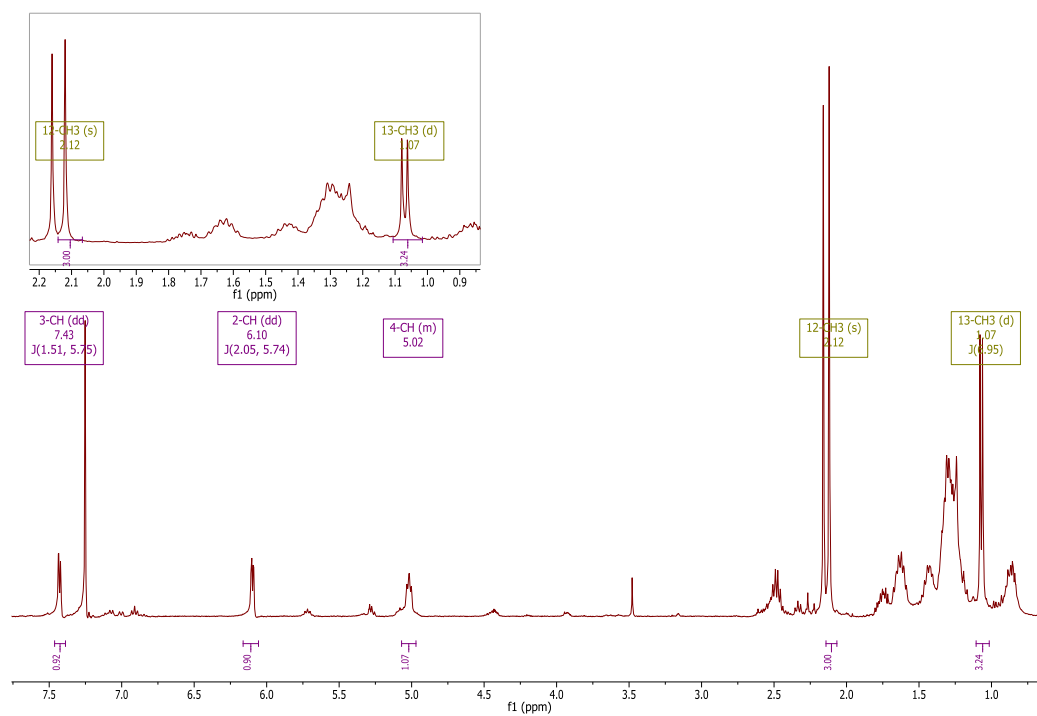


Figure 4-28: ^1H NMR of 127-156P (400 MHz, CDCl_3). Peaks common to the other butenolides are labelled in purple whereas those specific to butenolide 4 are labelled in olive.

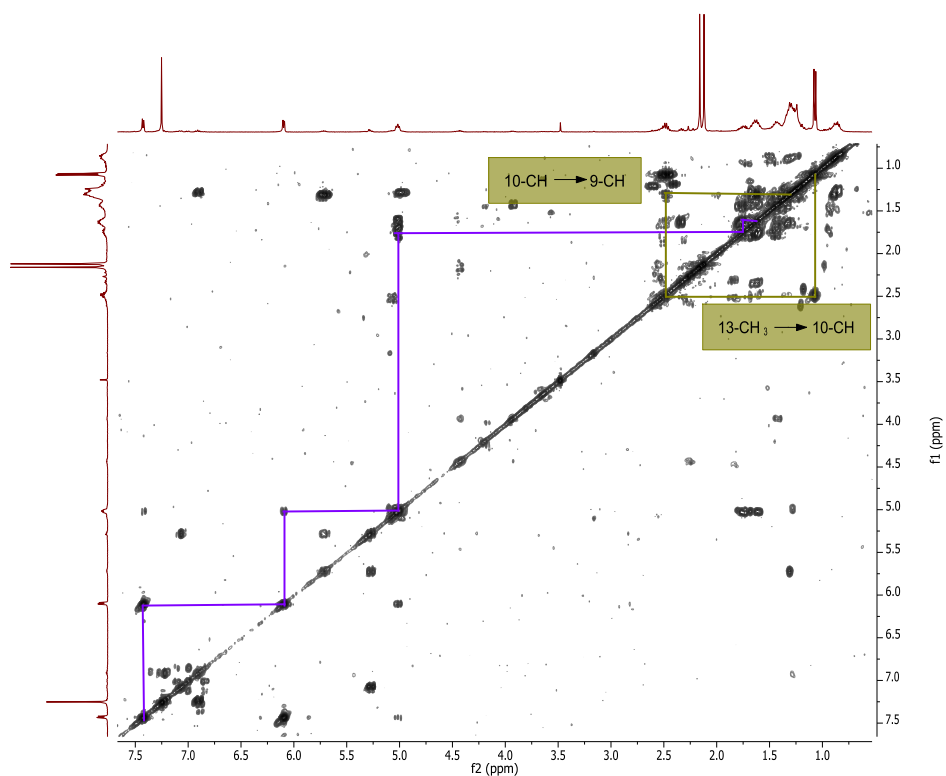


Figure 4-29: ^1H - ^1H COSY of 127-156P (400 MHz, CDCl_3). The spin system common to the three butenolides is marked in purple whereas the spin system specific to butenolide 4 is marked in olive.

NMR analysis indicated that the major components of S1 and S2 were butenolides 1 and 2, which possessed no activity when isolated in the previous fractionation (Fraction 110-126_D). However, the ^1H NMR spectra of P, S1 and S2 showed that they possessed impurities that could have been responsible for the antifungal activity (Figure 4-32). Analysis of the LC-HRFTMS spectra of the active antifungal fractions revealed the presence of antimycin A compounds (Figure 4-30).

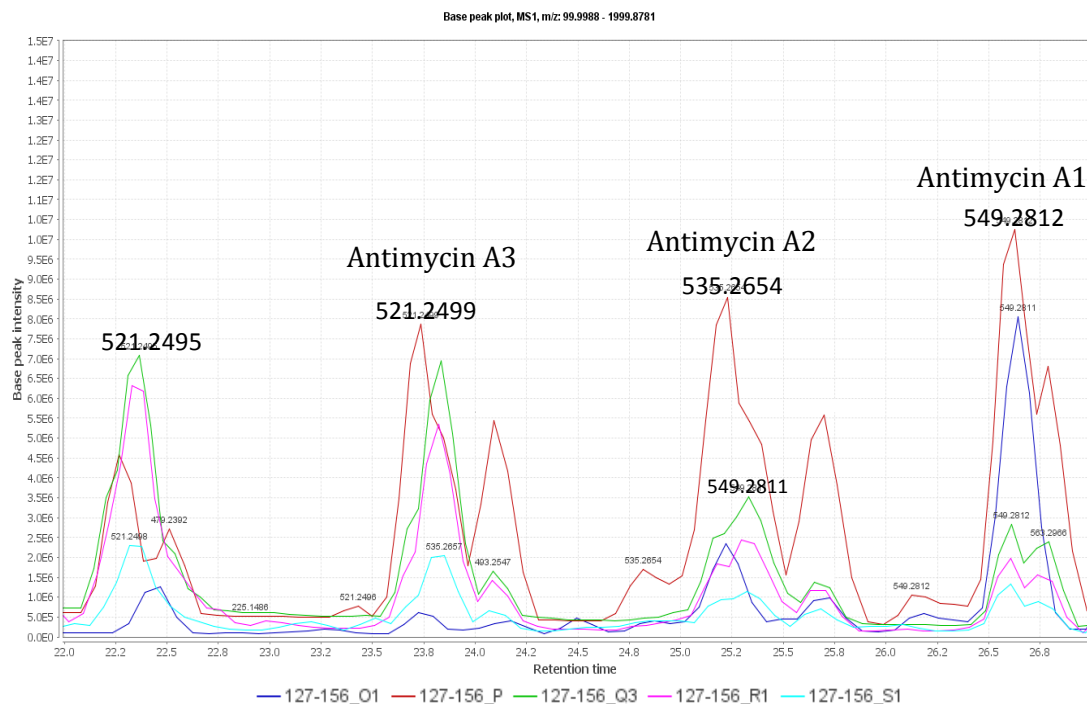


Figure 4-30: Total ion chromatograms of the antifungal 127-156 fractions showing the antimycin peaks. The samples are coloured as follows: O1 (dark blue), Q3 (green), P (red), R1 (pink), S1 (light blue).

Fraction P evidently had the greatest quantity of antimycins, particularly antimycin A2. This correlated well with the activity as P had the greatest antifungal activity. Fraction O1 possessed mostly antimycin A1 (549.2812 $[\text{M}+\text{H}]^+$). Fractions Q3 and R1 had very similar spectra. They had higher concentrations of antimycin A3 (521.2499 $[\text{M}+\text{H}]^+$) and lower concentrations of antimycin A1 and A2. S1 followed the same pattern but the peak areas were even less than those of Q3 and R1. Antimycins were also detected, albeit with much smaller peak areas, in fractions S2-W1. The comparison of the ^1H NMR spectra in Figure 4-31 below also confirmed the presence of antimycin A in Fraction 127-156P. Antimycin A peaks were also found in O1, S1 and faintly in S2. ^1H NMR analysis of Q3 and R1 was not performed.

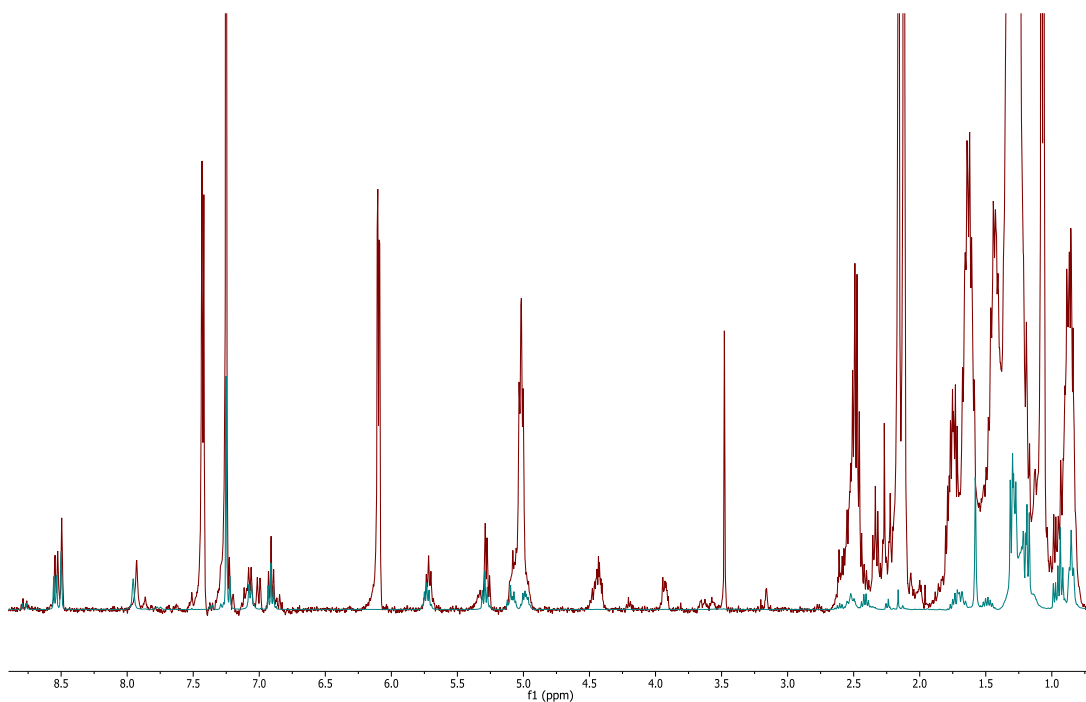


Figure 4-31: Overlap of ^1H NMR spectra of 127-156P (red) and antimycin A standard (teal). The similarity of the two spectra confirms the presence of antimycin compounds in 127-156P, accounting for its antifungal activity.

Fraction U1 was further separated using the Biotage[®] flash chromatography system. The weights and activities of the fractions are reported in Table 4-15 below. Fraction U1_320-349 was found to be a mixture of butenolides 1 and 2.

Table 4-15: Yields and activities of fractions from 127-156_U1 following Biotage® flash chromatography. The structure of 320-349, highlighted in grey, was elucidated.

Fraction	Yield (mg)	Antifungal activity (<i>C. albicans</i>)		Anti-calcineurin activity
		MIC µg/ml	Number of wells	
2-62	0.9	-	-	-
63-92	0.8	12.5	3	-
93-143	0.8	25	2	-
144-149	0.7	50	1	-
150-178	1.7	50	1	-
179-209	0.4	25	2	-
210-235	1.4	50	1	-
236-299	1.1	50	1	-
300-319	0.7	-	-	-
320-349	2.0	-	-	+
350-367	1.6	-	-	-
368-410	1.5	-	-	-
411-434	0.2	N/A*	N/A*	N/A*
435-443	0.4	-	-	-
444-455	0.6	-	-	-
456-468	1.5	-	-	-
469-484	1.6	-	-	-
485-504	2.3	50	1	-
505-516	2.0	50	1	-
517-532	1.8	50	1	-
Wash1-3	1.0	50	1	-
Wash4-9	8.0	25	2	-
90:10 E:M1	0.6	50	1	-
90:10 E:M2	4.3	50	1	+
80:20 E:M	4.2	50	1	+
50:50 A:M1	3.0	-	-	+
50:50 A:M2	1.6	-	-	-
50:50 A:M3	1.5	-	-	-
100% A	0.3	-	-	-

* - assay was not performed on this fraction due to the small quantity.

The NMR spectra of Fractions 127-156P, 127-156S1, 127-156S2, and 127-156U1_320-349 were similar to that of Fraction 110-126_D, indicating that these fractions also contained butenolides. However, unlike Fraction 110-126_D, these fractions had anti-calcineurin activity. Although 127-156P possessed a different butenolide from all of the other fractions, for the others the only difference lay in the ratio of the two compounds within each fraction as clearly illustrated in Figure 4-33.

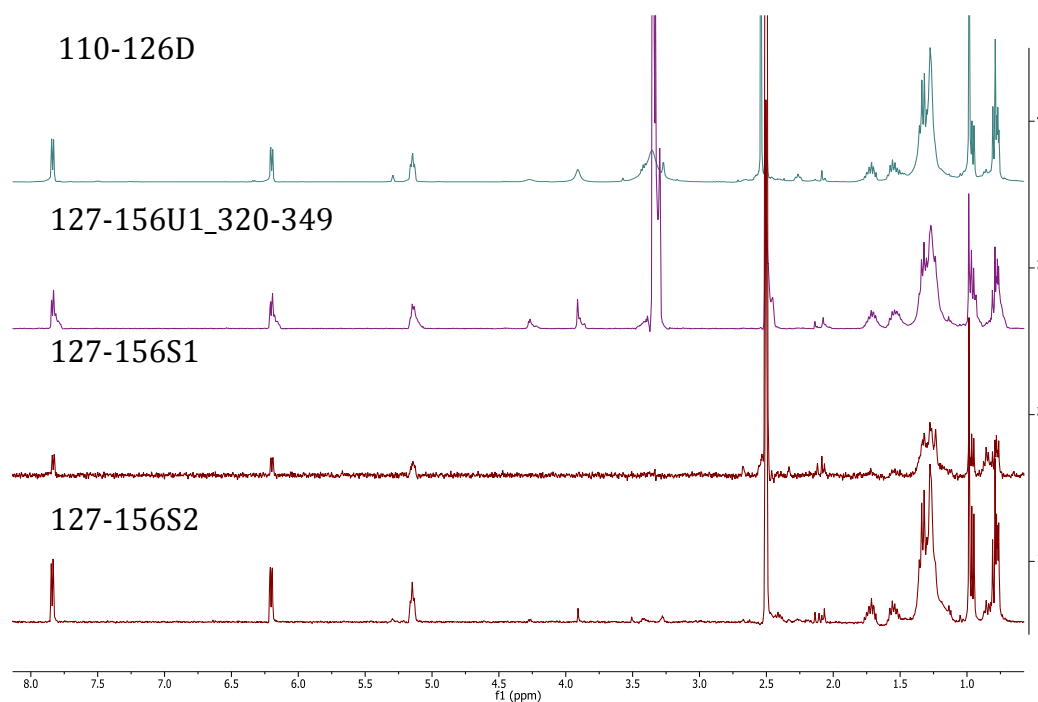


Figure 4-32: ^1H NMR spectra of the SM8 fractions containing butenolides **1** and **2**. They were all dissolved in DMSO and analysed at 400 MHz except 127-156U1_320-349 which was at 600 MHz. It is clearly evident from the spectra that all of the fractions contain butenolides.

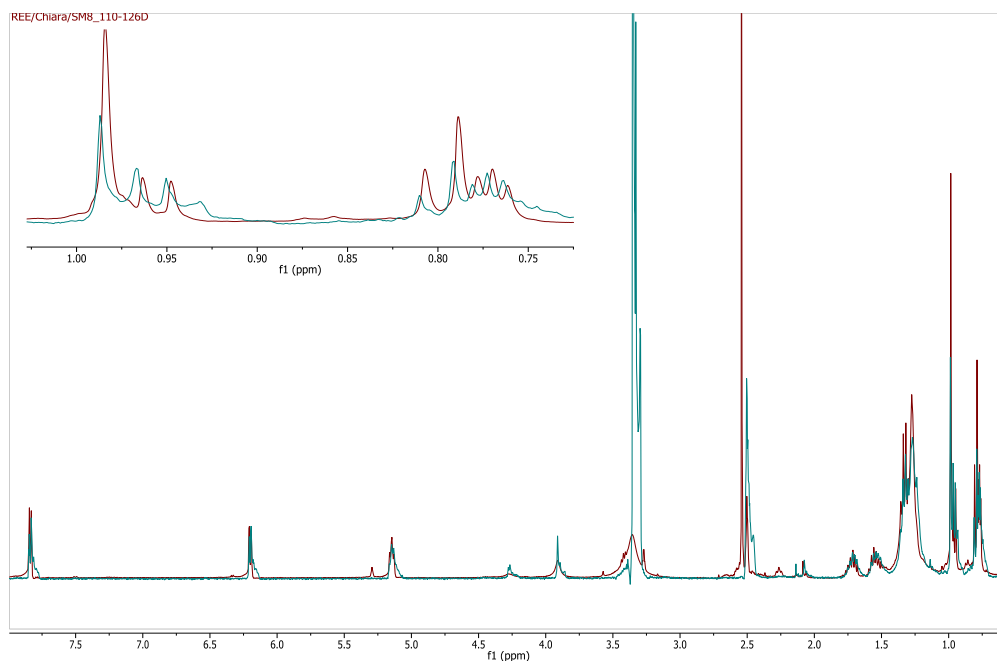


Figure 4-33: ^1H NMR spectra of Fraction 110-126_D (inactive) in red and Fraction 127-156_U1_320-349 (active) in teal. The expansion in the upper right corner shows the peaks in the aliphatic region. Although the peaks corresponding to the butenolide ring are approximately the same height, the peaks in the aliphatic region differ in intensity, denoting differences in the ratio of the two components.

It can be seen from Figure 4-33 above that the red singlet at 0.99 ppm, belonging to 13-CH₃ of butenolide 1, was of higher intensity than that of the teal singlet at the same chemical shift. The two peaks belonging to the doublet beside it, at 0.95 and 0.96 ppm, however, were almost the same intensity for the two fractions. This doublet corresponded to 12-CH₃ of butenolide 2. This indicated that the ratio of the two butenolides in each fraction varied. The ratios were calculated by getting the integration of the peaks.

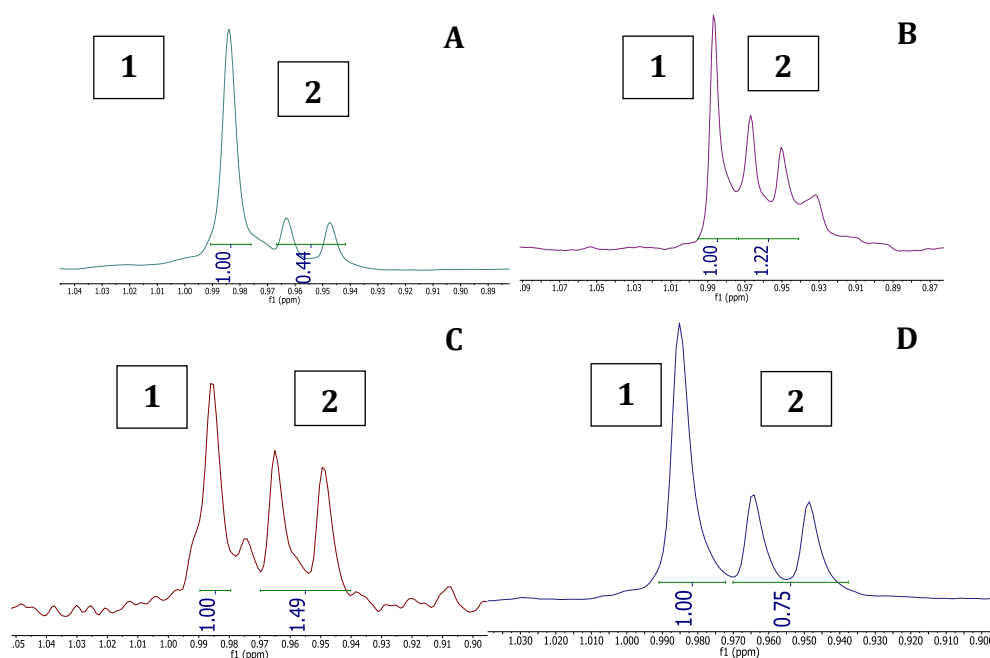


Figure 4-34: The integration of peaks 1 and 2 in (A) Fractions 110-126D, (B) 127-156U1_320-349, (C) 127-156S1 and (D) 127-156S2. Peak 1, which belonged to butenolide 1, was consistently given an integration value of 1.00. The corresponding value of peak 2 varied according to the ratio of the two butenolides.

In Figure 4-34 above, the peak labelled ‘1’ belongs to butenolide 1 (as labelled in Table 4-11), whereas the peaks labelled ‘2’ belong to butenolide 2. Peak 1 was assigned the value of 1 proton in each spectrum, and the number of protons represented in peak 2 was calculated as a ratio to peak 1. The integration values and corresponding percentages are shown in Table 4-16.

Table 4-16: Integration values and percentages of butenolides 1 and 2 in Fraction 110-126D, Fraction 127-156U1_320-349, Fraction 127-156S1 and Fraction 127-156S2.

Fraction	Anti-calcineurin activity	Peak 1	Peak 2	Butenolide 1 (%)	Butenolide 2 (%)
D	-	1.00	0.44	69.44	30.56
320-349	+	1.00	1.22	45.05	54.95
S1	+++	1.00	1.49	40.16	59.84
S2	+	1.00	0.75	57.14	42.86

The amount of butenolide 2 was significantly less in the inactive fraction (D) but was present in greater quantities in all of the active fractions. Fraction S1 had the greatest percentage of butenolide 2 and also possessed the greatest anti-calcineurin activity. It is therefore likely that butenolide 2 was the isomer that was active against calcineurin signalling. Although S2 appeared to contain a greater amount of butenolide 1, the fraction still had mild activity indicating that a sufficient amount of butenolide 2 was present in the fraction. The presence of these butenolides in each fraction was confirmed using high resolution LC-MS. The extracted ion chromatogram of each fraction can be seen in Figure 4-35 below.

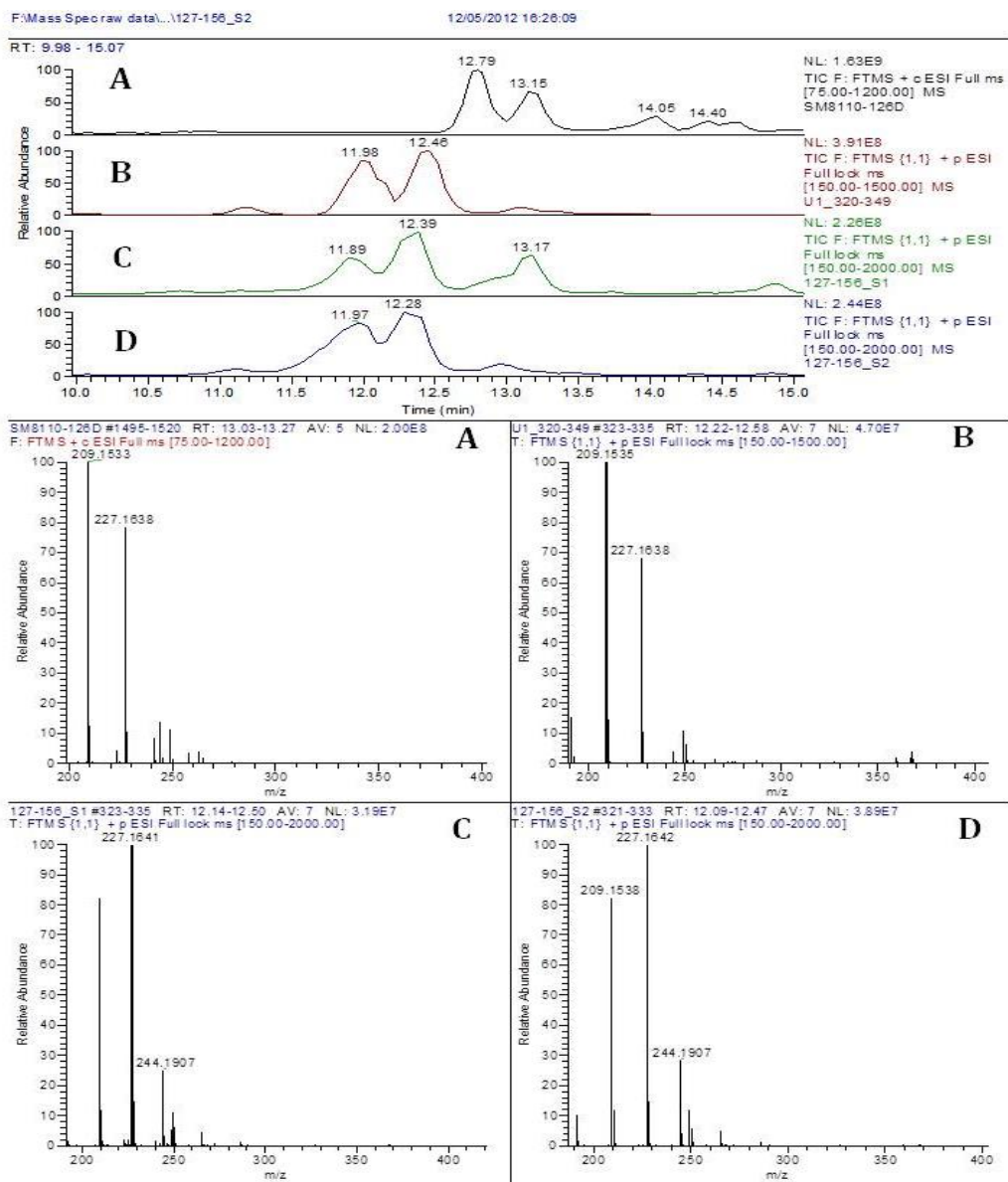


Figure 4-35: Extracted ion chromatogram and mass spectra of butenolide-containing fractions showing m/z 227.16-227.18 $[M+H]^+$. (A) 110-126D, (B) 127-156U1_320-349, (C) 127-156S1, (D) 127-156S2. 110-126D was analysed on a different instrument hence the shift in retention time.

SM8_110-126D and SM8_127-156S1 were tested for quorum signalling activity against *Chromobacterium violaceum* CV026. Figure 4-36 showed the results of the TLC overlay assay. *C. violaceum* CV026 is a modified strain that lacks the ability to produce N-hexanoyl-homoserine lactone (HHL), the signalling molecule it requires in order to produce a violet pigment called violacein. The weak violet colouration seen on the TLC plate proved that the butenolides were mild activators of the quorum signalling pathway of *C. violaceum* CV026. The LC-MS data of fraction D

and S1 were analysed to determine the presence of any acylhomoserine lactones (AHLs), the autoregulatory factors of *C. violaceum*. AHLs are typical products of Gram-negative bacteria and none have been isolated from *Streptomyces* strains before. It was therefore not surprising that no AHLs were detected in the LC-MS spectra, indicating that the quorum signalling activity came wholly from the butenolides. Several butenolides isolated from *S. antibioticus* TÛ 99 have also shown stimulatory activity towards the production of violacein in *C. violaceum* CV026 (Grossmann et al., 2003), although other butenolides from the same strain inhibit violacein production (Martinelli et al., 2004).

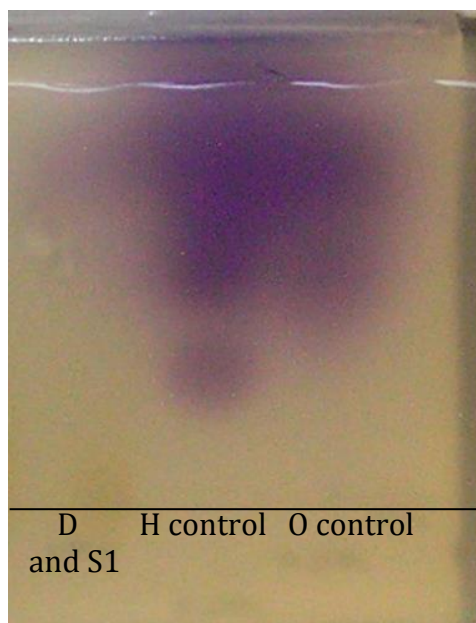


Figure 4-36: Reverse phase TLC plate overlaid with *C. violaceum* CV026. The violet spots indicate activation of violacein production by *C. violaceum* even without the presence of endogenous HHL, the regulator of *C. violaceum*.

4.3.5 Comparison of Endosymbiont and Host Sponge Metabolic Profiles

The extracts of SM8 were compared with those of the host sponge, *H. simulans*. This was performed using LC-HRFTMS. There were many compounds that were present in both the sponge and the bacterial extracts as evidenced in Figure 4-37.

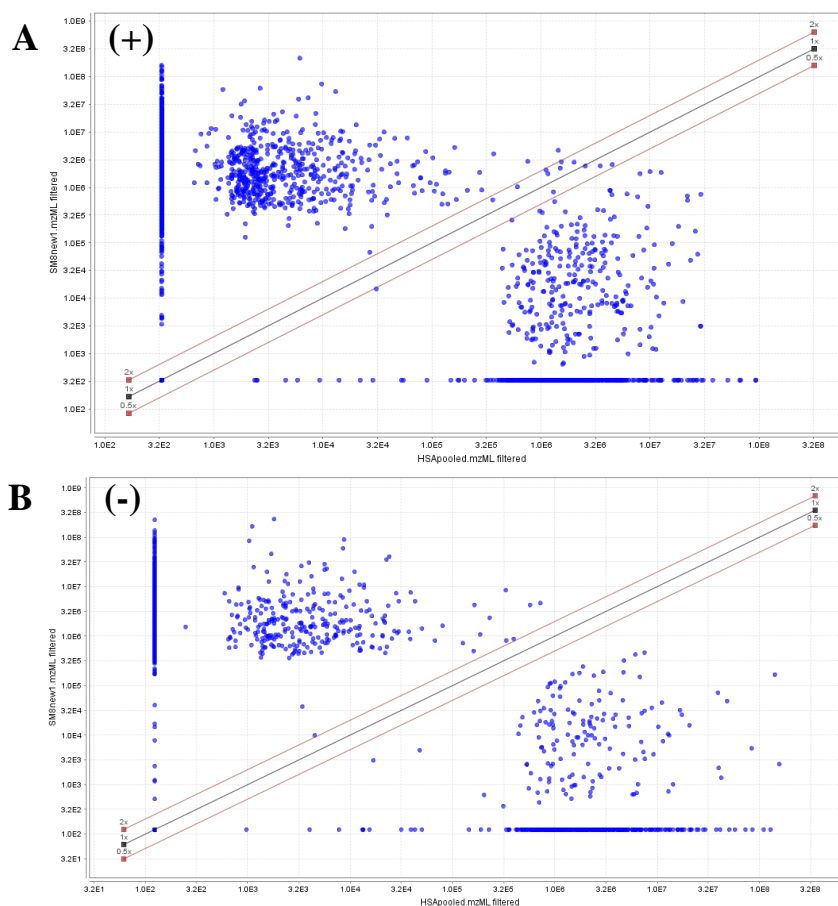


Figure 4-37: Scatter plot comparisons of HSA (x-axis) and SM8_1 (y-axis) in (A) positive ionisation and (B) negative ionisation mode. The peaks along the x-axis and y-axis are present solely in the sponge and SM8 extracts, respectively, whereas those in the middle of the graph are common to both samples.

The scatter plots showed that there were common metabolites present in the sponge and bacteria, as well as metabolites that were more specific to the sponge or to the bacteria. Metabolites that lie in the middle of the graph are common to both HSA and SM8. Those that lie above the diagonal are more intense in SM8 whereas those that lie below the diagonal are more intense in HSA. The compounds that form a line along the y-axis are found only in SM8 whereas those that form a line along the x-axis are only found in HSA. The common metabolites which were most intense in both HSA and SM8_1 (peak area $\geq 1.0E5$) are shown in Figure 4-38. The identification is shown in Table 4-17 and Table 4-18.

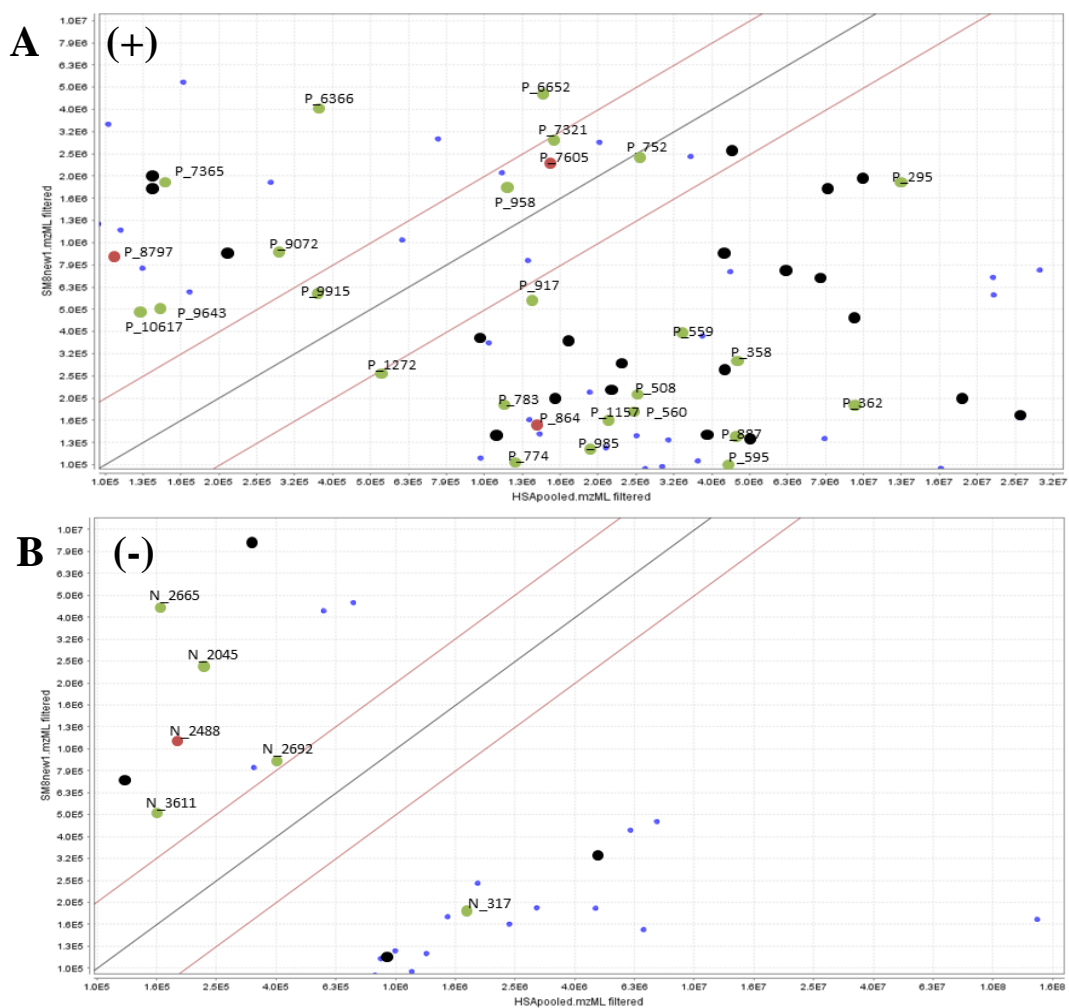


Figure 4-38: Common metabolites in HSA and SM8_1 extracts with peak areas $\geq 1.0E5$. (A) Positive ionisation mode. (B) Negative ionisation mode. Blue circles are unidentified; black circles are metabolites previously isolated from fungi, algae and other marine invertebrates; green circles are those previously isolated from sponges and/or bacteria; red circles are those isolated from *Haliclona* sp.

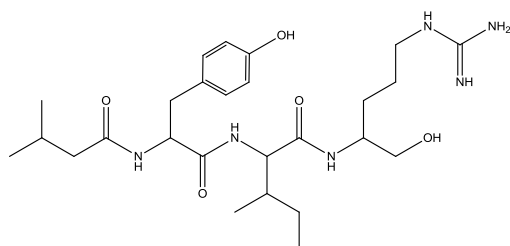
Table 4-17: Common metabolites present in the extracts of HSA and SM8_1 (positive ionisation). The compounds were putatively identified using the AntiMarin 2012 database. Only those from sponges or bacteria are included in the table.

Mol_ID	m/z	RT	Formula	Name	Source	Reference
P_6552	521.3450	19.69	C ₂₆ H ₄₄ N ₆ O ₅	[27] WA-3854-D	[B] <i>Streptomyces</i> sp. WA3854 P11784	
P_752	295.1649	4.00	C ₁₅ H ₂₂ N ₂ O ₄	[28] 1328-3; Cyclocarbamide B	[B] <i>Streptoverticillium</i> sp.	(Isogai et al., 1986)
				[29] (2S,3R)-3-Amino-2-hydroxy-1-phenylbutanoyl-L-valine	[B] <i>Streptomyces neyagawaensis</i> SL-387 + DL-3-amino-3-phenylpropionic	(Chung et al., 1996)
P_7321	295.1651	4.00	C ₁₅ H ₂₂ N ₂ O ₄	[28] 1328-3; Cyclocarbamide B	[B] <i>Streptoverticillium</i> sp.	(Isogai et al., 1986)
				[29] (2S,3R)-3-Amino-2-hydroxy-1-phenylbutanoyl-L-valine	[B] <i>Streptomyces neyagawaensis</i> SL-387 + DL-3-amino-3-phenylpropionic	(Chung et al., 1996)
P_7605	206.0812	6.62	C ₁₁ H ₁₁ NO ₃	[30] Indole-3-lactic acid	[B] <i>Streptomyces</i> sp. L083; marine <i>Streptomyces</i> sp. 7919	(Narayanan and Rao, 1976, Rigaud, 1970, Kaper and Veldstra, 1958)
				[31] 1-(3-Indolyl)-2,3-dihydroxypropan-1-one	[B] <i>Streptomyces violaceus</i> , marine	(Volkman et al., 1995)
				[32] 1-Hydroxymethyl-7-methoxyisoquinolinol	Porifera <i>Haliclona</i> sp	(Rashid et al., 2001)
P_958	243.1338	5.27	C ₁₁ H ₁₈ N ₂ O ₄	[33] Bicycloamid; tet+	[B] <i>Streptomyces albus</i> Tue 2031	
				[34] 3,7-Dihydroxy-cis,cis-1,8-nonadiene-1,9-dicarboxylic acid diamide	[B] marine actinomycete B 1758	(Smelcerovic et al., 2001)
				[35], [36]	Porifera <i>Asteropus</i> sp.	
P_9915	320.1852	14.93	C ₁₈ H ₂₅ NO ₄	[37] 9-(4-Aminophenyl)-7-hydroxy-2,4,6-trimethyl-9-oxo-non-2-enoic acid	[B] <i>Streptomyces griseus</i> subsp.	(Guan et al., 2005)
				[38]	Actinobacteria <i>Streptomyces</i> sp	(Guan et al., 2005)
P_6366	277.1181	6.65	C ₁₄ H ₁₆ N ₂ O ₄	[39] cyclo-(L-Tyrosyl-cis-4-hydroxy-D-proline)	[B] <i>Ruegeria</i> sp. from cell culture of sponge <i>Suberites domuncula</i>	(Mitova et al., 2004)
				[40] cyclo-(L-Tyrosyl-trans-4-hydroxy-L-proline)	[B] <i>Ruegeria</i> sp. from cell culture of sponge <i>Suberites domuncula</i>	
P_7365	232.0968	9.47	C ₁₃ H ₁₃ NO ₃	[41]	Porifera <i>Halichondria melanodocia</i>	(Gopichand and Schmitz, 1979)
				[42] 4-Hydroxy-5-(indole-3-yl)-5-oxopentanone	Porifera <i>Dysidea etheria</i> , Porifera <i>Ulosa ruetzleri</i>	(Cardellina et al., 1986)
				[43] Anthosamine A	Porifera <i>Anthosigmella raromicrosclera</i>	(Tsukamoto et al., 1995)
P_8797	247.1332	15.57	C ₁₅ H ₁₈ O ₃	[44] Hirsutanol-A	[F] marine fungus from sponge	(Wang et al., 1998)
				[45] Hirsutanol-B	<i>Haliclona</i> sp.	
				[46] Parahigginol D	Porifera <i>Epipolasis</i> sp, Porifera <i>Parahigginia</i> sp.	(Chen et al., 1999)
P_9072	734.4320	15.87	C ₃₇ H ₅₉ N ₅ O ₁₀	[47] Onnamide E	Porifera <i>Theonella</i> sp	(Matsunaga et al., 1992)
P_9897	229.1004	5.06	C ₁₀ H ₁₆ N ₂ O ₂ S	[48] Cyclo-(L-Pro-L-Met)	[B] sponge-associated <i>Pseudomonas aeruginosa</i>	(Jayatilake et al., 1996)
				[49] Cyclo-(L-proline-L-methionine)	Proteobacteria <i>Pseudomonas aeruginosa</i>	(Jayatilake et al., 1996)
P_10617	242.1498	3.13	C ₁₁ H ₁₉ N ₃ O ₃	[50] Leuhistin	[B] <i>Bacillus laterosporus</i>	(Yoshida et al., 1991)

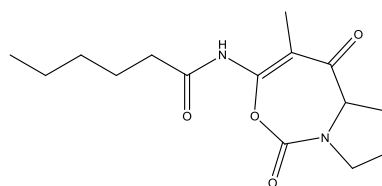
					bmi156-14f1	
P_9643	499.2886	14.11	C ₂₆ H ₄₂ O ₉	[51] Pseudomonic acid D	[B] <i>Pseudomonas fluorescens</i> (ncib 10586)	(O'Hanlon et al., 1983)
P_407	233.1171	14.63	C ₁₄ H ₁₆ O ₃	[52] Pichiafuran A	[Y] sponge-derived <i>Pichia membranaefaciens</i>	(Elbandy et al., 2008)
P_295	482.3230	18.97	C ₂₃ H ₄₈ NO ₇ P	[53] Pichiafuran C	Porifera <i>Stelletta</i> sp	(Zhao et al., 2003)
P_1272	175.0867	4.02	C ₁₀ H ₁₀ N ₂ O	[54] Stellettacholine B	[M] myxobacteria	(Bohlendorf et al., 1996)
				[55] 3-Indolylacetaldoxime	[An] Porifera <i>Dysidea etheria</i> , <i>Ulosa ruetzleri</i>	(Cardellina et al., 1986)
P_917	265.1545	5.02	C ₁₄ H ₂₀ N ₂ O ₃	[56] 3-Indolylacetic acid amide; indole-3-acetamide	[B] <i>Streptomyces albospinus</i> A19301, marine Actinomycete CNH741	(Makkar et al., 1995)
				[57] Phenamide	[B] marine-derived <i>Streptomyces</i> sp.	(Bugni et al., 2006)
				[58] Bohemamine B		
				[59] Bohemamine C		
P_783	288.2032	1.48	C ₁₂ H ₂₅ N ₃ O ₃	[60] Ile-Arg		
P_559	263.1388	5.29	C ₁₄ H ₁₈ N ₂ O ₃	[61] Bohemamine	[B] <i>Actinosporangium</i> sp.	(Doyle et al., 1980, Nettleton et al., 1980)
P_358	432.2382	17.80	C ₂₄ H ₃₃ NO ₆	[62] Nakijiquinone C	Porifera	(Kobayashi et al., 1995a)
				[63] Metachromin P	Porifera <i>Spongia</i> sp	(Takahashi et al., 2007)
				[64] Metachromin Q		
P_864	206.0811	6.72	C ₁₁ H ₁₁ NO ₃	[65] 4,7-Dihydro-6-methoxy-2,5-dimethyl-2H-isoindole-4,7-dione	[An] sponge <i>Reniera</i> sp.	(Frincke and Faulkner, 1982)
				[30] beta-Indole-lactic acid; Indole-3-lactic acid	[B] <i>Agrobacterium tumefaciens</i> , <i>Acetobacter xylinum</i> ., [B] <i>Streptomyces</i> sp. L083; marine <i>Streptomyces</i> sp. 7919	(Narayanan and Rao, 1976, Rigaud, 1970, Kaper and Veldstra, 1958)
				[31] 1-(3-Indolyl)-2,3-dihydroxypropan-1-one	<i>Streptomyces</i> sp. B8042	(Volkman et al., 1995)
				[32] 1-Hydroxymethyl-7-methoxyisoquinolinol	Porifera <i>Haliclona</i> sp	(Rashid et al., 2001)
P_774	318.1809	7.88	C ₁₇ H ₂₃ N ₃ O ₃	[66] (-)-2-Oxyindolactam V	[B] <i>Streptoverticillium blastmyceticum</i>	(Koshimizu et al., 1985)
P_1157	328.2230	4.45	C ₁₆ H ₂₉ N ₃ O ₄	[67] Valylprolylisoleucine; Diprotin C	[B] <i>Bacillus cereus</i>	
				[68] Valylprolylleucine; Diprotin B	[B] <i>Bacillus cereus</i> bmf 673-rf1 (FERM-p 6623)	(Umezawa et al., 1984)
P_985	468.3086	21.88	C ₂₉ H ₄₁ NO ₄	[69] Cyclo-Delaminomycin A	[B] <i>Streptomyces albulus</i> MJ202-72F3	(Ueno et al., 1993a, Ueno et al., 1993b, Ueno et al., 1993c)
P_508	437.1925	17.62	C ₂₁ H ₂₈ N ₂ O ₈	[70] Deisovalerylblastmycin	[B] S. sp. 5140-a; marine <i>Streptomyces</i> sp. B1751	
P_560	608.3780	17.53	C ₃₃ H ₅₃ NO ₉	[71] 3-O-Acetyl M-4365 G2	[B] <i>Streptoverticillium kitasatoensis</i> ka-429, <i>Streptomyces</i>	(Sadakane et al., 1982)
P_595	189.1233	2.97	C ₈ H ₁₆ N ₂ O ₃	[72] Ne-Acetyl-beta-lysine	[B] <i>Methanosarcina thermophila</i> (nonmarine archaeobacterium)	(Sowers et al., 1990)
P_887	342.2386	5.75	C ₁₇ H ₃₁ N ₃ O ₄	[73] Diprotin A	[B] <i>Bacillus cereus</i> bmf 673-rf1 (FERM-p 6623)	(Umezawa et al., 1984)
P_362	279.1700	6.67	C ₁₅ H ₂₂ N ₂ O ₃	[74] 2-(1-Amino-2-hydroxy-4-enyl)-5-methoxy-N-methylbenzamide	[B] <i>Pseudomonas cepacia</i> 5798	(Smirnov et al., 1991)
				[75] Terragine C	[B] DNA isolated from soil expressed in a <i>Streptomyces lividans</i> host	(Wang et al., 2000)

Table 4-18: Common metabolites present in the extracts of HSA and SM8_1 (negative ionisation). The compounds were putatively identified using the AntiMarin 2012 database. Only those from sponges or bacteria are included in the table.

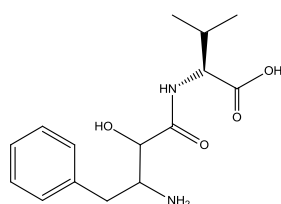
Mol_ID	m/z	RT	Formula	Name	Source	Structure
N_2665	381.2654	21.63	C ₂₂ H ₃₈ O ₅	[76] 3-Anteisoheptadecanoyl-5-hydroxymethyl tetronic acid	[B] Actinomycete strain DSM 7357	(Roggo et al., 1994a)
N_2045	230.0825	8.55	C ₁₃ H ₁₃ NO ₃	[41]	Porifera <i>Halichondria melanodocia</i>	(Gopichand and Schmitz, 1979)
				[42] 4-Hydroxy-5-(indole-3-yl)-5-oxopentanone	Porifera <i>Dysidea etheria</i> , Porifera <i>Ulosa ruetzleri</i>	(Cardellina et al., 1986)
				[43] Anthosamine A	Porifera <i>Anthosigmella raromicrosclera</i> , Chordata <i>Halocynthia roretzi</i>	(Tsukamoto et al., 1995)
N_2488	204.0669	8.19	C ₁₁ H ₁₁ NO ₃	[65] 4,7-Dihydro-6-methoxy-2,5-dimethyl-2H-isoindole-4,7-dione	Porifera <i>Reniera</i> sp	(Frincke and Faulkner, 1982)
				[32] 1-Hydroxymethyl-7-methoxyisoquinolinol	Porifera <i>Haliclona</i> sp	(Rashid et al., 2001)
N_3611	335.2235	21.42	C ₂₀ H ₃₂ O ₄	[77] Shahamine E	Porifera <i>Dysidea</i> sp	(Carmely et al., 1988)
				[78] Halilactone	Porifera <i>Halichondria okadai</i>	(Niwa et al., 1989)
				[79] Topsentolide B2	Porifera <i>Topsentia</i> sp	(Luo et al., 2006a)
				[80] Topsentolide B3		
[81] Phorbasin K	Porifera <i>Phorbas</i> sp	(Zhang et al., 2008)				
N_2692	271.2282	26.21	C ₁₆ H ₃₂ O ₃	[82] 2-Methoxypentadecanoic acid	Porifera <i>Callispongia fallax</i>	(Carballeira and Pagán, 2001)
N_317	241.1198	5.18	C ₁₁ H ₁₈ N ₂ O ₄	[35], [36]	Porifera <i>Asteropus</i> sp.	



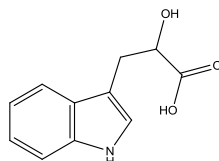
[27]



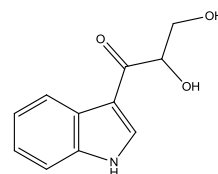
[28]



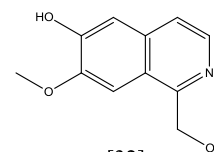
[29]



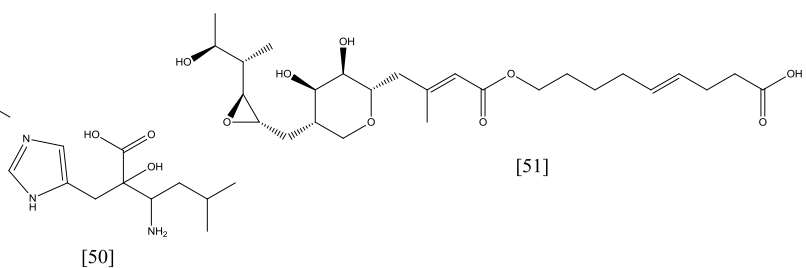
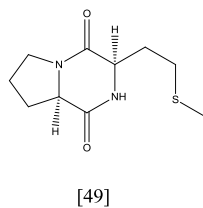
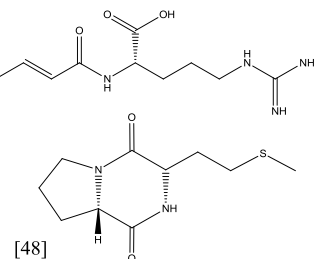
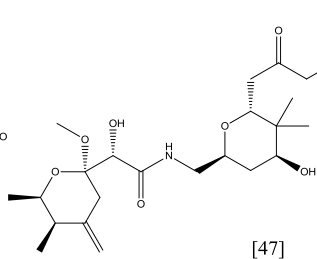
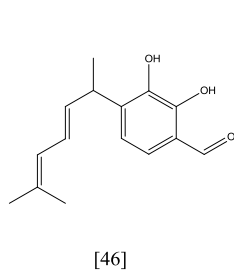
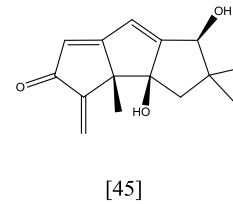
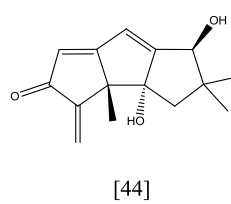
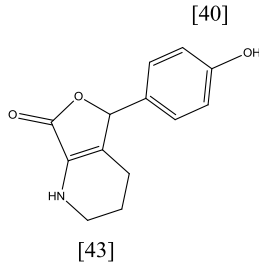
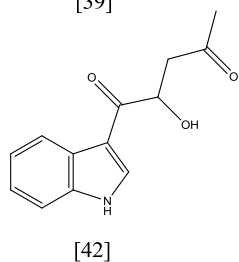
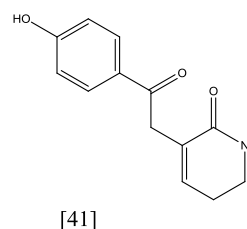
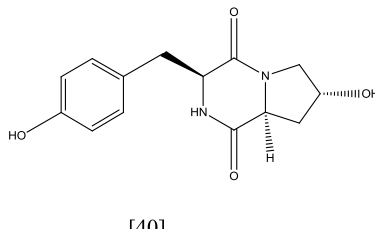
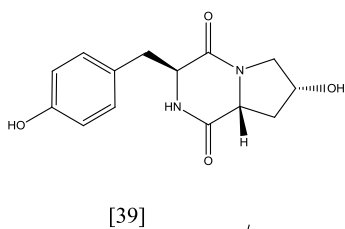
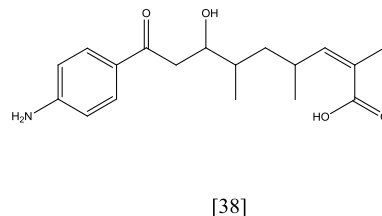
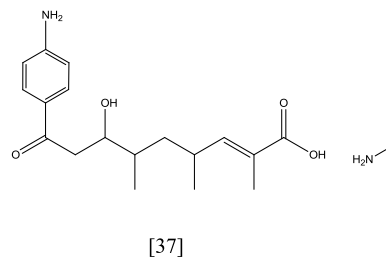
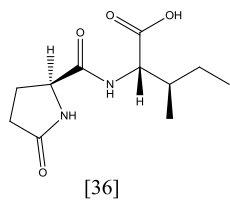
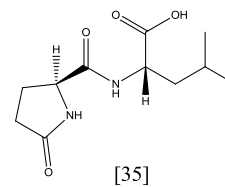
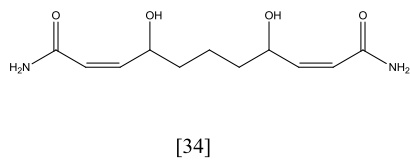
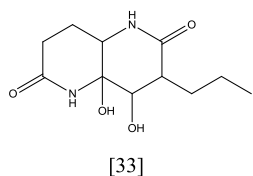
[30]



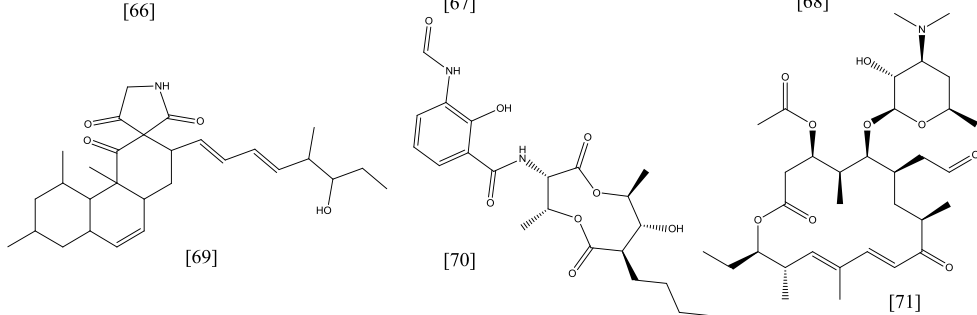
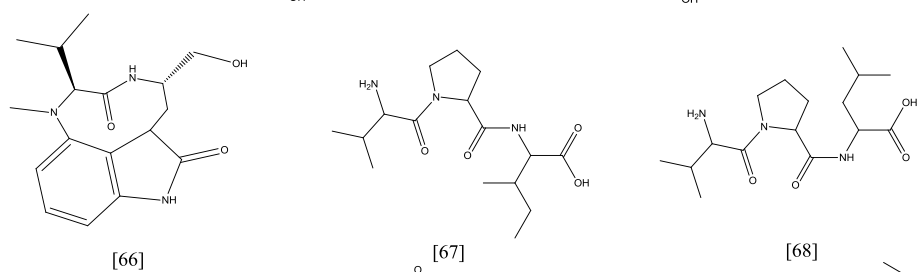
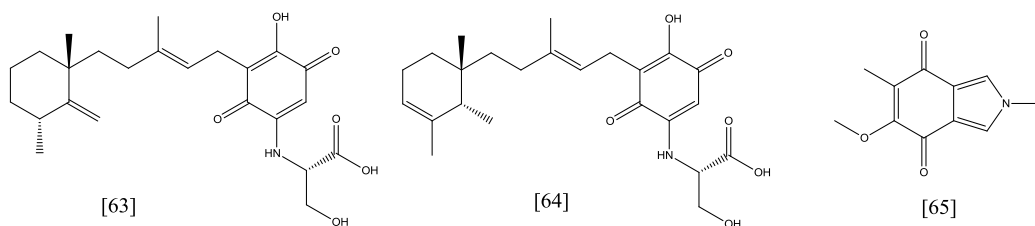
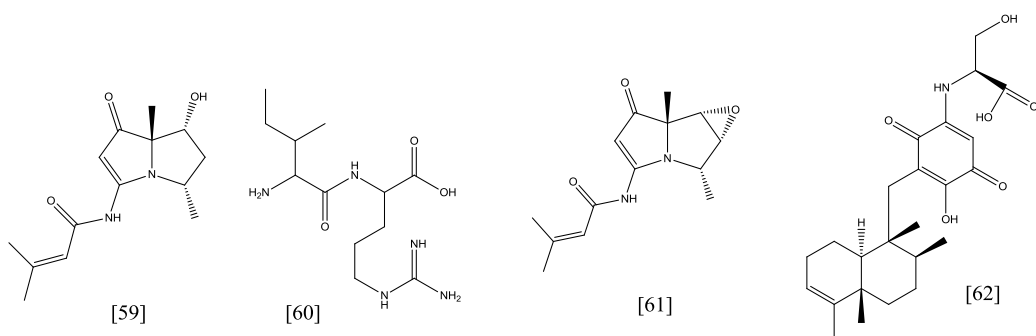
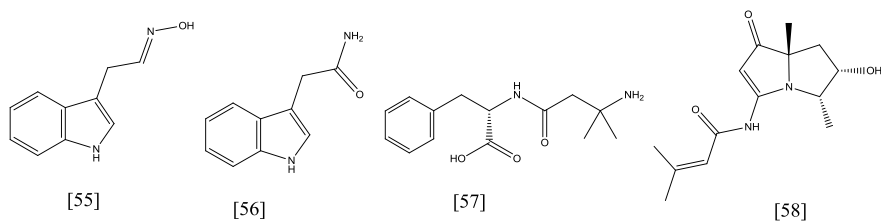
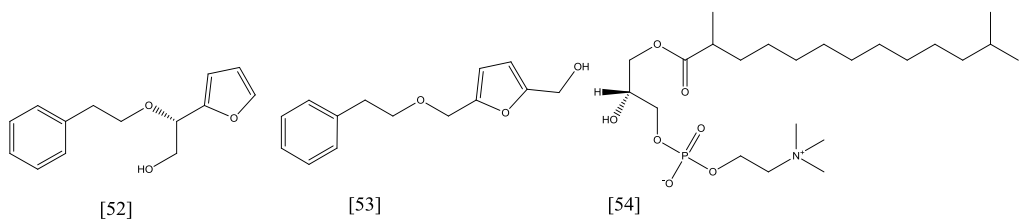
[31]



[32]



[51]



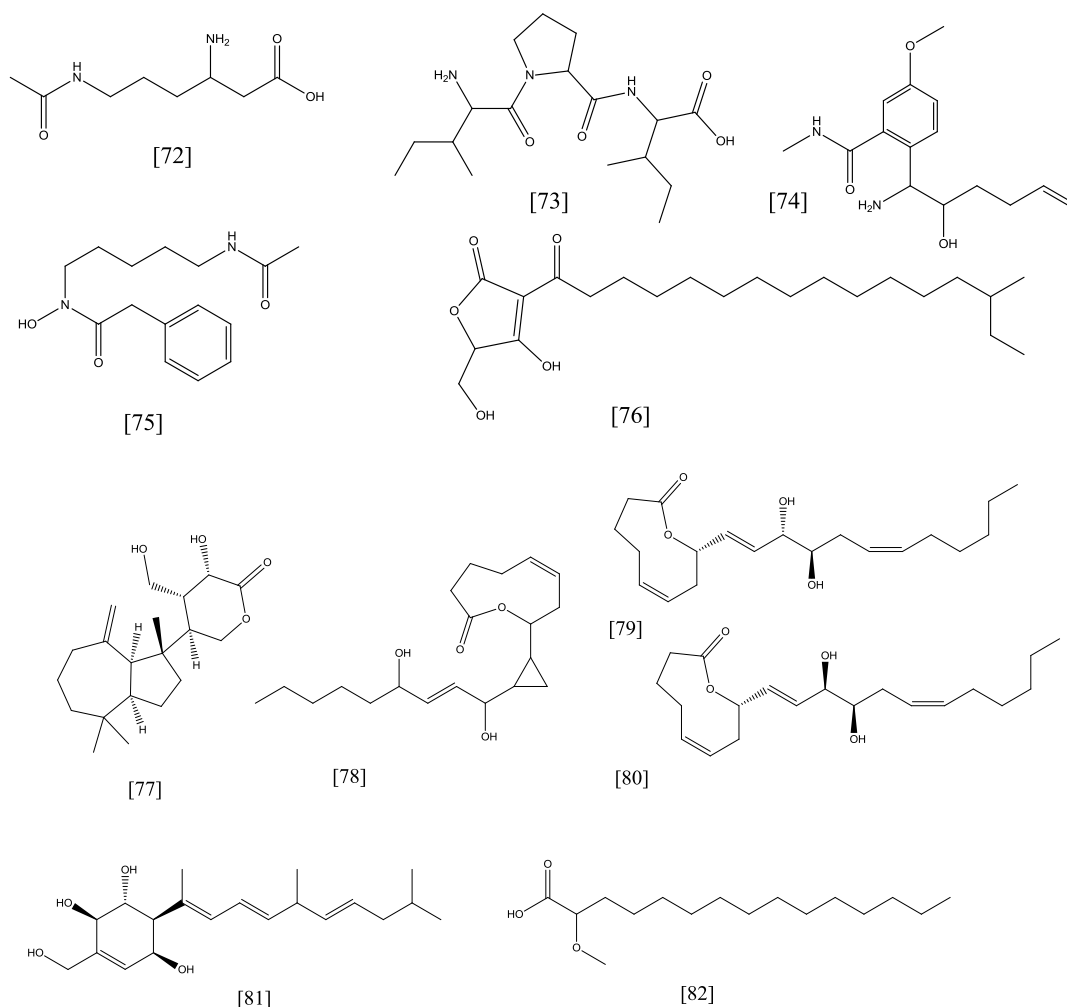


Figure 4-39: Structures of compounds from sponges and bacteria that have been putatively identified using the AntiMarin 2012 database.

As observed in Table 4-17 and Table 4-18, many of the identified metabolites have previously been isolated from other sponge species or *Streptomyces* sp. Although the structures of these compounds have yet to be proven through isolation of the compounds, it is likely that these or related isomers are being produced by SM8. Several of the putative compounds are low molecular weight peptides (**27**, **29**, **39**, **40**, **48**, **49**, **60**, and **65**) that are possibly produced by one of the NRPS gene clusters in SM8. Indeed, both WA-3854-D (**27**) and (2S,3R)-3-amino-2-hydroxy-1-phenylbutanoyl-L-valine (**29**) are products of other *Streptomyces* strains. 9-(4-Aminophenyl)-7-hydroxy-2,4,6-trimethyl-9-oxo-non-2-enoic acid (**37**) is a truncated version of candicidin and may be a product of the candicidin pathway or as a degradation product. A candicidin gene cluster was found in SM8 but candicidin was not detected in any of the extracts. The antimycins that were identified as antifungal

compounds produced by SM8 were shown to be present in the *H. simulans* extract as well. Most of them were observed only in the SM8 extract but two (antimycin A1b and deisovaleryl-antimycin-A3) were present in HSA. The butenolides 1 and 2 were also observed in the HSA extract (Figure 4-40).

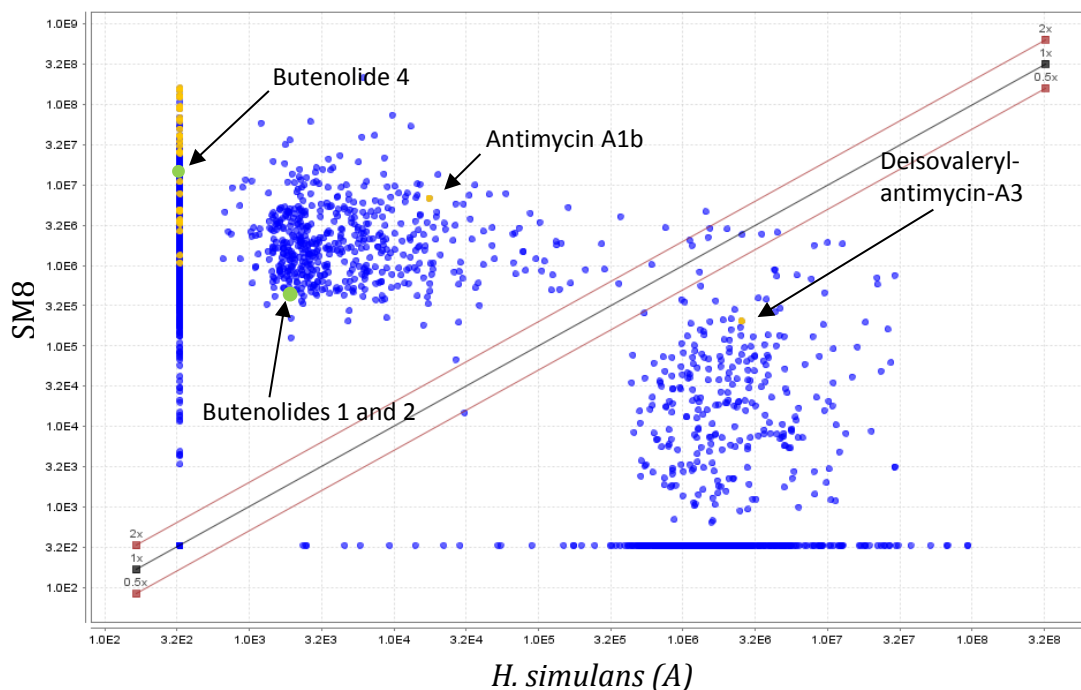


Figure 4-40: Scatter plot (positive ionisation) of HSA vs SM8_1. Metabolites identified as belonging to the antimycin family of compounds are highlighted in yellow whereas the isolated butenolides are highlighted in green.

Multivariate analysis was also performed using SIMCA 13. PCA was used initially to check for outliers and to ensure that the samples clustered together prior to their classification. OPLS-DA was then performed (Figure 4-41). An S-plot was generated and compared with the scatter plots to show the peak areas of the common metabolites (Figure 4-42).

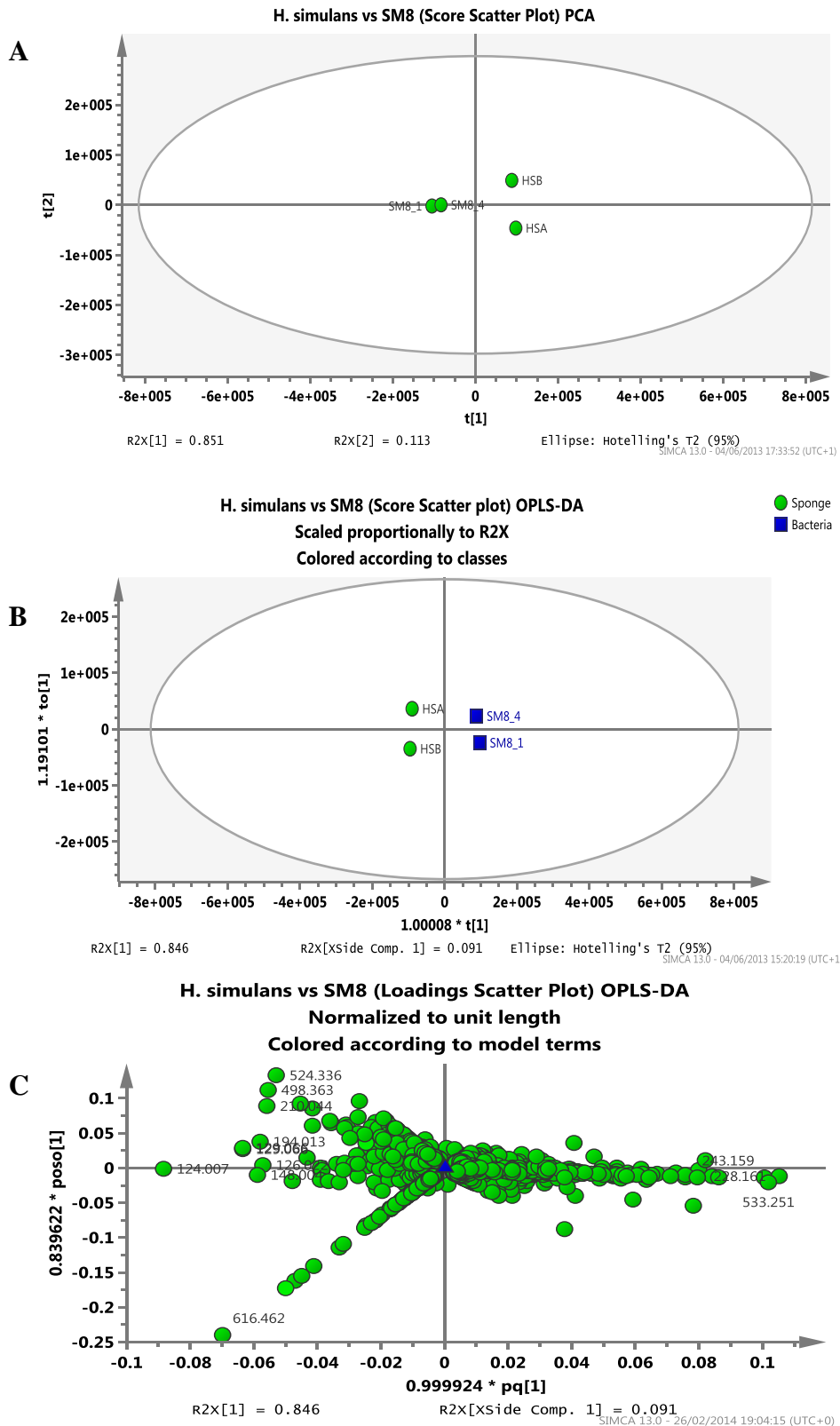


Figure 4-41: PCA and OPLS-DA of the *H. simulans* and SM8 extracts. (A) PCA scores plot of *H. simulans* vs. SM8. $R2(\text{cum})= 0.965$, $Q2(\text{cum})= 0.98$. (B) Scores plot and (C) loadings plot of the OPLS-DA model of *H. simulans* vs SM8. $R2X(\text{cum})= 0.937$, $R2Y(\text{cum})= 0.998$, $Q2(\text{cum})= 0.99$.

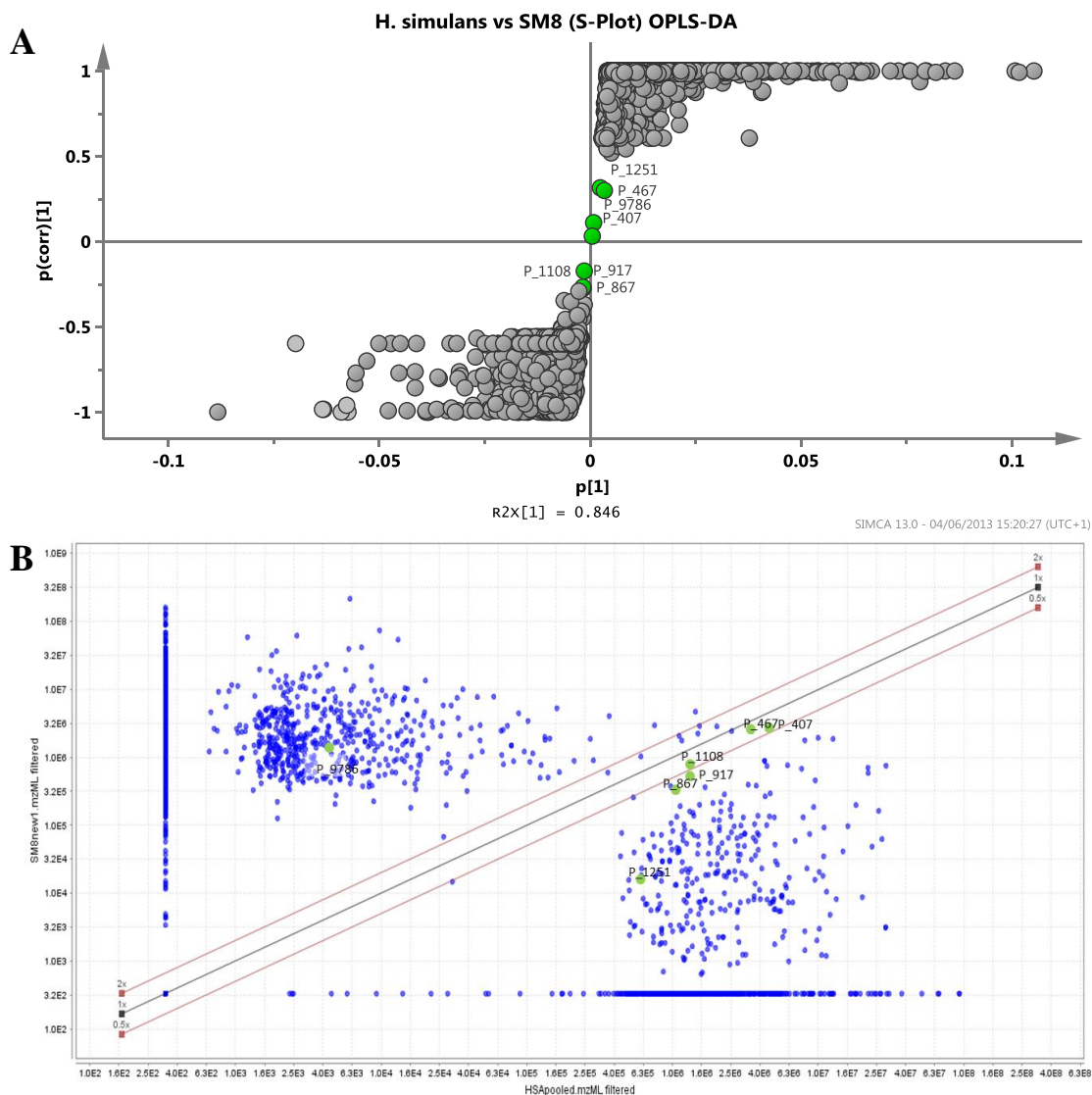


Figure 4-42: (A) S-plot and (B) positive ionisation mode scatter plot of *H. simulans* vs SM8. The peaks highlighted in green show the presence of common metabolites.

The S-plot is generally used to show the metabolites that contribute most to the separation of the classes. However, in this instance, the metabolites at the centre of the S-curve are of most interest as these are the ones that are present in both the host sponge and the sponge-associated bacteria. Only two of these metabolites (P_407 and P_917) were identified using the AntiMarin database. Two isomers of P_407 were found; these were pichiafuran A (**52**) and pichiafuran C (**53**). These two metabolites were first obtained from the yeast *Pichia membranifaciens* which was isolated from a sponge, *Petrosia* sp. (Elbandy et al., 2008). P_917 was putatively

identified as phenamide (**57**), bohemamine B (**58**) or bohemamine C (**59**). These three compounds are all products of *Streptomyces* strains (Makkar et al., 1995, Bugni et al., 2006).

The ethyl acetate-soluble components of *H. simulans* and SM8 were compared using GC-MS. Figure 4-43 shows the GC-MS chromatograms of *H. simulans* and SM8. It is evident that the sponge produces compounds with peaks that elute later from the column; that is, less volatile compounds that require a higher temperature to elute.

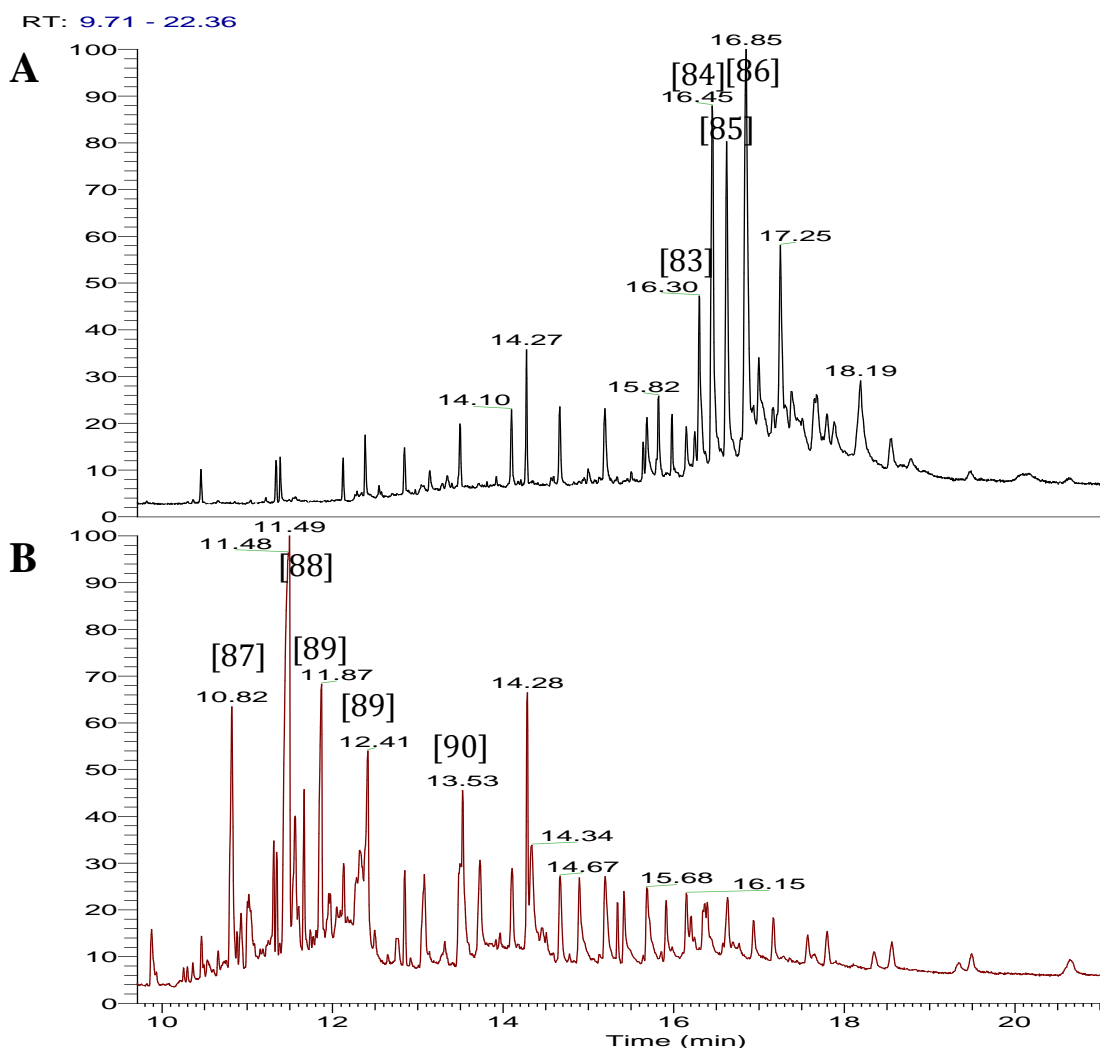


Figure 4-43: GC-MS chromatograms of *H. simulans* (A) and SM8 (B). Identified peaks are labelled. The sponge extract contained less volatile compounds that eluted from the column later than the SM8 metabolites.

The peaks present in the *H. simulans* sample at 15-17 minutes were identified using the in-house libraries. These were all determined to be steroids. In contrast, the SM8 extract contained smaller molecules that had retention times of 10-13 minutes.

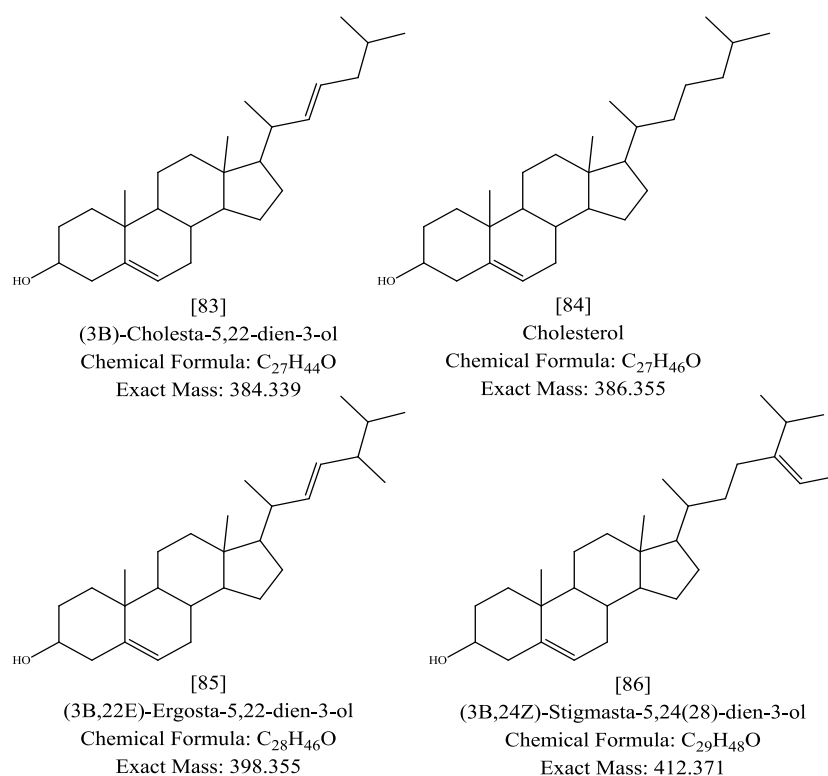


Figure 4-44: Steroids identified from the *H. simulans* extract using the NIST library.

These steroids were not isolated from the sponge, indicating that they may be present in smaller quantities than the three steroids that were isolated from *H. simulans*. All four (**83-86**) have previously been found in marine sources including sponges. The isolated *H. simulans* steroids 24-vinyl-cholest-9-ene-3 β ,24-diol and 5 α ,8 α -epidioxy-20-methyl-pregn-6-en-3 β -ol possess a greater number of oxygen atoms, increasing their polarity and thus making them more difficult to ionise in the GC-MS without derivatisation. One peak with an m/z of 398 [M]⁺ was putatively identified as ergosta-5,22-dien-3-ol (**85**). Although the m/z is the same as 24-methylenecholesterol, the fragmentation pattern matched that of ergosta-5,22-dien-3-ol more closely (Figure 4-45), hence proving that the peak indeed was ergosta-5,22-dien-3-ol and not 24-methylenecholesterol which was previously isolated from *H. simulans*.

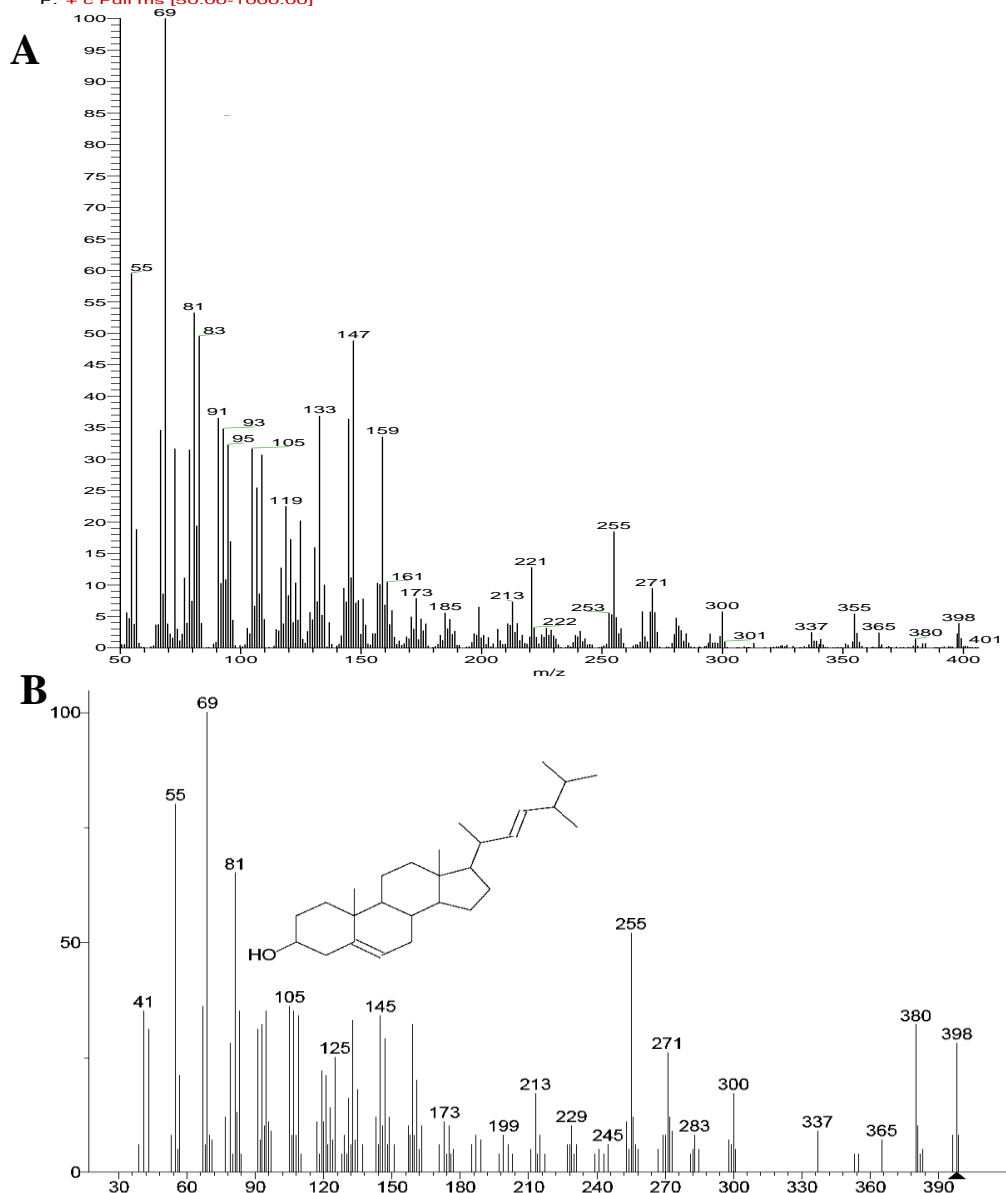


Figure 4-45: Comparison of (A) GC-MS spectrum of the peak with m/z 398 $[M^+]$ and (B) predicted spectrum for ergosta-5,22-dien-3-ol. The high degree of similarity between the two spectra proves the presence of ergosta-5,22-dien-3-ol in the sponge extract.

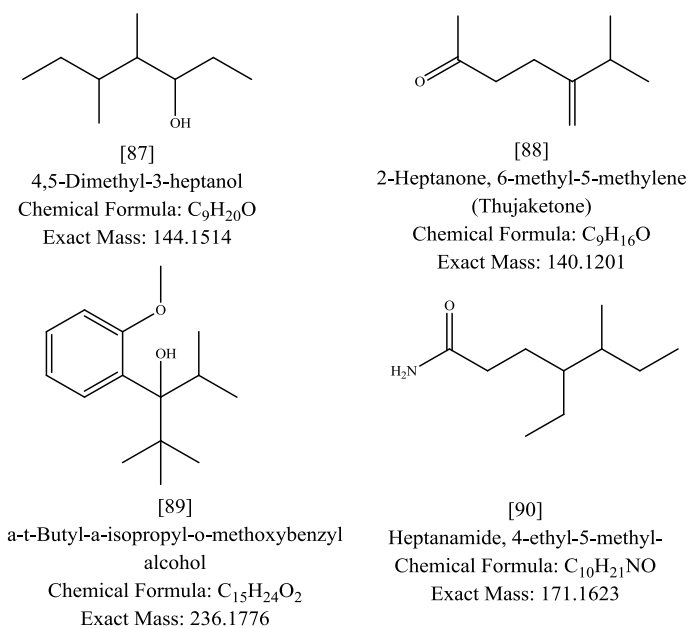


Figure 4-46: Expansion of the GC-MS chromatogram and the small molecules putatively identified in the SM8 extract using the in-house libraries.

Thujaketone (**88**) is commonly obtained from plants. However, its carbon skeleton is the same as the side chain of ergosterol (Werner and Bogert, 1938). It is possible that such small molecules produced by the bacteria are utilised by the sponge in the production of other compounds such as steroids. 4-Ethyl-5-methyl-heptanamide (**90**) has previously been isolated from a terrestrial *Streptomyces* sp. (Abdalla et al., 2011) as well as from freshwater green alga (Dembitsky et al., 2000). The spectrum for this compound, a fatty acid amide, contains a peak at m/z 59 that is characteristic of aliphatic primary amides (Dembitsky et al., 2000).

4.4 Discussion

The up-scale extracts of SM8 were found to produce more metabolites than the small-scale extracts hence they were selected for initial fractionation using normal phase MPLC. Similar to the extract of *H. simulans*, the non-polar fractions showed greater microbial activity. The fractions of SM8 were tested against *B. subtilis* and *C. albicans* and showed activity against both, although they possessed greater antifungal activity. None of the known compounds putatively identified by using MZmine 2.10 and the AntiMarin 2012 database appeared to be predominant in the active fractions, as evidenced by the NMR spectra that showed polyhydroxylated saturated fatty acids

as the major compounds. Polyhydroxy saturated fatty acids have previously been isolated from fungi such as *Ulocladium botrytis* and *Haematomma ventosum* (Girisham et al., 1986, Turner and Aldridge, 1983). The tetrahydroxy saturated fatty acids also comprise the aglycone portion of the deacetyl glykenins A-C which are glycosidic antibiotics produced by *Basidiomycetes* sp. (Nishida et al., 1988). They have also been found as degradation products of guanidylfungin A and B, metabolites of *S. hygrosopicus* that are active against fungi and Gram-negative bacteria (Takesako and Beppu, 1984a, Takesako and Beppu, 1984b). The structures can be seen in Figure 4-47. Guanidylfungins are similar in structure to nystatin, a polyene antibiotic isolated from *S. noursei*. A BLAST search was conducted through which homologues of the NysA, NysB, NysC, NysI and NysJ proteins were searched for within the SM8 genome. The alignments and conserved domains are shown in Appendix V. The high sequence similarities within the conserved domains implies that SM8 is capable of producing compounds similar in structure to nystatin, and it may be during this process that the polyhydroxylated saturated fatty acids are produced. Alternatively, the fatty acids may be degradation products of polyene compounds.

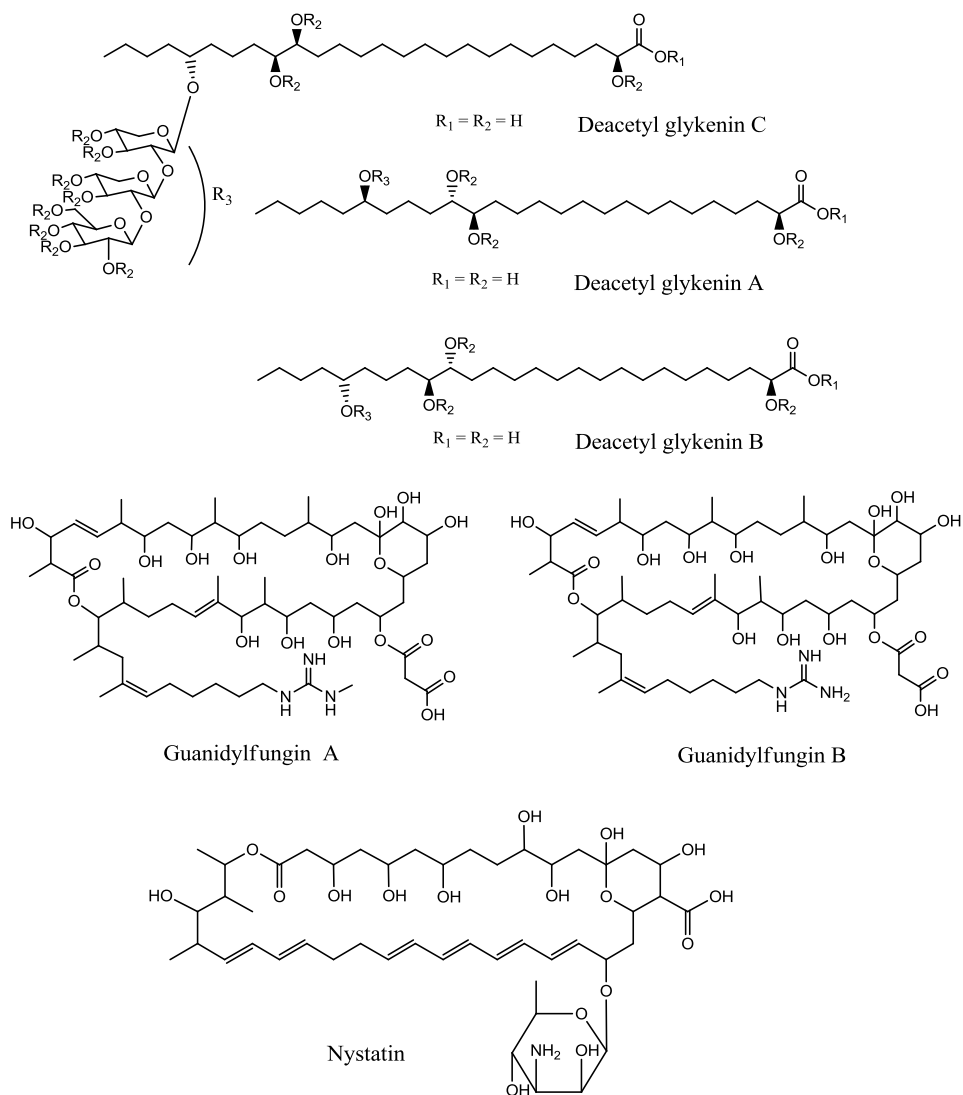


Figure 4-47: Structures of compounds containing polyhydroxylated saturated fatty acids. Tetrahydroxy saturated fatty acids comprise the aglycone portion of the deacetylglykenins and were also found to be degradation products of the guanidylfungins, which are similar in structure to nystatin.

Although fatty acids were the major compounds of the MPLC fractions, a comparison of the LC-HRFTMS spectra of the active fractions with that of an antimycin A standard confirmed the production of two isomers, antimycin A2 and A3, by SM8. Unfortunately the quantities obtained in each fraction were insufficient for further analyses.

The crude extracts of wildtype SM8 and of mutant SM8 from which the *antC* gene had been deleted were compared to an antimycin A standard from Sigma-Aldrich, USA using LC-HRFTMS in order to confirm the identities of the antimycins being

produced. The antimycin A standard that was obtained from a *Streptomyces* species was a mixture of antimycin A1, A2, A3 and A4. However, it was not stated whether these were the 'a' or 'b' homologues of antimycin A (e.g. antimycin A1a or A1b). All four antimycins were produced by the wildtype SM8, as well as some other antimycin isomers.

Antimycin A was first isolated from an unknown soil *Streptomyces* sp. (Dunshee et al., 1949). It was discovered to be a mixture of four components, named A1 to A4, which were then purified and characterised. Antimycin A3 was found to be the most active component (Liu and Strong, 1959, van Tamelen et al., 1961) although this appears to be due to its diffusion coefficient in agar (Kluepfel et al., 1970). Since then, many other compounds falling under the antimycin A family have been isolated from other *Streptomyces* species (Shiomi et al., 2005). These compounds possess antifungal activity and act by blocking the electron transport chain. Bacterial cytochrome c does not have an antimycin A-sensitive site and hence bacteria are not affected by antimycin A (Rehacek et al., 1968). The production of antimycin A1-A4 by SM8 was proven by combined genomics and metabolomic techniques. Aside from being a well-known antifungal, antimycin A is also a fish toxicant (Abidi et al., 1990), and hence could be of value to a sponge when produced by an endosymbiont.

The antimycin gene cluster is a hybrid NRPS/PKS (polyketide synthase). It can consist of 15 (short-form), 16 (intermediate-form), or 17 (long-form) genes. The *antFGHIJKLN* genes encode the biosynthesis of the 3-aminosalicylate moiety, *antCD* encode the NRPS/PKS modules, *antE* and *antM* encode a crotonyl-CoA reductase and a ketoreductase, respectively, *antB* and *antO* encode tailoring enzymes, and *antA* encodes an extracytoplasmic function (ECF) RNA polymerase σ factor (Seipke and Hutchings, 2013). The antimycin gene cluster of SM8 can be seen in Figure 4-48 together with the proposed biosynthetic pathway for antimycin biosynthesis.

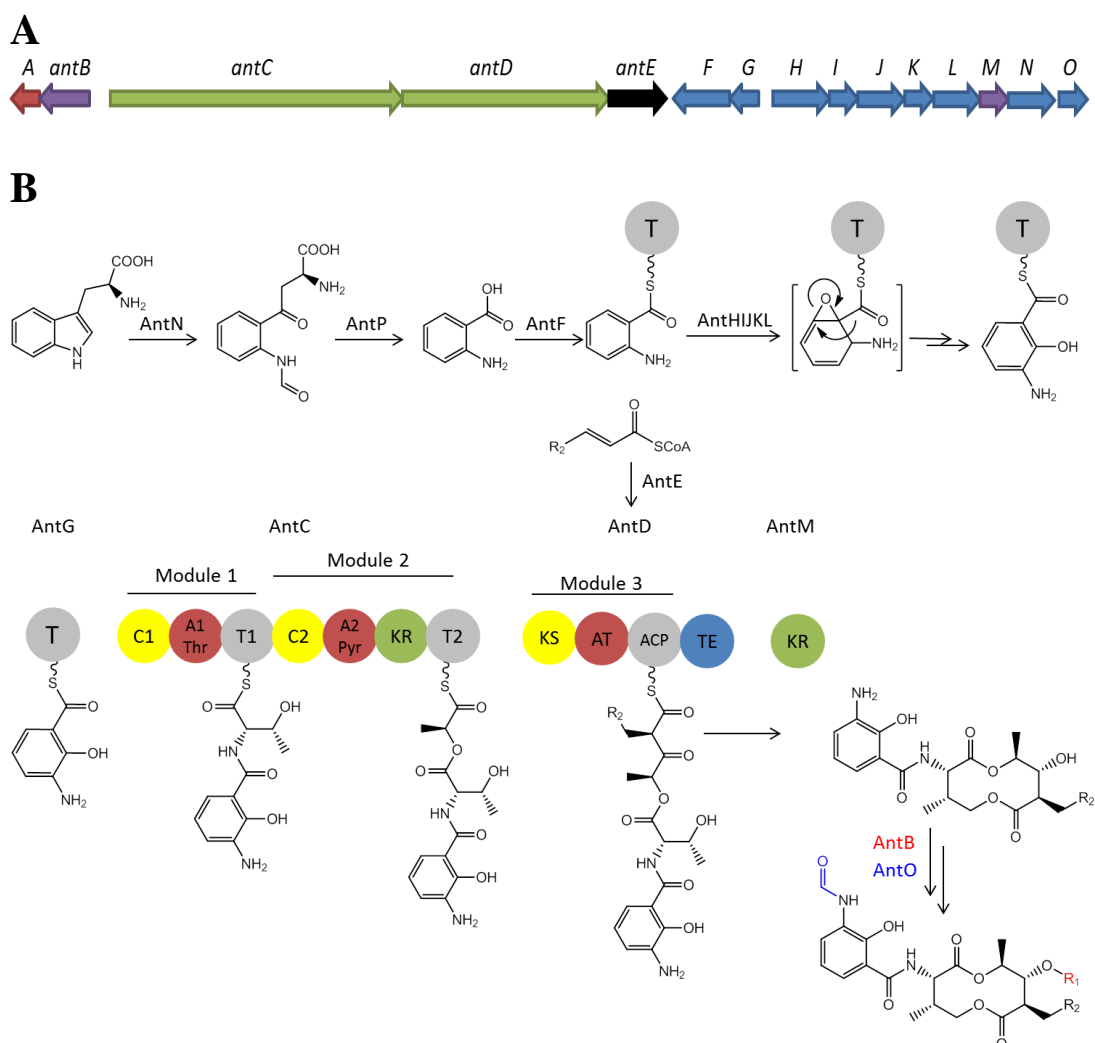


Figure 4-48: (A) Antimycin gene cluster in SM8 and (B) proposed biosynthetic pathway for antimycins (adapted from Seipke and Hutchings, 2013). (A) The antimycin gene cluster of SM8 was provided by ERI at the UCC. Genes are colour coded according to their roles in the pathway: regulation (red), NRPS and PKS scaffold biosynthesis (green), 3-formamidosalicylic acid starter unit biosynthesis (blue), post-PKS/NRPS tailoring (purple), PKS extender unit supply (black). (B) The antimycin biosynthetic pathway follows the conversion of tryptophan to 3-aminosalicylic acid, which is then condensed with threonine and pyruvate. Tailoring in the proposed pathway is performed by AntB and AntO. The domains are labelled as follows: C = condensation; A = adenylation, T = thiolation, KR = ketoreduction; KS = ketosynthase, AT = acyltransferase, ACP = acyl carrier protein, TE = thioesterase. AntP is only found in long- and intermediate-form gene clusters (Seipke and Hutchings, 2013).

Tryptophan is first converted to *N*-formyl-L-kynurenine by AntN. This then is converted to anthranilate by AntP in organisms containing the long- or intermediate-form gene cluster, or by kynureninase from the primary tryptophan metabolic pathway for those containing short-form gene clusters. Anthranilate is activated by AntF and loaded by AntG. It is then converted into 3-aminosalicylate by AntHIJKL. This molecule is passed on to AntC, the NRPS cluster. The adenylation

(A1) domain loads threonine onto the thiolation domain (T1), after which the condensation domain (C1) condenses 3-aminosalicylate with threonine. The A2 domain loads pyruvate onto T2, which is reduced by the ketoreductase (KR) domain and condensed with the threonine moiety by the C2 domain. The AntD gene cluster encodes for the PKS module. The acetyltransferase (AT) domain of AntD transfers an acyl-CoA to the acyl carrier protein (ACP). The acyl-CoAs that are transferred are the products of AntE. AntD^{AT} can accept acyl-CoAs with varying R₂-groups and thereby introduces structural diversity into the molecule. Ketosynthase (KS) condenses the 2-carboxy-acyl moiety on ACP with the aminoacyl thioester on T2 of the AntC module. AntM reduces the β-keto group, after which the AntD^{TE} closes the dilactone ring and releases the molecule. AntB causes a transesterification reaction that adds the R₁ group onto the molecule and thus is also responsible for the structural diversity of antimycins. AntO catalyses the addition of the *N*-formyl group to create the 3-formamidosalicylate moiety (Seipke and Hutchings, 2013). From the biosynthetic pathway it can be seen that antimycins A1-A4 are not intermediates of each other but possess varying side chains through the different acyl-CoA moieties introduced by AntD and AntB.

SM8 was initially grown on SYP (starch-yeast extract-peptone) medium, but the antifungal activity was found to increase when it was grown on oatmeal medium. The reason for this was evident when the extracts were compared using high resolution LC-MS, as the production of antimycin A was clearly increased when SM8 was grown on oatmeal medium. The optimum conditions for antimycin production have previously been studied (Neft and Farley, 1972); therefore it is known that the pH of the media and certain components such as tryptophan have an effect on antimycin production. For example, when tryptophan was added to the medium, the antimycin production of *S. antibioticus* increased with increasing tryptophan concentration up to 2 mg/mL after which there was decreased antimycin production. Tryptophan, as previously mentioned, is the precursor from which the 3-formamidosalicylate moiety is formed. In this study, tryptophan was present in the yeast extract that was included in SYP medium, but to what extent this affected antimycin A production in SM8 is unknown. Tryptophan was not found in the mass spectrum of the blank oatmeal medium, however. Both SYP and OM media

contained Instant Ocean[®] salt as SM8 does not survive in the absence of salt. The reason SM8 produces greater quantities of antimycin A when grown on OM medium is therefore not clear, but this is certainly the medium of choice, compared to SYP, if the antimycins are the desired compounds for isolation. If antifungal compounds other than the antimycins are desired, SM8 could be cultured on SYP medium.

A new batch of SM8 extracts was received from ERI. Following Sephadex[®] LH-20 separation the antibacterial, antifungal and anti-calcineurin fractions were pooled according to their bioactivities. An MPLC separation of the pooled antibacterial fractions yielded a fraction that contained two furanone isomers. These furanones, or butenolides, have previously been isolated from marine *Streptomyces* sp. (Mukku et al., 2000). Butenolide 1 has also been isolated from a *Streptomyces* sp. cultivated from a Mediterranean sponge *Tethya* sp. and has been proven to have inhibitory activity against *T. b. brucei* (Pimentel-Elardo et al., 2010). Butenolides 1 and 2 were also present in the antifungal fractions, although the antifungal activity can be attributed to the antimycins that were likewise present in the fractions. Other butenolides, including some synthetic ones, have been found to have antifungal activity (Gamard et al., 1997, Husain et al., 2010). Some furanones also have quorum signalling activity (Martinelli et al., 2004). It is possible that these butenolides synthesized by SM8 play a defensive or regulatory role. They did not possess antibacterial or antifungal activity against the strains tested in this study, but they did show mild quorum signalling activity (Figure 4-36).

Quorum signalling is a mechanism by which bacteria communicate with each other through the use of autoregulators. Autoregulators, or autoregulatory factors, can be defined as “*low-molecular-weight chemical substances effective at extremely low concentrations and are essentially required as intrinsic factors for triggering secondary metabolite formation and/or morphogenesis*” (Horinouchi and Beppu, 1992). In the case of *C. violaceum*, the autoinducer HHL accumulates as the cell density of the culture increases, until the critical concentration is reached at which point the genes involved in violacein production are expressed. *C. violaceum* contains homologues of the *luxR* and *luxI* genes which were first described in *Vibrio fischeri* (McClellan et al., 1997). The *luxR* gene in *V. fischeri* encodes for the LuxR

protein, which is the transcriptional activator of bioluminescence. The *luxI* gene encodes the protein that synthesizes the *V. fischeri* autoinducer (VAI), which is *N*-3-(oxohexanoyl)homoserine lactone (OHHL). At low cell densities of *V. fischeri*, *luxI* is transcribed and the VAI is produced and diffuses through the cell membrane into the culture medium or surrounding seawater. As the cell density of *V. fischeri* increases, VAI accumulates and the LuxR protein is activated, resulting in bioluminescence (Fuqua et al., 1994). A similar mechanism is involved in the production of violacein by *C. violaceum*. In *C. violaceum* CV026, however, the *luxI* homologue has been disrupted, resulting in the inability of the strain to produce endogenous HHL and, consequently, violacein. The application of exogenous HHL, or indeed, other stimulatory molecules allows the production of violacein (McClellan et al., 1997). The SM8 butenolides resulted in mild violacein production. It may have been due to the structural similarities of the butenolides to AHLs and the high concentration of butenolides used. Although it is unexpected for Gram-positive regulatory molecules to affect the Gram-negative regulatory system of *C. violaceum* CV026, it is not unprecedented, as two butenolides isolated from *S. antibioticus* Tü 99 have also shown weak stimulatory activity towards *C. violaceum* CV026 (Grossmann et al., 2003).

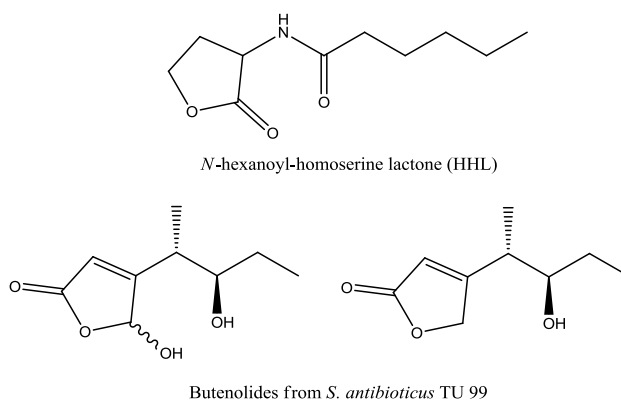


Figure 4-49: Structure of HHL, the autoregulatory molecule of *C. violaceum*, and of butenolides isolated from *S. antibioticus* Tü 99. The two butenolides showed weak stimulatory activity for the production of violacein in *C. violaceum* CV026, a genetically engineered strain that does not produce endogenous HHL.

Butenolides are similar in structure to the γ -butyrolactones, the main differences being the position of the side chain, the presence of a double bond in the butenolides,

and the presence of an alcohol functional group on the γ -butyrolactones. The latter are analogous to AHLs in that they are autoregulators. An example of a *Streptomyces* autoregulator is the A-factor, the first and best-known autoregulatory butyrolactone, isolated from *S. griseus*. It induces the production of secondary metabolites, such as streptomycin, and also induces cell differentiation, such as the formation of aerial mycelia (Horinouchi and Beppu, 1992). The receptor proteins of γ -butyrolactones are often repressor proteins, and binding of the γ -butyrolactones results in the expression of the genes (Takano, 2006). Approximately 60% of *Streptomyces* may produce these butyrolactones, although their roles in each of the strains have not been determined (Yamada, 1995). These compounds may not have antibacterial or antifungal activity by themselves but could be responsible for the regulation of metabolite production, such as in the case of the virginiae butanolides (VBs) isolated from *S. virginiae* that are responsible for regulating the production of the antibiotic virginiamycin (Kondo et al., 1989). Conversely, another γ -butyrolactone from a *Streptomyces* species, butalactin, possesses no inducing activity but is mildly antibacterial (Franco et al., 1991). γ -Butyrolactones have also been identified from actinomycetes belonging to genera other than *Streptomyces*. For example, *Actinoplanes teichomyceticus*, which yields vancomycin, and *Amycolatopsis mediterranei*, which yields rifamycin, were found to produce butyrolactone autoregulators (Choi et al., 2003).

Avenolide is a butenolide autoregulator produced by *S. avermitilis* that regulates the production of the antihelmintic compound avermectin (Kitani et al., 2011). It is closer in structure to the butenolides isolated from SM8 than the γ -butyrolactones and represents another class of *Streptomyces* autoregulators. The biosynthetic gene cluster of avenolide consisted of a regulatory gene, a cytochrome P450 hydroxylase, and an acyl-CoA oxidase (Kitani et al., 2011). However, this arrangement was not found in the SM8 genome, indicating that the biosynthesis of the butenolides in SM8 occurs through a different pathway. In addition, volatile butenolides and other furanone derivatives have been identified as products of antimycin degradation (Riclea et al., 2012). The three SM8 butenolides differed from these degradation products in that, unlike the volatile butenolides, they lacked the 2-alkyl group and possessed an alkyl chain rather than a methyl group on C-4. That the SM8

butenolides arose from a different pathway unrelated to the antimycin pathway was further confirmed as their production was undiminished in the SM8 $\Delta antC$ mutants.

It must be noted that other autoregulatory factors exist, aside from the γ -butyrolactones. The C-factor, for instance, is a protein that induces sporulation in *S. griseus*, and pamamycin-607, a macrodiolide, affects aerial mycelium formation (Horinouchi and Beppu, 1992).

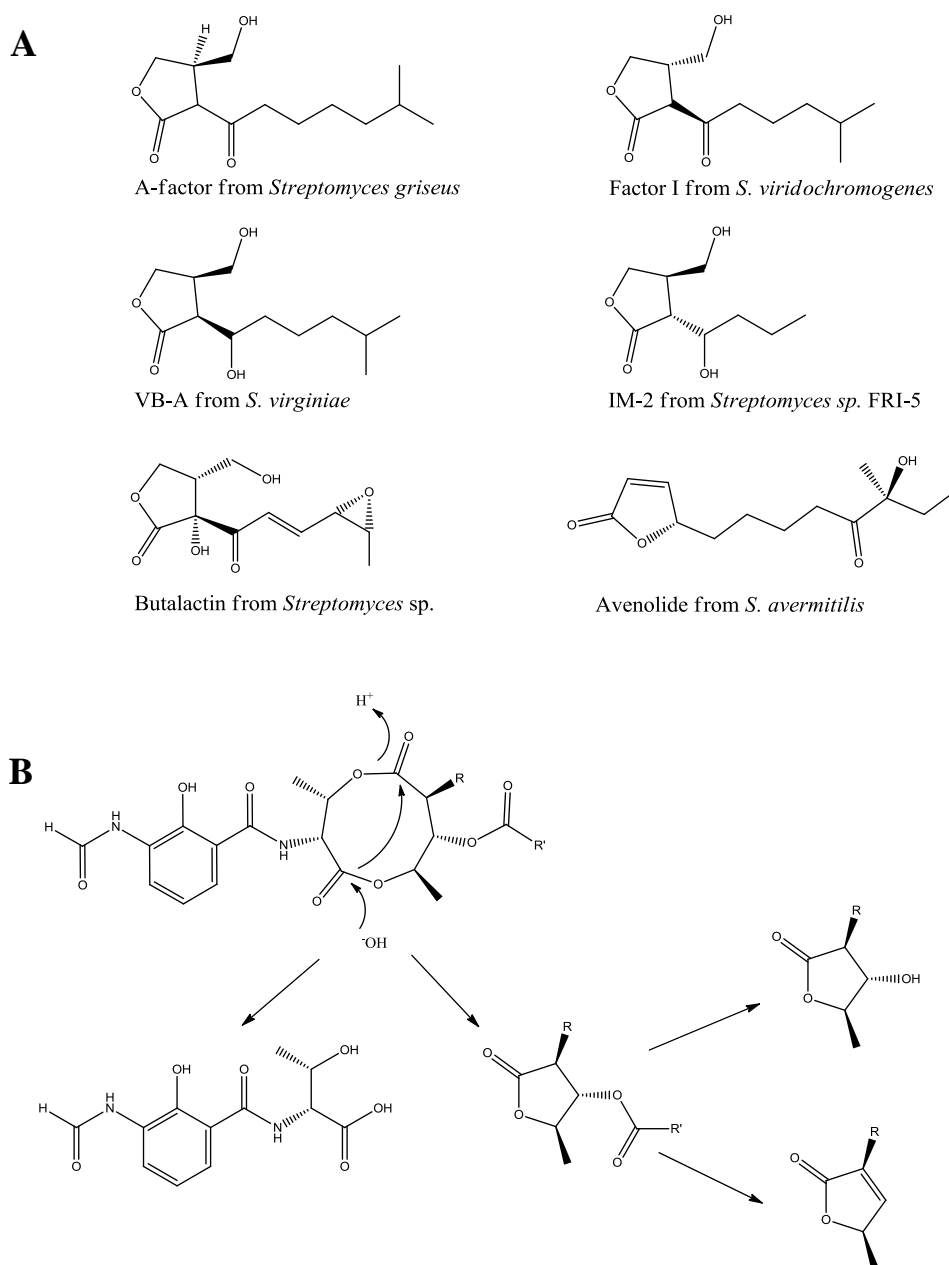


Figure 4-50: Examples of butyrolactones from *Streptomyces sp.* (A) Butyrolactone-containing metabolites from *Streptomyces sp.* A-factor, Factor I, VB-A and IM-2 are all γ -butyrolactone autoregulators. Butalactin is a butanolide that does not act as an autoregulator but possesses mild antibacterial activity. Avenolide is a non- γ -butyrolactone autoregulator that is closer in structure to the

SM8 butenolides than the γ -butyrolactones. (B) Degradation of antimycin to produce volatile butyrolactones (adapted from Riclea et al., 2012). The butenolides isolated from SM8 differ structurally and thus are not products of antimycin degradation.

Butenolides have also been isolated from sponges (Faulkner, 2002) (Figure 4-51). Research has shown that furanones may be used by eukaryotic host organisms to interfere with prokaryotic signalling, thereby regulating the colonies they play host to (Givskov et al., 1996, Kjelleberg et al., 1997). The butenolides found from SM8 were evident in the *H. simulans* extract as well, albeit in much reduced quantities, as expected.

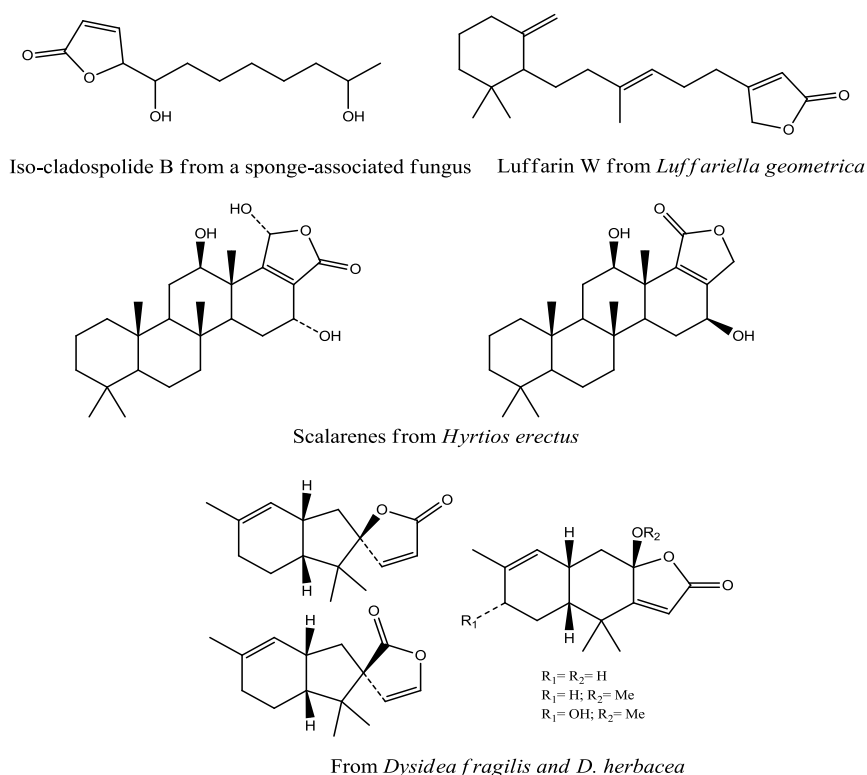


Figure 4-51: Some butenolides previously isolated from sponges (Faulkner, 2002).

Two of the butenolides, named here as butenolide 2 and butenolide 4 (Table 4-11 and Table 4-14) inhibits calcineurin signalling. Calcineurin is a calcium-activated phosphatase and is the key rate-limiting enzyme in the T-cell signalling cascade. It is the target enzyme of immunosuppressant drugs such as cyclosporin A, tacrolimus and pimecrolimus (Clipstone and Crabtree, 1992, Nghiem et al., 2002). Calcineurin is widely distributed in eukaryotes. As prokaryotes such as bacteria do not have calcineurin, it is believed that some bacteria evolved to produce calcineurin

inhibitors and thereby gain an edge against their fungal competitors. Tacrolimus and pimecrolimus are produced by *Streptomyces tsukubaensis* and *S. hygroscopicus* respectively, whereas cyclosporin A is produced by the fungus *Beauveria nivea*. Calcineurin also plays an important role in mammals, being involved in memory, renal function and immune response (Nghiem et al., 2002). Indeed, calcineurin is so-named because it binds calcium and was initially believed to be specific to the nervous system (Klee et al., 1979). However, the phosphatase is actually present in many other systems, although in much lower quantities in the cells of the immune system. This, in addition to the necessity of calcineurin to the signalling cascade, leads to the relative selectivity of calcineurin inhibitors as immunosuppressants, although side effects include nephrotoxicity and psychiatric disturbances (Nghiem et al., 2002).

As previously mentioned, calcineurin is the key enzyme in the T-cell signalling cascade. It is regulated by calmodulin and Ca^{2+} . When intracellular levels of Ca^{2+} are low, calmodulin is unable to bind to calcineurin and the enzyme is inactive. However, when an antigen binds to the T lymphocyte, thereby activating it and causing a Ca^{2+} to enter the cell, the Ca^{2+} binds to calmodulin, resulting in a conformational change and allowing calmodulin to bind to calcineurin (Rusnak and Mertz, 2000). This opens the active site of calcineurin which then allows it to dephosphorylate target proteins. In T cells calcineurin dephosphorylates the cytoplasmic portion of NFAT (nuclear factor of activated T cells), which is termed NFATc. The dephosphorylated NFATc enters the nucleus and binds to its nuclear counterpart, then allowing production of several cytokines (Nghiem et al., 2002).

A review by Sieber and Baumgrass lists several small molecules that act as inhibitors of the calcineurin signalling pathway (Sieber and Baumgrass, 2009). Although none of these are furanones, some are heterocyclic small molecules with aliphatic chains (Figure 4-52). Dibefurin is a benzofuran dimer that inhibits calcineurin (Brill et al., 1996). 1,5-Dibenzoyloxymethyl-norcantharidin is a synthetic compound that was created to specifically target calcineurin without affecting other serine/threonine protein phosphatases (Baba et al., 2003). WIN 53071 (Baine et al., 1995) does not act against calcineurin itself but rather on NFATc-DNA complex formation. NFAT-68,

an aromatic compound derived from a *Streptomyces* sp., also does not act on calcineurin itself but prevents NFAT-dependent transcription (Burres et al., 1995), as do some quinolones with aliphatic side chains. The methylated quinolones with longer side chains had greater inhibitory activity than those with shorter side chains (Jin et al., 2004).

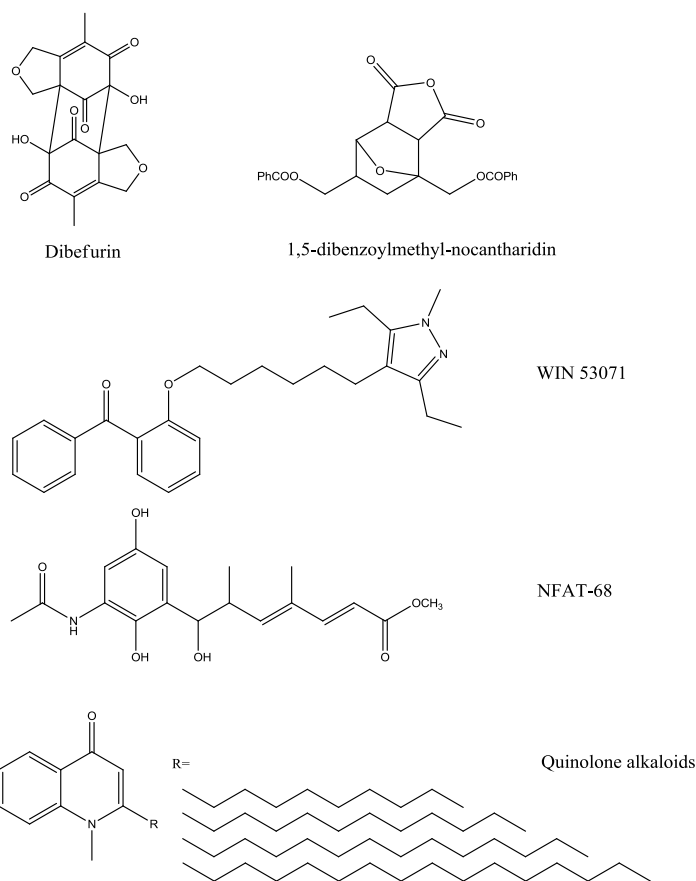


Figure 4-52: Structures of some small-molecule inhibitors of the calcineurin signalling pathway (Sieber and Baumgrass, 2009).

The assay for calcineurin inhibition that was used in this study does not determine which part of the calcineurin signalling pathway is affected by the butenolides (Margassery et al., 2012); therefore, further work must be performed to determine the mechanism of action of the SM8 butenolides.

Comparison of the extracts of the host sponge *H. simulans* and its endosymbiont, SM8, using high resolution LC-MS revealed the presence of common metabolites in both extracts. This confirmed that SM8 is indeed associated with *H. simulans*. It is expected that the metabolome of SM8 would differ when it is cultured in the

laboratory as opposed to when it grows within the sponge. Further analysis into the common metabolites may lead to the elucidation of the roles of these compounds in the survival of SM8 within *H. simulans*. Although no common metabolites were found using GC-MS, one of the small molecules in the SM8 extract that was identified by the in-house library, thujaketone, is identical to the side chain of ergosterol. It is possible that *H. simulans* uses some of the metabolites of SM8 as part of its chemical defence or as building blocks for the production of its own compounds. Although no novel compounds were isolated from SM8, largely due to the small quantity of starting material (<1 gram), three known furanones, two of which have a novel activity, were isolated using bioassay-guided fractionation, and the production of antimycin A by SM8 was confirmed using metabolomics and gene knockout studies.

Chapter 5 Dereplication, Metabolic Profiling and Analysis of Compounds from Bacteria Isolated from Marine Sponges

5. Dereplication, Metabolic Profiling and Analysis of Compounds from Bacteria Isolated from Marine Sponges

5.1 Introduction

The multitude of known chemical structures derived from natural sources is still insufficient to fulfil the needs of human therapy. As such, the search for novel bioactive compounds continues. This is constrained, however, both by limitations in screening methodologies as well as depletion of new biological sources from which to isolate new compounds (Berdy, 2005). To combat the latter problem, researchers have turned to the marine environment, which has been said to have a greater chemical and biological diversity than the terrestrial environment (Haefner, 2003). Although extracting metabolites from marine invertebrates and microorganisms does not guarantee the novelty of the compounds, the probability of obtaining a previously undiscovered compound is much higher. Nevertheless, dereplication is still an important part of any screening process in order to save time and costs. Dereplication is the elimination of natural product sources (in this instance, microorganisms) that have previously been studied or that contain many known compounds (Lang et al., 2008, Dieckmann et al., 2005). In this work the dereplication of novel marine actinobacteria was performed using LC-HRFTMS.

Once compounds of interest have been successfully identified, the production of these metabolites by the microorganisms can be enhanced by optimising the culture conditions. For example, substituting glycerol for glucose as the carbon source of a sponge-associated *Microbacterium* sp. resulted in an increase both in biomass as well as in the yield of the desired anti-tumour glucosylmannosyl-glycerolipid (Lang et al., 2004). Another strategy used to improve biomass and yield is fermentation. Fermentation is “*any process for the production of product by the mass culture of a microorganism*” (Stanbury et al., 1995). During fermentation of *Microbacterium* sp. HP2 (DSM 12583) the production of the glucosylmannosyl-glycerolipid remained the same as the shake flask culture at 25 mg/gram of biomass; however, the biomass increased from 10 g/L after three days to 12 g/L in 32 hours (Lang et al., 2004).

This chapter describes the dereplication of six novel marine actinomycetes and the selection of one actinomycete for further study. EG4, a novel *Microbacterium* sp.,

was up-scaled for compound isolation. The metabolic profile of the bacteria over time, under different media conditions, and during fermentation was also analysed to assist in the optimisation of the production of bioactive metabolites.

5.2 Methodology

5.2.1 Screening and Dereplication of Bacterial Isolates

5.2.1.1 Acquisition of Bacterial Extracts

The bacterial extracts CO105, CO155, EG4, EG7, EG37, and EG45 were obtained from the University of Würzburg, Germany. These were acquired from agar cultures. An extract from the blank M1 agar was also provided, as were extracts from CO155 and EG37 broth cultures and their corresponding blank M1 broth.

The bacteria prefixed with ‘CO’ were isolated from sponges and sediment collected from El Morro, Santa Marta Bay, Colombia in December 2008 (Tabares et al., 2011). Those prefixed with ‘EG’ were isolated from sponges collected from the Red Sea, Ras Mohamed, Sinai, Egypt in August 2006 (Abdelmohsen et al., 2010).

EG4, a *Microbacterium sp.*, was cultured by the University of Würzburg from a *Callyspongia aff. implexa* sponge collected from the Red Sea, Egypt (Abdelmohsen et al., 2010). Samples of EG4 on M1 agar plates were acquired from the University of Würzburg for reinoculation.

5.2.1.2 Screening of Samples with LC-HRFTMS and NMR

The extracts were dissolved in deuterated DMSO for ¹H NMR analysis. Extracts that did not dissolve completely were centrifuged and the supernatant liquid was used.

After NMR analysis, the extracts were subsequently freeze-dried and re-dissolved in enough 50:50 pure-grade H₂O:MeOH (HPLC grade) to give a final concentration of 1 mg/mL. The samples which did not dissolve completely were centrifuged at 10,000 rpm for 10 minutes and the supernatant was removed for LC-HRFTMS. The UltiMate 3000-Exactive Orbitrap was used following the method in 2.4.1. Dereplication was performed using the MZmine 2.10 parameters outlined in 2.4.2.

The peaks that had a peak area greater than or equal to 1.00E4 in the blank media and solvent were subtracted from those of the extracts, and the remaining peaks were compared to the AntiMarin 2012 database for identification. EG4 was selected for further work because it produced many unidentified metabolites.

5.2.2 Isolation and Analysis of Antibiotic Compounds from EG4

5.2.2.1 Small-scale Growth of EG4 on Agar Plates

5.2.2.1.1 Preparation of M1 Agar

The University of Würzburg provided the protocols for the preparation of the artificial seawater and M1 agar medium.

5.2.2.1.1.1 Artificial Seawater

NaCl (VWR International, Belgium)	234.70 g
Na ₂ SO ₄ (Alfa Aesar, UK)	39.20 g
MgCl ₂ •6 H ₂ O (BDH Laboratory Supplies, England)	106.40 g
CaCl ₂ (Sigma-Aldrich Co. Ltd, UK)	11.0 g
NaHCO ₃ (Alfa Aesar, UK)	1.92 g
KCl (BDH Ltd., England)	6.64 g
KBr (BDH Ltd., England)	0.96 g
H ₃ BO ₃ (Alfa Aesar, UK)	0.26 g
SrCl ₂ (Alfa Aesar, UK)	0.24 g
NaF (Alfa Aesar, UK)	0.03 g
H ₂ O _{dd}	ad 10.0 L

5.2.2.1.1.2 M1 Agar

Soluble starch (Sigma Chemical Co. USA)	10.0 g
Yeast extract (Oxoid, England)	4.0 g
Peptone (Fisher Scientific UK Ltd, UK)	2.0 g
Agar (Oxoid, England)	18.0 g
Artificial seawater	ad 1.0 L

The agar was sterilized by autoclaving and allowed to cool slightly before being poured into petri dishes. M1 broth was prepared according to the same protocol albeit without the addition of agar.

5.2.2.1.2 Inoculation of EG4

EG4 was inoculated on M1 agar plates using the single streak method to obtain a pure colony for the preparation of a bacterial stock. Some plates were also inoculated using the multiplication method to allow the bacteria to grow and cover as much of the agar surface as possible. The plates were incubated at 30°C for 5-10 days.

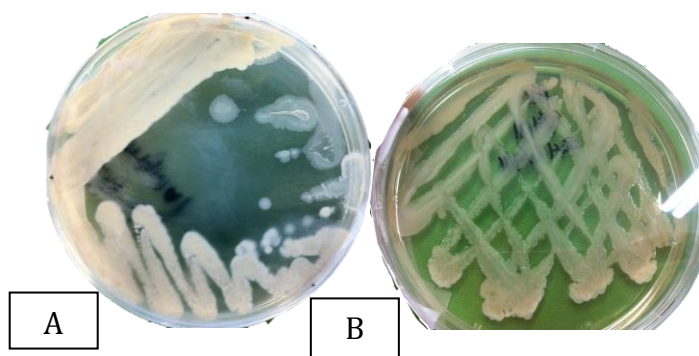


Figure 5-1: (A) Single streak method to obtain a pure colony, and (B) multiplication method to cover as much of the agar surface as possible.

5.2.2.1.3 Preparation of EG4 Stock

A pure colony of EG4 was inoculated onto M1 agar medium and allowed to grow for five days. Fifteen millilitres of sterile pure-grade water was added on top of the agar and mixed gently to suspend the bacteria. One millilitre of the bacterial suspension

was placed into each sterile cryotube containing 1 mL 30% sterile glycerol solution. They were then mixed and stored in the -80°C freezer.

5.2.2.1.4 Extraction and Analysis of EG4 Metabolites

The M1 agar plates were sliced into smaller pieces to be transferred into conical flasks then covered with 200 mL of ethyl acetate or methanol. The flasks were covered with aluminium foil to prevent solvent evaporation and were left to stand overnight before being homogenised and vacuum-filtered through a Millipore filter. The upper ethyl acetate layer was collected while the aqueous layer was shaken with ethyl acetate twice to further extract the non-polar metabolites. The ethyl acetate fractions were combined and dried under vacuum. When methanol was used to kill the cells, the methanol was saturated with water after filtration. This aqueous methanol layer was then treated as the aqueous phase and was extracted thrice with ethyl acetate. However, many sugars were obtained in the organic layer, hence the extract was subjected to HP20 chromatography using 100% water, 50:50 water:MeOH and 100% methanol in sequence to elute the column.

The extracts were dissolved in deuterated DMSO and analysed using NMR. They were then dried and prepared for LC-HRFTMS using the UltiMate 3000-Exactive Orbitrap. The spectra were compared to those obtained from the M1 agar blank as well as to the original anti-trypanosomal active extract received from the University of Würzburg.

5.2.2.2 Up-scaling of EG4 Culture

EG4 was inoculated onto M1 agar plates and incubated at 30°C. After five days, one plate was placed in the refrigerator (8°C) to stop the growth of the bacteria whereas the other plate was maintained at 30°C for ten days. This was to determine whether or not the age of the inoculum affected the metabolite production of the culture.

A quarter of each plate was placed into 500 mL of M1 broth. Two of the flasks containing the 5-day incubated culture and two of the flasks containing the 10-day

incubated culture were shaken at 150 rpm for 7 days at 30°C. The other similar set of four flasks was left to stand at 30°C for 7 days.

After the incubation period the flasks were covered in ethyl acetate and left to stand overnight. The metabolites were then extracted following the same procedure as in **5.2.2.1.4**. The extracts from flasks of similar culture conditions were combined resulting in four extracts: shake 5-day, shake 10-day, stand 5-day and stand 10-day. These were submitted for NMR, LC-MS and anti-trypanosomal assay.

5.2.2.3 MPLC Fractionation of EG4 Extracts

Analysis of the shake and stand cultures NMR spectra revealed no difference in the major compounds produced; the advantage of using the shake cultures was predominantly in the amount of extract obtained. As such, the four extracts were combined to give a total weight of 196.5 mg and subjected to MPLC in an attempt to isolate and identify bioactive compounds. The combined extracts were loaded onto a Versa Flash silica column and fractionated with the BÜCHI MPLC instrument using the following method:

Column: VersaPak Silica (Spherical) 23x53 mm (11 g)

Solvents: Dichloromethane (A), methanol (B) (HPLC grade)

Gradient: 0-5 min	0% B
5-35 min	0-30% B
35-40 min	30% B
40-45	50:50 acetone:methanol wash

Flow rate: 10 mL/min

Fractions were collected at a rate of four test tubes per minute, aside from the wash, which was collected in its entirety. The fractions were pooled according to the similarities of their TLC chromatograms, after which they were dried and prepared for NMR, LC-MS and anti-trypanosomal and anti-mycobacterium assays.

5.2.3 Chemical Profiling of EG4 in Shake Flask Cultures Over the Course of Seven Days

EG4 was grown in 21 flasks containing 200 mL of M1 broth at 30°C and 150 rpm for 0-8 and 15 days. Each day two flasks were checked for contamination by visual inspection using a microscope. They were covered with ethyl acetate to kill the cells and then extracted the following day through liquid-liquid partitioning. The broth and ethyl acetate layers were filtered through cotton, instead of a Millipore filter, before being poured into the separatory funnel. This was because it was found that the starch blocked the Millipore filter.

The ethyl acetate extracts were dissolved in deuterated DMSO and subjected to ¹H NMR as well as COSY and TOCSY. LC-MS was also performed using the UltiMate 3000-Exactive Orbitrap. The extracts were submitted for anti-trypanosomal and anti-mycobacterium assays.

5.2.4 Isolation of Bioactive Compounds from EG4 Extract

EG4 was grown in 500 mL conical flasks containing 200 mL of M1 broth and were incubated at 30°C for seven days with shaking at 150 rpm. A total of 16 L of inoculated broth was extracted with ethyl acetate, giving 1.2478 g of extract.

5.2.4.1 MPLC Fractionation of EG4 Extract Using BÜCHI Flash Chromatography System

The crude extract was subjected to MPLC using a VersaPak silica column (53x110 mm) with a flow rate of 10 mL/min.

Solvents: Hexane (A), ethyl acetate (B)

Gradient: 0-5 minutes	15% B
5-45 minutes	15-100% B
45-50 minutes	100% B

The fractions were pooled based on the similarity of their TLC patterns and submitted for anti-trypanosomal and anti-mycobacterium assay. NMR and MS analyses were also performed.

5.2.4.2 Fractionation of EG4_569-573 Using Conventional Chromatography

Fraction 569-573 was selected for further purification. It was loaded into a conventional silica column that was left to elute overnight with 80:20 dichloromethane:methanol at a flow rate of 1 ml/5min. The column was then washed with 50:50 dichloromethane:methanol. The test tubes were analysed by TLC and pooled according to their similarities.

5.2.4.3 MPLC Fractionation of EG4_215-392 using Biotage[®] Flash Chromatography System

A 25 g (30x72 mm) SNAP silica cartridge was used for further fractionation of fraction 215-392. The sample was loaded onto a frit and dried under nitrogen before being fitted onto the column. The sample was then eluted at a flow rate of 25 mL/min using the following method:

Solvents: Hexane (A), ethyl acetate (B)

Gradient:	0-15 minutes	0% B
	15-27 minutes	0-10% B
	27-45 minutes	10% B
	45-57 minutes	10-20% B
	57-73 minutes	20% B
	73-83 minutes	20-30% B
	83-93 minutes	30% B

The UV detector was set to 204 nm and 365 nm with a threshold of 10 mAU. Once again, the fractions were analysed and pooled by TLC.

5.2.4.4 Preparative TLC of EG4_215-392_wash and EG4_615-626

The wash of EG4_215-392 after fractionation with the Biotage[®] was pooled and spotted onto preparative TLC plates (Merck, Germany). The plates were eluted three times with 80:20 dichloromethane:ethyl acetate. In a similar manner, EG4_615-626 was spotted onto preparative TLC plates and eluted once with 80:20 DCM:MeOH. The plates were viewed under short wavelength and long wavelength UV. The bands were cut, placed into 100 mL conical flasks and extracted with acetone (HPLC grade) three times. These were stirred for an hour, after which the acetone was filtered and fresh acetone was placed into the flasks. The pooled filtrate was then evaporated under vacuum and the compounds were analysed using LC-HRFTMS and NMR.

5.2.5 Metabolic Profiling of EG4 Under Different Media Conditions

5.2.5.1 Cultivation of EG4 on Variations of M1 Agar

EG4 was inoculated onto variations of M1 agar to test the response of EG4 to the replacement of starch with glucose monohydrate (Alfa Aesar, UK) as a carbon source, the removal of salt or the addition of N-acetylglucosamine (GlcNAc) (Sigma-Aldrich Co., USA). The salt used during this experiment was a pre-formulated aquarium salt, Royal Nature (Royal Nature, Israel). A summary of the media used is presented in Table 5-1 below.

Table 5-1: Composition of the different types of M1 agar used

Media Name	Starch (1%)	Yeast Extract (0.4%)	Peptone (0.2%)	RN (2.3%)	Glucose (1%)	GlcNAc (50mM)
M1 control	✓	✓	✓	✓		
M1+Gluc		✓	✓	✓	✓	
M1-salt	✓	✓	✓			
GWOSW		✓	✓		✓	
GlcNAc_A	✓	✓	✓	✓		✓ (Added after autoclaving)
GlcNAc_B	✓	✓	✓	✓		✓ (Added before autoclaving)

A media blank was also prepared for each type of M1 agar used. GlcNAc that was added after autoclaving was sterilised under UV radiation prior to addition to the media. The metabolites were extracted with ethyl acetate according to **5.2.2.1.4** and were analysed using LC-HRFTMS and NMR. The extracts were also tested for activity against *T. b. brucei* and *M. marinum*.

5.2.5.2 Shake Cultures of EG4 Comparing Artificial Seawater and Royal Nature

One vial of EG4 glycerol stock was inoculated onto two M1 agar plates. After 7 days incubation at 27°C a quarter of a plate was aseptically transferred to a conical flask containing 200 mL of M1 broth with ASW or M1 broth with Royal Nature. The flasks were shaken at 150 rpm and 30°C for seven days. On the seventh day 20 mL from each flask was used to inoculate another 200 mL of M1 containing the appropriate salt. This was done in triplicate for each type of media. The flasks were incubated at 30°C and shaken at 150 rpm for seven days. On the seventh day the flasks were taken out and covered with ethyl acetate. The extraction then followed the standard procedure and the extracts were analysed using LC-HRFTMS and NMR and were submitted for anti-trypanosomal and anti-mycobacterium assays.

5.2.5.3 Shake Cultures of EG4 using Variations of M1 Broth

EG4 grew and maintained activity in M1 agar that contained glucose as the carbon source as well as in M1 agar that was absent of salt. Therefore EG4 was next grown in M1 broth that contained different concentrations of salt, starch and glucose. 200mL of each M1 broth variation was placed into a 500 mL conical flask. Two flasks for each media were inoculated with EG4 for each media and one flask served as the blank. The salt used was Royal Nature. The composition of the media used is shown in Table 5-2 below.

Table 5-2: Composition of various types of M1 broth to make 200mL

Media Name	Starch (g)	Glucose (g)	Salt (g)	Yeast Extract (g)	Peptone (g)
M1+G	-	2.0	4.6	0.8	0.4
M1-RN	2.0	-	-	0.8	0.4
50G50S	1.0	1.0	2.3	0.8	0.4
M1 control	2.0	-	4.6	0.8	0.4
GWOSW	-	2.0	-	0.8	0.4

5.2.6 Fermentation of EG4

5.2.6.1 Parameters

EG4 batch fermentation was carried out in duplicate in a Biostat Q fermenter (Braun, Switzerland) with vessels having a total volume of 1 L and a working volume of 0.75 L. pH and dissolved oxygen tension (DOT) were monitored but not maintained at a constant level. The temperature was set to 30°C and the broth was stirred at 150 rpm. 75 mL of M1 broth containing a 7-day shaken culture of EG4 was used as the inoculum. One millilitre of polypropylene glycol was added to the broth to prevent foaming. Ten mL of broth was taken from each vessel every 12 hours. Of this, 1 mL was used for the cell count and the other 9 mL were used for the extraction of metabolites. The fermentation occurred for 108 hours before being terminated.

5.2.6.2 Cell Count

5.2.6.2.1 Cell Count Using Haemocytometer

The samples from Vessel 2 were diluted as necessary and stained with crystal violet to facilitate ease of counting. The sample was loaded onto the haemocytometer and viewed under a microscope. It was considered properly diluted when there were an average of 50-100 cells per large square and they were uniformly distributed and not overlapping. The large squares were counted diagonally, the middle square being counted twice, and the average number of cells was determined. The cell count was then calculated using the formula below:

$$\text{Cell count (cell/mL)} = \text{Average no. of cells} \times \text{dilution factor} \times \frac{1}{4} \times 10^6$$

5.2.6.2.2 Viable Cell Count Using Spread Plate Technique

The samples from Vessel 3 were diluted with sterile artificial seawater. Three concentrations were selected and 100 µL of each concentration was used to inoculate three plates of M1 agar. The inoculum was carefully spread over the plate until dry. The plates were incubated at 30°C and the colonies from the most suitable concentration were counted.

5.2.6.3 Metabolic Profiling of EG4 Bioreactor Extracts

The sample taken from Vessel 2 at 0 hours was divided into two parts. 4.5 mL was placed in the cell disruptor and the other 4.5 mL was covered with ethyl acetate and homogenized. This was to compare the efficiency of the two techniques. As there appeared to be no real advantage to either in terms of killing the cells, the subsequent samples were treated with ethyl acetate and homogenized as this was less time-consuming. The extraction proceeded in the same manner as **5.2.2.1.4**. The extracts were analysed using NMR and LC-HRFTMS and were also submitted for anti-trypanosomal and anti-mycobacterium assays.

5.3 Results

5.3.1 Dereplication of Marine Actinomycetes

Eight bacterial extracts from six marine actinomycetes were obtained from the University of Würzburg, Germany. Six were agar extracts whereas two were broth extracts. The summary of the taxonomy and sources of these bacteria can be seen in Table 5-3.

Table 5-3: Taxonomy and sources of the six marine actinomycetes received for dereplication

Extract	Identification	Source	Location
CO105	<i>Sphingobium</i> sp.	<i>Discodermia dissoluta</i>	El Morro, Santa Marta Bay, Colombia (Tabares et al., 2011)
CO155	<i>Rhodococcus</i> sp.	Marine sediment	
EG4	<i>Microbacterium</i> sp.	<i>Callyspongia</i> aff. <i>implexa</i>	Red Sea, Ras Mohamed, Sinai, Egypt (Abdelmohsen et al., 2010)
EG7	<i>Brachybacterium</i> sp.		
EG37	<i>Brevibacterium</i> sp.	<i>Hyrtios erecta</i>	
EG45	<i>Micrococcus</i> sp.	<i>Sphaciospongia vagabunda</i>	

The eight bacterial extracts and two blank media extracts were analysed using NMR and LC-HRFTMS. The mass spectra of the agar extracts were then compared using MZmine 2.10, which picked out significant peaks from each sample. Peaks that were present in the media and the blank solvent as well as in the samples were disregarded. The peaks were compared to the AntiMarin 2012 database to facilitate identification of compounds. Table 5-4 summarises the numbers of identified compounds from each bacterial extract.

Table 5-4: Summary of total peaks detected and peaks identified using the AntiMarin database for each bacterial isolate

Isolate	Positive		Negative		Percentage of compounds identified
	Total peaks detected	Total identified	Total peaks detected	Total identified	
CO105	550	203	201	114	42.21
CO155	642	146	143	72	27.77
EG4	1086	333	256	130	34.50
EG7	1256	396	195	118	35.42
EG37	323	112	112	67	41.15
EG45	475	180	140	82	42.60

CO155, *Rhodococcus* sp., had the lowest percentage of identified compounds; however, it produced just over half of the total number of metabolites of EG4 and EG7. EG37, *Brevibacterium* sp., produced the least number of metabolites, and many of them were identified from the database. The two bacteria from the sponge *C. aff. implexa*, EG4 and EG7, were the most proliferative producers of metabolites. EG4, a

sponge-associated *Microbacterium* sp., was selected for further work as it had a lower percentage of identified compounds than EG7.

The major identified compounds from each bacterial isolate are shown in Table 5-5. These compounds were putatively identified from the AntiMarin 2012 database based on their m/z ratios. However, it must be noted that the presence of these metabolites has yet to be confirmed by isolation and structural elucidation and it is possible that the m/z values correspond to unknown structural isomers. In addition, where several hits have been found in the database for one peak, the first hit was displayed in the table.

Table 5-5: Major compound putatively identified from each bacterial isolate

Sample		m/z	RT	Name	Source	Reference
CO105	[M+H] ⁺	305.1283	14.56	[1] Neihumicin	[B] <i>Micromonospora neihuensis</i> ; marine bacterium NPS0002/0014	(Wu et al., 1988)
	[M-H] ⁻	491.2866	20.62	[2] Actinoramide C	[B] <i>Streptomyces</i> sp	
CO155	[M+H] ⁺	267.1127	18.99	[3] Cyclopiamide	[F] <i>Penicillium cyclopium</i>	(Holzapfel et al., 1990)
	[M-H] ⁻	403.2261	24.15	[4]	[S] <i>Physarum polycephalum</i> MCI 2526 (FERM P-11576)	
EG4	[M+H] ⁺	249.1386	9.55	[5] Brasilidine A	[B] <i>Nocardia brasiliensis</i>	(Kobayashi et al., 1997)
	[M-H] ⁻	322.0725	9.28	[6] Stealthin-A; CA39-A	[B] <i>Streptomyces viridochromogenes</i> 2220-SV2 (FERM BP-3504)	(Shinya et al., 1992)
EG7	[M-H] ⁺	254.1902	10.46	[7] Herbindole C	Porifera <i>Axinella</i> sp	(Herb et al., 1990)
	[M-H] ⁻	464.2787	20.33	[8] 16-Deethylindanomycin; A-83094A	[B] <i>Streptomyces setonii</i>	(Larsen et al., 1988)
EG37	[M+H] ⁺	296.1392	6.93	[9] Isonaamine-A	Porifera <i>Leucetta chagosensis</i>	(Carmely and Kashman, 1987)
	[M-H] ⁻	179.0716	8.87	[10] Adriadysiolide	Porifera <i>Dysidea</i> sp	(Mancini et al., 1987)
EG45	[M+H] ⁺	471.272	19.08	[11] Bacilysocin	[B] <i>Bacillus subtilis</i> 168	(Tamehiro et al., 2002)
	[M-H] ⁻	281.1761	16.23	[12] Mycinonic Acid IV	[B] <i>Micromonospora griseorubida</i>	(Kinoshita et al., 1991)

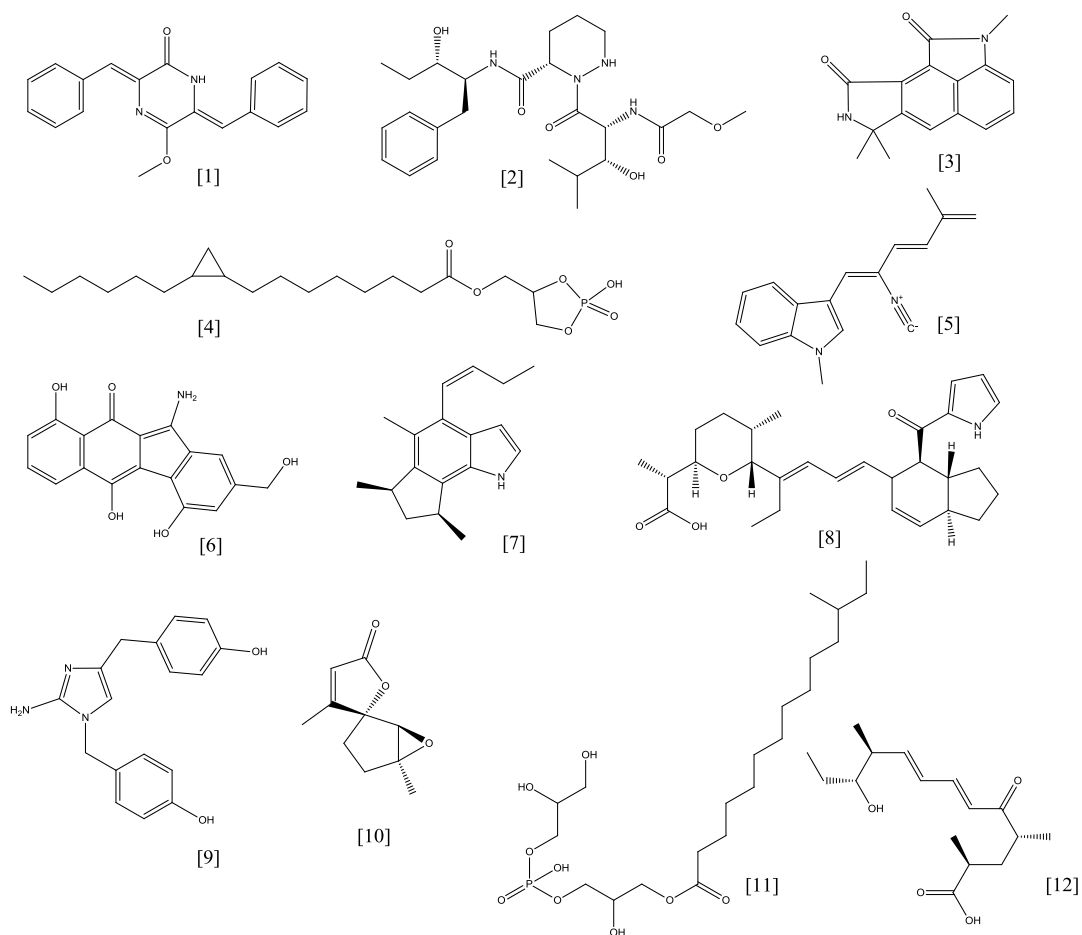


Figure 5-2: Structures of putatively identified compounds from marine actinomycetes.

EG4 is a novel strain of the genus *Microbacterium*. Small-scale cultures in M1 agar medium yielded round, cream-coloured colonies, as shown in Figure 5-3. A Gram stain of the bacteria showed small, Gram-positive rods.

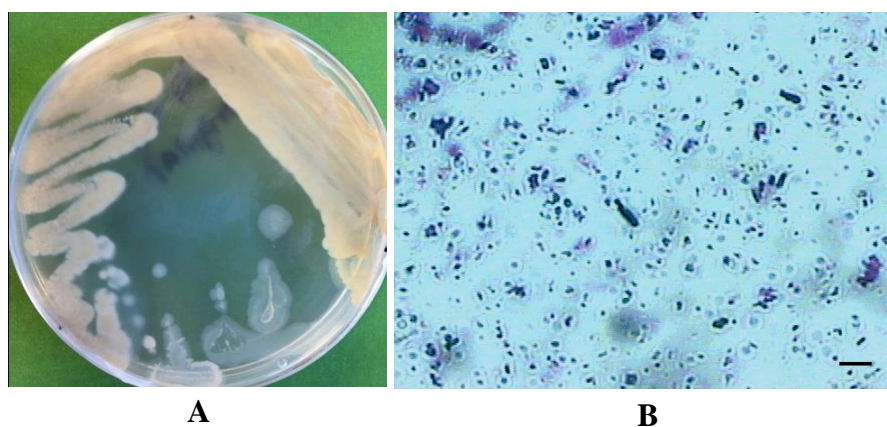


Figure 5-3: (A) EG4 (*Microbacterium* sp.) grown on M1 agar medium. (B) Gram stain of EG4. The scale bar is equivalent to 1 μ m.

5.3.2 Optimisation of Extraction Method

The ethyl acetate and methanol extracts were compared to the EG4 extract received from the University of Würzburg. The NMR spectra are depicted in Figure 5-4. The weights of the extracts are shown in Table 5-6.

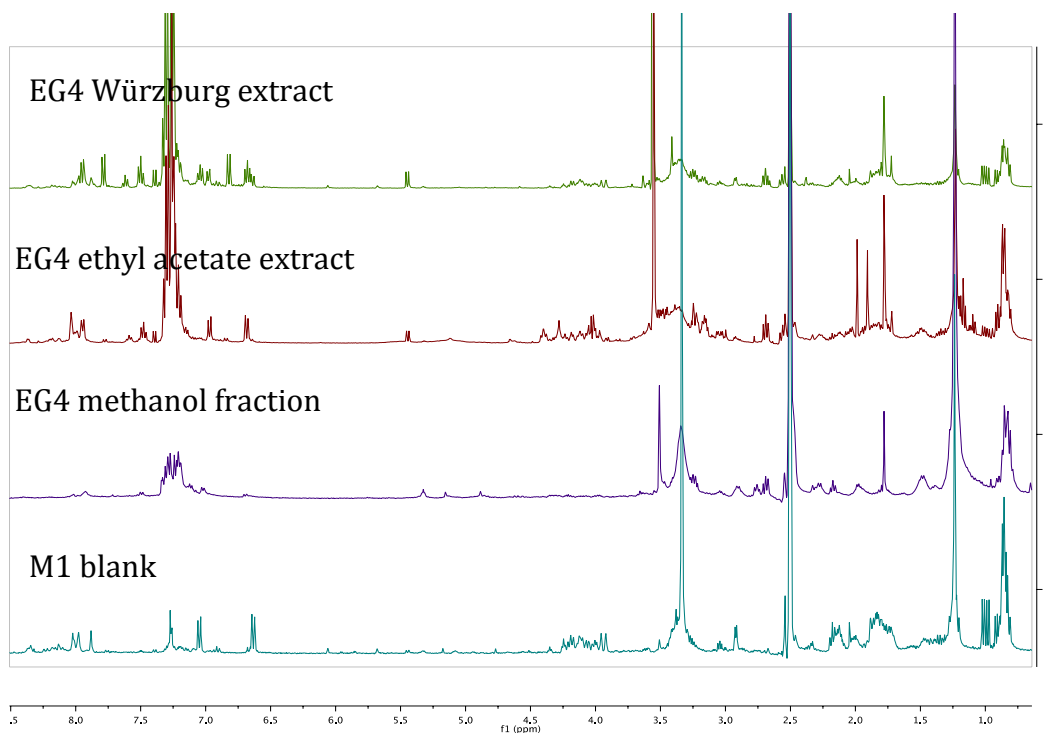


Figure 5-4: Comparison of the ^1H NMR spectra of the EG4 extracts (400 MHz, DMSO). The spectra are coloured as follows: EG4 extract sent from University of Würzburg (green), EG4 ethyl acetate extract (red), methanol fraction of the EG4 methanol extract after being subjected to HP20 chromatography (purple), and the M1 blank (teal).

Table 5-6: Yields of extracts obtained from EG4 agar cultures using different extraction procedures.

Extraction method	Yield (mg)
Ethyl acetate	15.8
Total methanol extract	59.2
Methanol extract after HP20 chromatography (100% MeOH)	2.4
Methanol extract after HP20 chromatography (50:50 H ₂ O:MeOH)	6.5
Methanol extract after HP20 chromatography (100% H ₂ O)	44.9

The ethyl acetate extraction required fewer steps and provided a larger yield than the methanol extract after HP20 chromatography. It was more similar to the original extract sent from Würzburg than the methanol extract, which required an additional step to remove the salt and sugars present from the media. It was therefore concluded that the extraction using ethyl acetate is a better procedure.

5.3.3 Up-scaling of EG4 Cultures

EG4 was then cultured in M1 broth. The bacteria were initially grown on M1 agar for five or ten days before being transferred to M1 broth. Half of the flasks were shaken and the other half were stationary in order to observe if shaking had any effect on the growth and metabolite production of the bacteria (Figure 5-5). The NMR spectra and heatmap representation of the LC-MS spectra of the extracts are shown in Figure 5-6 and Figure 5-7 respectively, and the resulting weights are shown in Table 5-7.



Figure 5-5: Stand (A) and shake (B) cultures of EG4 after 7 days incubation at 30°C. The stand cultures remained yellow, similar to the colour of un-inoculated M1, whereas the shake cultures foamed and became a darker in colour.

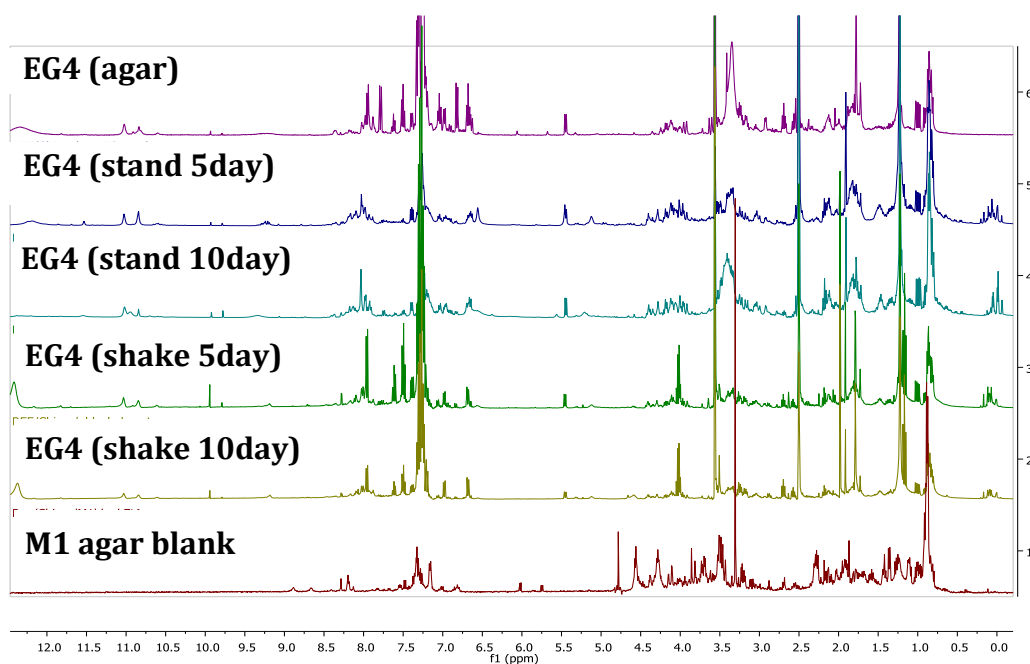


Figure 5-6: Comparison of various EG4 extracts (400 MHz, DMSO). Top to bottom: EG4 extract from agar, EG4 stand culture inoculated from 5-day incubated agar, EG4 stand culture inoculated from 10-day incubated agar, EG4 shake culture inoculated from 5-day incubated agar, EG4 shake culture inoculated from 10-day incubated agar, M1 agar blank. The extracts were broadly similar; however, the peaks in the aromatic region of the spectra (6.5-8.5 ppm) were more defined in the shake cultures than the stand cultures.

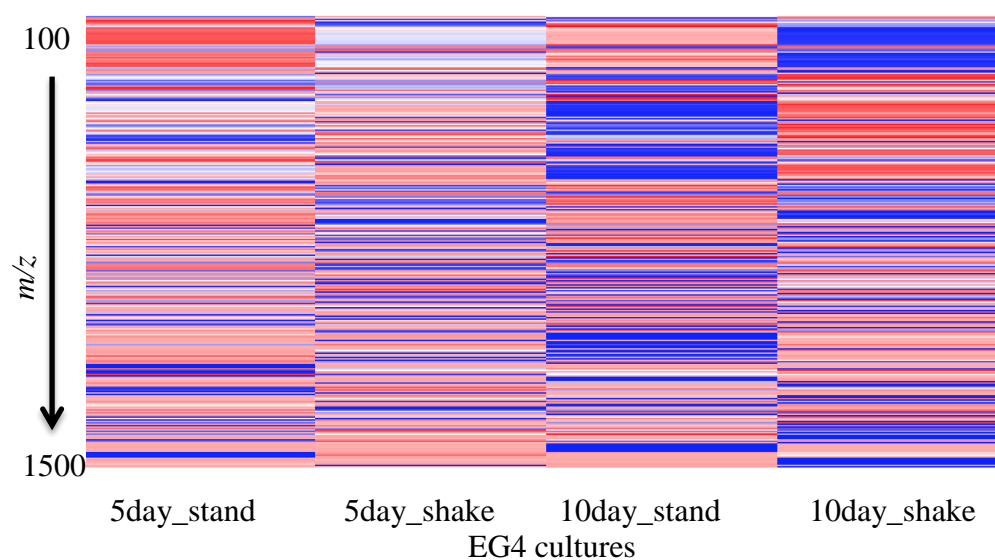


Figure 5-7: Heatmap representation of the LC-MS results of the EG4 extracts. Blue bands indicate a large peak area whereas red bands indicate low peak area. The ten day cultures appeared to produce more metabolites than the five day cultures. The ten day shake culture produced metabolites with lower molecular weights than the stand culture. In addition, the ten day stand culture produced more metabolites than the five day stand culture.

Table 5-7: Yields of up-scaled EG4 extracts

Culture	Yield (mg)	%inhibition of <i>T. brucei</i>
Stand culture from 5-day incubated agar	30.1	64.4
Stand culture from 10-day incubated agar	36.3	7.5
Shake culture from 5-day incubated agar	66.1	23.5
Shake culture from 10-day incubated agar	64	68.5

The anti-trypanosomal activities of the broth extracts are shown in Table 5-7. For the stand cultures, the one inoculated from a 5-day inoculum was more active whereas for the shake cultures the opposite was true. Nevertheless it was decided that it was better to grow EG4 in shake cultures because twice as much extract was produced compared to the stand culture. This was because shaking allowed the broth to be aerated and thus the growth of bacteria increased. Figure 5-5 also shows that the colours of the cultures were different; the stand culture remained yellow whereas the shake culture turned a darker shade of orange or pink. The NMR spectra in Figure 5-6 show that the metabolic profile of the cultures were similar; however, the shake cultures resulted in more peaks in the aromatic region (approximately 7-8 ppm). The heatmap in Figure 5-7 shows that the 10-day inocula resulted in the production of more metabolites as evidenced by the greater number and intensity of the blue bands. The two shake cultures had similar results, although the 10-day inoculum gave rise to a larger quantity of low-molecular weight metabolites. The 10day_stand culture evidently produced more metabolites than the 5day_stand culture, indicating that, should stand cultures be used, the inoculum should be cultured for a longer period of time if more metabolites are desired. However, the 5day_stand culture would be sufficient for the production of anti-trypanosomal compounds.

5.3.4 Medium Pressure Liquid Chromatography of Up-scaled EG4 Extracts

The up-scaled broth extracts were pooled, giving a total weight of 196.5 mg. This was then fractionated using normal phase MPLC. Although no pure compounds were obtained due to the small amount of starting material, it was evident that some fractions possessed anti-trypanosomal or anti-mycobacterial activity. The compounds

responsible for this activity may have been present in the crude extract in minute quantities; hence the activity was not so obvious until the extract was fractionated.

Table 5-8: Yields and activities of bioactive fractions following normal phase MPLC of EG4 up-scaled extracts. Active fractions are highlighted in grey (%Inhibition < 90). MIC determination was not performed against *M. marinum*.

Fraction	Yield (mg)	Inhibition of <i>T. b. brucei</i> (20 µg/mL)	MIC against <i>T. b. brucei</i> (µg/mL)	%Inhibition of <i>M. marinum</i> (100 µg/mL)
6	0.7	38.2	-	94.3
9	0.6	68.1	-	92.0
10	0.1	100.1	Insufficient sample	95.6
11	0.2	87.6	-	90.4
13	0.3	100.7	3.12	97.4
14	0.6	61.2	-	93.3
16	1.4	33.9	-	98.2
17	1.3	55.4	-	99.4
19	1.1	43.5	-	94.5
20	0.9	96.6	12.5	96.0
21	0.3	96.8	25	89.9
23	0.3	100.1	12.5	89.0
24	0.4	96.5	12.5	88.0
30	0.8	98.3	50	56
31	0.1	99.6	25	87.9
39	0.9	96.4	25	83.8
40	6.7	10.2	-	90.6
41	0.5	10.7	-	98.7

As seen in Table 5-8, the quantities obtained for each fraction were very small. Because the first fractions were extremely non-polar, these were unable to be dissolved in a suitable solvent for LC-MS. Fractions 17, 19-21, 23, 24, 30, 31 and 39-41 were analysed by LC-HRFTMS and processed using MZmine 2.10 to determine whether the major metabolites in each fraction had previously been identified. The results are in Table 5-9 and Figure 5-8.

Table 5-9: Metabolites with the largest peak area identified from bioactive EG4 fractions.

Fraction		<i>m/z</i>	RT	Name	Source	Reference
17	[M-H] ⁻	144.0457	8.63	[13] Indole-3-carboxaldehyde	Porifera <i>Dysidea etheria</i> , Porifera <i>Ulosa ruetzleri</i>	(Cardellina et al., 1986)
19	[M-H] ⁻	160.0408	8.41	[14] 5-methylindole-4,7-quinone	Mollusca <i>Drupella fragum</i>	(Fukuyama et al., 1998)
20	[M-H] ⁻	174.0565	6.94	[15] methyl indole-3-carboxylate	Actinobacteria <i>Streptomyces</i> sp.	(Hu et al., 2005)
21	[M+H] ⁺	225.1385	9.66	[16] Metabolite 3	[B] marine <i>Streptomyces</i> sp. (BL-49-58-005) from invertebrate	(Lopez et al., 2003)
	[M-H] ⁻	174.0563	7.55	[15] methyl indole-3-carboxylate	Actinobacteria <i>Streptomyces</i> sp.	(Hu et al., 2005)
23	[M+H] ⁺	256.1331	10.99	[17] Carbazomycin A	[B] <i>Streptomyces</i> sp. h 1051-my 10	(Sakano et al., 1980, Sakano and Nakamura, 1980, Kaneda et al., 1981, Yamasaki et al., 1983)
	[M-H] ⁻	311.2237	19.19	[18] Plakortin	[An] <i>Plakortis halichondrioides</i> , Sponge	(Higgs and Faulkner, 1978, Stierle and Faulkner, 1980)
24	[M+H] ⁺	150.0914	8.46	[19] Benzylacetamide; Phenylmethylacetamide	[B] marine <i>Streptomyces</i> sp. B 6921	(Maskey et al., 2004)
	[M-H] ⁻	347.2003	19.71	[20] Plakortether C	Porifera <i>Plakortis simplex</i>	(Campagnuolo et al., 2002)
30	[M+H] ⁺	164.107	8.67	[21] N-(2-Phenylethyl)acetamide	[M] [B] marine <i>Streptomyces</i> sp. B706, <i>Myxococcus fulvus</i> S110	(Daoud and Foster, 1993)
	[M-H] ⁻	315.2547	20.36	[22]	Porifera <i>Stelletta</i> sp.	(Zhao et al., 2003)
31	[M-H] ⁻	487.3068	6.68	[23] Heteronemin	Porifera <i>Cacospongia</i> sp, Porifera <i>Spongia</i> sp	(Kashman and Rudi, 1977)
39	[M+H] ⁺	245.1284	6.92	[24] cis-cyclo(L-Phe,L-Pro)	[B] arctic ice bacterium ANT V/2 132, ANT	(Barrow and Sun, 1994)
	[M-H] ⁻	329.2342	13.08	[25] Plakortether E	Porifera <i>Plakortis simplex</i>	(Campagnuolo et al., 2002)
40	[M-H] ⁻	329.2342	13.08	[25] Plakortether E	Porifera <i>Plakortis simplex</i>	(Campagnuolo et al., 2002)
41	[M+H] ⁺	219.1128	5.83	[26] beta-Hydroxy-Nbeta-acetyltryptamine	[B] <i>Streptomyces staurosporeus</i>	(Yang and Cordell, 1997)

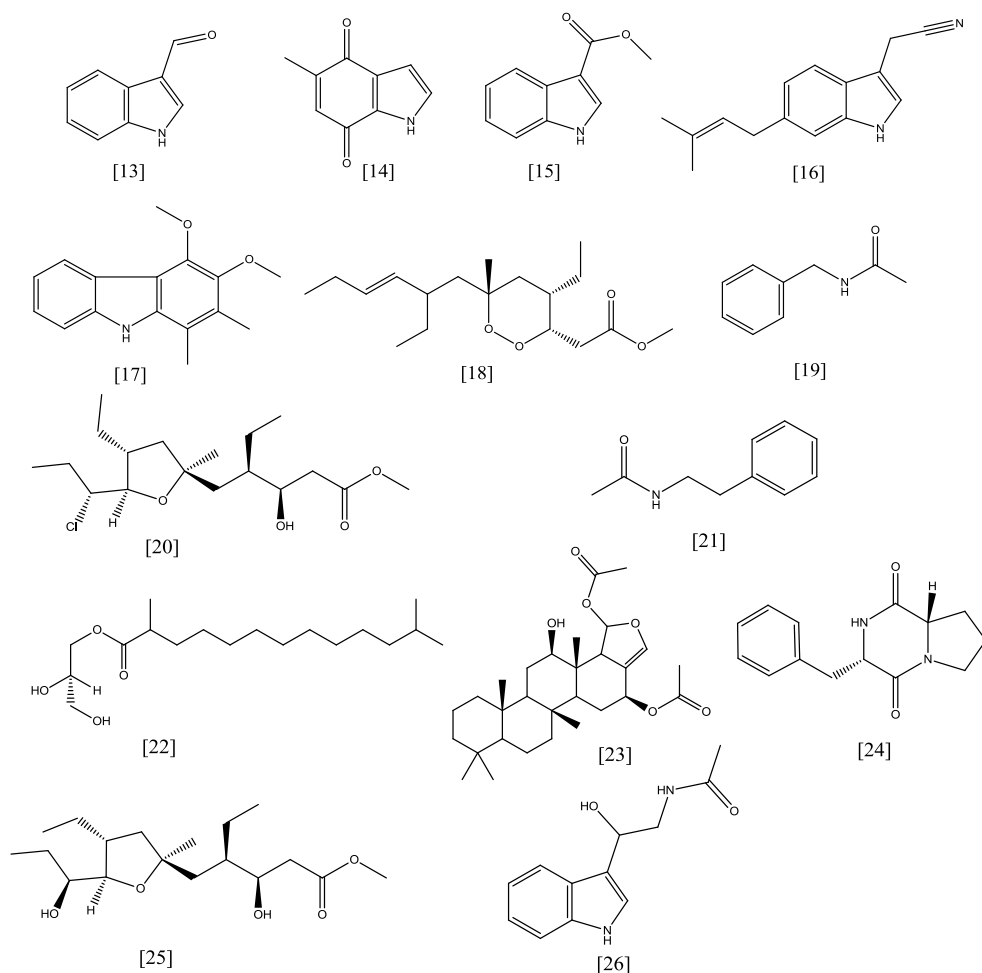


Figure 5-8: Structures of compounds identified from the bioactive EG4 MPLC fractions using the AntiMarin 2012 database.

Many of the identified compounds contained indole rings, as seen in Figure 5-8. It is also interesting to note that many of the compounds had previously been isolated from actinobacteria such as *Streptomyces* sp. and also from different species of sponges. It is possible that these compounds isolated from sponges were actually being produced by bacteria living in the sponge. As the quantities of the fractions were too small to obtain well-resolved ^1H NMR spectra, a large scale culture of EG4 was necessary to isolate and prove the presence of some of the compounds.

5.3.5 Metabolic Profiling of EG4 Over Time

Once the best method for the culture and extraction of EG4 was established, the metabolite production of EG4 over the course of two weeks was studied. This was to

determine the optimal duration of the culture. Two replicates were used for each day, spanning from Day 0 until Day 8 and Day 15. The weights of the extracts and their activities are listed below.

Table 5-10: Yields and activities of extracts obtained each day.

Extract	Yield (mg)	%Inhibition of <i>T. brucei</i> (20 µg/mL)	%Inhibition of <i>M. marinum</i> (100 µg/mL)
Day 0A	7.9	9.9	68.3
Day 0B	10.0	52.0	11.8
Day 1A	8.2	33.2	86.0
Day 1B	10.1	55.0	79.9
Day 2A	21.3	6.0	50.5
Day 2B	14.7	56.2	74.7
Day 3A	13.5	33.2	72.5
Day 3B	14.0	9.4	79.2
Day 4A	18.4	7.0	79.0
Day 4B	11.6	23.3	84.7
Day 5A	13.2	23.3	86.0
Day 5B	14.2	1.2	0
Day 6A	12.5	20.3	83.9
Day 6B	18.1	13.5	83.7
Day 7A	12.9	51.4	84.8
Day 7B	14.0	17.2	84.1
Day 8A	13.9	-1.5	83.9
Day 8B	16.3	-23.6	75.5
Day 15A	11.4	-21.5	68.8
Day 15B	12.8	-26.2	82.1
M1 Blank	14.8	18.0	79.0

The antimicrobial activities of the extracts fluctuated from day to day and between samples. The anti-trypanosomal activity was less than the anti-mycobacterial activity; however, the M1 blank itself had greater anti-mycobacterial activity than anti-trypanosomal activity indicating that compounds present in the media could be responsible for the bioactivity of the extracts. From Day 6 the anti-mycobacterial activity became more consistent. Anti-trypanosomal activity disappeared in Days 8 and 15.

Changes in metabolite production were evident in the ¹H NMR spectra, as seen in Figure 5-9. The most prominent variations occurred in the amide, aromatic and

allylic regions of the spectra. The production of metabolites appeared to be significant beginning on Day 2.

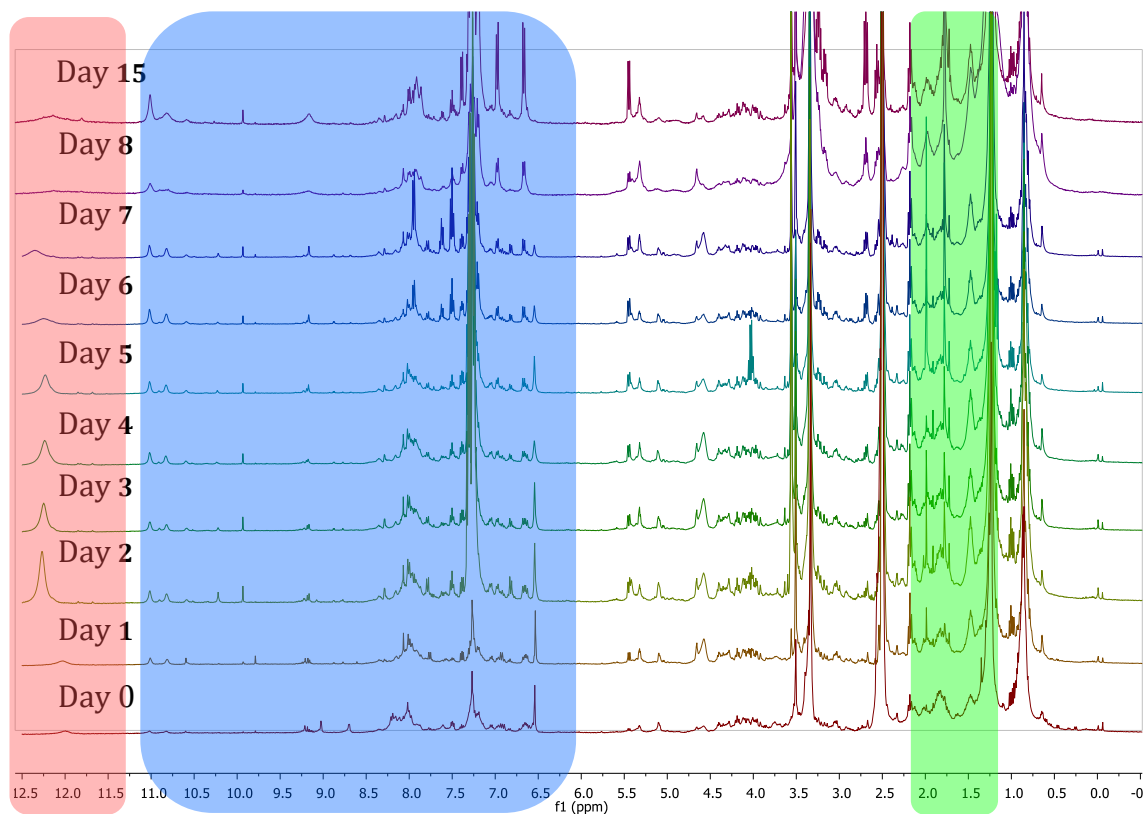


Figure 5-9: ^1H NMR of extracts across days (400 MHz, DMSO). The regions where changes occurred are highlighted in red (amide), blue (aromatic) and green (allylic).

Two-dimensional NMR, such as COSY and TOCSY, was performed on the extracts. Several spin systems were thereby identified, including those of tyrosine and phenylalanine.

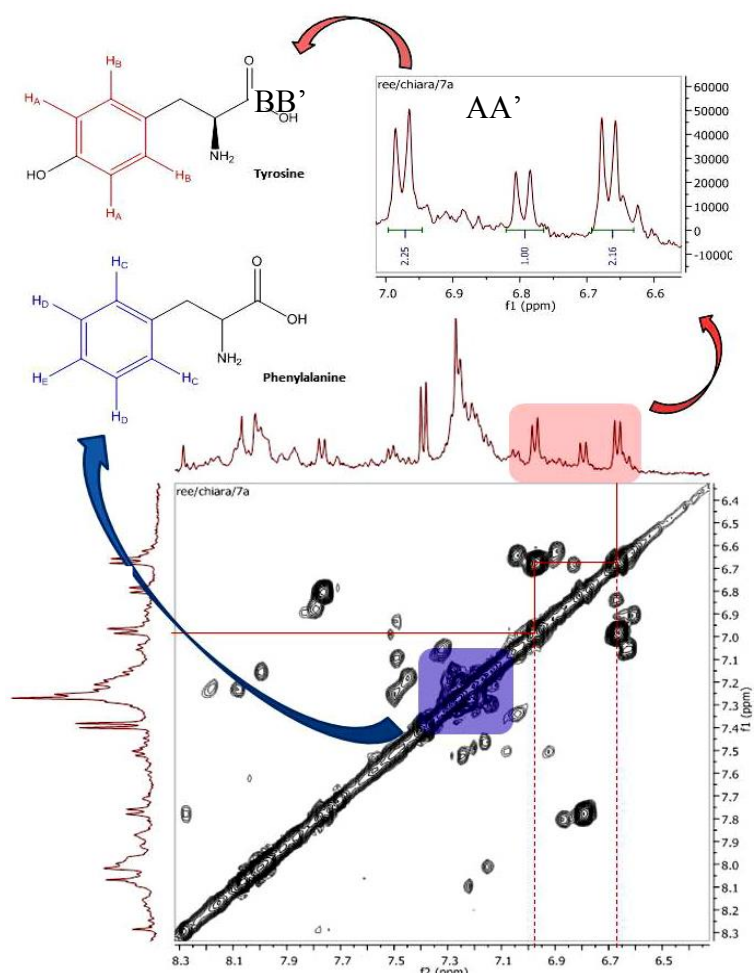


Figure 5-10: Expansion of the COSY spectrum of Day 1A. The peak correlations imply the presence of phenylalanine and tyrosine-like molecules.

An AA'BB' system in the aromatic region was derived from para-disubstituted benzenes similar to that of tyrosine. This was indicated by the two coupling peaks at δ_{H} 6.98 and 6.67 ppm. The cluster of peaks at δ_{H} 7.1–7.3 ppm is characteristic of the correlation between two groups of equivalent protons such as in phenylalanine, a monosubstituted benzene.

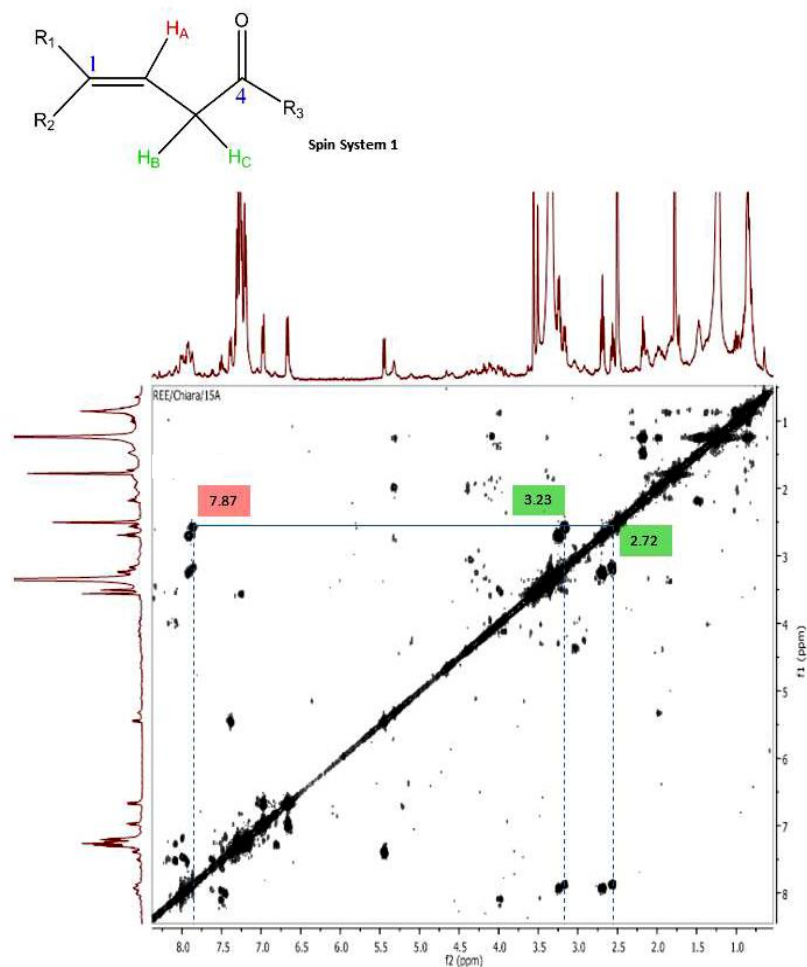


Figure 5-11: COSY spectrum of Day 15A. The lines show the correlations between the peaks that correspond to the above substructure.

The correlating amide and allylic region at δ_{H} 7.87 (H_{A}), 3.23 and 2.72 ppm (H_{B} and H_{C}) led to the elucidation of the substructure in Figure 5-11. 2D TOCSY spectra confirmed the spin system (Figure 5-12). The crosspeak for H_{A} appeared at Day 7 and was constant in the succeeding days. The signals for H_{B} and H_{C} became visible at Day 8 and all signals intensified on Day 15, indicating an increase in the concentration of that compound.

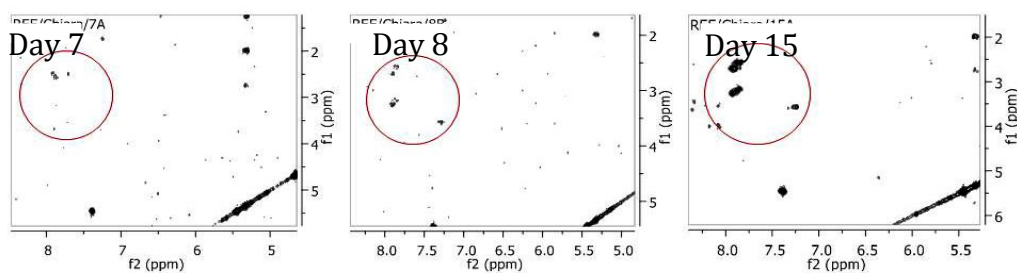


Figure 5-12: 2D-TOCSY spectra of Day 7, Day 8 and Day 15 extracts. The signals intensify as the days progress, implying the production of that compound from Day 7 onwards.

LC-MS was also performed on the extracts. Analysis of the resulting data showed that there was an increase in the production of small molecules as the days progressed, as depicted in Figure 5-13.

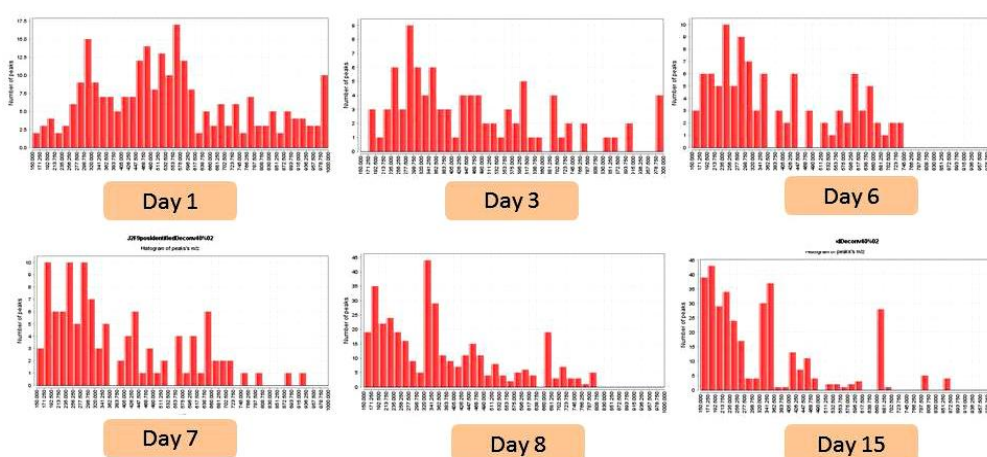


Figure 5-13: Histograms showing the shift towards small molecule production over time. The x-axis of the histograms represents the m/z ranges. As the days progress the histograms become skewed to the left, denoting an increase in small molecules (m/z 200-450) and a decrease in larger molecular weight compounds (m/z : 700-1000).

Multivariate analysis using SIMCA 13 was performed on the LC-HRFTMS data to detect the metabolites that correlated with the anti-trypanosomal and anti-mycobacterial activity. Principal component analysis (PCA), an unsupervised form of multivariate analysis, was used to portray the data in a graphical form, highlighting the similarities and differences between the samples. In Figure 5-14, PCA showed that there was good reproducibility between the extracts taken for each day, but that there was a difference between the first batch, Days 0-7, and the second batch, Days 8 and 15. It is possible that this was the progression of the metabolite

production; however, it is also possible that part of the difference was the result of inter-batch variation. There was no obvious difference in metabolite production from Day 0 to Day 2. Days 3, 4 and 5 clustered together indicating that during those days the bacteria produced the same metabolites. Different metabolites were produced in Day 6 and Day 7, as well as Days 8 and 15.

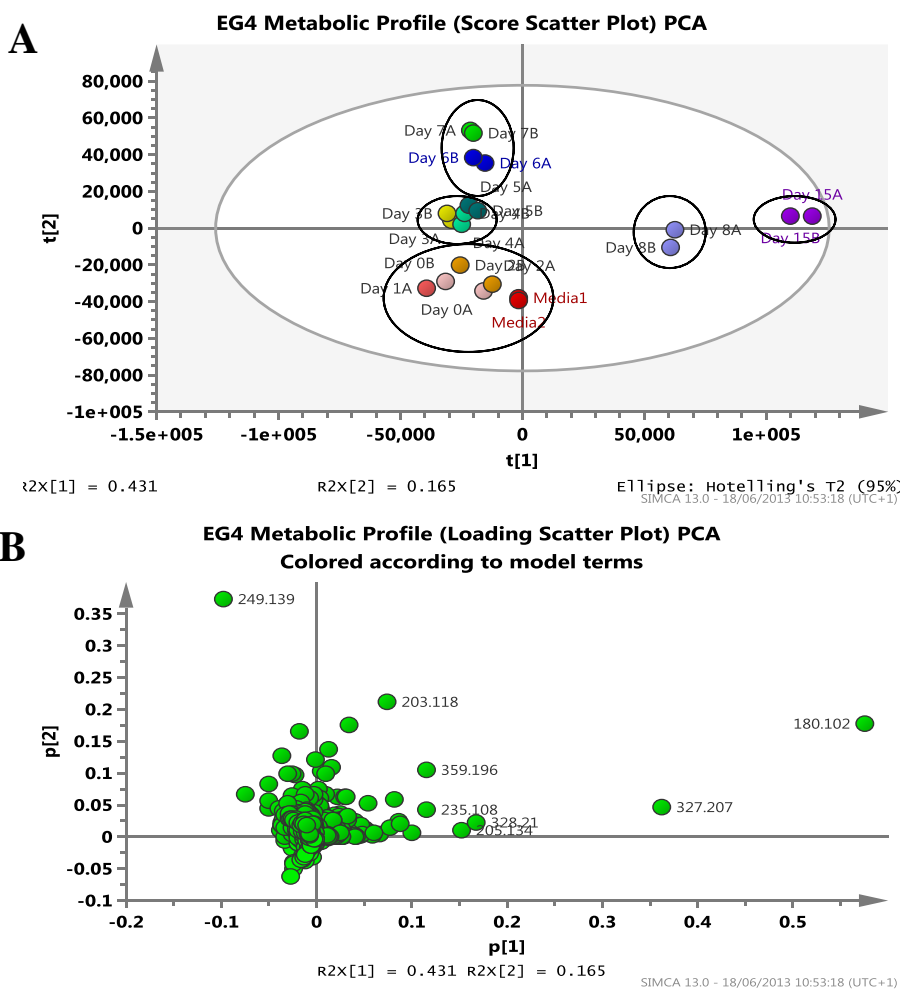


Figure 5-14: PCA of EG4 extracts grown over the course of two weeks. (A) PCA score plot showing the relationships between the extracts (coloured by day). (B) PCA loading plot showing the distribution of metabolites among the extracts. R2X(cum)= 0.762, Q2(cum)= 0.525.

OPLS-DA, a supervised form of multivariate analysis, was also performed. The anti-trypansomal activity fluctuated between the different days, but it was still possible to identify the metabolites contributing to the anti-trypansomal activity by classifying each extract as active or inactive according to whether or not they inhibited the trypanosome growth compared to the media blank. The score scatter plot in Figure 5-15 below shows the classification of the samples as active and

inactive. Day 6A, having an activity similar to the M1 broth blank, lay close to the inactive samples although it was classified as active. The loading scatter plot of the OPLS-DA highlights the metabolites that are more prominent in the inactive (left) and active (right) samples. The S-plot in Figure 5-16 gives a clearer indication of the metabolites that contribute to activity. Table 5-11 summarizes the distribution of the highlighted compounds across the extracts. The table is portrayed as a heatmap to facilitate viewing and to show, at a glance, at which day the production of that metabolite peaks. Those metabolites that were putatively identified by the AntiMarin database are listed in Table 5-12 and Figure 5-17.

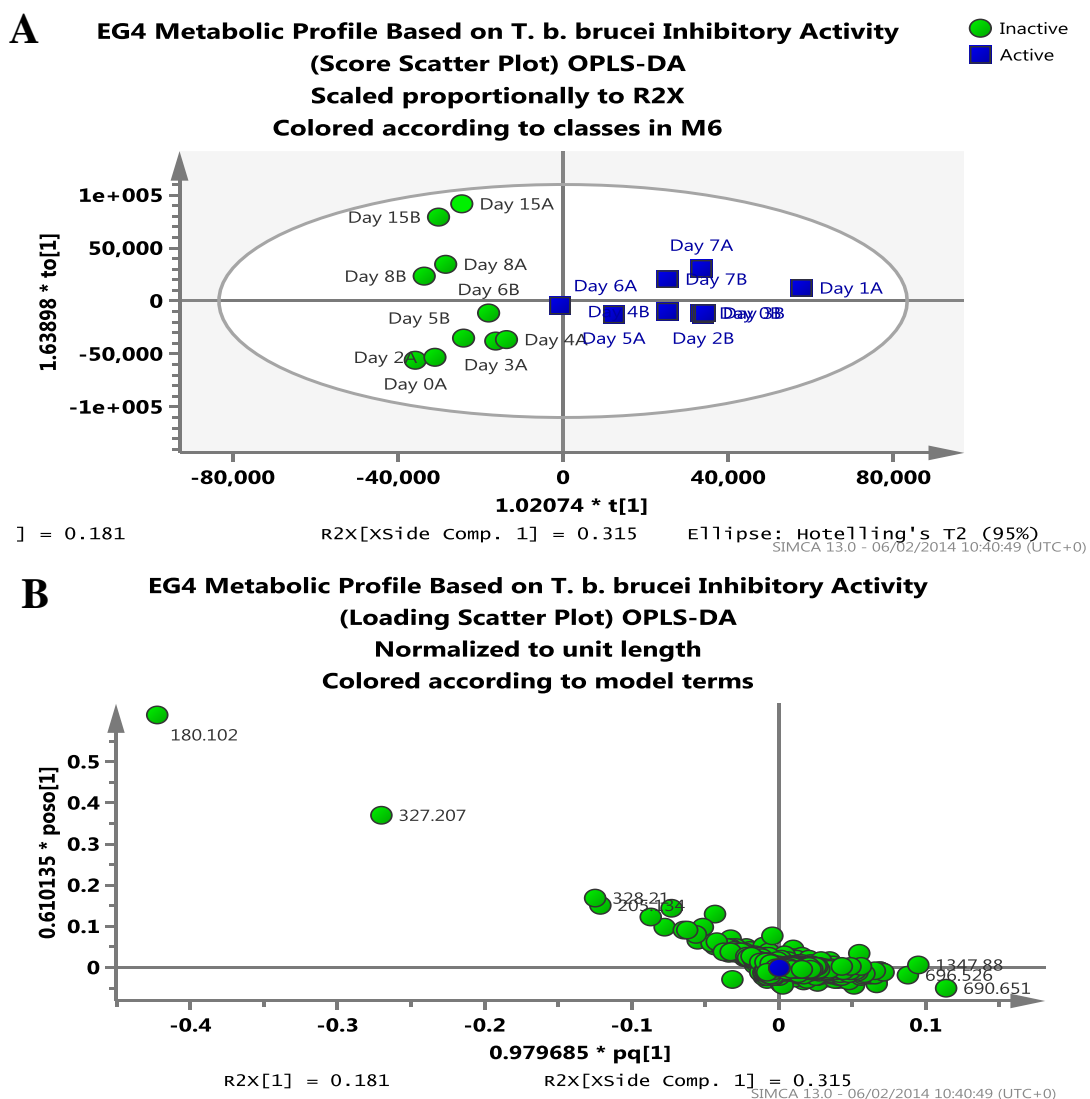


Figure 5-15: OPLS-DA of EG4 extracts grown over the course of two weeks based on their inhibitory activity against *T. b. brucei*. (A) Scores plot showing the classification of the extracts. (B) Loading plot showing the distribution of metabolites between the active and inactive extracts. $R^2X(cum)=0.633$, $R^2Y(cum)=0.839$, $Q^2(cum)=0.262$.

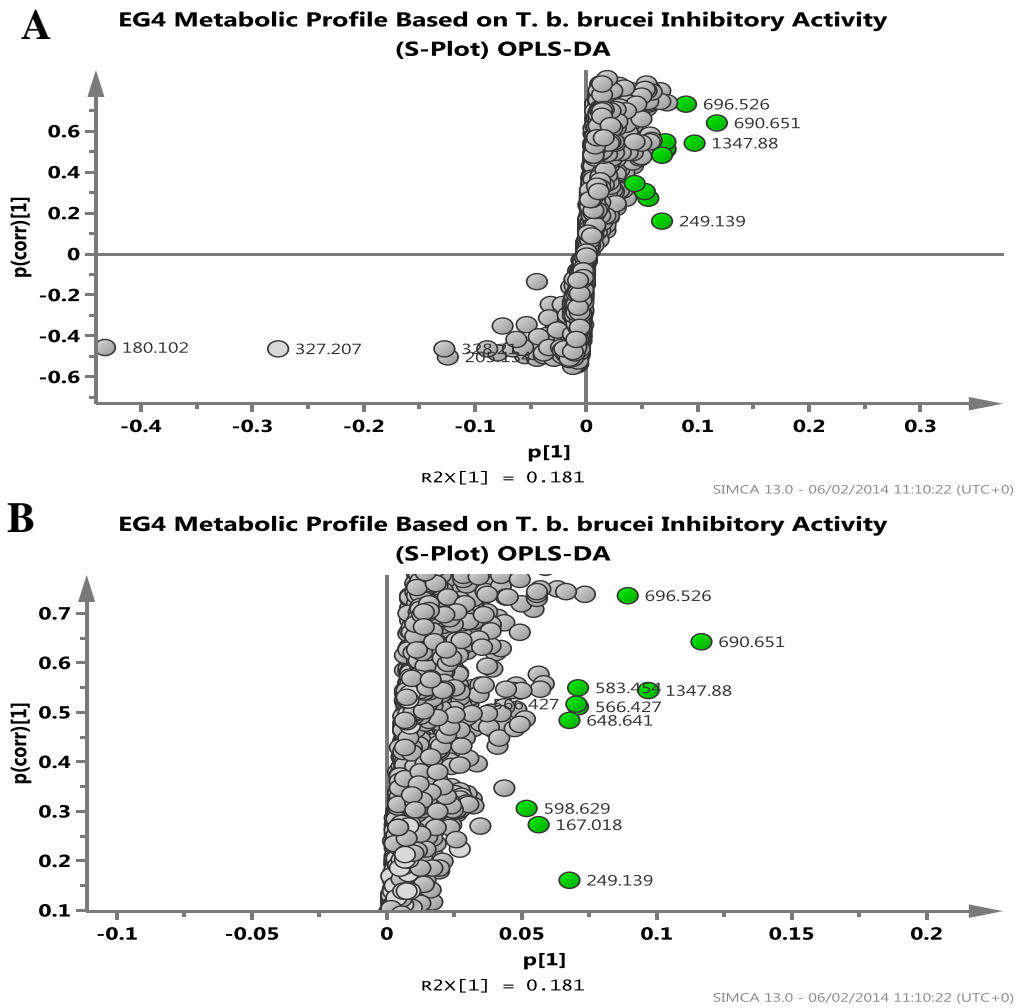


Figure 5-16: S-Plot showing the metabolites that contribute to the *T. b. brucei* inhibitory activity of the extracts. (A) Full S-plot. (B) Expansion of the upper right quadrant, showing the m/z of the highlighted metabolites, which are those that are most likely to contribute to the anti-trypanosomal activity of the extracts.

Table 5-11: Peak areas of peaks showing the greatest contribution to anti-trypanosomal activity as represented by the growing intensity of red from yellow. Cells highlighted in light grey were putatively identified by the AntiMarin database.

ID	m/z	RT	Day 0A	Day 0B	Day 1A	Day 2A	Day 2B	Day 3A	Day 3B	Day 4A	Day 4B	Day 5A	Day 5B	Day 6A	Day 6B	Day 7A	Day 7B	Day 8A	Day 8B	Day 15A	Day 15B
N_1090	167.0175	12.80	4.75E5	4.41E5	5.00E5	7.75E5	1.59E6	2.36E6	2.87E6	9.98E6	1.24E7	1.77E7	2.21E7	7.13E7	2.01E7	1.09E8	1.27E8	5.51E6	6.42E6	1.19E7	9.09E6
P_4336	249.1385	10.53	1.19E6	2.41E6	1.47E7	1.88E7	1.82E7	2.22E8	2.25E8	9.85E7	1.53E8	1.60E8	2.73E8	4.62E8	4.04E8	3.16E8	3.68E8	8.15E6	7.97E6	3.20E7	2.13E7
P_1597	566.4265	22.05	4.10E6	5.89E6	5.29E7	1.53E7	5.86E7	1.56E6	1.89E6	1.25E6	2.86E6	5.99E6	1.88E6	1.81E6	1.92E6	2.46E6	1.83E6	1.82E6	1.01E6	8.51E5	4.06E5
P_5506	566.4274	21.55	1.37E5	1.59E5	5.10E7	1.47E7	5.59E7	1.81E6	2.81E6	1.76E6	6.13E6	1.54E6	1.40E6	1.70E6	5.52E6	1.46E6	4.90E6	4.35E5	6.15E5	2.34E5	3.36E5
P_4331	583.4541	21.54	1.08E5	1.14E5	4.65E7	1.26E7	4.83E7	1.44E6	6.26E6	1.50E6	8.47E6	2.92E6	1.15E6	1.44E6	1.73E6	1.24E6	1.60E6	3.59E5	4.30E5	1.85E5	2.37E5
P_5170	598.6289	33.02	0	0	0	2.22E7	6.20E7	4.48E7	2.13E7	9.91E6	6.24E7	6.87E7	4.70E7	4.45E7	3.05E7	5.07E7	1.88E7	1.05E4	2.15E3	2.91E3	2.79E3
P_3348	648.6411	30.88	0	4.91E+07	1.29E7	3.05E7	1.32E7	4.77E6	3.99E7	4.72E7	3.20E7	2.46E7	2.17E7	3.45E7	1.46E7	1.72E7	4.36E7	0	0	0	0
P_2156	690.6515	31.63	8.71E6	5.19E7	5.37E7	3.02E6	8.02E7	3.93E7	2.79E7	7.14E7	5.79E7	7.89E7	6.53E7	4.59E7	2.85E7	4.84E7	6.58E7	1.95E4	6.05E3	2.23E4	1.03E4
P_904	696.5263	31.06	7.61E6	3.21E7	3.16E7	2.70E6	2.43E7	2.86E7	1.90E7	1.55E7	1.41E7	2.43E7	1.01E7	1.35E7	3.24E7	4.00E7	3.19E7	2.11E6	1.03E6	8.65E5	7.77E5
P_3289	1347.882	37.14	0	4.89E7	1.14E8	7.28E4	3.17E4	3.05E4	1.05E4	0	1.48E4	0	5.27E4	0	0	0	0	0	0	0	0

Table 5-12: Identification of peaks showing the greatest contribution to anti-trypanosomal activity using AntiMarin database.

ID	Exact mass	Formula	Name	Source	Reference
P_4336	248.1312	C ₁₇ H ₁₆ N ₂	[5] Brasilidine A	[B] <i>Nocardia brasiliensis</i>	(Kobayashi et al., 1997)
P_1597	565.4193	C ₃₀ H ₅₅ N ₅ O ₅	[27] Viscumamide	[F] endophytic <i>Paecilomyces</i> sp. From mangroves	(Guo et al., 2007)

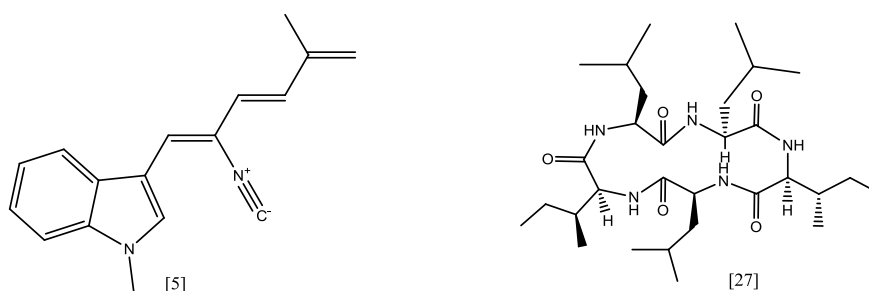


Figure 5-17: Metabolites putatively identified in the AntiMarin database that are potentially active against *T. b. brucei*.

The extracts were then classified based on their activity against *M. marinum*. Although there were varying degrees of activity throughout the time period that EG4 was cultivated, the anti-mycobacterial activity became more consistent from Day 6 onwards. Hence, Days 6, 7, 8 and 15 were classified as active against *M. marinum* whereas the others were considered inactive. The S-plot in Figure 5-18 shows some metabolites, such as m/z 180.102 [M+H]⁺ and 327.207 [M+H]⁺, which were strongly evident in the anti-mycobacterial extracts. These had previously been identified as metabolites that do not contribute to anti-trypanosomal activity (Figure 5-16), thus indicating that they may have selective anti-mycobacterial activity. Table 5-13 shows the distribution of these highlighted compounds across the extracts whereas Table 5-14 and Figure 5-19 show the putatively identified metabolites.

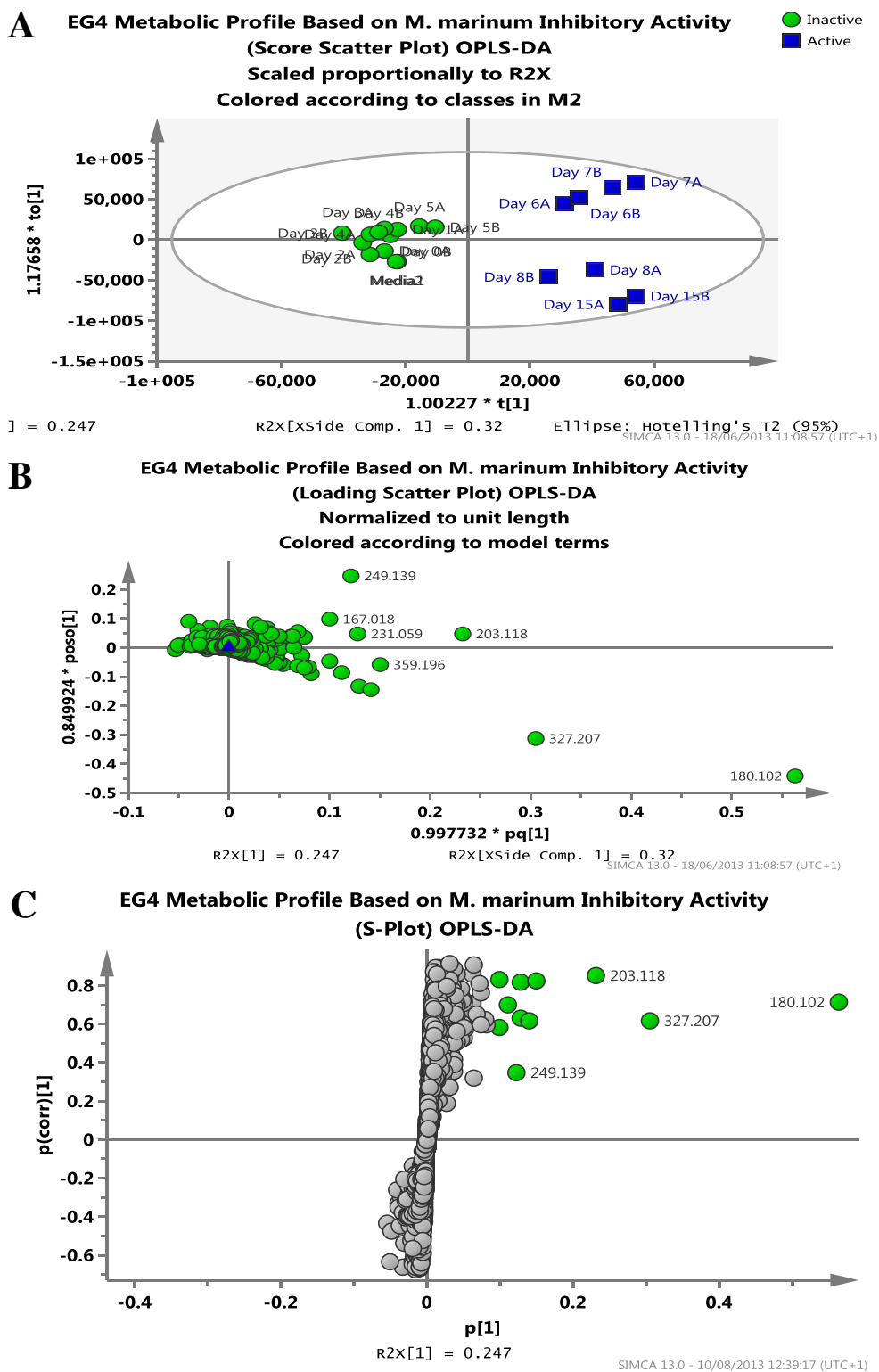


Figure 5-18: OPLS-DA of EG4 extracts grown over the course of two weeks based on their inhibitory activity against *M. marinum*. (A) Score plot showing the classification of the extracts. (B) Loading plot showing the distribution of metabolites between the active and inactive extracts. (C) S-Plot showing the metabolites that contribute to the *M. marinum* inhibitory activity of the extracts. $R^2X(\text{cum})=0.66$, $R^2Y(\text{cum})=0.939$, $Q^2(\text{cum})=0.853$.

Table 5-13: Peak areas of peaks showing the greatest contribution to anti-mycobacterium activity as represented by the growing intensity of red from yellow. Cells highlighted in light grey were putatively identified by the AntiMarin database.

ID	m/z	RT	Day 0A	Day 0B	Day 1A	Day 2A	Day 2B	Day 3A	Day 3B	Day 4A	Day 4B	Day 5A	Day 5B	Day 6A	Day 6B	Day 7A	Day 7B	Day 8A	Day 8B	Day 15A	Day 15B
N_1090	167.0175	12.80	4.75E5	4.41E5	5.00E5	7.75E5	1.59E6	2.36E6	2.87E6	9.98E6	1.24E7	1.77E7	2.21E7	7.13E7	2.01E7	1.09E8	1.27E8	5.51E6	6.42E6	1.19E7	9.09E6
P_302	180.1018	4.59	1.38E8	1.30E8	1.78E8	1.31E8	1.86E8	2.08E8	2.21E8	1.95E8	2.59E8	3.18E8	2.25E8	4.35E8	4.56E8	4.77E8	4.98E8	1.58E9	1.51E9	2.62E9	2.41E9
P_951	203.1178	9.39	5.90E6	8.80E6	1.82E7	5.37E6	8.37E6	1.54E7	1.73E7	9.40E6	1.70E7	3.12E7	2.46E7	1.30E8	1.72E8	2.63E8	1.60E8	2.67E8	1.26E8	2.37E7	1.94E8
P_816	205.1335	8.68	3.96E5	8.45E4	2.96E5	5.10E5	4.53E5	1.05E6	4.15E5	1.63E6	2.02E6	2.80E6	2.67E6	3.83E6	5.55E6	1.12E6	4.56E6	1.06E8	1.03E8	1.56E8	1.45E8
P_2526	207.1128	6.92	2.36E6	2.28E6	2.56E6	1.78E6	2.83E6	4.64E6	4.59E6	6.63E6	7.47E6	1.24E7	1.07E7	2.22E7	2.58E7	1.78E7	1.66E7	3.76E7	3.22E7	6.22E7	5.46E7
P_5168	231.0586	13.84	3.42E5	2.71E5	1.13E6	1.37E7	2.40E7	3.74E7	3.32E7	3.13E7	4.62E7	2.70E7	3.06E7	5.89E7	6.56E7	9.93E7	9.81E7	5.59E7	3.72E7	5.89E7	6.92E7
P_1625	235.1076	6.33	1.77E6	1.18E6	4.08E6	5.06E6	6.78E6	8.18E6	9.78E6	1.05E7	1.23E7	1.67E7	1.21E7	2.03E7	1.98E7	1.64E7	1.60E7	6.31E7	5.23E7	1.11E8	9.62E7
P_4336	249.1385	10.53	1.19E6	2.41E6	1.47E7	1.88E7	1.82E7	2.22E8	2.25E8	9.85E7	1.53E8	1.60E8	2.73E8	4.62E8	4.04E8	3.16E8	3.68E8	8.15E6	7.97E6	3.20E7	2.13E7
P_4375	327.2065	8.69	5.74E6	1.71E6	3.47E6	8.26E6	5.71E6	1.15E7	2.91E6	1.77E7	1.85E7	2.38E7	2.57E7	3.54E7	4.74E7	9.63E6	4.24E7	4.40E8	4.24E8	1.02E9	8.91E8
P_2276	328.2102	8.70	1.21E6	3.37E5	7.35E5	1.69E6	1.15E6	2.44E6	5.79E5	3.67E6	3.83E6	4.83E6	5.27E6	7.52E6	9.94E6	1.92E6	8.76E6	9.15E7	8.86E7	2.16E8	1.91E8
P_1027*	359.1964	4.59	1.06E7	1.05E7	1.61E7	1.53E7	2.11E7	2.25E7	2.51E7	2.34E7	3.09E7	3.91E7	2.60E7	5.41E7	5.60E7	6.15E7	6.45E7	7.46E7	6.66E7	1.55E8	1.35E8

*P_1027 is a [2M]^{-H} of P_302.

Table 5-14: Identification of peaks showing the greatest contribution to anti-mycobacterial activity using AntiMarin database.

ID	Exact mass	Formula	Name	Source	Reference
P_302	179.0946	C ₁₀ H ₁₃ NO ₂	[28] 5-Butylpyridine-2-carboxylic acid; 5-Butylpicolinic acid; Fusaric acid	[F] <i>Gibberella fujikuroi</i> , <i>Fusarium oxysporum</i> , <i>Fus.sp.</i> , <i>Fus.solani</i>	(Biland et al., 1960, Hardegger and Nikles, 1957b, Hardegger and Nikles, 1957a, Claydon et al., 1977, Desaty et al., 1968, Mutert et al., 1981)
			[29] N-Acetyl-tyramine	[B] marine <i>Streptomyces</i> B7939, <i>S. griseus</i> , <i>Mycobacterium tuberculosis</i>	(Comin and Kellerschierlein, 1959)
			[30] N-Hydroxy-dihydro-abikoviromycin	[B] <i>Streptomyces</i> species SANK 65986	(Takahashi et al., 1986)
			[31] U-77864	[B] <i>Streptomyces griseoluteus</i> strain ws6724	(Harper and Welch, 1992)
			[32] 3-(p-Hydroxyphenyl)-N-methylpropionamide; N-Methylphloretamide	[B] <i>Micromonospora</i> sp. P1068	(Gutierrez-Lugo et al., 2005)
			[33] 4'-tolyl-3-aminopropanoate	<i>Magnoliophyta Heritiera littoralis</i> , Actinobacteria <i>Streptomyces</i> sp	(Xie et al., 2008)
P_951	202.1106	C ₁₂ H ₁₄ N ₂ O	[34] Nb-Acetyltryptamine	[B] myxobacteria, marine Bacterium sp. GBF GW	(Bohlendorf et al., 1996)
P_816	204.1263	C ₁₂ H ₁₆ N ₂ O	[35] Bufotenin; N,N-Dimethylserotonin	[F] basidiomycete <i>Amanita mappa</i> , amphibians	(Nishida et al., 1990, Daly and Witkop, 1967)
			[36] Psilocin	[F] <i>Psilocybe cubensis</i> , <i>Stropharia semilanceata</i> and many others	(Hofmann et al., 1959)
P_2526	206.1055	C ₁₁ H ₁₄ N ₂ O ₂	[37] a-Amino-beta-(1-indoline)-propionic acid	[B] <i>Escherichia coli</i> t4-3	(Kanamitsu et al., 1987)
			[38] N-Acetylkynuramine	[B] marine <i>Janibacter limosus</i> Hel 1, arctic ice bacterium isolate ANT Actinobacteria <i>Janibacter limosus</i>	(Asolkar et al., 2004)
			[39] (S*R*)-2-(1-Hydroxyethyl)-2-methyl-2,3-dihydro-1H-quinazolin-4-one	[B] <i>Streptomyces</i> sp. GW23/1540	(Maskey et al., 2004)
			[40] (R*R*)-2-(1-Hydroxyethyl)-2-methyl-2,3-dihydro-1H-quinazolin-4-one	[B] <i>Streptomyces</i> sp. isolate GW23/1540	(Maskey et al., 2004)
P_1625	234.1003	C ₁₂ H ₁₄ N ₂ O ₃	[41] Cyclo-L-phenylalanin-L-serin	[F] <i>Hyalodendron</i> sp. (fsc-601)	(Boente et al., 1991)
			[42] 4-Methoxytryptophan	Synthetic	(van Wickern et al., 1997)
			[43] Nd-Acetyl-N2-formylkynuramine		
P_4336	248.1312	C ₁₇ H ₁₆ N ₂	[5] Brasilidine A	[B] <i>Nocardia brasiliensis</i>	(Kobayashi et al., 1997)

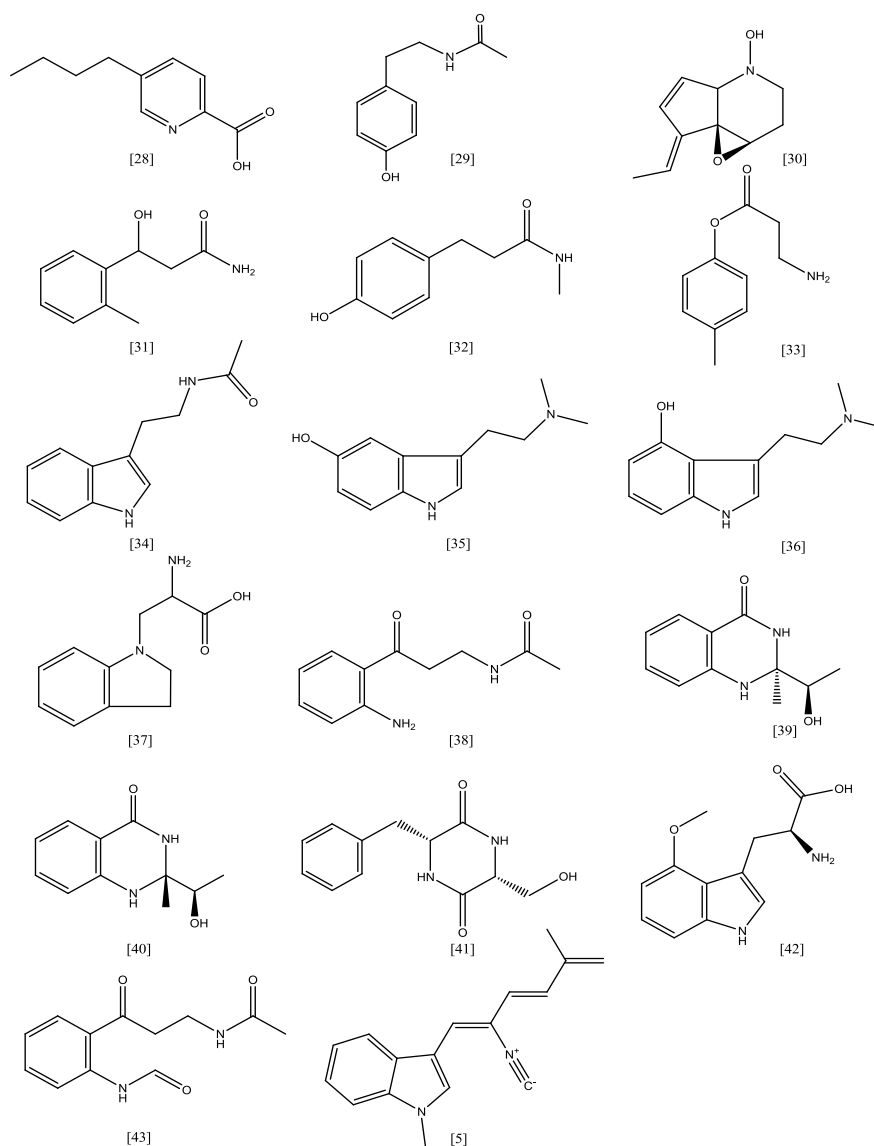


Figure 5-19: Structures of compounds identified from the EG4 extracts using the AntiMarin database. These compounds are possibly active against *M. marinum*. Many of the hits are indolic or aromatic compounds.

5.3.6 Isolation of Compounds from EG4

EG4 was grown in a total of 16 L of M1 broth. The resulting extract weighed 1.2478 g. Nine relatively pure compounds were isolated from this crude extract using a combination of bioassay- and metabolomics-guided techniques to identify target metabolites for purification. The flowchart in Figure 5-20 summarises the steps performed to isolate the compounds.

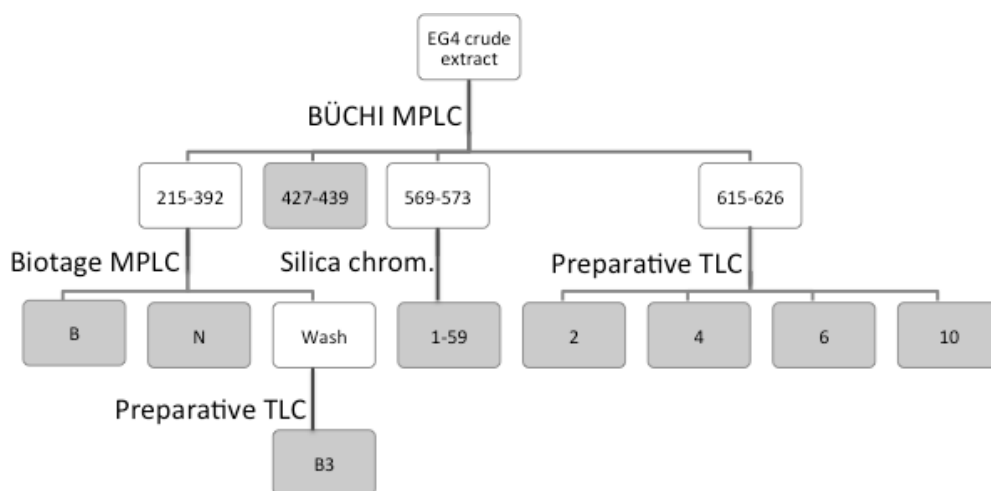


Figure 5-20: Flowchart of isolation work. Cells in grey were obtained as pure compounds.

5.3.6.1 Normal Phase MPLC of EG4 Up-scaled Extract

EG4 was grown in a total of 16 L of M1 broth. The resulting extract weighed 1.2478 g. This was fractionated using MPLC. The TLC summary plate of the resulting fractions is pictured in Figure 5-21 below. The fractions were subjected to anti-trypansomal and anti-mycobacterium assays. The weights and activities of each fraction are shown in Table 5-15.

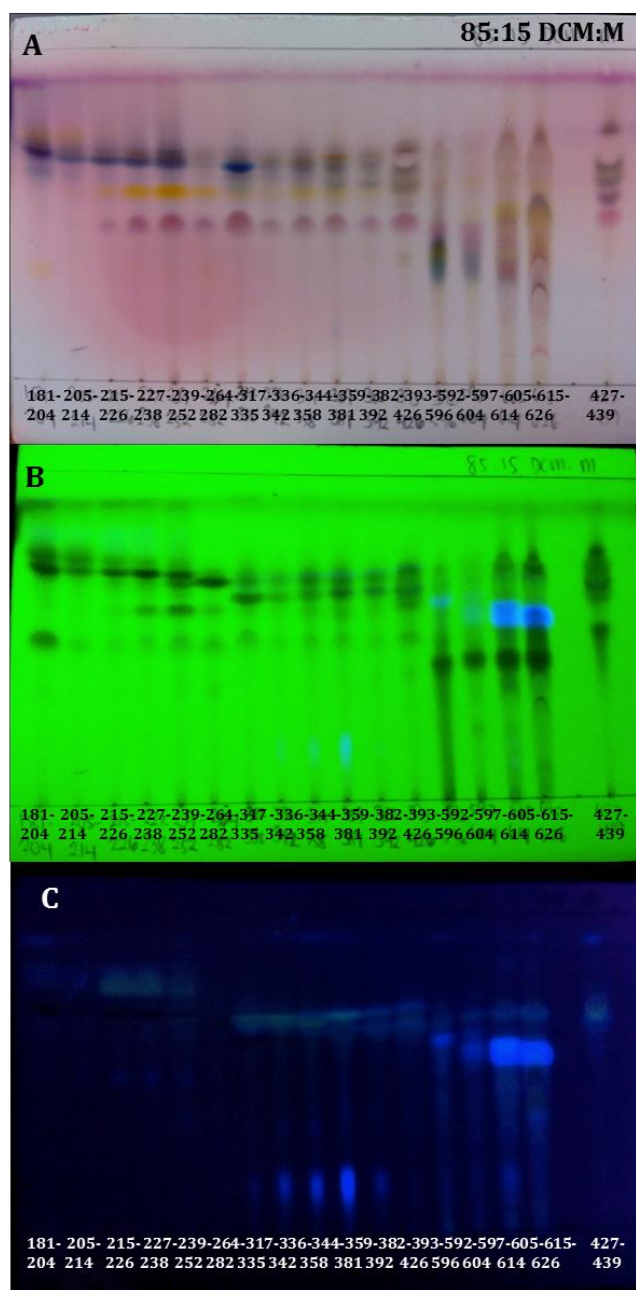


Figure 5-21: TLC summary plate of the fractions showing anti-trypanosomal and anti-mycobacterium activity. The plates were visualised by (A) spraying with anisaldehyde spray reagent, (B) viewing under short wavelength (254 nm) UV, and (C) viewing under long wavelength (365 nm) UV.

Table 5-15: Yields and activities of pooled fractions from EG4 extract. Grey cells highlight samples with %inhibition > 90%. The fraction in red was found to be relatively pure but inactive. The fractions in yellow were pooled together for further fractionation; likewise the fractions highlighted in green and blue were subjected to further purification.

Fraction	Yield (mg)	Average growth inhibition of <i>T. b. brucei</i> (%) n=2	MIC ($\mu\text{g/mL}$) against <i>T. b. brucei</i> n=2	Average growth inhibition of <i>M. marinum</i> (%) n=2
1-15	20.0	60.0		84.0
16-24	73.8	60.8		67.2
25-29	7.2	76.8		64.15
30-47	20.6	100.4	20	63.85
48-54	8.2	89.45		60.95
55-62	24.8	100.65	20	73.25
63-82	20.0	84.75		81.1
83-92	22.3	25.45		78.55
93-111	32.4	4.25		81.3
112-116	7.7	13.0		21.75
117-119	5.2	1.45		22.35
120-133	21.2	87.75	20	52.95
134-140	12.3	102.4	20	61.2
141-160	20.1	101.3	20	72.5
161-168	4.8	100.4	20	70.45
169-180	7.4	101.8	20	97.65
181-204	4.7	103.15	20	97.7
205-214	1.7	96.6	20	95.4
215-226	2.5	102.5	20	96.25
227-238	3.3	104.0	20	92.35
239-252	3.7	98.4	20	92.4
253-263	2.8	102.65	20	89.05
264-282	8.1	101.1	20	90.2
283-291	4.9	94.6	20	82.7
292-304	5.3	58.4		78.85
305-316	5.5	101.05	20	84.45
317-335	8.6	103.65	10	96.3
336-342	1.5	103.5	15	95.95
344-358	2.2	103.25	15	91.4
359-381	3.7	103.9	15	90.55
382-392	2.3	103.85	20	95.95
393-426	21.1	100.2	20	98.4
427-439	34.7	21.05		45.75
440-486	48.9	40.0		78.75
487-510	89.3	14.85		42.8
511-568	8.4	14.25		53.55
569-573	73.2	101.25	20	92.15
574-580	142.6	30.75		68.4

581-591	92.1	18.35		49.35
592-596	20.1	103.25	20	96.0
597-604	21.9	98.8	20	95.9
605-614	15.4	99.05	20	100.5
615-626	15.2	99.5	20	100.05
627-645	16.6	69.8		72.85
646-663	15.0	87.75		68.1
664-666	0.5	97.3	10	62.1
667-675	3.8	99.85	20	49.3
676-682	10.1	99.05	20	65.45
684-689	4.1	52.0		73.5
690-694	1.4	70.35		87.95
695-709	4.3	99.25	20	58.2
710-757	13.3	100.05	10	45.0
50:50 and 70:30 dichloromethane: methanol wash	4.6	32.25		73.75
50:50 acetone: methanol washing	13.6	2.95		77.25
100% methanol wash	2.4	7.7		59.2

The fractions had greater inhibitory activities than the crude EG4 extracts. This was because the active compounds were present in greater concentrations in the fractions relative to the extracts. Because the active fractions were still not of sufficient purity to identify the bioactive constituents, further purification was performed where the quantities of the fractions allowed it.

Fraction 427-439 was relatively pure and its major component was identified as N-phenethylacetamide (**21**) (Table 5-16). This was confirmed using NMR and MS. Although the NMR spectra showed that the Fraction 427-439 was a pure compound, several bands were observed on the TLC plate. This was due to the acidic nature of the silica plate protonating the amide group, which thereby resulted in more than one band on the TLC plate. The NMR chemical shifts and correlations are detailed in Table 5-17. These are similar to those previously reported for N-phenethylacetamide (Zhao et al., 2007). However, this fraction was found to be inactive against *T. b. brucei* and *M. marinum*.

Table 5-16: N-Phenethylacetamide

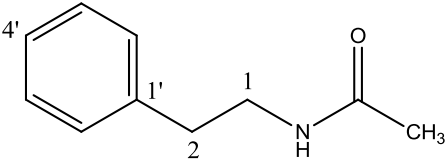
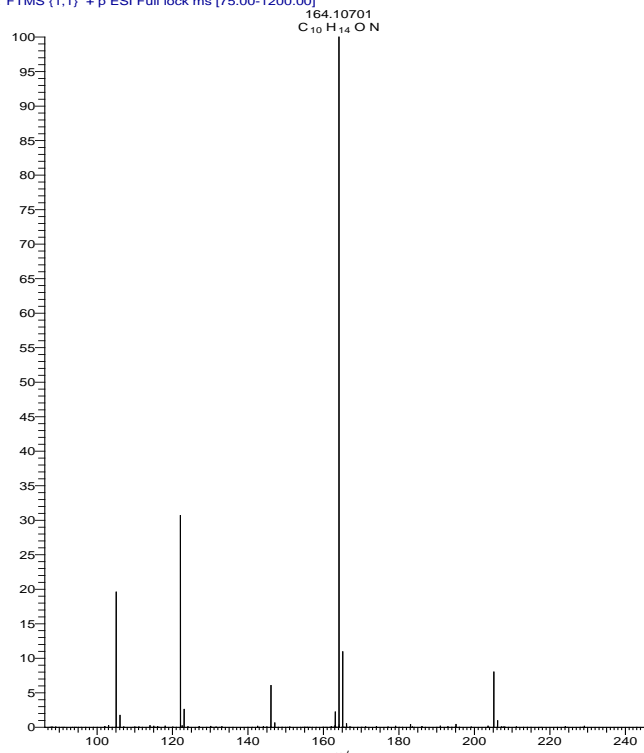
N-Phenethylacetamide													
Synonyms	Acetamide, <i>N</i> -(2-phenylethyl)-; N-(β-Phenylethyl)acetamide; N-Acetyl-2-phenylethylamine; NSC 7177												
Sample Code	427-439												
Sample Amount	34.7 mg												
Physical Description	Orange solid												
Molecular Formula	C ₁₀ H ₁₃ NO												
Molecular Weight	163 g/mol												
Optical Rotation [α]_D²⁶	+7												
Retention time (LC-MS)	8.18 min												
													
HRFTMS spectra [M+H]⁺													
<p style="font-size: small; text-align: center;">427-439 #66-86 RT: 1.13-1.23 AV: 5 NL: 1.22E8 T: FTMS (1,1) + p ESI Full lock ms [75.00-1200.00]</p>  <table border="1" style="margin-top: 10px; font-size: x-small;"> <caption>Peak Data from HRFTMS Spectrum</caption> <thead> <tr> <th>m/z</th> <th>Relative Intensity (%)</th> </tr> </thead> <tbody> <tr> <td>105</td> <td>~20</td> </tr> <tr> <td>121</td> <td>~30</td> </tr> <tr> <td>147</td> <td>~5</td> </tr> <tr> <td>164.10701</td> <td>100</td> </tr> <tr> <td>205</td> <td>~8</td> </tr> </tbody> </table>		m/z	Relative Intensity (%)	105	~20	121	~30	147	~5	164.10701	100	205	~8
m/z	Relative Intensity (%)												
105	~20												
121	~30												
147	~5												
164.10701	100												
205	~8												

Table 5-17: ^{13}C and ^1H NMR chemical shifts and correlations of EG4_427-439

Position	δ_{C} (ppm)	δ_{H} ppm (multiplicity, J)	^1H - ^1H COSY	HMBC (^1H - ^{13}C)
1'-C	139.0	-	-	-
2'/6'-CH	128.8	7.18 (d, 7.7 Hz)	3'/5', 4'	2, 4'
3'/5'-CH	128.7	7.31 (t, 7.2 Hz)	2'/6', 4'	1', 2'/6'
4'-CH	126.6	7.24 (d, 9.5 Hz)	2'/6', 3'/5'	
2-CH ₂	35.7	2.81 (t, 6.9 Hz)	1	1', 2'/6', 1
1-CH ₂	40.8	3.51 (q, 6.4 Hz)	2, NH	1', 2, CO
NH	-	5.47 (s)	1	-
CO	170.2	-	-	-
CH ₃	23.4	1.93 (s)	-	CO

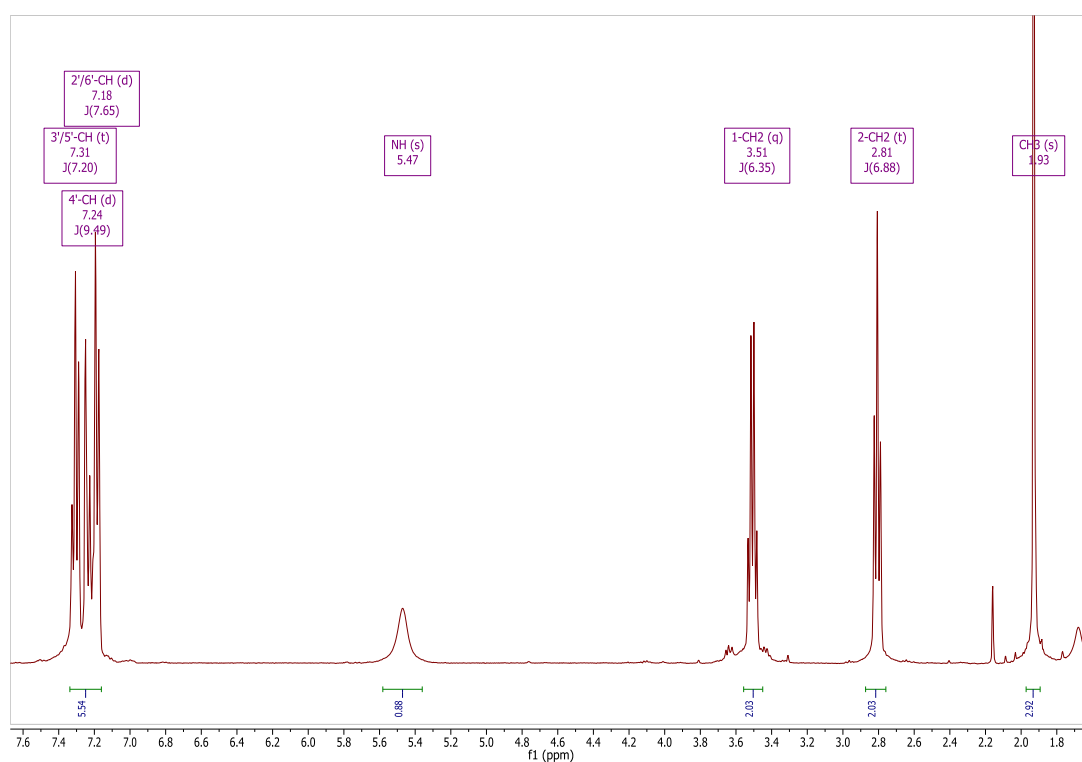


Figure 5-22: ^1H NMR spectrum of EG4_427-439 (400 MHz, CDCl_3).

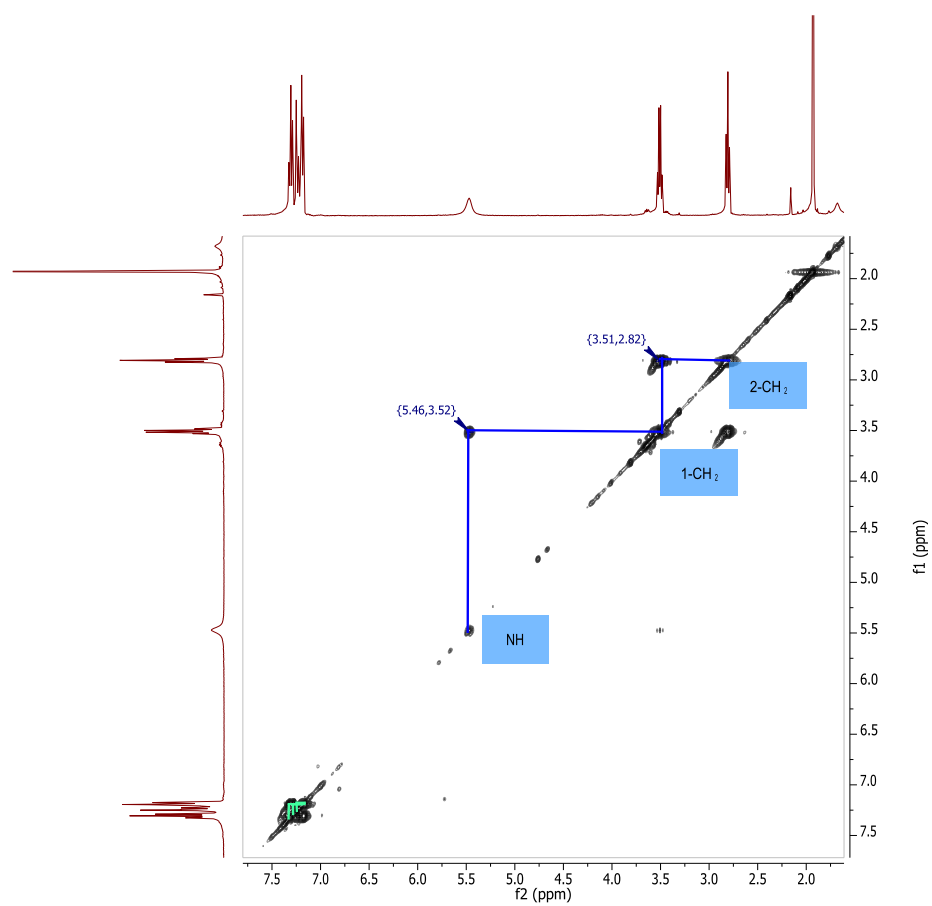


Figure 5-23: ^1H - ^1H COSY of EG4_427-439 (400 MHz, CDCl_3). The spin systems are labelled in green (phenyl system) and blue (aliphatic system).

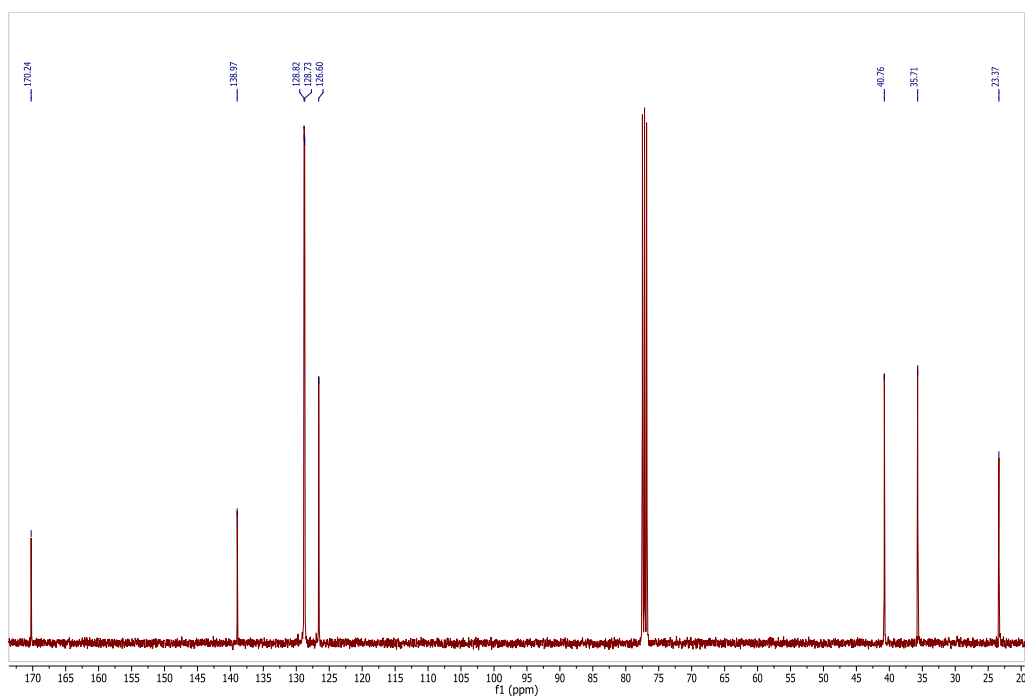


Figure 5-24: ^{13}C NMR spectrum of EG4_427-439 (100 MHz, CDCl_3).

The peaks at the aromatic region (δ_{H} 7.18-7.24) for the phenyl system overlapped and hence a doublet, rather than a triplet, was seen for 4'-CH. Nevertheless the peaks evidently belonged to a monosubstituted benzene ring. The integration of 5 protons confirmed this. The triplet at δ_{H} 2.81 (2-CH₂) and the quartet at δ_{H} 3.51 (1-CH₂) were seen in the COSY to couple to each other as well as to the broad singlet at δ_{H} 5.47 which was an amide group (NH). The singlet at δ_{H} 1.93 was a methyl group (CH₃) attached to a carbonyl carbon (CO) as seen in the HMBC. CO had a relatively upfield chemical shift (δ_{C} 170.2) indicating that it was attached to the amide group. In the HMBC 1-CH₂ correlated with CO, and likewise 2-CH₂ correlated with the carbons of the aromatic ring, thereby confirming the structure of the compound. In addition, direct injection of the fraction and analysis by MS showed that the molecule had an m/z of 164.1070 $[\text{M}+\text{H}]^+$ and a predicted formula of C₁₀H₁₄NO (Table 5-16).

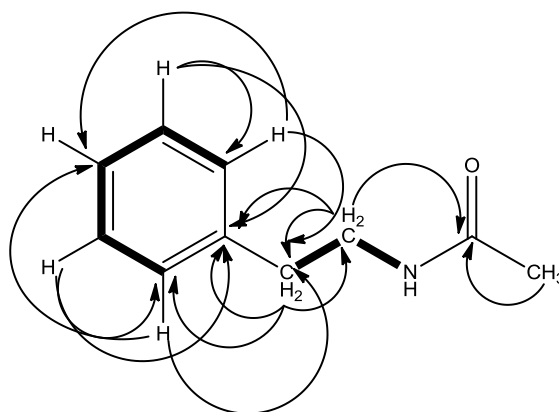


Figure 5-25: Structure of N-phenethylacetamide. The ¹H-¹H COSY correlations of N-phenethylacetamide are depicted by the bold lines and the ¹H-¹³C HMBC correlations are indicated by the arrows.

5.3.6.2 Conventional Silica Chromatography of EG4_569-573

Fraction 569-573 was chosen for further purification using a conventional silica column due to the large quantity of the fraction (73.2 mg) and its high anti-trypanosomal and anti-mycobacterium activity. A TLC summary plate was prepared using 85:15 dichloromethane:methanol as the mobile phase. The plate can be seen in Figure 5-26 below. The weights and activities of the resulting fractions are shown in Table 5-18. No pure compounds were obtained from this fractionation.

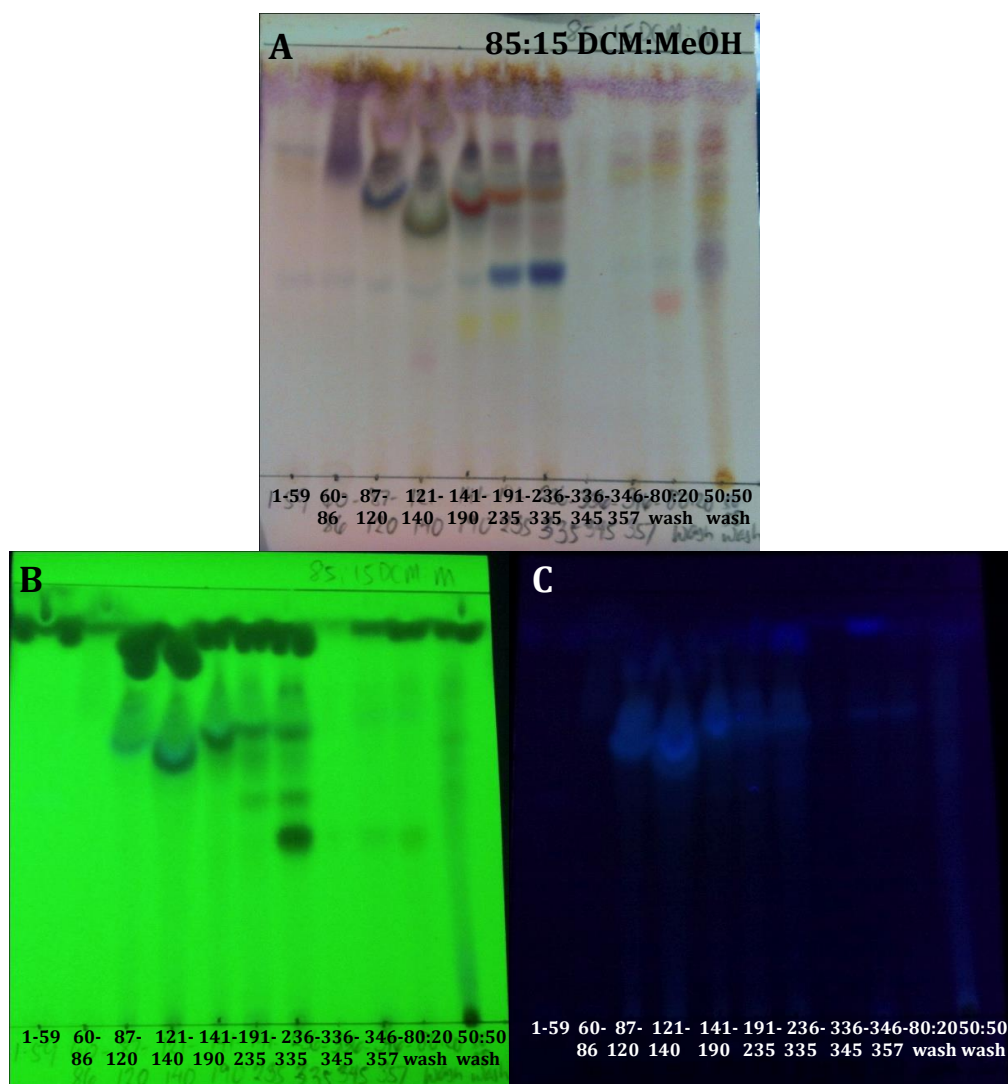


Figure 5-26: TLC summary plate of the fractions of 569-573. The plate was visualised by (A) spraying with anisaldehyde, (B) viewing under short wavelength (254 nm) UV, and (C) viewing under long wavelength (365 nm) UV.

Table 5-18: Yields and activities of pooled fractions following fractionation of 569-573. Cells highlighted in grey show the greatest activities. MIC determination was not performed against *M. marinum*.

Fraction	Yield (mg)	Average growth inhibition of <i>T. b. brucei</i> (%) n=2	MIC ($\mu\text{g/mL}$) against <i>T. b. brucei</i> n=2	Average growth inhibition of <i>M. marinum</i> (%) n=2
1-59	5.8	99.05	50	83.55
60-86	5.3	96.5	20	79.605
87-120	49.5	99.85	10	83.82
121-140	28.3	100.1	10	75.905
141-190	32.8	99.75	10	80.505
191-235	15.2	99.55	17.5	82.705
236-335	7.6	101.1	10	78.075
336-345	0.8	99.7	10	73.15
346-357	0.9	96.0	20	48.07
80:20 dichloromethane: methanol wash	15.2	99.35	10	64.06
50:50 dichloromethane: methanol wash	14.5	100.85	10	73.77

NMR analysis of Fraction 1-59 showed that it was relatively pure. GCMS analysis coupled to the NIST 2011 database putatively identified the compound as diisooctyl phthalate, otherwise called 1,2-benzenedicarboxylic acid, diisooctyl ester. This compound was found as a sodium adduct (m/z 413.27 $[\text{M}+\text{Na}]^+$) in the crude extract as well as in the blank media. Due to the abundance of possible isomers, however, it is difficult to definitively identify the phthalate. Comparison with standards and different techniques such as positive chemical ionisation MS with retention-time locked GC (George and Prest, 2002) should be attempted if the absolute identity of the phthalate in terms of chain length and branching position is desired. However, as this compound was discovered in the blank media, its identity was not pursued further.

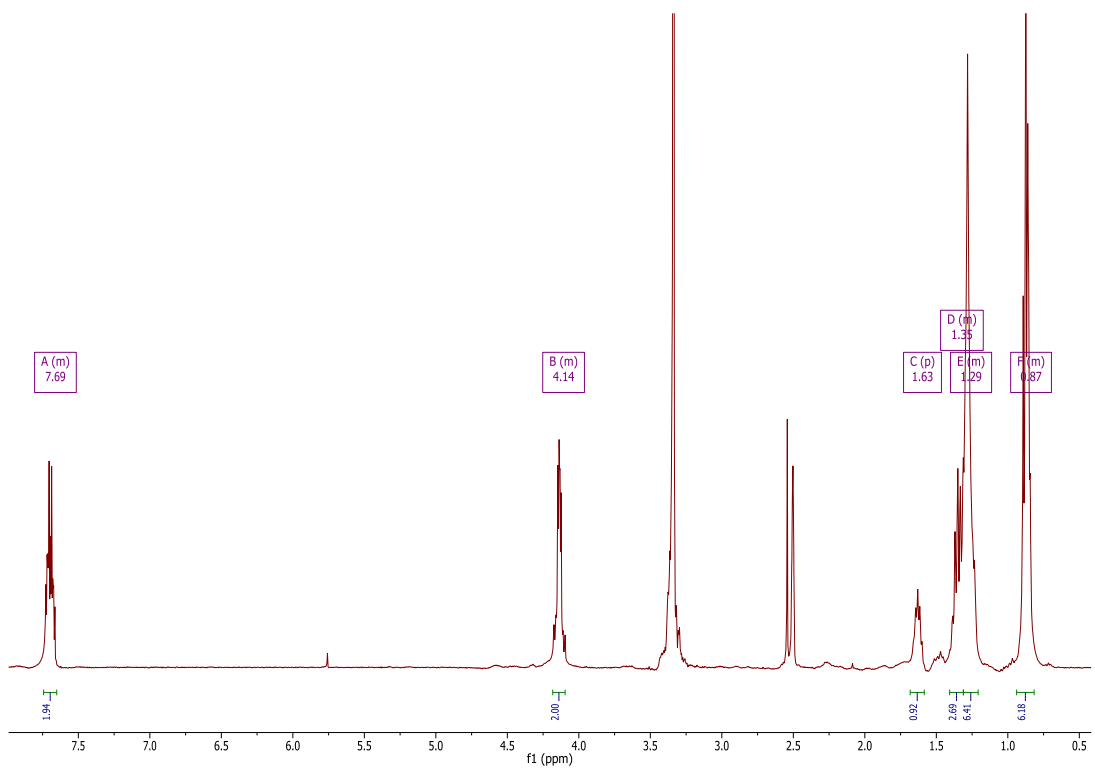


Figure 5-27: ¹H NMR spectrum of EG4_569-573_1-59 (400 MHz, DMSO).

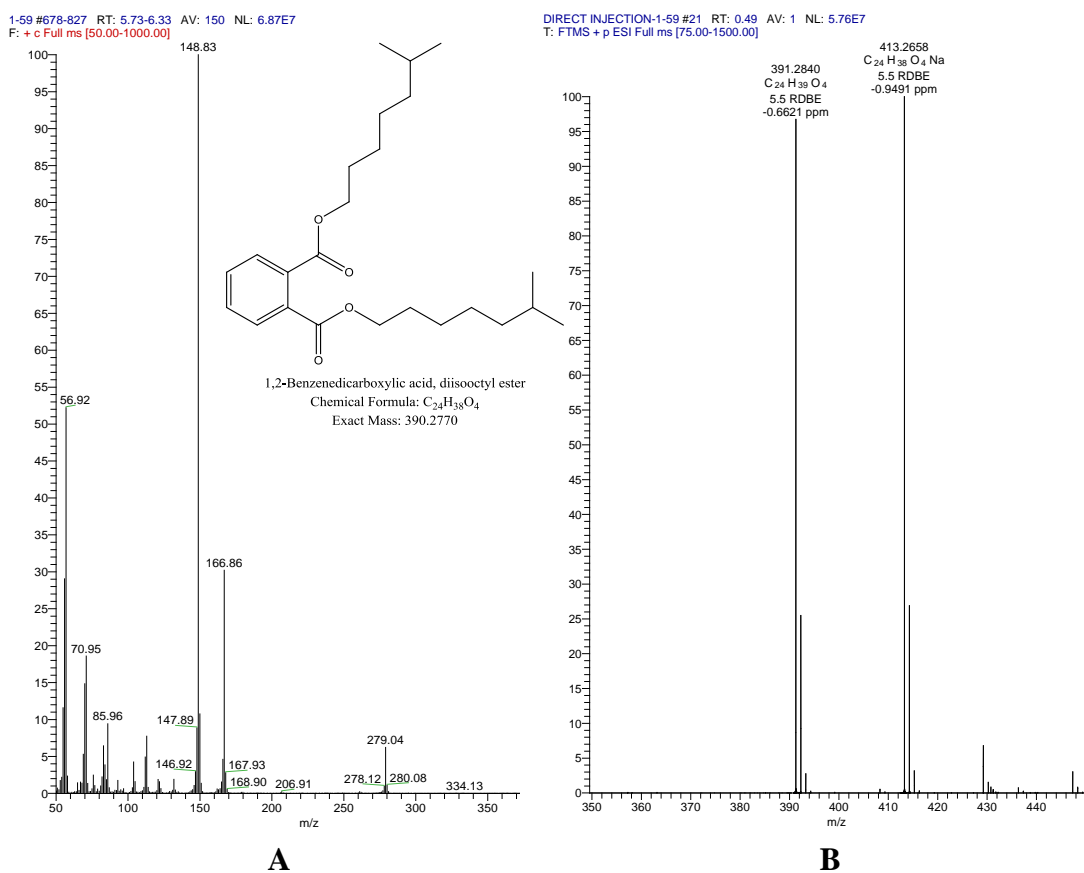


Figure 5-28: GC-MS and LC-MS spectra of EG4_569-573_1-59. (A) GCMS spectrum and structure of diisooctyl phthalate, the compound identified by the NIST database using the mass spectrum; (B) LCMS spectrum showing the [M+H]⁺ and [M+Na]⁺ ions of the phthalate.

Analysis of the LC-HRFTMS spectra showed that a compound with m/z 180.1017 [M+H]⁺ was present in some of the fractions, particularly in EG4_569-573_191-235 (Figure 5-29). This compound had previously been highlighted as one of the possible contributors to anti-mycobacterial activity (Figure 5-18). It was found to be present in the blank media; however, the time-course study showed that it increased in quantity from Day 0 to Day 15.

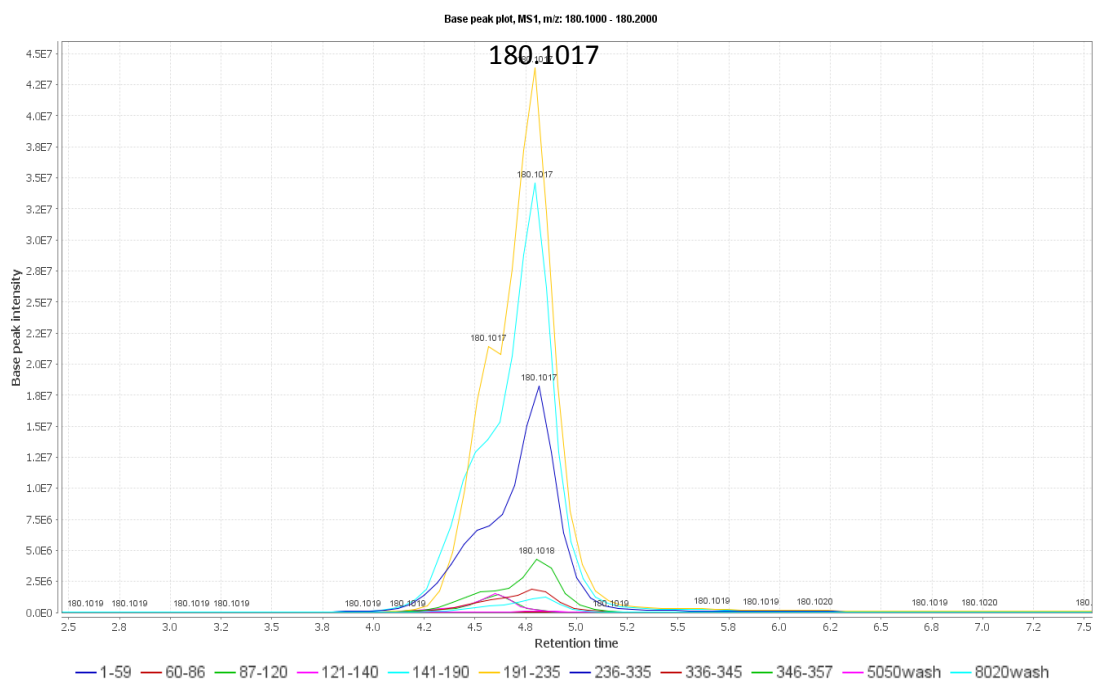


Figure 5-29: Extracted ion chromatogram showing m/z 180.1017 $[M+H]^+$ in fractions of EG4_569-573. Fraction 191-235 (yellow), followed by fraction 141-190 (light blue) and fraction 236-335 (dark blue), had the highest peak intensity, indicating that it contained the largest amount of the compound.

The AntiMarin database identified several hits for this ion. NMR spectroscopy of the extract and fragmentation of this ion confirmed the identity of this compound as N-acetyltyramine (**29**).

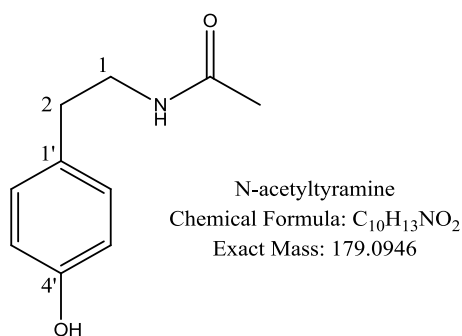


Figure 5-30: Structure of N-acetyltyramine. The identity of the peak with an m/z of 180.1017 $[M+H]^+$ was proven to be N-acetyltyramine based on NMR spectroscopy and LC-MS/MS.

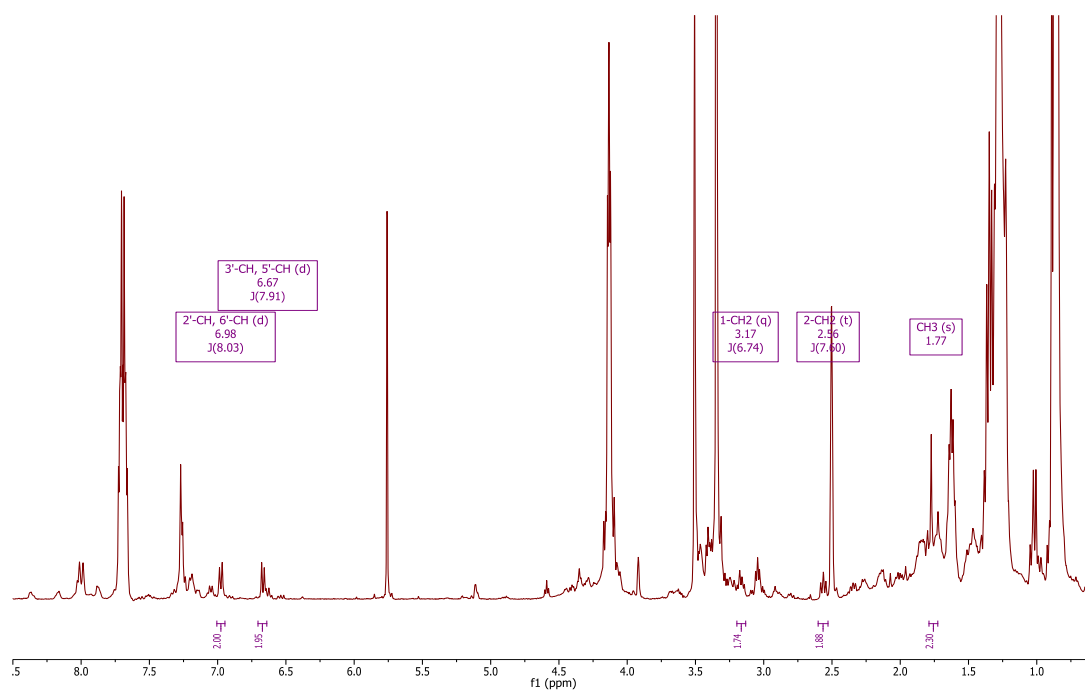


Figure 5-31: ^1H NMR spectrum of EG4_569-573_191-235 (400 MHz, DMSO). Peaks belonging to N-acetyltyramine are labelled. These values are similar to those previously reported (Sobolevskaya et al., 2007).

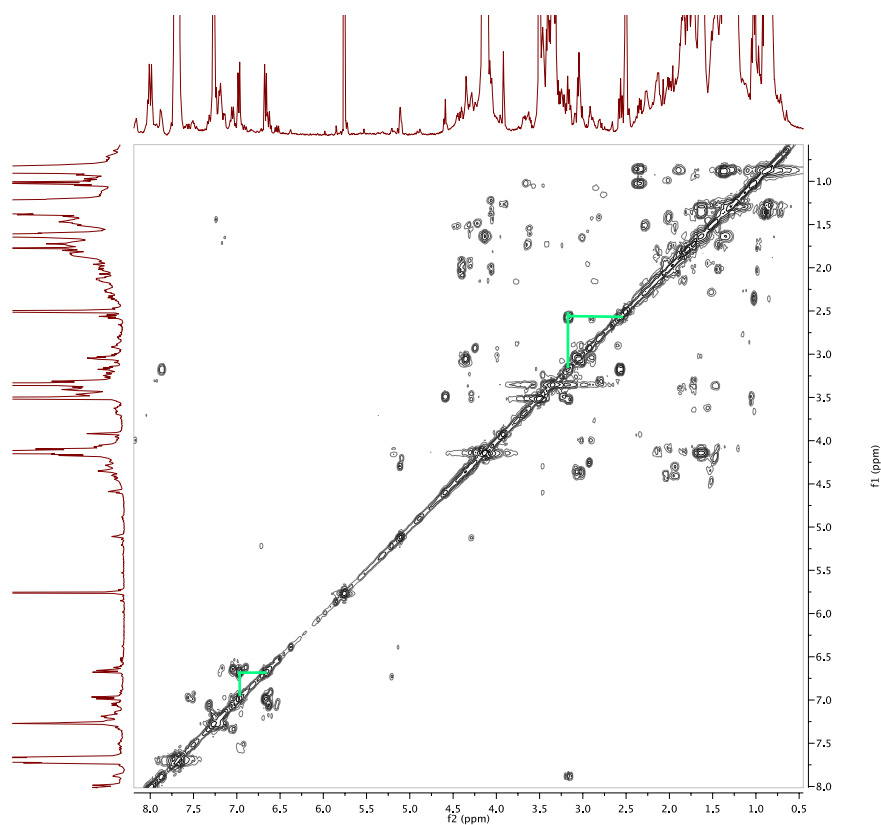
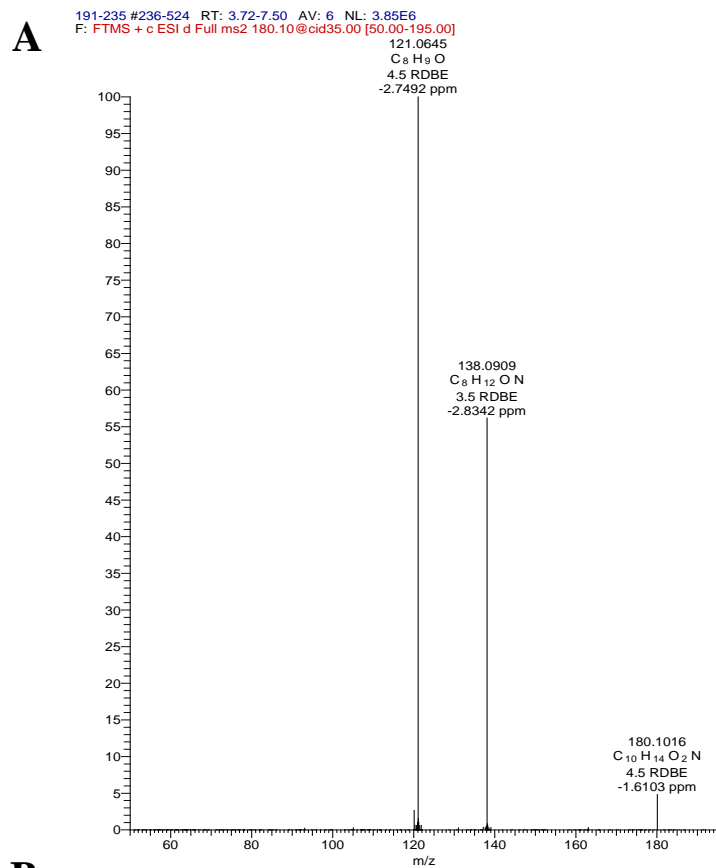


Figure 5-32: ^1H - ^1H COSY spectrum of EG4_569-573_191-235 (400 MHz, DMSO). The correlations of the aromatic and aliphatic spin systems of N-acetyltyramine are outlined in green.



B

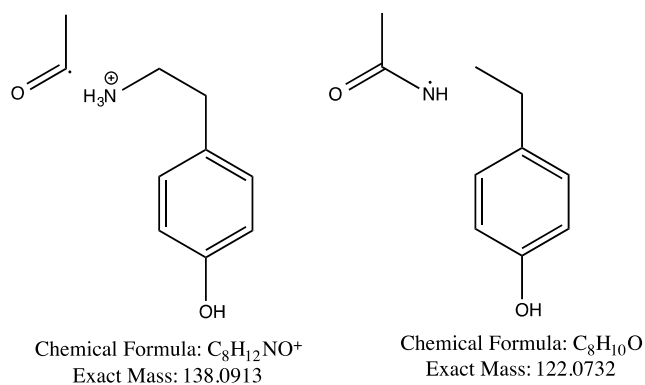


Figure 5-33: Fragmentation of m/z 180.10 [M+H]⁺. (A) Mass spectrum after fragmentation of the selected ion using the LTQ-Orbitrap. (B) Structures showing the fragmentation of N-acetyltyramine to form the fragment ions seen in the spectrum.

Another peak which had previously been found to correlate with anti-mycobacterial activity was m/z 203.1178 [M+H]⁺ which was identified as N-acetyltryptamine (**34**) using the AntiMarin database. Fraction EG4_569-573_141-190 had the largest peak area for this compound, as seen in an extracted ion chromatogram of the EG4_569-573 fractions (Figure 5-34).

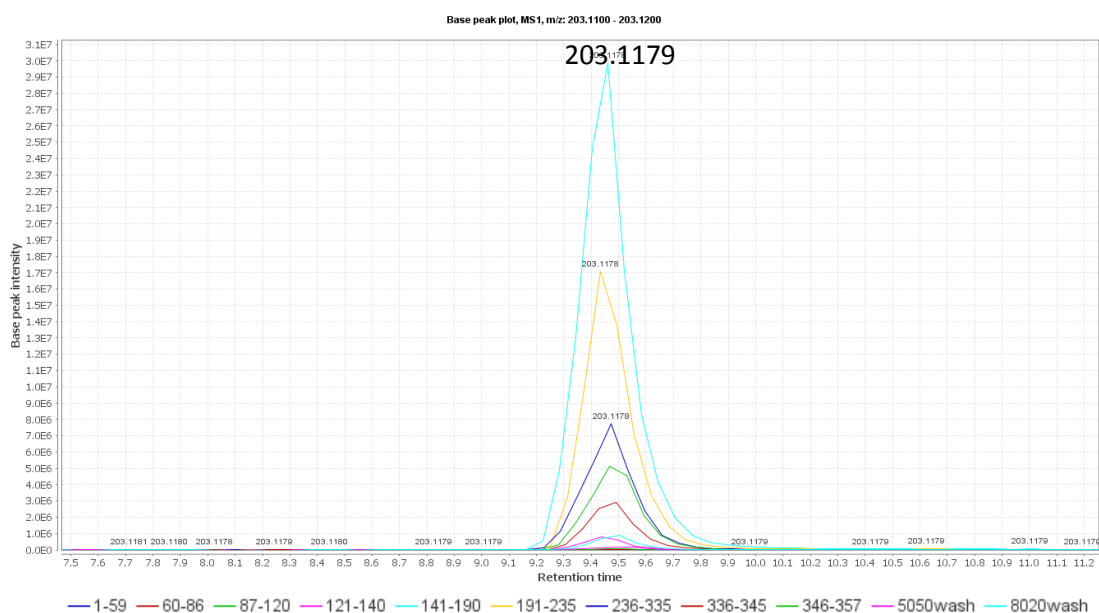


Figure 5-34: Extracted ion chromatogram showing m/z 203.1179 $[M+H]^+$ in fractions of EG4_569-573. Fraction 141-190 (light blue) had the largest intensity and therefore possessed the greatest amount of this compound.

However, as evidenced by the TLC plate in Figure 5-26, EG4_569-573_141-190 was still a mixture of at least four compounds. The total ion chromatogram of this fraction in Figure 5-35 showed that the peak with m/z 203.1178 $[M+H]^+$ was only a minor component and as such further purification was not attempted.

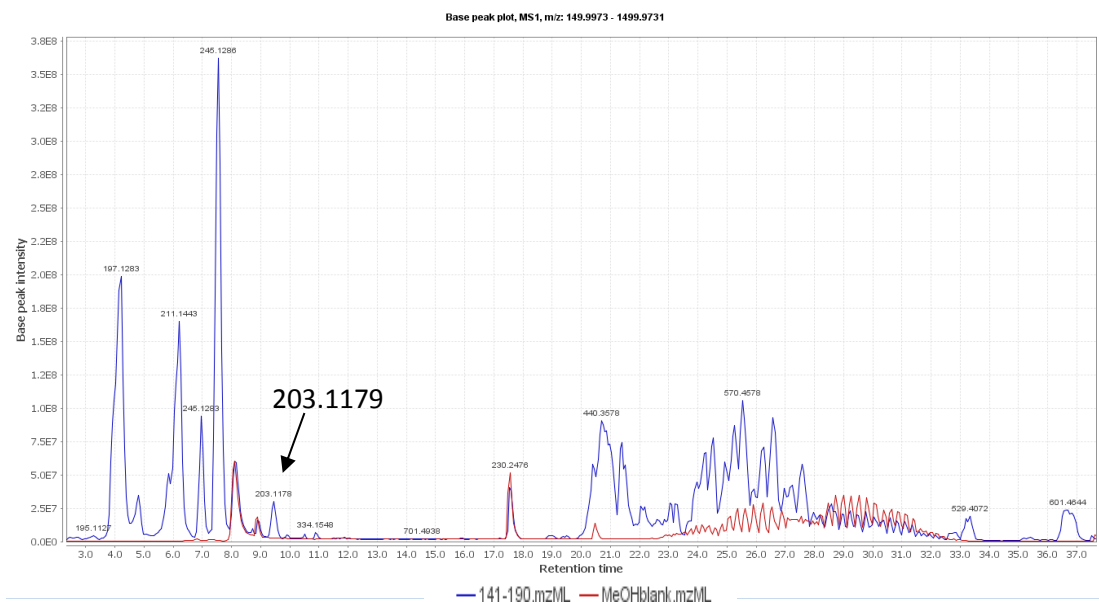


Figure 5-35: Total ion chromatogram of EG4_569-573_141-190 (blue). The chromatogram of the solvent blank, MeOH, is shown in red. The peak with m/z 203.1178 $[M+H]^+$ is indicated by the black arrow. Despite the extracted ion chromatogram showing high peak intensity for this peak, the total ion chromatogram indicated that the fraction was still a mixture and that there were several other compounds that were present in greater concentrations.

In order to confirm the presence of N-acetyltryptamine in the fraction, the COSY and ^1H NMR spectra of the fraction were compared to that of a tryptamine standard (Sigma-Aldrich Co. LLC, USA) (Figure 5-37 and Figure 5-38). The comparison confirmed that N-acetyltryptamine was indeed produced by EG4 and was present in EG4_569-573_141-190.

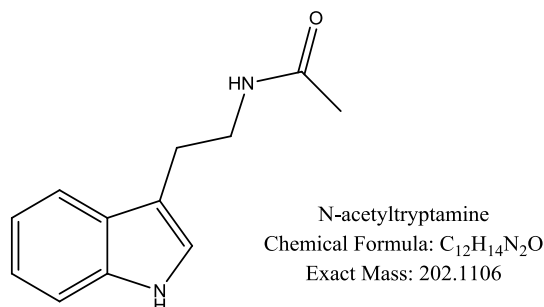


Figure 5-36: *N*-(2-(1-*H*-indol-3-yl)ethyl)acetamide (**N-acetyltryptamine**). The identity of the peak with m/z 203.1179 was proven to be N-acetyltryptamine based on NMR spectroscopy and LC-MS/MS. This compound was present only in fractions with anti-mycobacterial activity.

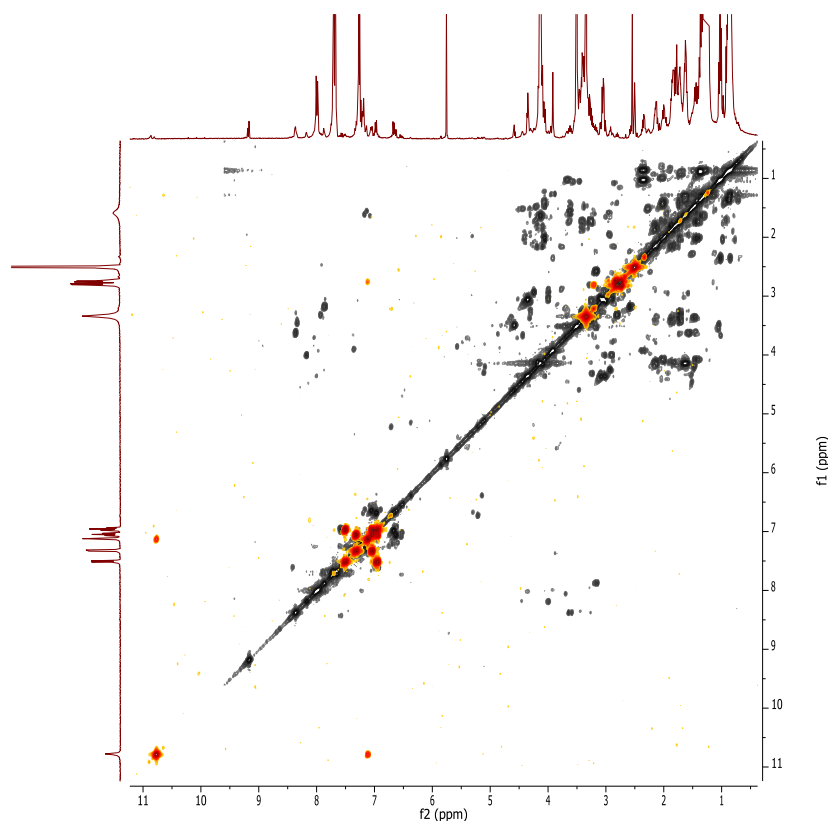


Figure 5-37: Overlapping COSY spectra of EG4_569-573_141-190 (grey) and the tryptamine standard (orange) (400 MHz, DMSO). The ^1H NMR spectrum of the fraction is on the x-axis and that of the standard is on the y-axis.

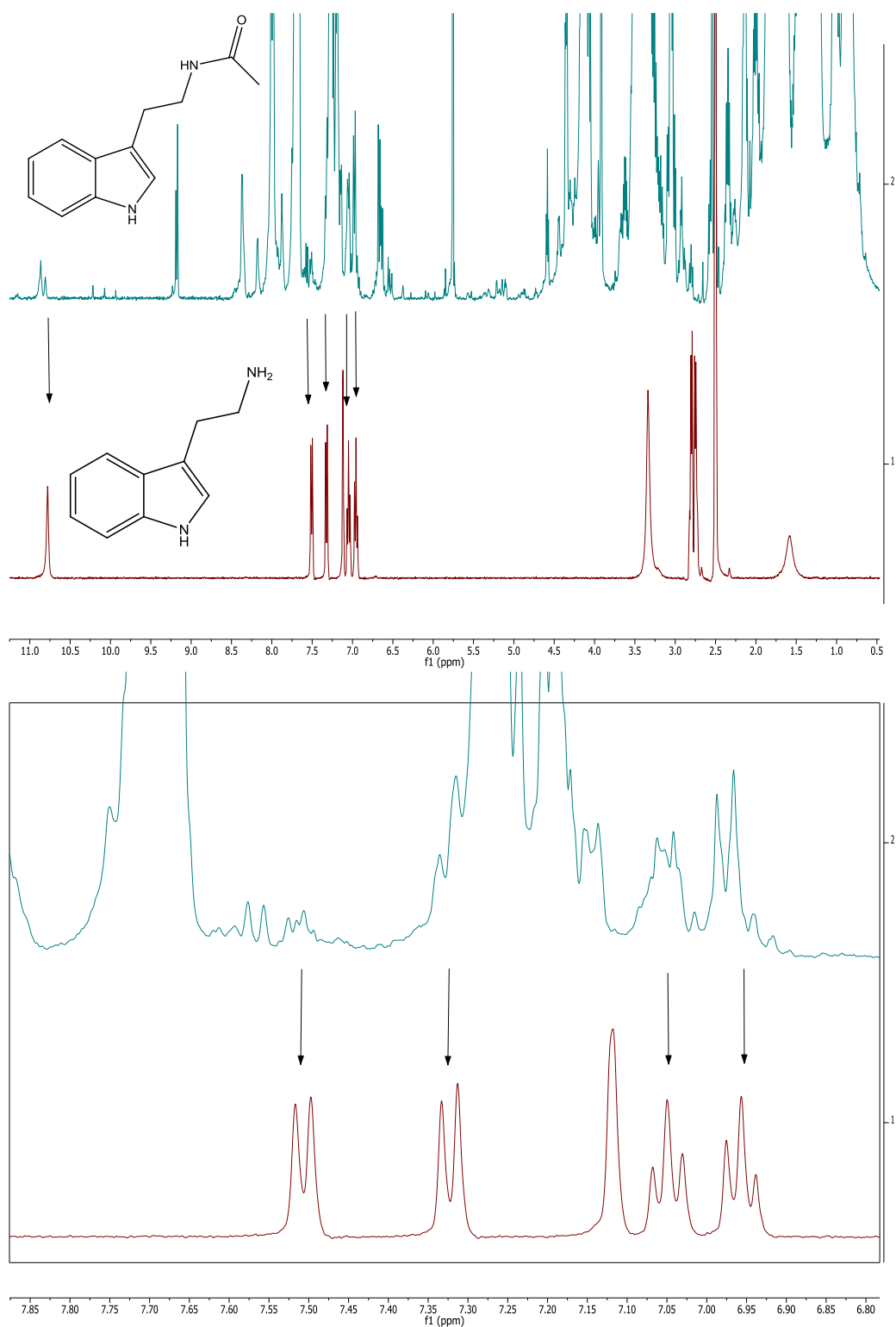


Figure 5-38: ¹H NMR spectra of EG4_569-573_141-190 (teal) and tryptamine standard (red) (400 MHz, DMSO). The expansion in the bottom spectrum shows the peaks in the aromatic region. Arrows mark the peaks from the fraction that match those in the standard, showing the presence of the indole ring in the fraction. The aliphatic regions of the two compounds are different, hence they were not compared.

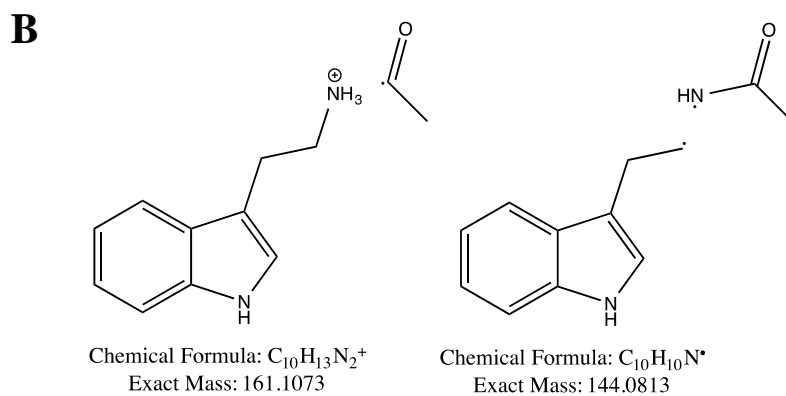
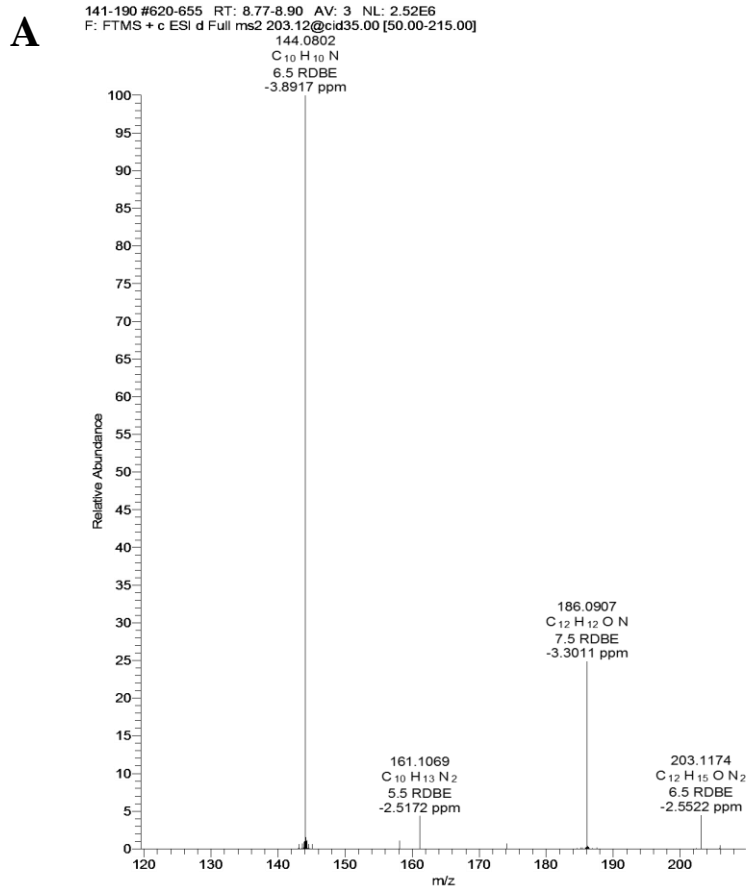


Figure 5-39: Fragmentation of N-acetyltryptamine. (A) Mass spectrum following fragmentation of an ion with m/z 203.12 $[M+H]^+$. (B) Structures of the fragments generated upon fragmentation of the ion.

This fraction also contained cyclo-L-phenylalanine-L-serine (**41**) (Figure 5-40). This compound had putatively been identified as a metabolite of EG4 that correlated with anti-mycobacterium activity as it was observed to increase in quantity as time progressed during the time-course study (Table 5-13).

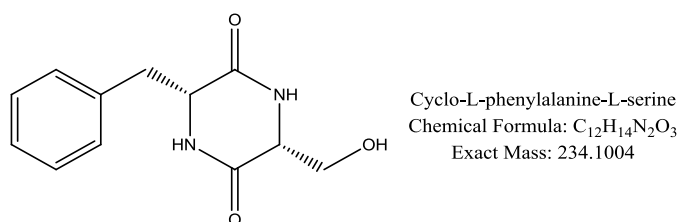


Figure 5-40: Structure of cyclo-L-phenylalanine-L-serine. This compound was identified by the AntiMarin database and corresponded to the peak with m/z 235.11 [M+H]⁺. The structure was confirmed by LC-MS/MS. The compound was putatively identified as a contributor to anti-mycobacterium activity.

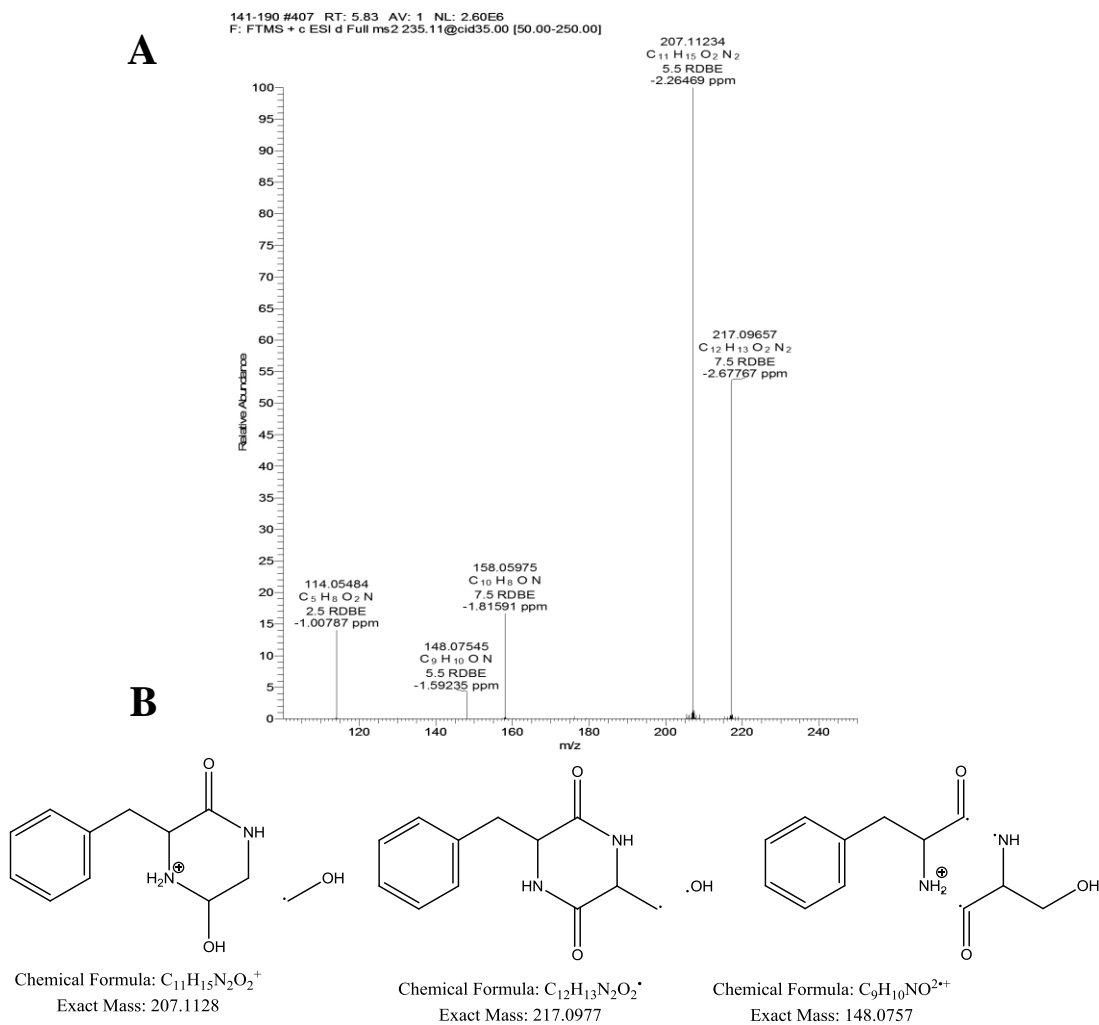


Figure 5-41: Fragmentation of cyclo-L-phenylalanine-L-serine. (A) Mass spectrum obtained upon fragmentation of m/z 235.11 [M+H]⁺. (B) The structures of some of the fragment ions generated.

The presence of the diketopiperazine in this fraction was also confirmed by fragmentation using the LTQ-Orbitrap as seen in Figure 5-41 above. However, analysis of the blank media indicated the presence of 235.11 [M+H]⁺, suggesting that

it was a component of the media and not solely produced by EG4. On the other hand, the study of the metabolic changes of EG4 over time proved that it was indeed a metabolite of EG4 as its production increased over time.

Two pathways are currently known for diketopiperazine biosynthesis. One involves cyclodipeptide synthases (CDPS), such as in the production of albonoursin from *S. noursei*, pulcherriminic acid from *B. subtilis*, and mycocyclosin from *M. tuberculosis* (Belin et al., 2012). A BLAST search for the CDPSs involved in the synthesis of these metabolites (AlbC, YmvC, and Rv2275, respectively) yielded no homologues within the *Microbacterium testaceum* StLB037 genome. This genome was utilised for all BLAST searches as the genome of EG4, itself a *Microbacterium* sp., has not been sequenced. The other pathway of diketopiperazine biosynthesis is NRPS-dependent. Gliotoxin, a fungal metabolite, is an example of a diketopiperazine produced through this pathway (Belin et al., 2012). Cyclo-L-phenylalanine-L-serine is an intermediate in the production of gliotoxin and hyalodendrin (Kirby et al., 1978, Boente et al., 1991). A BLAST search for the detection of homologues of GliK, the protein responsible for gliotoxin biosynthesis in *Aspergillus fumigatus* showed there were no homologues in the *M. testaceum* StLB037 sequence. Thaxtomin A is a bacterial diketopiperazine produced through the NRPS-dependent pathway (Belin et al., 2012). Homologues for thaxtomin synthetase A and B, the proteins responsible for the production of thaxtomin A in *S. ascidiscabies* (Healy et al., 2000), were detected in the *M. testaceum* StLB037 genome (Table 5-19). The alignments and conserved domains can be seen in Appendix VI.

Table 5-19: Homology results of thaxtomin biosynthetic clusters in the *M. testaceum* StLB037 genome

Protein	Accession number	<i>M. testaceum</i> protein accession number	Identity	E-value
TxtA	AAG27087	YP_004225560	36%	2E-46
TxtB	AAG27088	YP_004225560	38%	2E-50

The conserved domains in the thaxtomin A synthetase proteins include an adenylation domain of NRPS, an S-adenosylmethionine-dependent methyltransferase

domain, an adenylate forming domain, a phosphopantetheine attachment site, a condensation domain, and an HxxPF repeated domain. The sequence of the NRPS module found in the *M. testaceum* genome only have 36% and 38% identity with txtA and txtB, respectively. It is more probable, however, that the diketopiperazines produced by EG4 were synthesised through the NRPS-dependent pathway as opposed to the CDPS pathway.

5.3.6.3 Biotage® Flash Chromatography and Preparative TLC of EG4_215-392

Fractions EG4_215-226 until EG4_382-392 were pooled and fractionated again using the Biotage® flash chromatography system. The TLC summary plate can be seen in Figure 5-42 below.

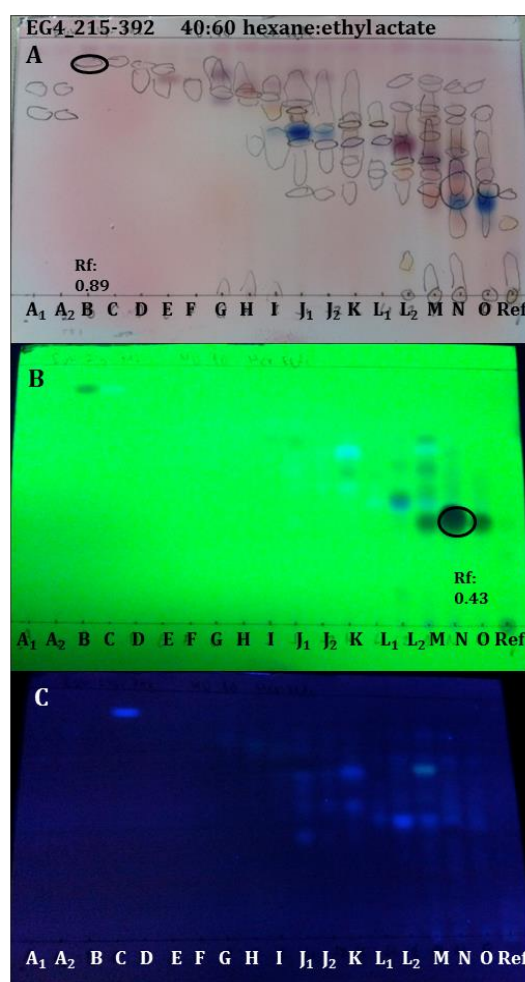


Figure 5-42: TLC summary plate of EG4_215-392 after Biotage® fractionation. The plate was eluted with 40:60 hexane:ethyl acetate. The spots were detected (A) by spraying with anisaldehyde-sulphuric acid, (B) under short wavelength UV (254 nm), and (C) under long wavelength UV (365 nm). The encircled spots are pure compounds that were later identified using NMR and LC-MS.

The wash was further purified using preparative TLC. The TLC summary plate of the bands obtained can be seen in Figure 5-43 below. The activity of all the EG4_215-392 fractions is displayed in Table 5-20.

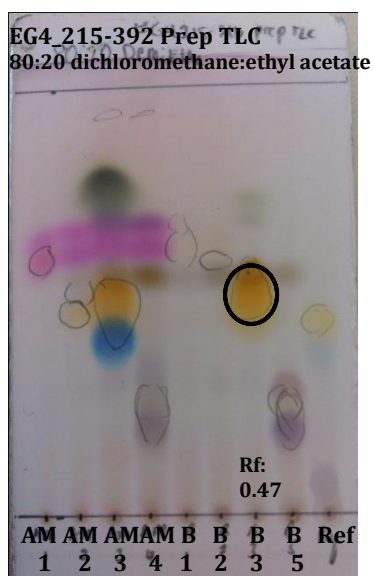


Figure 5-43: TLC summary plate of EG4_215-392 wash fractions after preparative TLC. The plate was sprayed with anisaldehyde-sulphuric acid to detect the spots. The encircled spot in fraction B3 is the major compound of that fraction, the structure of which was identified using LC-MS and NMR.

Table 5-20: Yields and activities of fractions from EG4_215-392. Fractions in yellow were obtained as relatively pure cultures and their structures were elucidated. Cells highlighted in grey indicate the most active fractions. The MICs against *M. marinum* were not determined.

Fraction	Yield (mg)	%Inhibition of <i>T.b. brucei</i> (20µg/mL)	MIC against <i>T. b. brucei</i> (µg/mL)	%Inhibition of <i>M. marinum</i> (100µg/mL)
A1	0.4	-1.9		-5.5
A2	0.2	-3.7		6.9
B	1.4	106.1	50	56.2
C	0.2	63.5		50.0
D	0.2	39.7		54.8
E	0.1	-		-
F	<0.1	-		-
G	<0.1	-		-
H	<0.1	-		-
I	0.1	-		-
J1	0.2	-4.9		11.3
J2	<0.1	-		-
K	0.5	105.1	25	99.6
L1	1.0	107.9	12.5	99.0
L2	1.7	102.8	50	99.1
M	2.0	105.5	25	99.8
N	2.6	45.4		80.1
O	2.6	89.7		78.9
1ppt	0.6	104.3	25	63.1
1wash	2.0	102.9	12.5	94.6
2ppt	<0.1	-		-
2wash	0.3	98.3	3.12	91.9
3ppt	0.3	-4.9		1.2
3wash	0.2	104.3	25	46.5
4-7wash	1.0	98.1	25	91
8-11wash	1.0	52.3		59.4
AM2-1	1.7	18.8		39.4
AM2-2	1.7	39.9		39.9
AM2-3	2.1	31.8		47.5
AM2-4	1.6	51.5		36.5
B1	1.1	-5.9		-43.6
B2	1.0	-3.5		41.2
B3	1.2	10.7		57.8
B4	2.2	2.3		45.0
B5	1.4	25.2		82.7
AMB1	0.9	9.8		14.5

Fractions 215-392_K until _M were the most active against both *T. b. brucei* and *M. marinum*. However, these fractions still contained mixtures of compounds and were of too small quantities to purify further. One of the components in Fraction 215-392_N which was identified as indole-3-carboxaldehyde was also evident in Fraction

215-392_M. Fractions B and B3 were obtained as pure compounds. B was active against *T. b. brucei* with an MIC of 50 $\mu\text{g}/\text{mL}$. N, which was a mixture of two compounds, and B3 had mild activity against *M. marinum*, inhibiting 80.1 and 57.8% of the cells respectively.

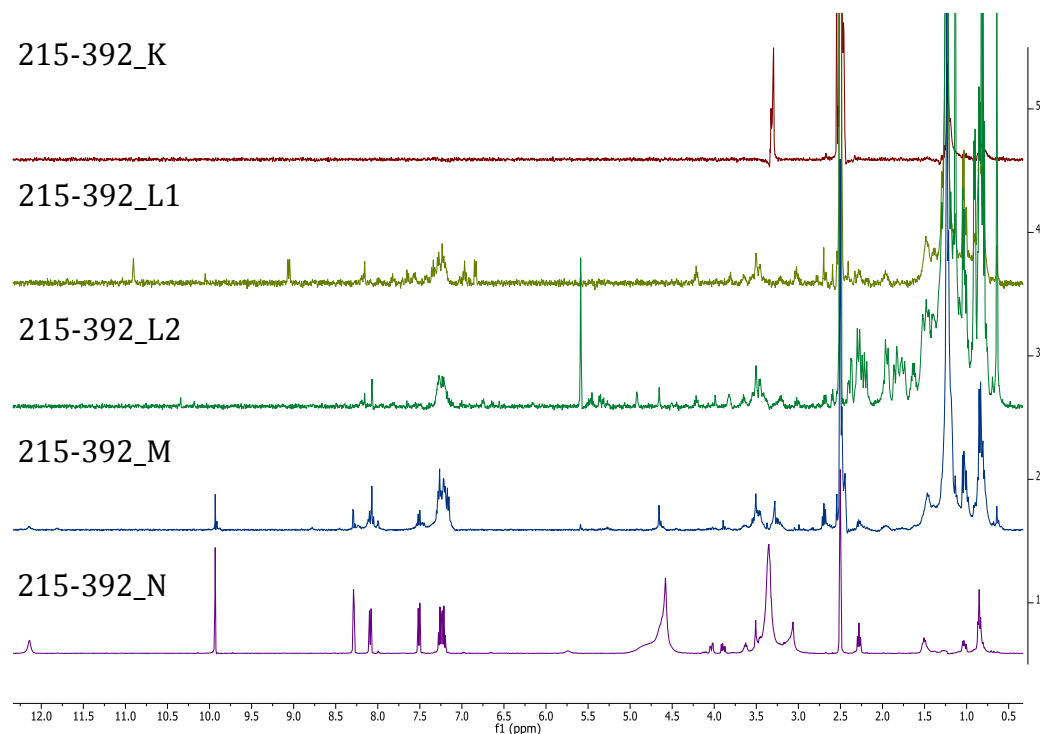


Figure 5-44: ^1H NMR spectra of the most active 215-392 fractions (400 MHz, DMSO). The peaks of indole-3-carboxaldehyde in fraction 215-392_N are also evident in 215-392_M. The presence of other aromatic compounds can be seen in fractions 215-392_L1 and _L2.

5.3.6.3.1 215-392_B

The NMR spectrum of EG4_215-392_B was similar to that of EG4_569-573_1-59, which was identified as a phthalate. Using 2D NMR the branching on the aliphatic side chains was determined, and the compound putatively identified as di(2-propylpentyl)phthalate. The NMR data is summarised in Table 5-22 and selected spectra can be seen from Figure 5-45 and Figure 5-46. The NMR values are similar to those found for phthalates in the literature (Hoang et al., 2008).

Table 5-21: 1,2-Benzenedicarboxylic acid, 1,2-bis(2-propylpentyl) ester

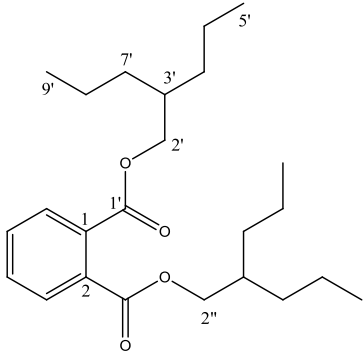
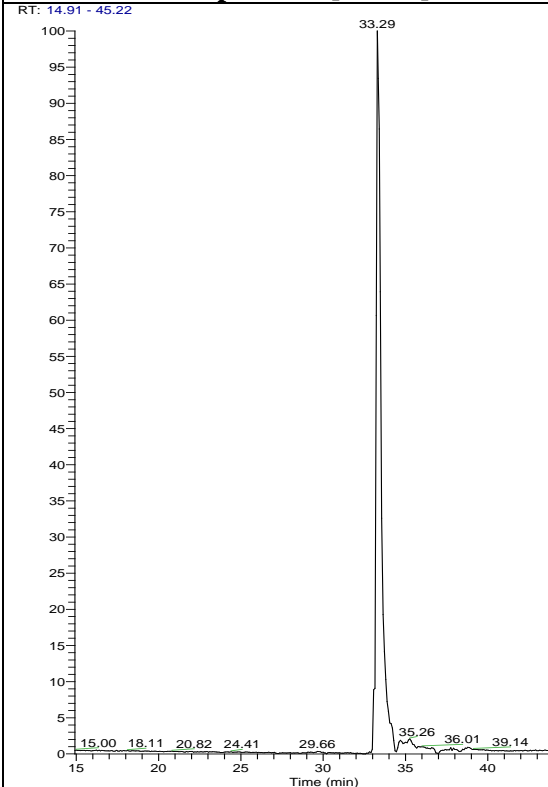
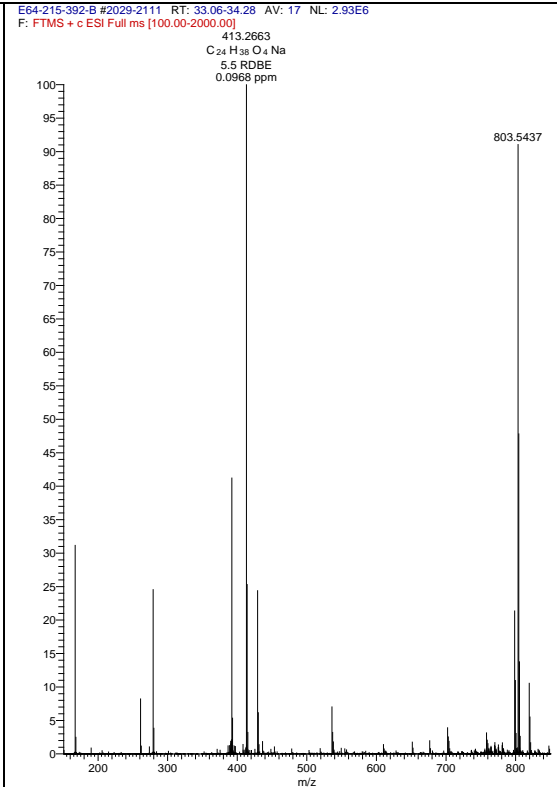
1,2-Benzenedicarboxylic acid, 1,2-bis(2-propylpentyl) ester	
Synonyms	1,2-Benzenedicarboxylic acid, bis(2-propylpentyl) ester; Di(2-propylpentyl) phthalate
Sample Code	215-392_B
Sample Amount	1.4 mg
Physical Description	White solid
Molecular Formula	C ₂₄ H ₃₈ O ₄
Molecular Weight	390 g/mol
Rf (TLC silica)	0.89 (40:60 hexane:ethyl acetate)
Retention time (LC-MS)	33.29 min
	
LC-HRFTMS Spectrum [M+Na]⁺	
<p>RT: 14.91 - 45.22</p> 	<p>E64-215-392-B #2029-2111 RT: 33.06-34.28 AV: 17 NL: 2.93E6 F: FTMS + c ESI Full ms [100.00-2000.00]</p> 

Table 5-22: NMR data of EG4_215-392_B

Position	δ_C (ppm)	δ_H ppm (multiplicity, <i>J</i>)	1H - 1H COSY	HMBC (1H - ^{13}C)
1-C	131.9	-	-	-
2-C	131.9	-	-	-
3- and 6-C	129.1	7.72 (dd, 3.3, 5.8 Hz)	-	1 and 2
4-and 5-C	132.1	7.69 (dd, 3.2, 5.7 Hz)	-	1 and 2
1'- and 1''COO	167.0	-	-	-
2'- and 2''-CH ₂	67.9	4.14 (dq, 5.7 and 11.0 Hz)	3', 3''	1', 3', 4', 5' 1'', 3'', 4'', 5''
3'- and 3''-CH	38.4	1.64 (m)	2', 4', 7' 2'', 4'', 7''	4' 4''
4'- and 4''-CH ₂	30.3	1.29 (p, 15.7 and 14.9 Hz)	3', 5' 3'', 5''	
7'- and 7''-CH ₂	28.8		3', 8' 3'', 8''	
5'- and 5''-CH ₂	23.7	1.36 (m)	4', 6' 4'', 6''	
8'- and 8''-CH ₂	22.8		7', 9' 7'', 9''	
6'- and 6''-CH ₃	14.3	0.88 (q, 7.3 Hz)	5' and 5''	3', 5' 3'', 5''
9'- and 9''-CH ₃			8' and 8''	3', 8' 3'', 8''

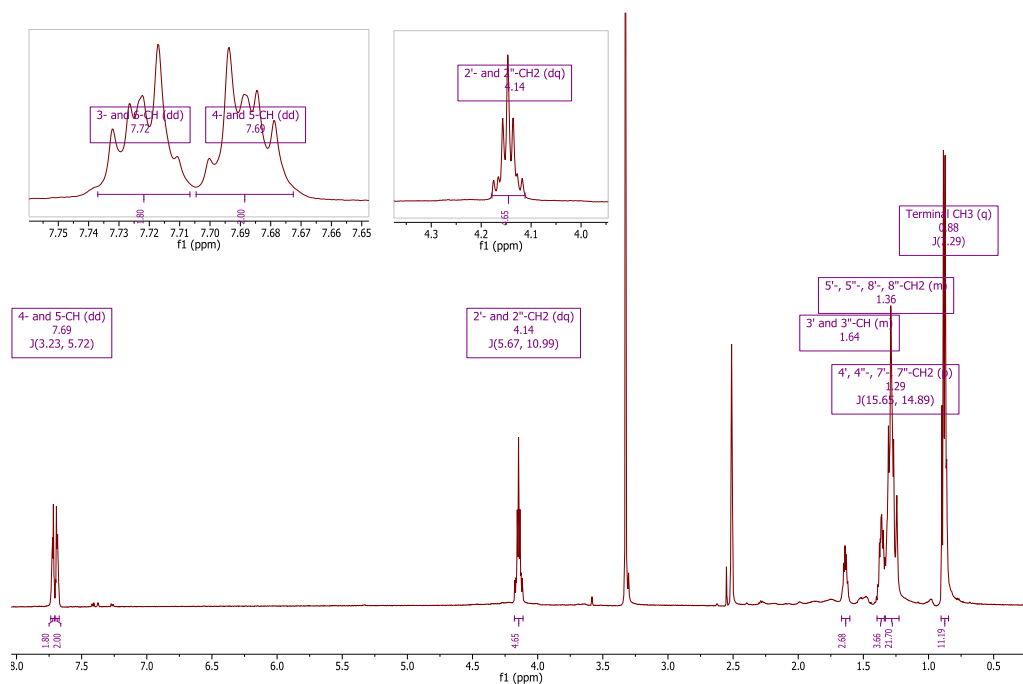


Figure 5-45: ^1H NMR spectrum of EG4_215-392_B (600 MHz, DMSO). The expansions in the upper left corner show the aromatic and oxygenated peaks, respectively. The integrations of the peaks prove the presence of the disubstituted benzene and the symmetrical aliphatic chains.

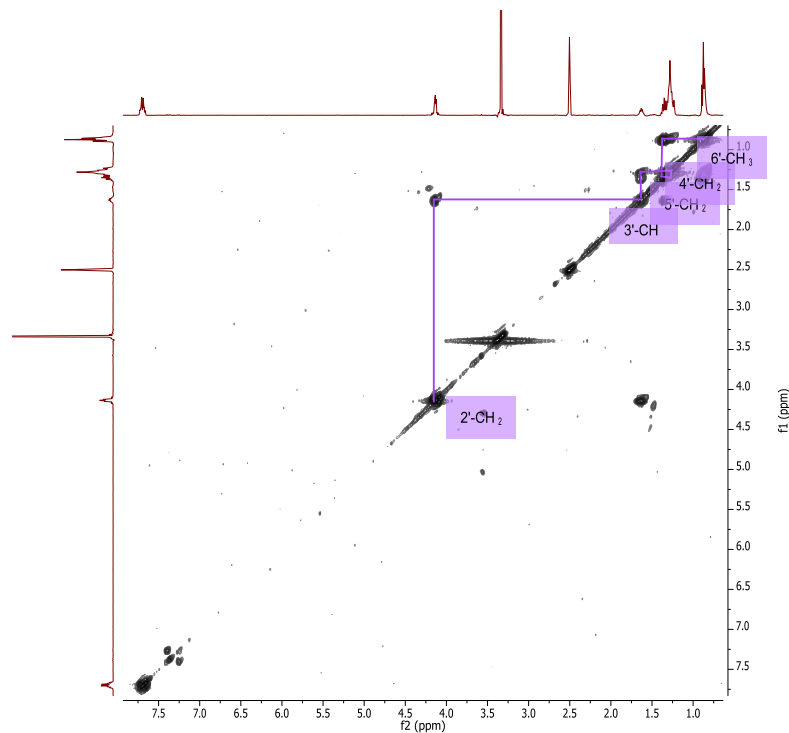


Figure 5-46: ^1H - ^1H COSY of EG4_215-392_B (400 MHz, DMSO). The spin system of one of the aliphatic chains is labelled. As the molecule is symmetrical, the spin system of the other chain would be identical.

The ^1H NMR spectrum of EG4_215-392_B was relatively simple; however, the integrations showed that there were many overlapping peaks that belonged to equivalent protons. This indicated that the compound was symmetrical. The aromatic region showed two peaks at δ_{H} 7.72 and 7.69, both of which had integrations of two protons. This suggested an ortho-substituted benzene ring, as a para-substituted ring would have resulted in one peak of four equivalent protons and a meta-substituted ring would not have yielded a symmetrical structure. The peak at δ_{H} 4.14 was shown in the heteronuclear single quantum coherence (HSQC) spectrum to be a CH_2 and to have a ^{13}C shift of δ_{C} 67.9, indicating that it was attached to an oxygen. In the HMBC the proton peak correlated to a peak at δ_{C} 167.0, an ester ($1'$ -COO). The COSY also showed a correlation with the $3'$ -CH peak at δ_{H} 1.64. Because the HSQC confirmed this peak as a $-\text{CH}$, it was evident that branching occurred at this point. The LC-MS spectrum showed a peak with m/z 413.2663 $[\text{M}+\text{Na}]^+$, corresponding to a predicted formula of $\text{C}_{24}\text{H}_{38}\text{O}_4\text{Na}$. The number of carbons on the side chains could thus be counted and the structure of the molecule determined.

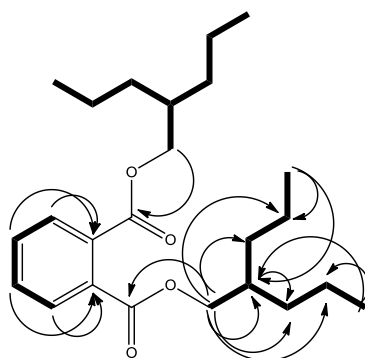


Figure 5-47: Structure of the phthalate. The COSY correlations are depicted with bold lines and the HMBC correlations with arrows. The HMBC correlations of only one side chain were marked for simplicity.

The UV absorption spectrum and MS/MS fragmentation of the ion peak in the LTQ-Orbitrap, along with the structures of the fragments generated, are depicted in Figure 5-48. The peak at 234 nm in the UV spectrum confirmed the presence of the aromatic ring. The ion with m/z 149.0234 $[\text{M}]^+$ is characteristic of phthalate esters with saturated non-oxygenated side chains (George and Prest, 2002). The structure of this fragment is also shown in Figure 5-48. Di(2-propylpentyl)phthalate was also

discovered in the blank media, however, proving that this compound was not a product of EG4.

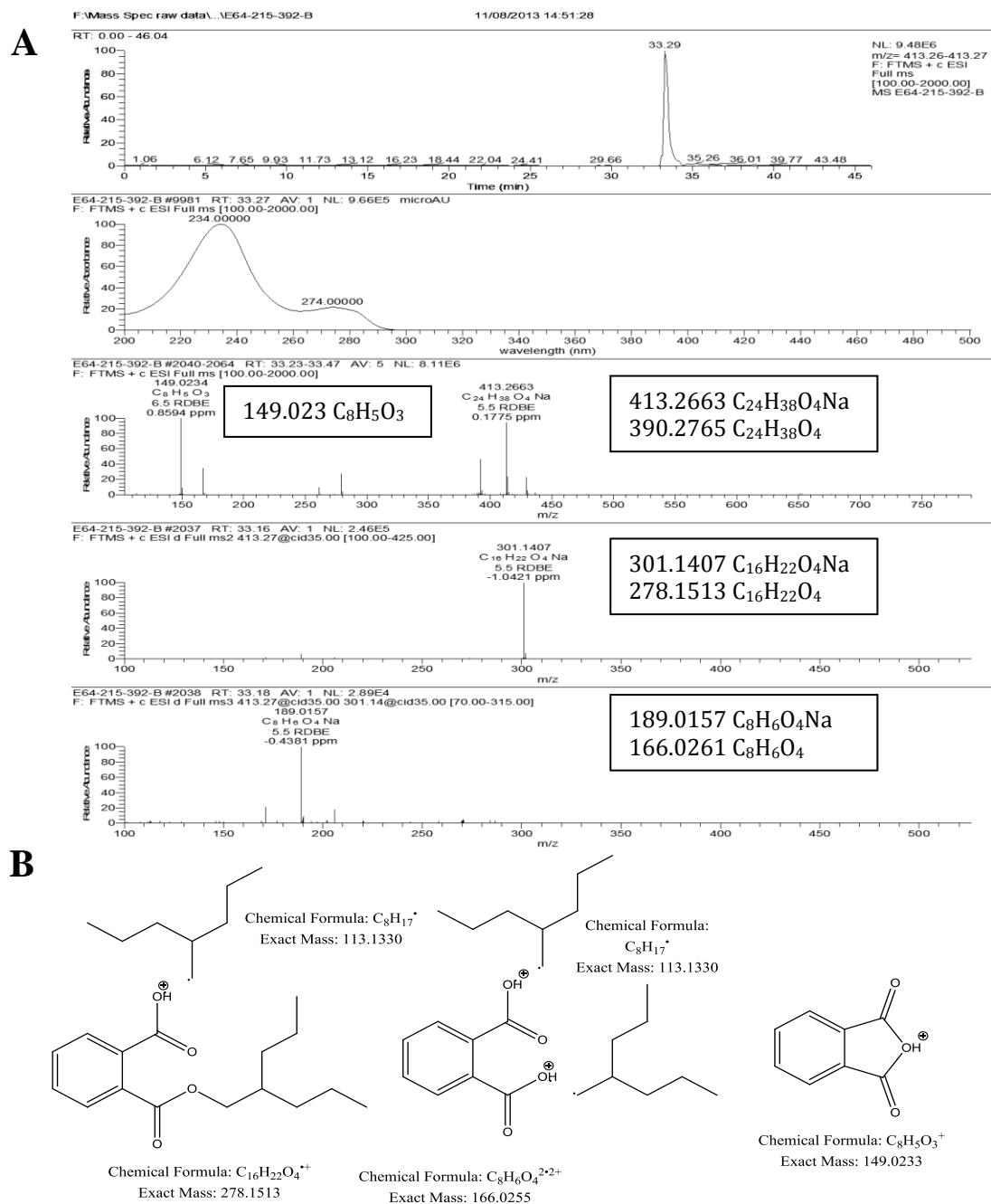


Figure 5-48: (A) MS/MS spectrum and photodiode array (PDA) of EG4_215-392_B and (B) the structure of fragment ions generated. The peak at 234 nm in the PDA spectrum confirms the presence of the aromatic ring. The MS/MS fragmentation resulted in the fragmentation of the side chains and the formation of the fragment with m/z 149.023 [M⁺], which is characteristic of phthalate esters with saturated non-oxygenated side chains.

As previously mentioned, 215-392_B and 569-573_1-59 had identical ^1H NMR spectra and both produced ion peaks at m/z 413.266 $[\text{M}+\text{H}]^+$ with retention times of approximately 33 minutes. The NIST 2011 database putatively identified the compound as diisooctylphthalate ester based on the GCMS spectrum, but analysis of the NMR data showed that branching occurs earlier on in the side chain; that is, closer to the ester group. The identities of the phthalates can be confirmed by comparing them with standards and also, as stated, by making use of more advanced techniques such as positive chemical ionisation MS with retention-time locking GC.

5.3.6.3.2 Indole-3-Carboxaldehyde and Octadecanoic Acid, 2,3-Dihydroxypropyl Ester

EG4_215-392_N was seen in the NMR as a mixture of two compounds, an indole and a monoacyl glycerol. The NMR data are shown in Table 5-25 and Table 5-26 and some NMR spectra can be seen from Figure 5-49 to Figure 5-54.

Table 5-23: Indole-3-Carboxaldehyde

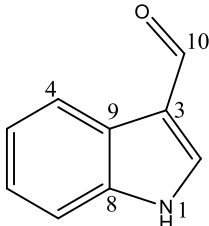
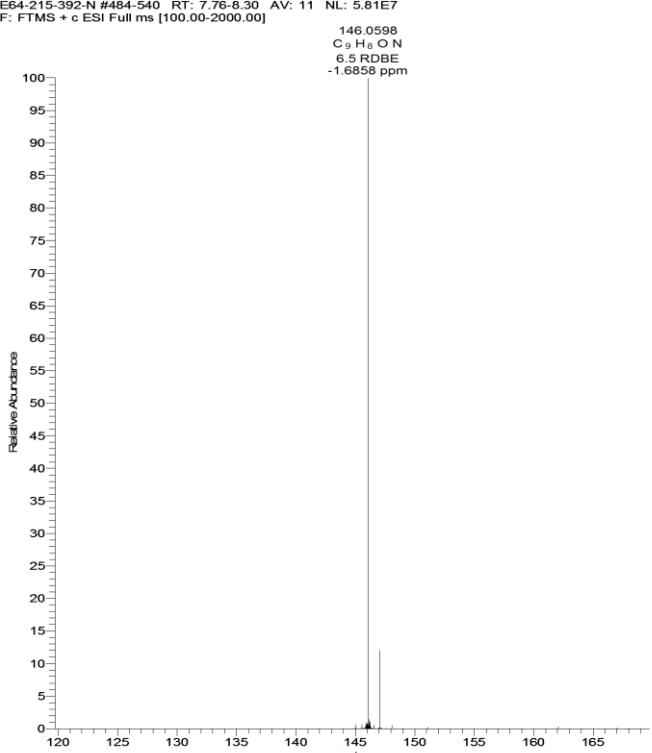
Indole-3-Carboxaldehyde	
<p>Synonyms</p> <p>Sample Code</p> <p>Sample Amount</p> <p>Physical Description</p> <p>Molecular Formula</p> <p>Molecular Weight</p> <p>Rf (TLC silica)</p> <p>Retention time (LC-MS)</p>	<p>1<i>H</i>-Indole-3-carboxaldehyde; 1<i>H</i>-Indole-3-aldehyde; 1<i>H</i>-Indole-3-carbaldehyde; 3-Formyl-1<i>H</i>-indole; 3-Formylindole; 3-Indolylformaldehyde; Indole-3-aldehyde; Indole-3-carbaldehyde; NSC 10118; β-Indolylaldehyde</p> <p>215-392_N</p> <p>2.6 mg</p> <p>-</p> <p>C₉H₇NO</p> <p>146 g/mol</p> <p>0.43 (40:60 hexane: ethyl acetate)</p> <p>8.25 min</p>
	
<p>HRFTMS Spectrum [M+H]⁺</p> <p>E64-215-392-N #484-540 RT: 7.76-8.30 AV: 11 NL: 5.81E7 F: FTMS + c ESI Full ms [100.00-2000.00]</p>  <p>146.0598 C₉H₇O N 6.5 RDBE -1.6858 ppm</p>	

Table 5-24: Octadecanoic acid, 2,3-dihydroxypropyl ester

Octadecanoic acid, 2,3-dihydroxypropyl ester	
<p>Synonyms</p> <p>Sample Code</p> <p>Sample Amount</p> <p>Molecular Formula</p> <p>Molecular Weight</p> <p>Retention time (LC-MS)</p>	<p>1-Monostearin; Stearin, 1-mono-; α-Monostearin; (\pm)-2,3-Dihydroxypropyl octadecanoate; 1-Glyceryl stearate; 1-Monooctadecanoylglycerol; 1-Monostearoylglycerol; 3-Stearoyloxy-1,2-propanediol; Aldo 33; Aldo 75; Aldo MSD; Aldo MSLG; Emerest 2407; Glycerin 1-monostearate; Glycerol 1-monostearate; Glycerol 1-stearate; Glycerol α-monostearate; Glyceryl 1-octadecanoate; NSC 3875; Sandin EU, Stearic acid α-monoglyceride; Tegin 55G</p> <p>215-392_N</p> <p>2.6 mg</p> <p>C₂₁H₄₂O₄</p> <p>358 g/mol</p> <p>32.48 min</p>
<p>HRFTMS Spectrum [M+H]⁺</p> <p>N #917 RT: 32.42 AV: 1 NL: 2.57E5 T: FTMS {1,1} + p ESI Full lock ms [150.00-1500.00]</p> <p>359.3156 C₂₁ H₄₃ O₄ 0.5 RDBE</p>	

Table 5-25: NMR data of EG4_215-392_N (indole-3-carboxaldehyde)

Position	δ_C (ppm)	δ_H ppm (multiplicity, <i>J</i>)	1H - 1H COSY	HMBC (1H - ^{13}C)
1-NH	-	12.14 (s)		
2-CH	138.7	8.29 (d, 3.0 Hz)		3, 8, 9
3-C	118.6	-	-	-
4-CH	121.2	8.10 (d, 7.7 Hz)	5	6, 8
5-CH	122.6	7.22 (t, 7.4 Hz)	4, 6	7, 9
6-CH	123.8	7.27 (t, 7.6Hz)	5, 7	4, 8
7-CH	112.8	7.52 (d, 8.0 HZ)	6	5, 6, 9
8-C	137.4	-	-	-
9-C	124.5	-	-	-
10-CHO	189.8	9.94 (s)		3

Table 5-26: NMR data of EG4_215-392_N (1-monostearin)

Position	δ_C (ppm)	δ_H ppm (multiplicity, <i>J</i>)	1H - 1H COSY	HMBC (1H - ^{13}C)
1-OH	-	4.63 (t, 5.6 Hz)	2	
2-CH ₂	63.1	3.36 (m)	3	
3-CH	69.8	3.64 (dt, 5.5 and 10.7 Hz)	2, 4a, 4b	
3-OH	-	4.86 (d, 5.1 Hz)	3-CH	
4a-CH ₂	65.9	4.04 (dd, 4.2 and 11.1 Hz)	3, 4b	
4b-CH ₂	65.9	3.90 (dd, 6.6 and 11.2 Hz)	4a, 5	3, 5
5-CO	173.3	-	-	-
6-CH ₂	34.0	2.29 (t, 7.4 Hz)	7	5, 7, 8
7-CH ₂	24.9	1.52 (p, 7.2 Hz)	6, 8	8
8-CH ₂	29.4	1.24 (bs)	6	
9-CH ₂ - 20-CH ₂	31.7	1.24 (bs)	8-21	8, 9-20
21-CH ₂	22.7	1.24 (bs)	22	22
22-CH ₃	14.4	0.86 (t, 6.7 Hz)	21	20, 21

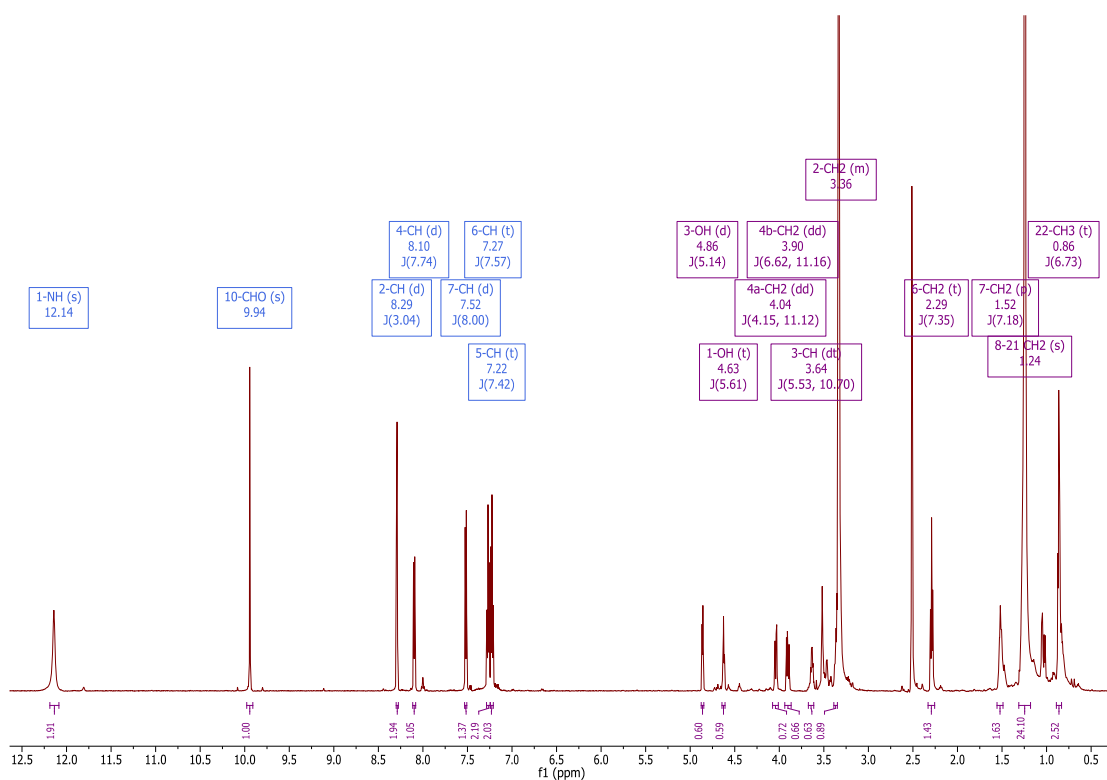


Figure 5-49: ^1H NMR spectrum of EG4_215-392_N (600 MHz, DMSO). The peaks of indole-3-carboxaldehyde are labelled in blue and those of 1-monostearin are labelled in purple.

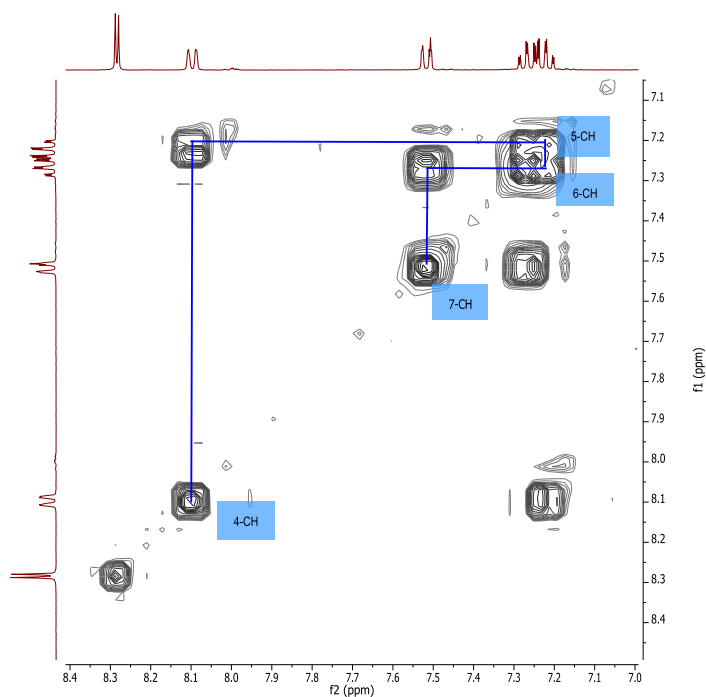


Figure 5-50: Expansion of the COSY showing the correlations of the protons in the indole ring (ABCD spin system) (600 MHz, DMSO).

The above spin system (d-t-t-d) was characteristic of an ABCD aromatic ring system. The ^1H and ^{13}C chemical shifts as seen in the ^1H , HSQC and HMBC spectra indicated that the compound was an indole. The doublet at δ_{H} 8.29 ppm (2-CH) did not correlate to any other peak in the COSY but as it was a doublet it must have been split by another proton, likely the exchangeable proton attached to the nitrogen (1-NH) at δ_{H} 12.14. In the HMBC it was seen that the hydrogen of 2-CH correlated with three quaternary carbons at δ_{C} 118.6 (3-C), 124.5 (9-C) and 137.4 ppm (8-C), confirming the indole substructure. The singlet at δ_{H} 9.94 was attached to an oxygenated carbon (δ_{C} 189.8) and was thus proven to be an aldehyde. It was seen to correlate with C-3 in the HMBC. The COSY and HMBC correlations are shown in Figure 5-51 and the confirmation of the structure using ESI-MS and fragmentation is shown in Figure 5-52. The UV absorption spectrum in Figure 5-52 obtained using the photodiode array (PDA) detector shows the wavelengths at which maximum UV absorption occurs.

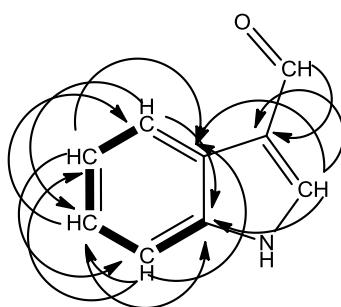


Figure 5-51: Structure of indole-3-carboxaldehyde. The COSY correlations are marked with bold lines whereas the HMBC correlations are marked with arrows.

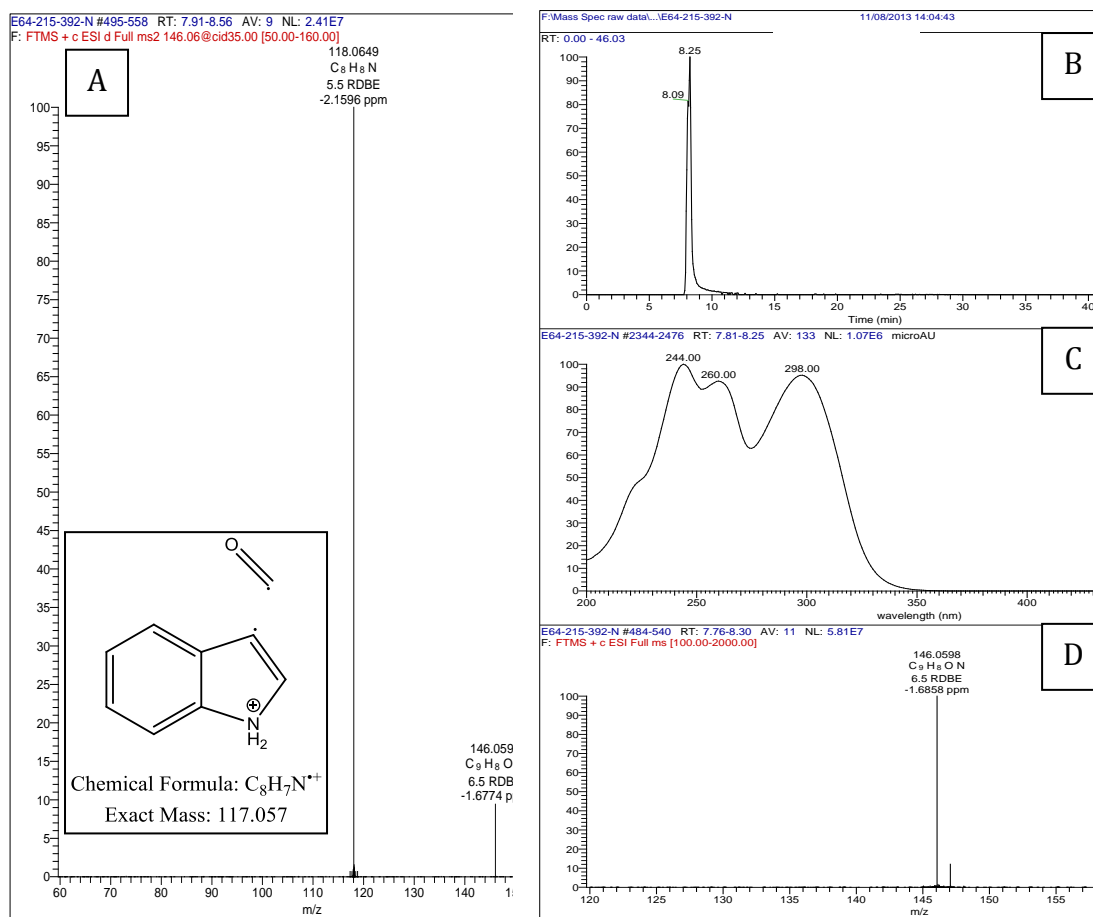


Figure 5-52: LC-MS/MS and PDA of EG4_215-392_N. (A) Mass spectrum showing the parent ion of indole-3-carboxaldehyde with m/z 146.0598 $[M+H]^+$ and the fragment with m/z 118.0649 $[M+H]^+$. The inset shows the structure of the fragment. (B) Extracted ion chromatogram, (C) PDA scan, and (D) mass spectrum of indole-3-carboxaldehyde.

The structure of the monoacyl glycerol was also elucidated. One spin system is highlighted in the COSY in Figure 5-53 below. The triplet at δ_H 4.63 (1-OH) was at one end of the spin system. It coupled to the multiplet at δ_H 3.36 which, based on the HSQC, was a CH_2 (δ_C 63.1). This was therefore assigned as 2- CH_2 . 2- CH_2 also coupled to the peak at δ_H 3.64 (3-CH). The HSQC showed that this hydrogen was attached to an oxygenated carbon (δ_C 69.8) and the COSY confirmed this as it showed the correlation of 3-CH to an OH group (doublet at δ_H 4.86). The spin system continued as 3-CH was also attached to 4- CH_2 (δ_H 4.04 and 3.90). The chemical shift of 4-C (δ_C 65.9) indicated that it was oxygenated, hence it was assigned as being attached to the ester functional group. This was confirmed by the HMBC as one of the protons from 4- CH_2 correlated with the carbonyl carbon (δ_C 173.3).

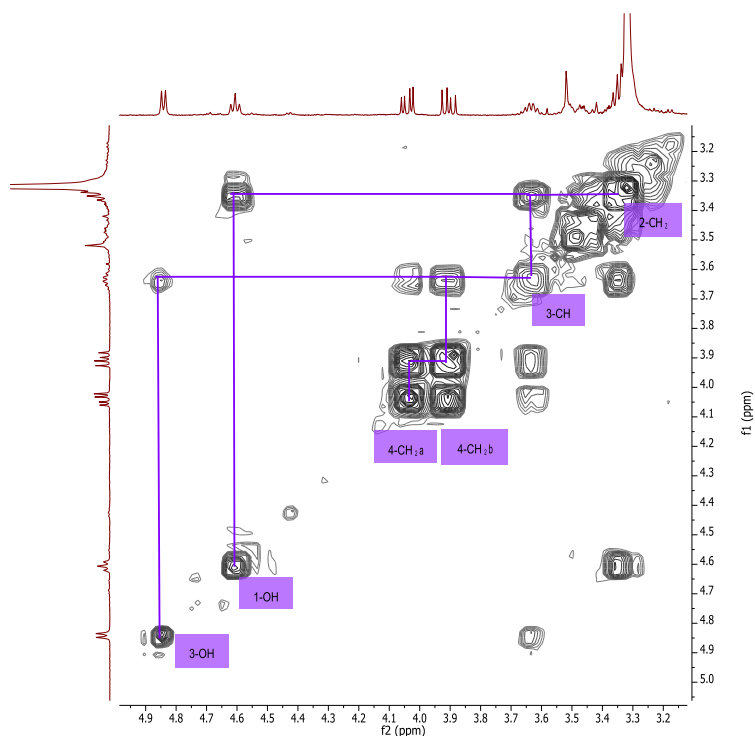


Figure 5-53: Expansion of the COSY of EG4_215-392_N showing the correlations of the protons in the glycerol moiety of the monoacyl glycerol (600 MHz, DMSO).

Figure 5-54 below is another expansion of the COSY showing the aliphatic chain attached to the ester. The triplet at δ_{H} 2.29 (6-CH₂) correlated with the carbonyl carbon in the HMBC. It also coupled with 7-CH₂ (δ_{H} 1.52), which then correlated to the CH₂ chain represented by the large peak at δ_{H} 1.24. This then ended with a terminal methyl group (δ_{H} 0.86). When the integration of the methyl group was set to 3, the broad singlet at δ_{H} 1.24 had a corresponding integration value of 28 protons, indicating that there were 14 overlapping CH₂ groups under that one peak. The proposed structure was confirmed by using the LC-HRFTMS spectrum in which a peak with m/z 359.3156 [M+H]⁺ was found.

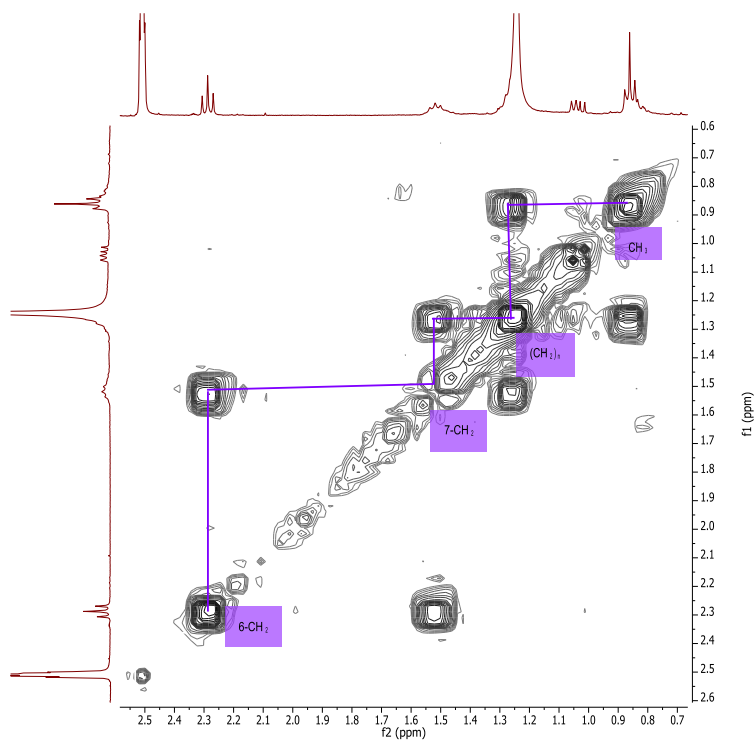
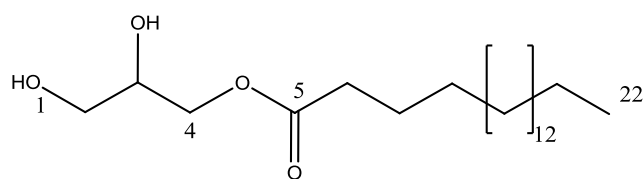


Figure 5-54: Expansion of the COSY of EG4_215-392_N showing the correlation of the protons in the aliphatic chain of 1-monostearin (600 MHz, DMSO).



Octadecanoic acid, 2,3-dihydroxypropyl ester

Chemical Formula: $C_{21}H_{42}O_4$

Exact Mass: 358.3083

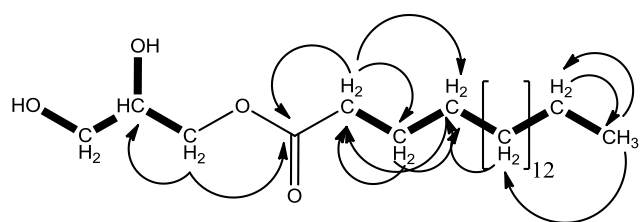


Figure 5-55: Structure of 1-monostearin found in EG4_215-392_N. The bottom structure shows the correlations seen in the COSY (bold lines) and in the HMBC (arrows).

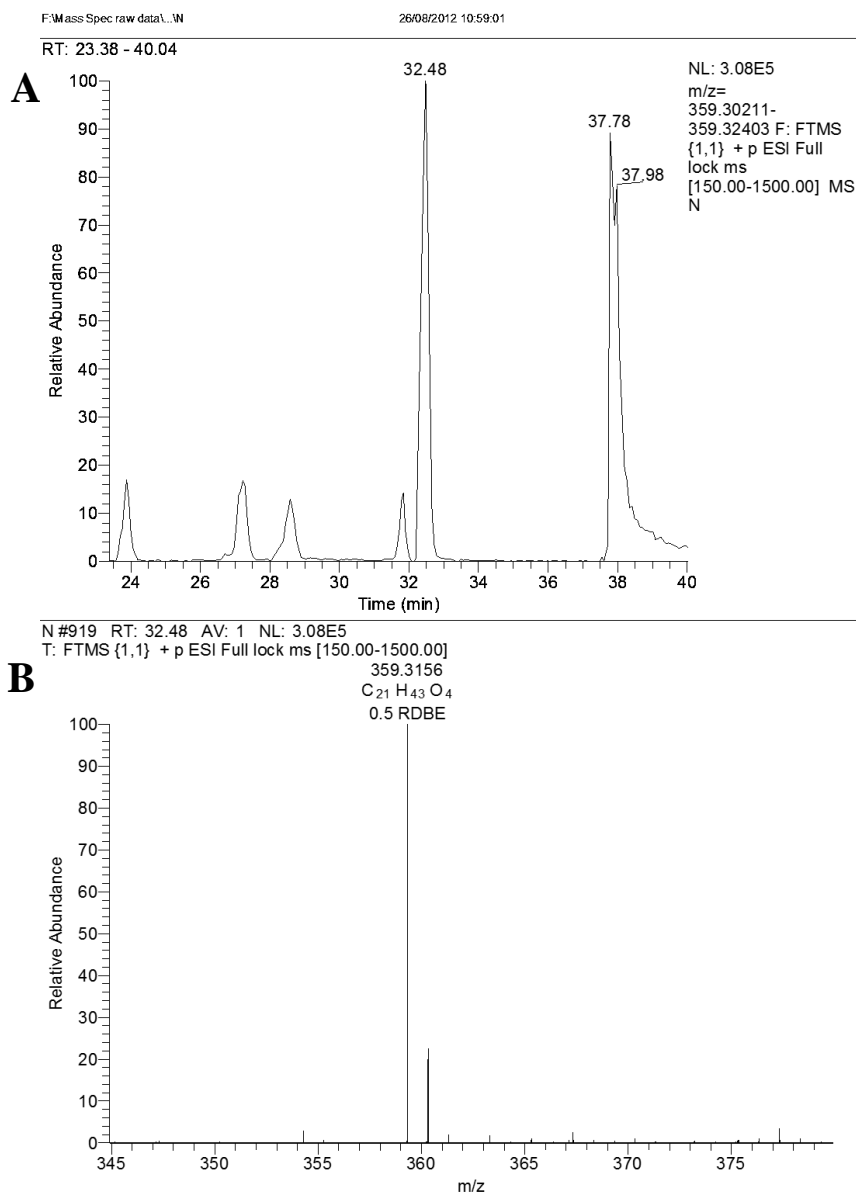


Figure 5-56: (A) Extracted ion chromatogram and (B) mass spectrum of EG4_215-392_N. The peak with m/z 359.3156 $[M+H]^+$ corresponds to 1-monostearin.

5.3.6.3.3 3,4-Dihydroxy-5,6-bis(1*H*-indol-3-yl)-3,5-cyclohexadiene

Fraction EG4_215-392_B3 was obtained after purification of the 215-392 wash fractions through preparative TLC. The NMR spectral data is shown in Table 5-28 and selected NMR spectra can be seen in Figure 5-57 to Figure 5-59.

Table 5-27: 3,4-Dihydroxy-5,6-bis(1H-indol-3-yl)-3,5-cyclohexadiene

3,4-dihydroxy-5,6-bis(1H-indol-3-yl)-3,5-cyclohexadiene (NEW)	
Synonyms	-
Sample Code	215-392_B3
Sample Amount	1.2 mg
Physical Description	-
Molecular Formula	C ₂₂ H ₁₄ N ₂ O ₄
Molecular Weight	370 g/mol
Rf (TLC silica)	0.47 (80:20 CH ₂ Cl ₂ :Ethyl acetate)
Retention time (LC-MS)	29.85 min
LC-HRFTMS spectra [M+H]⁺	
<p>RT: 19.67 - 42.45</p> <p style="text-align: center;">29.85</p> <p style="text-align: center;">Time (min)</p>	<p>EG4-B3 #675-886 RT: 29.66-29.97 AV: 6 NL: 2.78E6 T: FTMS (1,1) + p ESI Full lock ms [150.00-1500.00]</p> <p style="text-align: center;">371.1010 C₂₂H₁₅O₄N₂ 16.5 RDBE -4.3087 ppm</p> <p style="text-align: center;">m/z</p>

Table 5-28: NMR data of EG4_215-392_B3

Position	δ_C ppm	δ_H ppm (multiplicity, J)	1H - 1H COSY	HMBC (1H - ^{13}C)
1-CO	182.9	-	-	-
2-CO				
3-COH	165.9	8.06 (s)		
4-COH		7.69 (s)		
5-C	166.0			
6-C		-	-	-
1'-NH	-	12.20 (s)	2'	
1''-NH	-	11.81 (s)	2''	
2'	138.2	8.68 (d, 2.5 Hz)	1'	3', 8', 9'
2''	132.2	7.99 (s)	1''	3'', 9''
3'	112.2	-	-	-
3''	107.3	-	-	-
4'	121.2	8.22 (d, 6.7 Hz)	5', 6', 7'	6', 8'
4''	120.5	7.99 (d, 11.3 Hz)	5''	6'', 8''
5'	122.4	7.24 (m)	4'	7', 9'
5''	120.9	7.15 (m)	6''	7'', 9''
6'	123.3	7.26 (m)	4', 7'	4', 8'
6''	122.1	7.17 (m)	7''	4'', 8''
7'	112.5	7.53 (dd, 2.0 and 6.4 Hz)	4'6'	5', 9'
7''	112.1	7.45 (d, 7.8 Hz)	6''	5'', 9''
8'	136.4	-	-	-
8''	136.3	-	-	-
9'	126.1	-	-	-
9''	126.0	-	-	-

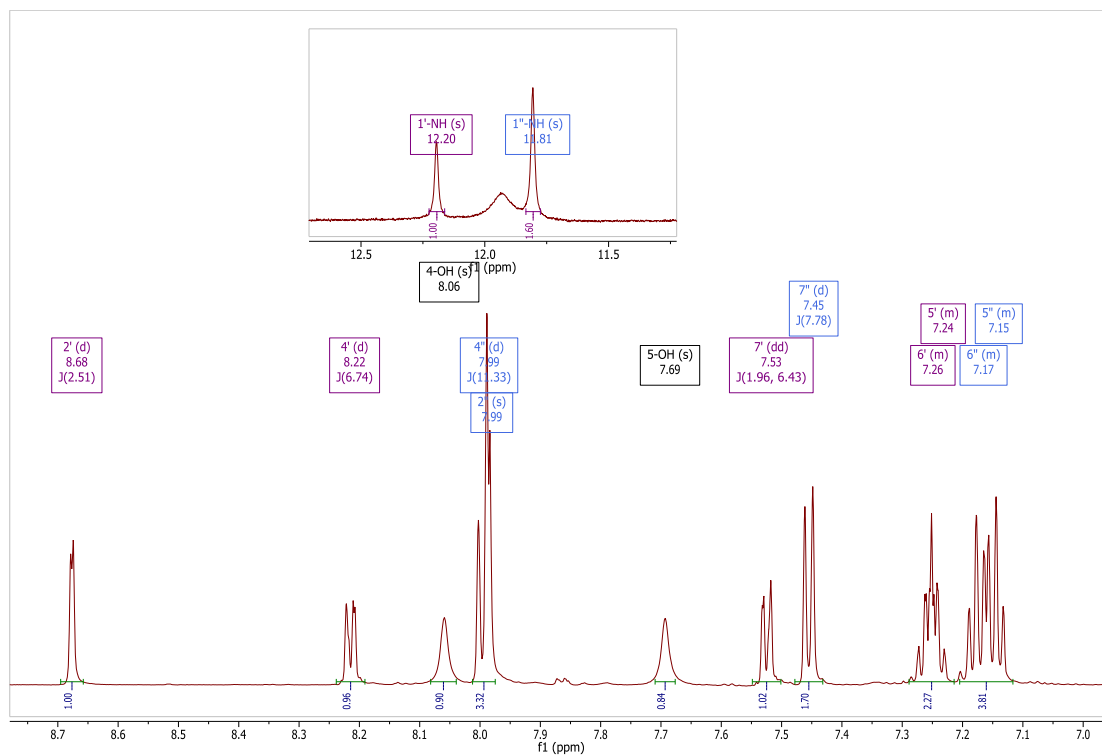


Figure 5-57: Expansion of the ^1H NMR spectrum of EG4_215-392_B3 (600 MHz, DMSO). The inset shows the downfield signals near 12 ppm. The blue and purple labels correspond to signals belonging to two indole rings whereas the black labels correspond to the signals of the cyclohexane ring.

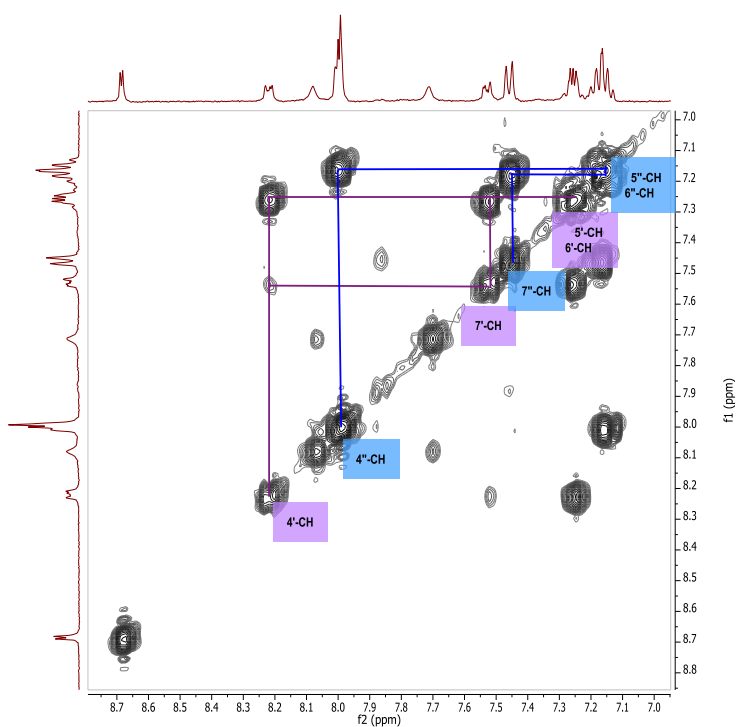


Figure 5-58: Expansion of the COSY of EG4_215-392_B3 (400 MHz, DMSO). The spin systems of the two indole rings are labelled in different colours.

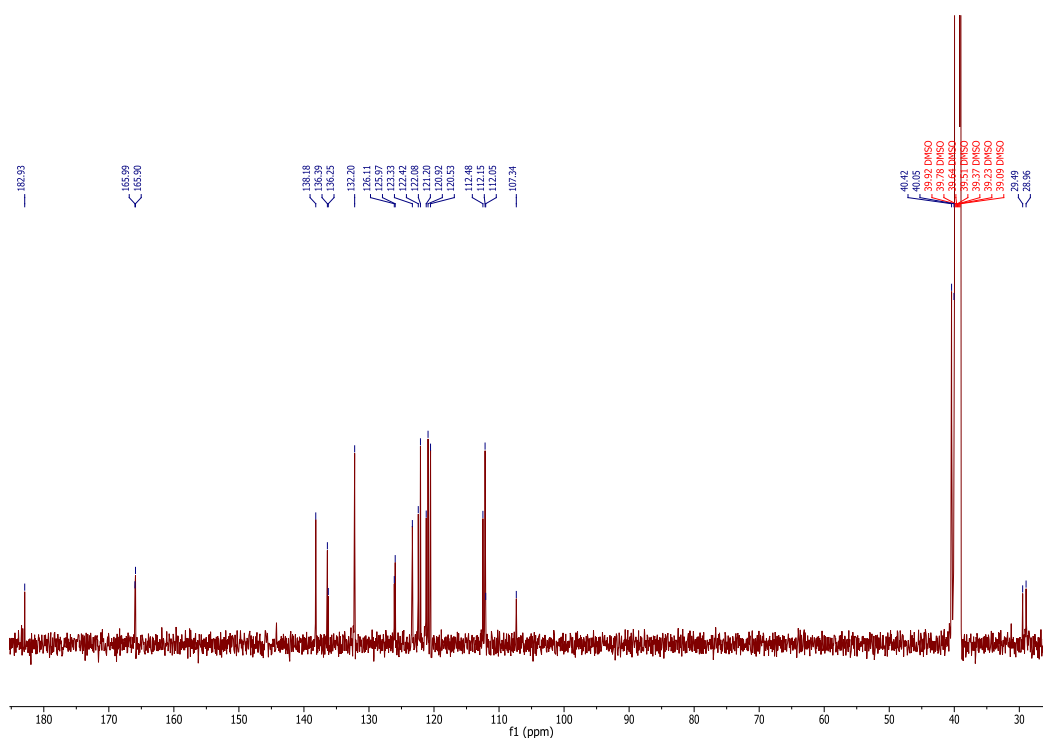


Figure 5-59: ^{13}C NMR spectrum of EG4_215-392_B3 (150 MHz, DMSO).

The ^1H NMR spectrum of EG4_215-392_B3 contained the peaks of two indole rings. Some of the peaks overlapped but the differing chemical shifts indicated that the two rings were in different environments; that is, the molecule was non-symmetrical. The ABCD spin system of one indole was traced in the COSY (Figure 5-58) where the doublet of 4'-CH at δ_{H} 8.22 correlated with the multiplets (overlapping triplets) of 5'-CH and 6'-CH at δ_{H} 7.24 and 7.26 respectively. 6'-CH then related to the doublet at δ_{H} 7.45 (7'-CH). The HMBC confirmed this substructure. The correlation of 2'-CH to 3'-C, 8'-C and 9'-C (δ_{C} 112.2, 136.4 and 126.1 respectively) was also observed in the HMBC.

The second indole ring was determined in a similar manner. The COSY showed the ABCD spin system (d-t-t-d) between 4''-CH (δ_{H} 7.99), 5''-CH (δ_{H} 7.15), 6''-CH (δ_{H} 7.17) and 7''-CH (δ_{H} 7.53). The HMBC once again confirmed this, as well as the position of 2''-CH (δ_{H} 7.99) as it correlated with 3''-C and 9''-C (δ_{C} 107.3 and 126.0 respectively).

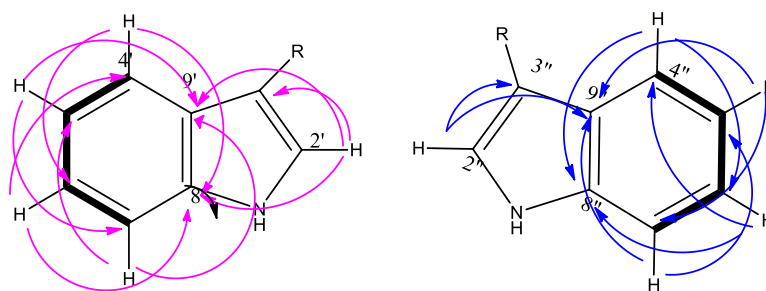


Figure 5-60: Indole rings of EG4_215-392_B3. The HMBC correlations of indole 1 (pink) and 2 (blue) are marked with arrows. The COSY correlations are marked with bold lines.

Analysis of the mass spectrum of B3 indicated that the compound had a predicted formula of $C_{22}H_{15}O_4N_2 [M+H]^+$ (Table 5-27), which thereby suggested that an additional 6 quaternary carbons – a substituted benzene ring – connected the two indole rings. There were four oxygens attached to the ring, two of which were hydroxyl groups. A 1D nuclear overhauser effect spectroscopy (NOESY) experiment irradiating the hydroxyl group at δ_H 7.69 resulted in an nOe correlation at δ_H 8.06, showing that the two hydroxyl groups were close to each other spatially (Figure 5-61). The indole rings rotate, hence no nOe correlation was visible between the OH and a proton from the indole ring.

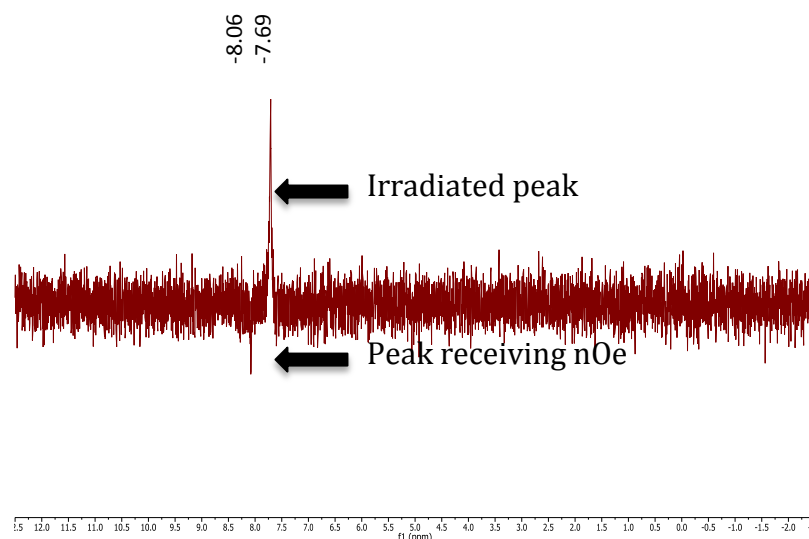


Figure 5-61: 1D NOE showing the through-space correlation between the two OH groups (400 MHz, DMSO). The two hydroxyl groups correlated with each other; however, neither of them correlated with any of the protons of the indole rings due to the rotation of the rings.

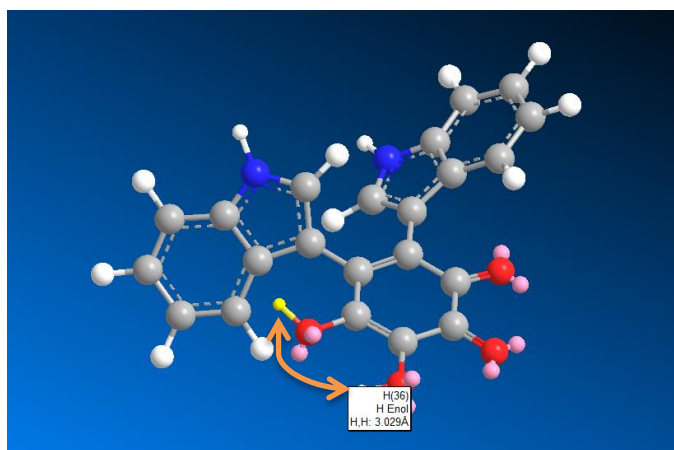


Figure 5-62: 3D depiction of EG4_215-392_B3. The hydrogens attached to the OH groups of the benzene ring had a distance of 3.029Å between them (marked by the orange arrow). The nOe correlation between the two was therefore visible.

5.3.6.4 Preparative TLC of EG4_615-626

Fraction 615-626 was also purified using preparative TLC. The TLC summary plate can be seen in Figure 5-63. EG4_615-626_2 and _4 were obtained as pure compounds. 615-626_6 and _10 were still mixtures, and although the structure of the latter was determined, that of the former was not completely elucidated. The fractions were sent for anti-trypanosomal and anti-mycobacterium assays. An assay against *Nocardia farcinica* was also performed. The antibiotic activities and weights of the fractions are seen in Table 5-29.

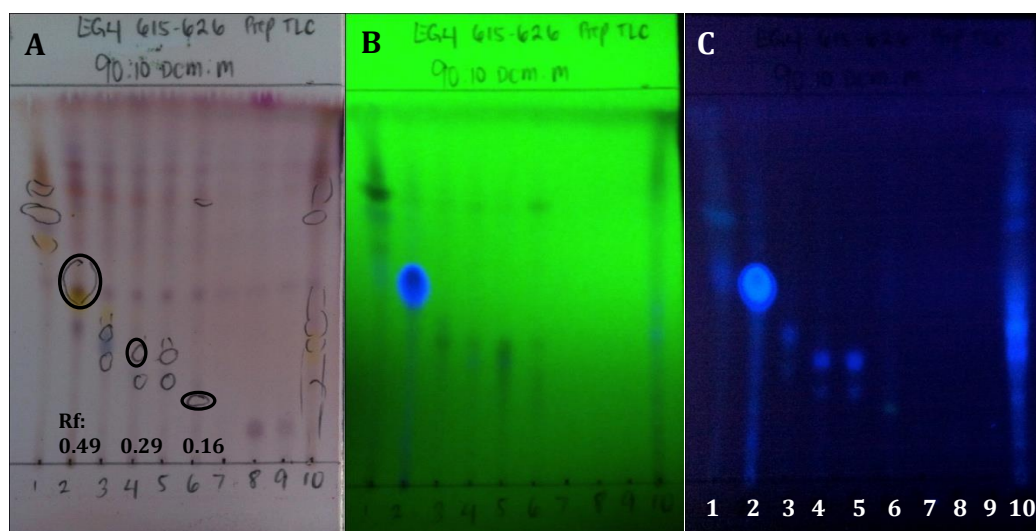


Figure 5-63: TLC summary plate of EG4_615-626 fractions obtained after preparative TLC. The plate was eluted with 90:10 dichloromethane:methanol and was viewed by (A) spraying with anisaldehyde-sulphuric acid, (B) under short wavelength UV, and (C) under long wavelength UV. The encircled spots indicate the isolated compounds whose structures were elucidated.

Table 5-29: Yields and activities of EG4_615-626 fractions after preparative TLC

Fraction	Identification	Yield (mg)	% Inh. <i>T.b.brucei</i> (20µg/mL)	MIC <i>T.b.brucei</i> (µg/mL)	% Inh. <i>M. marinum</i> (100µg/mL)	MIC <i>M. marinum</i> (µg/mL)	% Inh. <i>N. farcinica</i> (100µg/mL)	MIC <i>N. farcinica</i> (ug/mL)
1		6.3	74.6	-	97.8	100	6.3	-
2	1-Methyl-β-carboline	0.6	15.5	-	82.8	-	3.9	-
3		0.5	6.2	-	-35.8	-	2.8	-
4	Uracil	0.7	1.8	-	16.4	-	4.1	-
5		0.5	14.4	-	-23.0	-	4.6	-
6	Dianiline	0.4	0	-	51.6	-	100.3	
7		0.3	29.9	-	32.9	-	6.6	-
8		0.4	56.0	-	92.7	100	101.2	50
9		0.4	33.1	-	62.0	-	101.3	100
10	1,4-dibenzyl-imidazolidine	3.4	97.1		100.6	100	100.8	100

5.3.6.4.1 1-Methyl-β-Carboline

EG4_615-626_2 was identified as 1-methyl-β-carboline (also called harman or harmine). The NMR data can be seen in Table 5-31 and selected spectra can be seen in Figure 5-64 and Figure 5-65.

Table 5-30: 1-Methyl-β-Carboline

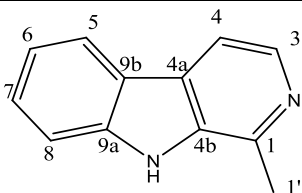
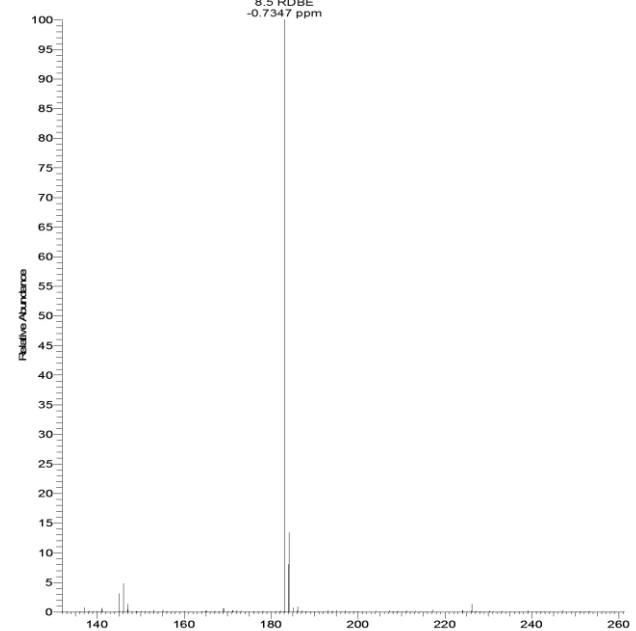
1-Methyl-β-carboline	
Synonyms	9 <i>H</i> -Pyrido[3,4- <i>b</i>]indole, 1-methyl; 2,9-Pyridindole, 1-methyl- (3 <i>CD</i>); Harman; Harmane; Aribin; Aribine; Indoter; Locuturin; Locuturine; NSC 54439; Zygofabagine
Sample Code	615-626_2
Sample Amount	0.6 mg
Physical Description	Orange solid
Molecular Formula	C ₁₂ H ₁₀ N ₂
Molecular Weight	182 g/mol
R_f (TLC silica)	0.49 (90:10 CH ₂ Cl ₂ :MeOH)
Retention time (LC-MS)	6.14 min
	
HRFTMS Spectra [M+H]⁺	
<p>EG461506262 #36-159 RT: 0.65-2.06 AV: 13 NL: 6.96E6 T: FTMS (1,1) + p ESI Full lock ms [75.00-1200.00] 183.0915 C₁₂H₁₁N₂ 9.5 RDBE -0.7347 ppm</p> 	

Table 5-31: NMR data of EG4_615-626_2 (harman) compared to that from literature

Position	δ_C ppm	δ_H ppm (multiplicity, J)	1H - 1H COSY	HMBC (1H - ^{13}C)	^{13}C from literature (Pouchert and Behnke, 1993)
1-C	142.6	-	-	-	142.04
2-N	-	-	-	-	-
3-CH	138.0	8.21 (d, 5.3 Hz)	4	4	137.42
4-CH	113.1	7.94 (d, 5.3 Hz)	3	4b	112.51
4a-C		-	-	-	126.76
4b-C	135.0	-	-	-	134.42
5-CH	122.3	8.20 (d, 7.8 Hz)	6	7, 9a	121.59
6-CH	119.7	7.24 (t, 7.4 Hz)	5, 7	8, 9b	119.07
7-CH	128.4	7.54 (t, 7.5 Hz)	6, 8	5, 9a	127.67
8-CH	112.5	7.60 (d, 8.2 Hz)	7	9b, 6	111.84
9-NH	-	11.56 (s)	-	-	-
9a-C	140.6	-	-	-	140.26
9b-C	121.6	-	-	-	121.02
1'-CH ₃	20.8	2.77 (s)	-	1, 4b	20.44

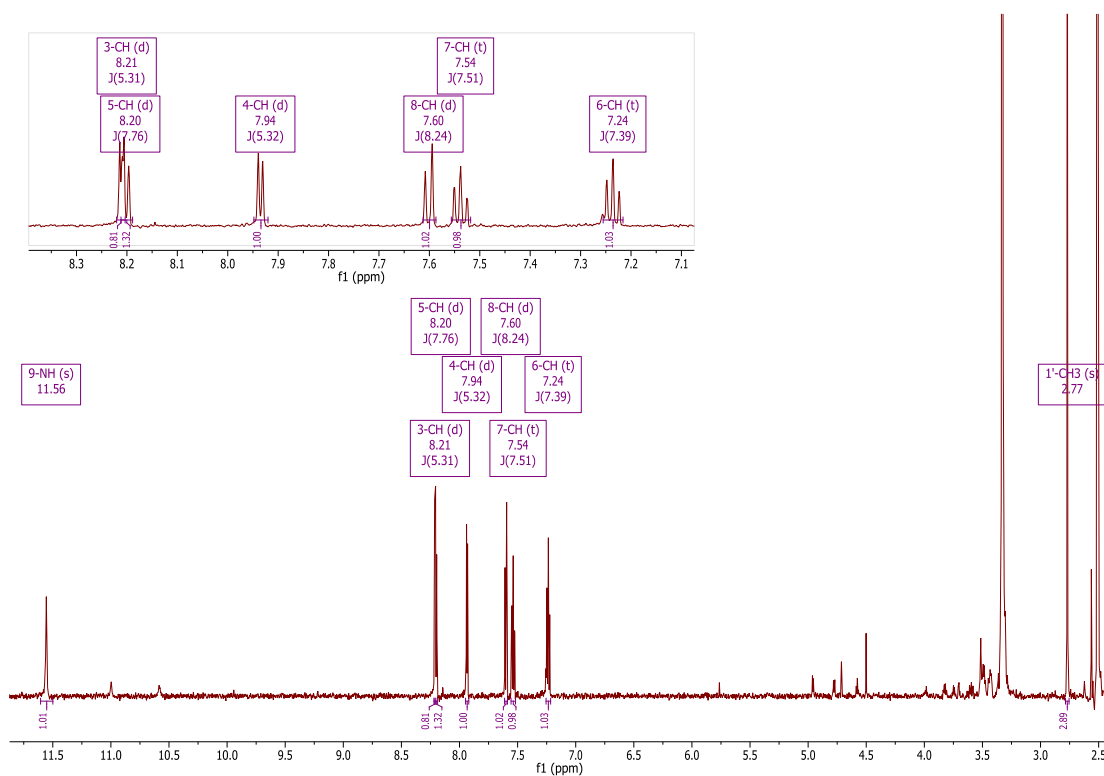


Figure 5-64: 1H NMR spectrum of EG4_615-626_2 (600 MHz, DMSO). The inset in the upper left corner shows an expansion of the aromatic region.

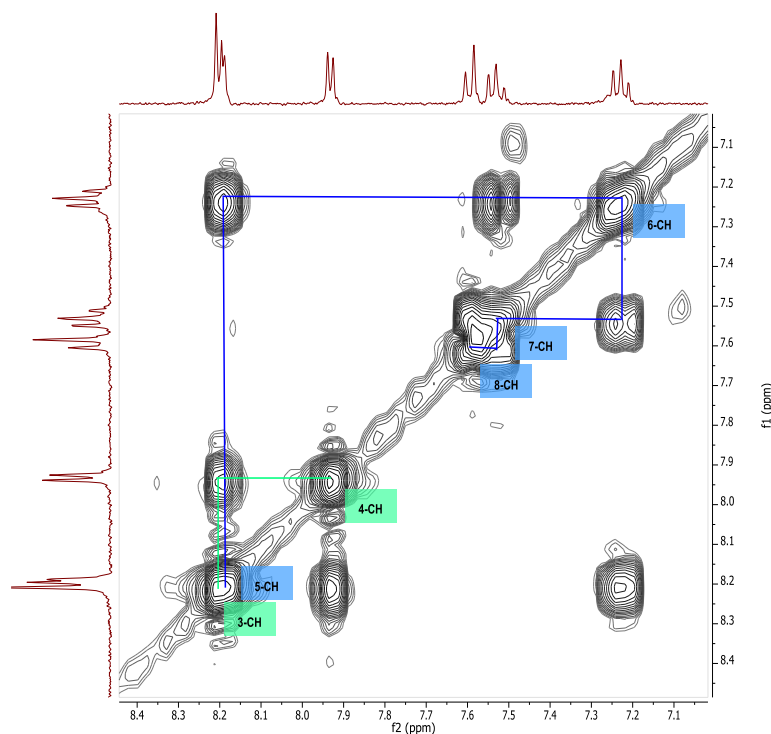


Figure 5-65: ^1H - ^1H COSY spectrum showing the correlations in the two spin systems (400 MHz, DMSO).

Once again, an ABCD spin system was evident in the COSY (Figure 5-65). The d-t-t-d pattern began from the doublet of 5-CH (δ_{H} 8.20) to the triplets of 6-CH and 7-CH (δ_{H} 7.24 and 7.54 respectively) and ended at the doublet of 8-CH (δ_{H} 7.60). This spin system was confirmed by the HMBC correlations. 5-CH and 7-CH also correlated with 9a-C (δ_{C} 140.6) in the HMBC, while 6-CH and 8-CH correlated with 9b-C (δ_{C} 121.6). The other spin system in Figure 5-65 highlighted in green showed the two protons, 3-CH and 4-CH, that were part of the C ring. The 3J value of approximately 5 Hz indicated that a heteroatom (nitrogen) was present in the ring as the normal coupling constant for protons in the ortho position, without the presence of nitrogen, is 7-9 Hz. The HMBC also showed a correlation between 4-CH and 4b-C (δ_{C} 135.0). The methyl group of 1'-CH₃ (δ_{H} 2.77) was a singlet and did not correlate with any other peak in the COSY, but the HMBC showed a correlation to 1-C and 4b-C (δ_{C} 142.6 and 135.0 respectively). The COSY and HMBC correlations can be seen in Figure 5-66.

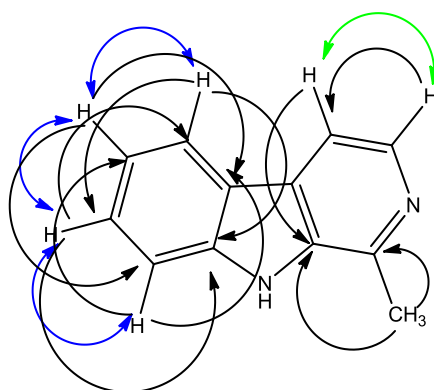


Figure 5-66: Structure of EG4_615-626_2 (harman). The COSY correlations were marked with blue and green arrows and the HMBC correlations by black arrows.

This proposed structure was confirmed by HRFTMS of the compound. The results can be seen in Table 5-30. Analysis of the M1 media blank indicated that this compound was a component of the media, and thus not a product of EG4. Harman did have activity against *M. marinum* but was not significantly active against *T. b. brucei* and *N. farcinica*.

5.3.6.4.2 Uracil

EG4_615-626_4 was also obtained as a pure compound. The structure was elucidated and the identity was confirmed as uracil (Table 5-32). The NMR data can be seen in Table 5-33 and selected NMR spectra are shown in Figure 5-67 and Figure 5-68.

Table 5-32: Uracil

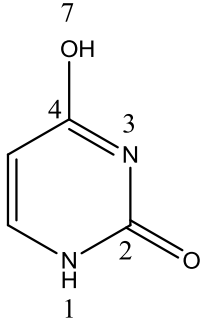
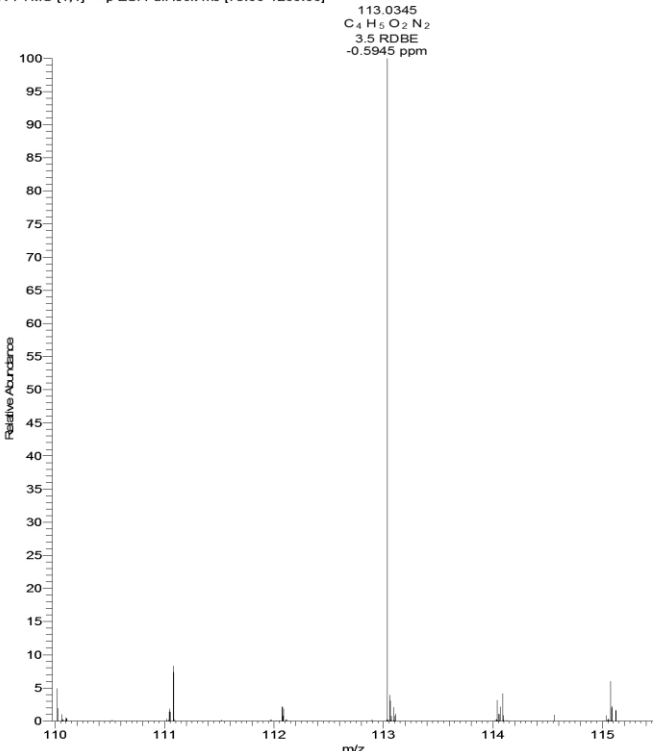
Uracil	
Synonyms	2,3(1 <i>H</i> ,3 <i>H</i>)-Pyrimidinedione; 2,4-Dihydroxypyrimidine; 2,4-Dioxypyrimidine; 2,4-Pyrimidinediol; 2,4-Pyrimidinedione; 4-Hydroxyuracil; Hybar X; NSC 3970; Pirod; Pyrod
Sample Code	615-626_4
Sample Amount	0.4 mg
Physical Description	-
Molecular Formula	C ₄ H ₄ N ₂ O ₂
Molecular Weight	112 g/mol
R_f (TLC silica)	0.29 (90:10 CH ₂ Cl ₂ :MeOH)
Retention time (LC-MS)	1.31 min
	
HRFTMS Spectra [M+H]⁺	
<p style="font-size: small;">EGH615-6264 #35-48 RT: 0.57-0.62 AV: 3 NL: 3.91E5 T: FTMS (1,1) + p ESI Full lock ms [75.00-1200.00]</p>  <p style="font-size: small;">113.0345 C₄H₅O₂N₂ 3.5 RDBE -0.5945 ppm</p>	

Table 5-33: NMR data for EG4_615-626_4 (Uracil) and comparison with values from literature

Position	δ_C ppm	δ_H ppm (multiplicity, J)	1H - 1H COSY	HMBC (1H - ^{13}C)	^{13}C from literature (Pouchert and Behnke, 1993)
1-NH	-	10.81 (s)	6		-
2-CO	151.9	-	-	-	151.43
3-N	-	-	-	-	-
4-C	164.6	-	-	-	164.26
5-CH	100.7	5.45 (dd, 1.9 and 7.6 Hz)	6, 7 (long-range)		100.13
6-CH	142.7	7.39 (dd, 5.6 and 7.6 Hz)	1, 5	4, 2	142.10
7-OH	-	11.01 (s)	3		-

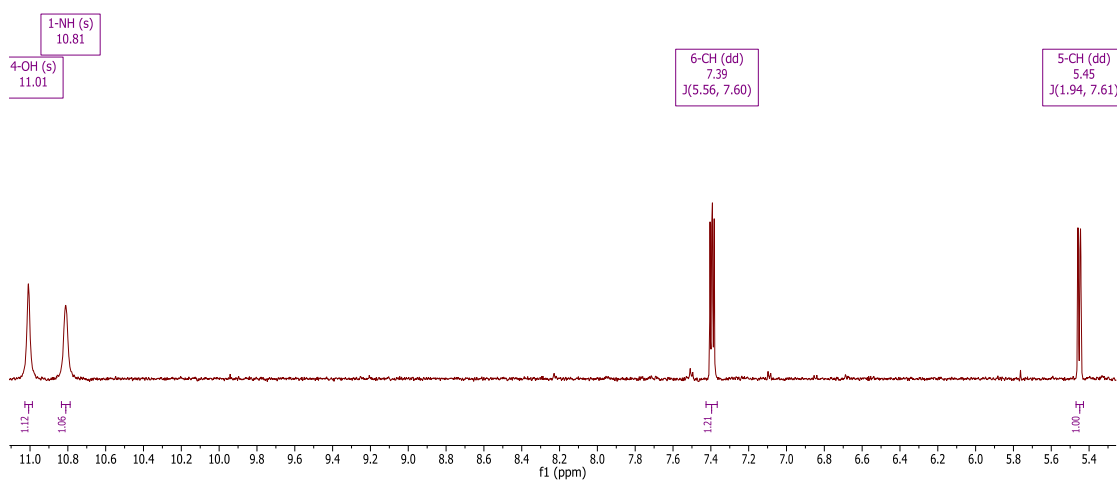


Figure 5-67: 1H NMR spectrum of EG4_615-626_4 (600 MHz, DMSO).

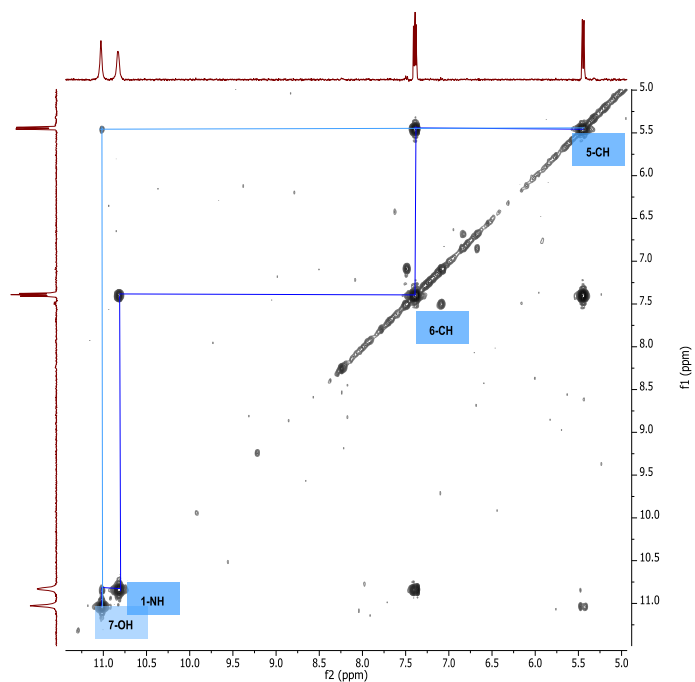


Figure 5-68: ^1H - ^1H COSY spectrum of EG4_615-626_4.

The structure of uracil was confirmed by the COSY (Figure 5-68). The COSY showed correlations between 1-NH (broad singlet at δ_{H} 10.81), and 6-CH and 5-CH (doublet of doublets at δ_{H} 7.39 and 5.45). 5-CH also had ^3J correlation with a peak at δ_{H} 11.01, which belonged to the hydroxyl group attached to 4-C. The HMBC allowed the assignment of the other two carbons as 6-CH correlated with both 2-CO and 4-C (δ_{C} 151.9 and 164.6 respectively). The structure was confirmed with HRFTMS (Table 5-32). Uracil was inactive against all three microorganisms tested.

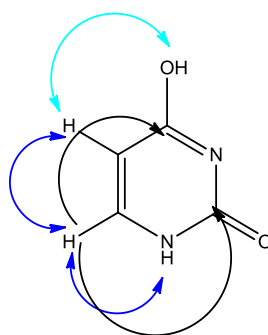
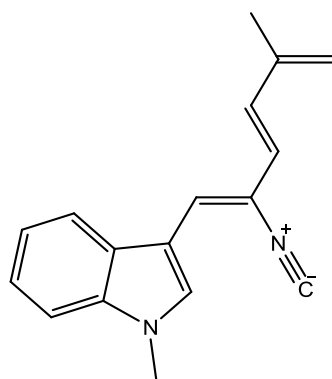


Figure 5-69: Structure of EG4_615-626_4 (uracil). The COSY correlations are marked with blue arrows and the HMBC correlations by black arrows.

5.3.6.4.3 615-626_6

EG4_615-626_6 was obtained as a mixture. This fraction contained an ion with m/z 249.138 $[M+H]^+$, a metabolite of interest because it had previously been identified as a contributor to bioactivity. However, the fraction possessed no inhibitory activity against *T. b. brucei* and inhibited only approximately 50% of *M. marinum*. Nevertheless, it was active against *N. farcinica*. Unfortunately, due to the low amount recovered, further purification of the compound was not performed. The AntiMarin database putatively identified the peak as brasilidone A (5), an isonitrile-bearing indole compound (Kobayashi et al., 1997), but the NMR spectra disproved this. Peaks corresponding to indoles were observed in the 1H and COSY spectra, but the LC-UV-MS spectra confirmed these as indole-3-carboxaldehyde (m/z 146.06 $[M+H]^+$) and indole-3-carboxylic acid (m/z 162.06 $[M+H]^+$) (Figure 5-76). The primary spin system seen in the 1H NMR spectrum is an AA'BB' spin system at δ_H 6.94 and 6.67 ppm. The J value of approximately 8 Hz confirmed the ortho coupling of the AA' and BB' protons. The benzene ring was also evident in the UV spectrum as shown by the peak at 225 nm (Figure 5-76).



Brasilidone A
Chemical Formula: $C_{17}H_{16}N_2$
Exact Mass: 248.1313

Figure 5-70: Structure of Brasilidone A [5]. This compound was identified by the AntiMarin database as a hit for the peak with an m/z of 249.138 $[M+H]^+$; however, NMR and LC-MS analysis proved that the compound produced by EG4 was not brasilidone A.

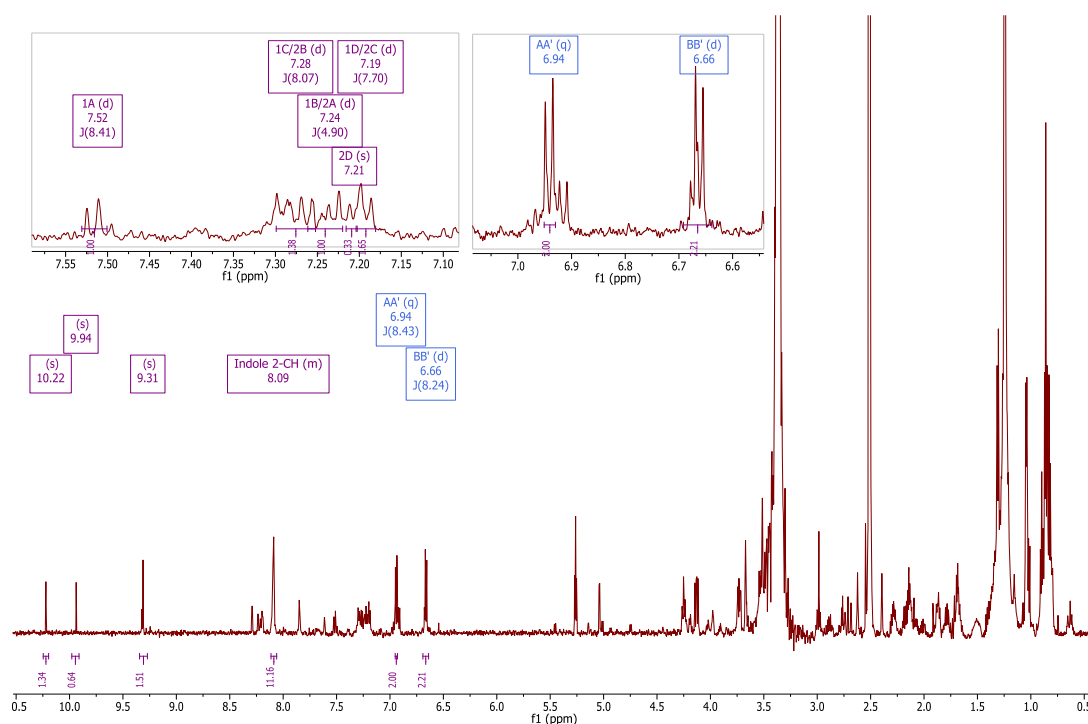
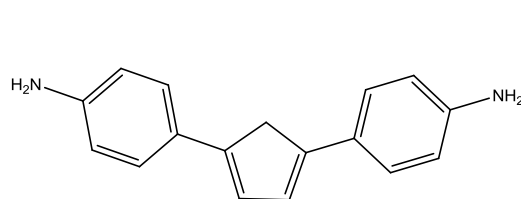
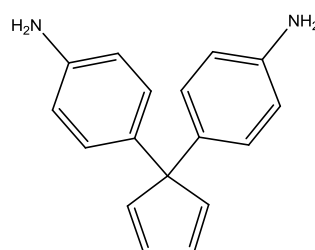


Figure 5-71: ^1H NMR spectrum of EG4_615-626_6 (600 MHz, DMSO). The peaks belonging to the AA'BB' system of m/z 249.138 $[\text{M}+\text{H}]^+$ are labelled in blue while the peaks belonging to the indoles are labelled in purple.

It was thus known that the molecule had an AA'BB' spin system and generated an ion peak with m/z 249.138 $[\text{M}+\text{H}]^+$ with a predicted molecular formula of $\text{C}_{17}\text{H}_{16}\text{N}_2$ and 10.5 RDBE. The high number of double bonds implied the presence of several unsaturated ring systems, whereas the lack of other aromatic signals indicated a symmetrical molecule in which the aromatic rings were equivalent. Two structures were therefore proposed:



4,4'-(cyclopenta-3,5-diene-1,3-diyl)dianiline
Chemical Formula: $\text{C}_{17}\text{H}_{16}\text{N}_2$
Exact Mass: 248.1313



4,4'-(cyclopenta-2,4-diene-1,1-diyl)dianiline
Chemical Formula: $\text{C}_{17}\text{H}_{16}\text{N}_2$
Exact Mass: 248.1313

Figure 5-72: Proposed structures for EG4_615-626_6.

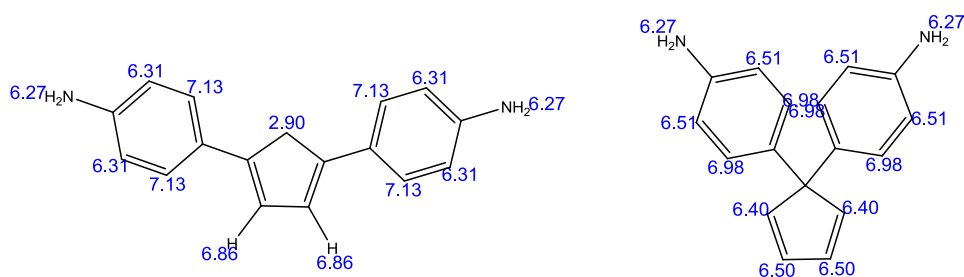


Figure 5-73: Predicted ^1H NMR chemical shifts for the proposed structures of EG4_615-626_6.

Figure 5-73 above shows the ^1H NMR signals of the proposed structures predicted using the software ChemBioDraw. For the first proposed structure, in which the aniline rings are attached to the cyclopentadiene ring at positions 1 and 3, the signals in the ^1H spectrum corresponding to the protons of the cyclopentadiene ring may be overlapping with the signals of the other indole metabolites. On the other hand, the peaks could be overlapping with those of the AA'BB' spin system of the aniline rings (Figure 5-74). A greater quantity of the pure compound must be obtained to ascertain the structure.

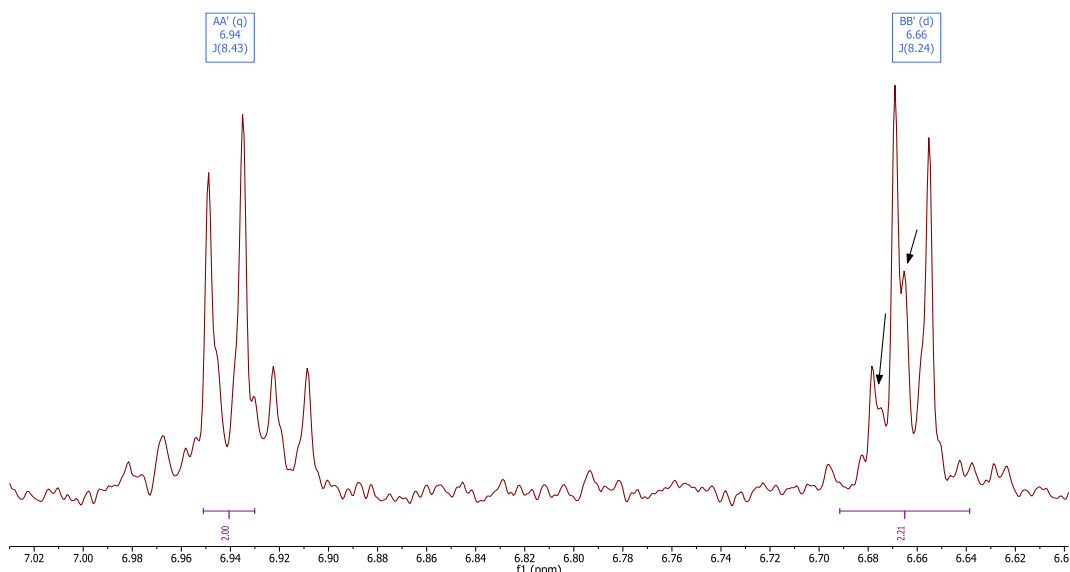


Figure 5-74: Expansion of the ^1H NMR spectrum of EG4_615-626_6. The AA'BB' spin system of aniline is evident. Black arrows point to the potential overlapping peaks of the cyclopentadiene ring.

The spin systems of at least two indoles were observed in the COSY spectrum, as shown in Figure 5-75 below. These belong to indole-3-carboxaldehyde and indole-3-carboxylic acid. Their UV spectra and mass spectra are shown in Figure 5-76. Some signals belonging to aldehydes may be seen in the downfield region (9.3-10.2 ppm)

of the ^1H spectrum (Figure 5-71). Although the structure of 615-626_6 was unable to be confirmed, Table 5-34 contains a summary of the fraction and the metabolite of interest. Searches of the DNP and the AntiMarin database have returned compounds, such as brasilidine A, which do not match the NMR data obtained for this fraction. The compound produced by EG4 may therefore be novel or may be a synthetic compound discovered in nature for the first time.

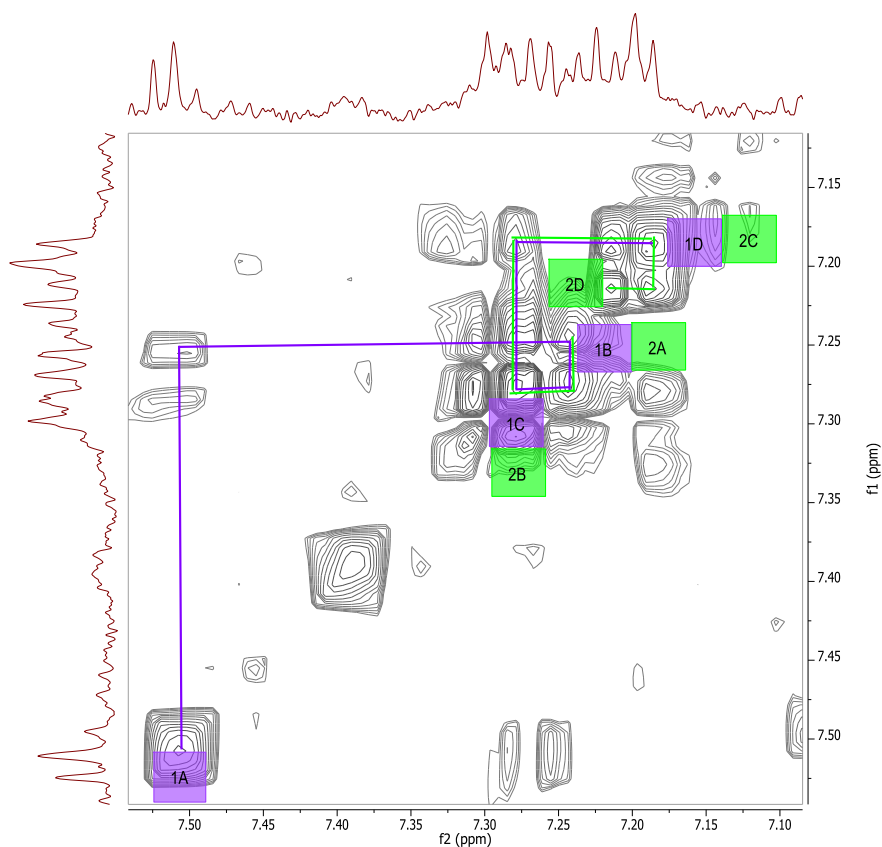


Figure 5-75: ^1H - ^1H COSY spectrum of EG4_615-626_6. The spin systems of the different indoles are coloured in purple and green.

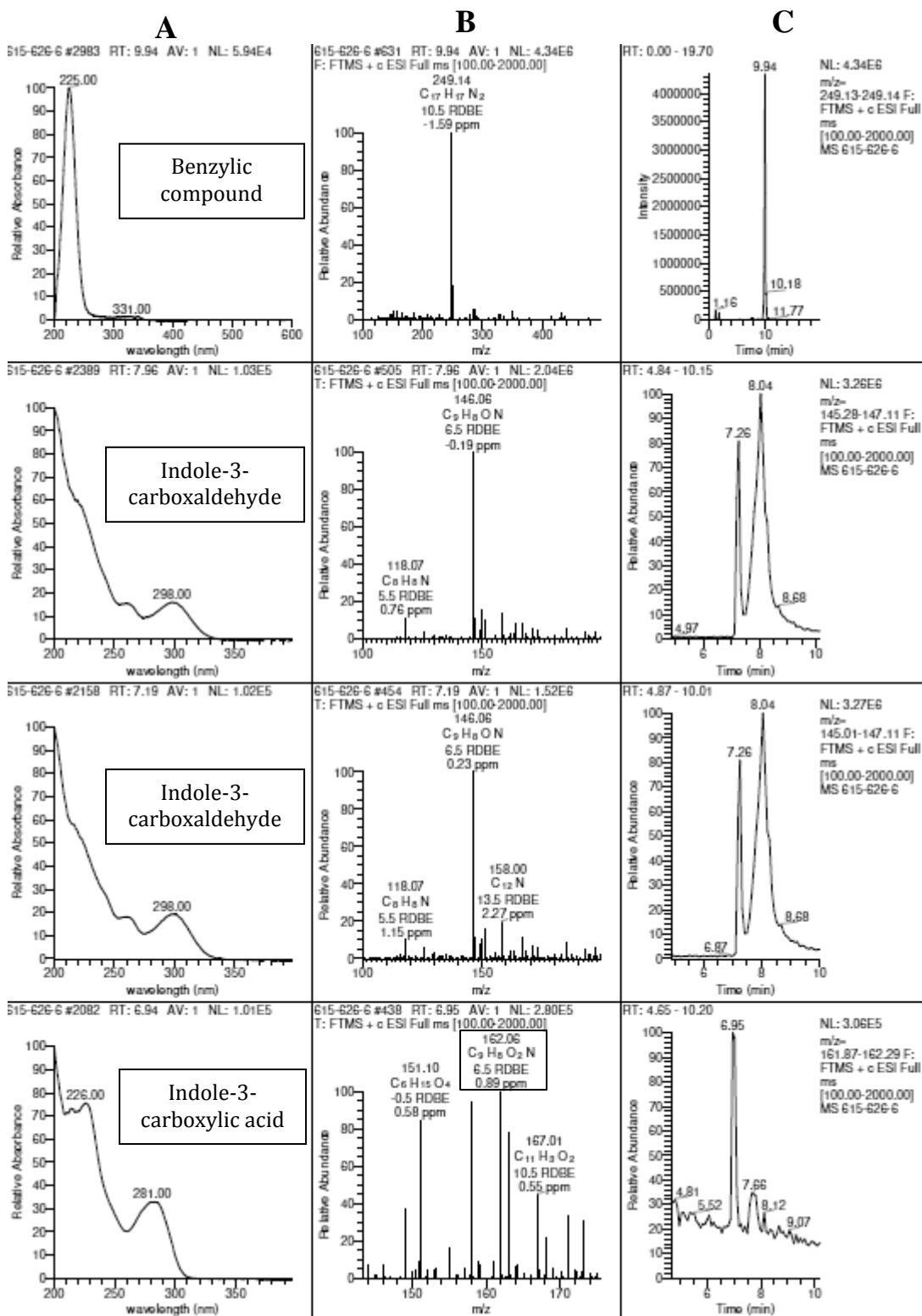
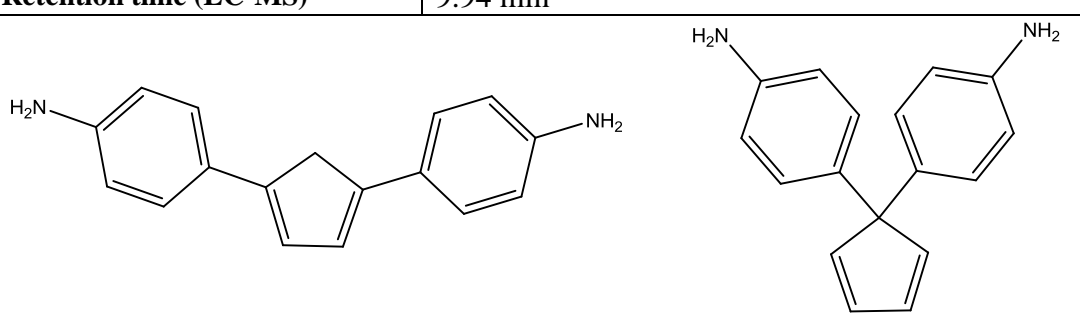
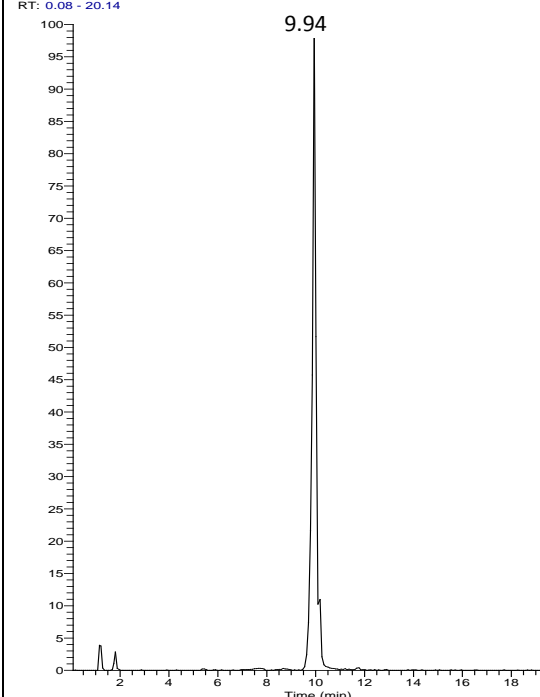
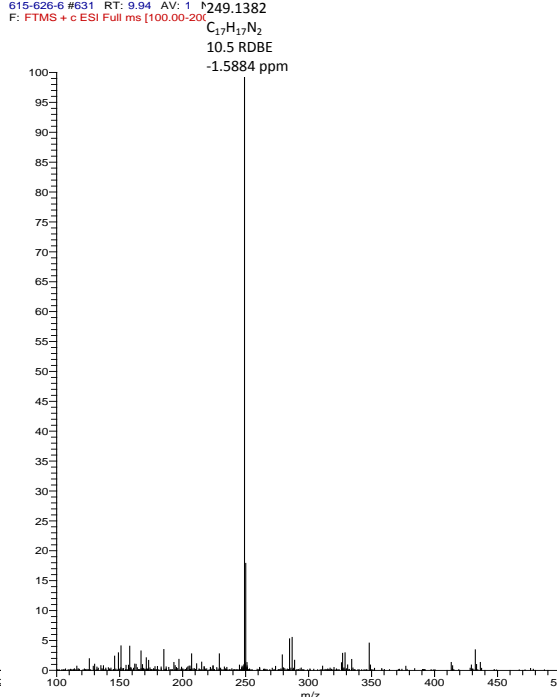


Figure 5-76: (A) PDA spectra, (B) MS spectra and (C) extracted ion chromatograms of metabolites found in EG4_615-626_6. The peak with m/z 249.138 $[M+H]^+$ had a peak at 225 nm in the PDA scan indicating that the compound is benzylic, not indolic as it would be for brasilidine A. The peaks for the indoles appear at longer wavelengths, as seen in the spectra for indole-3-carboxaldehyde and indole-3-carboxylic acid.

Table 5-34: EG4_615-626_6

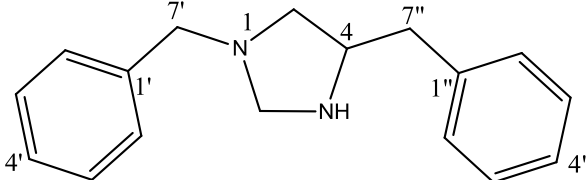
615-626_6	
Synonyms	-
Sample Code	615-626_6
Sample Amount	0.4 mg
Physical Description	Orange solid
Molecular Formula	C ₁₇ H ₁₆ N ₂
Molecular Weight	248 g/mol
R_f (TLC silica)	0.16 (90:10 CH ₂ Cl ₂ :MeOH)
Retention time (LC-MS)	9.94 min
	
<div style="display: flex; justify-content: space-around;"> 4,4'-(cyclopenta-3,5-diene-1,3-diyl)dianiline 4,4'-(cyclopenta-2,4-diene-1,1-diyl)dianiline </div>	
LC-HRFTMS Spectra [M+H]⁺:	
<div style="display: flex; justify-content: space-between;"> <div style="width: 48%;"> <p>RT: 0.08 - 20.14</p>  <p style="text-align: center;">9.94</p> </div> <div style="width: 48%;"> <p>615-626-6 #631 RT: 9.94 AV: 1 M249.1382 F: FTMS + c ESI Full ms [100.00-200]</p>  <p style="text-align: center;">249.1382 C₁₇H₁₇N₂ 10.5 RDBE -1.5884 ppm</p> </div> </div>	

5.3.6.4.4 1,4-Dibenzylimidazolidine

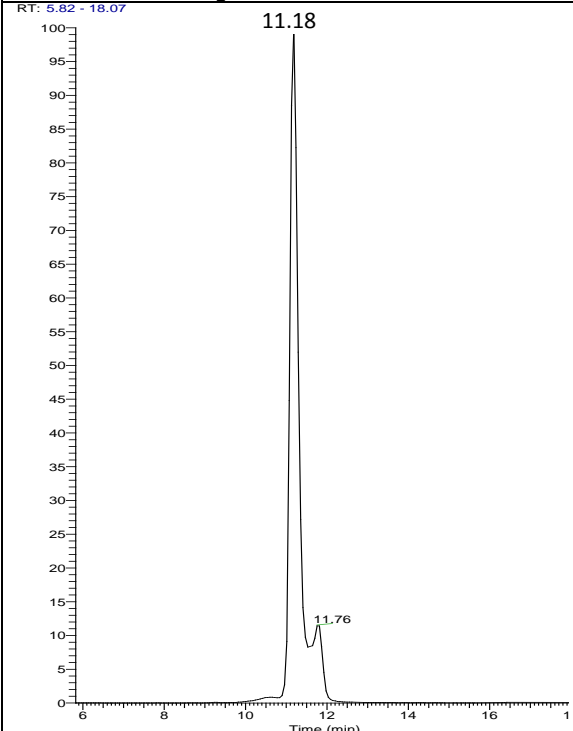
EG4_615-626_10 was the last band in the preparative TLC; therefore it contained the most polar compounds. Although it was still a mixture of compounds, NMR spectroscopy was used to elucidate the structure of the major component. The NMR data can be seen in Table 5-36 and selected NMR spectra are shown from Figure 5-77 to Figure 5-80.

Table 5-35: 1,4-Dibenzylimidazolidine

1,4-Dibenzylimidazolidine	
Synonyms	-
Sample Code	615-626_10
Sample Amount	3.4 mg
Physical Description	Orange solid
Molecular Formula	C ₁₇ H ₂₀ N ₂
Molecular Weight	252 g/mol
Retention time (LC-MS)	11.18 min



LC-HRFTMS Spectra [M+H]⁺:

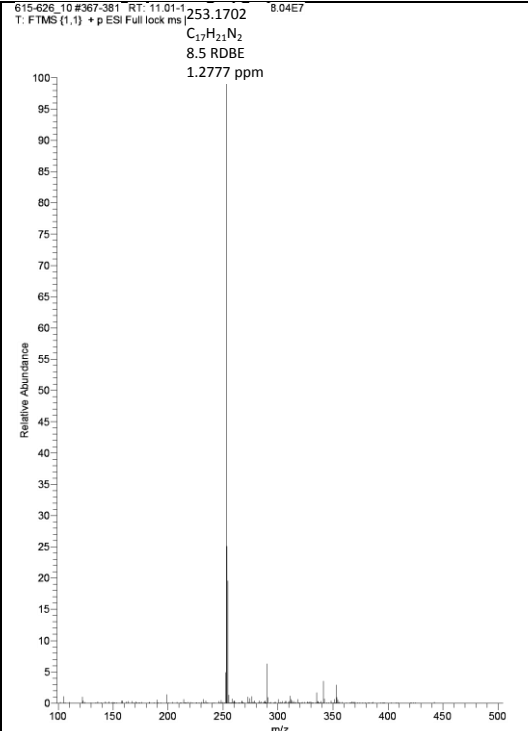


RT: 5.82 - 18.07

11.18

11.76

Time (min)



615-626_10 #367-381 RT: 11.01-11.253.1702 8.04E7

T: FTMS (1.1) + p ESI Full lock ms

C₁₇H₂₁N₂
8.5 RDBE
1.2777 ppm

Relative Abundance

m/z

Table 5-36: NMR data of EG4_615-626_10

Position	δ_C ppm	δ_H ppm	1H - 1H COSY	HMBC (1H , ^{13}C)
1', 1''-C	139.1	-	-	-
2'/6'-CH, 2''/6''-CH	127-129	7.17-7.32	Coupling within the aromatic ring	5, 7', 7''
3'/5'-CH, 3''/5''-CH				
4', 4''-CH				
7'-CH ₂ a,b	36.9	2.68-2.92	Geminal coupling	1', 2'/6', 5
7''-CH ₂ a,b	36.9			1'', 2''/6'', 5
1-N	-	-	-	
2-CH ₂		7.17-7.32	-	
3-NH	-	-		
4-CH			5	
5-CH ₂	52.5	3.38	4	

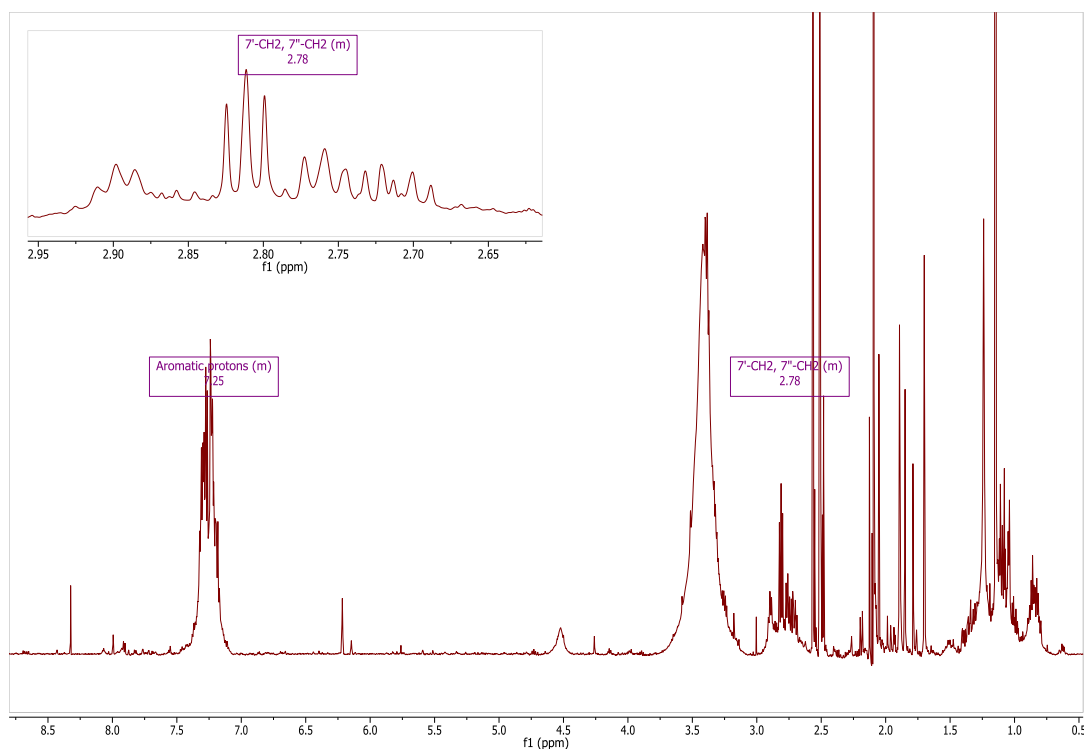


Figure 5-77: 1H NMR spectrum of EG4_615-626_10 (600 MHz, DMSO).

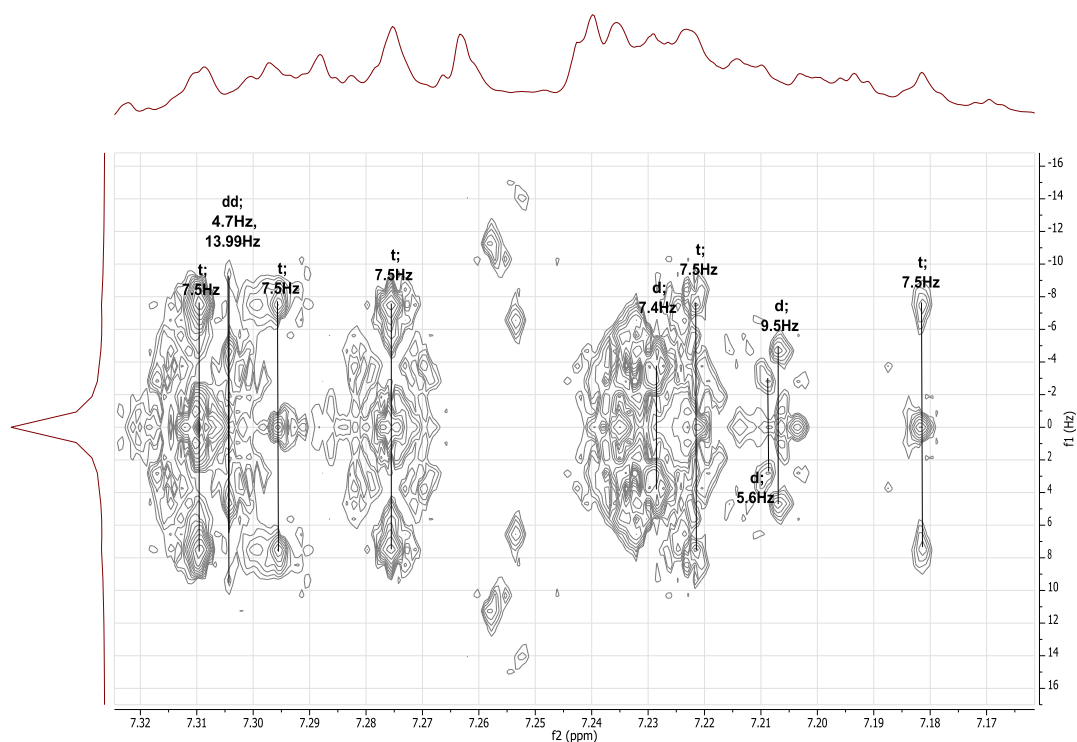


Figure 5-78: Expansion of the aromatic region of the J -resolved ^1H NMR spectrum of EG4_615-626_10 (600 MHz, DMSO). The J values approximating 7 Hz indicate the 3J (ortho) coupling in a monosubstituted benzene ring. The greater ratio of triplets to doublets attest to this.

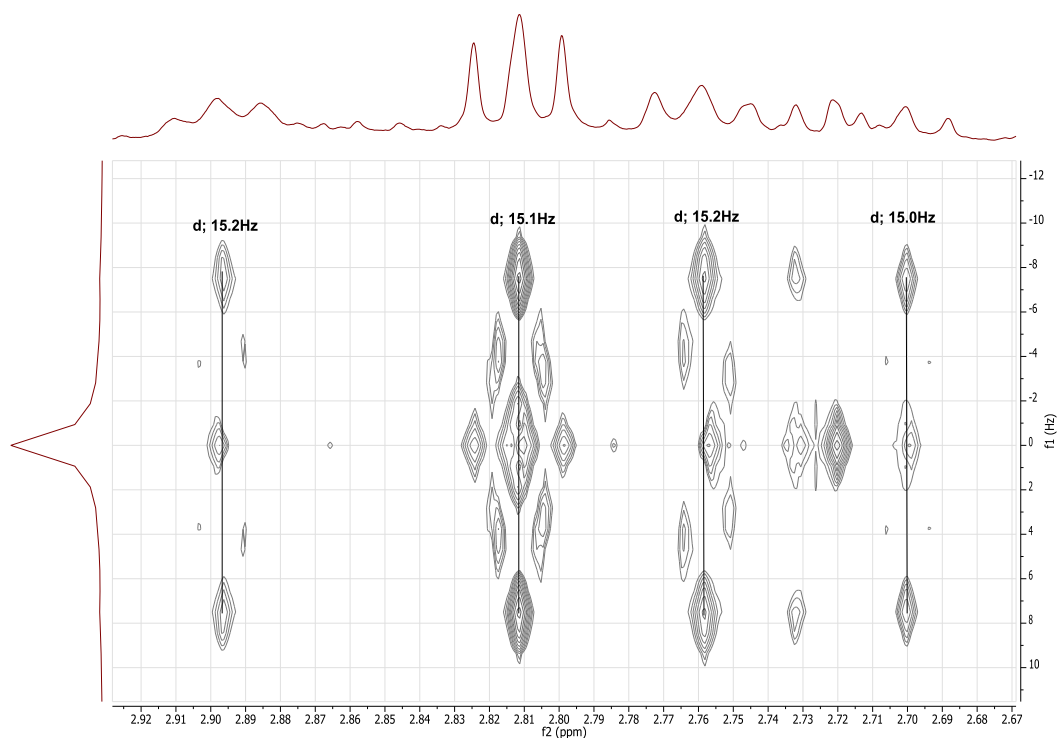


Figure 5-79: Expansion of the aliphatic region of the J -resolved of the ^1H NMR spectrum of EG4_615-626_10. The J values of the doublets indicate the geminal coupling of the 7'-CH₂ and 7''-CH₂ protons.

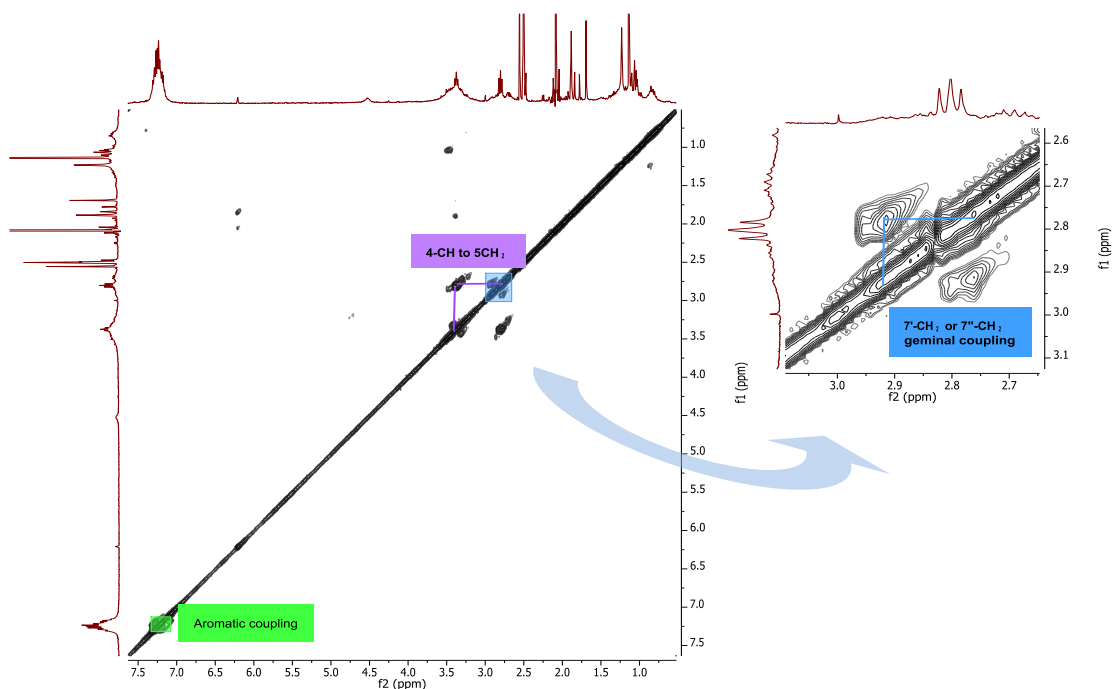


Figure 5-80: ^1H - ^1H COSY NMR spectrum of EG4_615-626_10 (400 MHz, DMSO). The full spectrum is on the left and an expansion of 2.6-3.1 ppm on the right highlights the geminal coupling of 7'-CH₂ or 7''-CH₂.

The multiplet at δ_{H} 7.17-7.32 was indicative of overlapping monosubstituted benzene rings. The *J*-resolved (Figure 5-78) showed the presence of triplets and doublets having coupling constants of approximately 7 Hz-9 Hz, characteristic of ortho coupling on monosubstituted benzene rings. Theoretically the ratio of the peaks should be 3 triplets:2 doublets for a monosubstituted benzene. The *J*-resolved did indeed show that there were more triplets than doublets. Figure 5-79 shows an expansion of the *J*-resolved of the aliphatic region. The *J*-values of approximately 15 Hz confirmed the geminal coupling that was also seen in the COSY above (Figure 5-80).

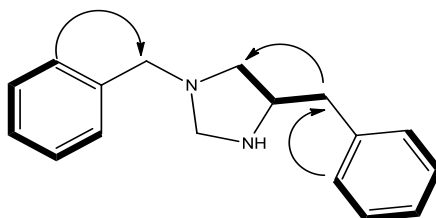
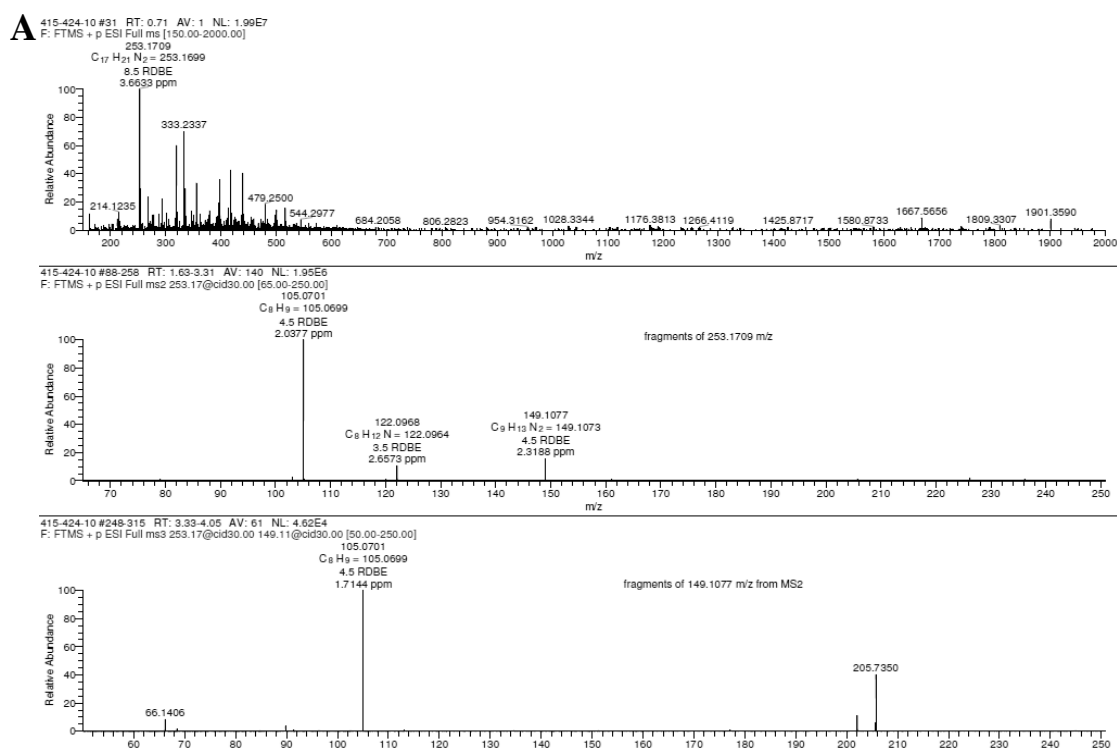


Figure 5-81: Structure of 1,4-dibenzylimidazolidine. The COSY correlations are marked by bold lines and HMBC correlations by arrows.

The LC-HRFTMS data showed a peak with m/z 253.1709 $[M+H]^+$ and a predicted formula of $C_{17}H_{21}N_2$, confirming the proposed structure. The parent ion was also fragmented, giving the following molecular ion fragments:



B

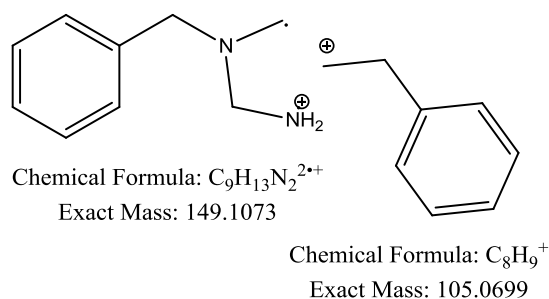


Figure 5-82: Fragmentation of m/z 253.1709 $[M+H]^+$. (A) Mass spectrum following fragmentation of the selected ion using the LTQ-Orbitrap. (B) The fragmentation of 1,4-dibenzylimidazolium to form the fragment ions seen in the spectrum.

5.3.7 Metabolic Profiling of EG4 on Variations of M1 Agar

In order to optimise the growth of EG4 and the production of bioactive compounds, EG4 was grown on M1 agar with different amounts of starch and salt and with N-acetylglucosamine (GlcNAc), a compound believed to stimulate secondary metabolite production by acting on the DasR regulatory protein (Rigali et al., 2008). The LC-MS spectra of the bacterial extracts can be seen in Figure 5-83.

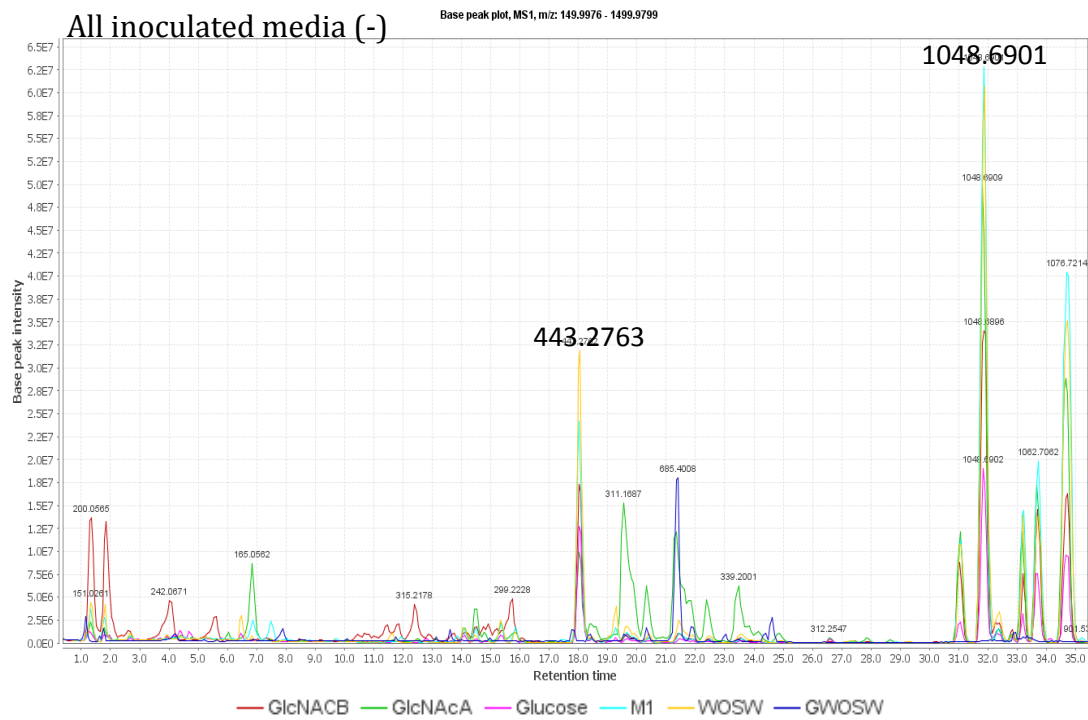
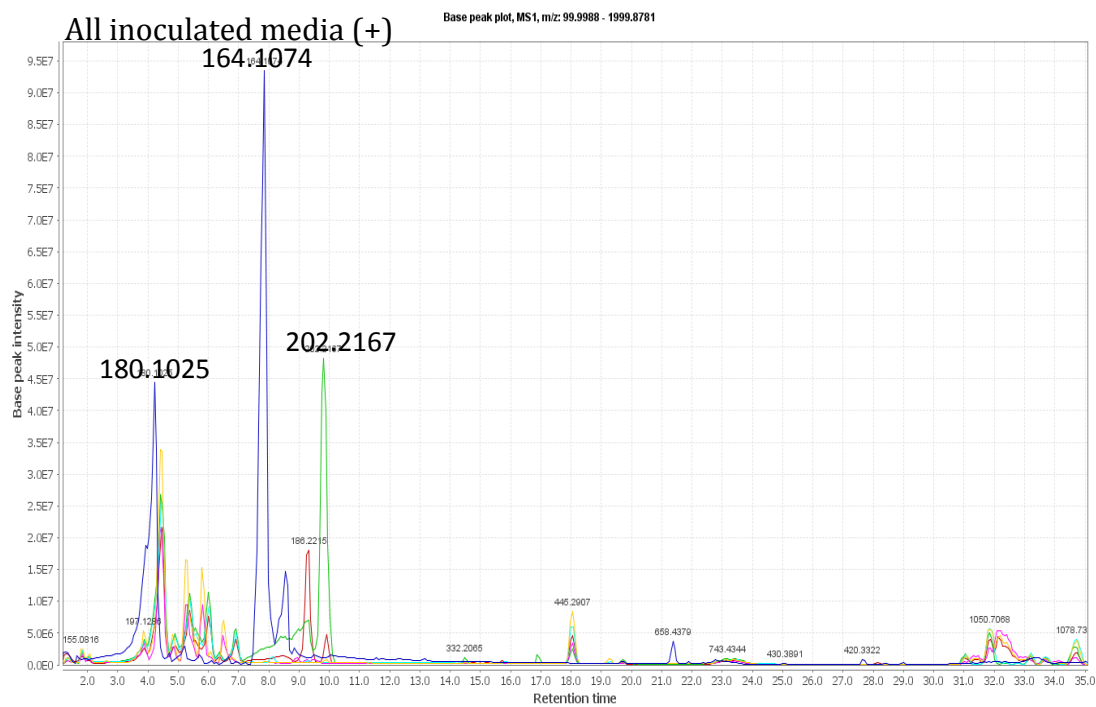


Figure 5-83: LC-HRFTMS spectra of EG4 grown on different media. GlcNACB: M1 with GlcNAC added before autoclaving (red); GlcNAC: M1 with GlcNAC added after autoclaving (green), Glucose: M1 with glucose replacing starch as the carbon source (pink); M1: control M1 (light blue), WOSW: M1 without salt (yellow), GWOSW: M1 without salt and with glucose replacing starch (dark blue). The peaks seen in the positive ionisation mode (top) were more polar and had smaller m/z values compared to the peaks seen in the negative ionisation mode (bottom). N-phenethylacetamide (m/z 164.1074 $[M+H]^+$) and N-acetyltyramine were the major compounds that were evident in the positive ionisation mode; these were most intense in the extract of EG4 grown on M1 without salt or starch. The higher molecular weight compounds detected in the negative ionisation mode that eluted after 30 minutes were putatively identified as peptides.

EG4 was grown on the following variations of M1 media: Glucose, in which glucose rather than starch is used as the carbon source, GlcNAcB and GlcNAcA, in which GlcNAc was added to the M1 medium before and after autoclaving, respectively, WOSW, which is M1 medium without the addition of salt, and GWOSW, which is M1 medium without salt and using glucose as the carbon source. The metabolites that ionised in the positive mode were more polar and eluted from the column earlier, whereas those that ionised in the negative mode eluted later and were therefore more non-polar. Moreover, peaks that eluted after 30:00 minutes in the negative mode had higher molecular weights than the more polar metabolites. A heatmap of the LC-MS results with the media peaks deleted is shown in Figure 5-84.

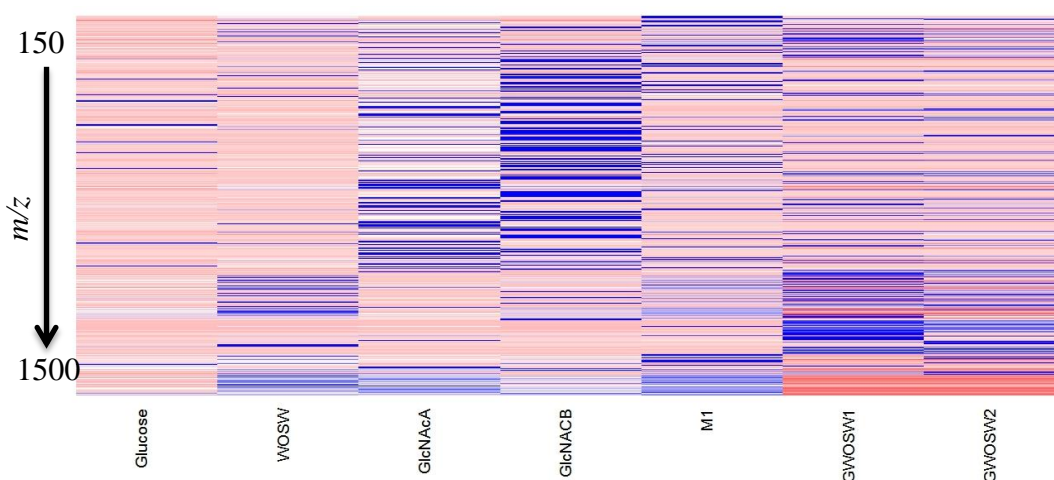


Figure 5-84: Heatmap depiction of the metabolites found in the EG4 agar extracts. Blue signifies a large peak area whereas red indicates a small peak area. The peaks are arranged in order of increasing m/z . Glucose: M1 with glucose replacing starch; WOSW: M1 without seawater; GlcNAcA and GlcNAcB: M1 with GlcNAc added after and before autoclaving, respectively; M1: control; GWOSW: M1 with glucose and without seawater. EG4 cultured on Glucose produced the least metabolites whereas EG4 cultured on GlcNAcB produced the most. EG4 cultured on GWOSW media produced higher molecular weight metabolites.

The heatmap above summarises the metabolite production of EG4 when grown on variations of M1 agar. The colours of the metabolites range from red (least intense) to blue (most intense). EG4 grown on M1 with glucose (Glucose) evidently produced the fewest metabolites whereas that grown on GlcNAcB produced the most. The exclusion of salt from the medium (WOSW) resulted in fewer metabolites than M1, particularly those with a lower m/z . EG4 grown on GWOSW appeared to produce more compounds with higher molecular weights, albeit not as high as those produced by WOSW, GlcNAcA and M1. Both GlcNAcA and GlcNAcB resulted in more low-

molecular weight metabolites than M1, but EG4 cultured on GlcNAcB yielded more, thereby proving that the autoclaving of GlcNAc does indeed have an effect on the metabolome of EG4.

GlcNAc stimulates antibiotic production in *Streptomyces* species by acting on the DasR protein (Rigali et al., 2008). A BLAST search was performed on the *M. testaceum* StLB037 genome to detect DasR homologues. The query sequence used was DasR from *S. coelicolor* A3(2) (accession number Q9K492). The best hit from the *M. testaceum* genome was a sequence for a transcriptional regulator (accession number YP_004225454) with 30% identity and an E-value of 4E-14. The alignment can be seen in Appendix VII. Although the similarity is not high, it is nevertheless possible that EG4 contains a repressor protein similar to DasR that is acted upon by GlcNAc.

The m/z ratios of the compounds isolated from the EG4 were searched for to determine whether the changes in conditions affected the production of these metabolites.

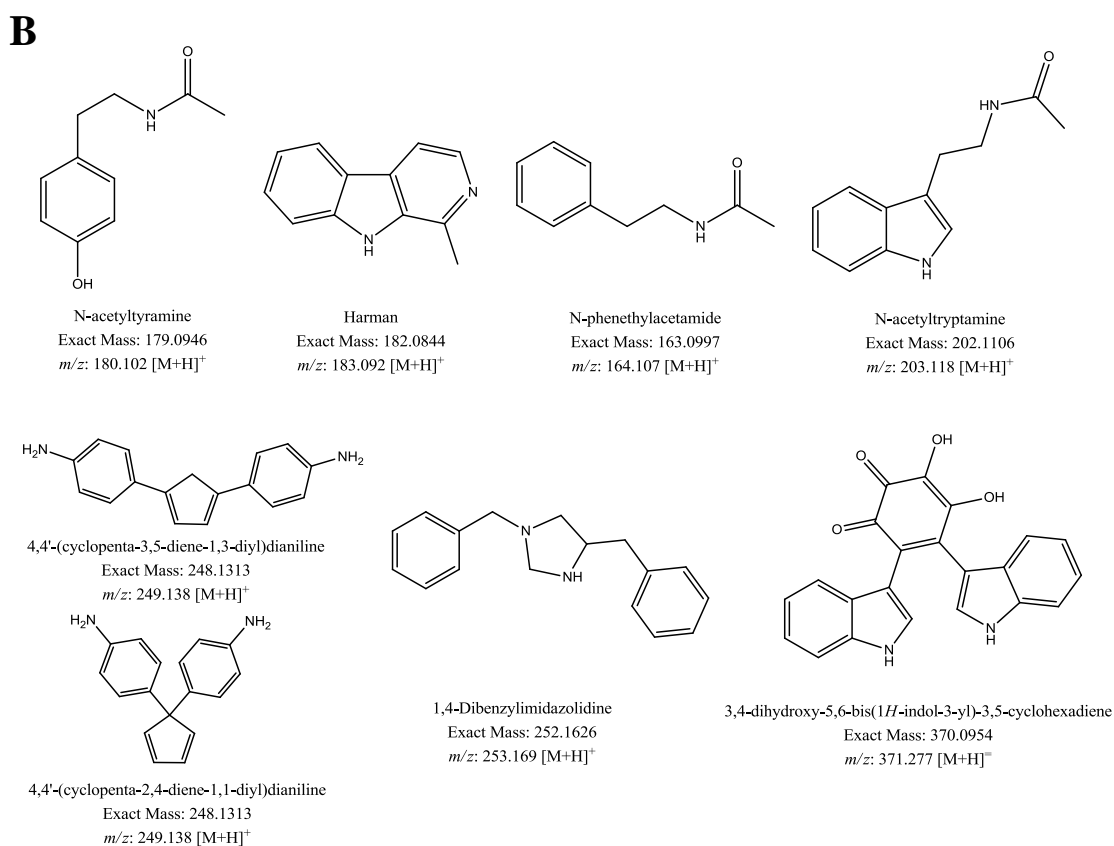
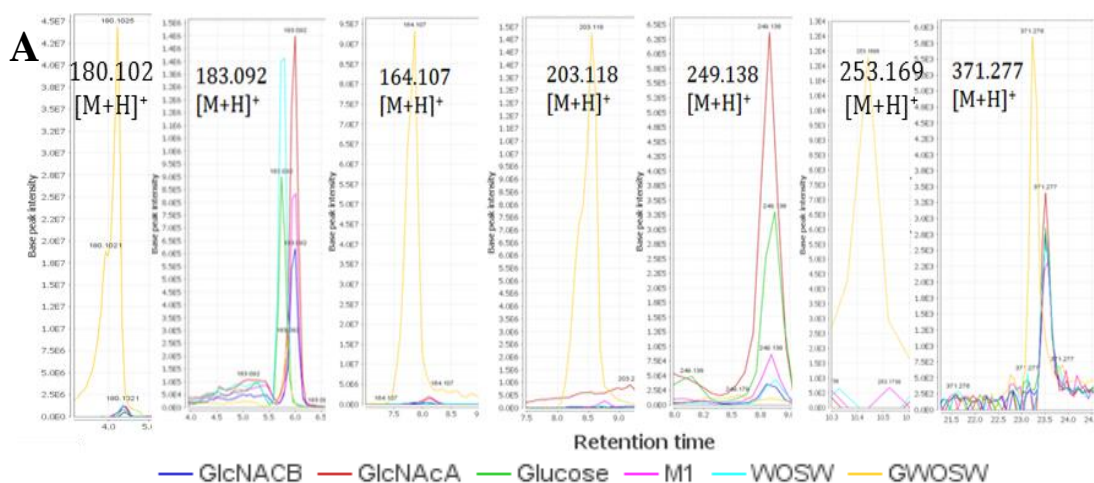


Figure 5-85: (A) Extracted ion chromatogram and (B) structures of the compounds isolated from EG4. GlcNACB: M1 with GlcNAc added before autoclaving (dark blue); GlcNAcA: M1 with GlcNAc added after autoclaving (red), Glucose: M1 with glucose replacing starch as the carbon source (green); M1: control M1 (pink), WOSW: M1 without salt (light blue), GWOSW: M1 without salt and with glucose replacing starch (yellow).

Harman (m/z 183.0915 $[M+H]^+$) was found to be present in all of the blank media. The peak for this compound appeared consistently more intense in all blank media types than in the inoculated extracts. It is therefore likely that harman was metabolised by the bacteria during growth. The bis-indole (m/z 371.277 $[M+H]^+$) also appeared in the blank but at approximately the same intensity as the samples. N-phenethylacetamide (m/z 164.107 $[M+H]^+$) was present in greatest quantity in the GWOSW bacterial extracts. This appeared to be the major metabolite being produced by the bacteria. As determined by the assay, this compound was inactive against *T. b. brucei* and *M. marinum*. N-Acetyltyramine (m/z 180.120 $[M+H]^+$) and N-acetyltryptamine (m/z 203.118 $[M+H]^+$) were also present in greatest quantities in the bacterial extracts of GWOSW, although the former was also found in lower quantities in the blank agar. The dianiline compound with m/z 249.138 $[M+H]^+$ was not found in any of the blank media and was most intense in the GlcNAcA extracts. The GWOSW media resulted in the least amount of this compound. 1,4-Dibenzylimidazolidine with m/z 253.1699 $[M+H]^+$ was present in low intensities in GWOSW but not in the other samples. It is possible that this compound is produced in greater quantities by EG4 that is cultured in broth as compared to agar.

Figure 5-86 shows the ^1H NMR spectra of the extracts and the M1 blank to determine the peaks that resulted from bacterial growth. The GlcNAcB extract appeared to have the greatest number of peaks but in reality these belonged to the medium, as evidenced in Figure 5-87. There were more peaks in both the media and the extract when GlcNAc was added before autoclaving (GlcNAcB). This indicated that the GlcNAc was not stable in the high pressure and temperature required for autoclaving.

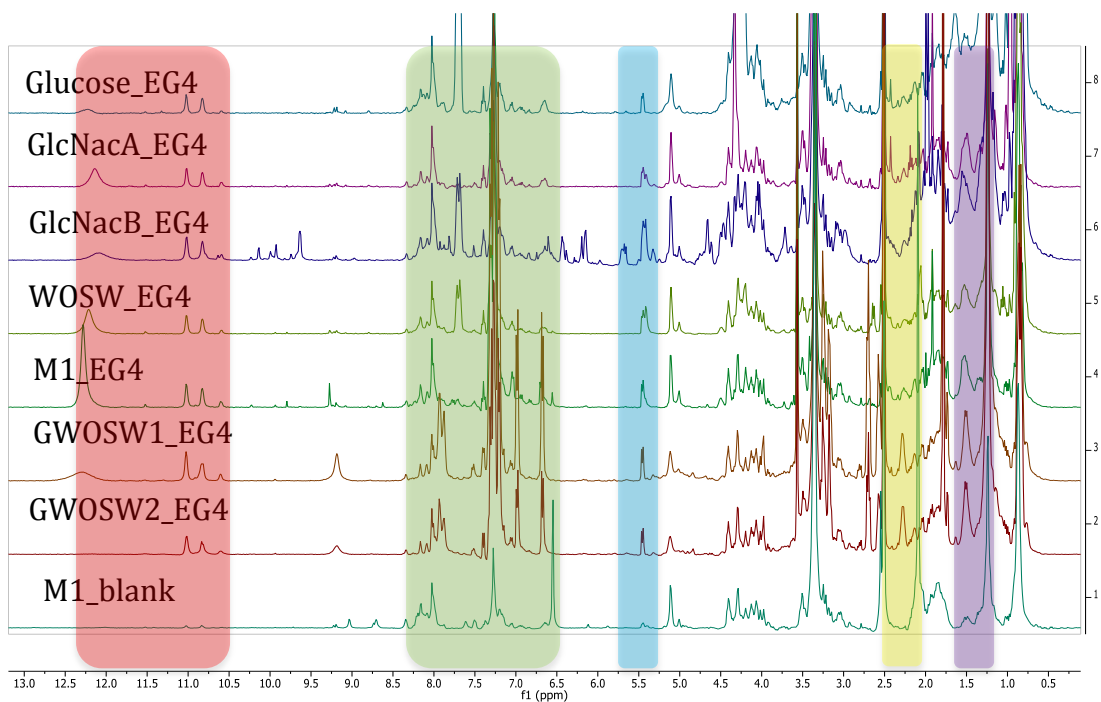


Figure 5-86: ^1H NMR spectra of EG4 M1 agar extracts (400 MHz, DMSO). Glucose: M1 with glucose replacing starch; GlcNacA and GlcNacB: M1 with GlcNac added after and before autoclaving, respectively; WOSW: M1 without seawater; M1: control; GWOSW: M1 with glucose and without seawater; M1_blank: uninoculated M1 agar. Areas where peaks are present in the bacterial samples but not in the blank media are highlighted. The spectrum of EG4 cultured on GlcNacB had the most peaks but many of these belonged to the blank GlcNacB medium.

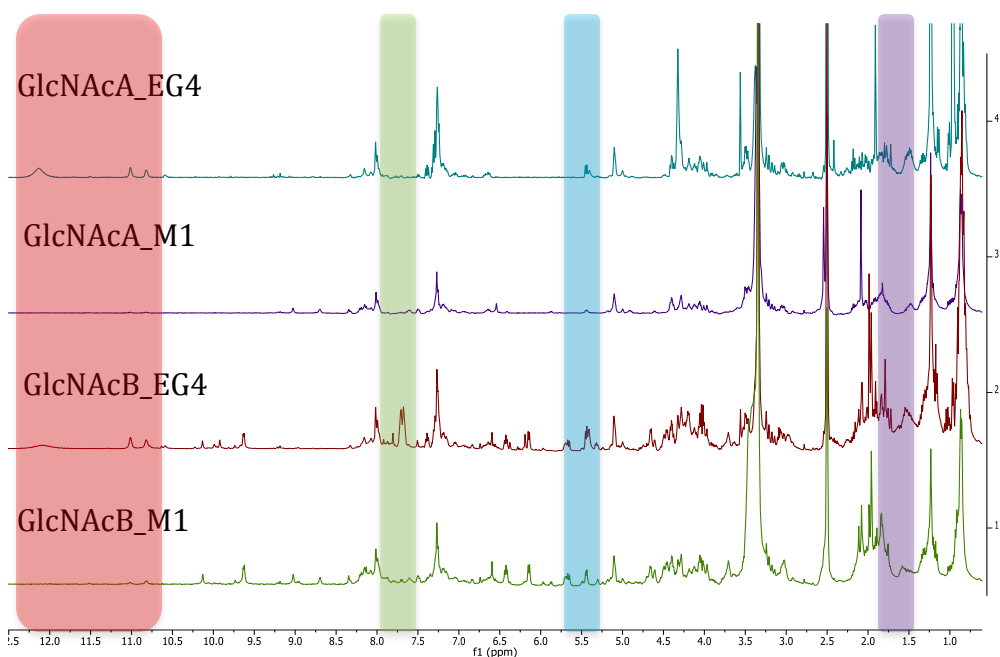


Figure 5-87: ^1H NMR spectra comparing GlcNacA and GlcNacB with their respective media blanks (400 MHz, DMSO). GlcNacA and GlcNacB: M1 with GlcNac added after and before autoclaving, respectively. Samples suffixed with ‘_EG4’ indicate bacterial cultures whereas those with ‘_M1’ are uninoculated media blanks. Areas where there are differences between the blank agar and the inoculated agar extracts are highlighted.

Table 5-37: Yields and activities of agar and bacterial extracts comparing different types of M1 media. Glucose: M1 with glucose replacing starch; GlcNAcA and GlcNAcB: M1 with GlcNAc added after and before autoclaving, respectively; WOSW: M1 without seawater; M1: control; GWOSW: M1 with glucose and without seawater. Samples suffixed with ‘_M1’ are uninoculated media blanks; samples suffixed with ‘_EG4’ are bacterial extracts. Highlighted cells indicate activity. (Activity=>50% inhibition)

Sample	Yield (mg)	%Inhibition of <i>T. b. brucei</i> (20µg/mL)	%Inhibition of <i>M. marinum</i> (100µg/mL)
Glucose_M1	4.6	0	11.55
Glucose_EG4	15.2	90.25	21.25
GlcNAcA_M1	3.3	10.3	0
GlcNAcA_EG4	8.6	64.25	76.85
GlcNAcB_M1	4.9	0	0
GlcNAcB_EG4	12.6	37.05	35.6
WOSW_M1	3.0	0	0
WOSW_EG4	10.7	111.85	69.5
M1_M1	4.4	0	0
M1_EG4	12.1	48.7	70.05
GWOSW_M1	6.3	6.5	7.5
GWOSW_EG4 (1)	11.9	10.5	0
GWOSW_EG4 (2)	11.1	13.6	0

The extract from the bacteria grown on M1 media without starch and seawater (GWOSW) had the least activity against *T. b. brucei* and *M. marinum*. However, growing EG4 on media in which starch was replaced by glucose (Glucose) or in which seawater was excluded entirely (WOSW) resulted in increased activity against *T. b. brucei* compared to the M1 control. Activity against *M. marinum* was unaffected in WOSW but was reduced in Glucose. The addition of N-acetylglucosamine to M1 before autoclaving (GlcNAc_B) resulted in decreased activity against both microorganisms, despite EG4 producing the greatest number of metabolites in this media (Figure 5-84), whereas addition of GlcNAc after autoclaving (GlcNAc_A) led to increased anti-trypanosomal activity and mildly increased anti-mycobacterium activity. The %inhibition of the extract from GlcNAc_B medium was approximately half that of GlcNAc_A for both organisms.

Multivariate analysis was performed on these samples to detect differences between the bacteria grown under varying media conditions. PCA and OPLS-DA were used to compare the extracts and the media, as well as the extracts with the media peaks deleted.

5.3.7.1 PCA of EG4 and M1 Agar Extracts

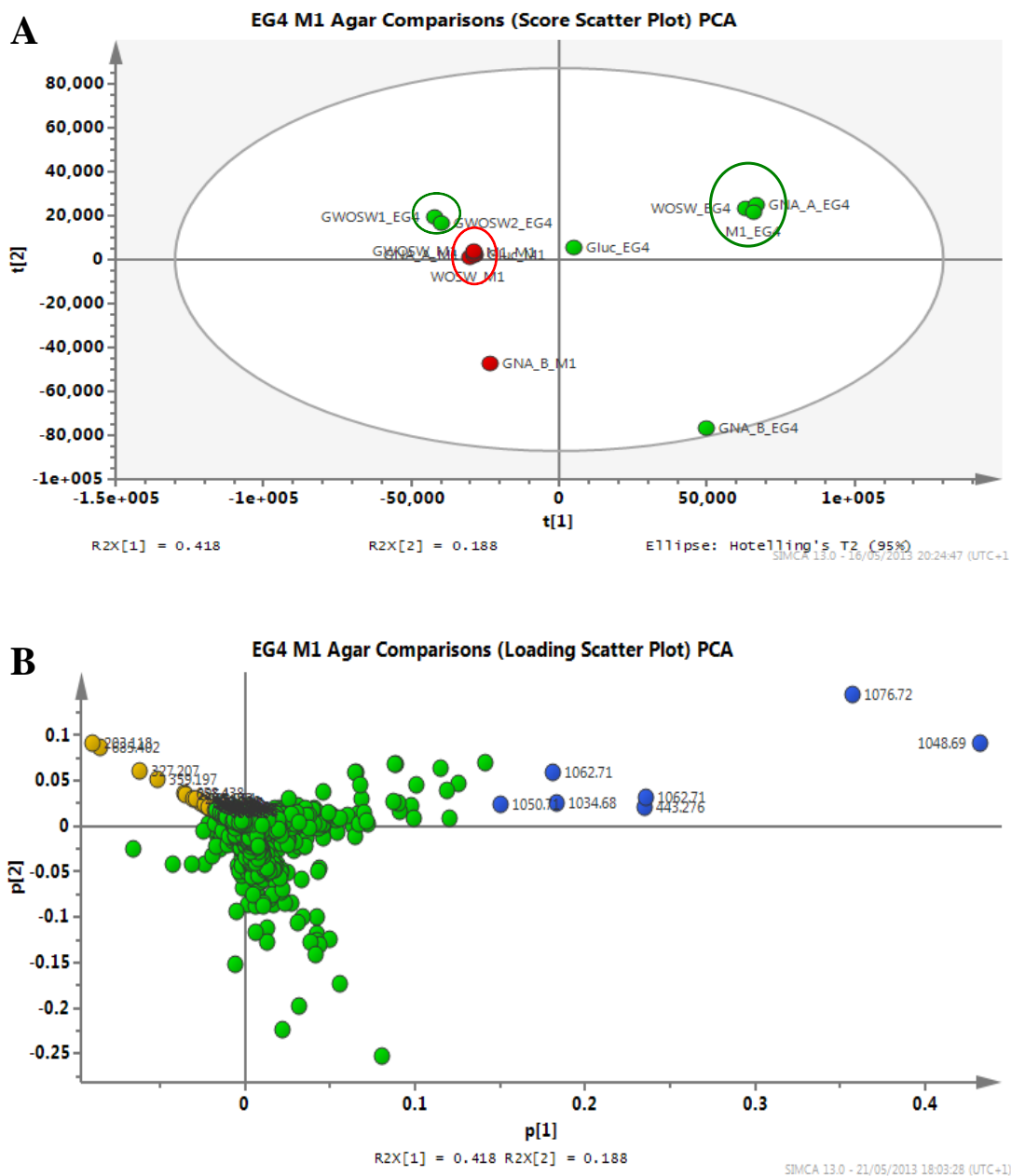


Figure 5-88: (A) PCA score scatter plot and (B) loading scatter plot of EG4 and M1 agar extracts. Gluc: M1 with glucose replacing starch; GNA_A and GNA_B: M1 with GlcNAc added after and before autoclaving, respectively; WOSW: M1 without seawater; M1: control; GWOSW: M1 with glucose and without seawater. Samples suffixed with ‘_M1’ are uninoculated media blanks; samples suffixed with ‘_EG4’ are bacterial extracts. The score scatter plot shows three clusters: M1_EG4, GNA_A_EG4, and WOSW_EG4 clustered together in the upper right quadrant, the two GWOSW_EG4 extracts clustered together in the upper left quadrant, and the blank M1 media variations (red) clustered together near the GWOSW cluster. The loading scatter plot shows the distribution of the metabolites among all the samples. Metabolites found in high levels in the EG4 extracts are labelled with their m/z values. Those in orange are more intense in GWOSW extracts and those in blue are more intense in WOSW, M1 and GNA_A extracts. $R^2X(\text{cum})= 0.606$, $Q2(\text{cum})= 0.239$

Although PCA is an unsupervised method of multivariate analysis, some clusters were clearly evident in the scores plot. GWOSW1 and GWOSW2, cultures of EG4 on M1 without salt and with starch instead of glucose, were both inactive and clustered closer to the media extracts. The metabolites produced by these cultures were indeed different from those of cultures on other media, as seen in the loadings plot above and the heatmap in Figure 5-84. The EG4 grown on M1 in which starch was replaced with glucose (Glucose) also produced fewer metabolites compared to those grown on normal M1 medium, WOSW and GlcNAc_A. This could be because glucose is a monosaccharide whereas starch is a polysaccharide; glucose as a carbon source is more readily available thus the bacteria may have produced fewer secondary metabolites as EG4 was not 'starved'. The higher molecular weight compounds found in the M1, WOSW and GlcNAc_A extracts (coloured in blue in the loadings plot) were most likely peptides, putatively identified by the AntiMarin database as derivatives of pumilacidin. Both the GlcNAc_B medium blank and inoculated GlcNAc_B were separated from the other samples. This suggested that N-acetylglucosamine degraded upon autoclaving and hence caused differences in the medium, resulting in different peaks in the LCMS and a different metabolic profile for the bacteria grown on that agar. This was further confirmed in the dendrogram produced upon analysis of the model with hierarchical clustering (Figure 5-89). The media clustered together and were also closely related to the GWOSW bacterial extracts, showing that these samples did not differ greatly from the media and therefore indicating that EG4 produced fewer metabolites when grown with glucose and without salt. This was also evident in the heatmap after the media peaks were deleted (Figure 5-84); GWOSW1 and 2 produced fewer metabolites than M1, GlcNAcA and GlcNAcB, but they appeared to produce more than Glucose and WOSW. The Glucose_EG4 extract also clustered together with the media in the dendrogram. The GlcNAc_B M1 and EG4 extracts clustered with the media and bacterial extracts, respectively but evidently had some differences compared to the other samples.

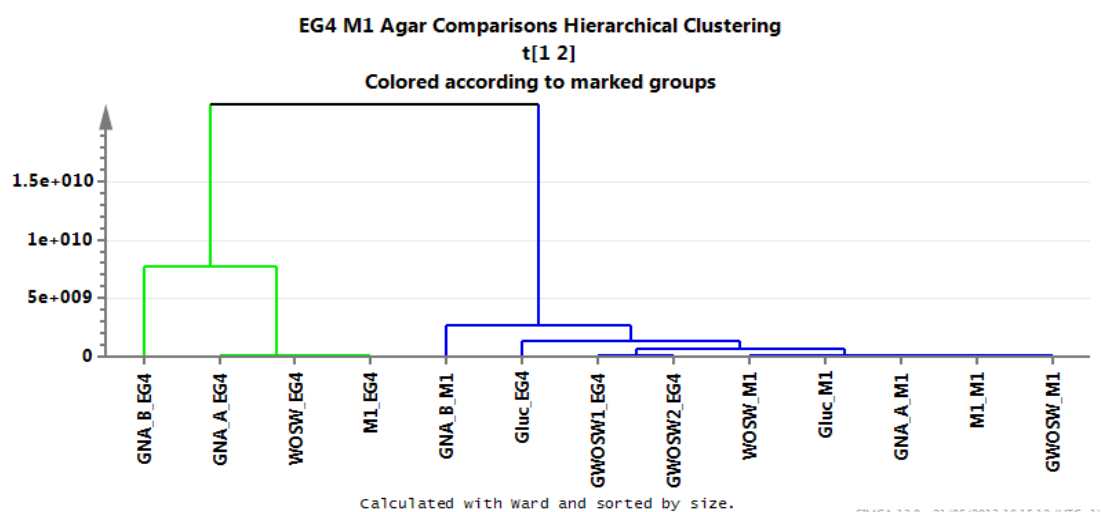


Figure 5-89: Dendrogram showing hierarchical clustering of EG4 M1 extracts. Bacterial extracts have the suffix ‘_EG4’ whereas media extracts are suffixed with ‘_M1’. GNA_B: GlcNAc was added before autoclaving; GNA_A: GlcNAc was added after autoclaving; WOSW: M1 media without seawater; Gluc: glucose is the carbon source; GWOSW: M1 containing glucose instead of starch and without seawater. Gluc_EG4 and the two GWOSW_EG4 extracts clustered with the blank media extracts as the bacteria did not produce many metabolites.

Derivatives of pumilacidin and surfactin were, as previously mentioned, putatively identified in the WOSW, M1 and GlcNAcA extracts (marked in blue in the loading plot in Figure 5-88). Surfactin and pumilacidin belong to the surfactin family of lipopeptide biosurfactants (LPBS). The biosynthetic gene cluster of surfactin is *srfA*. It encodes for SrfA-A, SrfA-B, and SrfA-C, which are NRPSs, and SrfA-Te, which is a type II thioesterase (Te) (Roongsawang et al., 2011). A BLAST search was conducted to find proteins in the *M. testaceum* StLB037 genome that were homologous to SrfA-A to -C (Table 5-38). The alignments of these sequences can be found in Appendix VIII.

Table 5-38: Homology results of surfactin biosynthetic clusters in the *M. testaceum* StLB037 genome

Protein	Accession number	<i>M. testaceum</i> StLB037 protein accession number	Identity	E-value
SrfAA	AGG59691	YP_004225560	31%	4E-62
SrfAB	AGG59692	YP_004225560	33%	2E-63
SrfAc	AGG59694	YP_004225560	32%	1E-54

One NRPS module gave the best alignment with all three SrfA synthetases. The identity similarity was not very high; however, it is still possible that EG4 is capable of producing LPBSs. As the identities of the peptides were not definitively determined, it may be that the LPBSs produced by EG4 belong to a different family and thus require other synthetases.

5.3.7.2 PCA of EG4 Extracts After Exclusion of Media Peaks

The analysis was repeated to compare the metabolic profiles of EG4 without including the media in the analysis. During pre-processing of the data with MZmine 2.10, the samples were all aligned together and media peaks deleted. The blanks were then deleted and the positive and negative modes combined using a macro on Microsoft Excel. Pre-processing of the data was also attempted in which each extract was aligned with its specific medium and the media peaks deleted, after which all extracts were aligned. However, the alignment was not as good and many peaks were repeated between samples, hence the former approach was used. The data were then analysed using SIMCA 13.0. The PCA results can be seen in Figure 5-90.

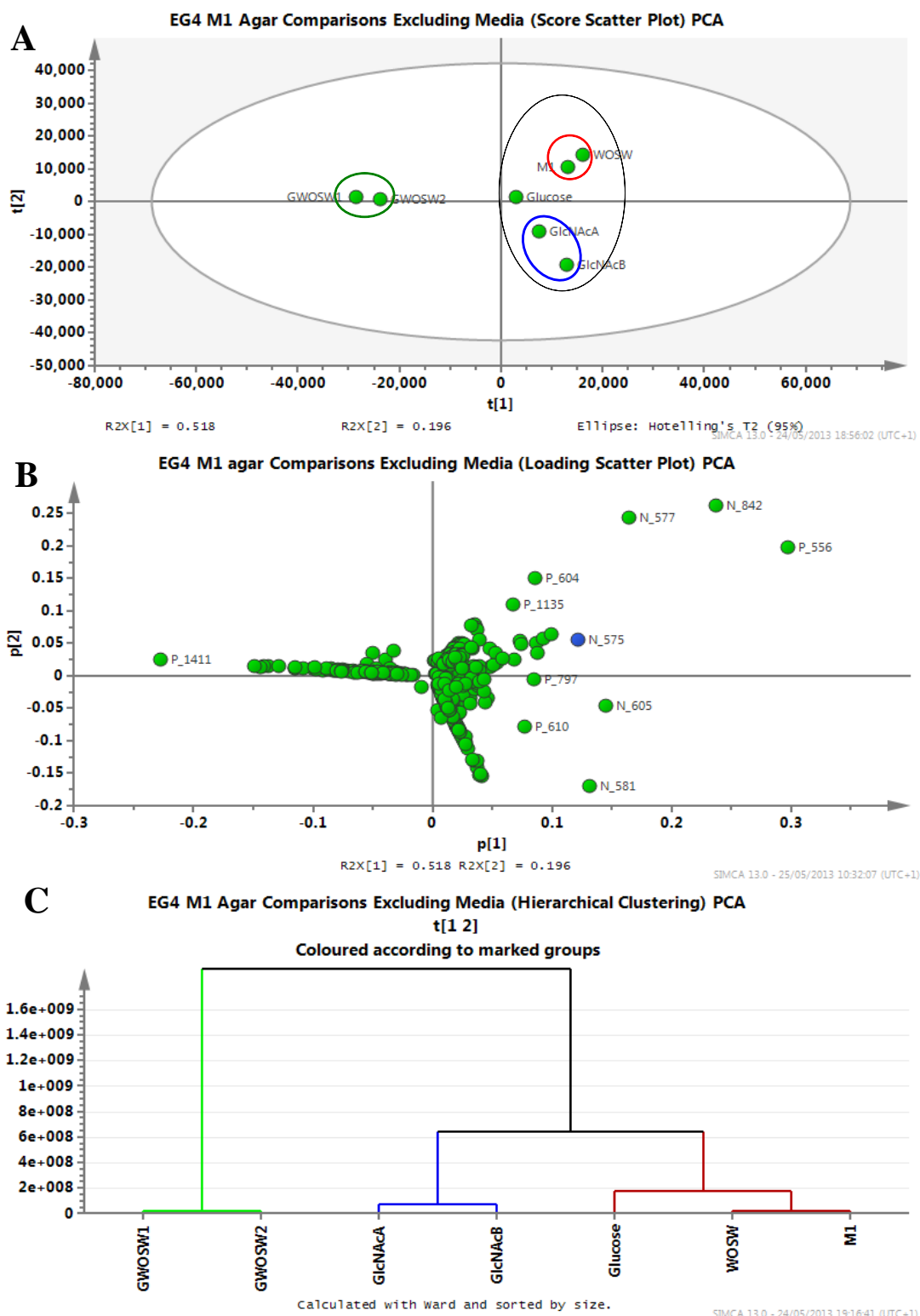


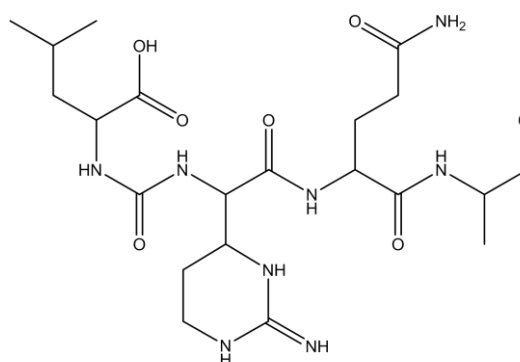
Figure 5-90: (A) Score scatter plot, (B) loading scatter plot, and (C) dendrogram following PCA of EG4 extracts after removal of media peaks. GlcNAcB: GlcNAc added before autoclaving; GlcNAcA: GlcNAc added after autoclaving; WOSW: M1 without seawater; Glucose: glucose as the carbon source; GWOSW: M1 containing glucose instead of starch and without seawater. Isolated variables that were more prominent in certain samples and thereby contributed more to the separation in the score plot are labelled with the primary IDs in the loading scatter plot. Only N_575, highlighted in blue, was identified using the AntiMarin 2012 database. R2X(cum)= 0.714, Q2(cum)= 0.334

The largest difference in the score scatter plot was seen between the clusters of the GWOSW samples, in which the media contained glucose instead of starch and did not contain salt, and the other M1 samples, that is, M1, WOSW, GlcNAc_A and GlcNAc_B. As determined in the previous analyses where the media were included, EG4 grown on GWOSW M1 produced different metabolites and therefore clustered separately from the other extracts. In the second rather loose cluster of the other extracts (encircled in black), two smaller clusters were seen: M1 and WOSW (M1 without salt) (encircled in red), and GlcNAc_A and GlcNAc_B (M1 with GlcNAc added after and before autoclaving, respectively) (encircled in blue). This was confirmed by the dendrogram which showed the hierarchical clustering.

The loading scatter plot shows the distribution of the metabolites among the samples. The variables that are towards the edges of the cluster occurred in greater intensities in certain samples and therefore contributed to the distribution of the samples in the score plot. These variables have been labelled with their primary ID and their distribution among the samples can be seen in Table 5-39. The cells of the table are coloured in the form of a heatmap to make it easier to compare the intensities of the metabolites. Primary IDs beginning with P ionised in the positive mode and those beginning with N ionised in the negative mode. Out of the listed metabolites, only one, N_575, was putatively identified by the AntiMarin2012 database. This compound was identified as elastatinal, a product of *S. griseoruber* (Umezawa et al., 1973) (Figure 5-91).

Table 5-39: Selected metabolites from the loading scatter plot of EG4 M1 agar comparison excluding media peaks. Glucose: M1 with glucose replacing starch; WOSW: M1 without seawater; GlcNAcA and GlcNAcB: M1 with GlcNAc added after and before autoclaving, respectively; M1: control; GWOSW: M1 with glucose and without seawater. The peak areas correspond to the colours in order of increasing intensity from yellow to red; red cells have the largest peak areas. The metabolite in blue has been identified as elastatinal.

ID	m/z	RT	Glucose	WOSW	GlcNAcA	GlcNAcB	M1	GWOSW1	GWOSW2
P_1411	225.0998	8.71	5.89E4	8.81E4	0	7.53E3	3.78E5	4.19E7	3.47E7
P_610	332.2065	14.54	1.96E6	3.59E6	1.38E7	7.03E6	6.90E6	0	0
N_581	330.1923	14.50	5.49E6	1.05E7	5.05E7	2.41E7	2.00E7	0	0
P_797	346.2223	15.74	1.31E6	5.33E6	5.25E6	6.16E6	7.60E6	6.75E2	8.24E2
N_605	344.2080	15.82	2.95E6	1.46E7	1.66E7	2.07E7	2.16E7	0	0
P_556	445.2909	18.05	4.09E7	1.03E8	3.09E7	5.82E7	7.76E7	0	0
P_1135	459.3062	19.43	2.16E6	9.88E6	5.90E5	1.68E6	5.26E6	0	0
P_604	459.3063	19.34	3.67E6	1.62E7	7.76E5	2.29E6	9.60E6	0	0
N_577	457.2921	19.38	9.65E6	5.62E7	6.94E6	1.11E7	2.89E7	0	0
N_575	511.2634	18.03	7.95E6	1.48E7	5.44E6	1.05E7	1.26E7	0	0
N_842	887.5589	18.03	1.91E7	9.24E7	1.32E7	3.35E7	5.68E7	0	0



Chemical Formula: $C_{21}H_{36}N_8O_7$
Exact Mass: 512.2707

Figure 5-91: Structure of elastatinal. Elastatinal was putatively identified as the metabolite with an m/z of 511.2634 [M-H]⁻. It was found in greatest quantities in the WOSW extract.

5.3.7.3 OPLS-DA of EG4 Extracts Classified According to Anti-trypanosomal Activity

OPLS-DA was performed on the bacterial extracts. The classes were set as active versus inactive against *T. b. brucei* based on the assay results in Table 5-37. Extracts that had a %inhibition of greater than 50% were considered to be active. The OPLS-DA results for *T. b. brucei* inhibition and *M. marinum* inhibition are presented in Figure 5-92 and Figure 5-96 respectively.

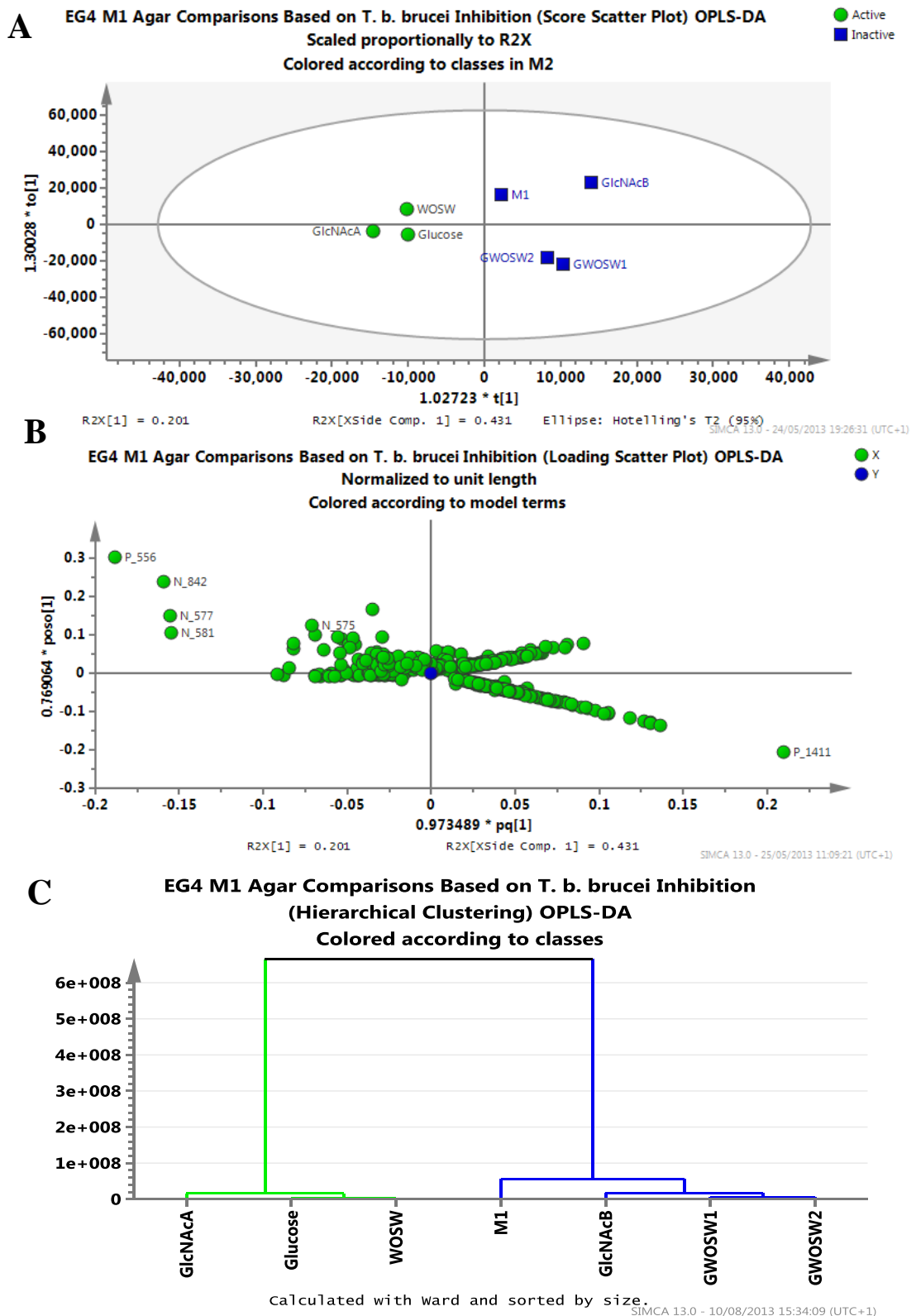


Figure 5-92: (A) Score scatter plot, (B) loading scatter plot, and (C) dendrogram of EG4 extracts after OPLS-DA based on *T. b. brucei* inhibitory activity. GlcNAcA: GlcNAc added after autoclaving; Glucose: glucose replaced starch as a carbon source; WOSW: M1 without salt added; GlcNAcB: GlcNAc added before autoclaving; GWOSW: M1 containing glucose instead of starch and without salt. $R2X(cum) = 0.632$, $R2Y(cum) = 0.89$, $Q2(cum) = 0.0617$.

Although the $R^2(\text{cum})$ values were at 0.632 and 0.89, the $Q^2(\text{cum})$ score for the OPLS-DA model was less than 0.1. This meant that the ability of the model to predict *T. b. brucei* inhibitory activity was not good. This was possibly because the EG4_M1 extract had an inhibitory activity of 48.7% compared to the control, and therefore could be considered as moderately active. In addition, having more samples or a greater number of replicates would also increase the predictability of the model. The dendrogram, also shown in Figure 5-92, placed the M1 EG4 extract as quite distant from the other inactive samples. This suggested that the extract contained low amounts of the anti-trypanosomal compounds; the production of these compounds was perhaps increased in GlcNAc_A, Glucose and WOSW.

The S-plot below (Figure 5-93) gives a clearer image of the contribution of each variable to the separation seen in the score plot. Variables at the ends of the S-curve have greater intensities in the relevant samples; that is, the coordinates in the S-plot match those of the score plot, therefore the variables in the left half of the S-plot are more strongly correlated with the active extracts (GlcNAc_A, Glucose and WOSW) and those on the right half of the S-plot are more strongly correlated with the inactive extracts (M1, GlcNAc_B, GWOSW1 and 2).

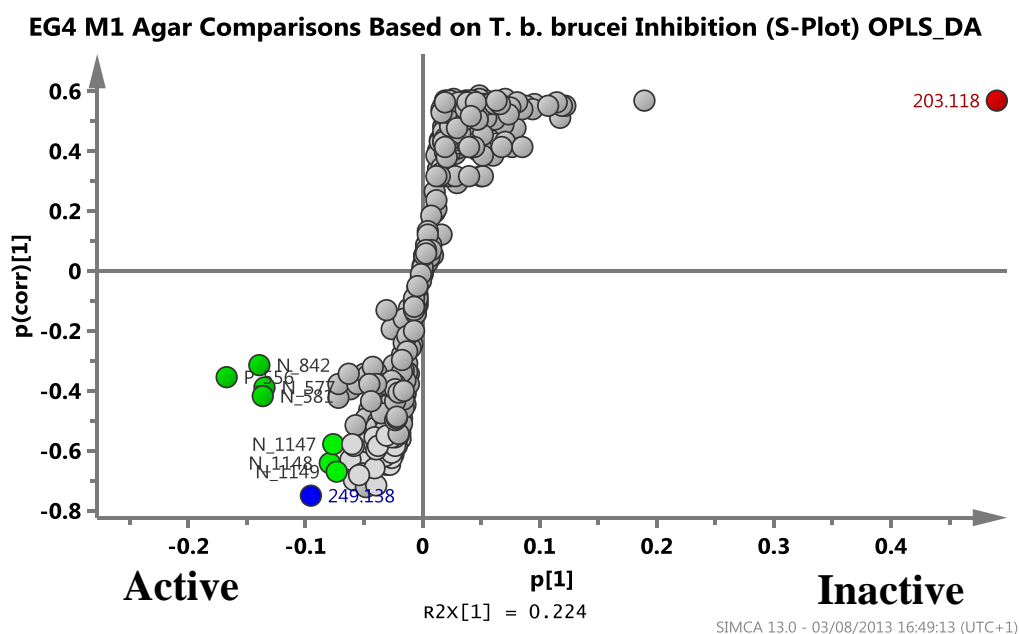


Figure 5-93: S-plot of the OPLS-DA model comparing EG4 extracts based on *T. b. brucei* inhibitory activity. The peaks in the lower left quadrant represent metabolites that are present in greater quantities in the active fractions and hence may be contributing to anti-trypanosomal activity.

The variable in red on the right side has an m/z of 203.118 $[M+H]^+$. This is N-acetyltryptamine. Although N-acetyltryptamine was identified in the Glucose, WOSW and M1 extracts, the fact that it was present in greater quantities in the inactive extracts, particularly GWOSW1 and 2, proved that it did not contribute to anti-trypanosomal activity. The variable in blue is 249.138 $[M+H]^+$. As previously mentioned, the fraction possessing this compound that was obtained during isolation did not have anti-trypanosomal activity, but it did have very mild inhibitory activity against *M. marinum* (51.6% at 100 $\mu\text{g/mL}$) and strong activity against *N. farcinica* (100.3% at 100 $\mu\text{g/mL}$). It is possible that 249.138 $[M+H]^+$ acts synergistically with another compound present in the extract, hence it is a greater contributor to activity in the extract than in its pure form. N-acetyltryptamine and cyclo-L-phenylalanine-L-serine were found to be present in the media blanks as well as in the samples. The other metabolites that were identified by the S-plot as contributing to the anti-trypanosomal activity of EG4 are shown in Table 5-40.

Table 5-40: Selected metabolites from the S-plot of OPLS-DA model comparing EG4 extracts based on *T. b. brucei* inhibitory activity. Glucose: M1 with glucose replacing starch; WOSW: M1 without seawater; GlcNAcA and GlcNAcB: M1 with GlcNAc added after and before autoclaving, respectively; M1: control; GWOSW: M1 with glucose and without seawater. The IDs highlighted in blue have been identified by the AntiMarin database. Peak areas are coloured according to their value with the largest peak areas in red and the lowest ones in white and yellow.

ID	m/z	RT	Glucose	WOSW	GlcNAcA	GlcNAcB	M1	GWOSW1	GWOSW2
P_556	445.2909	18.05	4.09E7	1.03E8	3.09E7	5.82E7	7.76E7	0	0
N_842	887.5589	18.03	1.91E7	9.24E7	1.32E7	3.35E7	5.68E7	0	0
N_577	457.2921	19.38	9.65E6	5.62E7	6.94E6	1.11E7	2.89E7	0	0
N_581	330.1923	14.50	5.49E6	1.05E7	5.05E7	2.41E7	2.00E7	0	0
N_1148	372.1458	6.72	1.13E5	1.47E6	7.16E6	7.93E3	8.11E5	1.04E4	2.48E5
N_1147	331.1191	6.72	1.42E5	3.76E5	8.08E6	6.85E3	8.78E5	5.24E3	1.13E5
N_1149	741.4363	18.05	2.99E5	2.14E6	5.77E6	7.42E5	1.21E6	0	0
P_586	249.1380	8.87	3.90E6	5.63E5	7.40E6	4.51E5	1.08E6	2.14E5	4.36E4
P_666	203.1180	8.72	7.01E5	8.60E5	0	1.71E5	3.74E6	2.84E8	2.25E8

N_1148 and N_1147 were putatively identified using the AntiMarin2012 database as naphthoquinone 2 and AH-17 respectively. Their structures can be seen in Figure 5-94 below. Naphthoquinone 2 has previously been isolated from a *Streptomyces* sp. (Kulanthaivel et al., 1999) whereas AH-17 has been isolated from *Spirillospora* sp. (Hacene and Lefebvre, 1995).

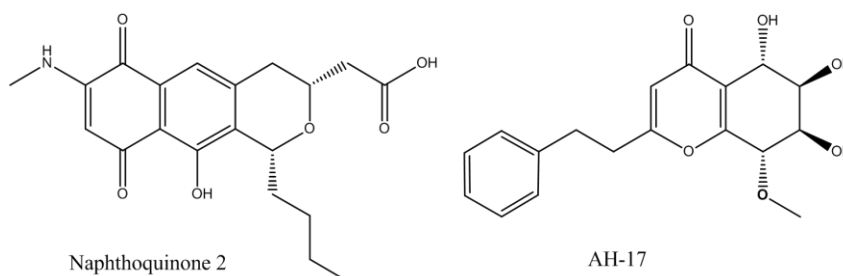


Figure 5-94: Putative identifications of N_1148 and N_1147, respectively.

When the analysis was repeated with M1 being considered as active rather than inactive against *T. b. brucei*, the R2X(cum), R2Y(cum) and Q2(cum) scores of the OPLS-DA model improved to 0.935, 1 and 0.999 respectively. The analysis was again performed with the M1 extract excluded from the samples. The scores also improved to 1 for both R2X(cum) and R2Y(cum) and 0.937 for Q2(cum). Both models gave better results than when M1 was considered inactive against *T. b. brucei*. However, the OPLS-DA model in which the M1 sample was considered active had better Q2(cum) scores than the model in which M1 was excluded, hence it would be better at predicting the anti-trypanosomal activities of extracts. This suggested that the metabolic profile of EG4_M1 was more similar to the active extracts than to the inactive ones.

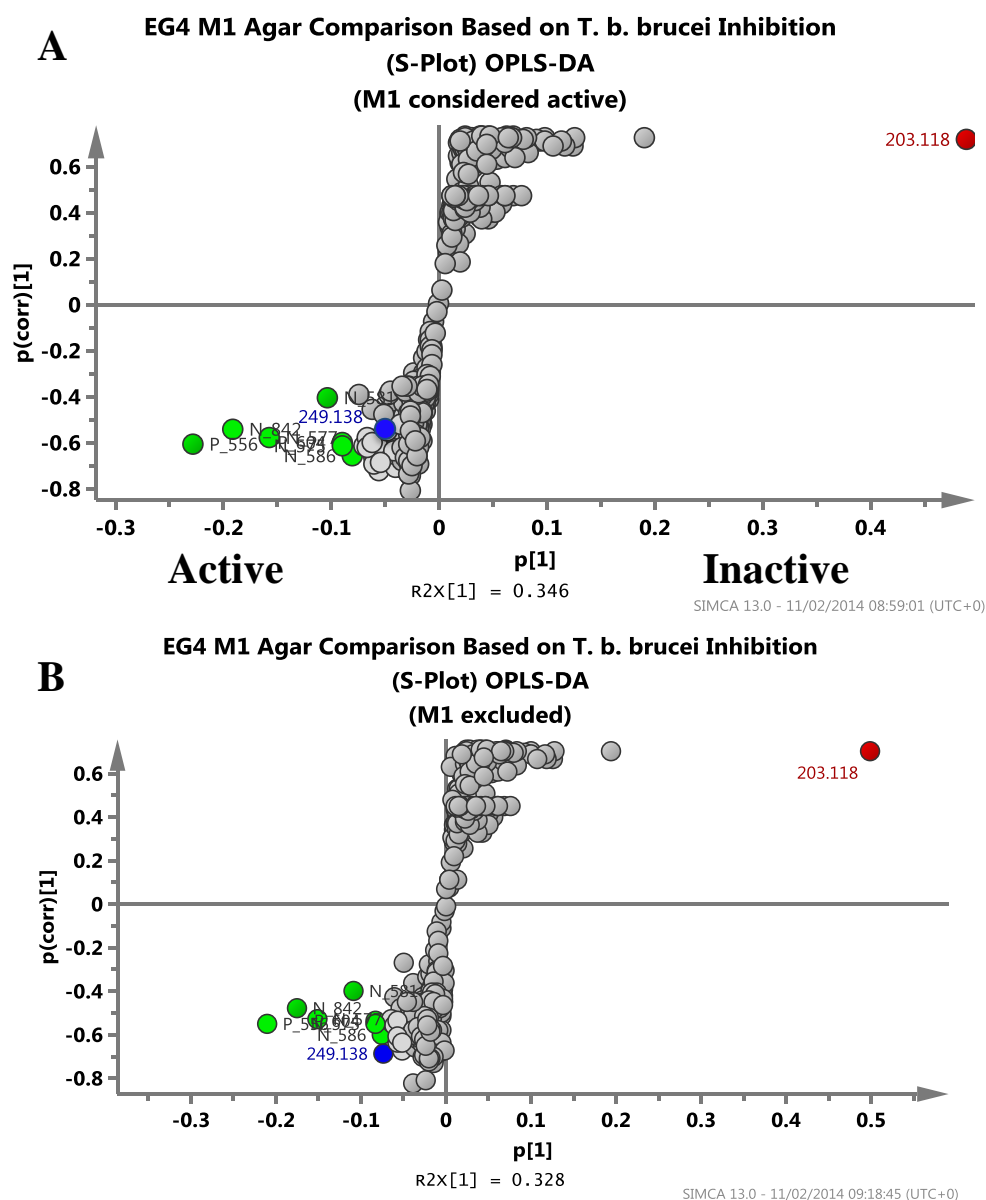


Figure 5-95: S-plots of OPLS-DA models with (A) M1 considered active against *T. b. brucei* and (B) M1 excluded from the model. Variables in the bottom left quadrant are more intense in the active extracts, hence the metabolites that they represent may be contributors to anti-trypanosomal activity. The red variable with m/z 203.118 $[M+H]^+$ in the upper right quadrant was identified as N-acetyltryptamine. It was most prevalent in the inactive extracts, hence it is unlikely that it contributes to anti-trypanosomal activity.

The S-plots of the three models (M1 considered inactive, M1 considered active and M1 excluded) did not vary greatly. The same three ions (P_556, N_842 and N_577) were identified as the greatest contributors to anti-trypanosomal activity. AH-17 (N_1147) and naphthoquinone 2 (N_1148), however, were not as prominent compared to when M1 was considered inactive. N_586 and P_604, both of which

were unidentified by the database, and elastatinal were determined to be greater contributors to activity than AH-17 and naphthoquinone 2 in the latter models.

5.3.7.4 OPLS-DA of EG4 Extracts Classified According to Anti-mycobacterium Activity

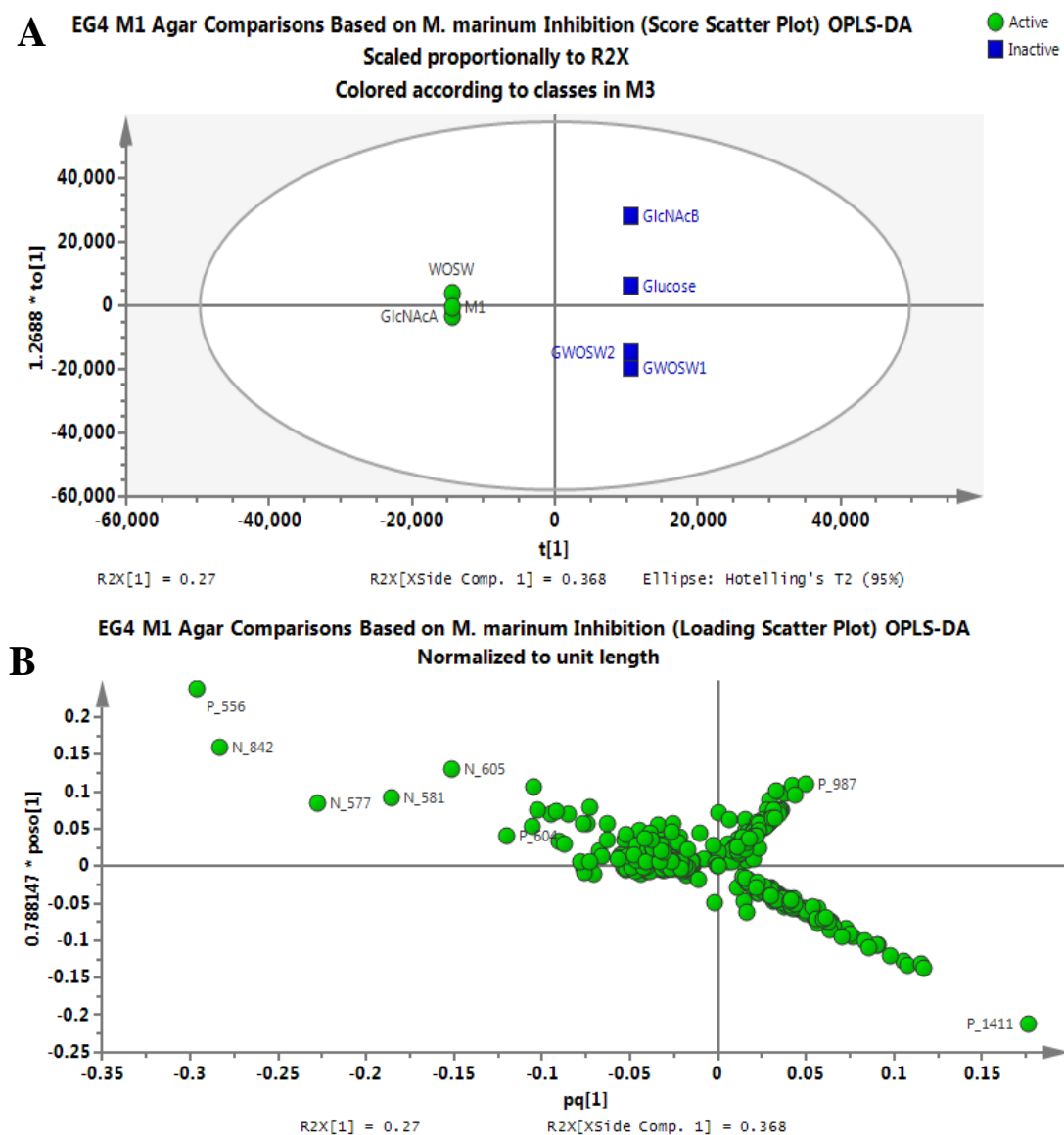


Figure 5-96: (A) Score plot and (B) loading plot of the OPLS-DA model of the EG4 extracts classified into those active against and those inactive against *M. marinum*. GlcNAcA: GlcNAc added to media after autoclaving; GlcNAcB: GlcNAc added to media before autoclaving; WOSW: M1 without salt; Glucose: M1 with glucose replacing starch; GWOSW: M1 with glucose instead of starch and without salt. R2X(cum)= 1, R2Y(cum)= 1, Q2(cum)=1

The OPLS-DA model classifying the extracts as active or inactive against *M. marinum* was better than that of *T. b. brucei*. Both the R2(cum) and Q2(cum) scores reached 1 at the fifth component. The activities of the extracts were better defined; that is, there was no sample that was close to the 50% limit by which activity was determined in this project. The closest was GlcNAc_B which inhibited 35% of *M. marinum* compared to the control, and was classified as inactive. The active fractions, (M1, WOSW and GlcNAc_A) all had similar activities (approximately 70%). Indeed, these clustered together very closely in the score plot, indicating that they were very similar. Some variables in the loading scatter plot that were more intense in certain extracts (corresponding to the distribution in the score plot) have been labelled. These were among those stated in Table 5-39. Those on the left side of the graph were also the metabolites identified in the S-plot (Figure 5-97) as being high contributors to the *M. marinum* activity.

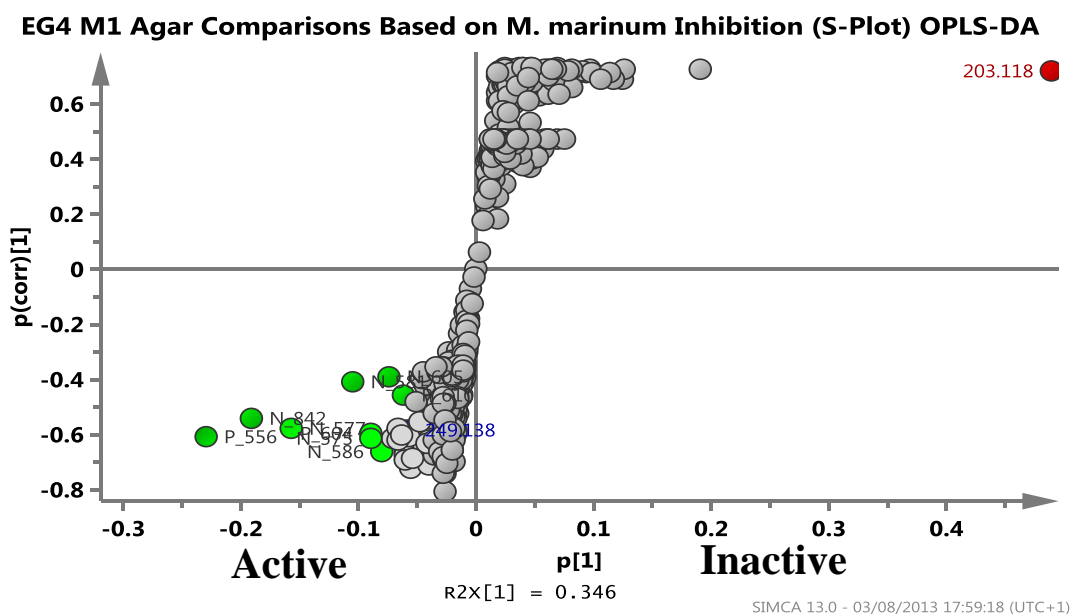


Figure 5-97: S-plot of the OPLS-DA model comparing EG4 extracts based on *M. marinum* inhibitory activity. Variables in the bottom left quadrant are more intense in the active extracts, hence the metabolites that they represent may be contributors to anti-mycobacterial activity. The red variable with m/z 203.118 $[M+H]^+$ in the upper right quadrant was identified as N-acetyltryptamine. It was most prevalent in the inactive extracts, hence it is unlikely that it contributes to anti-mycobacterial activity.

As with Figure 5-93, the metabolites on the left side of the graph were more strongly correlated with *M. marinum* inhibitory activity than those on the right side of the graph. N-acetyltryptamine was therefore not contributing to the anti-mycobacterial activity of EG4. The dianiline (249.138 [M+H]⁺), as previously mentioned, does possess mild anti-mycobacterium activity and its position in the S-plot confirmed it as a contributor to the activity of the crude extract. As mentioned above, N_575 was putatively identified as elastatinal (Figure 5-91). Table 5-41 summarises the distribution of selected metabolites:

Table 5-41: Selected metabolites from the S-plot of OPLS-DA model comparing EG4 extracts based on *M. marinum* inhibitory activity. Glucose: M1 with glucose replacing starch; WOSW: M1 without seawater; GlcNAcA and GlcNAcB: M1 with GlcNAc added after and before autoclaving, respectively; M1: control; GWOSW: M1 with glucose and without seawater. The cells are coloured according to peak area with the larger areas in red and the smaller ones in yellow and white.

ID	m/z	RT	Glucose	WOSW	GlcNAcA	GlcNAcB	M1	GWOSW1	GWOSW2
P_556	445.2909	18.05	4.09E7	1.03E8	3.09E7	5.82E7	7.76E7	0	0
N_842	887.5589	18.03	1.91E7	9.24E7	1.32E7	3.35E7	5.68E7	0	0
N_577	457.2921	19.38	9.65E6	5.62E7	6.94E6	1.11E7	2.89E7	0	0
N_581	330.1923	14.50	5.49E6	1.05E7	5.05E7	2.41E7	2.00E7	0	0
N_605	344.208	15.81	2.95E6	1.46E7	1.66E7	2.07E7	2.16E7	0	0
P_604	459.3063	19.34	3.67E6	1.62E7	7.76E5	2.29E6	9.60E6	0	0
N_575	511.2634	18.03	7.95E6	1.48E7	5.44E6	1.05E7	1.26E7	0	0
P_610	332.2065	14.54	1.96E6	3.59E6	1.38E7	7.03E6	6.90E6	0	0
N_586	506.2715	18.00	4.65E6	1.07E7	4.00E6	6.08E6	8.74E6	0	0
P_586	249.1380	8.87	3.90E6	5.63E5	7.40E6	4.51E5	1.08E6	2.14E5	4.36E4
P_666	203.1180	8.72	7.01E5	8.60E5	0	1.71E5	3.74E6	2.84E8	2.25E8

5.3.8 Comparison of EG4 Extracts when Grown on M1 Containing Artificial Seawater or Royal Nature Pre-formulated Salt

In order to facilitate upscale cultivation of EG4, a new salt formula was purchased. Royal Nature Advanced Pro Formula Salt (Royal Nature, Israel) is a pre-formulated aquarium salt that needs only to be dissolved in the culture broth, as opposed to the artificial seawater in which the ten inorganic salts were individually weighed and reconstituted in a required amount of deionised water. To determine whether the change in the artificial salt recipe had an effect on the bioactivity and metabolic

profile of EG4, a shake flask culture was performed in which three flasks containing M1 with artificial seawater (ASW) and three flasks containing M1 with Royal Nature (RN) were inoculated with EG4. A fourth flask containing each type of medium served as the blank. The blanks were labelled ‘-1’ whereas the inoculated flasks were labelled ‘-2’, ‘-3’, and ‘-4’.

Table 5-42: Yields and activities of EG4 grown on M1 with Royal Nature (RN) or artificial seawater (ASW). Samples suffixed with ‘-1’ are blank media extracts whereas those suffixed with ‘-2’ to ‘-4’ are EG4 extracts. Active extracts (% inhibition \geq 50%) are highlighted in grey.

Sample	Yield (mg)	% Inhibition of <i>T. b. brucei</i> (20 μ g/mL)	% Inhibition of <i>M. marinum</i> (100 μ g/mL)
M1-ASW-1	9.0	3.91	88.37
EG4-ASW-2	12.5	73.48	84.96
EG4-ASW-3	9.6	32.36	64.13
EG4-ASW-4	10.2	39.31	55.45
M1-RN-1	8.9	15.95	82.27
EG4-RN-2	13.5	95.09	84.56
EG4-RN-3	15.1	86.10	80.76
EG4-RN-4	10.6	50.35	72.70

A t-test showed that, at 95% confidence, there was no significant difference between the two salts for either activity, despite the RN samples appearing to have slightly higher activity. This was probably due to the variation across the replicates. Furthermore, the scatter plot in Figure 5-98 below showed that EG4 grown on M1 with RN produced more or less the same compounds as EG4 grown on M1 with ASW, albeit in slightly increased concentrations. This could account for the slight increase in bioactivity seen in the extracts of M1 grown with RN. The compounds that have been isolated from EG4 lie along the diagonal, however, indicating that their production was unaffected by the salt used. As a result of this experiment it was determined that RN can be used to replace ASW as it is easier to use, has no detrimental effect on the bioactivity of the extracts, and even potentially increases the production of the bioactive compounds. It is unknown whether this increase in metabolite production was a result of the salts present in the Royal Nature mixture or whether it was due to the reduction in salt concentration used as the RN samples have approximately half the amount of salt that the ASW samples have. 200 mL of

ASW contains 8.03 g of salt whereas only 4.6 g of RN is dissolved to make 200 mL of M1 broth.

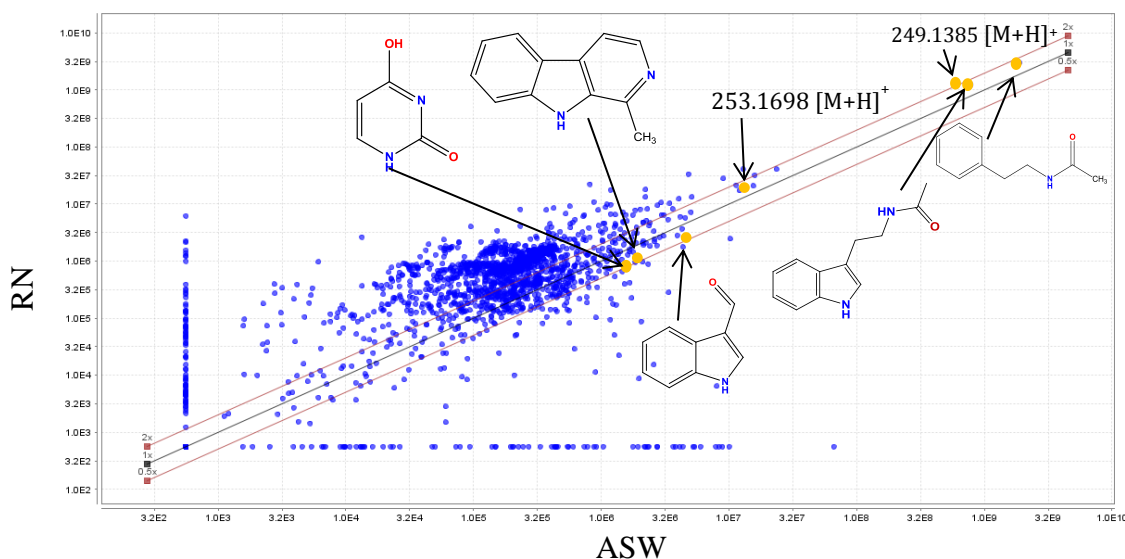


Figure 5-98: Scatter plot comparing the metabolites found in EG4 grown on M1 with different types of salt. The slight shift of the metabolites above the diagonal denotes increased production of the metabolites in the Royal Nature (RN) cultures as opposed to the artificial seawater (ASW) extracts. The compounds that have been isolated from EG4 are highlighted. They all lie along the diagonal, as their production was not affected by the change in salt used.

5.3.9 Metabolic Profiling of EG4 Cultured in Variations of M1 Broth

Following the results of EG4 cultured on M1 agar variations, an up-scaled experiment was performed in which EG4 was grown in 200 mL of M1 broth using different amounts of salt and glucose. The concentrations of starch/glucose and salt used can be seen in the methodology section in Table 5-2. The experiment concentrated on optimising the amounts of starch, glucose and salt and hence GlcNAc was not included. The activity of the extracts against *T. b. brucei* and *M. marinum* as well as the weights of the extracts can be seen in Table 5-43 below. As with the previous experiments, the blanks were labelled ‘-1’ and the inoculated cultures ‘-2’ and ‘-3’.

Table 5-43: Yields and activities of media and bacterial extracts comparing M1 broth with different concentrations of starch, glucose and salt. M1+G: M1 with glucose instead of starch; M1-RN: M1 without salt; 50G50S: M1 in which the carbon source is halved between starch and glucose and which contains half of the usual amount of salt; M1: control M1; GWOSW: M1 which contains glucose instead of starch and does not contain salt. Samples suffixed with '-1' are media blanks whereas those suffixed with '-2' and '-3' are EG4 extracts. Cells highlighted in grey show the active extracts (%inhibition \geq 50%).

Sample	Yield (mg)	%Inhibition of <i>T. b. brucei</i> (20 μ g/mL) (n=2)	% Inhibition of <i>M. marinum</i> (100 μ g/mL) (n=2)
M1+G-1	10.5	-12.9	62.41
M1+G-2	18.7	60.06	30.09
M1+G-3	19.5	79.41	55.51
M1-RN-1	10.8	45.23	99.16
M1-RN-2	13.2	96.18	100.51
M1-RN-3	11.5	97.14	100.55
50G50S-1	12.1	40.83	87.87
50G50S-2	15.6	99.35	77.11
50G50S-3	19.3	98.08	93.09
M1-1	10.3	32.05	100.65
M1-2	13.9	98.18	69.60
M1-3	12.3	100.03	79.63
GWOSW-1	11.0	-13.91	45.2*
GWOSW-2	17.0	76.86	69.59
GWOSW-3	12.7	47.34	66.75

*n=1 due to outlying results

EG4 grown on M1 broth, M1-RN (M1 without salt), and 50G50S (50% glucose, 50% starch and 50% salt) had mean anti-trypanosomal activities of 99%, 96% and 98% respectively. However, after subtraction of the activity of the blank media from that of the bacterial extracts, the activities of the bacterial extracts all fell within a similar range: M1-RN (51.43%), 50G50S (57.89%), GWOSW (M1 without starch and salt) (62.1%), M1 (67.19%) and M1+G (M1 with glucose) (69.74%). As with the agar cultures, the substitution of starch with glucose resulted in increased anti-trypanosomal activity. The removal of salt from the media resulted in a decrease in activity, as opposed to the results obtained from the agar study. The anti-mycobacterium activity of these extracts was not as evident as before because the blank broth extracts inhibited *M. marinum* growth to the same extent, and in some cases, even more, than the bacterial extracts. The heatmap in Figure 5-99 below shows that 50G50S resulted in the most metabolites whereas GWOSW resulted in the fewest. EG4 grown on M1+G broth produced more compounds than that grown on M1+Glucose agar (Figure 5-84).

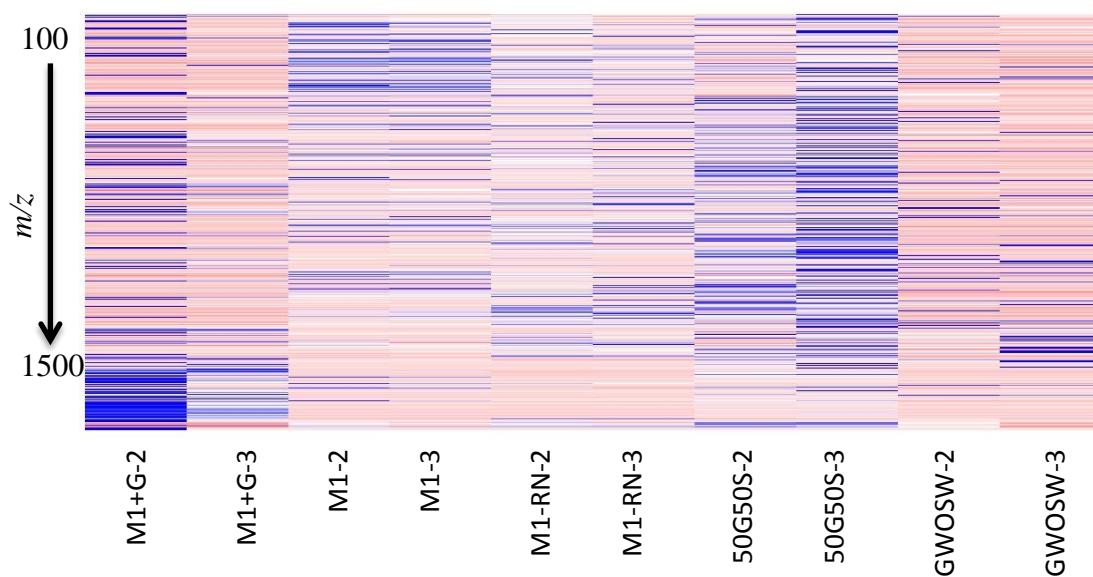


Figure 5-99: Heatmap depicting the relative peak areas of the metabolites produced by EG4 grown on various media. M1+G: M1 with glucose instead of starch; M1-RN: M1 without salt; 50G50S: M1 in which the carbon source is halved between starch and glucose and which contains half of the usual amount of salt; M1: control M1; GWOSW: M1 which contains glucose instead of starch and does not contain salt. The '-2' and '-3' suffixes denote that these are EG4 extract replicates. Blue: larger peak area, red: smaller peak area. EG4 cultured on M1+G produces higher molecular weight metabolites. The most prolific producer of metabolites is EG4 cultured on 50G50S medium.

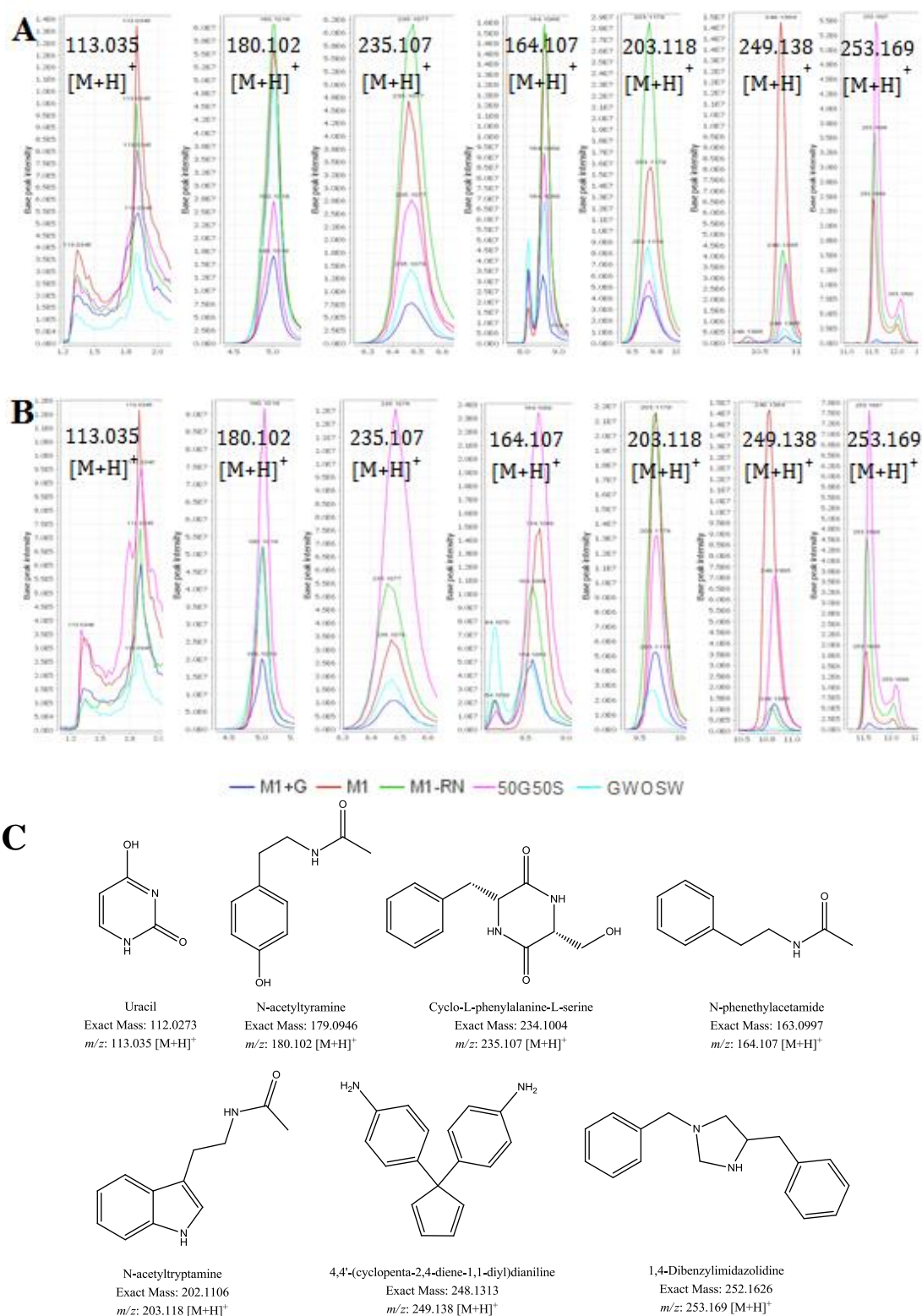


Figure 5-100: Extracted ion chromatogram of compounds isolated from EG4. (A) Comparison of "-2" flasks. (B) Comparison of "-3" flasks. M1+G: M1 with glucose instead of starch; M1: control; M1-RN: M1 without salt, 50G50S: M1 with equal amounts of starch and glucose and with half of the usual amount of salt; GWOSW: M1 with glucose replacing starch and without salt. (C) Structures of isolated compounds.

Figure 5-100 above shows the extracted ion chromatogram of the compounds isolated from the EG4 large scale culture when their corresponding m/z ratios were searched for in the M1 broth variation cultures. Indole-3-carboxaldehyde, harman and 3,4-dihydroxy-5,6-bis(1*H*-indol-3-yl)-3,5-cyclohexadiene were found in the media blanks and thus were not included in the graph. As can be seen in the figure above, the M1, M1-RN and 50G50S cultures often produced greater quantities of the desired metabolites; however, the media that resulted in the production of the greatest amount of each metabolite was not consistent between the duplicates. The M1+G and GWOSW cultures tended to produce smaller amounts of the metabolites, particularly 249.138 [M+H]⁺ (dianiline compound) and 253.169 [M+H]⁺ (1,4-dibenzylimidazolidine).

Aside from the dianiline (m/z 249.138 [M+H]⁺), the compounds that had been pinpointed in the agar cultures as contributing to the anti-trypanosomal and anti-mycobacterial activity (Table 5-40 and Table 5-41 respectively) were not found in the shake flask cultures. The antibiotic activities of the shake flask cultures were therefore due to compounds other than those previously determined using multivariate analysis. This also highlighted the fact that changes occur in the metabolic profile of EG4 when it is cultured in agar and in broth.

Multivariate analysis was performed to obtain an overview of the differences and similarities between the extracts as well as to determine the metabolites contributing to anti-trypanosomal activity. The anti-mycobacterial metabolites produced by EG4 were not analysed as the blank media also displayed anti-mycobacterial activity.

5.3.9.1 PCA of EG4 M1 Broth Extracts after Exclusion of Media Peaks

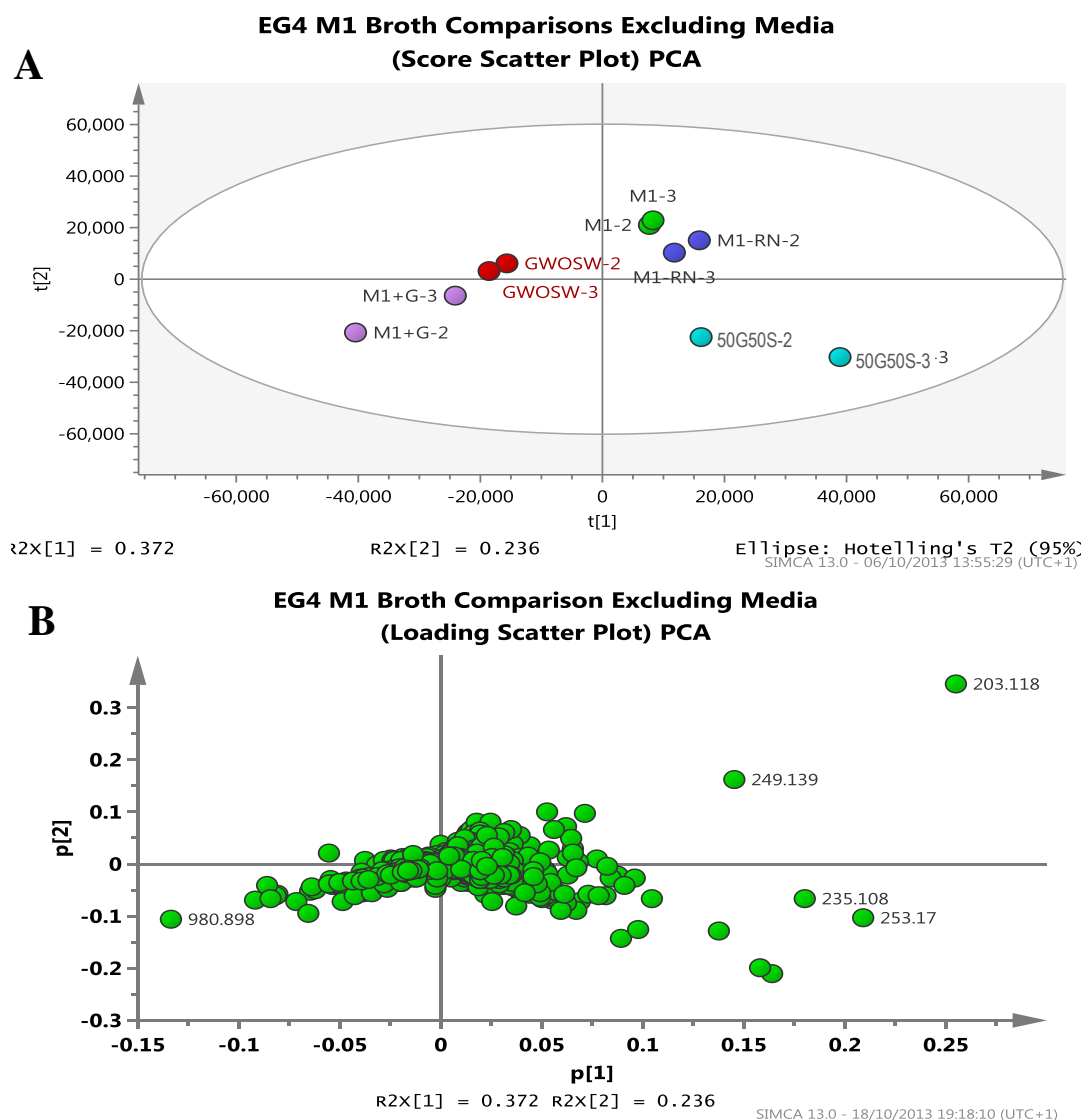


Figure 5-101: (A) PCA score scatter plot and (B) loading scatter plot of the EG4 M1 broth extracts following deletion of peaks belonging to the media. M1+G: M1 with glucose as the carbon source; GWOSW: M1 with glucose and without salt; M1-RN: M1 without salt, 50G50S: M1 with equal amounts of starch and glucose and with half of the standard amount of salt. The loading scatter plot shows the distribution of the metabolites among all the samples. The metabolites previously isolated and identified from EG4 have been labelled. $R^2X(\text{cum})=0.845$, $Q^2(\text{cum})=0.501$.

The score plot in Figure 5-101 was an indicator of the reproducibility of the extracts as the two samples from each media variation clustered together. M1+G (containing glucose) and M1 GWOSW (containing glucose but without salt) extracts formed a loose grouping on the left half of the graph whereas M1, M1-RN and 50G50S (50% glucose, 50% starch as the carbon source and containing 50% of the standard amount of salt) fell on the right half of the plot. EG4 cultured on the latter media produced greater quantities of N-acetyltryptamine, 1,4-dibenzylimidazolidine, cyclo-L-phenylalanine-L-serine, and the dianiline compound with m/z 249.138 $[M+H]^+$, as seen in the loading plot. This corroborated the results seen using MZmine 2.10.

5.3.9.2 OPLS-DA of Blank M1 Broth Extracts According to Anti-trypanosomal Activity

OPLS-DA was used to identify the metabolites contributing to anti-trypanosomal activity. The EG4 extracts all had similar anti-trypanosomal activity after the activities of the M1 blanks were subtracted from the samples. However, only some of the blank M1 broths had inhibitory activity whereas others did not. OPLS-DA was thus performed to compare the active and inactive media variations in order to identify the compounds in the media that contribute to the activity against *T. b. brucei*.

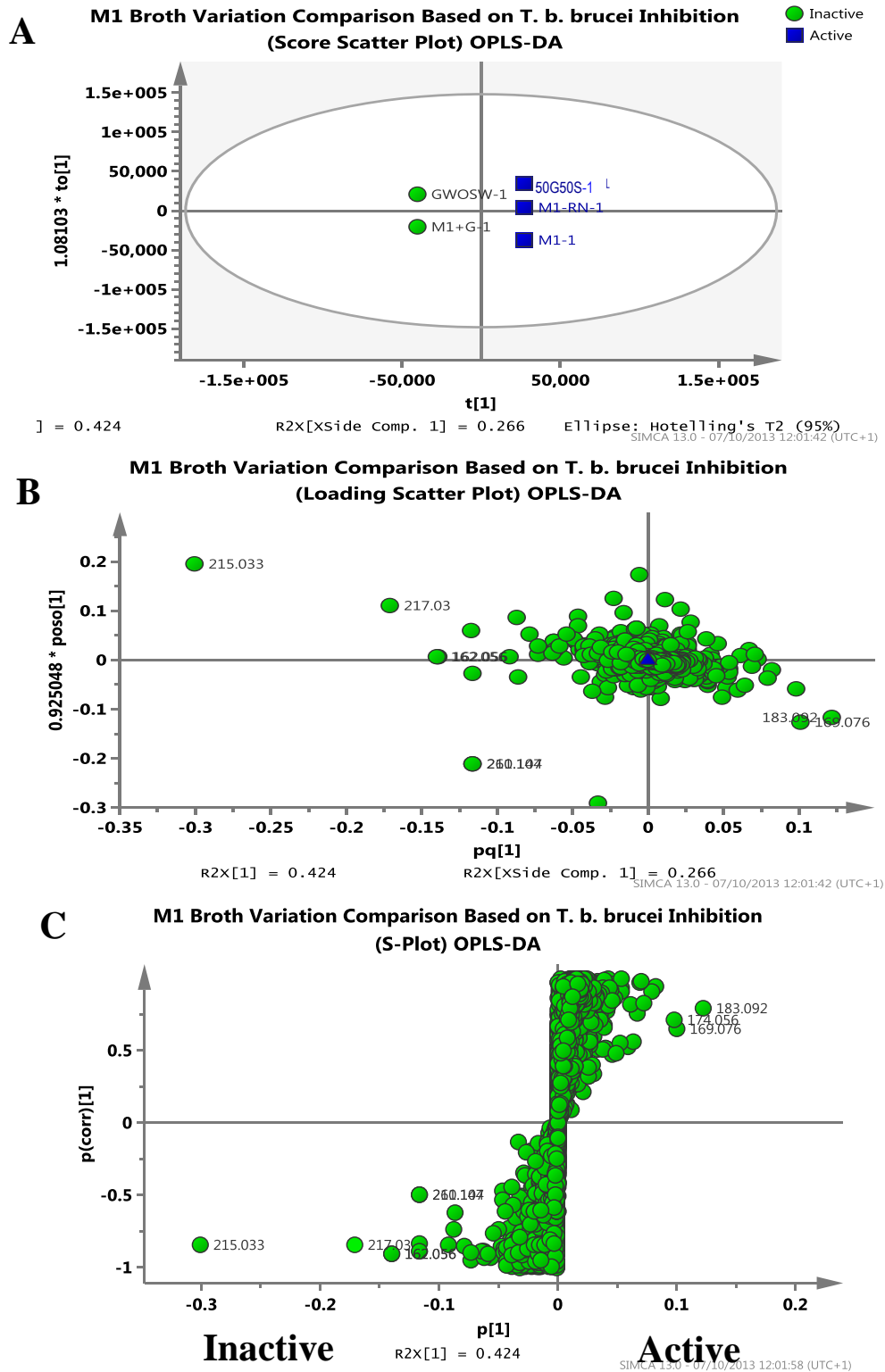


Figure 5-102: (A) Score plot, (B) loading plot, and (C) S-plot after OPLS-DA of the M1 media variations. GWOSW: M1 with glucose and without salt; M1+G: M1 with glucose as the carbon source; 50G50S: M1 with equal amounts of starch and glucose as the carbon source and with half of the standard amount of salt; M1-RN: M1 without salt; M1: control. M1+G and M1 GWOSW were classified as inactive and M1, M1-RN and 50G50S were classified as active against *T. b. brucei*. Metabolites at the upper right quadrant of the S-plot were considered contributors to anti-trypansomal activity. $R^2X(cum)=1$, $R^2Y(cum)=1$, $Q^2(cum)=1$

The metabolites that were identified as contributors to anti-trypanosomal activity were depicted on the right side of the S-plot in Figure 5-102 whereas those metabolites that were more strongly correlated to the inactive media were located on the left side of the S-plot. The three strongest contributors were identified using the AntiMarin database and are tabulated in Table 5-44.

Table 5-44: Compounds identified from the M1 broth as contributors to anti-trypanosomal activity

ID	m/z	RT	Name	M1+G-1	M1-1	M1-RN-1	50G50S-1	GWOSW-1
P_277	169.076	6.09	[44] Norharman	1.53E8	1.98E8	1.48E8	1.58E8	1.06E8
N_540	174.0561	7.42	[45] 3-(hydroxyacetyl)indole	3.18E7	9.39E7	4.16E7	6.72E7	3.54E7
			[15] methyl indole-3-carboxylate					
P_272	183.0918	6.56	[46] Harman	2.04E8	2.69E8	2.38E8	2.17E8	1.85E8

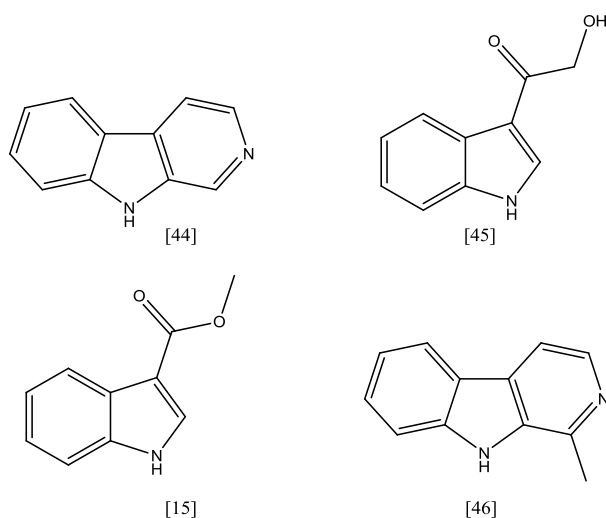


Figure 5-103: Contributors of anti-trypanosomal activity in the M1 broth variations.

It is evident in Table 5-44 that the compounds identified as contributors of anti-trypanosomal activity were still present in the inactive M1+G and GWOSW broths. It therefore cannot be concluded that these compounds were the only ones responsible for the anti-trypanosomal activity found in the media. However, norharman (**44**), 3-(hydroxyacetyl)indole (**45**) and harman (**46**) have all been proven to inhibit *T. cruzi* (Rivas et al., 1999, Martinez-Luis et al., 2012, Cavin et al., 1987).

Harman was indeed isolated and proved to possess very mild anti-trypanosomal activity (15% inhibition), although it did have stronger anti-mycobacterial activity. This could account for the strong inhibition of *M. marinum* observed in both the media blanks as well as the EG4 extracts.

5.3.10 Fermentation of EG4

EG4 was cultured in duplicate in a Biostat Q bioreactor. The pH and oxygen levels were monitored but not maintained at a certain target in order to determine the changes that occurred in the culture as EG4 grew. The temperature was set to 30°C and the stirrer speed was 150 rpm. These parameters showed slight fluctuations over the course of the fermentation but most likely did not affect the culture (Figure 5-104).

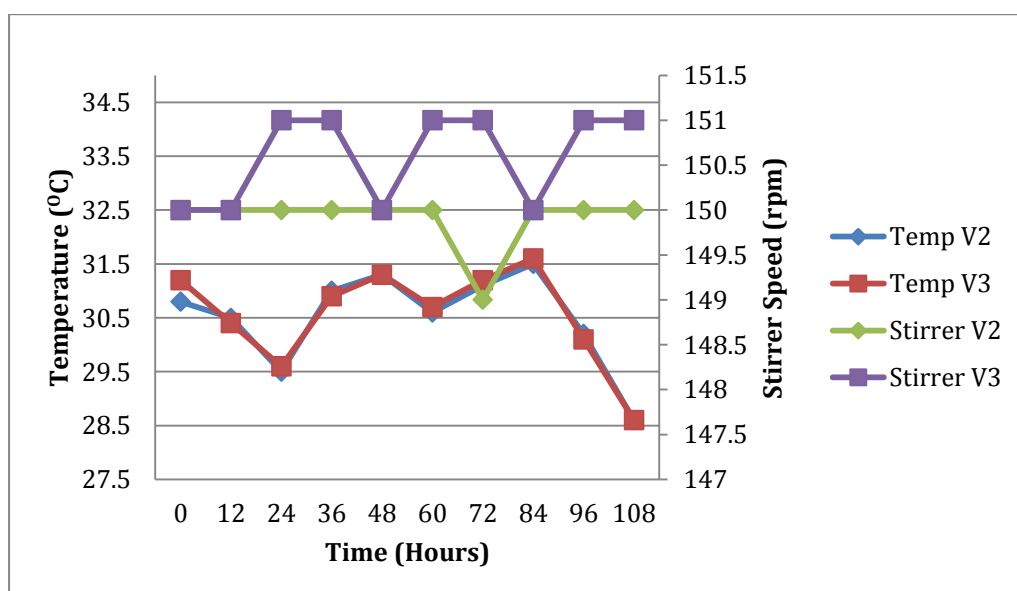


Figure 5-104: The temperature and stirrer speed for vessels 2 and 3 (V2 and V3) of the Biostat Q bioreactor over the duration of the fermentation. The temperature fluctuated slightly over the course of the fermentation, particularly towards the end as the water bath which regulated the temperature began to leak. However, the fluctuations were between $\pm 1.5^{\circ}\text{C}$ and were unlikely to affect the growth of EG4. The stirrer speeds also fluctuated slightly, with the stirrer in vessel 3 stirring 1 rpm faster than vessel 2; however, this was not a significant difference in speed.

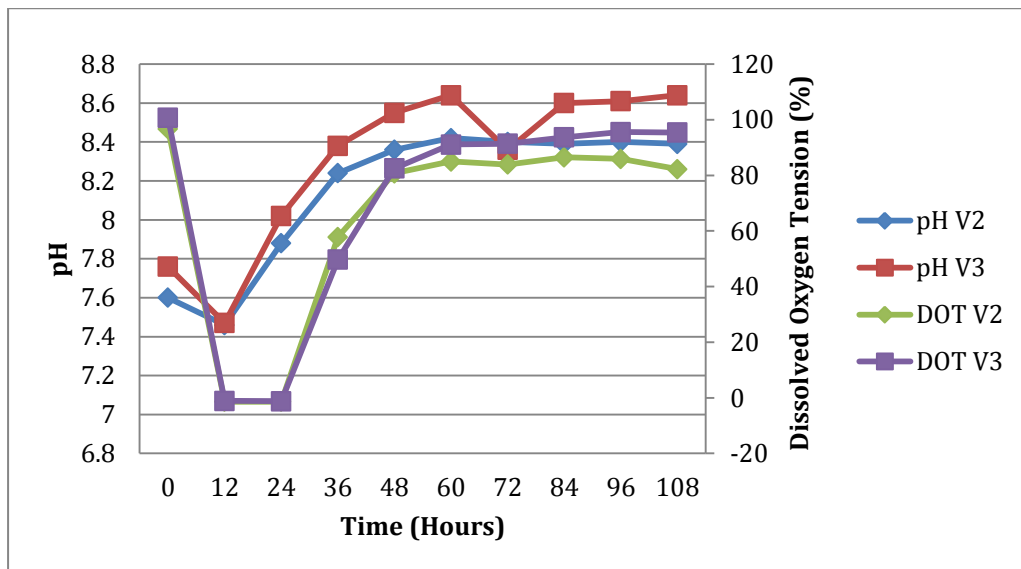


Figure 5-105: pH and dissolved oxygen tension (DOT) observed in vessels 2 and 3 (V2 and V3) during fermentation of EG4. The pH of the cultures decreased slightly during the first twelve hours of the fermentation, after which they increased before plateauing at approximately 60 hours. The DOT is a measure of the oxygen available in the broth. The drastic decrease in DOT during the first 24 hours indicated that the cells were utilising all of the available oxygen. The increase and subsequent plateau in DOT implied that the bacteria were using less oxygen and had begun to die.

The dissolved oxygen tension (DOT) gave an indication of the growth curve of the bacteria under the present conditions. The decrease in oxygen in the broth signalled that the cells were growing and were utilising the oxygen being supplied into the broth. The maximum growth of the cells appeared to occur within 12 hours and continued until 24 hours. This would correspond to the log phase of cell growth. The subsequent increase in DOT showed that the bacteria had stopped utilising as much oxygen, implying that they were not multiplying as rapidly and had reached the stationary phase of cell growth. The pH of the broths complemented the DOT as the same trend occurred. The pH decreased at 12 hours and gradually increased afterwards. These results correlated with the cell counts observed from each vessel (Figure 5-105).

Two methods were used to determine the growth curve of EG4 during fermentation (Figure 5-106). A haemocytometer was used to count cells from Vessel 2, whereas the spread plate technique was used to count cells from Vessel 3. The spread plate technique had the advantage of determining the number of viable cells in the culture whereas when the haemocytometer was used it was unknown whether the cells being counted were viable or not. However, the spread plate technique was subject to

contamination. Samples taken from Vessel 3 at 60 hours and from 84 hours onwards were unable to be counted due to contamination of the plates. The samples were examined under a microscope for contamination prior to plating so it is known that the microbial contaminant did not come from the fermenter. In addition, the contamination on the plates began from the edges of the plates and spread towards the center, and was not spread as evenly as the colonies of EG4.

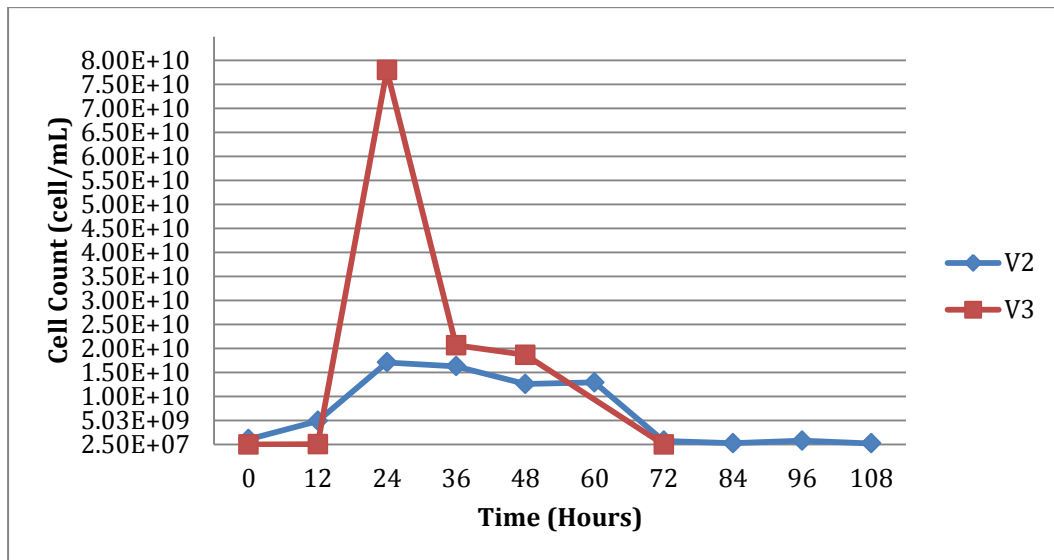


Figure 5-106: Cell counts of samples from Vessel 2 and Vessel 3. The cells from Vessel 2 were counted using a haemocytometer whereas the cells in Vessel 3 were counted using the spread plate technique. No cell count was obtained for Vessel 3 at 60, 84, 96 and 108 hours due to contamination of the plates.

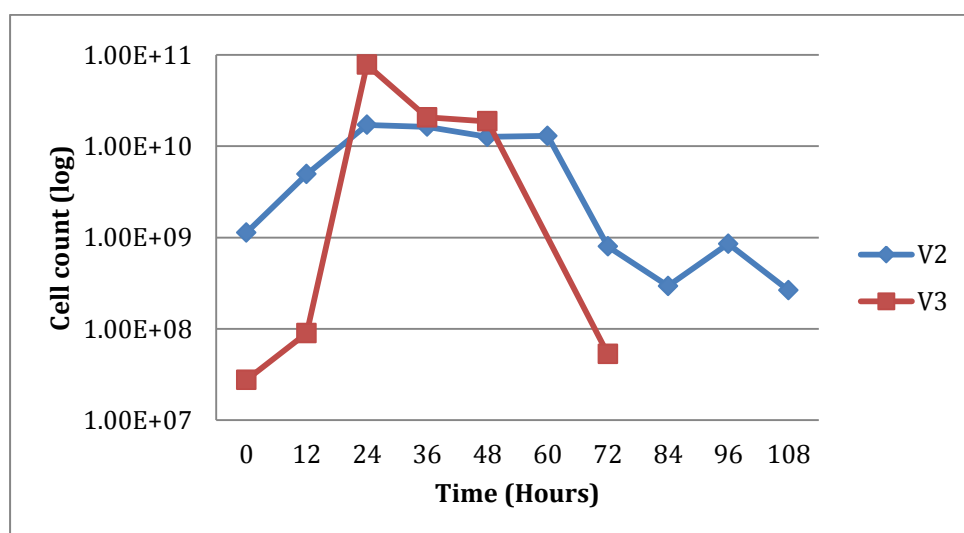


Figure 5-107: Growth curve of EG4 when grown in a bioreactor. The lag phase occurred from 0-12 hours, followed by the log phase from 12-24 hours and the stationary phase from 24-60 hours. The culture reached the death phase after 60 hours.

By transforming the y-axis of the graph into the log values of the cell counts it was possible to get the growth curve of EG4 (Figure 5-107). The four phases of bacterial growth were then evident. The lag phase, when the bacteria were adapting to the growth conditions, occurred from 0-12 hours. The log phase or exponential phase followed, from 12-24 hours, as the cells rapidly divided and utilised the available nutrients in the media. The stationary phase is the period in the growth curve during which the rate of cell death is the same as the rate of cell growth. This could be due to depletion certain nutrients required for growth or accumulation of inhibitory compounds. This phase occurred in Vessel 2 from 24-60 hours. As the cell count of Vessel 3 at 60 hours was unable to be determined, it was unknown if Vessel 3 would have followed the same pattern. However, as EG4 was grown in both vessels under identical conditions, it was likely that the stationary phase of EG4 in both vessels was the same, from 24-60 hours. The last phase, from 60 hours onwards, was the death phase during which the nutrients are exhausted and the bacteria die.

The metabolic changes during the course of the fermentation were tracked by analysing the extracts using NMR and LC-MS. The ^1H NMR spectra of the extracts from Vessel 2 and Vessel 3 are shown in Figure 5-108. The NMR spectra of both V2-0hrs samples extracted using a cell disrupter or a homogeniser were not included as the quantities were too small to obtain good spectra. The extracts were compared to the spectrum of a 7-day shake flask culture and an M1 blank containing polypropylene glycol, the antifoaming agent.

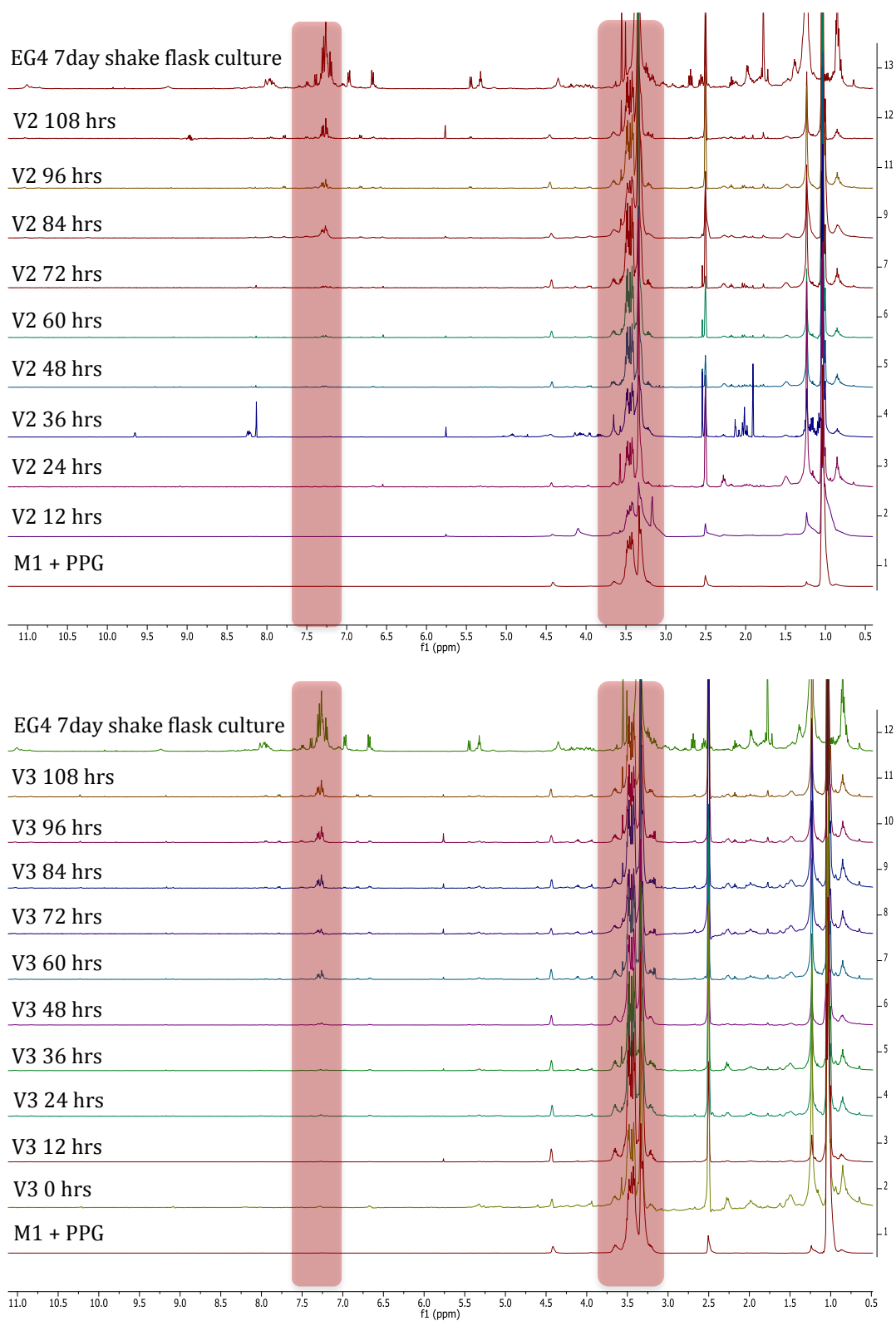


Figure 5-108: ^1H NMR spectra of Vessel 2 (top) and Vessel 3 (bottom) (400 MHz, DMSO). The spectra are compared to one obtained from a 7-day shake flask culture (top spectrum for each set) and blank M1 media containing polypropylene glycol (bottom spectrum for each set). The regions where changes occurred are highlighted. These are primarily at the aromatic region (7-7.5 ppm) and the olefinic region (3.0-4.0 ppm).

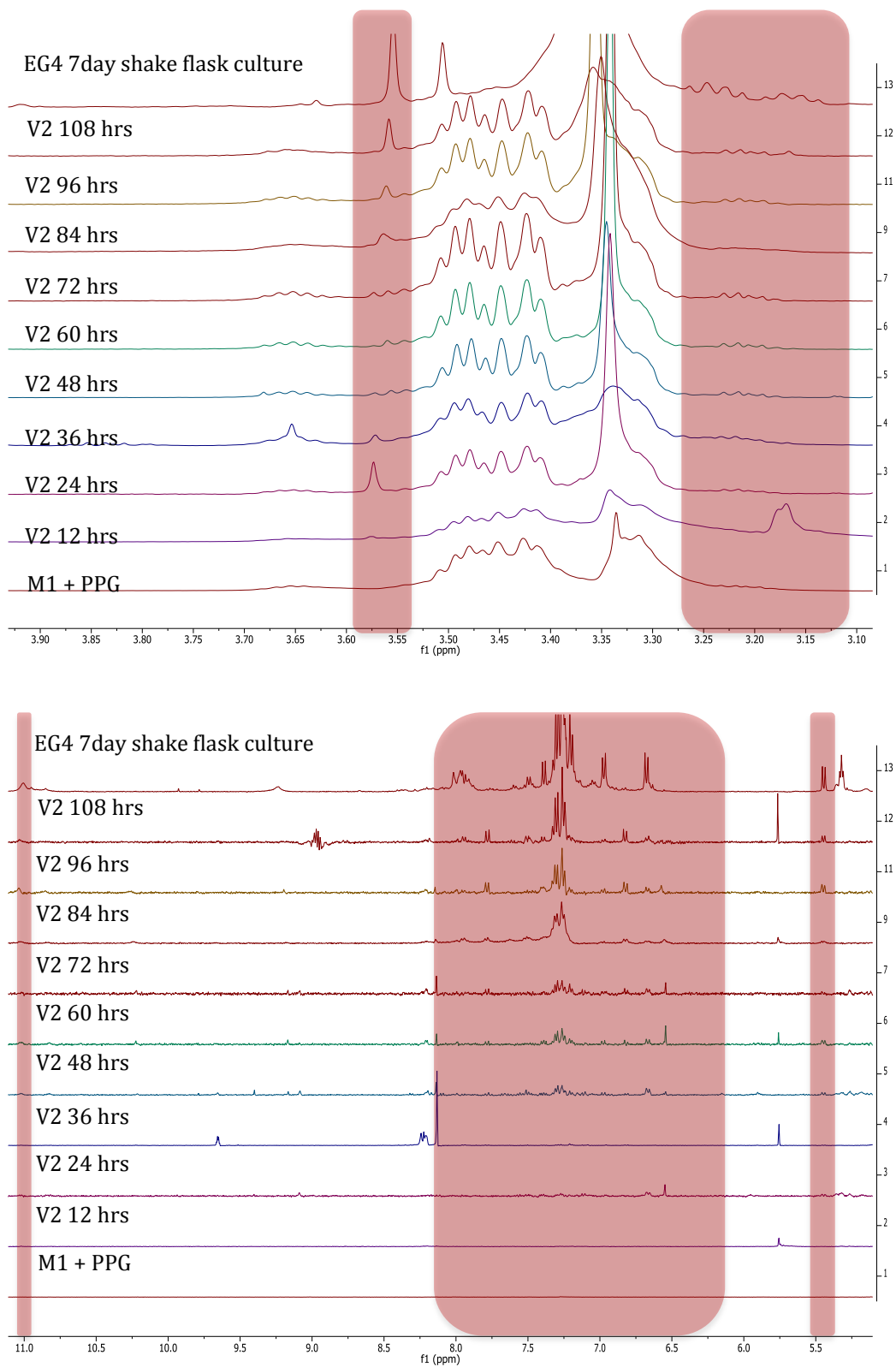
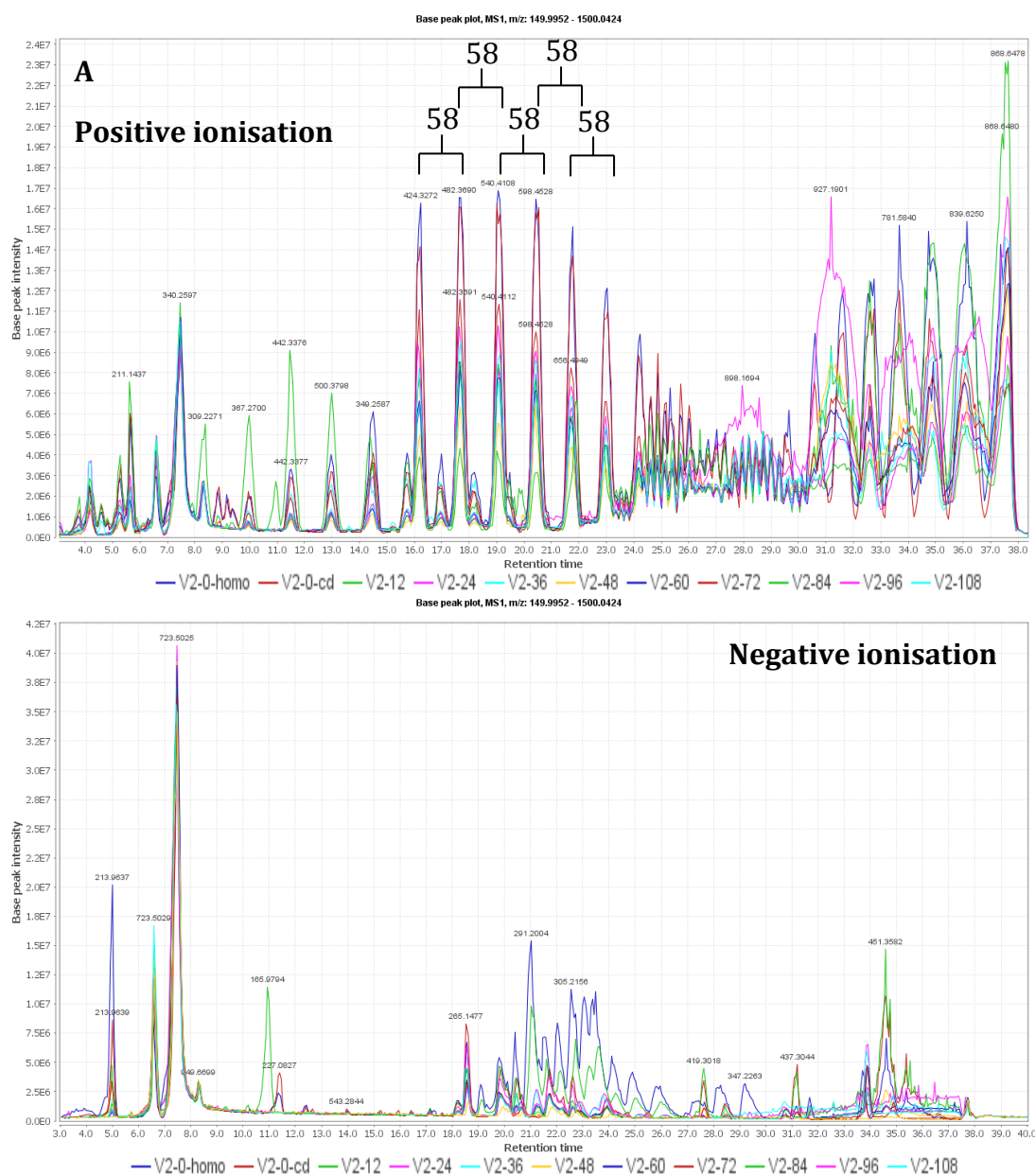


Figure 5-109: Expansion of the ^1H NMR spectra of the extracts from Vessel 2 showing the changes occurring from 3-4 ppm (top) and from 5-11 ppm (bottom). The spectra are compared to one obtained from a 7-day shake flask culture (top spectrum for each set) and blank M1 media containing polypropylene glycol (bottom spectrum for each set). The production of metabolites in the aromatic region began after 48 hours but became more evident during the cell death phase.

The production of metabolites with aromatic systems began after 48 hours, although the peaks were more obvious from 72 hours in Vessel 3 and 84 hours in Vessel 2. The production of aromatic metabolites therefore increased during the cell death phase, confirming that they were indeed secondary metabolites and not primary metabolites. The fermentation extracts possessed overlapping peaks between 3-4 ppm, which were proven to belong to the antifoam agent, polypropylene glycol (PPG). This was verified upon analysis of the HR-LCMS results.



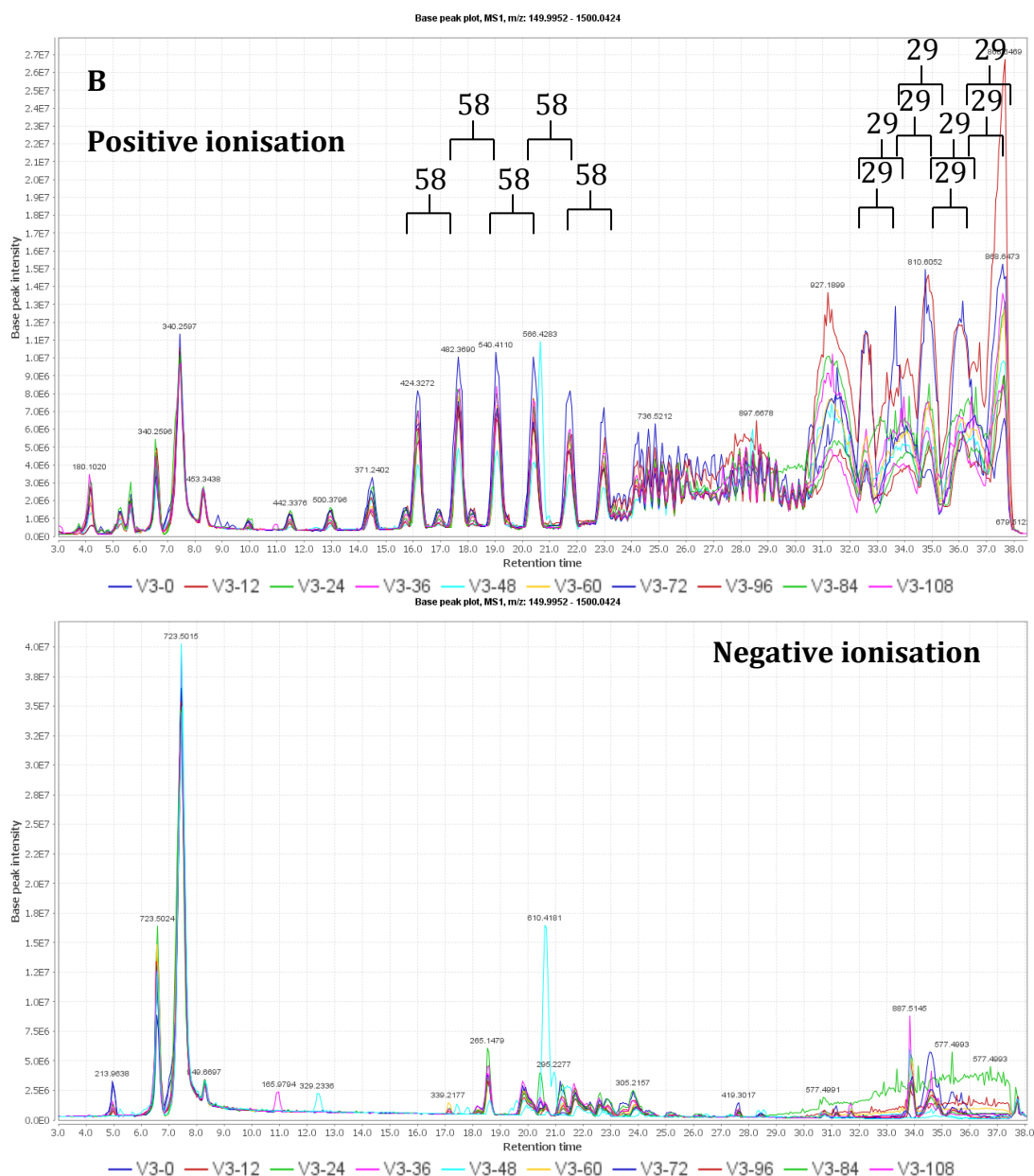


Figure 5-110: High-resolution LC-MS chromatograms of the extracts of A) Vessel 2 and B) Vessel 3. A polymer can be seen in the positive ionisation mode. It has repeating units of 58 Da ($z = 1$) and 29 Da ($z = 2$).

The LC-HRFTMS spectra looked different from the usual extracts of EG4 grown on agar and shake flasks. The middle of the spectra, from 14.5-23.0 minutes, had the pattern of a polymer with the repeating unit being 58 Da. Towards the end of the run, at 32.0-38.0 minutes, the polymer had a repeating unit of 29 Da, which indicated that these were doubly-charged species. This was validated by the Xcalibur software. The

predicted formula for a unit with a mass of 58 Da is C_3H_6O , the repeating unit of polypropylene glycol, the antifoam agent used.

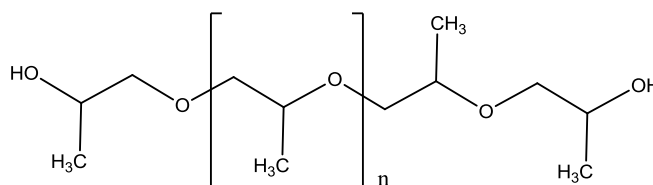


Figure 5-111: Structure of polypropylene glycol. Polypropylene glycol was the antifoam agent that was added to the M1 broth for the fermentation process. The repeating unit with a size of 58 Da is outlined by the brackets.

The peaks from the polypropylene glycol masked the other peaks being produced by EG4, particularly in the positive ionisation mode. However, by aligning the LC-MS data and subtracting the peaks from the media with antifoam added into it, a heatmap was generated which showed the differences in metabolite production between EG4 cultured in shake flasks or in a bioreactor.

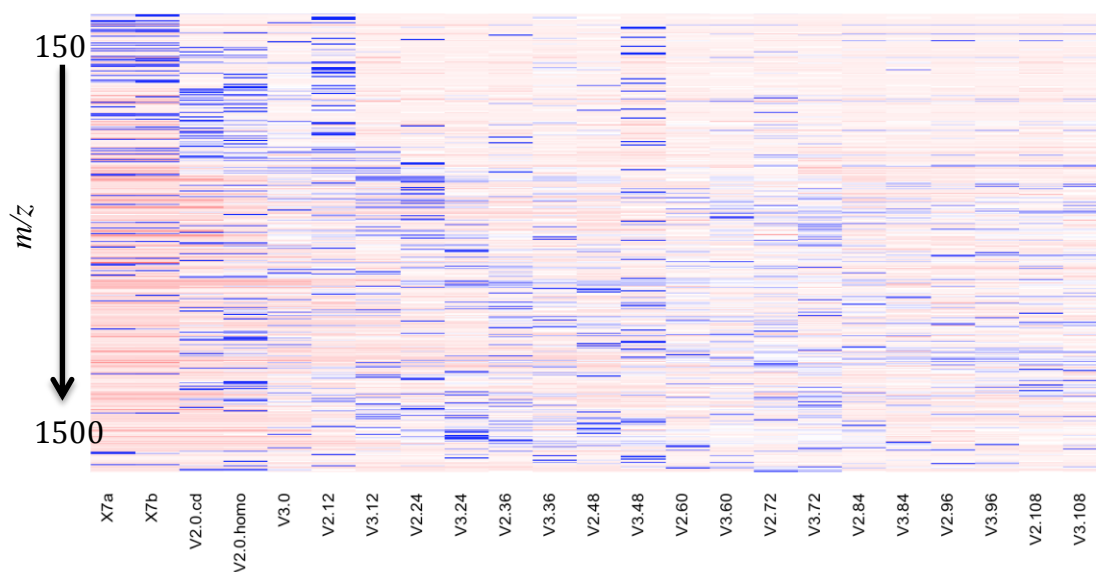


Figure 5-112: Heatmap comparing the LCMS results of two 7-day shake flask cultures (X7a and X7b) with those of the fermentation extracts. Blue bands denote a larger peak area whereas red bands denote a small peak area. Although the shake flask cultures produced lower molecular weight metabolites, EG4 when grown in the fermenter produced higher molecular weight metabolites as seen by the increasing incidence of blue bands in the later samples.

The heatmap in Figure 5-112 showed that EG4 grown in shake flasks produced more compounds with a lower m/z after seven days, whereas EG4 grown in the bioreactor

produced metabolites having a broader range of m/z values. As time went on, it appeared that the production of low molecular weight compounds decreased.

Using MZmine 2.10 it was possible to look for specific compounds, namely, the compounds isolated from EG4. The mass range for the mass spectrometer was only set for 150-1500; hence the smaller molecules such as uracil and indole-3-carboxaldehyde were unable to be detected. The dianiline, 249.1385 $[M+H]^+$, and the dibenzylimidazolidine, 253.17 $[M+H]^+$, were not found in any of the extracts, which led to the conclusion that EG4 stopped producing these compounds in the bioreactor. However, as seen in Figure 5-113, N-phenethylacetamide (164.107 $[M+H]^+$), N-acetyltyramine (180.1019 $[M+H]^+$), harman (183.0917 $[M+H]^+$), N-acetyltryptamine (203.1179 $[M+H]^+$) and the bis-indole (371.1012 $[M+H]^+$) were detected. N-phenethylacetamide had the greatest variation between fermentation vessels. There was an outlying peak at 84 hours from V2. Nevertheless, the other compounds were quite reproducible between vessels. Harman evidently was present in the media and the concentration decreased over time until 48 hours after which it stayed relatively constant. N-acetyltyramine was also present at a high intensity at 0 hours but it was clearly produced by EG4 as its concentration increased steadily over time. N-acetyltryptamine showed some fluctuations over time but the general trend was a slight increase in concentration. The bis-indole peaked at 12 hours followed by a gradual decrease in concentration. This implied that it could be a primary metabolite, essential to the growth of EG4, as it was being produced while EG4 was in the log phase.

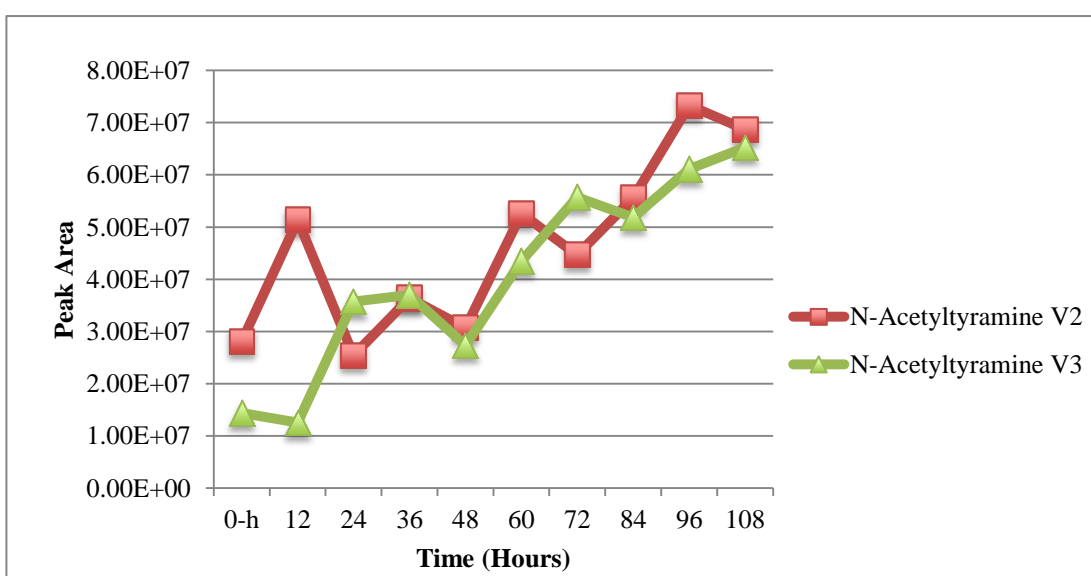
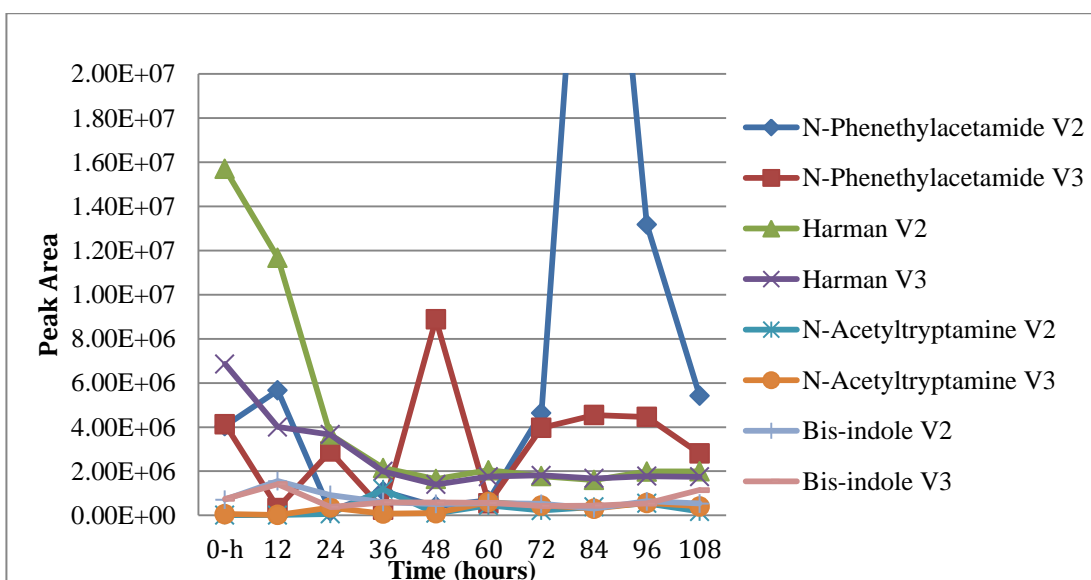


Figure 5-113: Peak areas of EG4 compounds produced during fermentation as determined by LC-MS. The production of N-phenethylacetamide fluctuated, ultimately increasing during the cell death phase. N-Acetyltryptamine showed a slight increase in concentration over time, whereas the peak area of harman decreased, implying that it was metabolised by EG4. Production of the bis-indole peaked during the lag phase, indicating that it was a primary metabolite. N-acetyltyramine was depicted in a separate graph as the intensities were much higher than the other compounds.

Table 5-45: Yields and activities of extracts of EG4 cultured in the bioreactor. Active extracts (% inhibition > 50%) are highlighted in grey. The MICs against *M. marinum* was not determined.

Sample (Vessel-hour)	Yield (mg)	<i>T. brucei</i>		% Inhibition of <i>M. marinum</i> (100 µg/mL)
		%Inhibition (20 µg/mL)	MIC (µg/mL)	
V2-0 (cell disrupter)	2.7	67.85	-	27.97
V2-0 (homogeniser)	2.3	91.30	50	45.7
V3-0	8.5	99.87	50	-5.36
V2-12	6.7	101.30	50	37.60
V3-12	14.9	100.58	25	12.04
V2-24	13.9	99.42	24	-7.54
V3-24	7.2	101.14	24	10.71
V2-36	10.7	101.15	25	15.49
V3-36	12.0	98.84	25	23.17
V2-48	12.9	99.51	50	12.92
V3-48	8.8	100.27	25	-13.15
V2-60	6.5	100.99	25	-30.63
V3-60	9.5	99.86	25	-33.39
V2-72	6.9	101.14	25	-16.99
V3-72	4.8	100.47	25	-1.18
V2-84	7.2	100.24	50	-20.81
V3-84	7.3	100.09	50	4.82
V2-96	5.7	99.24	50	-16.31
V3-96	7.8	100.45	25	-10.84
V2-108	5.7	100.49	25	-32.17
V3-108	7.0	99.15	50	-11.97

The bioreactor extracts proved to be much more active against *T. b. brucei* than the agar and shake flask extracts. The results suggested that the active compound was present in the samples from 0 until 108 hours. Conversely none of the extracts were active against *M. marinum*. Extracts of blank M1 broth containing 0.13% polypropylene glycol were assayed to determine whether or not the antifoam agent possessed antibiotic activity.

Table 5-46: Comparison of the inhibitory activity of M1 broth with and without polypropylene glycol. The active extract (% inhibition ≥ 50%) is highlighted in grey.

M1	%Inhibition against <i>T. b. brucei</i> (20 µg/mL) (n=2)	%Inhibition of <i>M. marinum</i> (100 µg/mL) (n=2)
(-) polypropylene glycol	-43.95	-5.8
(+) polypropylene glycol	104.7	-27.5

The addition of polypropylene glycol resulted in 104% inhibition of *T. b. brucei* and an increase in growth of *M. marinum*. The antifoam agent therefore resulted in false-positive anti-trypanosomal activity. As previously discussed, some of the compounds predicted to contribute to *M. marinum* activity were not produced by EG4 when grown in the bioreactor. It is evident that the conditions of EG4 cultivation in a bioreactor need to be optimised and a different antifoam agent used for succeeding fermentation experiments.

5.4 Discussion

The use of data processing software such as MZmine 2.10 greatly assisted the dereplication of the bacterial extracts sent from the University of Würzburg, making it possible to determine which strain produced the most number of compounds and what compounds, if any, had previously been identified. All bacteria were novel and were found to have biosynthetic genes that indicated that they were potential sources of bioactive secondary metabolites. Both EG4 and EG7, the most prolific producers of compounds out of the six bacteria, were isolated from the sponge *Callyspongia* aff. *implexa*. *C. implexa* is a marine sponge that has thus far only been found in the Red Sea (van Soest, 2013). To the best of the author's knowledge there have been no other studies involving microorganisms isolated from *C. implexa*. EG4 was selected for further work due to its abundance of metabolites.

EG4, a novel *Microbacterium* sp., is a fast-growing Gram-positive rod. A comparison of the NMR spectra of the extracts produced after various means of inoculation and culture showed that the major metabolites produced by a seven-day old EG4 broth culture that was inoculated from 5-day incubated bacteria or 10-day incubated bacteria were the same; the method of culture (i.e. stand or shake) had a more pronounced effect than the age of the inoculum. However, analysis of the heatmap of the LC-MS data indicated that, for the stand cultures, the one inoculated with a 10-day old inoculum resulted in more metabolites than that inoculated with the 5-day old inoculum. The 10-day_shake culture also had more intense blue bands than the 5day_shake culture; that is, the peak areas of the metabolites were larger, implying that a greater quantity of those metabolites was produced. There was also a

difference in the yield obtained from the extracts, as the shake cultures provided twice as much dried extract weight as the stand cultures. Shake cultures were therefore chosen for succeeding experiments. Fractionation of the extracts and subsequent bioassays showed that there were indeed many metabolites that were produced by EG4 and that some of these possessed anti-trypanosomal and anti-mycobacterium activities.

The metabolic profile of EG4 over a period of 15 days was analysed. Anti-mycobacterium activity was observed from Day 6 onwards. This coincided with increased production of *N*-(2-(1-*H*-indol-3-yl)ethyl)acetamide, also known as *N*-acetyltryptamine (**34**). This indolic compound is commonly found in plants and was first isolated from a microorganism in 1995 when it was isolated from *Streptoverticillium* sp., an actinomycete (Brambilla et al., 1995) and from *Corallococcus coralloides*, a myxobacteria (Bohlendorf et al., 1996). *N*-acetyltryptamine is also produced by marine bacteria such as *Roseivirga echinicomitans* KMM 6058^T (Oleinikova et al., 2006) and fungi (Li et al., 2003, Pedras et al., 2005, Park et al., 2006, Zou et al., 2011). It has also been isolated from *Streptomyces* sp. strain TN58 and has been shown to possess antifungal and antibacterial properties (Mehdi et al., 2009). Aside from antibiotic effects, the compound possesses anti-tumour activity, possibly due to its structural similarity to melatonin (Okudoh, 2010, Okudoh and Wallis, 2012). Other tryptamine derivatives have been found to have antibiotic activities, such as nematophin, a tryptamine-containing antibiotic with potent activity against some strains of MRSA (Paik et al., 2003). SAR studies have shown that the indole ring is not solely responsible for the anti-staphylococcal activity but it does contribute, as replacement of the indole group with a phenyl ring or an imidazole ring resulted in loss of activity (Himmler et al., 1998).

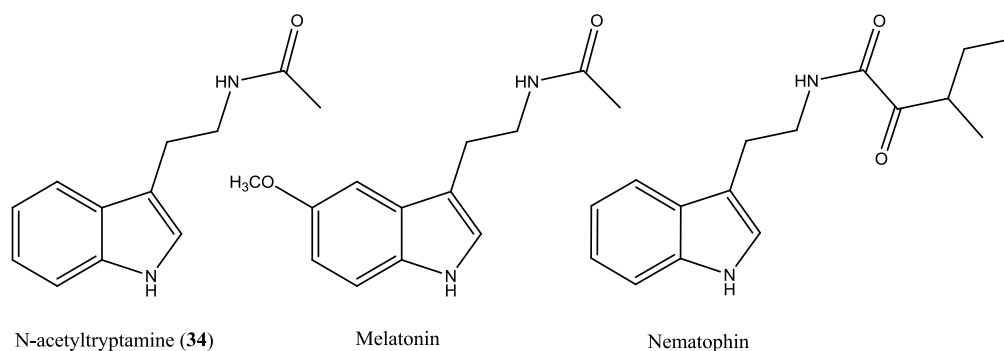


Figure 5-114: Structures of tryptamine derivatives possessing anti-tumour and antibiotic activity.

However, upon further experiments involving changing the culture media of EG4, it was determined that N-acetyltryptamine does not contribute to the anti-trypanosomal or anti-mycobacterial activity of EG4. N-acetyltryptamine was found in greatest quantities in the inactive samples. N-acetyltryptamine may have activity against other strains of bacteria and fungi but is not active against *T. b. brucei* and *M. marinum*.

Mass spectrometry showed that as time progressed there was an increase in the small molecules produced by EG4. The NMR spectra depicted the development of a diketopiperazine moiety. Diketopiperazines exhibit a wide range of biological activities, such as antibiotic, antiviral, antihyperglycaemic and antitumor activities, as well as the potent inhibition of plasminogen activator inhibitor -1 (PAI-1) and the blockage of μ -opioid receptors and calcium channels (Martins and Carvalho, 2007). The diketopiperazine cyclo-L-phenylalanine-L-serine (**41**) was found in the culture broth of EG4 from Day 3 onwards. It was also identified in one of the fractions after MPLC and silica gel chromatography, but was unable to be purified due to the small quantity of the fraction. No antimicrobial activity has been reported for cyclo-L-phenylalanine-L-serine. It is a known fungal metabolite and an intermediate in the production of gliotoxin and hyalodendrin (Boente et al., 1991, Kirby et al., 1978).

Two pathways have been identified for the biosynthesis of diketopiperazines. One involves small enzymes called cyclodipeptide synthases (CDPS). Examples of these are AlbC, which produces the antibacterial diketopiperazine albonoursin from *S. noursei*, YvmC, which produces pulcherriminic acid in *B. subtilis*, and Rv2275

which produces mycocyclosin, a compound believed to be necessary in the viability of *M. tuberculosis* (Figure 5-115). CDPSs use aminoacylated-tRNA (aa-tRNA) as substrates. The CDPS binds to the first aa-tRNA. It stores the aminoacyl moiety while releasing the tRNA. It then binds to the second aa-tRNA and catalyses the formation of a peptide bond between the two aminoacyl moieties (Belin et al., 2012). A BLAST search of AlbC, YvmC, and Rv2275 in the *M. testaceum* sequence yielded no homologues. CDPS sequences in general have only 19-27% sequence identity (Belin et al., 2012), however, so it is possible that another CDPS is present in the EG4 genome, although none were identified from *M. testaceum*. The other pathway of diketopiperazine biosynthesis is NRPS-dependent. Examples of diketopiperazines that are produced by NRPS proteins are erythrochelin and thaxtomin A, which are bacterial products, and gliotoxin, a fungal metabolite (Figure 5-115) (Belin et al., 2012). A BLAST search was performed using the *M. testaceum* StLB037 genome to detect homologues of NRPSs that are involved in the biosynthesis of these diketopiperazines. No homologues were identified for GliK, the protein responsible for gliotoxin biosynthesis in the fungus *Aspergillus fumigatus*. A search for TxtA and B, which are responsible for the production of thaxtomin A in *S. ascidiscabei* (Healy et al., 2000) yielded NRPS modules with 36% and 38% identities, respectively, and E-values of 2E-46 and 2E-50, respectively. The conserved domains that were putatively identified included the adenylation domain of an NRPS, an S-adenosylmethionine-dependent methyltransferase, phosphopantetheine attachment sites, condensation domains and an HxxPF repeated domain. The adenylation domain, the phosphopantetheine attachment site and the condensation domain are necessary in the biosynthesis of diketopiperazines through the NRPS-dependent pathway (Belin et al., 2012). Although the similarities of the *M. testaceum* sequence to that of TxtA and B were not very high, it is more probable that the diketopiperazines of EG4 are produced by the NRPS-pathway as opposed to the CDPS pathway.

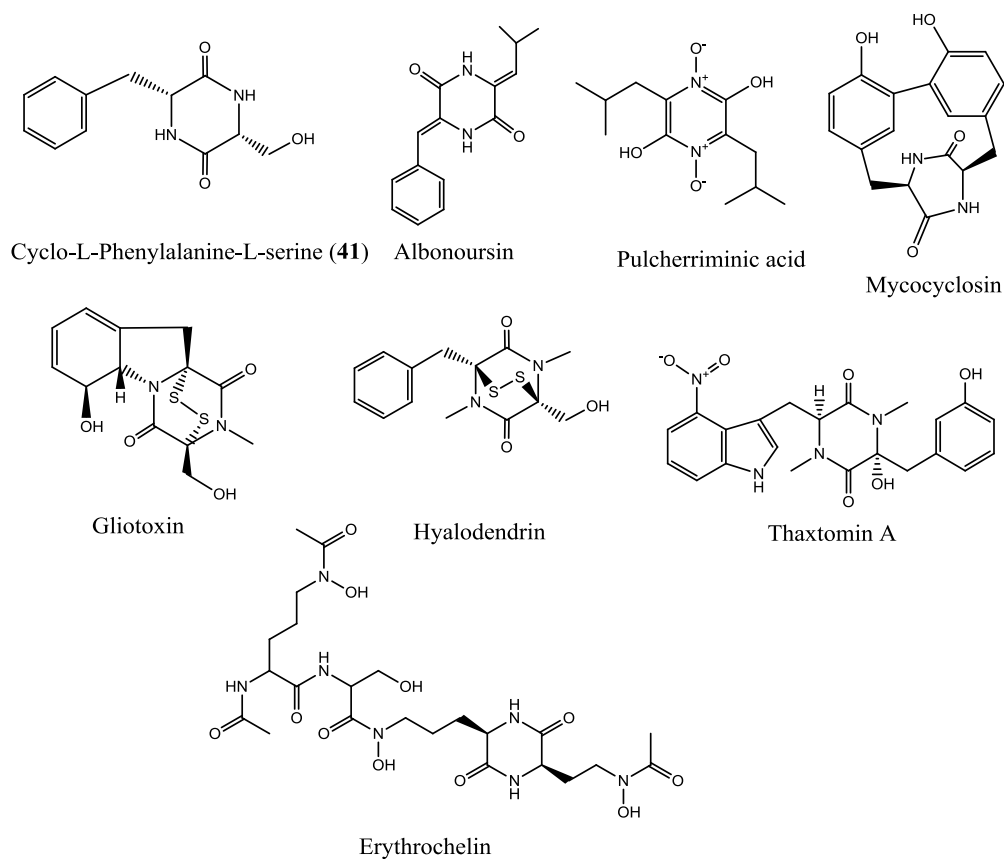
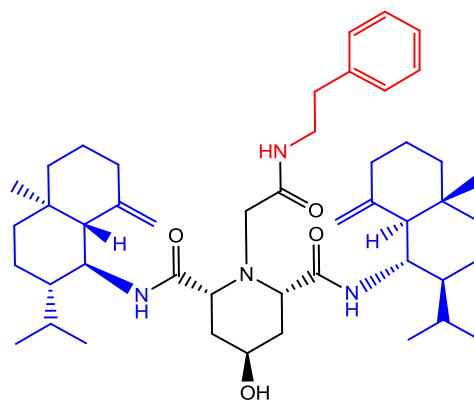


Figure 5-115: Structures of diketopiperazines. Cyclo-L-phenylalanine-L-serine (**41**) was detected in EG4 extracts. Albonoursin, pulcherrimic acid and mycocyclusin are produced by CDPSs whereas the fungal metabolites gliotoxin and hyalodendrin and the bacterial metabolites thaxtomin A and erythrochelin are produced by NRPSs.

Upon larger scale culture of EG4, the crude extracts began to show both anti-trypanosomal and anti-mycobacterium activity. The extract was fractionated using MPLC. N-Phenethylacetamide (**21**) was isolated but this compound proved to be inactive in the assays conducted. It has previously been isolated from a marine *Bacillus subtilis* and from seaweed (Lu et al., 2011) as well as from terrestrial *Streptomyces* sp. (Zhao et al., 2007). Freshwater *Bacillus* sp. produced both N-phenethylacetamide and N-acetyltryptamine (Maskey et al., 2002). N-phenethylacetamide is present as a substructure of the sponge sesquiterpenoid halichonadin L from an Okinawan sponge, *Halichondria* sp. The biogenetic pathway proposed for the synthesis of halichonadin L involves the addition of phenethylamine to an intermediate composed of halichonadin C, glyoxylic acid and lysine (Tanaka et al., 2012), and phenethylamine is listed on the KEGG database as a product of the hydrolysis of N-phenethylacetamide (Kanehisa and Goto, 2000, Kanehisa et al.,

2012). It may be that the sponge uses the N-phenethylacetamide synthesised by its symbiotic bacteria to produce this sesquiterpenoid.



Halichonadin L

Figure 5-116: Structure of halichonadin L. The halichonadin C and phenethylamine moieties are highlighted in blue and red, respectively. (Tanaka et al., 2012)

Another small molecule produced by EG4 was N-acetyltyramine (**29**). This compound was not purified but was proven to be present in bioactive fractions by NMR analysis and MS/MS fragmentation. N-acetyltyramine has previously been isolated from cultures of marine *Streptomyces* sp. (Hernandez et al., 2004, Sobolevskaya et al., 2007) and other marine bacteria such as *Pantoea agglomerans* (Gang et al., 2013). It has also been isolated from *S. griseus* and *M. tuberculosis*. No antimicrobial activity has been reported for N-acetyltyramine (Maehr and Berger, 1969).

EG4_215-392_B was identified as di(2-propylpentyl) phthalate. It possessed activity against both *T. brucei* and *M. marinum*, but it was found in both the blank media as well as the solvent blank. Although phthalates are commonly found in nature from sources such as algae (Sastry and Rao, 1995), plants (Rameshthangam and Ramasamy, 2007) and bacteria (Hoang et al., 2008, Al-Bari et al., 2005), they are also frequently used as plasticisers and are found in a variety of synthetic substances (George and Prest, 2002). These phthalates reported from these studies also have a range of bioactivities including antibacterial, antifungal and antiviral activity. It is likely that the phthalate isolated originated from various plastics used, including the

plastic containers used to store the media components as well as the plastic pipette tips used for solvents.

Indole-3-carboxaldehyde (**13**) (present in 215-392_N and 615-626_6) has previously been isolated from the sponge *Dysidea etheria* (Cardellina et al., 1986), algae (Ovenden et al., 2012), a marine pseudomonad (Wratten et al., 1977), and a marine *Bacillus* sp. (Martinez-Luis et al., 2012). It showed selective activity against *T. cruzi* compared to other protozoans such as *Plasmodium falciparum* and *Leishmania donovani* (Martinez-Luis et al., 2012). Indole-3-carboxaldehyde is an analogue and oxidative metabolite of indole-3-carbinol and indole-3-acetonitrile (Wortelboer et al., 1992). All are commonly isolated in plants from the Cruciferae family, particularly the *Brassica* genus (Devys and Barbier, 1991, Aggarwal and Ichikawa, 2005).

The BioCyc website (SRI international, USA) is a collection of pathway/genome databases (PGDB) that predicts metabolic pathways of sequenced organisms based on their genomic data. One such organism is *Microbacterium testaceum* StLB037. As EG4 is also a *Microbacterium* species but has not been sequenced, *M. testaceum* StLB037 was the organism database used to search for EG4 metabolites and pathways. Indole-3-carboxaldehyde was not found in the database, however; the closest structural analogue was indole-3-acetaldehyde.

Also present in 215-392_N was a monoacyl glycerol with a C-18 side chain. Monoacyl glycerols are known to have antimicrobial activity, particularly against Gram-positive bacteria and yeast, in addition to antitumour and haemolytic activity (Conley and Kabara, 1973). Monoacyl glycerols with chain lengths less than C₁₆ were proven to be more active than their free fatty acid counterparts (Kabara et al., 1977); however, di- and triacyl glycerols were not (Kabara et al., 1972). The activity of monoacyl glycerols against *S. aureus* varied according to the length of the side chain with the long-chain monoacyl glycerol (C18) being the least active: C12>C8>C14>C18 (Wakabayashi et al., 2002).

There are several proposed mechanisms of action for the antibacterial activities of fatty acids and monoglycerides. One theory postulates that cell membrane permeability and cell metabolism are affected (Kabara et al., 1972). Glycerol

monolaurate (GML) is also capable of inhibiting the production of exotoxins by streptococci, *S. aureus* and *B. anthracis* at concentrations less than those that inhibit the growth of the microorganisms (Schlievert et al., 1992, Vetter and Schlievert, 2005). GML, like lauric acid, does this by affecting the signal transduction of the cells (Ruzin and Novick, 2000). It is hypothesized that GML binds to the cell membrane and thereby causes changes to the structure of the transmembrane proteins involved in signal transduction (Projan et al., 1994). More recent research has also shown glycerol monocaprate (monocaprin) causes the disintegration of the cell membrane and cytoplasmic granules of *S. aureus* without evident effects on the cell wall (Bergsson et al., 2001).

Various fatty acids affect *Mycobacterium* sp. in different ways. Saturated fatty acids, aside from capric and lauric acid, are in general not inhibitory towards fast-growing mycobacteria. Unsaturated fatty acids, however, were much more active (Saito et al., 1984). Oleic acid and an ester of oleic acid were found to promote the growth of species such as *M. kansasii*, *M. marinum* and other pigment-producing mycobacteria. Lauric acid also promoted the growth of *M. kansasii* (Schaefer and Lewis, 1965). In contrast, *M. avium* was susceptible to capric, lauric, oleic and linolenic acids, although the susceptibility varied depending on the strain. It was found that the susceptibility of the *M. avium* strains were inversely correlated with their virulence; that is, the more virulent strain was the least affected by the fatty acids (Saito and Tomioka, 1988). This matched the observation that the pathogenic group IV mycobacteria strains, *M. fortuitum* and *M. chelonae* were the most resistant to fatty acids (Saito et al., 1984). The fraction 215-392_N caused 45% growth inhibition of *T. b. brucei* and 80% inhibition of *M. marinum*. As EG4_215-392_N was a mixture of indole-3-carboxaldehyde and 1-monostearin it is unknown how much each compound contributed to the activity.

It is also worth noting that one class of antibacterial agents includes the lipopeptides, which are composed of a fatty acid moiety attached to a peptide. The structures of several lipopeptides are shown in Figure 5-117. The best-studied lipopeptide is daptomycin, which is currently used to treat Gram-positive infections, including methicillin-resistant *Staphylococcus aureus* (MRSA) and vancomycin-resistant

Enterococcus faecalis (VRE). It acts through the insertion of the lipophilic tail into the cell membrane, resulting in membrane depolarisation and the release of potassium ions (Steenbergen et al., 2005). Other examples of lipopeptides are the lipopeptide biosurfactants (LPBS), such as pumilacidin and surfactin. Pumilacidin is a group of seven (A-G) antiviral LPBSs produced by *Bacillus pumilus* (Naruse et al., 1990), whereas surfactin was first isolated from *B. subtilis*. There are three families of LPBS from *Bacillus* strains: surfactin (to which surfactin and pumilacidin belong), fengyn, and iturin (Roongsawang et al., 2011). Derivatives of pumilacidin were putatively identified in the agar cultures of EG4, but not in the broth cultures. The biosynthetic gene cluster of surfactin is *srfA*. It encodes for SrfAA, SrfAB, and SrfAC, which are NRPSs, and SrfA-Te, which is a type II thioesterase (Te) (Roongsawang et al., 2011). A BLAST search was conducted to find homologous proteins in the sequence of *M. testaceum* StLB037. One NRPS module from *M. testaceum* was found to be homologous to SrfAA, SrfAB, and SrfAC. The alignments of these sequences can be found in Appendix VIII. The identity similarities were not very high, however. It is possible that EG4 contains proteins that are more similar to the SrfA synthetases than *M. testaceum*, or that EG4 produces LPBSs of a different family.

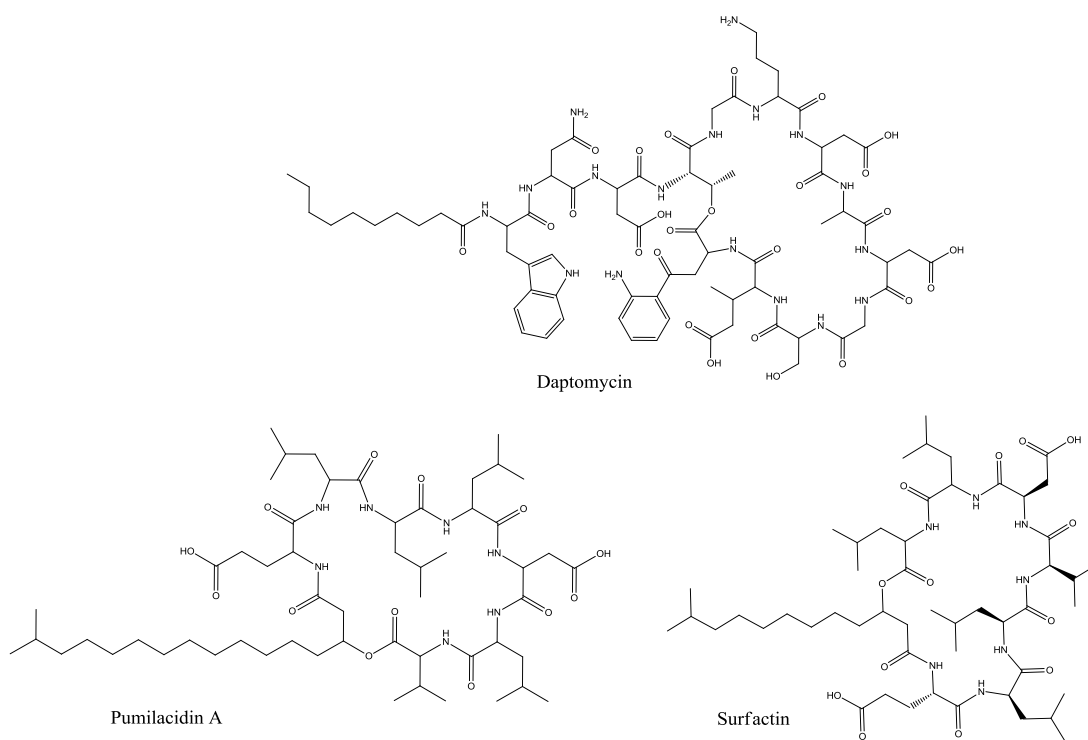


Figure 5-117: Structures of lipopeptides.

Harman (**46**), or 1-methyl- β -carboline, (615-626_2) was isolated using preparative TLC. Analysis of the M1 blank medium, however, showed the presence of harman; it is therefore likely that the harman isolated was from the medium and not a product of EG4. Harman is produced by other strains of bacteria such as *Pseudomonas* sp. and *Enterococcus* sp. (Aassila et al., 2003, Kodani et al., 2002). Harman is also produced by plants, fungi, mammals, and is also found in food, alcoholic beverages and tobacco smoke (Pfau and Skog, 2004). It is biologically active, having antibacterial, antifungal, anti-protozoal, anti-algae, anti-parasitic and anti-proliferative effects (Bratchkova et al., 2012, Arshad et al., 2008, Aassila et al., 2003, Kodani et al., 2002, Di Giorgio et al., 2004). Harman is active against both *T. cruzi* and *T. b. rhodesiense*, although the mechanism of action is unclear as the former could be due to respiratory chain inhibition and the latter to DNA intercalation (Rivas et al., 1999, Freiburghaus et al., 1996). The anti-*Leishmania* effects are caused by the intercalation of the planar structures with DNA (Di Giorgio et al., 2004). In this study, however, harman inhibited the growth of *M. marinum* by 83% but showed very small inhibitory activity against *T. b. brucei*. An earlier study of β -carboline

alkaloids against *T. cruzi* found harmaline and harmalol to be more active than harman, which in turn was more active than other β -carboline alkaloids that did not possess the 3,4 unsaturation on the pyridyl ring. It was therefore suggested that the 3,4 unsaturation was related to activity and that substitution of a methoxy or hydroxyl group at C-7 increases the activity against *T. cruzi* (Cavin et al., 1987).

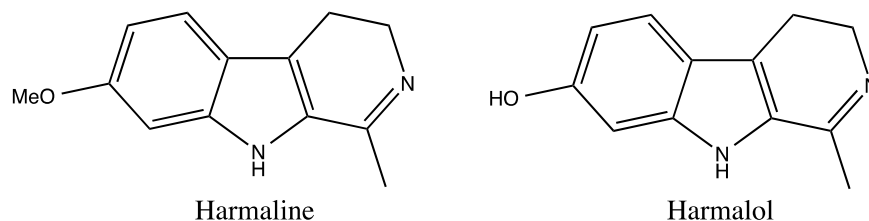
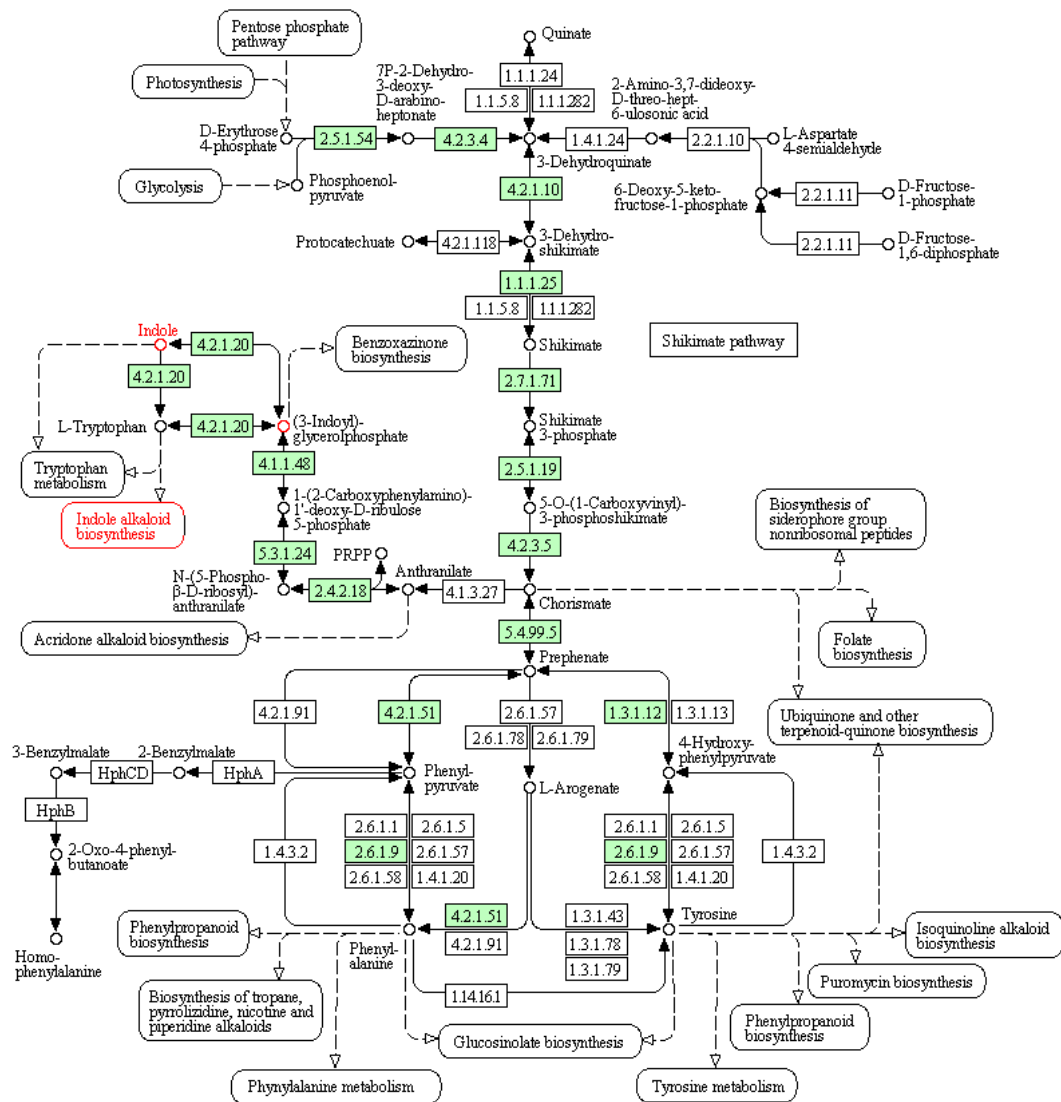


Figure 5-118: Structure of harmaline and harmalol. These are β -carboline alkaloids that are more active than harman against *T. cruzi* (Cavin et al., 1987).

β -carbolines are formed via Pictet-Spengler condensation of indoleamines, such as tryptamine, and aldehydes, such as acetaldehyde. The resulting product undergoes further metabolism to create a series of β -carboline alkaloids (Tse et al., 1991). An overview of indole alkaloid biosynthesis can be seen within the phenylalanine, tyrosine and tryptophan pathway in Figure 5-119. The green boxes represent genes of *M. testaceum* that encode for enzymes required for the pathway. The β -carboline alkaloids and indole derivatives are products of tryptamine in the shikimate pathway (Figure 5-120) (Kanehisa and Goto, 2000, Kanehisa et al., 2012).

PHENYLALANINE, TYROSINE AND TRYPTOPHAN BIOSYNTHESIS



00400 11/18/13
 (c) Kanehisa Laboratories

Figure 5-119: Phenylalanine, tyrosine and tryptophan pathway. Many of the genes that code for enzymes required for indole alkaloid biosynthesis and tryptophan metabolism were identified in *M. testaceum*. These are represented by the green boxes. The part of the pathway pertaining to indole alkaloid biosynthesis is in red. (Kanehisa and Goto, 2000, Kanehisa et al., 2012)

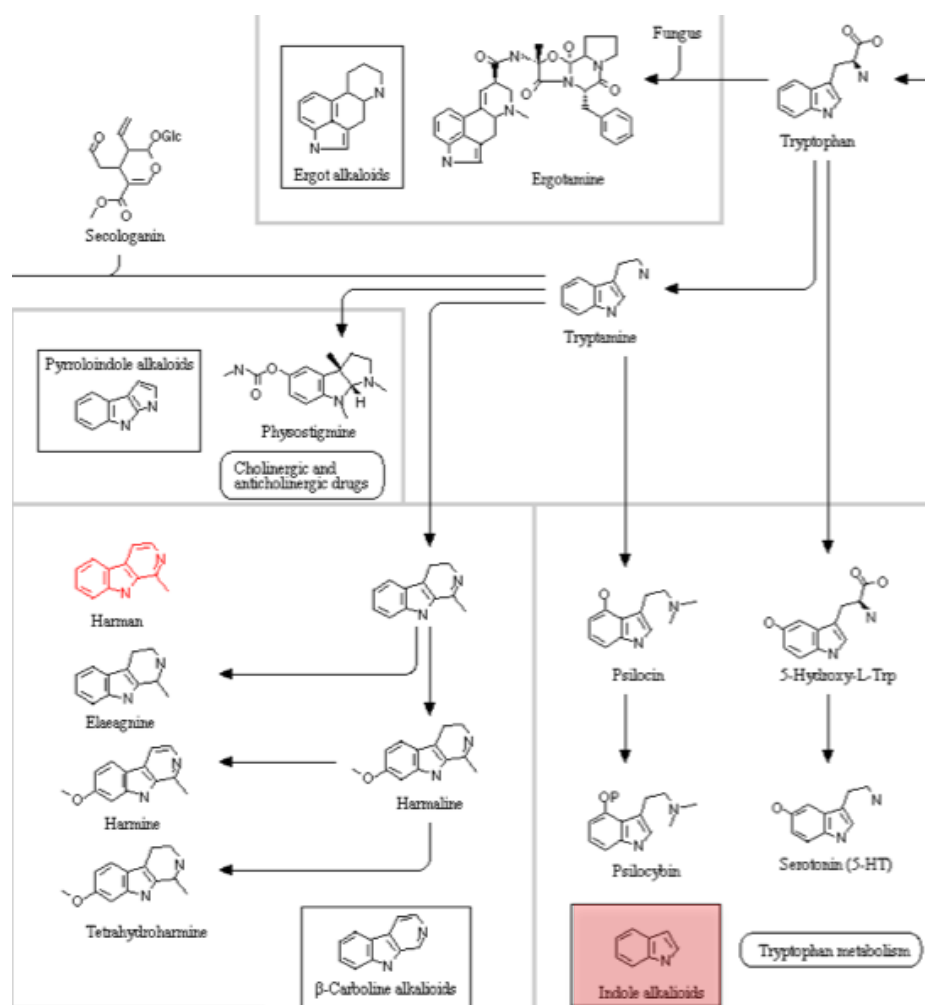


Figure 5-120: A closer look at alkaloid biosynthesis in the shikimate pathway. Harman and indole derivatives are highlighted in red (Kanehisa and Goto, 2000, Kanehisa et al., 2012).

Uracil (615-626_4) was also isolated from the crude extract. KEGG shows that *M. testaceum* has a gene for uracil phosphoribosyltransferase, an enzyme that catalyzes the reaction of uridine-5'-monophosphate and diphosphate to form 5-phospho- α -D-ribose 1-diphosphate and uracil. Uracil is involved in pyrimidine metabolism, as seen in Figure 5-121.

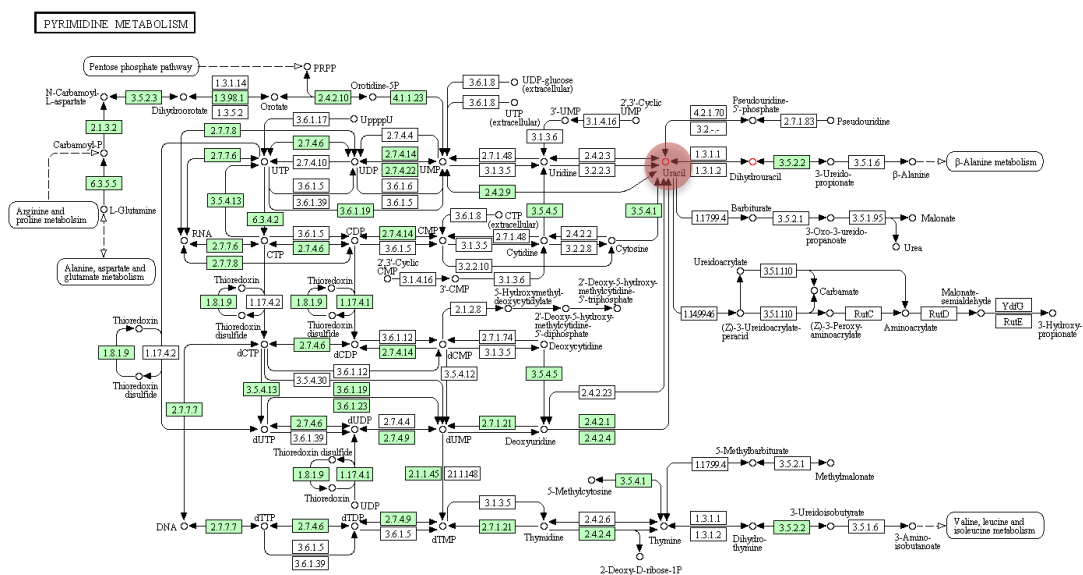


Figure 5-121: Pyrimidine metabolism pathway in *M. testaceum*. Uracil is highlighted in red. Boxes in green are enzymes that are present in *M. testaceum* (Kanehisa and Goto, 2000, Kanehisa et al., 2012).

Two structures were proposed for EG4_615-626_6. These were 4,4'-(cyclopenta-3,5-diene-1,3-diyl)dianiline and 4,4'-(cyclopenta-2,4-diene-1,1-diyl)dianiline, both with a molecular formula of $C_{17}H_{16}N_2$ and an m/z of 249.138 $[M+H]^+$. The exact structure of the compound was unable to be determined due to the low quantity of material recovered (0.4 mg). As such, the compound was not sufficiently purified and a number of essential NMR experiments, such as J-resolved, ^{13}C , HMBC and HMQC could not be performed.

Bacterial metabolites containing aniline moieties are not uncommon; members of the genus *Streptomyces* are particularly prolific in producing small molecules (Guan et al., 2005, Wang et al., 2010, Potterat et al., 1994) as well as polyketides and macrolides containing phenylamine substructures. It has been postulated that the small molecules are precursors of the macrolides (Guan et al., 2005). Norpicacetin is an antibacterial compound (Evans and Weare, 1977), whereas hamycin, trichomycin A and B, and levorin A2 exhibit antifungal activity (Shadomy et al., 1969, Komori, 1990, Kozhuharova et al., 2008).

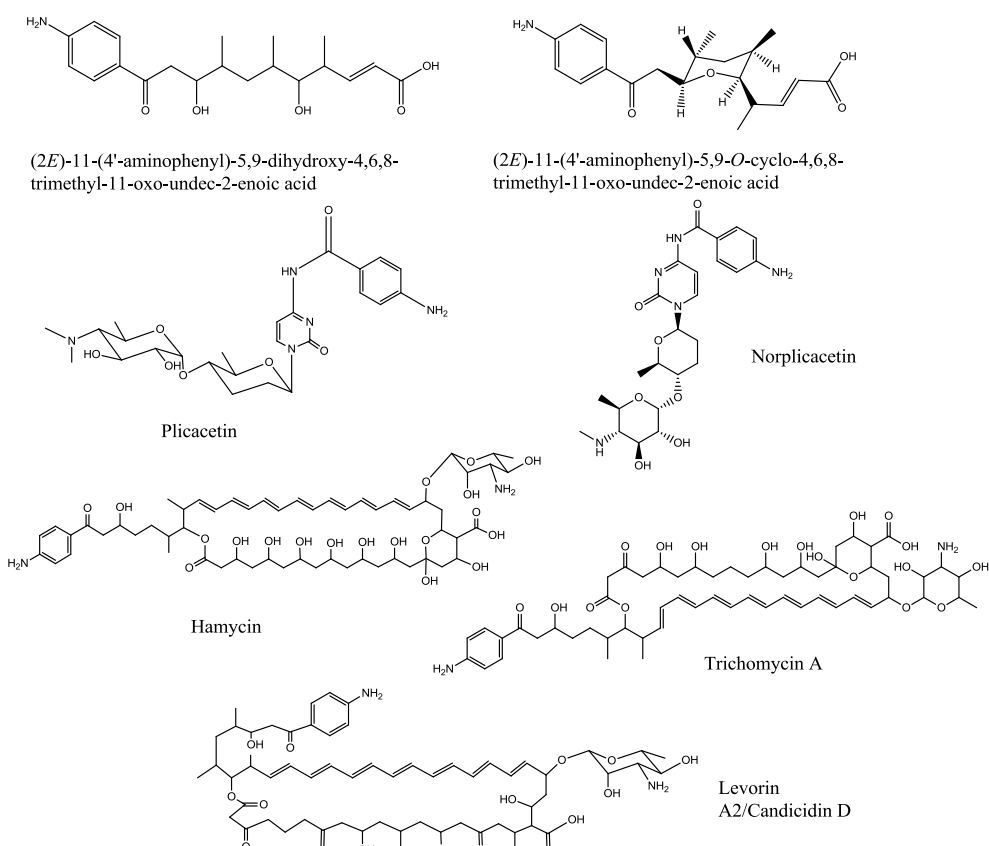


Figure 5-122: Examples of small molecules and macrolides produced by *Streptomyces* sp. that possess an aniline moiety. (Guan et al., 2005, Evans and Weare, 1977, Komori, 1990, Kozuharova et al., 2008, Haskell et al., 1958)

1,4-Dibenzylimidazolidine is a novel compound that was not found in any of the databases. It was, however, highly active against *T. b. brucei*, *M. marinum* and *N. farcinica*, inhibiting the growth of the microorganisms by 97%, 100% and 100% respectively compared to their corresponding control drugs.

After the isolation of compounds, EG4 was grown on variations of M1 media in an attempt to optimise the production of bioactive metabolites. EG4 is a halotolerant bacterium as it was able to grow without the presence of salt (WOSW). The extract proved to have greater anti-trypanosomal activity and similar anti-mycobacterium than that of EG4 grown on M1 that contained salt. Glucose was tried as an alternative carbon source due to the difficulties in working with starch. Starch is less soluble than glucose and hence causes turbidity in the media. This makes determining the growth curve of the bacteria using UV spectroscopy difficult, and the measurement of the bacterial biomass by filtration impossible due to the clogging of the filter paper by starch. In the small-scale experiment using variations of M1

agar, the use of glucose in the media resulted in the production of fewer metabolites as shown by the proximity of glucose_EG4 to the blank medium in the score plot (Figure 5-88). In spite of this, the anti-trypanosomal activity of EG4 on M1 with glucose was greater than that of EG4 grown on regular M1 that contained starch as a carbon source. Conversely, the anti-mycobacterial activity of EG4 on M1 with glucose decreased. This indicated that, at least in the case of EG4 grown on glucose, the metabolites responsible for anti-trypanosomal activity were different from the metabolites responsible for anti-mycobacterium activity.

Glucose has been known to interfere with antibiotic production due to carbon catabolite regulation (CCR), a regulatory mechanism that ensures that the microorganisms preferentially consume the most readily available carbon source; that is, the source that is easiest to catabolise and thus provides the most energy for growth. Actinomycetes such as *Streptomyces* sp. are susceptible to CCR. For example, glucose inhibits the production of some aminoglycoside antibiotics, as well as doxorubicin (Sanchez and Demain, 2002). In the case of EG4 the anti-trypanosomal compounds were still being produced despite the substitution of starch by glucose, but the production of the anti-mycobacterial compounds may have been affected by CCR.

N-Acetylglucosamine (GlcNAc) has been found to stimulate antibiotic production in *Streptomyces* species by acting on the DasR protein, a repressor protein belonging to the GntR family of transcription factors (Rigali et al., 2008). As the genome of EG4 has not been sequenced, a BLAST search was conducted using *M. testaceum* StLB037 to find a homologue of the DasR protein from *S. coelicolor* A3(2). The transcriptional regulator detected in the *M. testaceum* genome had 30% identity and an E-value of 4E-14. The aligned sequences can be seen in Appendix VII. An analysis of the conserved domains showed that portions of the WHTH_GntR (winged helix-turn-helix) DNA binding domain and a UTRA (UbiC transcription regulator-associated domain) were similar, indicating that a DasR homologue was indeed present in *M. testaceum* StLB037. A homologue of DasR is also therefore likely to be present in EG4, accounting for the increased anti-trypanosomal and anti-mycobacterial activity of the extract of the EG4 culture when GlcNAc was added

after the autoclaving of the medium. However, the addition of GlcNAc prior to autoclaving resulted in a decrease in both activities; it was therefore evident that GlcNAc is not stable upon autoclaving and should be added to the medium after autoclaving to have a positive effect on the production of bioactive metabolites.

Multivariate analysis was performed to identify the metabolites having the greatest contribution towards the bioactivity of the extracts. The majority of the metabolites that were predicted to be contributors were the same for both anti-trypanosomal and anti-mycobacterial activity. Most of these were unidentified, aside from naphthoquinone 2 and AH-17 that were putatively identified as contributors to anti-trypanosomal activity. Naphthoquinone 2 has previously been isolated from *Streptomyces* sp. and had weak activity against Cdc25A phosphatase, an enzyme involved in cell cycle progression (Kulanthaivel et al., 1999). Naphthoquinones have been reported to possess antiprotozoal activity, including anti-malarial, anti-leishmanial and anti-trypanosomal effects (Bringmann et al., 2000, Samant and Chakaingesu, 2013). AH17 was first isolated from *Spirillospora* strain 719. It possesses activity against both Gram-negative and Gram-positive bacteria, fungi and yeast (Hacene and Lefebvre, 1995). Elastatinal was putatively identified as a contributor to anti-mycobacterial activity. It is a microbial protease inhibitor that was isolated from *Streptomyces griseoruber*. It specifically inhibits elastase and has no antibacterial or antifungal activity, although the strains on which this compound was tested were not mentioned (Umezawa et al., 1973). It is cytotoxic to Chinese hamster cells (Paul and Fujiwara, 1981).

In order to make media preparation easier and less time consuming, an experiment was set up to determine if a change from artificial seawater to a pre-formulated aquarium salt, Royal Nature, had an effect on the metabolic profile and bioactivity of EG4. The experiment showed that Royal Nature had no detrimental effect on bioactivity; in contrast, the bioactivity appeared to increase slightly, albeit not significantly. A scatter plot of the LCMS results (Figure 5-98) showed that although the metabolites produced by EG4 remained the same with both salts, the metabolites were being produced in greater quantities when Royal Nature was used. The compounds isolated from EG4 were unaffected by the type of salt used. It is possible

that this increase in the quantity of the metabolites was caused by the decrease in salt, as the concentration of salt present in the broth when RN was used was approximately half of what was present in ASW.

The cultivation of EG4 in various M1 broths in shake flask cultures resulted in the loss of production of some metabolites previously identified in the agar cultures as contributors to anti-trypanosomal and anti-mycobacterial activity. All of the extracts possessed some degree of activity against *T. b. brucei* and, as such, OPLS-DA was unable to be performed on the extracts to identify contributors to anti-trypanosomal activity. Some of the blank media proved to be active and thus OPLS-DA was executed on the blank media. Harman (**46**), norharman (**44**), 3-(hydroxyacetyl)indole (**45**) and methyl indole-3-carboxylate (**15**), were identified as correlating with the anti-trypanosomal activity. Although no mention of anti-trypanosomal activity of methyl indole-3-carboxylate was found in the literature, the former three compounds all have been determined to possess activity against *T. cruzi* (Cavin et al., 1987, Rivas et al., 1999, Martinez-Luis et al., 2012). The anti-mycobacterial activity of EG4 in shake flask cultures was not evident because the blank M1 media had the same activity. Analysis of the previously isolated compounds produced by EG4 showed that these compounds were more prevalent in the M1, M1-RN and M1 50G50S extracts. The selection of the most appropriate media therefore depends on the objective for up-scaling. If the objective is the isolation of 1,4-dibenzylimidazolidine or one of the other previously isolated compounds, M1 without salt (M1-RN) or M1 with 50% starch, glucose and salt (M1 50G50S) would be suitable media as the compounds were produced in greatest quantities in these media and the reduction in salt would be beneficial for industrial upscaling. If the objective is the isolation of the aniline-type compounds (m/z 249.138 $[M+H]^+$), M1 is the best medium as EG4 grown on this medium produced the greatest quantity of that compound. However, M1 with glucose would be the most suitable medium for upscaling to continue the isolation of anti-trypanosomal compounds as the anti-trypanosomal activity of these extracts was the highest despite the fact that the compounds previously isolated were present in smaller quantities, thus indicating that there are other bioactive compounds to be discovered.

In this first attempt to grow EG4 in a bioreactor, the culture conditions were monitored but not adjusted or maintained. The bacteria grew rapidly, utilizing the available oxygen quickly as reflected in the DOT measurement (Figure 5-105). The decline in the DOT implied the lag and log phases of bacterial growth as the bacteria were then dividing and therefore metabolised the oxygen quickly. The subsequent rise in the amount of DO indicated that the cells were not dividing as rapidly and that the rate of death of the cells was greater than rate of division. This chart correlated with the growth curves obtained by counting the cells with the haemocytometer and by using the spread plate method (Figure 5-107). EG4 was in the lag phase before the 12th hour, utilizing the oxygen and resulting in a decrease in DOT. The log phase occurred between 12-24 hours, and the DOT levels began to rise again during the stationary phase as cell growth slowed. It was more reliable to use the haemocytometer as the spread plate method was vulnerable to contamination.

Bioreactor samples were collected for metabolite extraction to determine when anti-trypanosomal or anti-mycobacterial activity occurred; however, anti-trypanosomal activity was present in all extracts whereas anti-mycobacterial activity was absent in all extracts. Indeed, the metabolic profile looked quite different from that obtained from the shake flask cultures. This was not unexpected as the growth conditions were different from that in the shake flask. Molecules with lower m/z ratios were more prominent in the shake flask cultures whereas higher molecular weight compounds were more abundant in the bioreactor samples (Figure 5-112). Further experiments confirmed that the anti-trypanosomal activity seen in the extracts was a result of the presence of polypropylene glycol. For future fermentations it is recommended that no antifoaming agent be used if the metabolic profile is being studied.

EG4 was a prolific producer of indole alkaloids and other tryptophan derivatives. Further purification must be performed on the other active fractions. Other future experiments may include adding phenylalanine to the media to promote production of cyclic peptides as well as the optimisation of EG4 in a bioreactor once a suitable broth has been decided upon from the shake flask experiments.

Chapter 6 Conclusions and Future Work

6. Conclusions and Future Work

The primary objectives of this project were to use metabolomics to facilitate the isolation of antibiotics from a marine sponge, *Haliclona simulans*, and from sponge-associated bacteria. The sponge and two sponge-associated bacteria, SM8 and EG4, proved to be rich sources of bioactive compounds. Chromatographic methods were successfully applied for the isolation and purification of metabolites. The isolation work was guided both by the bioassay results as well as by metabolomic methods which identified target molecules. Dereplication of sponge-associated bacteria was performed using high-resolution mass spectrometry. Metabolic profiling and optimisation of culture conditions to enhance the production of bioactive secondary metabolites were performed using high-resolution analytical techniques, such as NMR and mass spectrometry, and multivariate analysis, such as PCA and OPLS-DA. The use of these techniques gave a glimpse into the metabolic changes that occurred due to varying growth conditions, allowing decisions to be made as to the best medium to be used for the large scale culture of the bacteria.

6.1 Conclusions

6.1.1 Isolation of Bioactive Steroids from *H. simulans*

Three steroids were isolated from *H. simulans* using cold extraction and flash chromatography. The Reveleris[®] Flash Forward system proved to be more efficient at purifying the compounds. Three pure steroids were obtained from the Reveleris fractionation, as opposed to the two steroids that were isolated using the BÜCHI Sepacore <<Easy Synthesis>> Purification System.

24-Methylenecholesterol, 24-vinyl-cholest-9-ene-3 β ,24-diol, and 20-methyl-pregn-6-en-3 β -ol, 5 α ,8 α -epidioxy were the three sterols isolated from *H. simulans*. The former is widely distributed in sponges whereas the latter two are novel. 24-Vinyl-cholest-9-ene-3 β ,24-diol was the most active against *T. brucei* with an MIC of 4.58 μ M followed by the epidioxy sterol which had an MIC of 9.01 μ M. 24-Methylenecholesterol was the least active anti-trypanosomal steroid (MIC: 11.87 μ M). It was, however, the most active against *M. marinum* (MIC: 156.90 μ M). 24-vinyl-cholest-9-ene-3 β ,24-diol was the next most active (MIC: 233.44 μ M), with the

epidioxy sterol being the least active against *M. marinum*. 24-Vinyl-cholest-9-ene-3 β ,24-diol showed no cytotoxic effects against normal human fibroblasts (Hs27) at concentrations of up to 100 μ M. However, both 24-methylenecholesterol and 5 α ,8 α -epidioxy-20-methyl-pregn-6-en-3 β -ol caused changes in cell morphology at 100 μ M. The former was the most cytotoxic, having an IC₅₀ of 58 μ M. This value is still higher than the MIC for anti-trypanosomal activity, thus it may still be considered as a lead compound for anti-trypanosomal drugs. The sterols all differ in their steroid nuclei and side chains, which is not unexpected as sponges are well-known for the diversity of steroids which they possess.

6.1.2 Identification of Bioactive Compounds from SM8

The genus *Streptomyces* is known for producing a large number of antibiotics. The extracts of SM8, a *Streptomyces* sp. isolated from *H. simulans*, did indeed possess antibacterial, antifungal and anti-calcineurin activity. Polyhydroxylated saturated fatty acids were identified as the major components present in the antibacterial fractions. Metabolomic techniques putatively identified members of the antimycin A family as those responsible for the antifungal activity of SM8. This was confirmed by comparison of the crude extracts and antifungal fractions with an antimycin A standard using NMR and LC-HRFTMS. A gene knockout study also validated the findings as SM8 from which the *antC* gene had been deleted had much less antifungal activity than SM8 that produced antimycins.

For the isolation of antimycins, oatmeal medium would be the optimal medium as SM8 grown on OM produced the most antimycins. Starch-yeast extract-peptone (SYP) medium may be used if antifungal compounds other than antimycins are desired for isolation.

Two isomeric butenolides, 4,10-dihydroxy-10-methyl-dodec-2-en-1,4-olide (butenolide 1) and 4,11-dihydroxy-10-methyl-dodec-2-en-1,4-olide (butenolide 2) were isolated from the crude extract. They co-eluted, hence they were isolated together, but in differing ratios in various fractions. Butenolide 2 was identified, using NMR spectroscopy, as the isomer that provided anti-calcineurin activity. The butenolides also produced mild quorum signalling activity when tested with

Chromobacterium violaceum CV026. A third butenolide, 4-hydroxy-10-methyl-11-oxo-dodec-2-en-1,4-olide (butenolide 4) was also isolated. It too possessed mild anti-calcineurin activity.

6.1.3 Comparison of the Metabolomes of SM8 and *H. simulans*

Metabolites produced by SM8 were identified in the extract of *H. simulans* using LC-HRFTMS. The antimycins A1 and A3, in addition to butenolides 1 and 2, were found in the sponge extract. This confirmed that SM8 is associated with *H. simulans*. Additionally, it provided insight into what metabolites were being produced by SM8 while it was within the sponge. As the environment in which SM8 is cultured in the laboratory differs from the environment within the sponge, the metabolome of the bacterium would also differ from when it is in its natural environment. The identification of SM8 metabolites within the sponge extract can lead to the elucidation of the ecological roles of the metabolites. No steroids were identified in the SM8 metabolome using GCMS, implying that the steroids are produced by the sponge itself or by associated fungi. However, thujaketone, a compound putatively identified from the SM8 extract using GC-MS, has the same carbon skeleton as ergosterol and could be an example of a small molecule produced by an endosymbiont that is utilised by the host sponge to produce larger compounds.

6.1.4 Dereplication of Marine Actinomycetes

LC-HRFTMS was successfully applied in the dereplication of six marine actinomycetes isolated from Colombia and from the Red Sea. All strains were reported to possess NRPS biosynthetic gene clusters indicating that they were potential sources of bioactive compounds. EG4 and EG7, both isolated from the sponge *Callyspongia* aff. *implexa*, produced the greatest number of metabolites. The coupling of HRFTMS data with the AntiMarin database allowed the putative identification of known compounds from the bacterial extracts. It was thus determined that fewer known metabolites were produced by EG4; therefore, the chances of isolating novel compounds from EG4 was higher than that of EG7. EG4, a *Microbacterium* sp., was consequently selected for further work.

6.1.5 Culture and Extraction of EG4

EG4 was up-scaled from M1 agar to M1 broth. The metabolic profile of EG4 grown in stand cultures at 30°C was compared with that of EG4 grown with shaking at 150 rpm at the same temperature. It was discovered that using an older inoculum (10 days) as opposed to a younger one (5 days) resulted in a slight increase in the production of metabolites. The difference was more evident in the stand cultures compared to the shake cultures. There was a two-fold increase in the amount of extract obtained when EG4 was grown in the shake flask cultures. As a result, it was decided that the large-scale culture of EG4 would be performed using shake flask cultures.

Extraction of EG4 was performed by liquid-liquid partitioning of the agar or broth using either ethyl acetate or methanol. The use of methanol was more time-consuming as the methanol required saturation with water prior to further partitioning with ethyl acetate. The resulting yield from the methanol extraction was greater than that obtained with ethyl acetate alone; however, due to the more polar nature of methanol, the extract contained a lot of sugars that originated from the medium. An additional step using HP20 chromatography was required to remove these medium components. It was therefore more efficient to extract the EG4 metabolites using ethyl acetate rather than methanol.

6.1.6 Isolation and Identification of Compounds from EG4

A combination of chromatographic and metabolomic techniques were employed in the isolation and identification of compounds from EG4. N-Phenethylacetamide, indole-3-carboxaldehyde, di(2-propylpentyl)phthalate, 1-monostearin, harman and uracil were known compounds isolated from the crude extract of EG4. The fraction containing indole-3-carboxaldehyde and 1-monostearin had activity against *M. marinum*, as did harman. However, harman was determined to be a component of the media and not a product of EG4. Di(2-propylpentyl)phthalate, which had an MIC of 50 µg/mL (128.21 µM) against *T. brucei*, was also discovered in the media. 3,4-Dihydroxy-5,6-bis(1*H*-indol-3-yl)-3,5-cyclohexadiene was identified as a novel compound; however, it was also detected in the blank media.

A dianiline compound and 1,4-dibenzylimidazolidine were two novel metabolites produced by EG4. The dianiline was active against *N. farcinica*. Due to the small quantity obtained after purification, however, the structure of this compound has not been fully elucidated. The proposed structures are 4,4'-(cyclopenta-3,5-diene-1,3-diyl)-dianiline and 4,4'-(cyclopenta-2,4-diene-1,1-diyl)-dianiline. 1,4-Dibenzylimidazolidine possessed activity against *T. b. brucei*, *M. marinum* and *N. farcinica* (MIC: 100 µg/mL for both *M. marinum* and *N. farcinica*).

N-Acetyltryptamine, N-acetyltyramine and cyclo-L-phenylalanine-L-serine were identified using the AntiMarin database and their presence was confirmed using NMR and MS/MS fragmentation. N-Acetyltryptamine was additionally confirmed by NMR comparison with a tryptamine standard. The production of N-acetyltyramine and N-acetyltryptamine correlated with the appearance of anti-mycobacterial activity. However, further studies showed that N-acetyltryptamine is also found in inactive EG4 crude extracts, thus proving that it was not responsible for the anti-mycobacterial activity. Multivariate analysis during the optimisation of EG4 culture conditions also did not identify N-acetyltyramine as one of the contributors to bioactivity. Indeed, no antimicrobial activity has been attributed to this compound in literature.

6.1.7 Optimisation of Culture Conditions of EG4 to Enhance the Production of Anti-trypanosomal and Anti-mycobacterial Metabolites

Although EG4 was isolated from the marine environment, it did not require salt to survive. M1 media prepared with Royal Nature Advanced Pro Formula salt possessed approximately half of the amount of salt present in media prepared with artificial seawater. Although the same metabolites were produced, they were produced in slightly larger quantities when EG4 was grown on media prepared with Royal Nature salt rather than artificial seawater. On average extracts from the former were slightly more active against *T. brucei* and *M. marinum* than the latter.

The substitution of starch with glucose in M1 agar (Glucose) resulted in the production of fewer metabolites; however, while the anti-trypanosomal activity increased compared to the control, the anti-mycobacterium activity decreased. The

removal of salt from the M1 agar (WOSW) did not significantly affect the anti-mycobacterium activity of EG4, but it caused an increase in the anti-trypanosomal activity compared to the control. The substitution of starch by glucose and simultaneous removal of salt (GWOSW) resulted in the loss of antimicrobial activity and the production of metabolites that differed from those of other cultures. N-acetylglucosamine added before autoclaving (GlcNAcB) resulted in a decrease in antimicrobial activity of EG4, whereas the addition of N-acetylglucosamine after autoclaving (GlcNAcA) led to an increase in both anti-trypanosomal and anti-mycobacterium activity. Although GlcNAcB caused increased metabolite production by EG4, the antibiotic activity of the extracts decreased. GlcNAc should therefore be added to the media after autoclaving to prevent its degradation and to enhance the production of bioactive metabolites by EG4.

EG4 cultured in broth led to the production of metabolites with smaller m/z ratios compared to when EG4 was cultured in agar. The use of M1 GWOSW caused a decrease in the metabolites produced. However, the bacterial extract had both anti-trypanosomal and anti-mycobacterium activity. Interestingly it was EG4 grown on 50% starch, 50% glucose and 50% salt (50G50S) that yielded the greatest number of metabolites.

Multivariate analysis using PCA and OPLS-DA was invaluable during the optimisation of the EG4 culture conditions as it allowed the comparison of the active and inactive extracts as well as the identification of contributors to activity. This approach allows the targeted isolation of the metabolites that are most likely to be bioactive.

As previously mentioned, the optimal medium for the culture of EG4 is dependent on the purpose of the up-scaling. For the isolation of 1,4-dibenzylimidazolidine, M1 without salt (M1-RN) or 50G50S may be used. M1 should be used for the isolation of the dianiline compound. M1 with glucose would be the media of choice for the isolation of other compounds possessing anti-trypanosomal activity.

6.1.8 Fermentation of EG4

The lag phase of the growth curve of EG4 occurred from 0 to 12 hours in the bioreactor. The log phase subsequently lasted from hour 12 to 24, after which the stationary phase ensued until hour 60.

The cultivation of EG4 in a bioreactor resulted in a change in the metabolic profile of EG4 with higher molecular weight compounds being produced compared to the shake flask cultures. 1,4-dibenzylimidazolidine and the dianiline were not produced by EG4 when it was grown in the bioreactor. The antifoam agent used, polypropylene glycol, gave rise to false-positive results in the anti-trypanosomal assay.

6.2 Future Work

Although three bioactive steroids were isolated from *H. simulans*, there were other non-steroidal fractions that possessed anti-trypanosomal and anti-mycobacterium activity. Further purification of these fractions can be performed to determine whether these compounds that are responsible for the activity are novel or are the same ones putatively identified in the AntiMarin database. In addition, MALDI-MS can be performed on slices of the freeze-dried sponge to ascertain the distribution of the metabolites in the sponge. The distribution of the SM8 metabolites within *H. simulans* would also provide further information on the roles these compounds play in the symbiosis of the sponge and bacterium.

Polyhydroxylated fatty acids, members of the antimycin A family, and butenolide 2 and 4 were identified as the compounds responsible for the antibacterial, antifungal, and anti-calcineurin activity, respectively, of SM8; however, further compounds may be discovered if a larger quantity of SM8 extract is obtained for fractionation. Further tests may be performed to validate the quorum signalling activity of the butenolides. It is possible that these butenolides act as autoregulators for SM8 or for other *Streptomyces* species, therefore it would be interesting to determine the biosynthetic pathway and potential autoregulatory roles of these compounds.

Experiments to determine the mechanism of action of butenolides 2 and 4 as calcineurin signalling inhibitors can also be performed.

Genomic sequencing of EG4 would greatly aid in understanding of the types of metabolites EG4 is capable of producing. For example, antiSMASH is an online tool that analyses the secondary metabolite biosynthetic gene clusters within a genome and can predict the core structures of the compounds the genes could code for (Blin et al., 2013). Cloning genes of interest and expressing them in other bacteria could enhance the yield of the target metabolite. In addition, the knowledge of the biosynthetic pathways may assist in the designing of experiments with the intention of increasing the production of target metabolites, such as in the case of the upregulation of antibiotic production through the activity of GlcNAc on the DasR homologue.

The fermentation of EG4 can be repeated using a variation of M1 media. It is recommended that no antifoam agent be used; or, if absolutely necessary, a different antifoam agent should be used. The antifoam agent should be assayed to ensure that it does not inhibit *T. b. brucei* or *M. marinum*. Further investigations may include spiking the media of EG4 with phenylalanine, tryptophan or tryptamine, as this may result in the increased production of indole alkaloids. The chemical synthesis of the proposed dianiline and dibenzylimidazolidine compounds may help to confirm the structure and activity of the compounds.

One area of research that has been gaining interest involves the co-culture of microorganisms. It has been found that the culturing of two different microorganisms together stimulates the production of antibiotics. It would thus be of interest to try co-culturing SM8 and EG4 with other strains of bacteria, particularly as their habitat within a sponge implies that they have evolved the necessary machinery to survive in a highly competitive environment. The application of advanced techniques such as imaging mass spectrometry (IMS) using MALDI (Gonzalez et al., 2011) would provide insight into the interactions of the different strains.

References

- AASSILA, H., BOURGUET-KONDRACKI, M. L., RIFAI, S., FASSOUANE, A. & GUYOT, M. 2003. Identification of harman as the antibiotic compound produced by a tunicate-associated bacterium. *Marine Biotechnology (NY)*, 5, 163-166.
- ABDALLA, M. A., WIN, H. Y., ISLAM, M. T., VON TIEDEMANN, A., SCHÜFFLER, A. & LAATSCH, H. 2011. Khatmiamycin, a motility inhibitor and zoosporicide against the grapevine downy mildew pathogen *Plasmopara viticola* from *Streptomyces* sp. ANK313. *Journal of Antibiotics*, 64, 655-659.
- ABDELMOHSEN, U., PIMENTEL-ELARDO, S., HANORA, A., RADWAN, M., ABOU-EL-ELA, S., AHMED, S. & HENTSCHEL, U. 2010. Isolation, phylogenetic analysis and anti-infective activity screening of marine sponge-associated actinomycetes. *Marine Drugs*, 8, 399-412.
- ABIDI, S. & ADAMS, B. 1987. ¹H and ¹³C resonance designation of antimycin A₁ by two-dimensional NMR spectroscopy. *Magnetic Resonance in Chemistry*, 25, 1078-1080.
- ABIDI, S. L., HA, S. C. & ROSEN, R. T. 1990. Liquid chromatography-thermospray mass spectrometric study of N-acylamino dilactones and 4-butyrolactones derived from antimycin A. *Journal of Chromatography*, 552, 179-194.
- ABURAKI, S. & KINOSHITA, M. 1979. Improved synthesis of antimycin A₃. *Bulletin of the Chemical Society of Japan*, 52, 198-203.
- ACKERS, R. G., MOSS, D., PICTON, B. E., STONE, S. M. K. & MORROW, C. C. 2007. *Sponges of the British Isles ("Sponge V"): A Colour Guide and Working Document*, Marine Conservation Society.
- AGGARWAL, B. B. & ICHIKAWA, H. 2005. Molecular targets and anticancer potential of indole-3-carbinol and its derivatives. *Cell Cycle*, 4, 1201-1215.
- AICHER, T., BUSZEK, K., FANG, F., FORSYTH, C., JUNG, S., KISHI, Y., MATELICH, M., SCOLA, P., SPERO, D. & YOON, S. 1992. Total synthesis of halichondrin B and norhalichondrin B. *Journal of the American Chemical Society*, 114, 3162-3164.
- AL-BARI, M., BHUIYAN, M., FLORES, M., PETROSYAN, P., GARCIA-VARELA, M. & UL ISLAM, M. 2005. *Streptomyces bangladeshensis* sp nov., isolated from soil, which produces bis-(2-ethylhexyl)phthalate. *International Journal of Systematic and Evolutionary Microbiology*, 55, 1973-1977.
- AOKI, S., CAO, L., MATSUI, K., RACHMAT, R., AKIYAMA, S. & KOBAYASHI, M. 2004. Kendarimide A, a novel peptide reversing P-glycoprotein-mediated multidrug resistance in tumor cells, from a marine sponge of *Haliclona* sp. *Tetrahedron*, 60, 7053-7059.
- APSIMON, J., BADRIPERSAUD, S., BUCCINI, J. & EENKHOORN, J. 1980. Marine organic chemistry. 4. Isolation of (20R)-5-alpha-pregn-9(11)-ene-3-beta,6-

alpha,20-triol from the saponins of the starfish, *Asterias forbesi* and *Asterias vulgaris*, and its synthesis. *Canadian Journal of Chemistry*, 58, 2703-2708.

APSIMON, J., BUCCINI, J. & BADRIPER, S. 1973. Marine organic chemistry. 1. Isolation of 3beta,6alpha-dihydroxy-5alpha-pregn-9(11)-en-20-one from saponins of starfish *Asterias forbesi*. A rapid method for extracting starfish saponins. *Canadian Journal of Chemistry*, 51, 850-855.

ARANIBAR, N., OTT, K., ROONGTA, V. & MUELLER, L. 2006. Metabolomic analysis using optimized NMR and statistical methods. *Analytical Biochemistry*, 355, 62-70.

ARSHAD, N., ZITTERL-EGLESEER, K., HASNAIN, S. & HESS, M. 2008. Effect of *Perganum harmala* or its β -carboline alkaloids on certain antibiotic resistant strains of bacteria and protozoa from poultry. *Phytotherapy Research*, 22, 1533-1538.

ASOLKAR, R. N., SCHRÖDER, D., HECKMANN, R., LANG, S., WAGNER-DÖBLER, I. & LAATSCH, H. 2004. Helquinoline, a new tetrahydroquinoline antibiotic from *Janibacter limosus* Hel 1+. *Journal of Antibiotics*, 57, 17-23.

AUBRY, A., CHOSIDOW, O., CAUMES, E., ROBERT, J. & CAMBAU, E. 2002. Sixty-three cases of *Mycobacterium marinum* infection: clinical features, treatment, and antibiotic susceptibility of causative isolates. *Archives of Internal Medicine*, 162, 1746-1752.

AYYAD, S. E., SOWELLIM, S. Z., EL-HOSINI, M. S. & ABO-ATIA, A. 2003. The structural determination of a new steroidal metabolite from the brown alga *Sargassum asperifolium*. *Zeitschrift fur Naturforschung C*, 58, 333-336.

BABA, Y., HIRUKAWA, N., TANOHIRA, N. & SODEOKA, M. 2003. Structure-based design of a highly selective catalytic site-directed inhibitor of Ser/Thr protein phosphatase 2B (calcineurin). *Journal of the American Chemical Society*, 125, 9740-9749.

BAINE, Y., STANKUNAS, B. M., MILLER, P., HOBBS, C., TIBERIO, L., KOCH, J., YOON, K., SAWUTZ, D. & SUROWY, C. 1995. Functional characterization of novel IL-2 transcriptional inhibitors. *Journal of Immunology*, 154, 3667-3677.

BAKER, B., SCHEUER, P. & SHOOLERY, J. 1988. Papuamine, an antifungal pentacyclic alkaloid from a marine sponge, *Haliclona* sp. *Journal of the American Chemical Society*, 110, 965-966.

BAKER, P., KENNEDY, J., DOBSON, A. & MARCHESI, J. 2009. Phylogenetic diversity and antimicrobial activities of fungi associated with *Haliclona simulans* isolated from Irish coastal waters. *Marine Biotechnology*, 11, 540-547.

BALLANTINE, J., WILLIAMS, K. & BURKE, B. 1977. Marine sterols. 4. C21-Sterols from marine sources. Identification of pregnane derivatives in extracts of sponge *Haliclona rubens*. *Tetrahedron Letters*, 1547-1550.

- BARNATHAN, G., KORNPORST, J. M., DOUMENQ, P. & MIRALLES, J. 1996. New unsaturated long-chain fatty acids in the phospholipids from the Axinellida sponges *Trikenrion loeve* and *Pseudaxinella* cf. *lunaecharta*. *Lipids*, 31, 193-200.
- BARRON, P., QUINN, R. & TUCKER, D. 1991. Structural elucidation of a novel scalarane derivative by using high-field (14.1-T) NMR spectroscopy. *Australian Journal of Chemistry*, 44, 995-999.
- BARROW, C. J., OLEYNEK, J. J., MARINELLI, V., SUN, H. H., KAPLITA, P., SEDLOCK, D. M., GILLUM, A. M., CHADWICK, C. C. & COOPER, R. 1997. Antimycins, inhibitors of ATP-citrate lyase, from a *Streptomyces* sp. *Journal of Antibiotics*, 50, 729-733.
- BARROW, C. J. & SUN, H. H. 1994. Spiroquinazoline, a novel substance P inhibitor with a new carbon skeleton, isolated from *Aspergillus flavipes*. *Journal of Natural Products*, 57, 471-476.
- BARROW, R. & CAPON, R. 1991. Alkyl and alkenyl resorcinols from an Australian marine sponge, *Haliclona* sp. (Haplosclerida: Halicltonidae). *Australian Journal of Chemistry*, 44, 1393-1405.
- BAZIN, M. A., LOISEAU, P. M., BORIES, C., LETOURNEUX, Y., RAULT, S. & EL KIHHEL, L. 2006. Synthesis of oxysterols and nitrogenous sterols with antileishmanial and trypanocidal activities. *European Journal of Medicinal Chemistry*, 41, 1109-1116.
- BEDAIR, M. & SUMNER, L. 2008. Current and emerging mass-spectrometry technologies for metabolomics. *Trac-Trends in Analytical Chemistry*, 27, 238-250.
- BELIN, P., MOUTIEZ, M., LAUTRU, S., SEGUIN, J., PERNODET, J. L. & GONDRY, M. 2012. The nonribosomal synthesis of diketopiperazines in tRNA-dependent cyclodipeptide synthase pathways. *Natural Product Reports*, 29, 961-979.
- BELLAMINE, A., MANGLA, A., DENNIS, A., NES, W. & WATERMAN, M. 2001. Structural requirements for substrate recognition of *Mycobacterium tuberculosis* 14 alpha-demethylase: implications for sterol biosynthesis. *Journal of Lipid Research*, 42, 128-136.
- BELLAMINE, A., MANGLA, A. T., NES, W. D. & WATERMAN, M. R. 1999. Characterization and catalytic properties of the sterol 14alpha-demethylase from *Mycobacterium tuberculosis*. *Proceedings of the National Academy of Sciences USA*, 96, 8937-8942.
- BERDY, J. 2005. Bioactive microbial metabolites - A personal view. *Journal of Antibiotics*, 58, 1-26.
- BERGMANN, W. & BURKE, D. 1955. Contributions to the study of marine products. 39. The nucleosides of sponges. 3. Spongothymidine and spongouridine. *Journal of Organic Chemistry*, 20, 1501-1507.

- BERGMANN, W. & FEENEY, R. 1950. The isolation of a new thymine pentoside from sponges. *Journal of the American Chemical Society*, 72, 2809-2810.
- BERGMANN, W. & FEENEY, R. 1951. Contributions to the study of marine products. 32. The nucleosides of sponges. 1. *Journal of Organic Chemistry*, 16, 981-987.
- BERGMANN, W., SCHEDL, H. & LOW, E. 1945. Contributions to the study of marine products. 19. Chalinasterol. *Journal of Organic Chemistry*, 10, 587-593.
- BERGQUIST, P. R. 1978. *Sponges*, Hutchinson & Co (Publishers) Ltd.
- BERGSSON, G., ARNFINNSSON, J., STEINGRÍMSSON, O. & THORMAR, H. 2001. Killing of Gram-positive cocci by fatty acids and monoglycerides. *APMIS*, 109, 670-678.
- BERN, C., MONTGOMERY, S. P., HERWALDT, B. L., RASSI, A., MARINETO, J. A., DANTAS, R. O., MAGUIRE, J. H., ACQUATELLA, H., MORILLO, C., KIRCHHOFF, L. V., GILMAN, R. H., REYES, P. A., SALVATELLA, R. & MOORE, A. C. 2007. Evaluation and treatment of Chagas disease in the United States: a systematic review. *JAMA*, 298, 2171-2181.
- BEUCHAT, L., NIELSEN, P., FRISVAD, J., NATORI, S., HASHIMOTO, K. & UENO, Y. 1989. Environmental factors influencing fumitremorgin production by *Neostartorya fischeri*. *Mycotoxins and Phycotoxins* 88, 10, 7-12.
- BILAND, H., LOHSE, F. & HARDEGGER, E. 1960. Welkstoffe und antibiotica. 22. Verwendung radioaktiver fusarinsäure und synthese von fusarinsäure-[2,51-14C]. *Helvetica Chimica Acta*, 43, 1436-1440.
- BLIN, K., MEDEMA, M. H., KAZEMPOUR, D., FISCHBACH, M. A., BREITLING, R., TAKANO, E. & WEBER, T. 2013. antiSMASH 2.0--a versatile platform for genome mining of secondary metabolite producers. *Nucleic Acids Research*, 41, W204-212.
- BLUNT, J. W., COPP, B. R., KEYZERS, R. A., MUNRO, M. H. & PRINSEP, M. R. 2013. Marine natural products. *Natural Products Reports*, 30, 237-323.
- BLUNT, J. W., COPP, B. R., KEYZERS, R. A., MUNRO, M. H. & PRINSEP, M. R. 2014. Marine natural products. *Natural Products Reports*, 31, 160-258.
- BLUNT, J. W., COPP, B. R., MUNRO, M. H., NORTHCOTE, P. T. & PRINSEP, M. R. 2004. Marine natural products. *Natural Products Reports*, 21, 1-49.
- BOENTE, M., KIRBY, G., PATRICK, G. & ROBINS, D. 1991. Biosynthesis of hyalodendrin and didethiobis(methylthio)hyalodendrin, sulfur-containing 2,5-dioxopiperazines of the 3S,6S series. *Journal of the Chemical Society-Perkin Transactions 1*, 1283-1290.

- BOHLENDORF, B., FORCHE, E., BEDORF, N., GERTH, K., IRSCHIK, H., JANSEN, R., KUNZE, B., TROWITZSCHKIENAST, W., REICHENBACH, H. & HOFLE, G. 1996. Antibiotics from gliding bacteria .73. Indole and quinoline derivatives as metabolites of tryptophan in myxobacteria. *Liebigs Annalen*, 49-53.
- BOROS, C., SMITH, C. J., VASINA, Y., CHE, Y., DIX, A. B., DARVEAUX, B. & PEARCE, C. 2006. Isolation and identification of the icosalides--cyclic peptolides with selective antibiotic and cytotoxic activities. *Journal of Antibiotics*, 59, 486-494.
- BOROUJERDI, A. F., VIZCAINO, M. I., MEYERS, A., POLLOCK, E. C., HUYNH, S. L., SCHOCK, T. B., MORRIS, P. J. & BEARDEN, D. W. 2009. NMR-based microbial metabolomics and the temperature-dependent coral pathogen *Vibrio coralliilyticus*. *Environmental Science & Technology*, 43, 7658-7664.
- BORRIS, R., BURG, R., HENSENS, O., HUANG, L., KELEMEN, L. & MOCHALES, S. 1989. *Sterol inhibitors of testosterone 5a-reductase*. US patent application US 07/023,015.
- BOURNE, R., HIMMELREICH, U., SHARMA, A., MOUNTFORD, C. & SORRELL, T. 2001. Identification of *Enterococcus*, *Streptococcus*, and *Staphylococcus* by multivariate analysis of proton magnetic resonance spectroscopic data from plate cultures. *Journal of Clinical Microbiology*, 39, 2916-2923.
- BRAEKMAN, J. & DALOZE, D. 1986. Chemical defense in sponges. *Pure and Applied Chemistry*, 58, 357-364.
- BRAITHWAITE, A. & SMITH, F. J. 1996. *Chromatographic Methods 5th ed.*, Glasgow, UK, Blackie Academic & Professional.
- BRAMBILLA, U., NASINI, G., PETROLINI, B., QUARONI, S., SARACCHI, M. & FEDELI, L. 1995. Prodigiosin-like and other metabolites produced by a *Streptovercillium* strain. *Actinomycetes*, 6, 63-70.
- BRATCHKOVA, A., IVANOVA, V., GOUSTEROVA, A. & LAATSCH, H. 2012. Beta-carboline alkaloid constituents from a *Thermoactinomyces* sp. strain isolated from Livingston Island, Antarctica. *Biotechnology & Biotechnological Equipment*, 26, 3005-3009.
- BRAUTASET, T., SEKUROVA, O. N., SLETTA, H., ELLINGSEN, T. E., STRLM, A. R., VALLA, S. & ZOTCHEV, S. B. 2000. Biosynthesis of the polyene antifungal antibiotic nystatin in *Streptomyces noursei* ATCC 11455: analysis of the gene cluster and deduction of the biosynthetic pathway. *Chemistry and Biology*, 7, 395-403.
- BRENER, Z. & KRETTLI, A. U. 1990. Immunology of Chagas' Disease. In: WYLER, D. J. (ed.) *Modern Parasite Biology: Cellular, Immunological and Molecular Aspects*. New York: W.H. Freeman and Company.
- BREWER, D., JERRAM, W., MEILER, D. & TAYLOR, A. 1970. Toxicity of cochliodinol, an antibiotic metabolite of *Chaetomium* spp. *Canadian Journal of Microbiology*, 16, 433-440.

BREWER, D., JERRAM, W. & TAYLOR, A. 1968. Production of cochliodinol and a related metabolite by *Chaetomium* species. *Canadian Journal of Microbiology*, 14, 861-866.

BRILL, G. M., PREMACHANDRAN, U., KARWOWSKI, J. P., HENRY, R., CWIK, D. K., TRAPHAGEN, L. M., HUMPHREY, P. E., JACKSON, M., CLEMENT, J. J., BURREN, N. S., KADAM, S., CHEN, R. H. & MCALPINE, J. B. 1996. Dibefurin, a novel fungal metabolite inhibiting calcineurin phosphatase activity. *Journal of Antibiotics*, 49, 124-128.

BRINGMANN, G., HAMM, A., GÜNTHER, C., MICHEL, M., BRUN, R. & MUDOGO, V. 2000. Ancistroealaines A and B, two new bioactive naphthylisoquinolines, and related naphthoic acids from *Ancistrocladus ealaensis*. *Journal of Natural Products*, 63, 1465-1470.

BRUSCA, R. C. & BRUSCA, G. J. 1990. *Invertebrates*, Massachusetts, Sinauer Associates, Inc.

BUGNI, T. S., WOOLERY, M., KAUFFMAN, C. A., JENSEN, P. R. & FENICAL, W. 2006. Bohemamines from a marine-derived *Streptomyces* sp. *Journal of Natural Products*, 69, 1626-1628.

BUNDY, J. G., WILLEY, T. L., CASTELL, R. S., ELLAR, D. J. & BRINDLE, K. M. 2005. Discrimination of pathogenic clinical isolates and laboratory strains of *Bacillus cereus* by NMR-based metabolomic profiling. *FEMS Microbiology Letters*, 242, 127-136.

BURREN, N. S., PREMACHANDRAN, U., HOSELTON, S., CWIK, D., HOCHLOWSKI, J. E., YE, Q., SUNGA, G. N., KARWOWSKI, J. P., JACKSON, M. & WHITTERN, D. N. 1995. Simple aromatics identified with a NFAT-lacZ transcription assay for the detection of immunosuppressants. *Journal of Antibiotics*, 48, 380-386.

BYLESJO, M., RANTALAINEN, M., CLOAREC, O., NICHOLSON, J., HOLMES, E. & TRYGG, J. 2006. OPLS discriminant analysis: combining the strengths of PLS-DA and SIMCA classification. *Journal of Chemometrics*, 20, 341-351.

CAMPAGNUOLO, C., FATTORUSSO, E., TAGLIALATELA-SCAFATI, O., IANARO, A. & PISANO, B. 2002. Plakortethers A-G: A new class of cytotoxic plakortin-derived metabolites. *European Journal of Organic Chemistry*, 61-69.

CARBALLEIRA, N. M. & PAGÁN, M. 2001. New methoxylated fatty acids from the Caribbean sponge *Callyspongia fallax*. *Journal of Natural Products*, 64, 620-623.

CARBALLERIA, N. M. & REYES, E. D. 1990. Identification of the new 23-methyl-5,9-pentacosadienoic acid in the sponge *Cribrochalina vasculum*. *Lipids*, 25, 69-71.

CARDELLINA, J., NIGH, D. & VANWAGENEN, B. 1986. Plant-growth regulatory indoles from the sponges *Dysidea etheria* and *Ulosa ruetzleri*. *Journal of Natural Products*, 49, 1065-1067.

CARLSON, R., POPOV, S., MASSEY, I., DELSETH, C., AYANOGLU, E., VARKONY, T. & DJERASSI, C. 1978. Minor and trace sterols in marine invertebrates. 6. Occurrence and possible origins of sterols possessing unusually short hydrocarbon side chains. *Bioorganic Chemistry*, 7, 453-479.

CARMELY, S., COJOCARU, M., LOYA, Y. & KASHMAN, Y. 1988. Ten new rearranged spongian diterpenes from two *Dysidea* species. *Journal of Organic Chemistry*, 53, 4801-4807.

CARMELY, S. & KASHMAN, Y. 1987. Naamines and naamides, novel imidazole alkaloids from the calcareous sponge *Leucetta chagosensis*. *Tetrahedron Letters*, 28, 3003-3006.

CATALAN, C., KOKKE, W., DUQUE, C. & DJERASSI, C. 1983. Synthesis of (24R)-5,28-stigmastadien-3-beta-ol and (24S)-5,28-stigmastadien-3-beta-ol and determination of the stereochemistry of their 24 hydroxy analogs, the saringosterols. *Journal of Organic Chemistry*, 48, 5207-5214.

CAVIN, J., KRASSNER, S. & RODRIGUEZ, E. 1987. Plant-derived alkaloids active against *Trypanosoma cruzi*. *Journal of Ethnopharmacology*, 19, 89-94.

CHARAN, R., GARSON, M., BRERETON, I., WILLIS, A. & HOOPER, J. 1996. Haliclonyclamines A and B, cytotoxic alkaloids from the tropical marine sponge *Haliclona* sp. *Tetrahedron*, 52, 9111-9120.

CHEN, C. Y., SHEN, Y. C., CHEN, Y. J., SHEU, J. H. & DUH, C. Y. 1999. Bioactive sesquiterpenes from a Taiwanese marine sponge *Parahigginsia* sp. *Journal of Natural Products*, 62, 573-576.

CHOI, S. U., LEE, C. K., HWANG, Y. I., KINOSITA, H. & NIHIRA, T. 2003. Gamma-butyrolactone autoregulators and receptor proteins in non-*Streptomyces* actinomycetes producing commercially important secondary metabolites. *Archives of Microbiology*, 180, 303-307.

CHUNG, M. C., LEE, H. J., CHUN, H. K., LEE, C. H., KIM, S. I. & KHO, Y. H. 1996. Bestatin analogue from *Streptomyces neyagawaensis* SL-387. *Bioscience, Biotechnology, and Biochemistry*, 60, 898-900.

CIMINO, G., SCOGNAMIGLIO, G., SPINELLA, A. & TRIVELLONE, E. 1990. Structural studies on saraine A. *Journal of Natural Products*, 53, 1519-1525.

CLARK, R., GARSON, M. & HOOPER, J. 2001. Antifungal alkyl amino alcohols from the tropical marine sponge *Haliclona* n. sp. *Journal of Natural Products*, 64, 1568-1571.

CLAYDON, N., GROVE, J. & POPLE, M. 1977. Fusaric acid from *Fusarium solani*. *Phytochemistry*, 16, 603-603.

CLIPSTONE, N. & CRABTREE, G. 1992. Identification of calcineurin as a key signaling enzyme in lymphocyte-T activation. *Nature*, 357, 695-697.

- COMIN, J. & KELLERSCHIERLEIN, W. 1959. Stoffwechselprodukte von actinomyceten. 19. N-acetyl-tyramin. *Helvetica Chimica Acta*, 42, 1730-1732.
- CONLEY, A. & KABARA, J. 1973. Antimicrobial action of esters of polyhydric alcohols. *Antimicrobial Agents and Chemotherapy*, 4, 501-506.
- CORDEIRO, A., THIEMANN, O. & MICHELS, P. 2009. Inhibition of *Trypanosoma brucei* glucose-6-phosphate dehydrogenase by human steroids and their effects on the viability of cultured parasites. *Bioorganic & Medicinal Chemistry*, 17, 2483-2489.
- CORPET, F. 1988. Multiple sequence alignment with hierarchical clustering. *Nucleic Acids Research*, 16, 10881-10890.
- CRANDALL, L. W. & HAMILL, R. L. 1986. Antibiotics Produced by *Streptomyces*: Major Structural Classes. In: QUEENER, S. W. & DAY, L. E. (eds.) *Antibiotic-Producing Streptomyces*. Orlando, Florida: Academic Press, Inc.
- DALY, J. & WITKOP, B. 1967. Selective exchange of nuclear protons in hydroxyindoles. *Journal of the American Chemical Society*, 89, 1032-1033.
- DAOUD, N. N. & FOSTER, H. A. 1993. Antifungal activity of *Myxococcus* species 1 production, physicochemical and biological properties of antibiotics from *Myxococcus fulvus* S110 (Myxobacterales). *Microbios*, 73, 173-184.
- DE ROSA, S., MILONE, A. & POPOV, S. 1999. Sterol composition of the sponge *Fasciospongia cavernosa*, from the Adriatic, Aegean and Tyrrhenian seas. *Comparative Biochemistry and Physiology B-Biochemistry & Molecular Biology*, 123, 235-239.
- DE SOUZA, W. & RODRIGUES, J. C. 2009. Sterol biosynthesis pathway as target for anti-trypanosomatid drugs. *Interdisciplinary Perspectives on Infectious Diseases*, 2009, 642502.
- DEFANT, A., MANCINI, I., RASPOR, L., GUELLA, G., TURK, T. & SEPCIC, K. 2011. New structural insights into Saraines A, B, and C, macrocyclic alkaloids from the Mediterranean sponge *Reniera (Haliclona) sarai*. *European Journal of Organic Chemistry*, 3761-3767.
- DELLA MONICA, C., RANDAZZO, A., BIFULCO, G., CIMINO, P., AQUINO, M., IZZO, I., DE RICCARDIS, F. & GOMEZ-PALOMA, L. 2002. Structural revision of halipeptins: synthesis of the thiazoline unit and isolation of halipeptin C. *Tetrahedron Letters*, 43, 5707-5710.
- DELPASSAND, E., CHARI, M., STAGER, C., MORRISETT, J., FORD, J. & ROMAZI, M. 1995. Rapid identification of common human pathogens by high-resolution proton magnetic resonance spectroscopy. *Journal of Clinical Microbiology*, 33, 1258-1262.

- DEMAIN, A. L. 2007. The Business of Biotechnology. *Industrial Biotechnology*, 3, 269-283.
- DEMBITSKY, V. M., SHKROB, I. & ROZENTSVET, O. A. 2000. Fatty acid amides from freshwater green alga *Rhizoclonium hieroglyphicum*. *Phytochemistry*, 54, 965-967.
- DESATY, D., MCINNES, A., SMITH, D. & VINING, L. 1968. Use of ¹³C in biosynthesis studies. Incorporation of isotopically labeled acetate and aspartate into fusaric acid. *Canadian Journal of Biochemistry*, 46, 1293-1300.
- DETTMER, K., ARONOV, P. A. & HAMMOCK, B. D. 2007. Mass spectrometry-based metabolomics. *Mass Spectrometry Reviews*, 26, 51-78.
- DEVYS, M. & BARBIER, M. 1991. Indole-3-carboxaldehyde in the cabbage *Brassica oleracea*: A systematic determination. *Phytochemistry*, 30, 389-391.
- DHARMARAJ, S. & SUMANTHA, A. 2009. Bioactive potential of *Streptomyces* associated with marine sponges. *World Journal of Microbiology & Biotechnology*, 25, 1971-1979.
- DI GIORGIO, C., DELMAS, F., OLLIVIER, E., ELIAS, R., BALANSARD, G. & TIMON-DAVID, P. 2004. In vitro activity of the beta-carboline alkaloids harmane, harmine, and harmaline toward parasites of the species *Leishmania infantum*. *Experimental Parasitology*, 106, 67-74.
- DIECKMANN, R., GRAEBER, I., KAESLER, I., SZEWZYK, U. & VON DOHREN, H. 2005. Rapid screening and dereplication of bacterial isolates from marine sponges of the Sula Ridge by Intact-Cell-MALDI-TOF mass spectrometry (ICM-MS). *Applied Microbiology and Biotechnology*, 67, 539-548.
- DIETZ, A. 1986. Structure and Taxonomy of *Streptomyces*. In: QUEENER, S. W. & DAY, L. E. (eds.) *Antibiotic-Producing Streptomyces*. Orlando, Florida: Academic Press, Inc.
- DOBRETISOV, S., DAHMS, H. & QIAN, P. 2004. Antilarval and antimicrobial activity of waterborne metabolites of the sponge *Callyspongia (Euplaccella) pulvinata*: evidence of allelopathy. *Marine Ecology Progress Series*, 271, 133-146.
- DOETSCH, R. N. & PELCZAR, M. J. 1948. The Microbacteria: I. Morphological and Physiological Characteristics. *Journal of Bacteriology*, 56, 37-49.
- DOPEÑO, J., QUIÑOJA, E., RIGUERA, R., DEBITUS, C. & BERGQUIST, P. 1994. Euryspongiols: Ten new highly hydroxylated 9, 11-secoosteroids with antihistaminic activity from the sponge *Euryspongia* sp. Stereochemistry and reduction. *Tetrahedron*, 50, 3813-3828.
- DOYLE, T. W., NETTLETON, D. E., BALITZ, D. M., MOSELEY, J. E., GRULICH, R. E., MCCABE, T. & CLARDY, J. 1980. Isolation and structure of bohemamine (1a. beta., 2. alpha., 6a. beta., 6b. beta.)-3-methyl-N-(1a, 6, 6a, 6b-

tetrahydro-2, 6a-dimethyl-6-oxo-2H-oxireno [a] pyrrolizin-4-yl)-2-butenamide. *Journal of Organic Chemistry*, 45, 1324-1326.

DUNSHEE, B., LEBEN, C., KEITT, G. & STRONG, F. 1949. The isolation and properties of Antimycin A. *Journal of the American Chemical Society*, 71, 2436-2437.

EL-MANSI, E. M. T., BRYCE, C. F. A., HARTLEY, B. S. & DEMAINE, A. L. 2007. Fermentation Microbiology and Biotechnology: An Historical Perspective. In: EL-MANSI, E. M. T., BRYCE, C. F. A., DEMAINE, A. L. & ALLMAN, A. R. (eds.) *Fermentation Microbiology and Biotechnology 2nd ed.* Florida: Taylor & Francis Group, LLC.

EL-TARABILY, K. A., SYKES, M. L., KURTBÖKE, I. D., HARDY, G. E. S. J., BARBOSA, A. M. & DEKKER, R. F. H. 1996. Synergistic effects of a cellulase-producing *Micromonospora carbonacea* and an antibiotic-producing *Streptomyces violascens* on the suppression of *Phytophthora cinnamomi* root rot of *Banksia grandis*. *Canadian Journal of Botany*, 74, 618-624.

ELBANDY, M., SHINDE, P. B., DANG, H. T., HONG, J., BAE, K. S. & JUNG, J. H. 2008. Furan metabolites from the sponge-derived yeast *Pichia membranifaciens*. *Journal of Natural Products*, 71, 869-872.

ELENKOV, I., MILKOVA, T., ANDREEV, S. & POPOV, S. 1994. Sterol composition and biosynthesis in the Black Sea sponge *Dysidea fragilis*. *Comparative Biochemistry and Physiology B-Biochemistry & Molecular Biology*, 107, 547-551.

ELYAKOV, G., KUZNETSOVA, T., MIKHAILOV, T., MALTSEV, I., VOINOV, V. & FEDOREYEV, S. 1991. Brominated diphenyl ethers from a marine bacterium associated with the sponge *Dysidea* sp. *Experientia*, 47, 632-633.

ENDO, T. & YONEHARA, H. 1970. Chemical studies on blastmycin. 3. Gas-liquid chromatography of antimycin A-blastmycin antibiotics. *Journal of Antibiotics*, 23, 91-95.

ERDMAN, T. & THOMSON, R. 1972. Sterols from sponges *Cliona celata* Grant and *Hymeniacidon perleve* Montagu. *Tetrahedron*, 28, 5163-5173.

ERICKSON, K., BEUTLER, J., CARDELLINA, J. & BOYD, M. 1997. Salicylhalamides A and B, novel cytotoxic macrolides from the marine sponge *Haliclona* sp. *Journal of Organic Chemistry*, 62, 8188-8192.

EVANS, J. R. & WEARE, G. 1977. Norplicacetin, a new antibiotic from *Streptomyces plicatus*. *Journal of Antibiotics*, 30, 604-606.

EVERITT, B. S. & DUNN, G. 2001. *Applied Multivariate Data Analysis 2nd Ed.*, London, UK, Arnold.

- FAHY, E., MOLINSKI, T., HARPER, M., SULLIVAN, B., FAULKNER, D., PARKANYI, L. & CLARDY, J. 1988. Haliclonadamine, an antimicrobial alkaloid from the sponge *Haliclona* sp. *Tetrahedron Letters*, 29, 3427-3428.
- FAULKNER, D. 2002. Marine natural products. *Natural Product Reports*, 19, 1-48.
- FIEHN, O. 2002. Metabolomics - the link between genotypes and phenotypes. *Plant Molecular Biology*, 48, 155-171.
- FINDLAY, J. & PATIL, A. 1985. Novel sterols from the finger sponge *Haliclona oculata*. *Canadian Journal of Chemistry*, 63, 2406-2410.
- FRANCO, C., BORDE, U., VIJAYAKUMAR, E., CHATTERJEE, S., BLUMBACH, J. & GANGULI, B. 1991. Butalactin, a new butanolide antibiotic: Taxonomy, fermentation, isolation and biological activity. *Journal of Antibiotics*, 44, 225-231.
- FREIBURGHHAUS, F., KAMINSKY, R., NKUNYA, M. & BRUN, R. 1996. Evaluation of African medicinal plants for their in vitro trypanocidal activity. *Journal of Ethnopharmacology*, 55, 1-11.
- FRIEDRICH, A., FISCHER, I., PROKSCH, P., HACKER, J. & HENTSCHEL, U. 2001. Temporal variation of the microbial community associated with the mediterranean sponge *Aplysina aerophoba*. *Fems Microbiology Ecology*, 38, 105-113.
- FRINCKE, J. M. & FAULKNER, D. J. 1982. Antimicrobial metabolites of the sponge *Reniera* sp. *Journal of the American Chemical Society*, 104, 265-269.
- FUKUYAMA, Y., IWATSUKI, C., KODAMA, M., OCHI, M. & KATAOKA, K. 1998. Antimicrobial indolequinones from the mid-intestinal gland of the muricid gastropod *Drupella fragum*. *Tetrahedron*, 54, 10007-10016.
- FUQUA, W., WINANS, S. & GREENBERG, E. 1994. Quorum sensing in bacteria: the LuxR-LuxI family of cell density-responsive transcriptional regulators. *Journal of Bacteriology*, 176, 269-275.
- GAMARD, P., SAURIOL, F., BENHAMOU, N., BELANGER, R. & PAULITZ, T. 1997. Novel butyrolactones with antifungal activity produced by *Pseudomonas aureofaciens* strain 63-28. *Journal of Antibiotics*, 50, 742-749.
- GAMIELDIEN, J., PTITSYN, A. & HIDE, W. 2002. Eukaryotic genes in *Mycobacterium tuberculosis* could have a role in pathogenesis and immunomodulation. *Trends in Genetics*, 18, 5-8.
- GANG, C., SHEN, M., XIN, W., FAN, X., MA, H., WU, H. & PEI, Y. 2013. Indole alkaloids from the marine bacterium *Pantoea agglomerans*. *Chemistry of Natural Compounds*, 49, 291-293.

GARG, M., GUPTA, R., HUSAIN, M., CHAWLA, S., CHAWLA, A., KUMAR, R., RAO, S., MISRA, M. & PRASAD, K. 2004. Brain abscesses: Etiologic categorization with in vivo proton MR spectroscopy. *Radiology*, 230, 519-527.

GAUVIN, A., SMADJA, J., AKNIN, M., FAURE, R. & GAYDOU, E. 2000. Isolation of bioactive 5 alpha,8 alpha-epidioxy sterols from the marine sponge *Luffariella cf. variabilis*. *Canadian Journal of Chemistry*, 78, 986-992.

GEORGE, C. & PREST, H. 2002. Determination of phthalate esters by positive chemical ionization MS with retention-time locked GC. *LC GC North America*, 20, 142-151.

GILLIGAN, P. 2002. Therapeutic challenges posed by bacterial bioterrorism threats. *Current Opinion in Microbiology*, 5, 489-495.

GINER, J. 1993. Biosynthesis of marine sterol side chains. *Chemical Reviews*, 93, 1735-1752.

GINER, J. & DJERASSI, C. 1990. Biosynthetic studies of marine lipids. 28. Use of sponge cell-free extracts in the study of marine sterol biosynthesis. *Tetrahedron Letters*, 31, 5421-5424.

GINER, J. & WIKFORS, G. 2011. "Dinoflagellate Sterols" in marine diatoms. *Phytochemistry*, 72, 1896-1901.

GIRISHAM, S., REDDY, S., RAO, G. & RAO, P. 1986. Metabolites from the Fermentation of *Ulocladium botrytis*. *Journal of Natural Products*, 49, 548-549.

GITLITZ, B., DAVIES, A., BELANI, C., ARGIRIS, A., RAMALINGAM, S., HOFFMAN, P., KOCZWAS, M., GROSHEN, S. & GANDARA, D. 2009. A phase II study of the halichondrin B analog, E7389, in patients (pts) with advanced non-small cell lung cancer (NSCLC) previously treated with a taxane. A California Consortium/University of Pittsburgh/University of Chicago NCI/CTEP sponsored trial. *Journal of Clinical Oncology*, 27, 8056.

GIVSKOV, M., DENYS, R., MANEFIELD, M., GRAM, L., MAXIMILIEN, R., EBERL, L., MOLIN, S., STEINBERG, P. & KJELLEBERG, S. 1996. Eukaryotic interference with homoserine lactone-mediated prokaryotic signaling. *Journal of Bacteriology*, 178, 6618-6622.

GJERSING, E. L., HERBERG, J. L., HORN, J., SCHALDACH, C. M. & MAXWELL, R. S. 2007. NMR metabolomics of planktonic and biofilm modes of growth in *Pseudomonas aeruginosa*. *Analytical Chemistry*, 79, 8037-8045.

GOAD, L. 1981. Sterol biosynthesis and metabolism in marine invertebrates. *Pure and Applied Chemistry*, 53, 837-852.

GOAD, L., GARNEAU, F., SIMARD, J., APSIMON, J. & GIRARD, M. 1985. Isolation of delta-9(11)-sterols from the sea cucumber *Psolus fabricii*. Implications for holothurin biosynthesis. *Tetrahedron Letters*, 26, 3513-3516.

- GONZALEZ, D. J., HASTE, N. M., HOLLANDS, A., FLEMING, T. C., HAMBY, M., POGLIANO, K., NIZET, V. & DORRESTEIN, P. C. 2011. Microbial competition between *Bacillus subtilis* and *Staphylococcus aureus* monitored by imaging mass spectrometry. *Microbiology*, 157, 2485-2492.
- GOPICHAND, Y. & SCHMITZ, F. 1979. Two novel lactams from the marine sponge *Halichondria melanodocia*. *Journal of Organic Chemistry*, 44, 4995-4997.
- GORDON, B. & LEGGAT, W. 2010. Symbiodinium-invertebrate symbioses and the role of metabolomics. *Marine Drugs*, 8, 2546-2568.
- GRIFFITHS, W., KARUA, K., HORNSHAW, M., WOFFENDIN, G. & WANGA, Y. 2007. Metabolomics and metabolite profiling: past heroes and future developments. *European Journal of Mass Spectrometry*, 13, 45-50.
- GROSSMANN, G., PONCIONI, M., BORNAND, M., JOLIVET, B., NEUBURGER, M. & SEQUIN, U. 2003. Bioactive butenolides from *Streptomyces antibioticus* TU 99: absolute configurations and synthesis of analogs. *Tetrahedron*, 59, 3237-3251.
- GUAN, L., SERA, Y., ADACHI, K., NISHIDA, F. & SHIZURI, Y. 2001. Isolation and evaluation of nonsiderophore cyclic peptides from marine sponges. *Biochemical and Biophysical Research Communications*, 283, 976-981.
- GUAN, S. H., SATTLER, I., LIN, W. H., GUO, D. A. & GRABLEY, S. 2005. p-Aminoacetophenonic acids produced by a mangrove endophyte: *Streptomyces griseus* subsp. *Journal of Natural Products*, 68, 1198-1200.
- GUNASEKERA, S., GUNASEKERA, M. & MCCARTHY, P. 1991. Discodermide - A new bioactive macrocyclic lactam from the marine sponge *Discodermia dissoluta*. *Journal of Organic Chemistry*, 56, 4830-4833.
- GUO, Z. Y., HUANG, Z. J., WEN, L., WAN, Q., LIU, F., SHE, Z. G., LIN, Y. C. & ZHOU, S. N. 2007. [The metabolites of cyclic peptides from three endophytic mangrove fungi]. *Zhong Yao Cai*, 30, 1526-1529.
- GUPTA, S., CORDEIRO, A. & MICHELS, P. 2011. Glucose-6-phosphate dehydrogenase is the target for the trypanocidal action of human steroids. *Molecular and Biochemical Parasitology*, 176, 112-115.
- GUTIERREZ-LUGO, M., WOLDEMICHAEL, G., SINGH, M., SUAREZ, P., MAIESE, W., MONTENEGRO, G. & TIMMERMANN, B. 2005. Isolation of three new naturally occurring compounds from the culture of *Micromonospora* sp P1068. *Natural Product Research*, 19, 645-652.
- HACENE, H. & LEFEBVRE, G. 1995. AH17, a new non-polyenic antifungal antibiotic produced by a strain of *Spirillospora*. *Microbios*, 83, 199-205.
- HAEFNER, B. 2003. Drugs from the deep: marine natural products as drug candidates. *Drug Discovery Today*, 8, 536-544.

- HAEGELE, K. D. & DESIDERIO, D. M. 1973. Structural elucidation of minor components in the antimycin A complex by mass spectrometry. *Journal of Antibiotics*, 26, 215-222.
- HAIR, J. F. J., BLACK, W. C., BABIN, B. J. & ANDERSON, R. E. 2010. *Multivariate Data Analysis: A Global Perspective 7th ed.*, New Jersey, Pearson Education, Inc.
- HAMILL, R., HOEHN, M., PITTENGER, G., CHAMBERLIN, J. & GORMAN, M. 1969. Dianemycin, an antibiotic of the group affecting ion transport. *Journal of Antibiotics*, 22, 161-164.
- HAN, Y., YANG, B., ZHANG, F., MIAO, X. & LI, Z. 2009. Characterization of antifungal chitinase from marine *Streptomyces* sp DA11 associated with South China Sea sponge *Craniella Australiensis*. *Marine Biotechnology*, 11, 132-140.
- HARDEGGER, E. & NIKLES, E. 1957a. Welkstoffe und antibiotica. 21. Mitteilung - Herstellung der fusarinsäure aus 2,5-lutidin. *Helvetica Chimica Acta*, 40, 2428-2433.
- HARDEGGER, E. & NIKLES, E. 1957b. Welkstoffe und Antibiotika. 19. Eine neue synthese der fusarinsäure. *Helvetica Chimica Acta*, 40, 1016-1021.
- HARPER, D. E. & WELCH, D. R. 1992. Isolation, purification, synthesis, and antiinvasive/antimetastatic activity of U-77863 and U-77864 from *Streptomyces griseoluteus*, strain WS6724. *Journal of Antibiotics*, 45, 1827-1836.
- HARRISON, B. & CREWS, P. 1997. The structure and probable biogenesis of helianane, a heterocyclic sesquiterpene, from the Indo-Pacific sponge *Haliclona fascigera*. *Journal of Organic Chemistry*, 62, 2646-2648.
- HASKELL, T., RYDER, A., FROHARDT, R., FUSARI, S., JAKUBOWSKI, Z. & BARTZ, Q. 1958. The isolation and characterization of 3 crystalline antibiotics from *Streptomyces plicatus*. *Journal of the American Chemical Society*, 80, 743-747.
- HATFIELD, G., WOODARD, R. & SON, J. 1992. Isolation and structure determination of new macrolide antibiotics. *Journal of Natural Products*, 55, 753-759.
- HATTORI, T., ADACHI, K. & SHIZURI, Y. 1998. New ceramide from marine sponge *Haliclona koremella* and related compounds as antifouling substances against macroalgae. *Journal of Natural Products*, 61, 823-826.
- HAYASHI, K. & NOZAKI, H. 1999. Kitamycins, new antimycin antibiotics produced by *Streptomyces* sp. *Journal of Antibiotics*, 52, 325-328.
- HEALY, F., WACH, M., KRASNOFF, S., GIBSON, D. & LORIA, R. 2000. The txtAB genes of the plant pathogen *Streptomyces acidiscabies* encode a peptide synthetase required for phytotoxin thaxtomin A production and pathogenicity. *Molecular Microbiology*, 38, 794-804.

HELMKE, E. & WEYLAND, H. 1984. *Rhodococcus marinonascens* sp. nov, an actinomycete from the sea. *International Journal of Systematic Bacteriology*, 34, 127-138.

HENTSCHEL, U., HOPKE, J., HORN, M., FRIEDRICH, A., WAGNER, M., HACKER, J. & MOORE, B. 2002. Molecular evidence for a uniform microbial community in sponges from different oceans. *Applied and Environmental Microbiology*, 68, 4431-4440.

HENTSCHEL, U., USHER, K. & TAYLOR, M. 2006. Marine sponges as microbial fermenters. *Fems Microbiology Ecology*, 55, 167-177.

HERB, R., CARROLL, A., YOSHIDA, W., SCHEUER, P. & PAUL, V. 1990. Polyalkylated cyclopentindoles - cytotoxic fish antifeedants from a sponge, *Axinella* sp. *Tetrahedron*, 46, 3089-3092.

HERNANDEZ, I., MACEDO, M., BERLINCK, R., FERREIRA, A. & GODINHO, M. 2004. Dipeptide metabolites from the marine derived bacterium *Streptomyces acrymici*. *Journal of the Brazilian Chemical Society*, 15, 441-444.

HERTIANI, T., EDRADA-EBEL, R., ORTLEPP, S., VAN SOEST, R., DE VOOGD, N., WRAY, V., HENTSCHEL, U., KOZYTSKA, S., MULLER, W. & PROKSCH, P. 2010. From anti-fouling to biofilm inhibition: New cytotoxic secondary metabolites from two Indonesian *Agelas* sponges. *Bioorganic & Medicinal Chemistry*, 18, 1297-1311.

HIGGS, M. & FAULKNER, D. 1978. Plakortin, an antibiotic from *Plakortis halichondrioides*. *Journal of Organic Chemistry*, 43, 3454-3457.

HIMMLER, T., PIRRO, F. & SCHMEER, N. 1998. Synthesis and antibacterial in vitro activity of novel analogues of nematophin. *Bioorganic & Medicinal Chemistry Letters*, 8, 2045-2050.

HIROTA, A., OKADA, H., KANZA, T., NAKAYAMA, M., HIROTA, H. & ISOGAI, A. 1989. Structure of Kaimonolide A, a novel macrolide plant growth inhibitor from a *Streptomyces* strain (Organic Chemistry). *Agricultural and Biological Chemistry*, 53, 2831-2833.

HOANG, V., LI, Y. & KIM, S. 2008. Cathepsin B inhibitory activities of phthalates isolated from a marine *Pseudomonas* strain. *Bioorganic & Medicinal Chemistry Letters*, 18, 2083-2088.

HOET, S., OPPERDOES, F., BRUN, R. & QUETIN-LECLERCQ, J. 2004. Natural products active against African trypanosomes: a step towards new drugs. *Natural Product Reports*, 21, 353-364.

HOET, S., PIETERS, L., MUCCIOLI, G. G., HABIB-JIWAN, J. L., OPPERDOES, F. R. & QUETIN-LECLERCQ, J. 2007. Antitrypanosomal activity of triterpenoids and sterols from the leaves of *Strychnos spinosa* and related compounds. *Journal of Natural Products*, 70, 1360-1363.

- HOFMANN, A., HEIM, R., BRACK, A., KOBEL, H., FREY, A., OTT, H., PETRZILKA, T. & TROXLER, F. 1959. Psilocybin und psilocin, zwei psychotrope Wirkstoffe aus mexikanischen Rauschpilzen. *Helvetica Chimica Acta*, 42, 1557-1572.
- HOLZAPFEL, C., BREDEKAMP, M., SNYMAN, R., BOEYENS, J. & ALLEN, C. 1990. Cyclopiamide, an isoindolo[4,6-CD]indole from *Penicillium cyclopium*. *Phytochemistry*, 29, 639-642.
- HORINOUCI, S. & BEPPU, T. 1992. Autoregulatory factors and communication in actinomycetes. *Annual Review of Microbiology*, 46, 377-398.
- HOSOTANI, N., KUMAGAI, K., NAKAGAWA, H., SHIMATANI, T. & SAJI, I. 2005. Antimycins A10 approximately A16, seven new antimycin antibiotics produced by *Streptomyces* spp. SPA-10191 and SPA-8893. *Journal of Antibiotics*, 58, 460-467.
- HOSOYA, T., HIROKAWA, T., TAKAGI, M. & SHIN-YA, K. 2012. Trichostatin analogues JBIR-109, JBIR-110, and JBIR-111 from the marine sponge-derived *Streptomyces* sp. RM72. *Journal of Natural Products*, 75, 285-289.
- HU, S., TAN, R., HONG, K., YU, Z. & ZHU, H. 2005. Methyl indole-3-carboxylate. *Acta Crystallographica Section E-Structure Reports Online*, 61, O1654-O1656.
- HUANG, X., GAO, Y., XUE, D., LIU, H., PENG, C., ZHANG, F., LI, Z. & GU, Y. 2011. Streptomycindole, an indole alkaloid from a marine *Streptomyces* sp DA22 associated with South China Sea sponge *Craniella australiensis*. *Helvetica Chimica Acta*, 94, 1838-1842.
- HUSAIN, A., ALAM, M., SHAHARYAR, M. & LAL, S. 2010. Antimicrobial activities of some synthetic butenolides and their pyrrolone derivatives. *Journal of Enzyme Inhibition and Medicinal Chemistry*, 25, 54-61.
- IKEKAWA, N., TSUDA, K. & MORISAKI, N. 1966. Saringosterol: A new sterol from brown algae. *Chemistry & Industry*, 1179-1180.
- IMAMURA, N., NISHIJIMA, M., ADACHI, K. & SANO, H. 1993. Novel antimycin antibiotics, Urauchimycins A and B, produced by marine actinomycete. *Journal of Antibiotics*, 46, 241-246.
- ISOGAI, A., SAKUDA, S., SHINDO, K., WATANABE, S. & SUZUKI, A. 1986. Structures of cyclocarbamides A and B, new plant growth regulators from *Streptoverticillium* sp. *Tetrahedron Letters*, 27, 1161-1164.
- ITO, S. & HIRATA, Y. 1977. The structure of ikarugamycin, an acyltetramic acid antibiotic possessing a unique asymmetric-hydrindacene skeleton. *Bulletin of the Chemical Society of Japan*, 50, 1813-1820.
- IZUMI, H., GAUTHIER, M., DEGNAN, B., NG, Y., HEWAVITHARANA, A., SHAW, P. & FUERST, J. 2010. Diversity of *Mycobacterium* species from marine

sponges and their sensitivity to antagonism by sponge-derived rifamycin-synthesizing actinobacterium in the genus *Salinispora*. *FEMS Microbiology Letters*, 313, 33-40.

IZUMIKAWA, M., KHAN, S., TAKAGI, M. & SHIN-YA, K. 2010. Sponge-derived *Streptomyces* producing isoprenoids via the mevalonate pathway. *Journal of Natural Products*, 73, 208-212.

JANG, K., KANG, G., JEON, J., LIM, C., LEE, H., SIM, C., OH, K. & SHIN, J. 2009. Haliclolin A, a new macrocyclic diamide from the sponge *Haliclona* sp. *Organic Letters*, 11, 1713-1716.

JASPARS, M., PASUPATHY, V. & CREWS, P. 1994. A tetracyclic diamine alkaloid, Halicyclamine A, from the marine sponge *Haliclona* sp. *Journal of Organic Chemistry*, 59, 3253-3255.

JAYATILAKE, G. S., THORNTON, M. P., LEONARD, A. C., GRIMWADE, J. E. & BAKER, B. J. 1996. Metabolites from an Antarctic sponge-associated bacterium, *Pseudomonas aeruginosa*. *Journal of Natural Products*, 59, 293-296.

JENSEN, P. R. & FENICAL, W. 2005. New Natural-Product Diversity from Marine Actinomycetes. In: ZHANG, L. & DEMAIN, A. L. (eds.) *Natural Products: Drug Discovery and Therapeutic Medicine*. Totowa, NJ: Humana Press Inc.

JERRAM, W., MCINNES, A., MAASS, W., SMITH, D., TAYLOR, A. & WALTER, J. 1975. The chemistry of cochliodinol, a metabolite of *Chaetomium* spp. *Canadian Journal of Chemistry*, 53, 727-737.

JIANG, S., SUN, W., CHEN, M., DAI, S., ZHANG, L., LIU, Y., LEE, K. & LI, X. 2007. Diversity of culturable actinobacteria isolated from marine sponge *Haliclona* sp. *Antonie Van Leeuwenhoek International Journal of General and Molecular Microbiology*, 92, 405-416.

JIN, H., LEE, J., LEE, D., LEE, H., HONG, Y., KIM, Y. & LEE, J. 2004. Quinolone alkaloids with inhibitory activity against nuclear factor of activated T cells from the fruits of *Evodia rutaecarpa*. *Biological & Pharmaceutical Bulletin*, 27, 926-928.

JONSSON, A. & TORSTENSSON, N. 1972. Protease inhibitors from *Streptomyces violascens*. 2. Production of the inhibitors. *Archiv Fur Mikrobiologie*, 83, 71-77.

JU, J., RAJSKI, S., LIM, S., SEO, J., PETERS, N., HOFFMANN, F. & SHEN, B. 2009. Lactimidomycin, iso-migrastatin and related glutarimide-containing 12-membered macrolides are extremely potent inhibitors of cell migration. *Journal of the American Chemical Society*, 131, 1370-1371.

KABARA, J., SWIECZKO, D., TRUANT, J. & CONLEY, A. 1972. Fatty acids and derivatives as antimicrobial agents. *Antimicrobial Agents and Chemotherapy*, 2, 23-28.

- KABARA, J., VRABLE, R. & LIEKENJIE, M. 1977. Antimicrobial lipids: Natural and synthetic fatty acids and monoglycerides. *Lipids*, 12, 753-759.
- KAGEYAMA, A., TAKAHASHI, Y., MATSUO, Y., ADACHI, K., KASAI, H., SHIZURI, Y. & OMURA, S. 2007a. *Microbacterium flavum* sp. nov. and *Microbacterium lactus* sp. nov., isolated from marine environments. *Actinomycetologica*, 21, 53-58.
- KAGEYAMA, A., TAKAHASHI, Y., MATSUO, Y., KASAI, H., SHIZURI, Y. & OMURA, S. 2007b. *Microbacterium sediminicola* sp nov and *Microbacterium marinilacus* sp nov., isolated from marine environments. *International Journal of Systematic and Evolutionary Microbiology*, 57, 2355-2359.
- KANAMITSU, O., KITAJIMA, N. & NAGOYA, I. 1987. A new enzymatic reaction for producing new-type amino acids by *Escherichia coli*: Production of α -amino- β -(1-indoline) propionic acid from indoline and L-serine. *Journal of Fermentation Technology*, 65, 395-403.
- KANAZAWA, A. 2001. Sterols in marine invertebrates. *Fisheries Science*, 67, 997-1007.
- KANEDA, M., SAKANO, K., NAKAMURA, S., KUSHI, Y. & IITAKA, Y. 1981. The structure of carbazomycin B. *Heterocycles*, 15, 993-998.
- KANEHISA, M. & GOTO, S. 2000. KEGG: Kyoto Encyclopedia of Genes and Genomes. *Nucleic Acids Research*, 28, 27-30.
- KANEHISA, M., GOTO, S., SATO, Y., FURUMICHI, M. & TANABE, M. 2012. KEGG for integration and interpretation of large-scale molecular data sets. *Nucleic Acids Research*, 40, D109-D114.
- KAPER, J. M. & VELDSTRA, H. 1958. On the metabolism of tryptophan by *Agrobacterium tumefaciens*. *Biochimica et Biophysica Acta*, 30, 401-420.
- KASHMAN, Y., KOREN-GOLDSHLAGER, G., GRAVALOS, G. & SCHLEYER, M. 1999. Halitulins, a new cytotoxic alkaloid from the marine sponge *Haliclona tulearensis*. *Tetrahedron Letters*, 40, 997-1000.
- KASHMAN, Y. & RUDI, A. 1977. C-13 NMR spectrum and stereochemistry of heteronemin. *Tetrahedron*, 33, 2997-2998.
- KAWASHIMA, H., OHNISHI, M. & OGAWA, S. 2011. Differences in sterol composition of gonads of the lottiid limpets *Nipponacmea concinna* and *Nipponacmea fuscoviridis* from Northeastern Japan. *Journal of Oleo Science*, 60, 501-504.
- KELL, D. 2004. Metabolomics and systems biology: making sense of the soup. *Current Opinion in Microbiology*, 7, 296-307.

KENNEDY, J., BAKER, P., PIPER, C., COTTER, P., WALSH, M., MOOIJ, M., BOURKE, M., REA, M., O'CONNOR, P., ROSS, R., HILL, C., O'GARA, F., MARCHESI, J. & DOBSON, A. 2009. Isolation and analysis of bacteria with antimicrobial activities from the marine sponge *Haliclona simulans* collected from Irish waters. *Marine Biotechnology*, 11, 384-396.

KENNEDY, J., CODLING, C., JONES, B., DOBSON, A. & MARCHESI, J. 2008. Diversity of microbes associated with the marine sponge, *Haliclona simulans*, isolated from Irish waters and identification of polyketide synthase genes from the sponge metagenome. *Environmental Microbiology*, 10, 1888-1902.

KERR, R., BAKER, B., KERR, S. & DJERASSI, C. 1990. Biosynthetic studies of marine lipids. 29. Demonstration of sterol side chain dealkylation using cell-free extracts of marine sponges. *Tetrahedron Letters*, 31, 5425-5428.

KERR, R., STOILOV, I., THOMPSON, J. & DJERASSI, C. 1989. Biosynthetic studies of marine lipids. 16. De novo sterol biosynthesis in sponges. Incorporation and transformation of cycloartenol and lanosterol into unconventional sterols of marine and freshwater sponges. *Tetrahedron*, 45, 1893-1904.

KHAN, S., KOMAKI, H., MOTOHASHI, K., KOZONE, I., MUKAI, A., TAKAGI, M. & SHIN-YA, K. 2011. *Streptomyces* associated with a marine sponge *Haliclona* sp.; biosynthetic genes for secondary metabolites and products. *Environmental Microbiology*, 13, 391-403.

KHAN, S., TAMURA, T., TAKAGI, M. & SHIN-YA, K. 2010. *Streptomyces tateyamensis* sp nov., *Streptomyces marinus* sp nov and *Streptomyces haliclona* sp nov., isolated from the marine sponge *Haliclona* sp. *International Journal of Systematic and Evolutionary Microbiology*, 60, 2775-2779.

KIM, D., BAEK, N., OH, S., JUNG, K., LEE, I., KIM, J. & LEE, H. 1997. Anticomplementary activity of ergosterol peroxide from *Naematoloma fasciculare* and reassignment of NMR data. *Archives of Pharmacal Research*, 20, 201-205.

KINGSTON, J., BENSON, E., GREGORY, B. & FALLIS, A. 1979. Sterols from the marine sponges *Orina arcoferus* and *Geodia megastrella*. *Journal of Natural Products*, 42, 528-531.

KINOSHITA, K., TAKENAKA, S. & HAYASHI, M. 1991. Mycinamicin biosynthesis - Isolation and structural elucidation of mycinonic acids, proposed intermediates for formation of mycinamicins - X-ray molecular structure of para-bromophenacyl 5-hydroxy-4-methylhept-2-enoate. *Journal of the Chemical Society-Perkin Transactions 1*, 2547-2554.

KINOSHITA, M., WADA, M., ABURAGI, S. & UMEZAWA, S. 1971. Total synthesis of antimycin A 3. *Journal of Antibiotics*, 24, 724-726.

KINOSHITA, M., WADA, M. & UMEZAWA, S. 1969. The total synthesis of a diastereomeric mixture of antimycin A₃ (blastmycin). *Journal of Antibiotics*, 22, 580-582.

KIRBY, G., PATRICK, G. & ROBINS, D. 1978. Cyclo-(L-phenylalanyl-L-seryl) as an intermediate in biosynthesis of gliotoxin. *Journal of the Chemical Society-Perkin Transactions 1*, 1336-1338.

KITAGAWA, I., KOBAYASHI, M. & SUGAWARA, T. 1978. Saponin and sapogenol. 25. Steroidal saponins from the starfish *Acanthaster planci* L. (Crown of Thorns). 1. Structures of two genuine sapogenols, Thornasterol A and Thornasterol B, and their sulfates. *Chemical & Pharmaceutical Bulletin*, 26, 1852-1863.

KITAGAWA, I., KOBAYASHI, M., SUGAWARA, T. & YOSIOKA, I. 1975. Thornasterol A and B, two genuine sapogenols from the starfish *Acanthaster planci*. *Tetrahedron Letters*, 967-970.

KITANI, S., MIYAMOTO, K. T., TAKAMATSU, S., HERAWATI, E., IGUCHI, H., NISHITOMI, K., UCHIDA, M., NAGAMITSU, T., OMURA, S., IKEDA, H. & NIHIRA, T. 2011. Avenolide, a *Streptomyces* hormone controlling antibiotic production in *Streptomyces avermitilis*. *Proceedings of the National Academy of Sciences USA*, 108, 16410-16415.

KJELLEBERG, S., STEINBERG, P., GIVSKOV, M., GRAM, L., MANEFIELD, M. & DENYS, R. 1997. Do marine natural products interfere with prokaryotic AHL regulatory systems? *Aquatic Microbial Ecology*, 13, 85-93.

KLEE, C., CROUCH, T. & KRINKS, M. 1979. Calcineurin: A calcium- and calmodulin-binding protein of the nervous system. *Proceedings of the National Academy of Sciences of the United States of America*, 76, 6270-6273.

KLUEPFEL, D., SEHGAL, S. & VEZINA, C. 1970. Antimycin A components. 1. Isolation and biological activity. *Journal of Antibiotics*, 23, 75-80.

KOBAYASHI, J. & ISHIBASHI, M. 1993. Bioactive metabolites of symbiotic marine microorganisms. *Chemical Reviews*, 93, 1753-1769.

KOBAYASHI, J., MADONO, T. & SHIGEMORI, H. 1995a. Nakijiquinones C and D, new sesquiterpenoid quinones with a hydroxy amino acid residue from a marine sponge inhibiting c-erbB-2 kinase. *Tetrahedron*, 51, 10867-10874.

KOBAYASHI, J., TSUDA, M., NEMOTO, A., TANAKA, Y., YAZAWA, K. & MIKAMI, Y. 1997. Brasilidine A, a new cytotoxic isonitrile-containing indole alkaloid from the actinomycete *Nocardia brasiliensis*. *Journal of Natural Products*, 60, 719-720.

KOBAYASHI, M., CHEN, Y., AOKI, S., IN, Y., ISHIDA, T. & KITAGAWA, I. 1995b. Four new beta-carboline alkaloids isolated from two Okinawan marine sponges of *Xestospongia* sp. and *Haliclona* sp. *Tetrahedron*, 51, 3727-3736.

- KOBAYASHI, M. & KITAGAWA, I. 1999. Marine spongean cytotoxins. *Journal of Natural Toxins*, 8, 249-258.
- KODANI, S., IMOTO, A., MITSUTANI, A. & MURAKAMI, M. 2002. Isolation and identification of the antialgal compound, harmaline (1-methyl-beta-carboline), produced by the algicidal bacterium, *Pseudomonas* sp K44-1. *Journal of Applied Phycology*, 14, 109-114.
- KOL, S., MERLO, M., SCHELTEMA, R., DE VRIES, M., VONK, R., KIKKERT, N., DIJKHUIZEN, L., BREITLING, R. & TAKANO, E. 2010. Metabolomic characterization of the salt stress response in *Streptomyces coelicolor*. *Applied and Environmental Microbiology*, 76, 2574-2581.
- KOMORI, T. 1990. Trichomycin B, a polyene macrolide from *Streptomyces*. *Journal of Antibiotics*, 43, 778-782.
- KONDO, K., HIGUCHI, Y., SAKUDA, S., NIHIRA, T. & YAMADA, Y. 1989. New virginiae butanolides from *Streptomyces virginiae*. *Journal of Antibiotics*, 42, 1873-1876.
- KOSHIMIZU, K., IRIE, K., HAGIWARA, N., HIROTA, HAYASHI, H., MURAO, S., TOKUDA, H. & ITO, Y. 1985. Structures and biological activities of indole alkaloid tumor promoters produced by *Streptoverticillium blastmyceticum*. *27th Symposium on the Chemistry of Natural Products*. Hiroshima.
- KOZHUHAROVA, L., GOCHEV, V. & KOLEVA, L. 2008. Isolation, purification and characterization of levorin produced by *Streptomyces levoris* 99/23. *World Journal of Microbiology & Biotechnology*, 24, 1-5.
- KOZONE, I., IZUMIKAWA, M., MOTOHASHI, K., NAGAI, A., YOSHIDA, M., DOI, T., TAKAGI, M. & SHIN-YA, K. 2011. Isolation of new hexapeptides - JBIR-39 and JBIR-40 - from a marine sponge-derived *Streptomyces* sp. Sp080513SC-24. *Journal of Marine Science: Research and Development*, 1, 101.
- KTARI, L. & GUYOT, M. 1999. A cytotoxic oxysterol from the marine alga *Padina pavonica* (L.) Thivy. *Journal of Applied Phycology*, 11, 511-513.
- KULANTHAIVEL, P., PERUN, T., BELVO, M., STROBEL, R., PAUL, D. & WILLIAMS, D. 1999. Novel naphthoquinones from a *Streptomyces* sp. *Journal of Antibiotics*, 52, 256-262.
- LABEDA, D., GOODFELLOW, M., BROWN, R., WARD, A., LANOOT, B., VANNCANNEYT, M., SWINGS, J., KIM, S., LIU, Z., CHUN, J., TAMURA, T., OGUCHI, A., KIKUCHI, T., KIKUCHI, H., NISHII, T., TSUJI, K., YAMAGUCHI, Y., TASE, A., TAKAHASHI, M., SAKANE, T., SUZUKI, K. & HATANO, K. 2012. Phylogenetic study of the species within the family *Streptomycetaceae*. *Antonie Van Leeuwenhoek International Journal of General and Molecular Microbiology*, 101, 73-104.

- LAMB, D., KELLY, D., MANNING, N. & KELLY, S. 1998. A sterol biosynthetic pathway in *Mycobacterium*. *FEBS Letters*, 437, 142-144.
- LANG, G., MAYHUDIN, N., MITOVA, M., SUN, L., VAN DER SAR, S., BLUNT, J., COLE, A., ELLIS, G., LAATSCH, H. & MUNRO, M. 2008. Evolving trends in the dereplication of natural product extracts: New methodology for rapid, small-scale investigation of natural product extracts. *Journal of Natural Products*, 71, 1595-1599.
- LANG, S., BEIL, W., TOKUDA, H., WICKE, C. & LURTZ, V. 2004. Improved production of bioactive glucosylmannosyl-glycerolipid by sponge-associated *Microbacterium* species. *Marine Biotechnology*, 6, 152-156.
- LARSEN, S. H., BOECK, L. D., MERTZ, F. P., PASCHAL, J. W. & OCCOLOWITZ, J. L. 1988. 16-Deethylindanomycin (A83094A), a novel pyrrole-ether antibiotic produced by a strain of *Streptomyces setonii*. Taxonomy, fermentation, isolation and characterization. *Journal of Antibiotics*, 41, 1170-1177.
- LAWSON, M., STOILOV, I., THOMPSON, J. & DJERASSI, C. 1988. Sterols in marine invertebrates. 59. Cell membrane localization of sterols with conventional and unusual side chains in two marine demosponges. *Lipids*, 23, 750-754.
- LEE, S., KIM, H., PARK, B., AHN, S., LEE, H. & AHN, J. 1997. Topical anti-inflammatory activity of dianemycin isolated from *Streptomyces* sp. MT 2705-4. *Archives of Pharmacal Research*, 20, 372-374.
- LEGROS, D., OLLIVIER, G., GASTELLU-ETCHEGORRY, M., PAQUET, C., BURRI, C., JANNIN, J. & BUSCHER, P. 2002. Treatment of human African trypanosomiasis - present situation and needs for research and development. *Lancet Infectious Diseases*, 2, 437-440.
- LI, K., LI, Q., JI, N., LIU, B., ZHANG, W. & CAO, X. 2011. Deoxyuridines from the marine sponge associated actinomycete *Streptomyces microflavus*. *Marine Drugs*, 9, 690-695.
- LI, Y., LI, X., KIM, D., CHOI, H. & SON, B. 2003. Indolyl alkaloid derivatives, N-b-acetyltryptamine and oxaline from a marine-derived fungus. *Archives of Pharmacal Research*, 26, 21-23.
- LIDGREN, G., BOHLIN, L. & CHRISTOPHERSEN, C. 1988. Studies of Swedish marine organisms. 10. Biologically active compounds from the marine sponge *Geodia baretii*. *Journal of Natural Products*, 51, 1277-1280.
- LIU, M., SEIDEL, V., KATERERE, D. R. & GRAY, A. I. 2007. Colorimetric broth microdilution method for the antifungal screening of plant extracts against yeasts. *Methods*, 42, 325-329.
- LIU, W. & STRONG, F. 1959. The chemistry of Antimycin A. 6. Separation and properties of Antimycin A subcomponents. *Journal of the American Chemical Society*, 81, 4387-4390.

- LOPEZ, J., INSUA, M., BAZ, J., PUENTES, J. & HERNANDEZ, L. 2003. New cytotoxic indolic metabolites from a marine *Streptomyces*. *Journal of Natural Products*, 66, 863-864.
- LORENTE, S., RODRIGUES, J., JIMENEZ, C., JOYCE-MENEKSE, M., RODRIGUES, C., CROFT, S., YARDLEY, V., DE LUCA-FRADLEY, K., RUIZ-PEREZ, L., URBINA, J., DE SOUZA, W., PACANOWSKA, D. & GILBERT, I. 2004. Novel azasterols as potential agents for treatment of leishmaniasis and trypanosomiasis. *Antimicrobial Agents and Chemotherapy*, 48, 2937-2950.
- LU, H., XIE, H., GONG, Y., WANG, Q. & YANG, Y. 2011. Secondary metabolites from the seaweed *Gracilaria lemaneiformis* and their allelopathic effects on *Skeletonema costatum*. *Biochemical Systematics and Ecology*, 39, 397-400.
- LUO, X., LI, F., HONG, J., LEE, C. O., SIM, C. J., IM, K. S. & JUNG, J. H. 2006a. Cytotoxic oxylipins from a marine sponge *Topsentia* sp. *Journal of Natural Products*, 69, 567-571.
- LUO, X., LI, F., SHINDE, P., HONG, J., LEE, C., IM, K. & JUNG, J. 2006b. 26,27-cyclosterols and other polyoxygenated sterols from a marine sponge *Topsentia* sp. *Journal of Natural Products*, 69, 1760-1768.
- MA, W., MUTKA, T., VESLEY, B., AMSLER, M., MCCLINTOCK, J., AMSLER, C., PERMAN, J., SINGH, M., MAIESE, W., ZAWOROTKO, M., KYLE, D. & BAKER, B. 2009. Norselic acids A-E, highly oxidized anti-infective steroids that deter mesograzers, from the Antarctic Sponge *Crella* sp. *Journal of Natural Products*, 72, 1842-1846.
- MACGREGOR, R. 1995. Cutaneous tuberculosis. *Clinics in Dermatology*, 13, 245-255.
- MADSEN, R., LUNDSTEDT, T. & TRYGG, J. 2010. Chemometrics in metabolomics-A review in human disease diagnosis. *Analytica Chimica Acta*, 659, 23-33.
- MAEHR, H. & BERGER, J. 1969. Production, isolation and characterization of a grisein-like sideromycin complex. *Biotechnology and Bioengineering*, 11, 1111-1123.
- MAKKAR, N. S., NICKSON, T. E., TRAN, M., BIEST, N., MILLER-WIDEMAN, M., LAWSON, J., MCGARY, C. I. & STONARD, R. 1995. Phenamide, a fungicidal metabolite from *Streptomyces albospinus* A19301. Taxonomy, fermentation, isolation, physico-chemical and biological properties. *Journal of Antibiotics*, 48, 369-374.
- MALIK, S., KERR, R. & DJERASSI, C. 1988. Biosynthesis of marine lipids. 19. Dealkylation of the sterol side chain in sponges. *Journal of the American Chemical Society*, 110, 6895-6897.

- MANCINI, I., GUELLA, G., GUERRIERO, A., BOLDRIN, A. & PIETRA, F. 1987. Adriadysiolide, the first monoterpene isolated from a marine sponge. *Helvetica Chimica Acta*, 70, 2011-2018.
- MANSFIELD, J. M. 1990. Immunology of African Trypanosomiasis. In: WYLER, D. J. (ed.) *Modern Parasite Biology: Cellular, Immunological and Molecular Aspects*. New York: W.H. Freeman and Company.
- MANSOOR, T., HONG, J., LEE, C., BAE, S., IM, K. & JUNG, J. 2005. Cytotoxic sterol derivatives from a marine sponge *Homaxinella* sp. *Journal of Natural Products*, 68, 331-336.
- MANSOOR, T. A., LEE, Y. M., HONG, J., LEE, C. O., IM, K. S. & JUNG, J. H. 2006. 5,6:8,9-diepoxy and other cytotoxic sterols from the marine sponge *Homaxinella* sp. *J Nat Prod*, 69, 131-134.
- MARGASSERY, L., KENNEDY, J., O'GARA, F., DOBSON, A. & MORRISSEY, J. 2012. A high-throughput screen to identify novel calcineurin inhibitors. *Journal of Microbiological Methods*, 88, 63-66.
- MARTINELLI, D., GROSSMANN, G., SEQUIN, U., BRANDL, H. & BACHOFEN, R. 2004. Effects of natural and chemically synthesized furanones on quorum sensing in *Chromobacterium violaceum*. *BMC Microbiology*, 4, 25.
- MARTINEZ-LUIS, S., GOMEZ, J., SPADAFORA, C., GUZMAN, H. & GUTIERREZ, M. 2012. Antitrypanosomal alkaloids from the marine bacterium *Bacillus pumilus*. *Molecules*, 17, 11146-11155.
- MARTINS, M. & CARVALHO, I. 2007. Diketopiperazines: biological activity and synthesis. *Tetrahedron*, 63, 9923-9932.
- MASKEY, R., ASOLKAR, R., KAPAUN, E., WAGNER-DOBLER, I. & LAATSCH, H. 2002. Phytotoxic arylethylamides from limnic bacteria using a screening with microalgae. *Journal of Antibiotics*, 55, 643-649.
- MASKEY, R. P., SHAABAN, M., GRÜN-WOLLNY, I. & LAATSCH, H. 2004. Quinazolin-4-one derivatives from *Streptomyces* isolates. *Journal of Natural Products*, 67, 1131-1134.
- MASUNO, M., PAWLIK, J. & MOLINSKI, T. 2004. Phorbasterones A-D, cytotoxic Nor-ring a steroids from the sponge *Phorbas amaranthus*. *Journal of Natural Products*, 67, 731-733.
- MATSUNAGA, S., FUSEYANI, N. & NAKAO, Y. 1992. Eight new cytotoxic metabolites closely related to onnamide A from two marine sponges of the genus *Theonella*. *Tetrahedron*, 48, 8369-8376.
- MAYER, A., GLASER, K., CUEVAS, C., JACOBS, R., KEM, W., LITTLE, R., MCINTOSH, J., NEWMAN, D., POTTS, B. & SHUSTER, D. 2010. The odyssey of

marine pharmaceuticals: A current pipeline perspective. *Trends in Pharmacological Sciences*, 31, 255-265.

MCCLEAN, K., WINSON, M., FISH, L., TAYLOR, A., CHHABRA, S., CAMARA, M., DAYKIN, M., LAMB, J., SWIFT, S., BYCROFT, B., STEWART, G. & WILLIAMS, P. 1997. Quorum sensing and *Chromobacterium violaceum*: Exploitation of violacein production and inhibition for the detection of N-acylhomoserine lactones. *Microbiology*, 143, 3703-3711.

MEHDI, R., SHAABAN, K., REBAI, I., SMAOUI, S., BEJAR, S. & MELLOULI, L. 2009. Five naturally bioactive molecules including two rhamnopyranoside derivatives isolated from the *Streptomyces* sp strain TN58. *Natural Product Research*, 23, 1095-1107.

MIKA, A., GOLEBIOWSKI, M., SKORKOWSKI, E. & STEPNOWSKI, P. 2012. Composition of fatty acids and sterols composition in brown shrimp *Crangon crangon* and herring *Clupea harengus membras* from the Baltic Sea. *Oceanological and Hydrobiological Studies*, 41, 57-64.

MITOVA, M., LANG, G., WIESE, J. & IMHOFF, J. 2008. Subinhibitory concentrations of antibiotics induce phenazine production in a marine *Streptomyces* sp. *Journal of Natural Products*, 71, 824-827.

MITOVA, M., POPOV, S. & DE ROSA, S. 2004. Cyclic peptides from a *Ruegeria* strain of bacteria associated with the sponge *Suberites domuncula*. *Journal of Natural Products*, 67, 1178-1181.

MOCO, S., BINO, R., VORST, O., VERHOEVEN, H., DE GROOT, J., VAN BEEK, T., VERVOORT, J. & DE VOS, C. 2006. A liquid chromatography-mass spectrometry-based metabolome database for tomato. *Plant Physiology*, 141, 1205-1218.

MORINO, T., SHIMADA, K., NAKATANI, A., NISHIKAWA, K., HARADA, T. & SAITO, S. 1995. Medelamines, novel anticancer agents which cancel RAS2-val19 induced heat shock sensitivity of yeast. *Journal of Antibiotics*, 48, 904-906.

MOTOHASHI, K., INABA, K., FUSE, S., DOI, T., IZUMIKAWA, M., KHAN, S., TAKAGI, M., TAKAHASHI, T. & SHIN-YA, K. 2011. JBIR-56 and JBIR-57, 2(1H)-Pyrazinones from a marine sponge-derived *Streptomyces* sp SpD081030SC-03. *Journal of Natural Products*, 74, 1630-1635.

MOTOHASHI, K., TAKAGI, M. & SHIN-YA, K. 2010a. Tetracenoquinocin and 5-Iminoaranciamycin from a sponge-derived *Streptomyces* sp Sp080513GE-26. *Journal of Natural Products*, 73, 755-758.

MOTOHASHI, K., TAKAGI, M. & SHIN-YA, K. 2010b. Tetrapeptides possessing a unique skeleton, JBIR-34 and JBIR-35, isolated from a sponge-derived actinomycete, *Streptomyces* sp Sp080513GE-23. *Journal of Natural Products*, 73, 226-228.

- MUKKU, V., SPEITLING, M., LAATSCH, H. & HELMKE, E. 2000. New butenolides from two marine streptomycetes. *Journal of Natural Products*, 63, 1570-1572.
- MUTERT, W., LUTFRING, H., BARZ, W. & STRACK, D. 1981. Formation of fusaric acid by fungi of the genus *Fusarium*. *Zeitschrift Fur Naturforschung C*, 36, 338-339.
- NARAYANAN, T. K. & RAO, G. R. 1976. Beta-indoleethanol and beta-indolelactic acid production by *Candida* species: their antibacterial and autoantibiotic action. *Antimicrobial Agents and Chemotherapy*, 9, 375-380.
- NARUSE, N., TENMYO, O., KOBARU, S., KAMEI, H., MIYAKI, T., KONISHI, M. & OKI, T. 1990. Pumilacidin, a complex of new antiviral antibiotics: Production, isolation, chemical properties, structure and biological activity. *Journal of Antibiotics*, 43, 267-280.
- NEEMAN, I., FISHELSON, L. & KASHMAN, Y. 1975. Isolation of a new toxin from the sponge *Latrunculia magnifica* in the Gulf of Aquaba (Red Sea). *Marine Biology*, 30, 293-296.
- NEFT, N. & FARLEY, T. 1972. Conditions influencing antimycin production by a *Streptomyces* species grown in chemically defined medium. *Antimicrobial Agents and Chemotherapy*, 1, 274-276.
- NETTLETON, D. E., BALITZ, D. M., DOYLE, T. W., BRADNER, W. T., JOHNSON, D. L., O'HERRON, F. A., SCHREIBER, R. H., COON, A. B., MOSELEY, J. E. & MYLLYMAKI, R. W. 1980. Antitumor agents from bohemic acid complex, III. The isolation of marcellomycin, musettamycin, rudolphomycin, mimimycin, collinemycin, alcindoromycin, and bohemicamine. *Journal of Natural Products*, 43, 242-258.
- NEWMAN, D. & CRAGG, G. 2004. Marine natural products and related compounds in clinical and advanced preclinical trials. *Journal of Natural Products*, 67, 1216-1238.
- NGHIEM, P., PEARSON, G. & LANGLEY, R. 2002. Tacrolimus and pimecrolimus: From clever prokaryotes to inhibiting calcineurin and treating atopic dermatitis. *Journal of the American Academy of Dermatology*, 46, 228-241.
- NICHOLSON, J., LINDON, J. & HOLMES, E. 1999. 'Metabonomics': understanding the metabolic responses of living systems to pathophysiological stimuli via multivariate statistical analysis of biological NMR spectroscopic data. *Xenobiotica*, 29, 1181-1189.
- NISHIDA, F., MORI, Y., ISOBE, S., FURUSE, T., SUZUKI, M., MEEVOOTISOM, V., FLEGEL, T. & THEBTARANONTH, Y. 1988. Structures of deacetyl glykenins-A, B and C, glycosidic antibiotics from *Basidiomycetes* sp. *Tetrahedron Letters*, 29, 5287-5290.

- NISHIDA, R., OHSUGI, T. & FUKAMI, H. 1990. Oviposition stimulant activity of tryptamine analogs on a Rutaceae-feeding swallowtail butterfly, *Papilio xuthus*. *Agricultural and Biological Chemistry*, 54, 1853-1855.
- NIWA, H., WAKAMATSU, K. & YAMADA, K. 1989. Halicholactone and neohalicholactone, two novel fatty acid metabolites from the marine sponge *Halichondria okadai* Kadota. *Tetrahedron Letters*, 30, 4543-4546.
- NOGLE, L. M. & GERWICK, W. H. 2002. Isolation of four new cyclic depsipeptides, antanapeptins A-D, and dolastatin 16 from a Madagascan collection of *Lyngbya majuscula*. *Journal of Natural Products*, 65, 21-24.
- O'HANLON, P. J., ROGERS, N. H. & TYLER, J. W. 1983. The chemistry of pseudomonic acid. Part 6. Structure and preparation of pseudomonic acid D. *Journal of the Chemical Society, Perkin Transactions 1*, 2655-2657.
- OHARA, T., ITOH, Y., ITOH, K. & TETSUKA, T. 2001. Analysis of methicillin-resistant *Staphylococcus aureus* isolates by proton magnetic resonance spectroscopy. *Journal of Infection*, 43, 116-121.
- OKAMI, Y. & HOTTA, K. 1988. Search and Discovery of New Antibiotics. In: GOODFELLOW, M., WILLIAMS, S. T. & MORDARSKI, M. (eds.) *Actinomycetes in Biotechnology*. London: Academic Press Ltd.
- OKUDOH, V. & WALLIS, F. 2012. Enhanced recovery and identification of a tryptamine-related antibiotic produced by *Intrasporangium* N8 from KwaZulu-Natal, South Africa. *Tropical Journal of Pharmaceutical Research*, 11, 729-737.
- OKUDOH, V. I. 2010. *Isolation and Characterization of Antibiotic(s) Produced by Bacteria from Kwazulu-Natal Soils*. PhD in Microbiology, University of Kwazulu-Natal.
- OLENIKOVA, G., IVCHUK, O., DENISENKO, V., CHAIKINA, E., MENZOROVA, N., NEDASHKOVSKAYA, O. & KUZNETSOVA, T. 2006. Indolic metabolites from the new marine bacterium *Roseivirga echinicomitans* KMM 6058(T). *Chemistry of Natural Compounds*, 42, 713-717.
- OOI, T. T. 2010. *Metabolomic Profiling of Anti-trypanosomal Active Sponge Extracts*. MPharm, University of Strathclyde.
- OSINGA, R., TRAMPER, J. & WIJFFELS, R. 1999. Cultivation of marine sponges. *Marine Biotechnology*, 1, 509-532.
- OVENDEN, S., NIELSON, J., LIPROT, C., WILLIS, R., TAPIOLAS, D., WRIGHT, A. & MOTTI, C. 2012. Update of spectroscopic data for 4-hydroxydictyolactone and dictyol E isolated from a *Halimeda stuposa* - *Dictyota* sp. assemblage. *Molecules*, 17, 2929-2938.
- PAIK, S., PARK, N., JHUN, S., PARK, H., LEE, C., CHO, B., BYUN, H., CHOE, S. & SUH, S. 2003. Isolation and synthesis of tryptamine derivatives from a

- symbiotic bacterium *Xenorhabdus nematophilus* PC. *Bulletin of the Korean Chemical Society*, 24, 623-626.
- PALERMO, J., BRASCO, M., HUGHES, E., SELDES, A., BALZARETTI, V. & CABEZAS, E. 1996. Short side chain sterols from the tunicate *Polizoa opuntia*. *Steroids*, 61, 2-6.
- PARK, Y., GUNASEKERA, S., LOPEZ, J., MCCARTHY, P. & WRIGHT, A. 2006. Metabolites from the marine-derived fungus *Chromocleista* sp isolated from a deep-water sediment sample collected in the Gulf of Mexico. *Journal of Natural Products*, 69, 580-584.
- PAUL, P. & FUJIWARA, Y. 1981. Elastatinal and leupeptin: Effects on UV-induced mutation and sister chromatid exchange in Chinese hamster cells. *Carcinogenesis*, 2, 255-259.
- PEDRAS, M., YU, Y., LIU, J. & TANDRON-MOYA, Y. 2005. Metabolites produced by the phytopathogenic fungus *Rhizoctonia solani*: Isolation, chemical structure determination, syntheses and bioactivity. *Zeitschrift Fur Naturforschung C*, 60, 717-722.
- PERAUD, O. 2006. *Isolation and Characterization of a Sponge-associated Actinomycete that Produces Manzamines*. PhD, University of Maryland.
- PEREIRA, M. E. A. 1990. Cell Biology of *Trypanosoma cruzi*. In: WYLER, D. J. (ed.) *Modern Parasite Biology: Cellular, Immunological and Molecular Aspects*. New York: W.H. Freeman and Company.
- PERIC-CONCHA, N. & LONG, P. 2003. Mining the microbial metabolome: a new frontier for natural product lead discovery. *Drug Discovery Today*, 8, 1078-1084.
- PETRINI, B. 2006. *Mycobacterium marinum*: Ubiquitous agent of waterborne granulomatous skin infections. *European Journal of Clinical Microbiology and Infectious Diseases*, 25, 609-613.
- PFAU, W. & SKOG, K. 2004. Exposure to beta-carbolines norharman and harman. *Journal of Chromatography B*, 802, 115-126.
- PHILLIPS, K. M., RUGGIO, D. M., EXLER, J. & PATTERSON, K. Y. 2012. Sterol composition of shellfish species commonly consumed in the United States. *Food Nutrition & Research*, 56, 18931.
- PIMENTEL-ELARDO, S., KOZYTSKA, S., BUGNI, T., IRELAND, C., MOLL, H. & HENTSCHEL, U. 2010. Anti-parasitic compounds from *Streptomyces* sp strains isolated from Mediterranean sponges. *Marine Drugs*, 8, 373-380.
- PINHEIRO, A., DETHOUP, T., BESSA, J., SILVA, A. & KIJJOA, A. 2012. A new bicyclic sesquiterpene from the marine sponge associated fungus *Emericellopsis minima*. *Phytochemistry Letters*, 5, 68-70.

- POTTERAT, O., ZAHNER, H., METZGER, J. & FREUND, S. 1994. Metabolic products of microorganisms. 269. 5-Phenylpentadienoic acid derivatives from *Streptomyces* sp. *Helvetica Chimica Acta*, 77, 569-574.
- POUCHERT, C. & BEHNKE, J. 1993. *The Aldrich Library of 13C and 1H NMR Spectra Edition 1*, USA, Aldrich Chemical Company, Inc.
- PRAWAT, H., MAHIDOL, C., WITTAYALAI, S., INTACHOTE, P., KANCHANAPOOM, T. & RUCHIRAWAT, S. 2011. Nitrogenous sesquiterpenes from the Thai marine sponge *Halichondria* sp. *Tetrahedron*, 67, 5651-5655.
- PROJAN, S., BROWNSKROBOT, S., SCHLIEVERT, P., VANDENESCH, F. & NOVICK, R. 1994. Glycerol monolaurate inhibits the production of beta-lactamase, toxic shock syndrome toxin-1, and other staphylococcal exoproteins by interfering with signal transduction. *Journal of Bacteriology*, 176, 4204-4209.
- PROKSCH, P. 1994. Defensive roles for secondary metabolites from marine sponges and sponge-feeding nudibranchs. *Toxicon*, 32, 639-655.
- PROKSCH, P., EDRADA, R. & LIN, W. H. 2006. Implications of Marine Biotechnology on Drug Discovery. In: PROKSCH, P. & MÜLLER, W. E. G. (eds.) *Frontiers in Marine Biotechnology*. Norfolk, UK: Horizon Bioscience.
- RADWAN, M., MANLY, S., EL SAYED, K., WALI, V., SYLVESTER, P., AWATE, B., SHAH, G. & ROSS, S. 2008. Sinulodurins A and B, antiproliferative and anti-invasive diterpenes from the soft coral *Sinularia dura*. *Journal of Natural Products*, 71, 1468-1471.
- RAMESHTHANGAM, P. & RAMASAMY, P. 2007. Antiviral activity of bis(2-methylheptyl)phthalate isolated from *Pongamia pinnata* leaves against White Spot Syndrome Virus of *Penaeus monodon* Fabricius. *Virus Research*, 126, 38-44.
- RANDAZZO, A., BIFULCO, G., GIANNINI, C., BUCCI, M., DEBITUS, C., CIRINO, G. & GOMEZ-PALOMA, L. 2001. Halipeptins A and B: Two novel potent anti-inflammatory cyclic depsipeptides from the vanuatu marine sponge *Haliclona* species. *Journal of the American Chemical Society*, 123, 10870-10876.
- RASHID, M., GUSTAFSON, K., BOSWELL, J. & BOYD, M. 2000. Haligramides A and B, two new cytotoxic hexapeptides from the marine sponge *Haliclona nigra*. *Journal of Natural Products*, 63, 956-959.
- RASHID, M. A., GUSTAFSON, K. R. & BOYD, M. R. 2001. A new isoquinoline alkaloid from the marine sponge *Haliclona* species. *Journal of Natural Products*, 64, 1249-1250.
- REEVES, E. K., HOFFMAN, E. P., NAGARAJU, K., DAMSKER, J. M. & MCCALL, J. M. 2013. VBP15: preclinical characterization of a novel anti-inflammatory delta 9,11 steroid. *Bioorganic and Medicinal Chemistry*, 21, 2241-2249.

- REHACEK, Z., RAMANKUTTY, M. & KOZOVA, J. 1968. Respiratory chain of Antimycin A-producing *Streptomyces antibioticus*. *Applied Microbiology*, 16, 29-32.
- REZANKA, T. & GUSCHINA, I. A. 2001. Glycoside esters from lichens of central Asia. *Phytochemistry*, 58, 509-516.
- RICLEA, R., AIGLE, B., LEBLOND, P., SCHOENIAN, I., SPITELLER, D. & DICKSCHAT, J. S. 2012. Volatile lactones from streptomycetes arise via the antimycin biosynthetic pathway. *Chembiochem*, 13, 1635-1644.
- RIGALI, S., TITGEMEYER, F., BARENDS, S., MULDER, S., THOMAE, A., HOPWOOD, D. & VAN WEZEL, G. 2008. Feast or famine: the global regulator DasR links nutrient stress to antibiotic production by *Streptomyces*. *EMBO Reports*, 9, 670-675.
- RIGAUD, J. 1970. [Indole-3-lactic acid and its metabolism by *Rhizobium*]. *Archiv fur Mikrobiologie*, 72, 297-307.
- RIVAS, P., CASSELS, B., MORELLO, A. & REPETTO, Y. 1999. Effects of some beta-carboline alkaloids on intact *Trypanosoma cruzi* epimastigotes. *Comparative Biochemistry and Physiology C-Pharmacology Toxicology & Endocrinology*, 122, 27-31.
- ROGGO, B., HUG, P., MOSS, S., RASCHDORF, F. & PETER, H. 1994a. 3-Alkanoyl-5-hydroxymethyl tetronic acid homologs - New inhibitors of HIV-1 protease. 2. Structure determination. *Journal of Antibiotics*, 47, 143-147.
- ROGGO, B., PETERSEN, F., DELMENDO, R., JENNY, H., PETER, H. & ROESEL, J. 1994b. 3-Alkanoyl-5-hydroxymethyl tetronic acid homologs and resistomycin - New inhibitors of HIV-1 protease. 1. Fermentation, isolation and biological activity. *Journal of Antibiotics*, 47, 136-142.
- ROONGSAWANG, N., WASHIO, K. & MORIKAWA, M. 2011. Diversity of nonribosomal peptide synthetases involved in the biosynthesis of lipopeptide biosurfactants. *International Journal of Molecular Sciences*, 12, 141-172.
- ROSENBLUM, E., TJEERDEMA, R. & VIANT, M. 2006. Effects of temperature on host-pathogen-drug interactions in red abalone, *Haliotis rufescens*, determined by 1H NMR metabolomics. *Environmental Science & Technology*, 40, 7077-7084.
- ROVIROSA, J., ASTUDILLO, L., RAMIREZ, M. & SAN MARTIN, A. 1991. Chemical relationship between *Aplysia dactylomela* and *Laurencia claviformis* Borgesen from Easter Island. *Boletin De La Sociedad Chilena De Quimica*, 36, 153-156.
- RUGUTT, J. K. & RUGUTT, K. J. 2002. Relationships between molecular properties and antimycobacterial activities of steroids. *Natural Product Letters*, 16, 107-113.

- RUSNAK, F. & MERTZ, P. 2000. Calcineurin: Form and function. *Physiological Reviews*, 80, 1483-1521.
- RUZIN, A. & NOVICK, R. 2000. Equivalence of lauric acid and glycerol monolaurate as inhibitors of signal transduction in *Staphylococcus aureus*. *Journal of Bacteriology*, 182, 2668-2671.
- SADAKANE, N., TANAKA, Y. & OMURA, S. 1982. Hybrid biosynthesis of derivatives of protylonolide and M-4365 by macrolide-producing microorganisms. *Journal of Antibiotics*, 35, 680-687.
- SAITO, H. & TOMIOKA, H. 1988. Susceptibilities of transparent, opaque and rough colonial variants of *Mycobacterium avium* complex to various fatty acids. *Antimicrobial Agents and Chemotherapy*, 32, 400-402.
- SAITO, H., TOMIOKA, H. & YONEYAMA, T. 1984. Growth of Group IV Mycobacteria on medium containing various saturated and unsaturated fatty acids. *Antimicrobial Agents and Chemotherapy*, 26, 164-169.
- SAITO, T., SUZUKI, Y., KOYAMA, K., NATORI, S., IITAKA, Y. & KINOSITA, T. 1988. Chetracin A and Chaetocins B and C, three new epipolythiodioxo-piperazines from *Chaetomium* spp. *Chemical and Pharmaceutical Bulletin*, 36, 1942-1956.
- SAKAI, R. & HIGA, T. 1986. Manzamine A, a novel antitumor alkaloid from a sponge. *Journal of the American Chemical Society*, 108, 6404-6405.
- SAKAI, R., KOHMOTO, S. & HIGA, T. 1987. Manzamine B and C, two novel alkaloids from the sponge *Haliclona* sp. *Tetrahedron Letters*, 28, 5493-5496.
- SAKANO, K., ISHIMARU, K. & NAKAMURA, S. 1980. New antibiotics, carbazomycins A and B. I. Fermentation, extraction, purification and physico-chemical and biological properties. *Journal of Antibiotics*, 33, 683-689.
- SAKANO, K. & NAKAMURA, S. 1980. New antibiotics, carbazomycins A and B. II. Structural elucidation. *Journal of Antibiotics*, 33, 961-966.
- SAMANT, B. & CHAKAINGESU, C. 2013. Novel naphthoquinone derivatives: Synthesis and activity against human African trypanosomiasis. *Bioorganic & Medicinal Chemistry Letters*, 23, 1420-1423.
- SANCHEZ, S. & DEMAIN, A. 2002. Metabolic regulation of fermentation processes. *Enzyme and Microbial Technology*, 31, 895-906.
- SARKER, S. D., NAHAR, L. & KUMARASAMY, Y. 2007. Microtitre plate-based antibacterial assay incorporating resazurin as an indicator of cell growth, and its application in the in vitro antibacterial screening of phytochemicals. *Methods*, 42, 321-324.

SASTRY, V. & RAO, G. 1995. Dioctyl phthalate, and antibacterial compound from the marine brown alga - *Sargassum wightii*. *Journal of Applied Phycology*, 7, 185-186.

SCBD. 2014. *Convention on biological diversity: History of the convention* [Online]. Secretariat of the Convention on Biological Diversity. Available: <http://www.cbd.int/history/> [Accessed 7 May 2014].

SCHAEFER, W. & LEWIS, C. 1965. Effect of oleic acid on growth and cell structure of mycobacteria. *Journal of Bacteriology*, 90, 1438-1447.

SCHEUERMAYER, M., PIMENTEL-ELARDO, S., FIESELER, L., GROZDANOV, L. & HENTSCHEL, U. 2006. Microorganisms of Sponges: Phylogenetic Diversity and Biotechnological Potential. In: PROKSCH, P. & MÜLLER, W. E. G. (eds.) *Frontiers in Marine Biotechnology*. Norfolk, UK: Horizon Bioscience.

SCHILLING, G., BERTI, D. & KLUEPFEL, D. 1970. Antimycin A components. II. Identification and analysis of antimycin A fractions by pyrolysis-gas liquid chromatography. *Journal of Antibiotics*, 23, 81-90.

SCHLIEVERT, P., DERINGER, J., KIM, M., PROJAN, S. & NOVICK, R. 1992. Effect of glycerol monolaurate on bacterial growth and toxin production. *Antimicrobial Agents and Chemotherapy*, 36, 626-631.

SCHMIDT, G., TIMM, C. & KOCK, M. 2009. New haliclamines E and F from the Arctic sponge *Haliclona viscosa*. *Organic & Biomolecular Chemistry*, 7, 3061-3064.

SCHMITZ, F., VANDERAH, D., HOLLENBEAK, K., ENWALL, C., GOPICHAND, Y., SENGUPTA, P., HOSSAIN, M. & VANDERHELM, D. 1983. Metabolites from the marine sponge *Tedania ignis*. A new atisanediol and several known diketopiperazines. *Journal of Organic Chemistry*, 48, 3941-3945.

SCHNEEMANN, I., KAJAHN, I., OHLENDORF, B., ZINECKER, H., ERHARD, A., NAGEL, K., WIESE, J. & IMHOFF, J. 2010. Mayamycin, a cytotoxic polyketide from a *Streptomyces* strain isolated from the marine sponge *Halichondria panicea*. *Journal of Natural Products*, 73, 1309-1312.

SEHGAL, S. N., SAUCIER, R. & VÉZINA, C. 1976. Antimycin A fermentation. II. Fermentation in aerated-agitated fermenters. *Journal of Antibiotics*, 29, 265-274.

SEIPKE, R. F. & HUTCHINGS, M. I. 2013. The regulation and biosynthesis of antimycins. *Beilstein Journal of Organic Chemistry*, 9, 2556-2563.

SELDES, A., ROVIROSA, J., SAN MARTIN, A. & GROS, E. 1985. A new sterol from the sponge *Haliclona chilensis* (Thiele). *Experientia*, 41, 34-35.

SELVAN, G. P., RAVIKUMAR, S., RAMU, A. & NEELAKANDAN, P. 2012. Antagonistic activity of marine sponge associated *Streptomyces* sp. against isolated fish pathogens. *Asian Pacific Journal of Tropical Disease*, 2, S724-S728.

- SERA, Y., ADACHI, K., FUJII, K. & SHIZURI, Y. 2002. Isolation of haliclonamides: New peptides as antifouling substances from a marine sponge species, *Haliclona*. *Marine Biotechnology*, 4, 441-446.
- SERA, Y., ADACHI, K., FUJII, K. & SHIZURI, Y. 2003. A new antifouling hexapeptide from a palauan sponge, *Haliclona* sp. *Journal of Natural Products*, 66, 719-721.
- SHADOMY, S., ROBERTSON, G. M., SHADOMY, H. J., UTZ, J. P. & GAMBLE, E. 1969. In vitro and in vivo activity of hamycin against *Blastomyces dermatitidis*. *Journal of Bacteriology*, 97, 481-487.
- SHEIKH, Y. & DJERASSI, C. 1974. Steroids from sponges. *Tetrahedron*, 30, 4095-4103.
- SHINYA, K., FURIHATA, K., TESHIMA, Y., HAYAKAWA, Y. & SETO, H. 1992. Structures of stealthins A and stealthins B, new free-radical scavengers of microbial origin. *Tetrahedron Letters*, 33, 7025-7028.
- SHIOMI, K., HATAE, K., HATANO, H., MATSUMOTO, A., TAKAHASHI, Y., JIANG, C., TOMODA, H., KOBAYASHI, S., TANAKA, H. & OMURA, S. 2005. A new antibiotic, antimycin A(9), produced by *Streptomyces* sp K01-0031. *Journal of Antibiotics*, 58, 74-78.
- SIEBER, M. & BAUMGRASS, R. 2009. Novel inhibitors of the calcineurin/NFATc hub - alternatives to CsA and FK506? *Cell Communication and Signaling*, 7, 25-43.
- SILVA, C., WUNSCHE, L. & DJERASSI, C. 1991. Biosynthetic studies of marine lipids. 35. The demonstration of de novo sterol biosynthesis in sponges using radiolabeled isoprenoid precursors. *Comparative Biochemistry and Physiology B-Biochemistry & Molecular Biology*, 99, 763-773.
- SINGH, K., SCHILLING, G., RAKHIT, S. & VÉZINA, C. 1972. Transformations of antibiotics. II. Transformation of antimycin A by hog kidney acylase. *Journal of Antibiotics*, 25, 141-143.
- SIPKEMA, D., HOLMES, B., NICHOLS, S. & BLANCH, H. 2009. Biological characterisation of *Haliclona* (?gellius) sp.: Sponge and associated microorganisms. *Microbial Ecology*, 58, 903-920.
- SMELCEROVIC, A., DORDEVIC, S. & PALIC, R. 2001. A new metabolite from marine bacteria. *Hemijska Industrija*, 55, 399-401.
- SMIRNOV, V. V., KIPRIANOVA, E. A., DODATKO, T. A., GARAGULIA, A. D. & KLIUEV, N. A. 1991. [Antibiotics of an aromatic nature from *Pseudomonas cepacia*]. *Mikrobiolohichnyĭ Zhurnal*, 53, 41-45.
- SOBOLEVSKAYA, M., DENISENKO, V., MOISEENKO, A., SHEVCHENKO, L., MENZOROVA, N., SIBIRTSEV, Y., KIM, N. & KUZNETSOVA, T. 2007.

Bioactive metabolites of the marine actinobacterium *Streptomyces* sp KMM 7210. *Russian Chemical Bulletin*, 56, 838-840.

SONG, Z. & NES, W. D. 2007. Sterol biosynthesis inhibitors: potential for transition state analogs and mechanism-based inactivators targeted at sterol methyltransferase. *Lipids*, 42, 15-33.

SOWERS, K. R., ROBERTSON, D. E., NOLL, D., GUNSALUS, R. P. & ROBERTS, M. F. 1990. N epsilon-acetyl-beta-lysine: an osmolyte synthesized by methanogenic archaeobacteria. *Proceedings of the National Academy of Sciences, USA*, 87, 9083-9087.

SPECK, M. L. 1943. A study of the genus *Microbacterium*. *Journal of Dairy Science*, 26, 533-543.

SPERRY, S. & CREWS, P. 1997. Haliclostanoic acid sulfate and halistanol sulfate from an indo-Pacific *Haliclona* sponge. *Journal of Natural Products*, 60, 29-32.

STANBURY, P. F., WHITAKER, A. & HALL, S. J. 1995. *Principles of Fermentation Technology 2nd ed.*, Oxford, Butterworth-Heinemann.

STEENBERGEN, J. N., ALDER, J., THORNE, G. M. & TALLY, F. P. 2005. Daptomycin: a lipopeptide antibiotic for the treatment of serious Gram-positive infections. *Journal of Antimicrobial Chemotherapy*, 55, 283-288.

STIERLE, A., CARDELLINA, J. & SINGLETON, F. 1988. A marine *Micrococcus* produces metabolites ascribed to the sponge *Tedania ignis*. *Experientia*, 44, 1021-1021.

STIERLE, D. & FAULKNER, D. 1979. Metabolites of the marine sponge *Chondrosia collectrix*. *Journal of Organic Chemistry*, 44, 964-968.

STIERLE, D. & FAULKNER, D. 1980. Metabolites of three marine sponges of the genus *Plakortis*. *Journal of Organic Chemistry*, 45, 3396-3401.

STILL, W., KAHN, M. & MITRA, A. 1978. Rapid chromatographic technique for preparative separations with moderate resolution. *Journal of Organic Chemistry*, 43, 2923-2925.

STINEAR, T., SEEMANN, T., HARRISON, P., JENKIN, G., DAVIES, J., JOHNSON, P., ABDELLAH, Z., ARROWSMITH, C., CHILLINGWORTH, T., CHURCHER, C., CLARKE, K., CRONIN, A., DAVIS, P., GOODHEAD, I., HOLROYD, N., JAGELS, K., LORD, A., MOULE, S., MUNGALL, K., NORBERTCZAK, H., QUAIL, M., RABBINOWITSCH, E., WALKER, D., WHITE, B., WHITEHEAD, S., SMALL, P., BROSCHE, R., RAMAKRISHNAN, L., FISCHBACH, M., PARKHILL, J. & COLE, S. 2008. Insights from the complete genome sequence of *Mycobacterium marinum* on the evolution of *Mycobacterium tuberculosis*. *Genome Research*, 18, 729-741.

- TABARES, P., PIMENTEL-ELARDO, S., SCHIRMEISTER, T., HUNIG, T. & HENTSCHEL, U. 2011. Anti-protease and immunomodulatory activities of bacteria associated with Caribbean sponges. *Marine Biotechnology*, 13, 883-892.
- TAKAHASHI, S., SERITA, K., ENOKITA, R., OKAZA, T. & HANEISHI, T. 1986. A new antibiotic, N-hydroxydihydroabikoviromycin. *Sankyo Kenkyusho Nempo*, 38, 105-108.
- TAKAHASHI, Y., KUBOTA, T., FROMONT, J. & KOBAYASHI, J. 2007. Metachromins L-Q, new sesquiterpenoid quinones with an amino acid residue from sponge *Spongia* sp. *Tetrahedron*, 63, 8770-8773.
- TAKANO, E. 2006. gamma-Butyrolactones: *Streptomyces* signalling molecules regulating antibiotic production and differentiation. *Current Opinion in Microbiology*, 9, 287-294.
- TAKESAKO, K. & BEPPU, T. 1984a. Studies on new antifungal antibiotics, guanidylfungins A and B. I. Taxonomy, fermentation, isolation and characterization. *Journal of Antibiotics*, 37, 1161-1169.
- TAKESAKO, K. & BEPPU, T. 1984b. Studies on new antifungal antibiotics, guanidylfungins A and B. II. Structure elucidation and biosynthesis. *Journal of Antibiotics*, 37, 1170-1186.
- TAMEHIRO, N., OKAMOTO-HOSOYA, Y., OKAMOTO, S., UBUKATA, M., HAMADA, M., NAGANAWA, H. & OCHI, K. 2002. Bacilysocin, a novel phospholipid antibiotic produced by *Bacillus subtilis* 168. *Antimicrobial Agents and Chemotherapy*, 46, 315-320.
- TANAKA, N., SUTO, S., ISHIYAMA, H., KUBOTA, T., YAMANO, A., SHIRO, M., FROMONT, J. & KOBAYASHI, J. 2012. Halichonadins K and L, New Dimeric Sesquiterpenoids from a Sponge *Halichondria* sp. *Organic Letters*, 14, 3498-3501.
- TAYLOR, M., RADAX, R., STEGER, D. & WAGNER, M. 2007. Sponge-associated microorganisms: Evolution, ecology, and biotechnological potential. *Microbiology and Molecular Biology Reviews*, 71, 295-347.
- TAYLOR, M., SCHUPP, P., DE NYS, R., KJELLEBERG, S. & STEINBERG, P. 2005. Biogeography of bacteria associated with the marine sponge *Cymbastela concentrica*. *Environmental Microbiology*, 7, 419-433.
- TENG, R., JUNANKAR, P., BUBB, W., RAE, C., MERCIER, P. & KIRK, K. 2009. Metabolite profiling of the intraerythrocytic malaria parasite *Plasmodium falciparum* by 1H NMR spectroscopy. *NMR in Biomedicine*, 22, 292-302.
- TIEMERSMA, E., VAN DER WERF, M., BORGDORFF, M., WILLIAMS, B. & NAGELKERKE, N. 2011. Natural history of tuberculosis: Duration and fatality of untreated pulmonary tuberculosis in HIV negative patients: A systematic review. *PLoS ONE*, 6, e17601.

- TIKUNOV, A., JOHNSON, C., LEE, H., STOSKOPF, M. & MACDONALD, J. 2010. Metabolomic investigations of American oysters using ¹H-NMR spectroscopy. *Marine Drugs*, 8, 2578-2596.
- TISCHLER, M., AYER, S., ANDERSEN, R., MITCHELL, J. & CLARDY, J. 1988. Anthosterone-A and anthosterone-B, ring-a contracted steroids from the sponge *Anthoracuata granceae*. *Canadian Journal of Chemistry*, 66, 1173-1178.
- TIZIANI, S., SCHWARTZ, S. & VODOVOTZ, Y. 2006. Profiling of carotenoids in tomato juice by one- and two-dimensional NMR. *Journal of Agricultural and Food Chemistry*, 54, 6094-6100.
- TJEERDEMA, R. 2008. Application of NMR-based techniques in aquatic toxicology: Brief examples. *Marine Pollution Bulletin*, 57, 275-279.
- TOLSTIKOV, V. V., FIEHN, O. & TANAKA, N. 2007. Application of Liquid Chromatography-Mass Spectrometry Analysis in Metabolomics: Reversed-Phase Monolithic Capillary Chromatography and Hydrophilic Chromatography Coupled to Electrospray Ionization-Mass Spectrometry. In: WECKWORTH, W. (ed.) *Metabolomics: Methods and Protocols*. Totowa, New Jersey: Humana Press.
- TOMIOKA, H., KAGAWA, M. & NAKAMURA, S. 1976. Some enzymatic properties of 3beta-hydroxysteroid oxidase produced by *Streptomyces violascens*. *Journal of Biochemistry*, 79, 903-915.
- TRETHEWEY, R., KROTZKY, A. & WILLMITZER, L. 1999. Metabolic profiling: a Rosetta Stone for genomics? *Current Opinion in Plant Biology*, 2, 83-85.
- TRIANTO, A., HERMAWAN, I., DE VOOGD, N. & TANAKA, J. 2011. Halioxepine, a new meroditerpene from an Indonesian sponge *Haliclona* sp. *Chemical & Pharmaceutical Bulletin*, 59, 1311-1313.
- TRYGG, J., HOLMES, E. & LUNDSTEDT, T. 2007. Chemometrics in metabolomics. *Journal of Proteome Research*, 6, 469-479.
- TSE, S., MAK, I. & DICKENS, B. 1991. Antioxidative properties of harmaline and beta-carboline alkaloids. *Biochemical Pharmacology*, 42, 459-464.
- TSUKAMOTO, S., KATO, H., HIROTA, H. & FUSEYANI, N. 1995. Pipecolate derivatives, anthosamines A and B, inducers of larval metamorphosis in ascidians, from a marine sponge *Anthosigmella* aff. *raromicrosclera*. *Tetrahedron*, 51, 6687-6694.
- TURNER, W. B. & ALDRIDGE, D. C. 1983. *Fungal Metabolites II*, London, Academic Press Inc. (London) Ltd.
- TWEEDDALE, H., NOTLEY-MCROBB, L. & FERENCI, T. 1998. Effect of slow growth on metabolism of *Escherichia coli*, as revealed by global metabolite pool ("Metabolome") analysis. *Journal of Bacteriology*, 180, 5109-5116.

UENO, M., AMEMIYA, M., IJIMA, M., OSONO, M., MASUDA, T., KINOSHITA, N., IKEDA, T., IINUMA, H., HAMADA, M. & ISHIZUKA, M. 1993a. Delaminomycins, novel nonpeptide extracellular matrix receptor antagonist and a new class of potent immunomodulator. I. Taxonomy, fermentation, isolation and biological activity. *Journal of Antibiotics*, 46, 719-727.

UENO, M., SOMENO, T., SAWA, R., IINUMA, H., NAGANAWA, H., ISHIZUKA, M. & TAKEUCHI, T. 1993b. Delaminomycins, novel nonpeptide extracellular matrix receptor antagonist and a new class of potent immunomodulator. II. Physico-chemical properties and structure elucidation of delaminomycin A. *Journal of Antibiotics*, 46, 979-984.

UENO, M., YOSHINAGA, I., AMEMIYA, M., SOMENO, T., IINUMA, H., ISHIZUAKA, M. & TAKEUCHI, T. 1993c. Delaminomycins, novel extracellular matrix receptor antagonists. V. Biosynthesis. *Journal of Antibiotics*, 46, 1390-1396.

UMEZAWA, H., AOYAGI, T., OGAWA, K., NAGANAWA, H., HAMADA, M. & TAKEUCHI, T. 1984. Diprotins A and B, inhibitors of dipeptidyl aminopeptidase IV, produced by bacteria. *Journal of Antibiotics*, 37, 422-425.

UMEZAWA, H., AOYAGI, T., OKURA, A., MORISHIMA, H., TAKEUCHI, T. & OKAMI, Y. 1973. Elastatinal, a new elastase inhibitor produced by actinomycetes. *Journal of Antibiotics*, 26, 787-789.

UNEP. 1992. *Convention on biological diversity* [Online]. Rio de Janeiro, Brazil: Secretariat of the Convention on Biological Diversity. Available: <http://www.cbd.int/doc/legal/cbd-en.pdf> [Accessed 7 May 2014].

UNEP. 2000. *Cartagena protocol on biosafety to the convention on biological diversity* [Online]. Montreal, Canada: Secretariat of the Convention on Biological Diversity. Available: <http://bch.cbd.int/database/attachment/?id=10694> [Accessed 7 May 2014].

UNEP. 2010. *Nagoya protocol on access to genetic resources and the fair and equitable sharing of benefits arising from their utilization to the convention on biological diversity* [Online]. Nagoya, Japan: Secretariat of the Convention on Biological Diversity. Available: <http://www.cbd.int/abs/doc/protocol/nagoya-protocol-en.pdf> [Accessed 7 May 2014].

USHER, K., FROMONT, J., SUTTON, D. & TOZE, S. 2004. The biogeography and phylogeny of unicellular cyanobacterial symbionts in sponges from Australia and the Mediterranean. *Microbial Ecology*, 48, 167-177.

VACELET, J. & DONADEY, C. 1977. Electron microscope study of the association between some sponges and bacteria. *Journal of Experimental Marine Biology and Ecology*, 30, 301-314.

VAN SOEST, R. 2013. *Callyspongia implexa* (Topsent, 1892) [Online]. Available: <http://www.marinespecies.org/porifera/porifera.php?p=taxdetails&id=166114> [Accessed 13 August 2013].

VAN TAMELEN, E. E., DICKIE, J. P., LOOMANS, M. E., DEWEY, R. S. & STRONG, F. M. 1961. The chemistry of Antimycin A. X. Structure of the antimycins. *Journal of the American Chemical Society*, 83, 1639-1646.

VAN WICKERN, B., MÜLLER, B., SIMAT, T. & STEINHART, H. 1997. Determination of γ -radiation induced products in aqueous solutions of tryptophan and synthesis of 4-, 6- and 7-hydroxytryptophan. *Journal of Chromatography A*, 786, 57-65.

VETTER, S. & SCHLIEVERT, P. 2005. Glycerol monolaurate inhibits virulence factor production in *Bacillus anthracis*. *Antimicrobial Agents and Chemotherapy*, 49, 1302-1305.

VIANI, M. 2007a. Metabolomics of aquatic organisms: the new 'omics' on the block. *Marine Ecology Progress Series*, 332, 301-306.

VIANI, M. R. 2007b. Revealing the Metabolome of Animal Tissues using ¹H Nuclear Magnetic Resonance Spectroscopy. In: WECKWERTH, W. (ed.) *Metabolomics: Methods and Protocols*. Totowa, New Jersey: Humana Press Inc.

VOLK, C., LIPPERT, H., LICHTER, E. & KOCK, M. 2004. Two new haliclamines from the arctic sponge *Haliclona viscosa*. *European Journal of Organic Chemistry*, 3154-3158.

VOLKMAN, J. 2003. Sterols in microorganisms. *Applied Microbiology and Biotechnology*, 60, 495-506.

VOLKMAN, C., HARTJEN, U., ZEECK, A. & FIEDLER, H. P. 1995. Biosynthetic capacities of actinomycetes. 3. Naphthgeranine F, a minor congener of the naphthgeranine group produced by *Streptomyces violaceus*. *Journal of Antibiotics*, 48, 522-524.

WACHTER, G., FRANZBLAU, S., MONTENEGRO, G., HOFFMANN, J., MAIESE, W. & TIMMERMANN, B. 2001. Inhibition of *Mycobacterium tuberculosis* growth by saringosterol from *Lessonia nigrescens*. *Journal of Natural Products*, 64, 1463-1464.

WAKABAYASHI, H., TERAGUCHI, S. & TAMURA, Y. 2002. Increased *Staphylococcus*-killing activity of an antimicrobial peptide, lactoferricin B, with minocycline and monoacylglycerol. *Bioscience Biotechnology and Biochemistry*, 66, 2161-2167.

WALL, P. E. 2005. *Thin-layer Chromatography: A Modern Practical Approach*, Cambridge, UK, The Royal Society of Chemistry.

- WALTON, M. & PENNOCK, J. 1972. Some studies on the biosynthesis of ubiquinone, isoprenoid alcohols, squalene and sterols by marine invertebrates. *Biochemical Journal*, 127, 471-479.
- WANG, B., LEE, K., ZHANG, S., JUNG, J. & LIU, Y. 2009. 2-Palmitamidoethanesulfonic acid, a taurine derivative from the marine sponge *Haliclona* sp. *Chemistry of Natural Compounds*, 45, 137-138.
- WANG, F., XU, M., LI, Q., SATTLER, I. & LIN, W. 2010. p-Aminoacetophenonic acids produced by a mangrove endophyte *Streptomyces* sp. (strain HK10552). *Molecules*, 15, 2782-2790.
- WANG, G., ABRELL, L., AVELAR, A., BORGESON, B. & CREWS, P. 1998. New hirsutane based sesquiterpenes from salt water cultures of a marine sponge-derived fungus and the terrestrial fungus *Coriolus consors*. *Tetrahedron*, 7335-7342.
- WANG, G. Y., GRAZIANI, E., WATERS, B., PAN, W., LI, X., MCDERMOTT, J., MEURER, G., SAXENA, G., ANDERSEN, R. J. & DAVIES, J. 2000. Novel natural products from soil DNA libraries in a streptomycete host. *Organic Letters*, 2, 2401-2404.
- WANG, K., YOUNG, L., WANG, Y. & LEE, S. 1990. Microbial transformation of cycloartenol and 24-methylene cycloartenol. *Tetrahedron Letters*, 31, 1283-1286.
- WARD, O. P. 1995. *Fermentation Biotechnology: Principles, Processes and Products*, Chichester, John Wiley & Sons Ltd.
- WASSERMAN, H. & GAMBALE, R. 1985. Synthesis of (+)-antimycin A3. Use of the oxazole ring in protecting and activating functions. *Journal of the American Chemical Society*, 107, 1423-1424.
- WATANABE, K., TSUDA, Y., HAMADA, M., OMORI, M., MORI, G., IGUCHI, K., NAOKI, H., FUJITA, T. & VAN SOEST, R. 2005. Acetylenic strongyloidiols from a *Petrosia* (*Strongylophora*) Okinawan marine sponge. *Journal of Natural Products*, 68, 1001-1005.
- WEI, X., RODRÍGUEZ, A. D., WANG, Y. & FRANZBLAU, S. G. 2008. Synthesis and in vitro biological evaluation of ring B abeo-sterols as novel inhibitors of *Mycobacterium tuberculosis*. *Bioorganic and Medicinal Chemistry Letters*, 18, 5448-5450.
- WERNER, J. & BOGERT, M. T. 1938. The synthesis from thujaketone of some new hydroterpenoids. *Journal of Organic Chemistry*, 3, 578-587.
- WHO 2008. *The Global Burden of Disease 2004 Update*, Geneva, World Health Organization.
- WHO 2012. *Global Tuberculosis Report 2012*, Geneva, World Health Organization.

WHO 2013. *Sustaining the Drive to Overcome the Global Impact of Neglected Tropical Diseases: Second WHO Report on Neglected Tropical Diseases*, Geneva, World Health Organization.

WICKE, C., HUNERS, M., WRAY, V., NIMTZ, M., BILITEWSKI, U. & LANG, S. 2000. Production and structure elucidation of glycoacylglycerolipids from a marine sponge-associated *Microbacterium* species. *Journal of Natural Products*, 63, 621-626.

WIKLUND, S. 2008. *Multivariate Data Analysis for Omics*. Umetrics.

WILTON, J. H., HOKANSON, G. C. & FRENCH, J. C. 1985. PD 118,576: a new antitumor macrolide antibiotic. *Journal of Antibiotics*, 38, 1449-1452.

WOLD, S., ESBENSEN, K. & GELADI, P. 1987. Principal component analysis. *Chemometrics and Intelligent Laboratory Systems*, 2, 37-52.

WOO, E. J., STARKS, C. M., CARNEY, J. R., ARSLANIAN, R., CADAPAN, L., ZAVALA, S. & LICARI, P. 2002. Migrastatin and a new compound, isomigrastatin, from *Streptomyces platensis*. *Journal of Antibiotics*, 55, 141-146.

WORTELBOER, H., VANDERLINDEN, E., DEKRUIF, C., NOORDHOEK, J., BLAAUBOER, B., VANBLADEREN, P. & FALKE, H. 1992. Effects of indole-3-carbinol on biotransformation enzymes in the rat - in vivo changes in liver and small intestinal mucosa in comparison with primary hepatocyte cultures. *Food and Chemical Toxicology*, 30, 589-599.

WRATTEN, S., WOLFE, M., ANDERSEN, R. & FAULKNER, D. 1977. Antibiotic metabolites from a marine pseudomonad. *Antimicrobial Agents and Chemotherapy*, 11, 411-414.

WU, R. Y., YANG, L. M., YOKOI, T. & LEE, K. H. 1988. Neihumicin, a new cytotoxic antibiotic from *Micromonospora neihuensis*. I. The producing organism, fermentation, isolation and biological properties. *Journal of Antibiotics*, 41, 481-487.

WU, Y., WU, M., WANG, C., WANG, X., YANG, J., OREN, A. & XU, X. 2008. *Microbacterium profundum* sp nov., isolated from deep-sea sediment of polymetallic nodule environments. *International Journal of Systematic and Evolutionary Microbiology*, 58, 2930-2934.

XIAO, X., YUAN, Z. & LI, G. 2013. Preparation of phytosterols and phytol from edible marine algae by microwave-assisted extraction and high-speed counter-current chromatography. *Separation and Purification Technology*, 104, 284-289.

XIE, X., MEI, W., ZENG, Y., LIN, H., ZHUANG, L., DAI, H. & HONG, K. 2008. Cytotoxic constituents from marine actinomycete *Streptomyces* sp 124092. *Chemical Journal of Chinese Universities-Chinese*, 29, 2183-2186.

XIN, Y., HUANG, J., DENG, M. & ZHANG, W. 2008. Culture-independent nested PCR method reveals high diversity of actinobacteria associated with the marine

sponges *Hymeniacidon perleve* and *Sponge* sp. *Antonie Van Leeuwenhoek International Journal of General and Molecular Microbiology*, 94, 533-542.

YAMADA, Y. 1995. Butyrolactone autoregulators, inducers of secondary metabolites, in *Streptomyces*. *Actinomycetologica*, 9, 57-65.

YAMASAKI, K., KANEDA, M., WATANABE, K., UEKI, Y., ISHIMARU, K., NAKAMURA, S., NOMI, R., YOSHIDA, N. & NAKAJIMA, T. 1983. New antibiotics, carbazomycins A and B. III. Taxonomy and biosynthesis. *Journal of Antibiotics*, 36, 552-558.

YANG, S. & CORDELL, G. 1997. Further metabolic studies of indole and sugar derivatives using the staurosporine producer *Streptomyces staurosporeus*. *Journal of Natural Products*, 60, 230-235.

YOSHIDA, S., AOYAGI, T. & TAKEUCHI, T. 1991. Biosynthetic study of leuhistin, a new inhibitor of aminopeptidase M. *Journal of Antibiotics*, 44, 683-684.

YU, C., YU, P., CHAN, P., YAN, Q. & WONG, P. 2004. Two novel species of tetrodotoxin-producing bacteria isolated from toxic marine puffer fishes. *Toxicon*, 44, 641-647.

YU, S., DENG, Z., PROKSCH, P. & LIN, W. 2006. Oculatol, oculatolide, and A-nor sterols from the sponge *Haliclona oculata*. *Journal of Natural Products*, 69, 1330-1334.

ZHANG, H., MAJOR, J. M., LEWIS, R. J. & CAPON, R. J. 2008. Phorbassins G-K: new cytotoxic diterpenes from a southern Australian marine sponge, *Phorbas* sp. *Organic and Biomolecular Chemistry*, 6, 3811-3815.

ZHAO, P., WANG, H., LI, G., LI, H., LIU, J. & SHEN, Y. 2007. Secondary metabolites from endophytic *Streptomyces* sp Lz531. *Chemistry & Biodiversity*, 4, 899-904.

ZHAO, Q., MANSOOR, T. A., HONG, J., LEE, C. O., IM, K. S., LEE, D. S. & JUNG, J. H. 2003. New lysophosphatidylcholines and monoglycerides from the marine sponge *Stelletta* sp. *Journal of Natural Products*, 66, 725-728.

ZHI, X. Y., LI, W. J. & STACKEBRANDT, E. 2009. An update of the structure and 16S rRNA gene sequence-based definition of higher ranks of the class *Actinobacteria*, with the proposal of two new suborders and four new families and emended descriptions of the existing higher taxa. *International Journal of Systematic and Evolutionary Microbiology*, 59, 589-608.

ZHU, P., LI, Q. & WANG, G. 2008. Unique microbial signatures of the alien hawaiian marine sponge *Suberites zeteki*. *Microbial Ecology*, 55, 406-414.

ZOU, X., LIU, S., ZHENG, Z., ZHANG, H., CHEN, X., LIU, X. & LI, E. 2011. Two new imidazolone-containing alkaloids and further metabolites from the ascomycete fungus *Tricladium* sp. *Chemistry & Biodiversity*, 8, 1914-1920.

Appendices

Appendix I NMR Spectra of Novel Steroids Isolated from *Haliclona simulans*

IA B-4/R-13 (24-vinyl-cholest-9-ene-3 β ,24-diol) (JEOL 400MHz, CDCl₃)

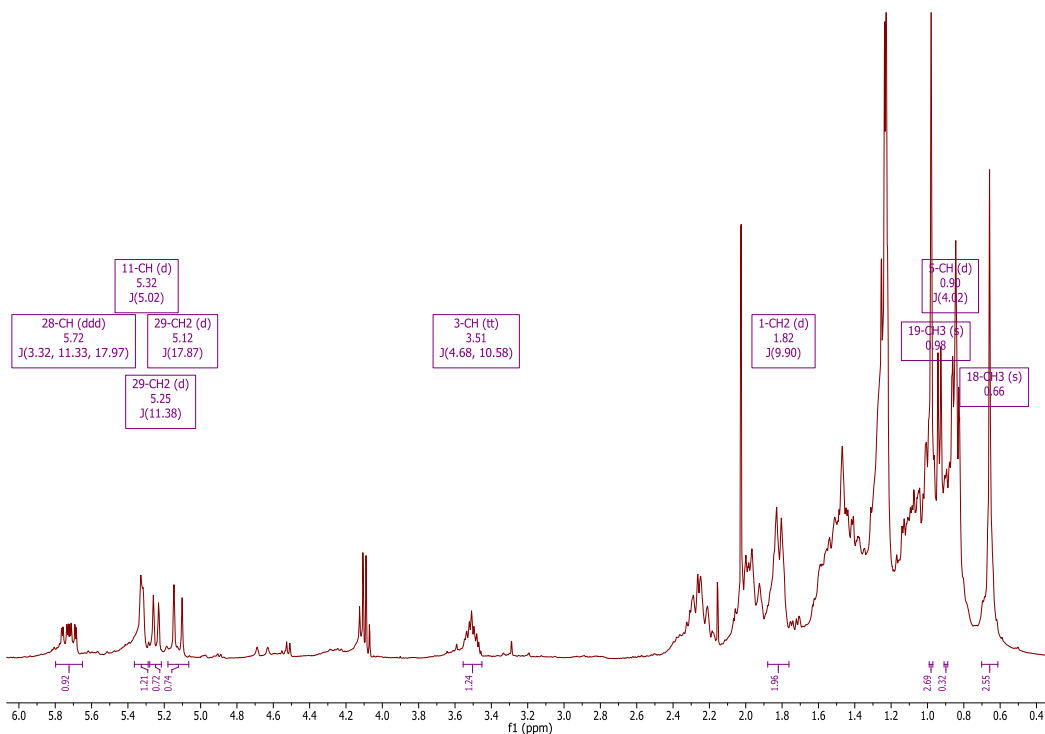


Figure 1: ¹H NMR spectrum of B-4 (400 MHz, CDCl₃)

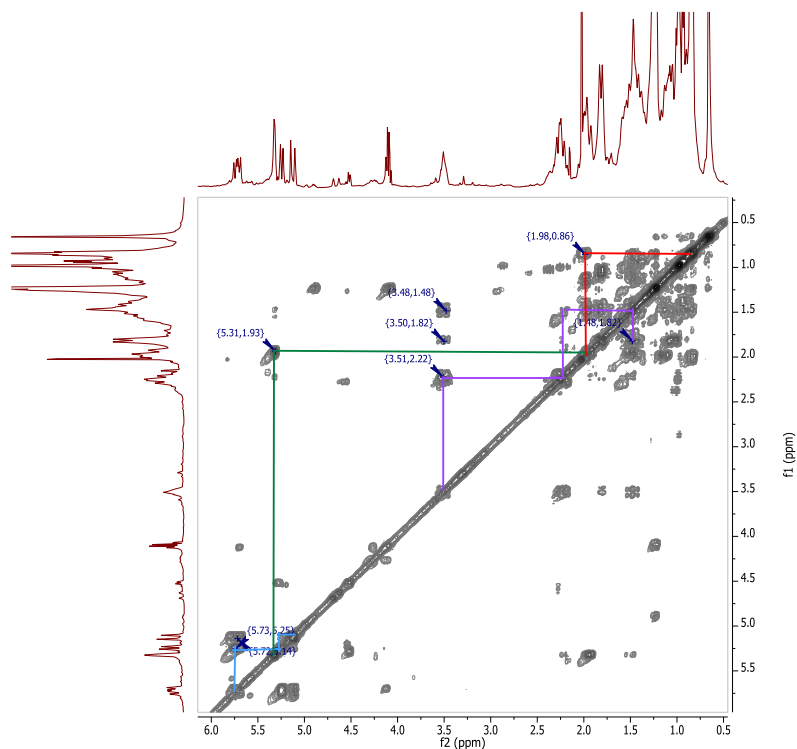


Figure 2: ¹H-¹H COSY spectrum of B-4 (400 MHz, CDCl₃)

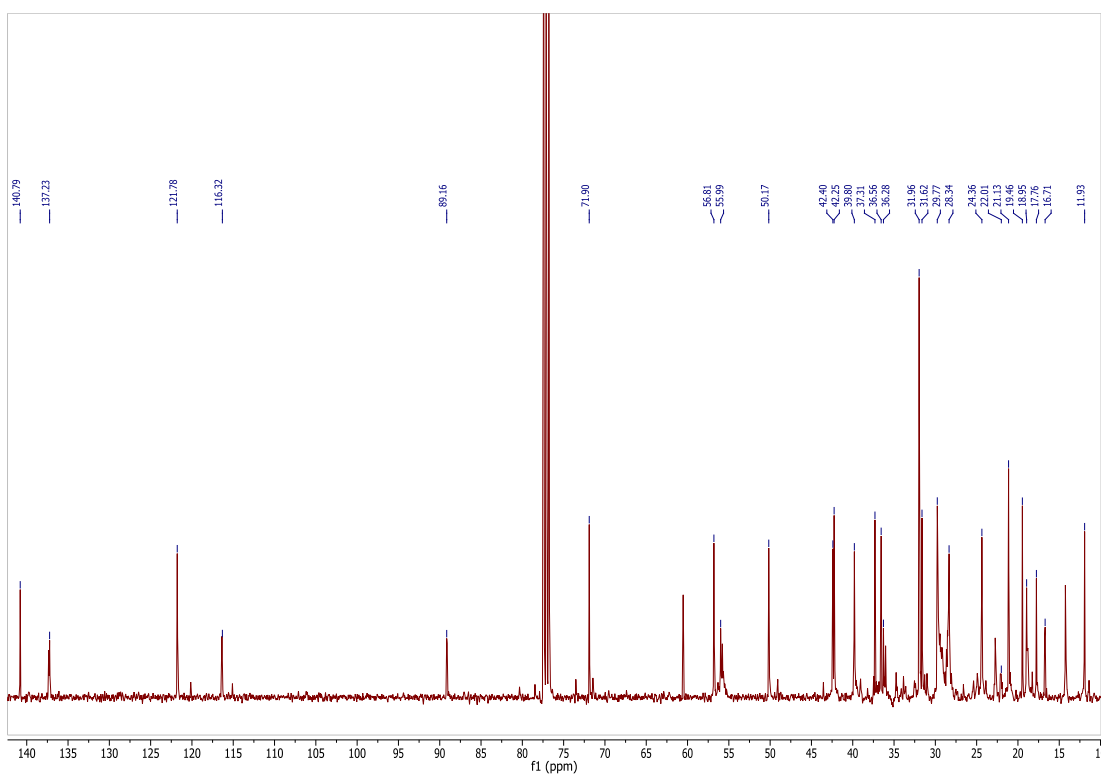


Figure 3: ^{13}C NMR spectrum of B-4 (100 MHz, CDCl_3)

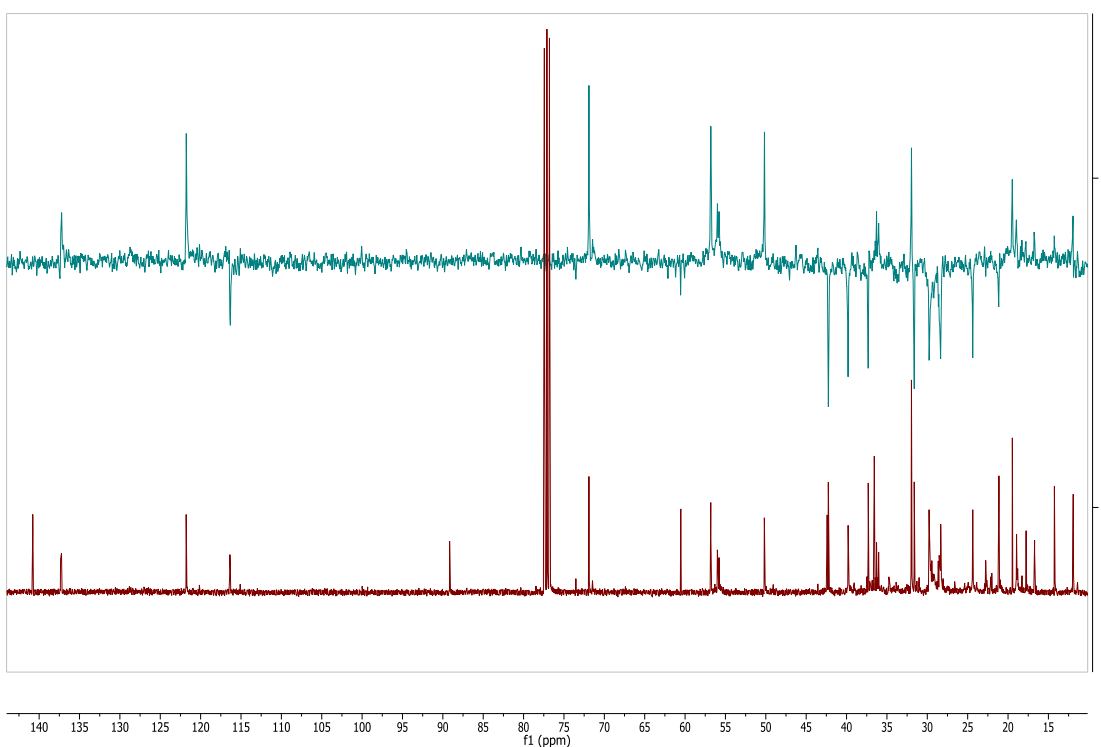


Figure 4: DEPT-135 (top) and ^{13}C (bottom) NMR spectra of B-4 (100 MHz, CDCl_3)

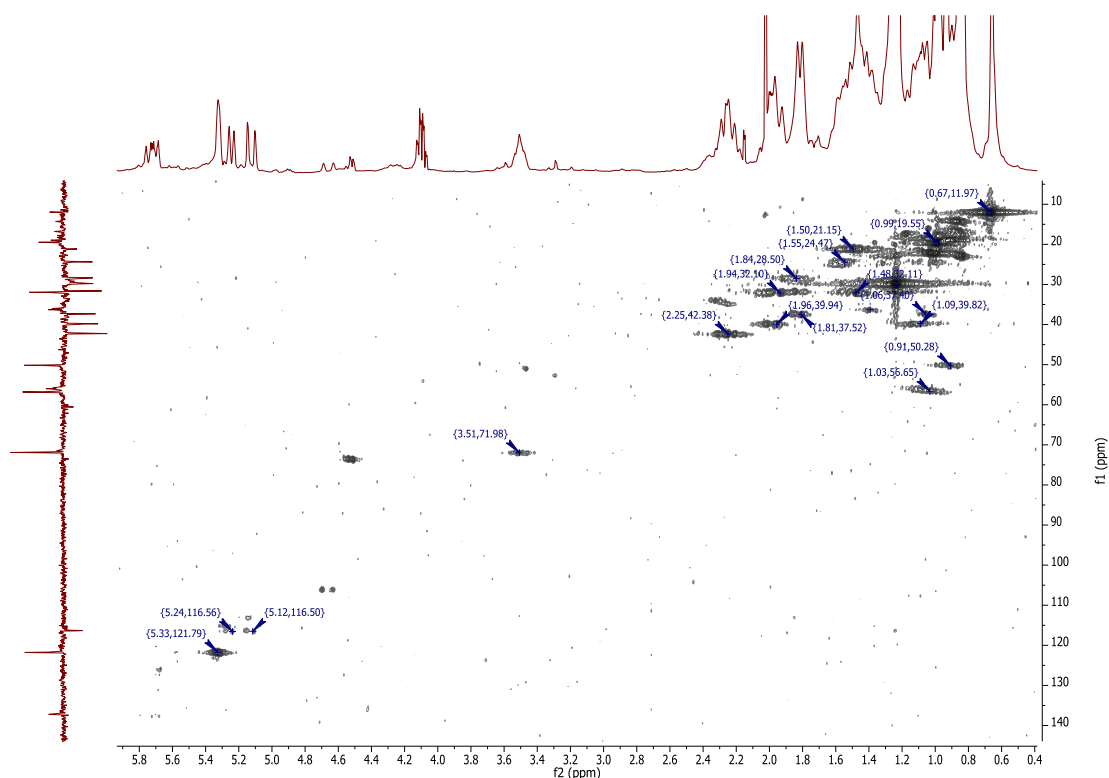


Figure 5: HMQC spectrum of B-4 showing direct C-H correlation (400 and 100 MHz, CDCl_3). The x-axis is the ^1H NMR spectrum and the y-axis is the DEPT-135 spectrum.

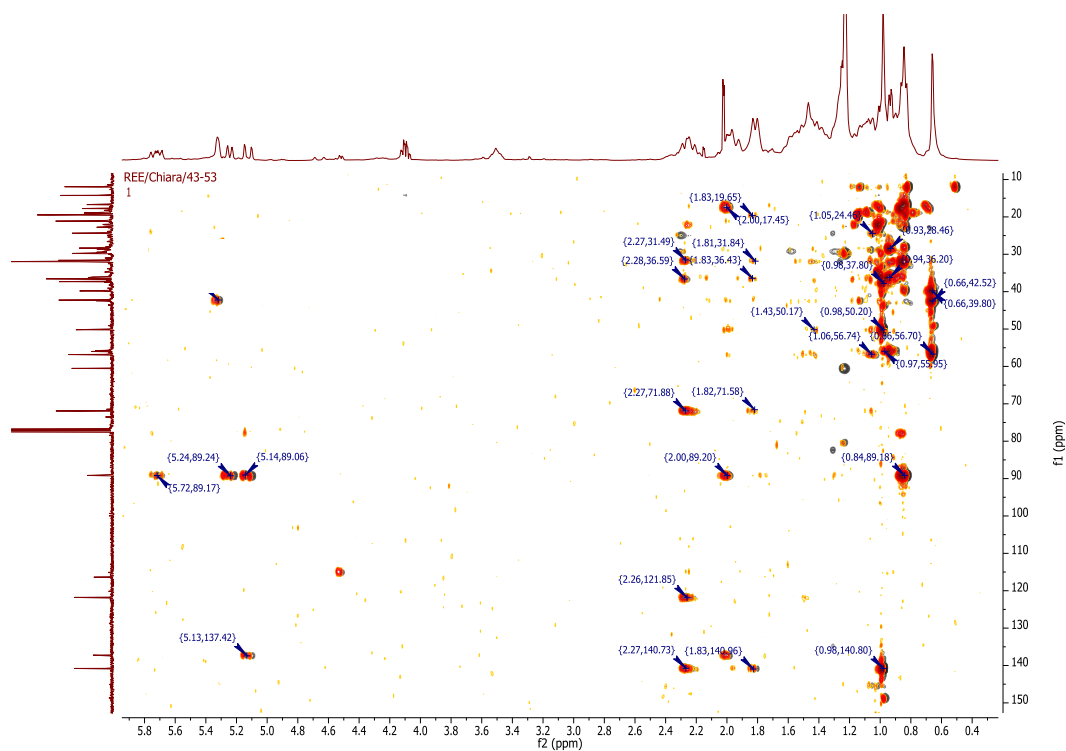


Figure 6: HMBC of B-4 (black) and R-13 (orange) (400 and 100 MHz, CDCl_3). The spectra are the same, confirming that the two fractions contain the same steroid. The HMBC shows long range C-H correlation. The y-axis is the ^{13}C spectrum whereas the x-axis is the ^1H spectrum of B-4.

IB R-17 (20-methyl-pregn-6-en-3 β -ol, 5 α ,8 α -epidioxy) (JEOL 400MHz, CDCl₃)

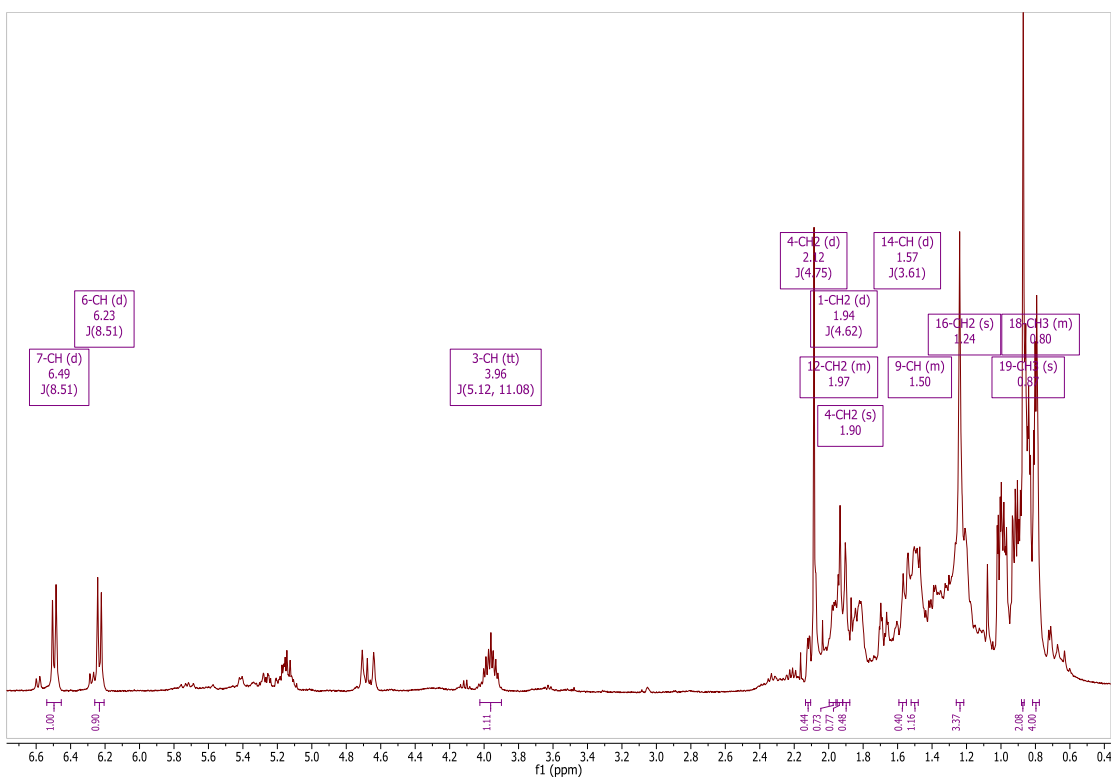


Figure 7: ¹H NMR spectrum of R-17 (400 MHz, CDCl₃)

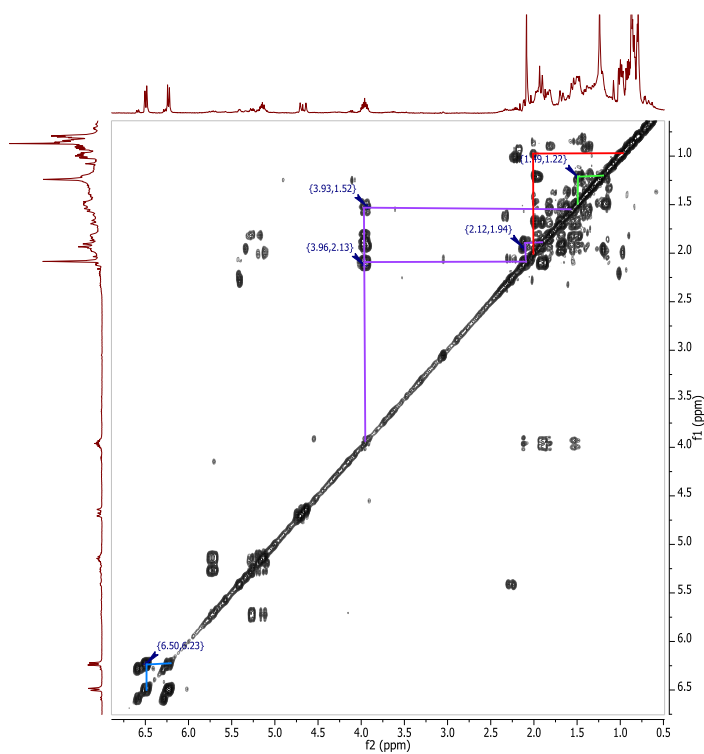


Figure 8: ¹H-¹H COSY spectrum of R-17 (400 MHz, CDCl₃)

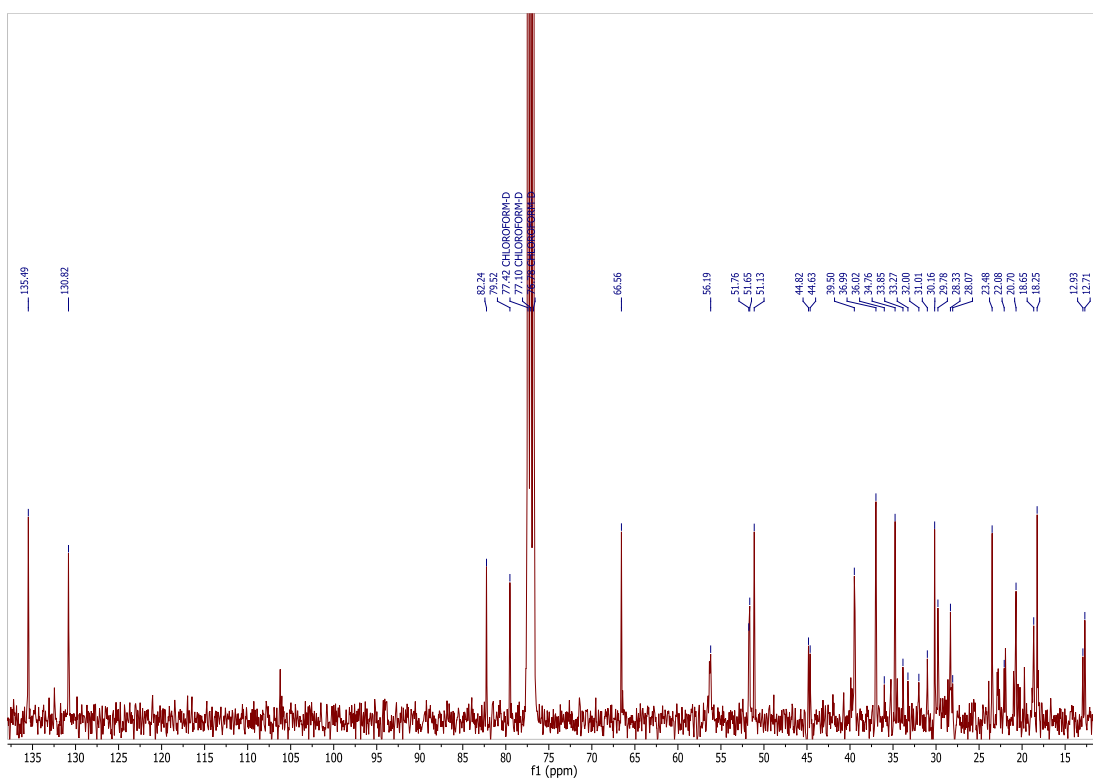


Figure 9: ^{13}C NMR spectrum of R-17 (100 MHz, CDCl_3)

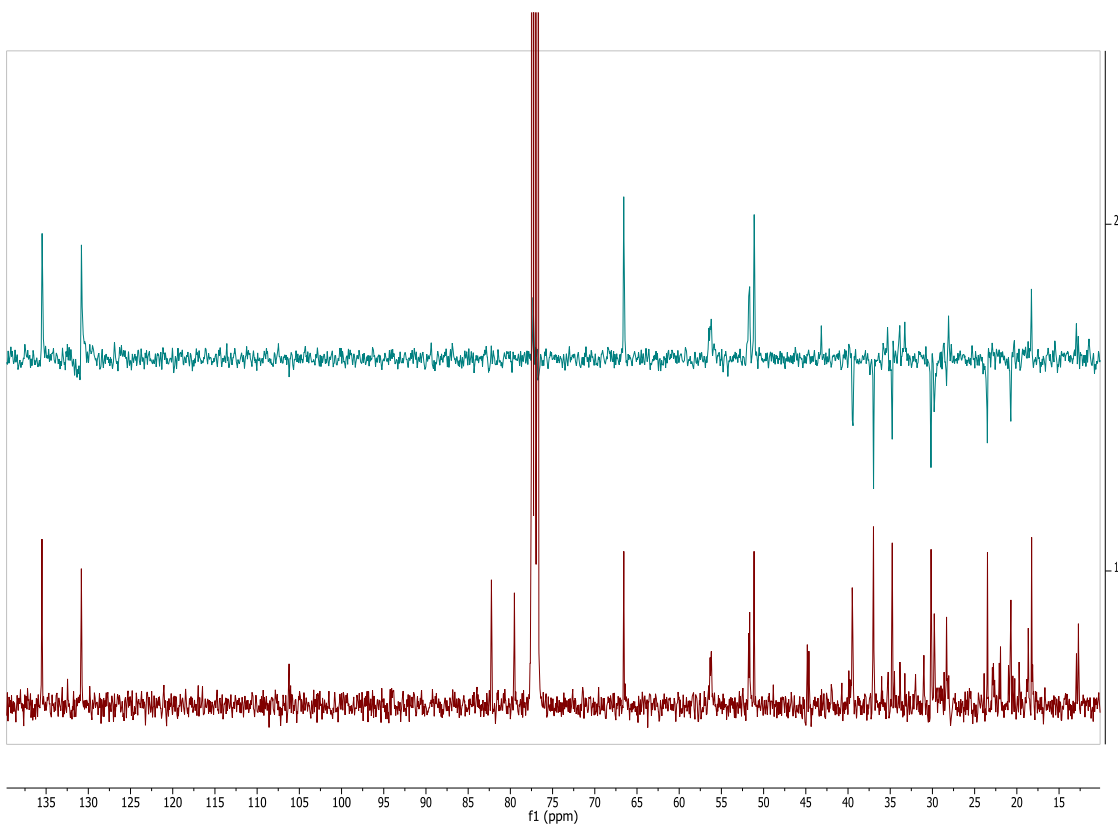


Figure 10: DEPT-135 (top) and ^{13}C (bottom) NMR spectra of R-17 (100 MHz, CDCl_3)

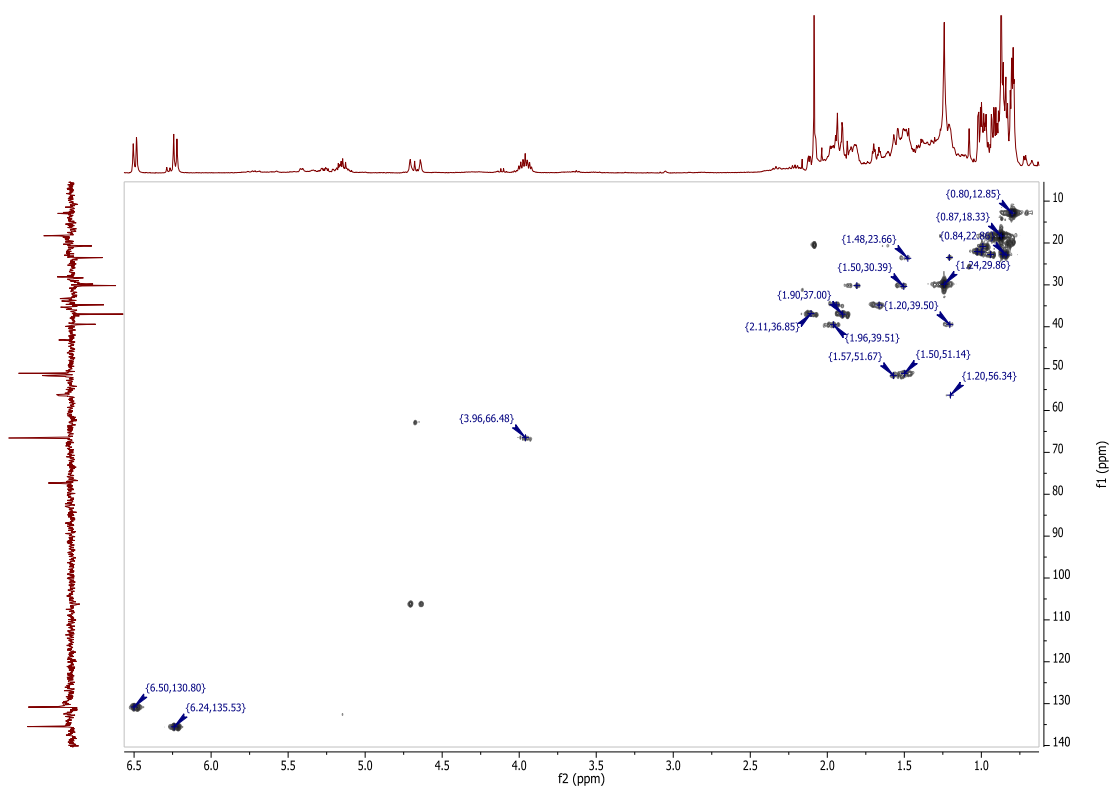


Figure 11: HMBC spectrum of R-17 showing direct C-H correlation (400 and 100 MHz, CDCl_3). The x-axis is the ^1H NMR spectrum and the y-axis is the DEPT-135 spectrum.

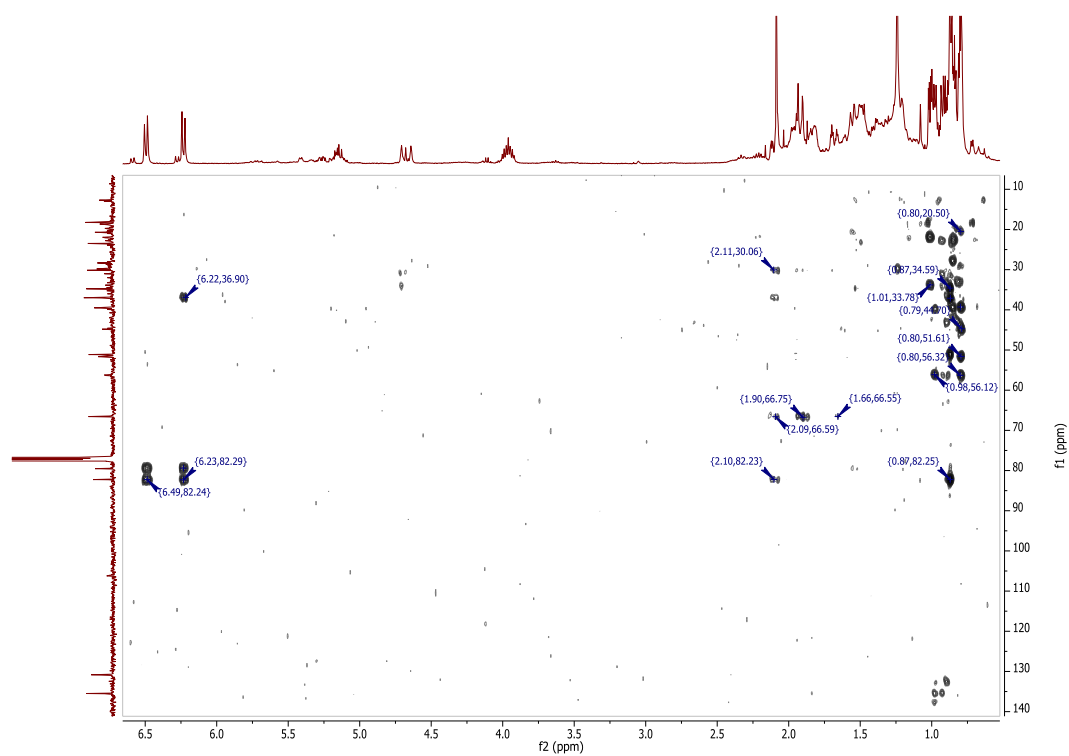


Figure 12: HMBC spectrum of R-17 showing through-bond H-C correlation (400 and 100 MHz, CDCl_3). The x-axis is the ^1H NMR spectrum and the y-axis is the ^{13}C NMR spectrum.

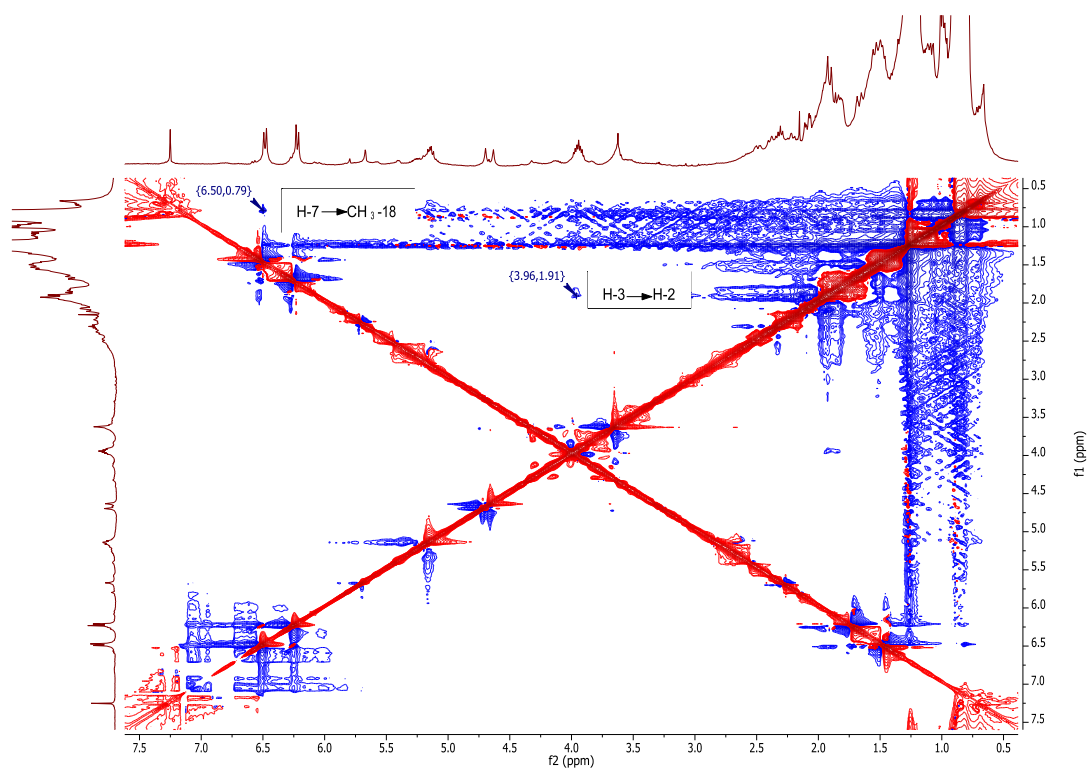


Figure 13: ROESY spectrum of B-5 (400 MHz, CDCl₃). The correlations between H-7 and CH₃-18, as well as H-3 and H-2 are labelled.

Appendix II NMR Spectra of the Butenolides from SM8 (*Streptomyces* sp.) (JEOL 400MHz, DMSO)

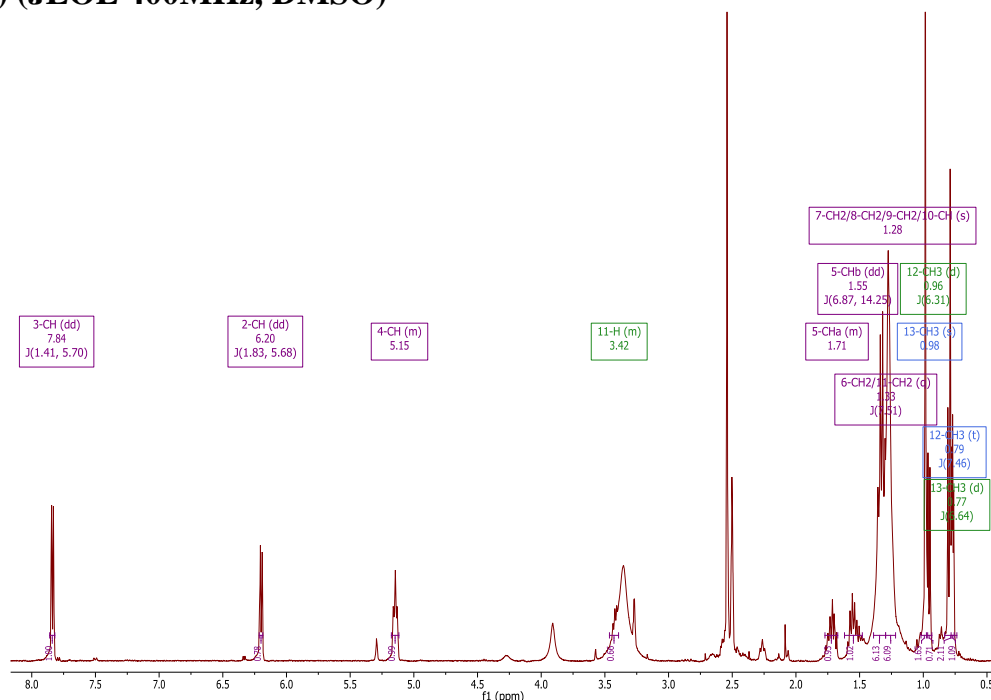


Figure 14: ^1H NMR of SM8_110-126D (400 MHz, DMSO). Peaks of Butenolide 1 are labelled in blue and those of butenolide 2 are labelled in green. Peaks common to both are labelled in purple.

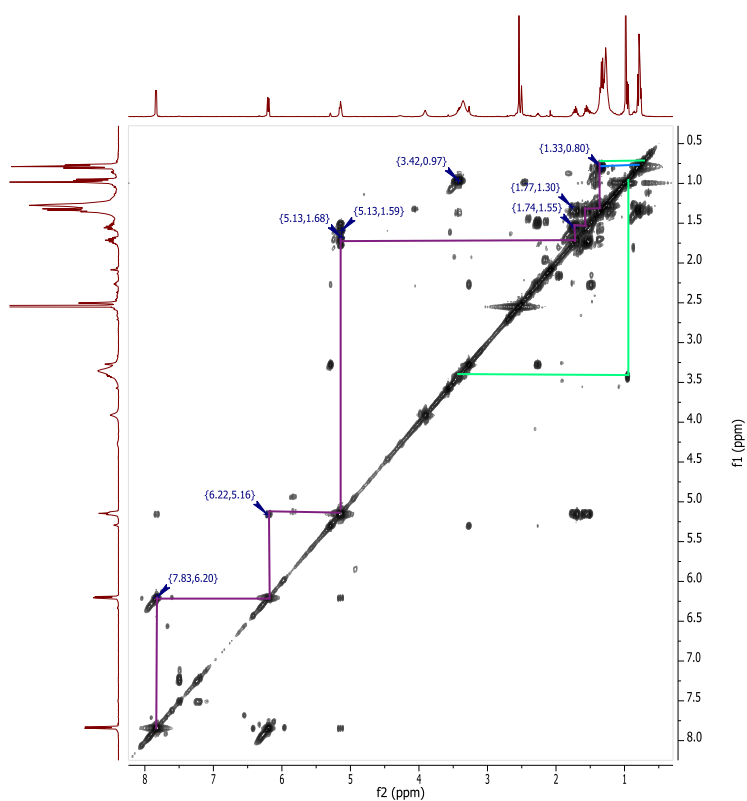


Figure 15: ^1H - ^1H COSY spectrum of SM8_110-126D (400 MHz, DMSO). The purple lines indicate the spin systems belonging to both compounds whereas the blue and green lines indicate spin systems specific to butenolide 1 and 2 respectively.

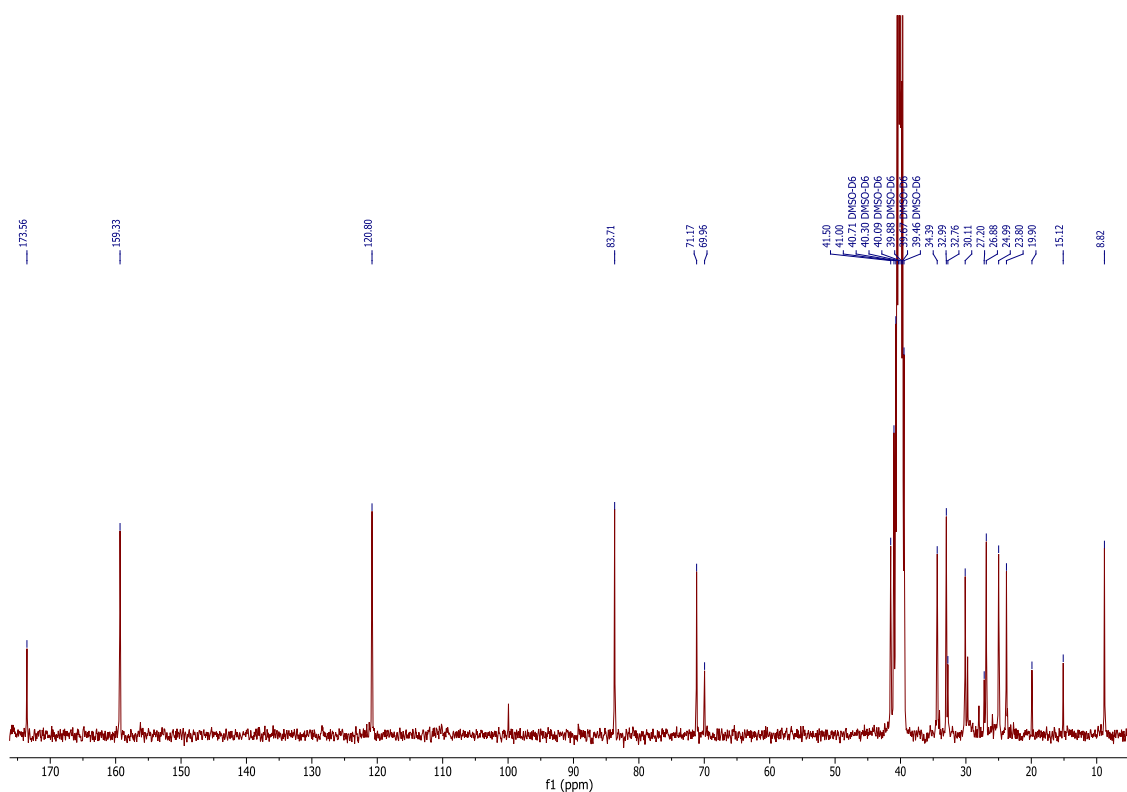


Figure 16: ^{13}C NMR spectrum of SM8_110-126D (100 MHz, DMSO)

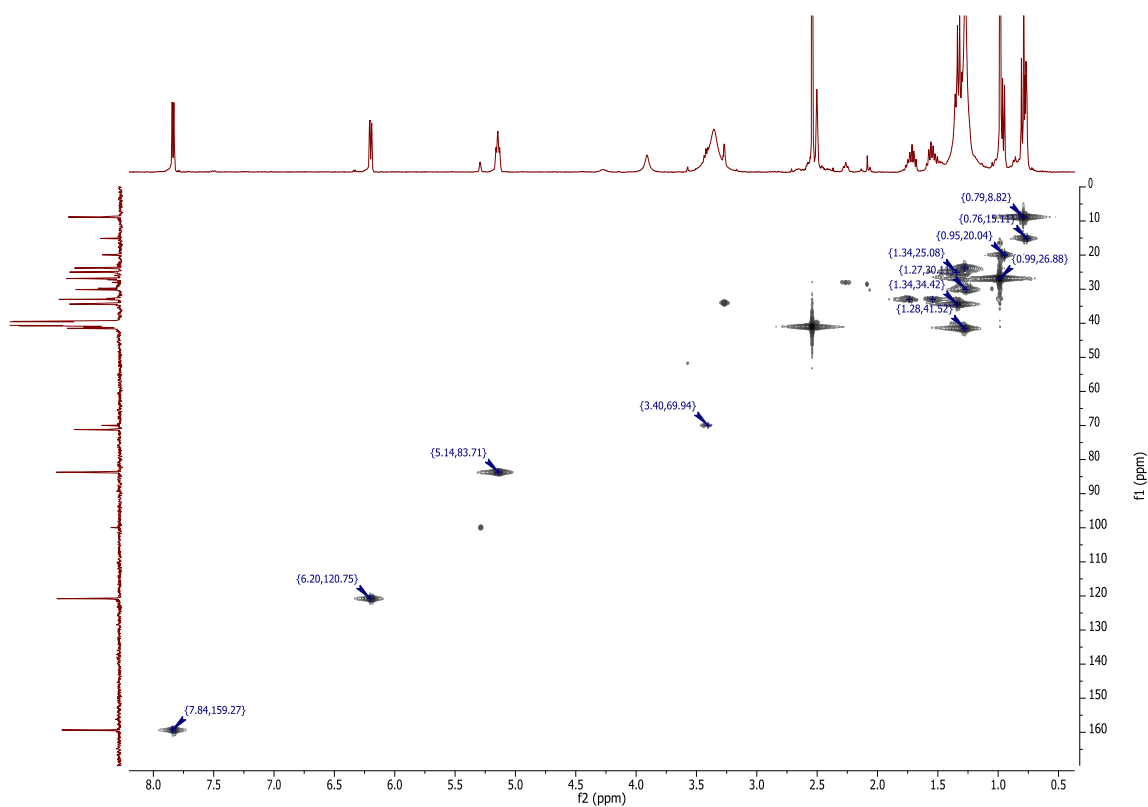


Figure 17: HMQC spectrum of SM8_110-126D showing direct C-H correlation (400 MHz and 100 MHz, DMSO). The x-axis is the ^1H NMR spectrum and the y-axis is the ^{13}C NMR spectrum.

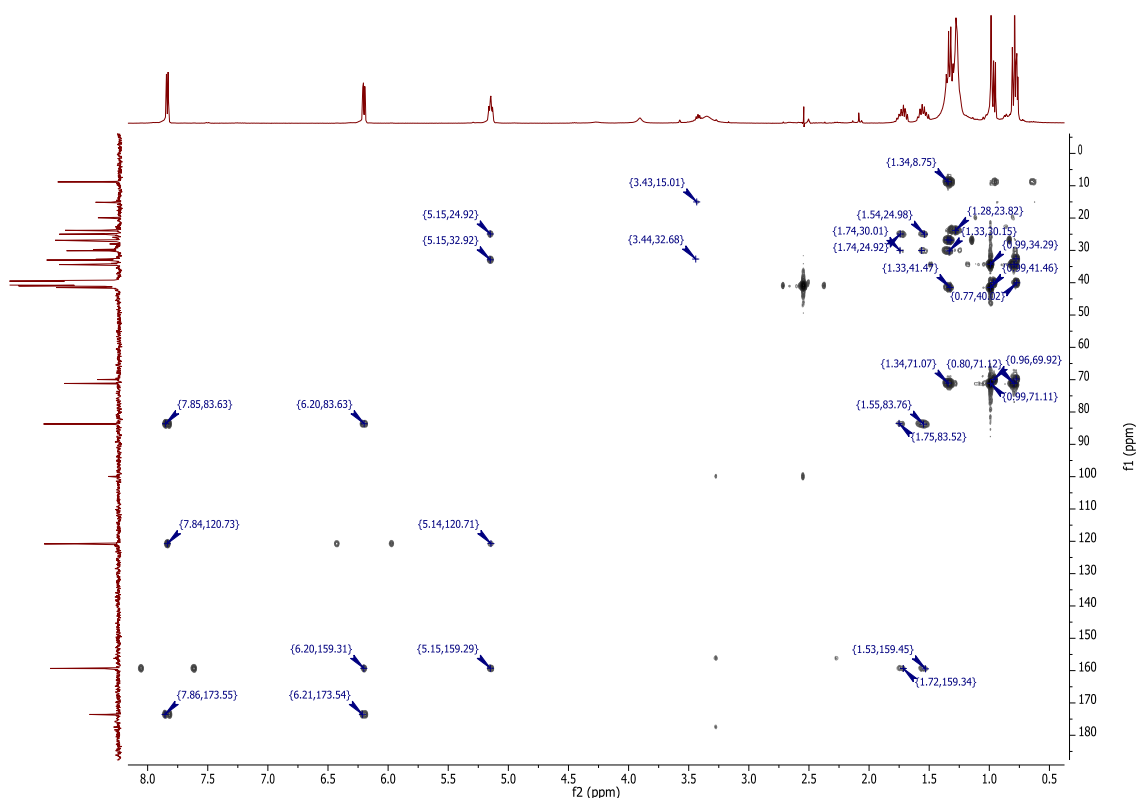


Figure 18: HMBC spectrum of Fraction 110-126D showing the ^3J and ^4J C-H coupling (400 and 100 MHz, DMSO). Some direct C-H coupling can be noted. The ^1H NMR spectrum is on the x-axis and the ^{13}C NMR spectrum is on the y-axis.

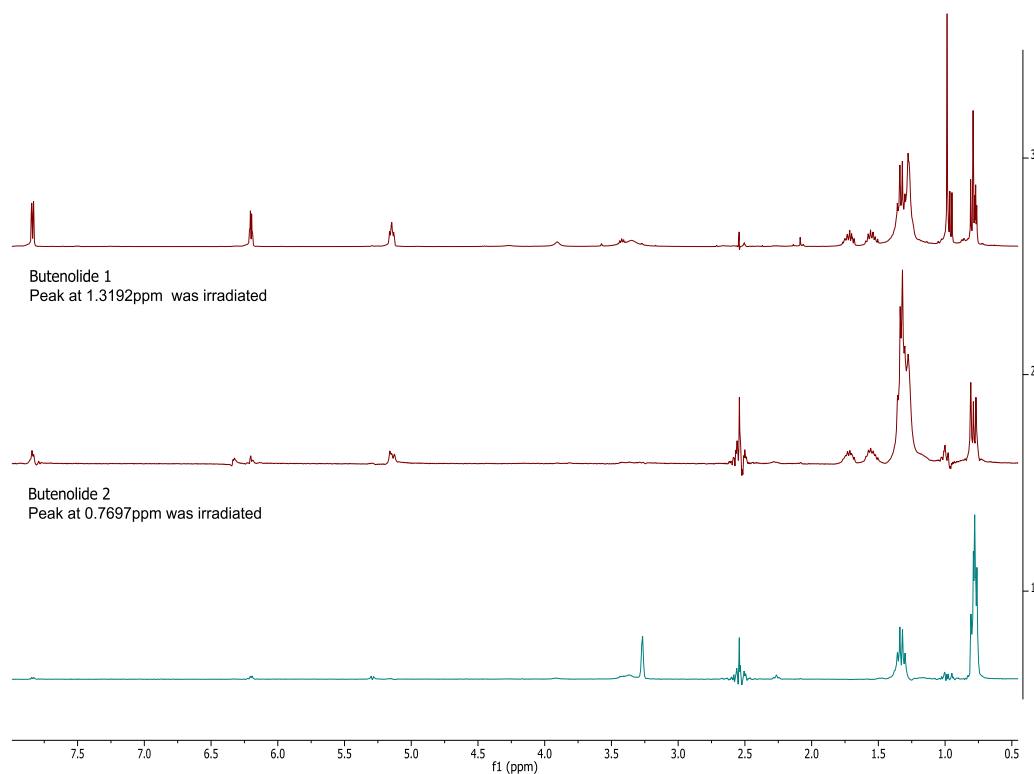


Figure 19: Comparison of ^1H NMR spectrum of SM8_110-126D (top) with 1D TOCSY spectra (middle and bottom) of the same fraction (400 MHz, DMSO). This shows the different spin systems belonging to butenolide 1 and butenolide 2.

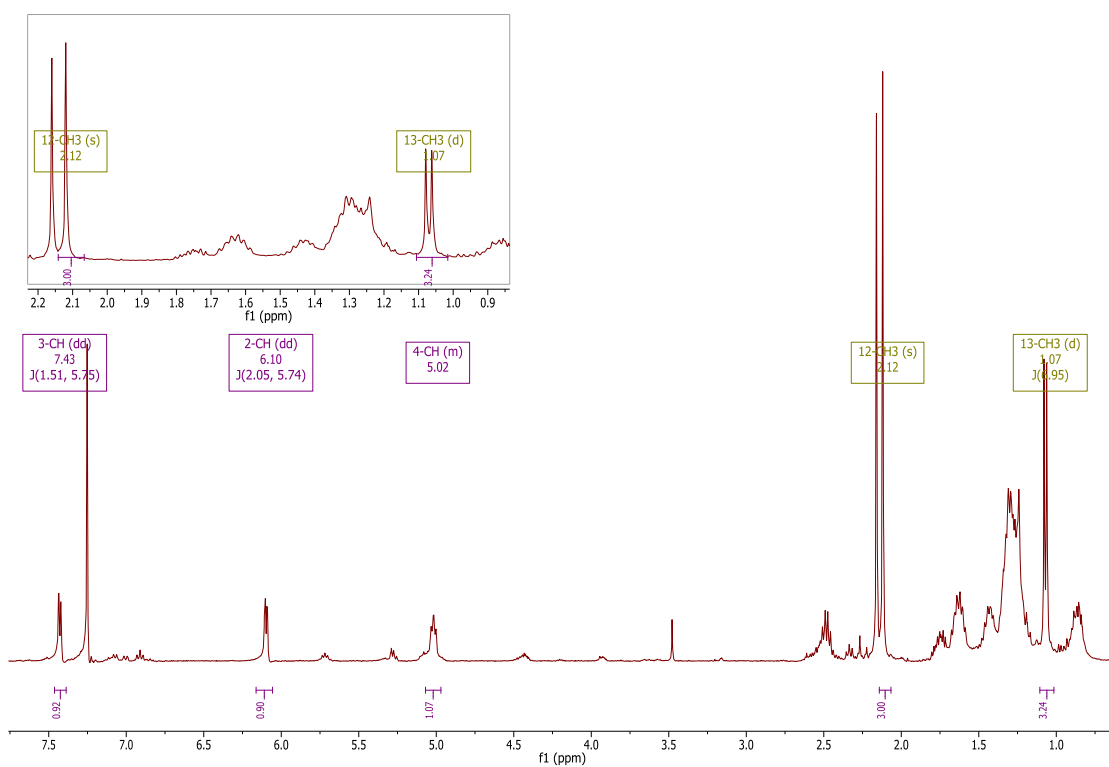


Figure 20: ^1H NMR of 127-156P (400 MHz, CDCl_3). Peaks common to the other butenolides are labelled in purple whereas those specific to butenolide 4 are labelled in olive.

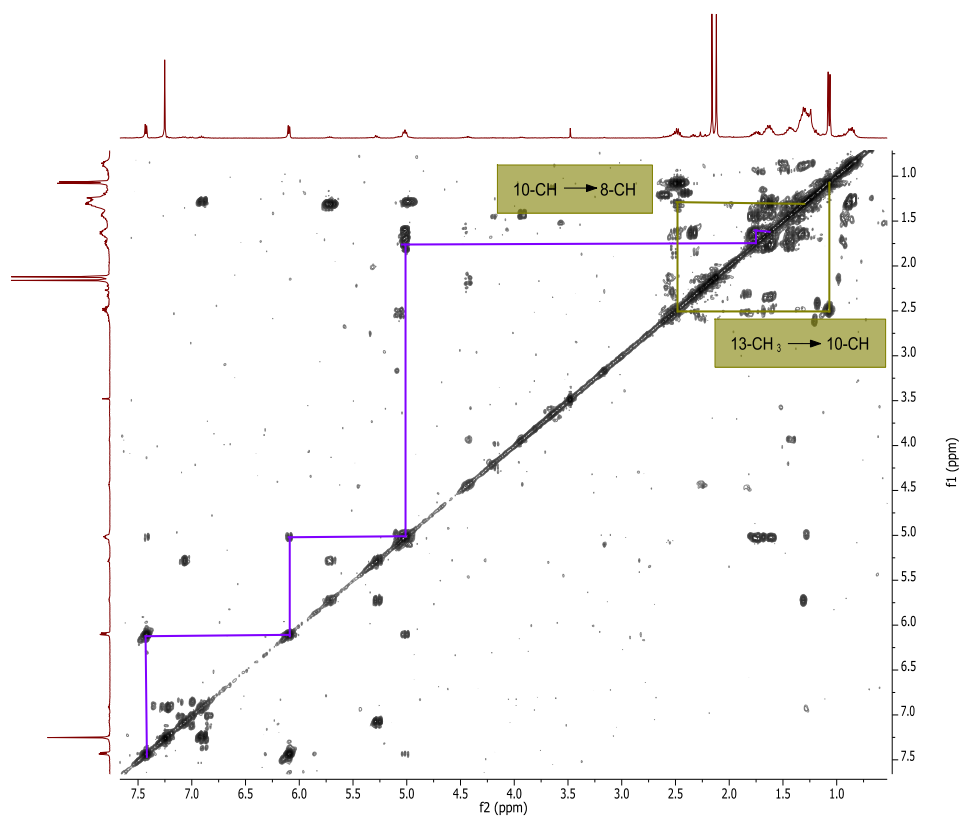


Figure 21: ^1H - ^1H COSY of 127-156P (400 MHz, CDCl_3)

Appendix III NMR Spectra of Novel Compounds Isolated from EG4 (*Microbacterium* sp.)

IIIA Fraction EG4_215-392_B3 (3,4-dihydroxy-5,6-bis(1H-indol-3-yl)-3,5-cyclohexadiene) (Bruker, 600MHz, DMSO)

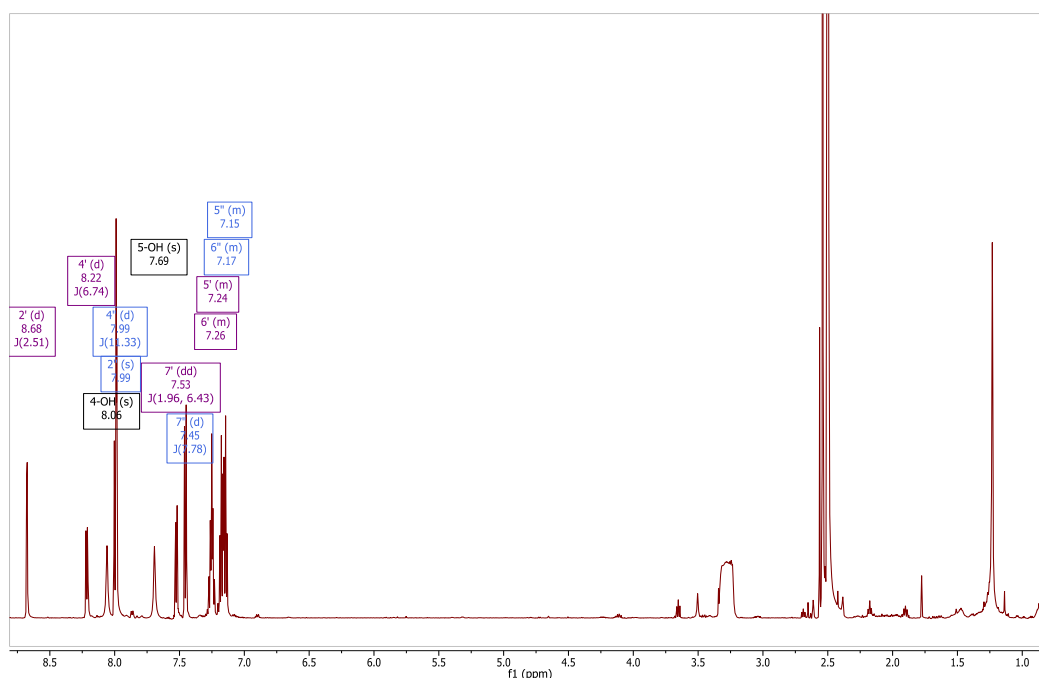


Figure 22: ^1H NMR spectrum of EG4_215-392_B3 (600 MHz, DMSO). The peaks belonging to different ring systems are labelled in different colours. The two indoles are in blue and purple and the middle benzene ring is in black.

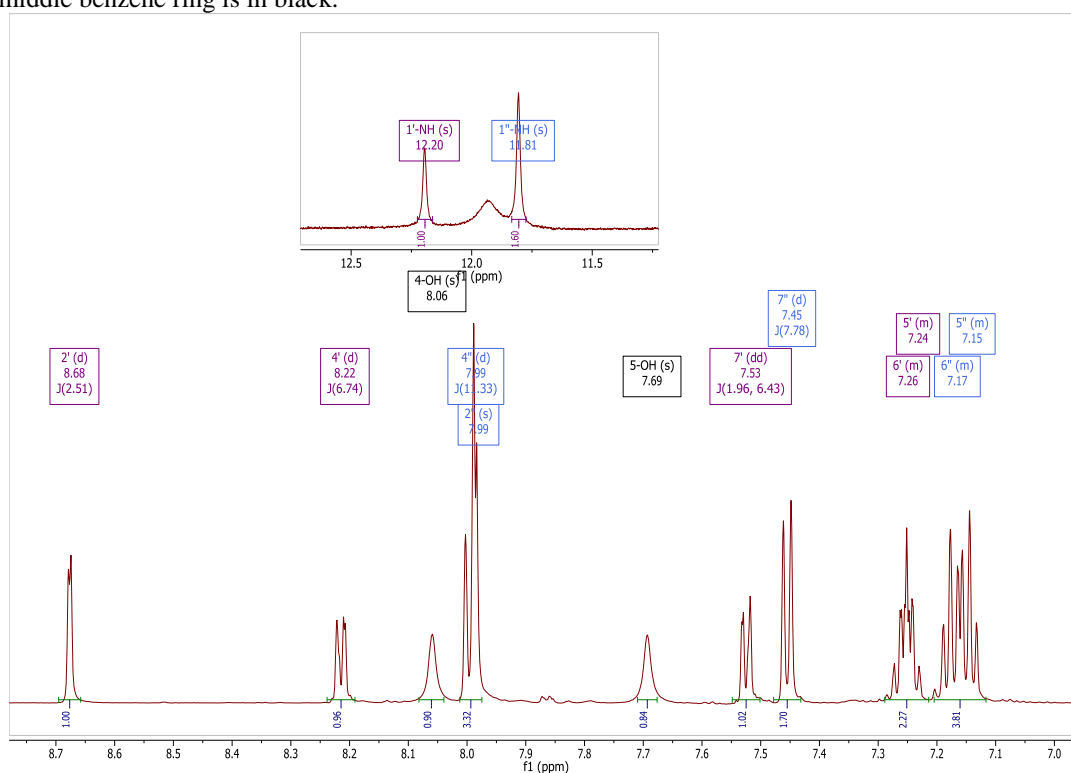


Figure 23: Expansion of the ^1H NMR spectrum

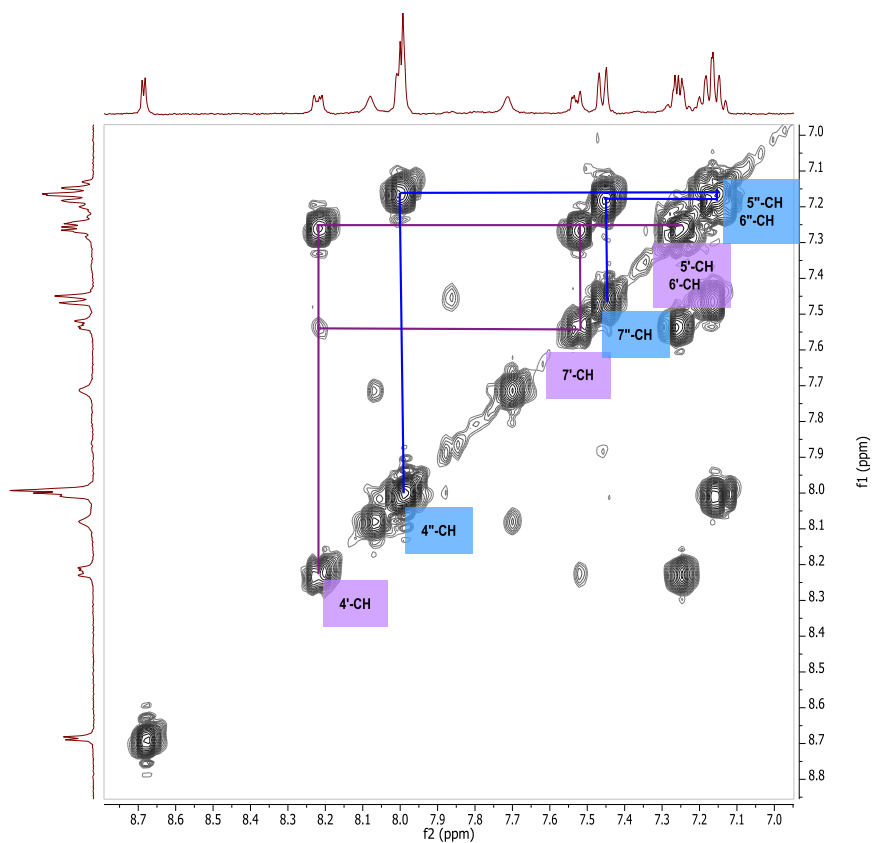


Figure 24: COSY of EG4_215-392_B3 showing the spin systems of the different indole rings. (400 MHz, DMSO)

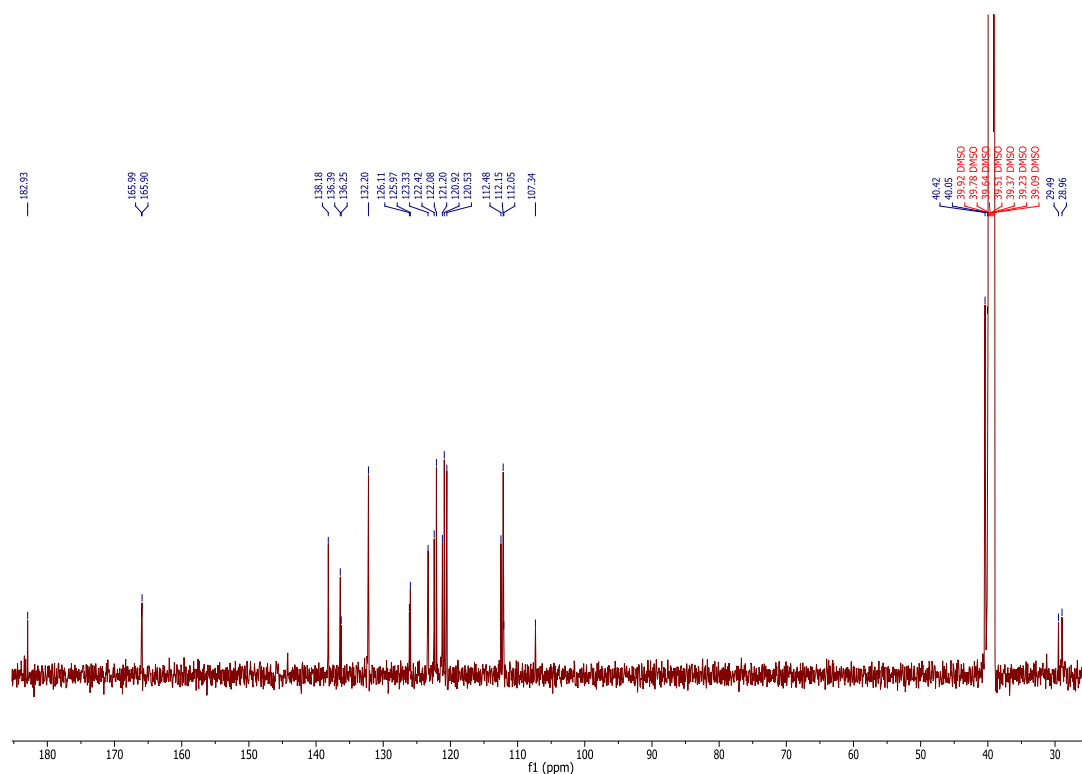


Figure 25: ^{13}C NMR spectrum of EG4_215-392_B3 (150 MHz, DMSO)

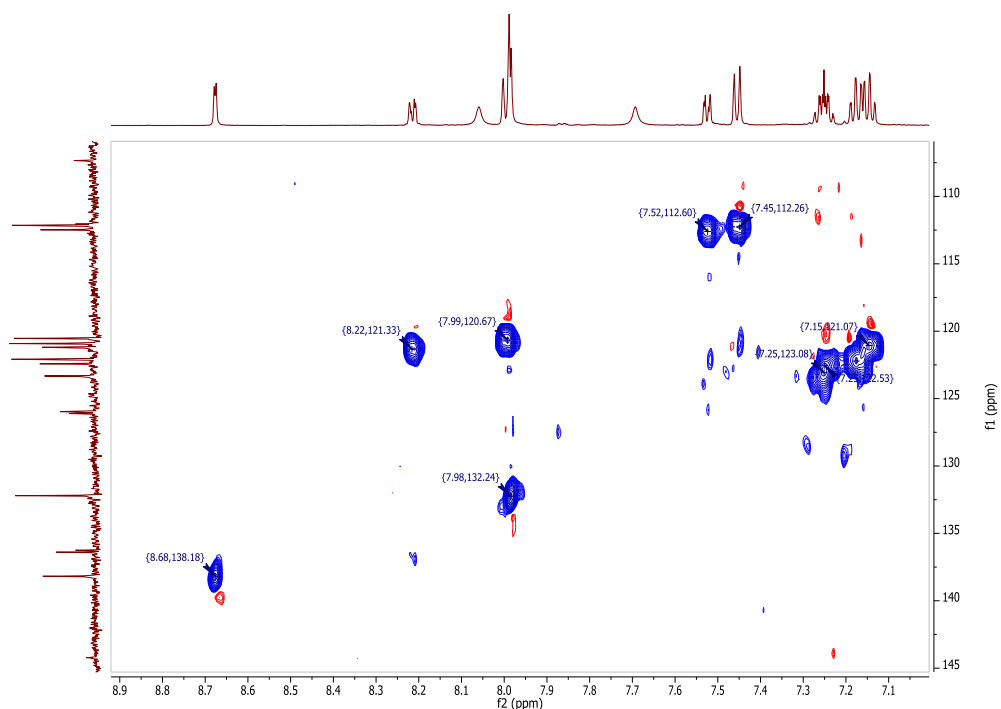


Figure 26: HSQC spectrum of EG4_215-392_B3 (600 and 150 MHz, DMSO). The blue spots indicate -CH groups.

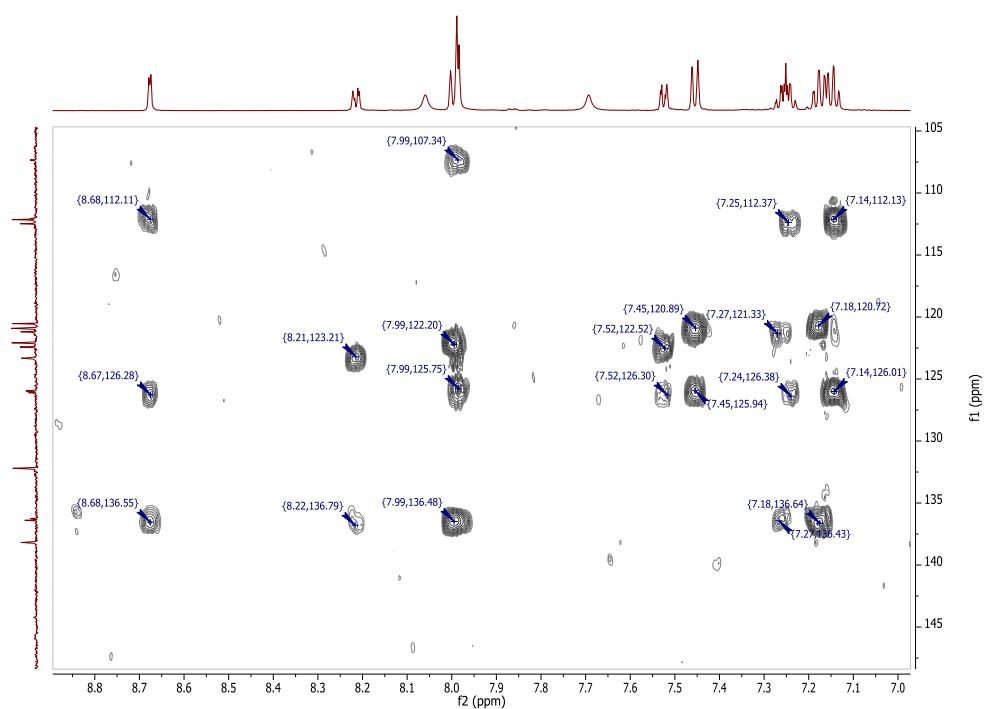


Figure 27: HMBC spectrum of EG4_215-392_B3 (600 and 150 MHz, DMSO).

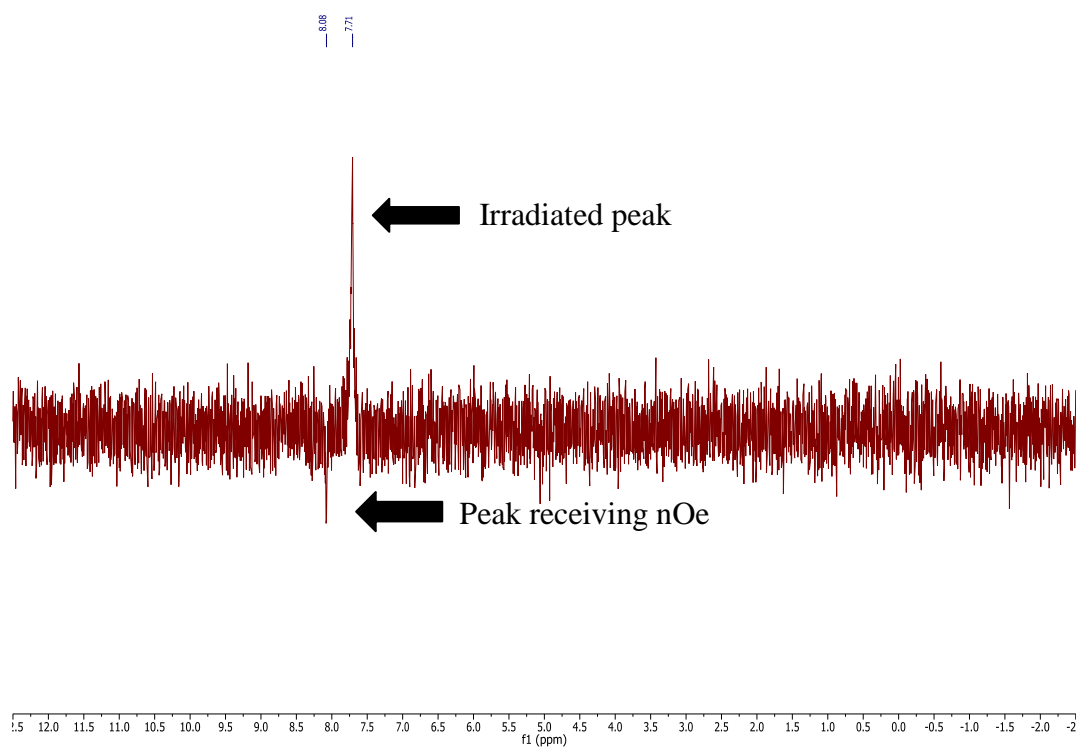


Figure 28: 1D-NOE of EG4_215-392_B3 (400 MHz, DMSO). This shows the through-space correlation of the OH peaks indicating that they are spatially close to each other. This spectrum was acquired on the JEOL 400MHz instrument.

IIB EG4_615-626_6 (Dianiline compound) (Bruker 600 MHz, DMSO)

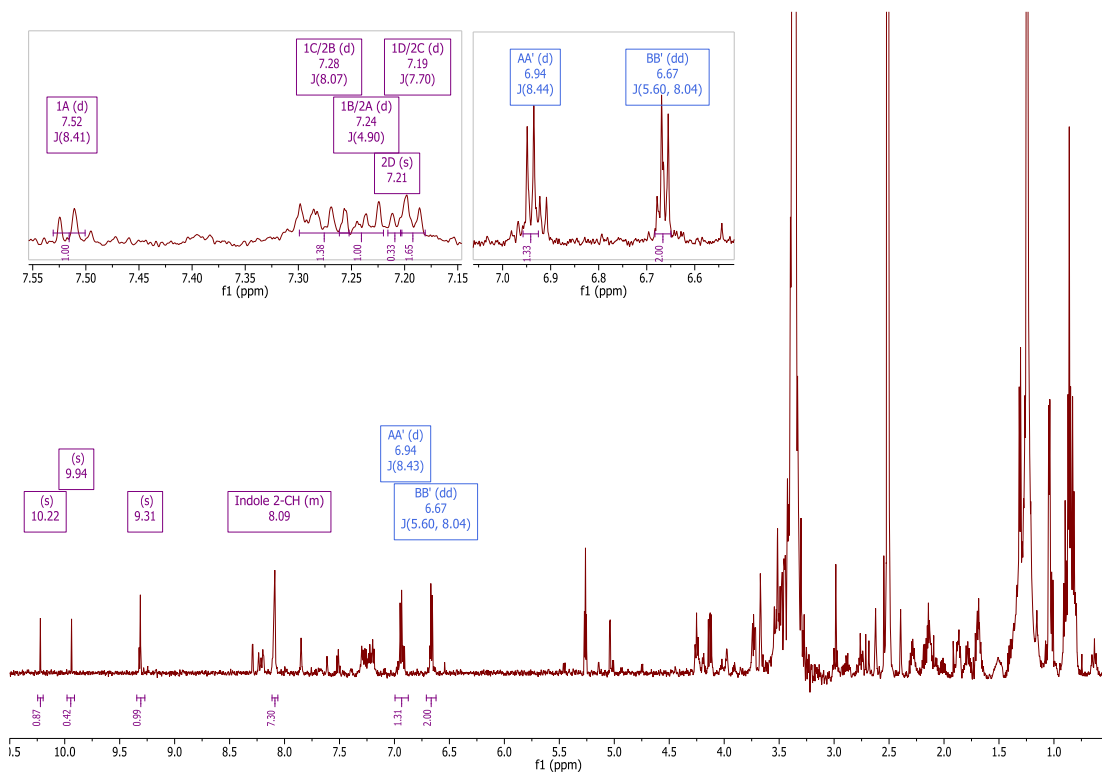


Figure 29: ^1H NMR spectrum of EG4_615-626_6 (600 MHz, DMSO)

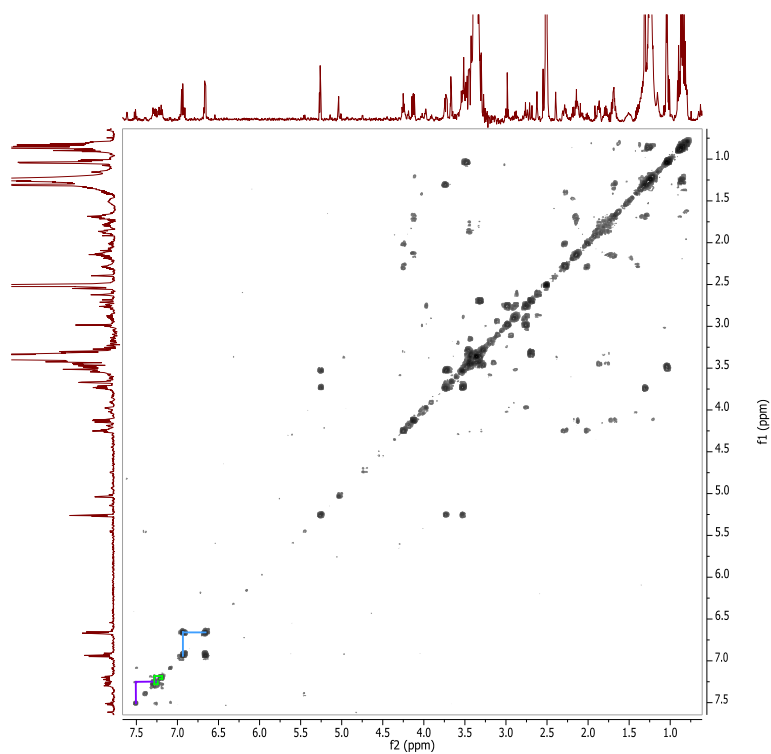


Figure 30: ^1H - ^1H COSY spectrum of EG4_615-626_6 (600 MHz, DMSO). The indole spin systems are highlighted in purple and green, and the AA'BB' system is highlighted in blue.

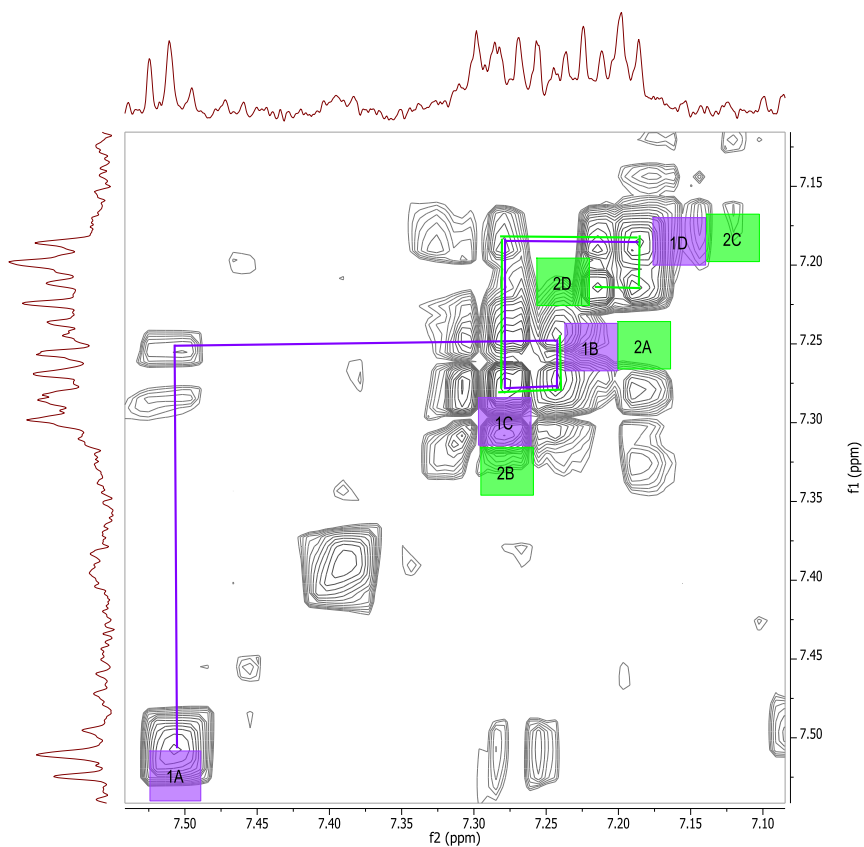


Figure 31: Expansion of the COSY spectrum showing the two indole spin systems in purple and green.

IIIC EG4_615-626_10 (1,4-dibenzylimidazolidine) (Bruker 600 MHz, DMSO)

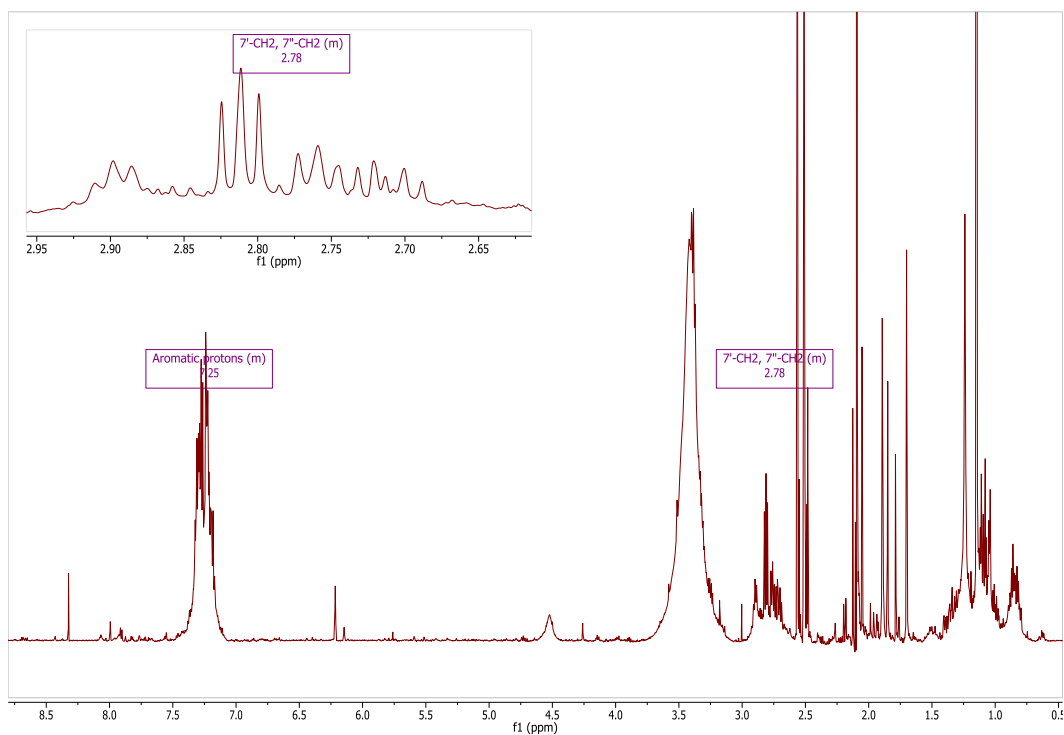


Figure 32: ¹H NMR spectrum of EG4_615-626_10 (600 MHz, DMSO)

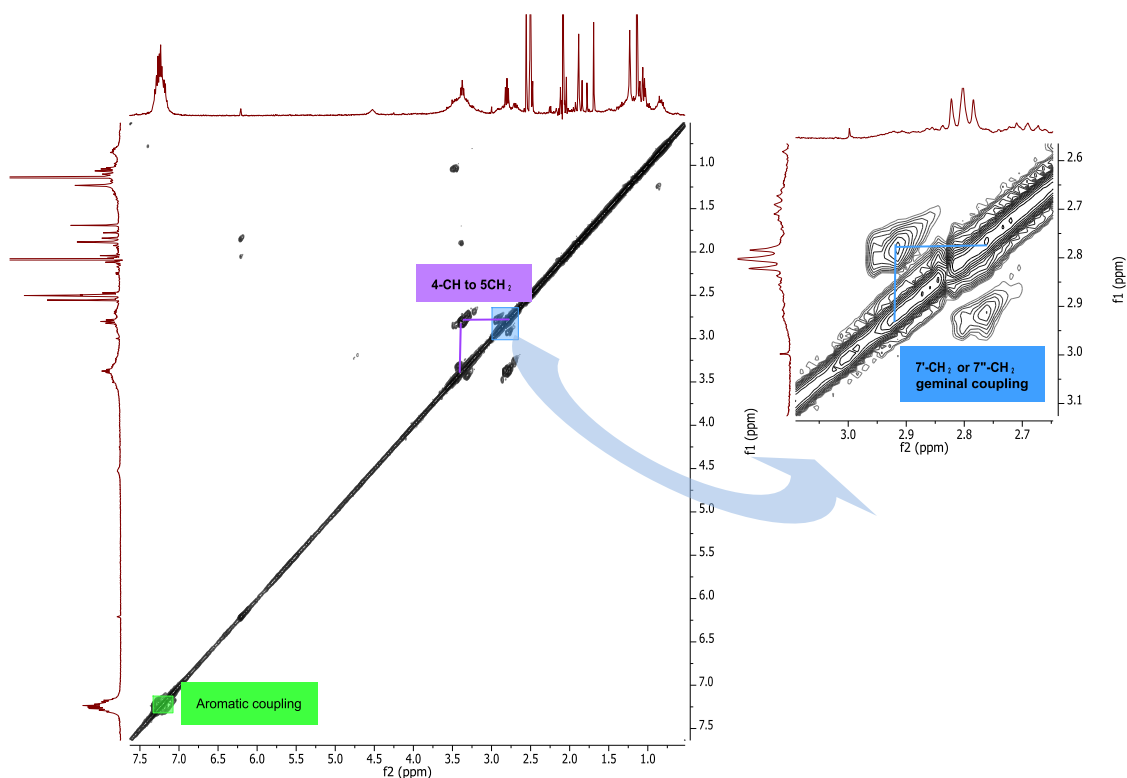


Figure 33: ¹H-¹H COSY NMR spectrum of EG4_615-626_10 (acquired on JEOL 400MHz, DMSO). The full spectrum is on the left and an expansion of 2.6-3.1ppm on the right highlights the geminal coupling between the protons of 7'-CH₂ or 7''-CH₂.

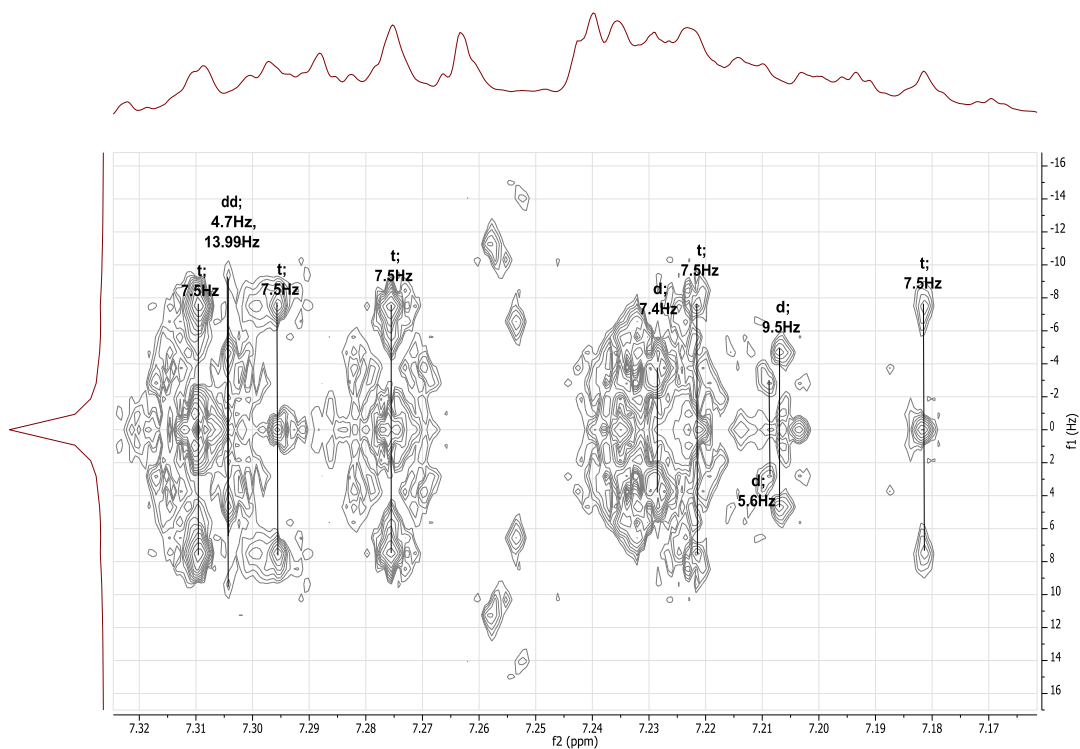


Figure 34: Expansion of the aromatic region of the J-resolved spectrum of EG4_615-626_10 (600 MHz, DMSO)

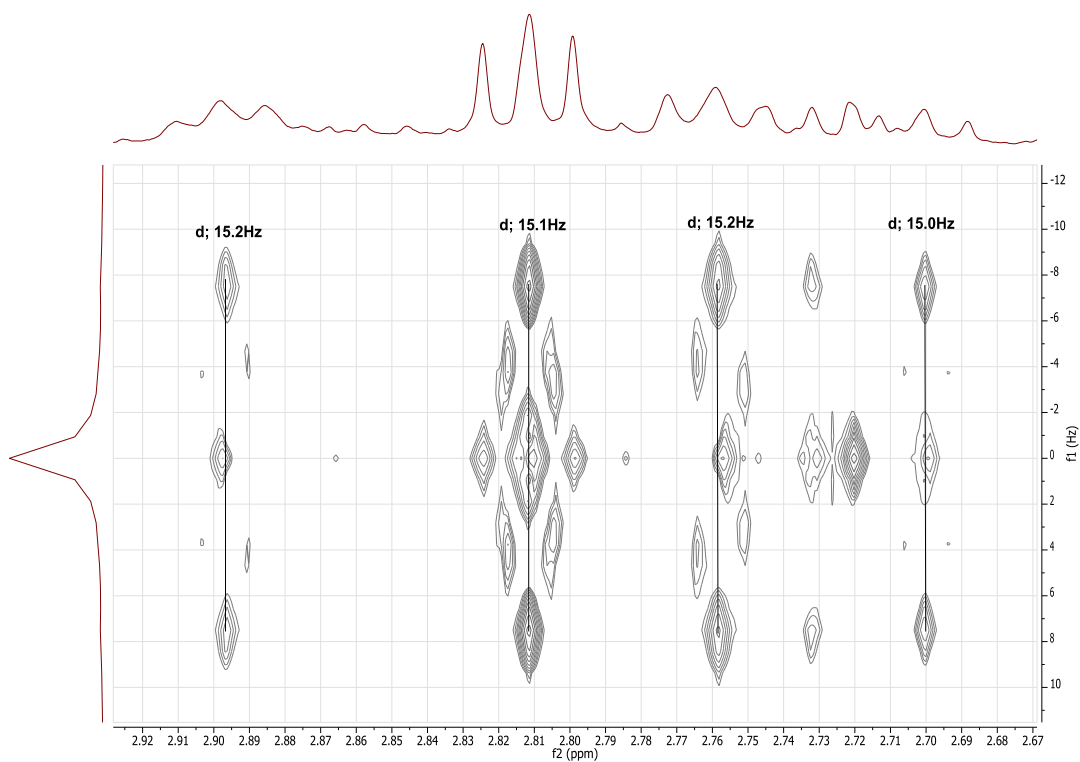


Figure 35: Expansion of the olefinic region of the J-resolved spectrum of EG4_615-626_10 (600 MHz, DMSO). The coupling constants of approximately 15 Hz indicate geminal coupling between the protons.

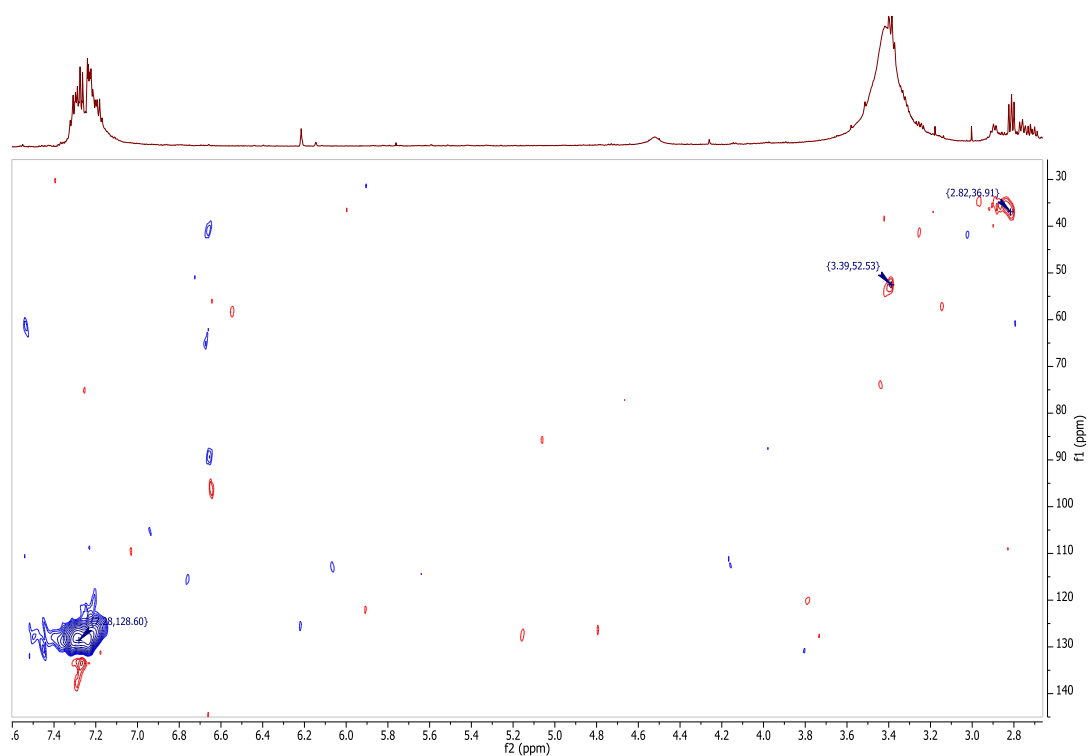


Figure 36: HSQC of EG4_615-626_10 (600 MHz, DMSO). The x-axis shows the ^1H NMR spectra and chemical shifts. The y-axis shows the ^{13}C chemical shifts. The blue spot indicates the $-\text{CH}$ groups of the phenyl rings and the red spot indicates the CH_2 groups connecting the benzene rings to the imidazolidine ring.

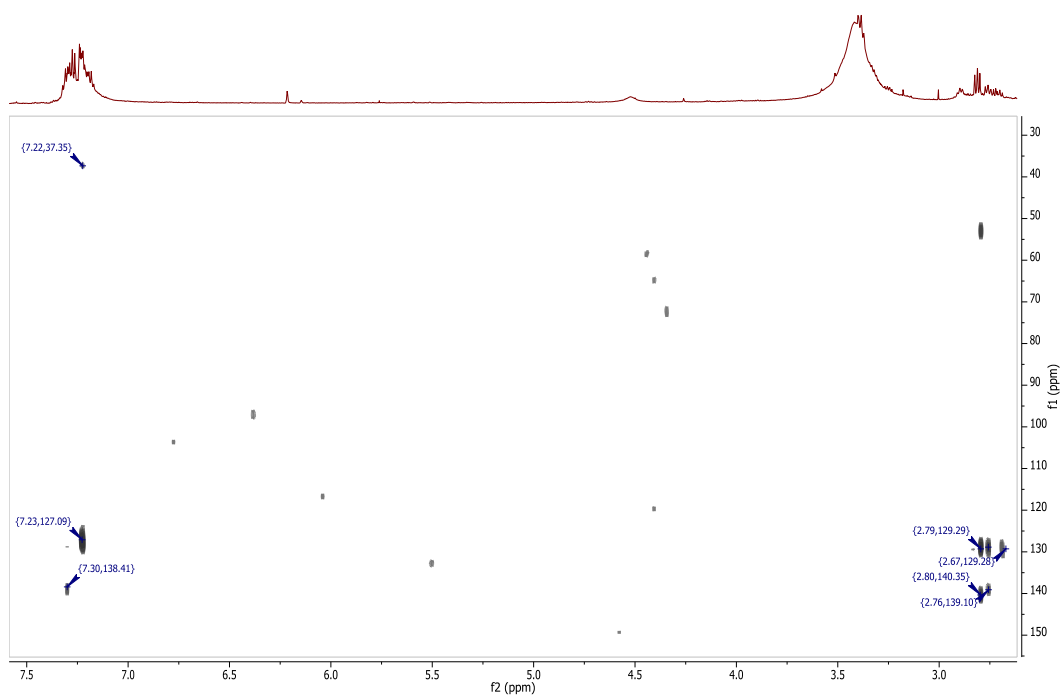


Figure 37: HMBC of EG4_615-626_10 (600 and 150 MHz, DMSO).

Appendix IV Antimicrobial Activities of Active SM8 Fractions Following Sephadex® LH-20 Chromatography

Table 0-1: Active fractions following size-exclusion chromatography of SM8 extract with Sephadex® LH-20. The specific activity is equivalent to the MIC, and the total activity is the number of wells for which the sample was active.

Fraction Nos.	Antifungal activity		Antibacterial activity			
	Specific activity (MIC) µg/mL	Total activity (Number of wells)	<i>P. aeruginosa</i>		<i>B. subtilis</i>	
			Specific activity (MIC) µg/mL	(Number of wells)	Specific activity (MIC) µg/mL	(Number of wells)
64					150	1
65					<50	1
66					150	1
67					250	1
68					100	1
69					200	1 (mild)
70					50	1
71					150	1
72					<50	1 (mild)
73					50	1 (mild)
74					100	1 (mild)
75					100	1 (mild)
76	-	-	300	1	300	1
77	225	2	450	1	225	2
78	200	1	-	-	100	1
79	350	1	-	-	175	1 (mild)
80	-	-	-	-	100	1 (mild)
81	300	1	-	-	150	1 (mild)
82	200	1	-	-	100	1 (mild)
83	150	1	75	1	75	1 (mild)
84	250	1	-	-	125	1
85	200	1	100	1	100	1
86	-	-	-	-	125	1 (mild)
87	250	1	125	1	125	1
88	250	1	62.5	1	62.5	2
89	250	1	6.25	1	62.5	2
90	-	-	50	1	25	2
91	-	-	75	1	37.5	2
92	-	-	<25	1	<12.5	2
93	-	-	25	1	12.5	2
94	-	-	<25	1	<012.5	2
95	-	-	50	1	25	2
96	-	-	50	1	25	2
97	-	-	25	1	25	1
98	-	-	75	1	37.5	2
99	-	-	75	1	37.5	2
100	250	1	125	1	62.5	2
101	250	1 (mild)	125	1	62.5	2

102	200	1	50	1	25	2
103	250	1	125	1	62.5	2
104	250	1 (mild)	125	1	62.5	2
105	250	1	125	1	62.5	2
106	350	1	175	1	87.5	2
107	300	1	150	1	75	2
108	-	-	125	1	62.5	2
109	-	-	100	1	50	2
110	150	1	75	1	37.5	2
111	150	1	75	1	37.5	2
112	100	1	50	1	25	2
113	250	1	125	1	62.5	2
114	50	1	25	1	12.5	2
115	-	-	50	1 (mild)	50	1
116	50	1	25	1	25	1
117	150	1	75	1	37.5	2
118	<50	1	<25	1	<12.5	2
119	50	1	25	1	12.5	2
120	100	1	50	1	25	2
121	150	1	75	1	37.5	2
122	100	1	50	1	50	1
123	250	1	125	1	62.5	2
124	6.25	5	50	1	25	2
125	9.375	5	75	1	75	1
126	9.375	5	75	1	75	1
127	6.25	5	-	-	-	-
128	6.25	5	-	-	-	-
129	9.375	5	-	-	-	-
130	6.25	5	-	-	-	-
131	6.25	5	-	-	-	-
132	6.25	5	-	-	-	-
133	3.125	5	-	-	-	-
134	<3.125	5	-	-	-	-
135	<3.125	5	-	-	-	-
136	6.25	5	-	-	-	-
137	<3.125	5	-	-	-	-
138	9.375	5	-	-	-	-
139	<3.125	5	-	-	-	-
140	3.125	5	-	-	-	-
141	3.125	5	-	-	-	-
142	<3.125	5	-	-	-	-
143	6.25	5	-	-	-	-
144	<3.125	5	-	-	-	-
145	6.25	5	-	-	-	-
146	6.25	5	-	-	-	-
147	6.25	5	-	-	-	-
148	25	3	-	-	-	-
149	12.5	3	-	-	-	-
150	25	3	-	-	-	-
151	6.25	4	-	-	-	-
152	25	4	-	-	-	-

153	18.75	4	-	-	-	-
154	37.5	3	-	-	-	-
155	37.5	3	-	-	-	-
156	50	3	-	-	-	-
157	62.5	3	-	-	-	-
158	50	3	-	-	-	-
159	50	3	-	-	-	-
160	50	2	-	-	-	-
161	50	2	-	-	-	-
162	50	2	-	-	-	-
163	150	1 (mild)	-	-	-	-
164	50	1	-	-	-	-
165	<50	1	-	-	-	-
166	<50	1	-	-	-	-
167	<50	1	-	-	-	-
168	<50	1	-	-	-	-
169	<50	1 (mild)	-	-	-	-

Appendix V BLAST Search of Nystatin Biosynthetic Clusters within *Streptomyces* sp. SM8 Genome

VA Alignment of the NysA and *Streptomyces* sp. SM8 PKS sequence

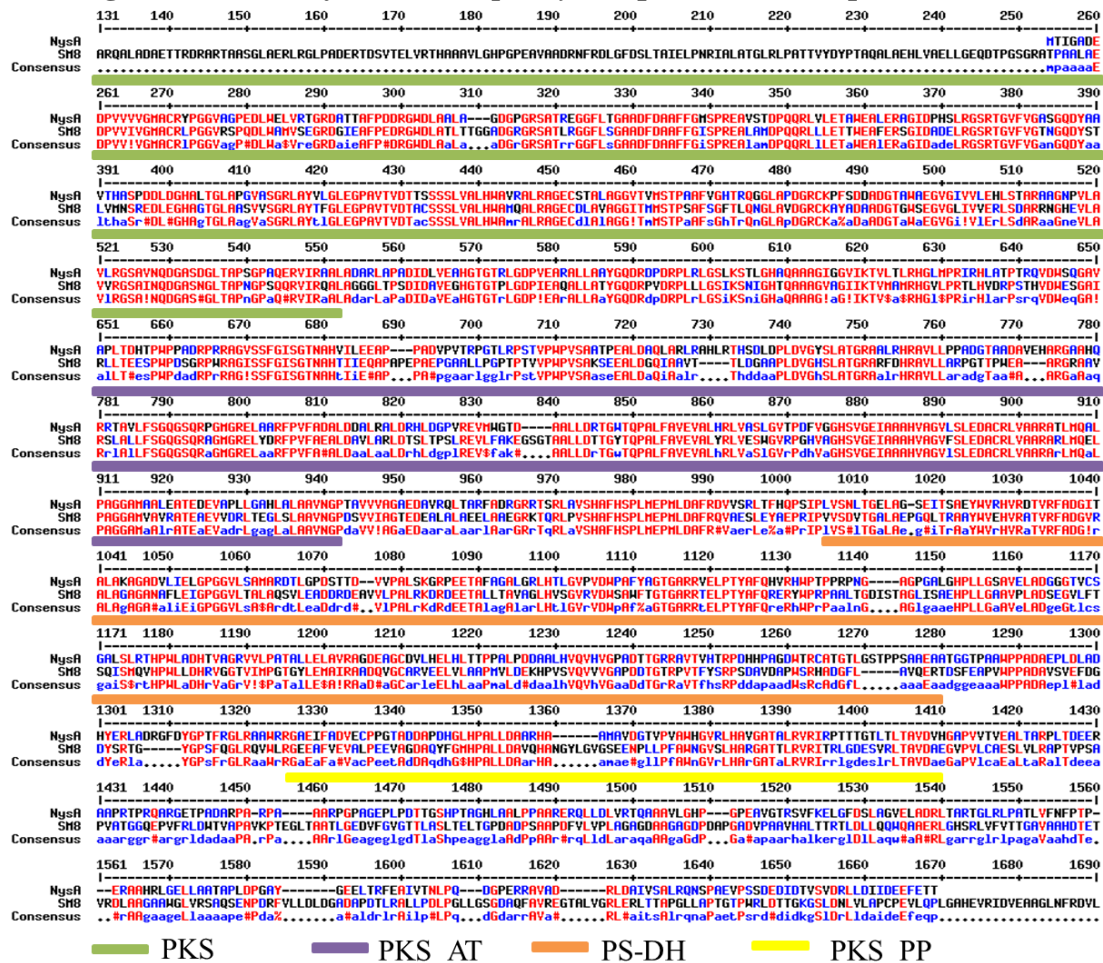


Figure 38: Alignment of the NysA sequence with that of a PKS sequence of SM8 (Identity: 57%, E-value: 0.0). Highly conserved regions are highlighted in red. Less conserved domains are highlighted in blue. The domains are designated according to their known functions in the NysA sequence and are indicated by colour, with PKS (green), the acetyltransferase domain in PKS (PKS_AT) (purple), PKS dehydratase (PS-DH) (orange) and phosphopantetheine attachment site (PKS_PP) domains identified.

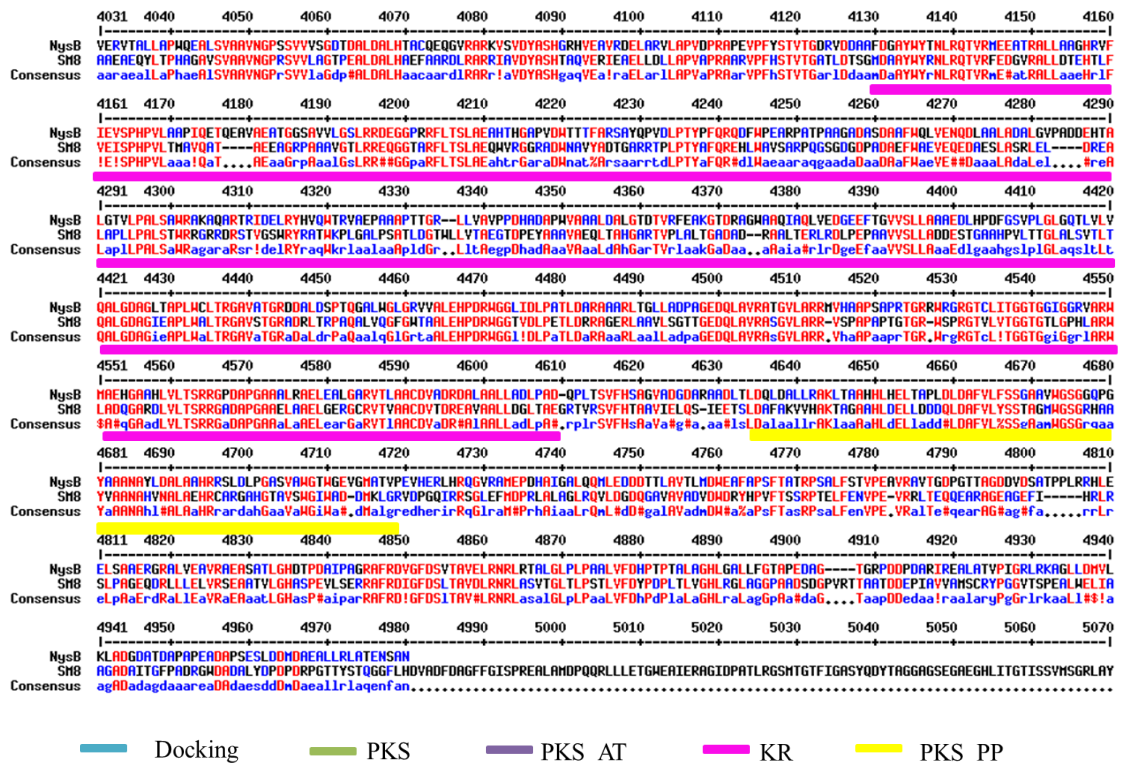


Figure 39: Alignment of the NysB sequence with that of a PKS sequence of SM8 (Identity: 53%, E-value: 0.0). Highly conserved regions are highlighted in red. Less conserved domains are highlighted in blue. The domains are designated according to their known functions in the NysB sequence and are indicated by colour, with the erythronolide synthase docking domain (teal), PKS (green), the acyltransferase domain in PKS (PKS_AT) (purple), a ketoreductase (pink) and phosphopantetheine attachment site (PKS_PP) (yellow) domains identified.

VC Alignment of the NysC and *Streptomyces* sp. SM8 PKS sequence

	5461	5470	5480	5490	5500	5510	5520	5530	5540	5550	5560	5570	5580	5590
NysC	DARLRTGSRALVPRDLAALRTGDIAPLLRGLVKAPIRRAARTTPGDTGLAEQLTRLQRAERDITLALVROQAAMVLTGSDGVDPSRAFRDLGDFSLTAVELNRRIGARTGLRLPATVDFVPTA													
SM8														
Consensus														
NysC	5591	5600	5610	5620	5630	5640	5650	5660	5670	5680	5690	5700	5710	5720
SM8	DAAALHLLTELLGPDRESOPDEPGDPTAGPTDIPVIYIGHSRCPGDIIGSPEDLHRLGGDGVYDFPTNRGMDLNLVYDPPAHAGTSYRRTGGFLHADRDFDFFGHSPREAHTDSQRLLLESSE													
Consensus														
NysC	5721	5730	5740	5750	5760	5770	5780	5790	5800	5810	5820	5830	5840	5850
SM8	MEIERERGLDPLTRDSRTGVFAGVHYSYGTRLDGRAE-FFGQGGQSSALSVASGRYSYTFEGEPMTVDTRCSSSLVALHLAQAALRGCECTLALAGGVVHNSPTDTEFSRQRGLADGRCKPFE													
Consensus														
NysC	5851	5860	5870	5880	5890	5900	5910	5920	5930	5940	5950	5960	5970	5980
SM8	SADGVNASEGVNHLLEQSDAVVNGHILLAVYRGSVAVNDGASNLGAPNGSQQRVTRQALASGGLTAGDGVYVEAHGTTGLDPIEQAALLATYGRDRDPEPLLLGSVKSNGLHTQARAGVYGI													
Consensus														
NysC	5981	5990	6000	6010	6020	6030	6040	6050	6060	6070	6080	6090	6100	6110
SM8	KYVHARRHGLVPSRLNITPESSHVDHSGAVELLEQTAPETGRARRRAGISSFISGTVNHHVILEQPEARRHSHPEEADTRAAKAPRATAPL-VNPHALSGKTEALRAQAARLLHLLQQRPELA-													
Consensus														
NysC	6111	6120	6130	6140	6150	6160	6170	6180	6190	6200	6210	6220	6230	6240
SM8	-PDDTALSLATQRSDFTHRAYVLSRDRETRALSLATTRASDPSALGTVYTHGRCAVLSFGQSSQLGNGRELVERFPVFAERLDVYIDHLDARLPAQAGREVHAGDGVVLLNETGTPALFAIEV													
Consensus														
NysC	6241	6250	6260	6270	6280	6290	6300	6310	6320	6330	6340	6350	6360	6370
SM8	ALFRLVESMGVYDFVAGHSIGTEAARHVAQVFLSDRACLRVARRRLLHQAALPAGGAMVAVQTEDEYIPL--DDEIARVAVNGPTSVYISGDEEAQTQVQHFADGRRTALRYSHAFHSPML--HL													
Consensus														
NysC	6371	6380	6390	6400	6410	6420	6430	6440	6450	6460	6470	6480	6490	6500
SM8	REFRVRVREGLSYRPTLPVYSNLGQVATDDELCSREYVHVRVREVRADGVTALAEQGVTFLELQPDGLAARHRETVADDIVVPLRRHPEERTLLTALGRLLTGTPDHAHLLAPDGRAPVD													
Consensus														
NysC	6501	6510	6520	6530	6540	6550	6560	6570	6580	6590	6600	6610	6620	6630
SM8	LPTYFQRHPFMP-SGPRDTAARVYVAGSHPLNGIYELADEEGLLFTGRSLQSNHPLADHVRVGVVLLPGLTLLLELRAGDEYVGDHVEELTLARPLVPCRGAVQTVQVYGVADTGRRTVII													
Consensus														
NysC	6631	6640	6650	6660	6670	6680	6690	6700	6710	6720	6730	6740	6750	6760
SM8	HSPRRRTTDSOHTGTPTPQHTAGVYVGLPATAVFPDRTVMPRAHPEVLDLAFYSRAGGEGYGFQGLRAARHDDGEVFDVAVLPCAGTEARAYGLHAPLLDAGLHARHVLVDPDGEPTR													
Consensus														
NysC	6761	6770	6780	6790	6800	6810	6820	6830	6840	6850	6860	6870	6880	6890
SM8	TGCVYFSGRQVFLASGASVVRVLRGDSQDLSLADDDTGGPVASVQALSRMYSVQVLSATAGLADRALFRLDASAPPCQPDPTVTVYVAVVYVGTESLTELTAALRAQADIVYRTLLST													
Consensus														
NysC	6891	6900	6910	6920	6930	6940	6950	6960	6970	6980	6990	7000	7010	7020
SM8	DEPAPALIALPLVSDQGTREARRVYVAVHDLTRRALALVQTLRQEQHFDTKFVFTVTRGATVGRDVAARVAVGLVRSQSENPGCFALVLDIPDQVGAARVAVLVSQEPQLVYRQVLRVRLVRR													
Consensus														
NysC	7021	7030	7040	7050	7060	7070	7080	7090	7100	7110	7120	7130	7140	7150
SM8	PLTEYVGGADGTDGEGVGGSGVFSGEGAVLYGTGGGLGAVLRHLLVREYGRDILLVSRSGERAVGAGELVYAEALGAVGRVRYVACDVTORAVVLEGGHAYSVAVHAGVLDGQVGLTGERLSA													
Consensus														
NysC	7151	7160	7170	7180	7190	7200	7210	7220	7230	7240	7250	7260	7270	7280
SM8	VLRPKVYHMLHEARTGLDLDARVYVSSLAGVFGSPGQRYARAFDLALTRARRRAGELPLSLAHGPNLSLDGTSMLADRALDTSQVYPLTQEQGLALFDALDGTCTVYPRDLASLRQ													
Consensus														
NysC	7281	7290	7300	7310	7320	7330	7340	7350	7360	7370	7380	7390	7400	7410
SM8	GEVPLRLSLIRGSRARRARESATATGLRRLVGLNPVERQEVLLDLVYRQVAVLGHADDDVHPRARFRELGFDSLVSVELNRLNTVITGLRLPATVFDYPTVEVLSYVLDLDTGDEAVTQV													
Consensus														
NysC	7411	7420	7430	7440	7450	7460	7470	7480	7490	7500	7510	7520	7530	7540
SM8	RAY-AVADDPVIVGACRYPGGVASPDMLRLVTDGVDVSPFTNRGADVESLHNPDPHLLTYSTRSGGFLHARGFDFPFFGHSPREALDTSQQRLLLESSEHATERGIDPDLRGSRTGVFAG													
Consensus														
NysC	7541	7550	7560	7570	7580	7590	7600	7610	7620	7630	7640	7650	7660	7670
SM8	VYNSYSAHLASPEFEGQESGSSPLASGRVYTLLEGAPVTVDTACSSSLVAMHQAARLRSQECGLALAGGVVHNSPTVYDFARQRLSPDGRCKFRADGRAGVHSGEGVGLLEQSDARVY													
Consensus														
NysC	7671	7680	7690	7700	7710	7720	7730	7740	7750	7760	7770	7780	7790	7800
SM8	GHEILAVYRGSVAVNDGASNLGAPNGSQQRVTRQALASGGLTAGDGVYVEAHGTTGLDPIEQAALLATYGRDRDPEPLLLGSVKSNGLHTQARAGVYGIKHYVHARRHGRPRTLHVADPSSHVD													
Consensus														
NysC	7801	7810	7820	7830	7840	7850	7860	7870	7880	7890	7900	7910	7920	7930
SM8	MSGAVELLEQRAMPETGRVRRAGVSSFGISGTVNHHVILEQPEARRRYPVHETNIVE--PSTVYVPLSGKTEALRAQAARLLSSIEERPELRLVYVNSLVTGRSTFHRVAVLADRDARALSAI													
Consensus														
NysC	7931	7940	7950	7960	7970	7980	7990	8000	8010	8020	8030	8040	8050	8060
SM8	BADDDAARATGRVAGRNHVLFSGQAGRLGNGRELVERFPVFAERLDVYVADHDLAPRQAGREVHAGDDELNETGTPALFAIEVALFRLESVHGVRPQVFAVHSGEIVGVSLEDR													
Consensus														

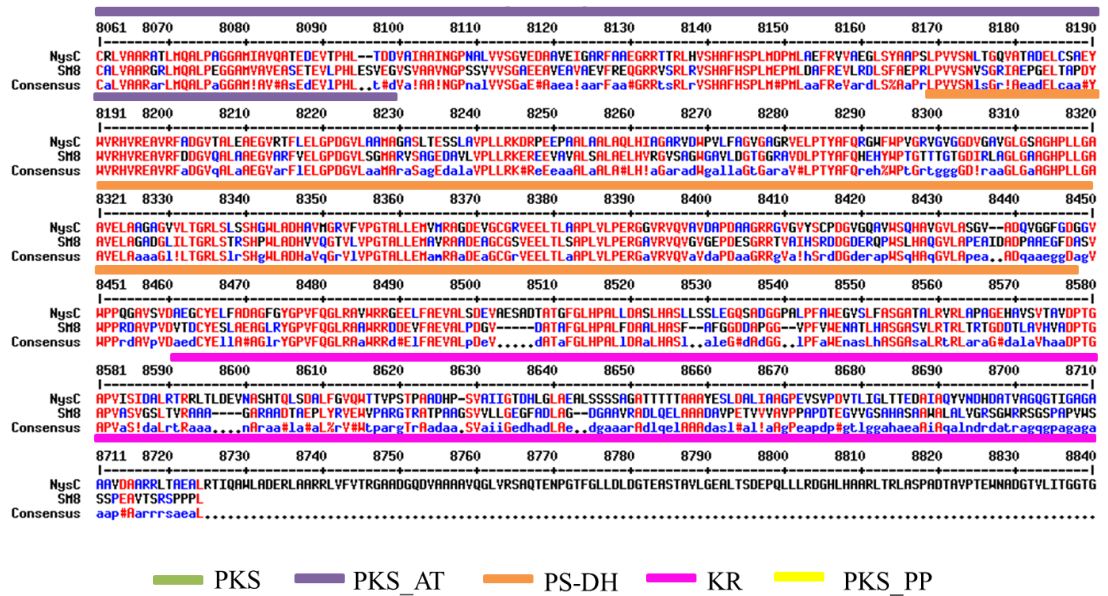
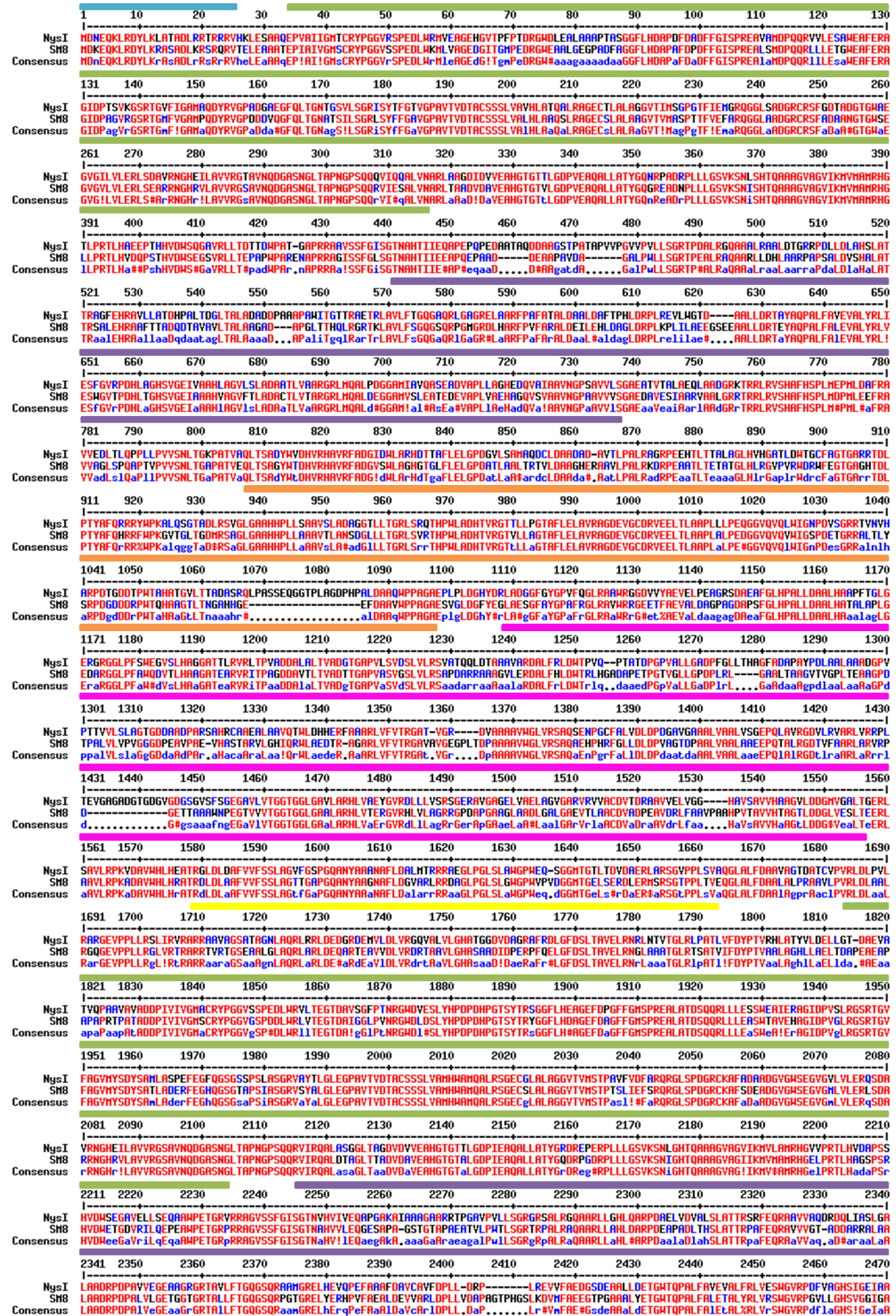


Figure 40: Alignment of the NysC sequence with that of a PKS sequence of SM8 (Identity: 61%, E-value: 0.0). Highly conserved regions are highlighted in red. Less conserved domains are highlighted in blue. The domains are designated according to their known functions in the NysC sequence and are indicated by colour, with the PKS (green), the acyltransferase domain in PKS (PKS_AT) (purple), PKS dehydratase (PKS-DH) (orange), a ketoreductase (pink) and phosphopantetheine attachment site (PKS_PP) (yellow) domains identified.

VD Alignment of the NysI and *Streptomyces* sp. SM8 PKS sequence



2471 2480 2490 2500 2510 2520 2530 2540 2550 2560 2570 2580 2590 2600
NgsI
Sf8
Consensus
2601 2610 2620 2630 2640 2650 2660 2670 2680 2690 2700 2710 2720 2730
NgsI
Sf8
Consensus
2731 2740 2750 2760 2770 2780 2790 2800 2810 2820 2830 2840 2850 2860
NgsI
Sf8
Consensus
2861 2870 2880 2890 2900 2910 2920 2930 2940 2950 2960 2970 2980 2990
NgsI
Sf8
Consensus
2991 3000 3010 3020 3030 3040 3050 3060 3070 3080 3090 3100 3110 3120
NgsI
Sf8
Consensus
3121 3130 3140 3150 3160 3170 3180 3190 3200 3210 3220 3230 3240 3250
NgsI
Sf8
Consensus
3251 3260 3270 3280 3290 3300 3310 3320 3330 3340 3350 3360 3370 3380
NgsI
Sf8
Consensus
3381 3390 3400 3410 3420 3430 3440 3450 3460 3470 3480 3490 3500 3510
NgsI
Sf8
Consensus
3511 3520 3530 3540 3550 3560 3570 3580 3590 3600 3610 3620 3630 3640
NgsI
Sf8
Consensus
3641 3650 3660 3670 3680 3690 3700 3710 3720 3730 3740 3750 3760 3770
NgsI
Sf8
Consensus
3771 3780 3790 3800 3810 3820 3830 3840 3850 3860 3870 3880 3890 3900
NgsI
Sf8
Consensus
3901 3910 3920 3930 3940 3950 3960 3970 3980 3990 4000 4010 4020 4030
NgsI
Sf8
Consensus
4031 4040 4050 4060 4070 4080 4090 4100 4110 4120 4130 4140 4150 4160
NgsI
Sf8
Consensus
4161 4170 4180 4190 4200 4210 4220 4230 4240 4250 4260 4270 4280 4290
NgsI
Sf8
Consensus
4291 4300 4310 4320 4330 4340 4350 4360 4370 4380 4390 4400 4410 4420
NgsI
Sf8
Consensus
4421 4430 4440 4450 4460 4470 4480 4490 4500 4510 4520 4530 4540 4550
NgsI
Sf8
Consensus
4551 4560 4570 4580 4590 4600 4610 4620 4630 4640 4650 4660 4670 4680
NgsI
Sf8
Consensus
4681 4690 4700 4710 4720 4730 4740 4750 4760 4770 4780 4790 4800 4810
NgsI
Sf8
Consensus
4811 4820 4830 4840 4850 4860 4870 4880 4890 4900 4910 4920 4930 4940
NgsI
Sf8
Consensus
4941 4950 4960 4970 4980 4990 5000 5010 5020 5030 5040 5050 5060 5070
NgsI
Sf8
Consensus

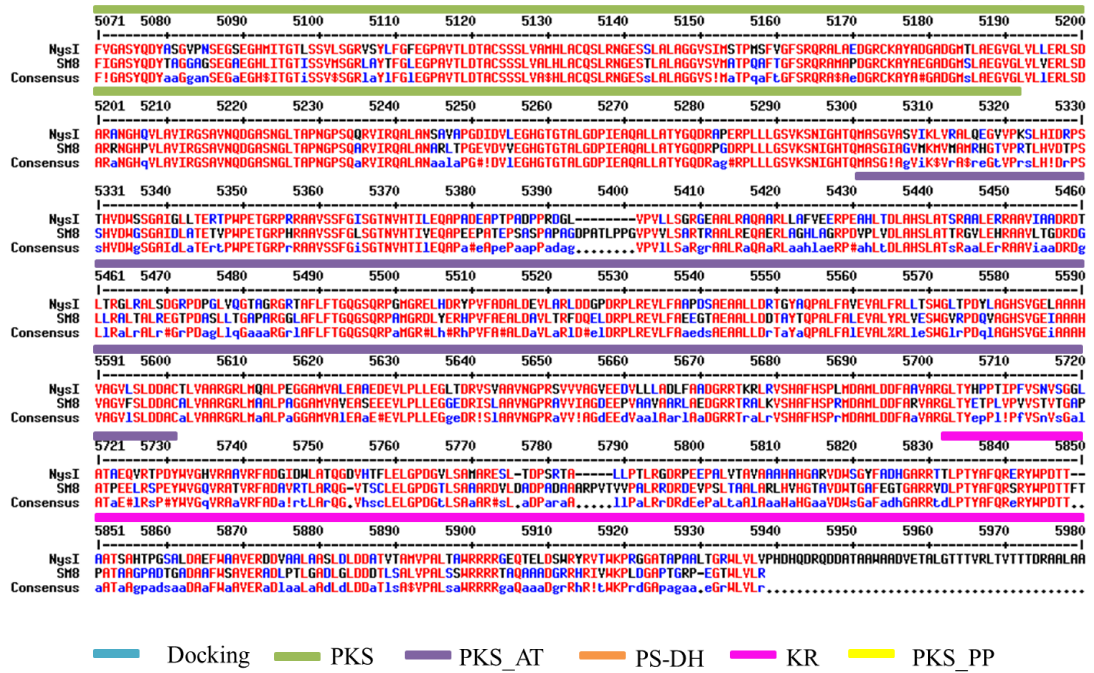


Figure 41: Alignment of the NysI sequence with that of a PKS sequence of SM8 (Identity: 65%, E-value: 0.0). Highly conserved regions are highlighted in red. Less conserved domains are highlighted in blue. The domains are designated according to their known functions in the NysI sequence and are indicated by colour, with the PKS (green), the acyltransferase domain in PKS (PKS_AT) (purple), PKS dehydratase (PKS-DH) (orange), a ketoreductase (pink) and phosphopantetheine attachment site (PKS_PP) (yellow) domains identified.

VE Alignment of the NysJ and *Streptomyces* sp. SM8 PKS sequence

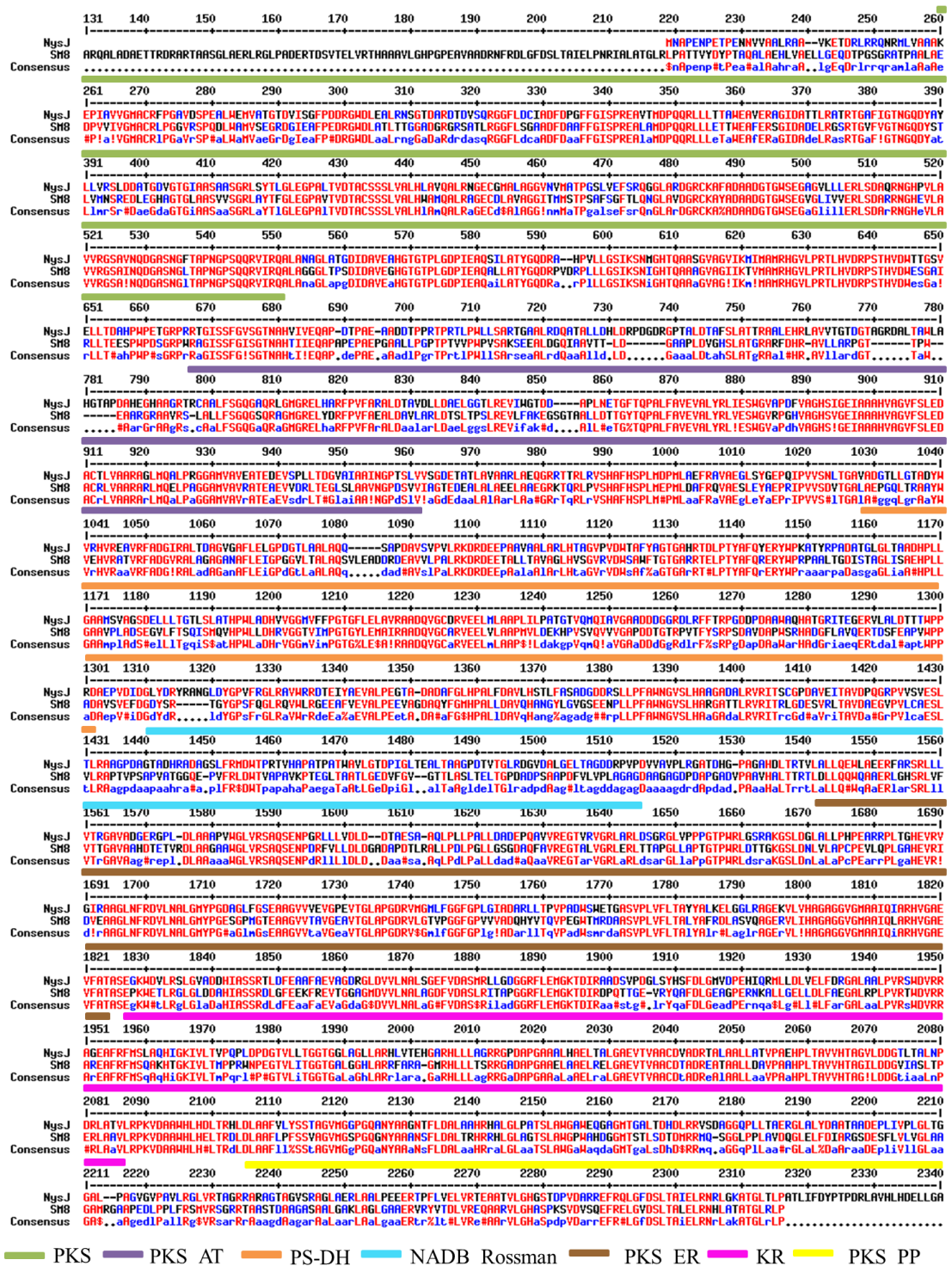


Figure 42: Alignment of the NysJ sequence with that of a PKS sequence of SM8 (Identity: 59%, E-value: 0.0). Highly conserved regions are highlighted in red. Less conserved domains are highlighted in blue. The domains are designated according to their known functions in the NysJ sequence and are indicated by colour, with the PKS (green), the acyltransferase domain in PKS (PKS_AT) (purple), PKS dehydratase (PKS-DH) (orange), Rossmann-fold NAD(P) (+) binding proteins (NADB_Rossmann) (light blue), enoylreductase of PKS (PKS_ER) (brown), a ketoreductase (pink) and phosphopantetheine attachment site (PKS_PP) domains identified.

Appendix VI BLAST Search for Thaxtomin Biosynthetic Clusters within the *Microbacterium testaceum* StLB037 Genome

VIA Alignment of the TxtA and *M. testaceum* StLB037 NRPS module sequence

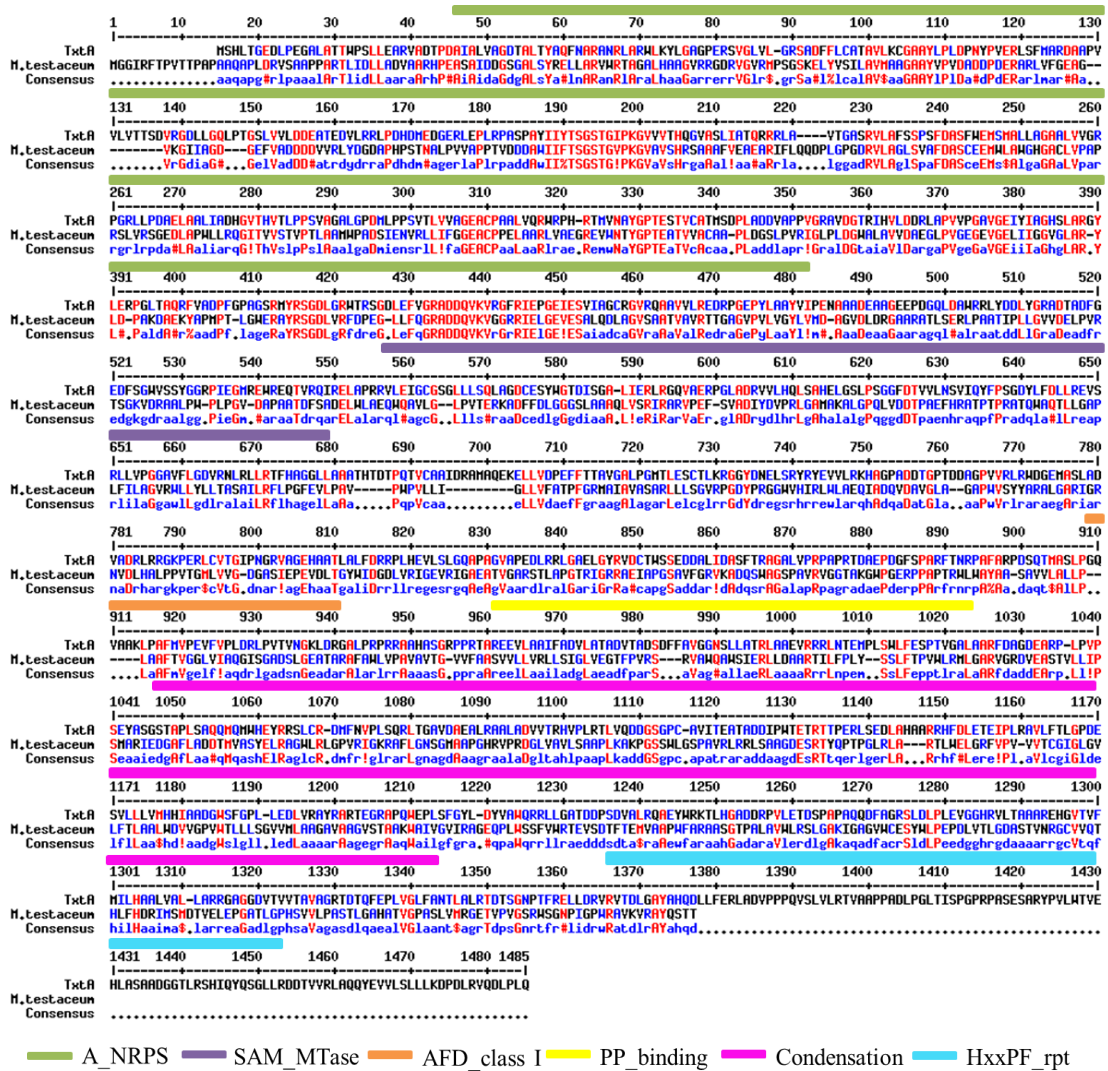


Figure 43: Alignment of the TxtA sequence with that of an NRPS module of *M. testaceum* StLB037 (Identity: 36%, E-value: 2E-46). Highly conserved regions are highlighted in red. Less conserved domains are highlighted in blue. The domains are designated according to their known functions in the TxtA sequence and are indicated by colour, with the adenylation domain of NRPS (A_NRPS) (green), the S-adenosylmethionase-dependent methyltransferase domain (SAM_MTase) (purple), adenylation forming domain (AFD_class I) (orange), phosphopantetheine attachment site (PP_binding) (yellow), a condensation domain (pink) and HxxPF-repeated (HxxPF_rpt) (light blue) domains identified.

VIB Alignment of the TxtB and *M. testaceum* StLB037 NRPS module sequence

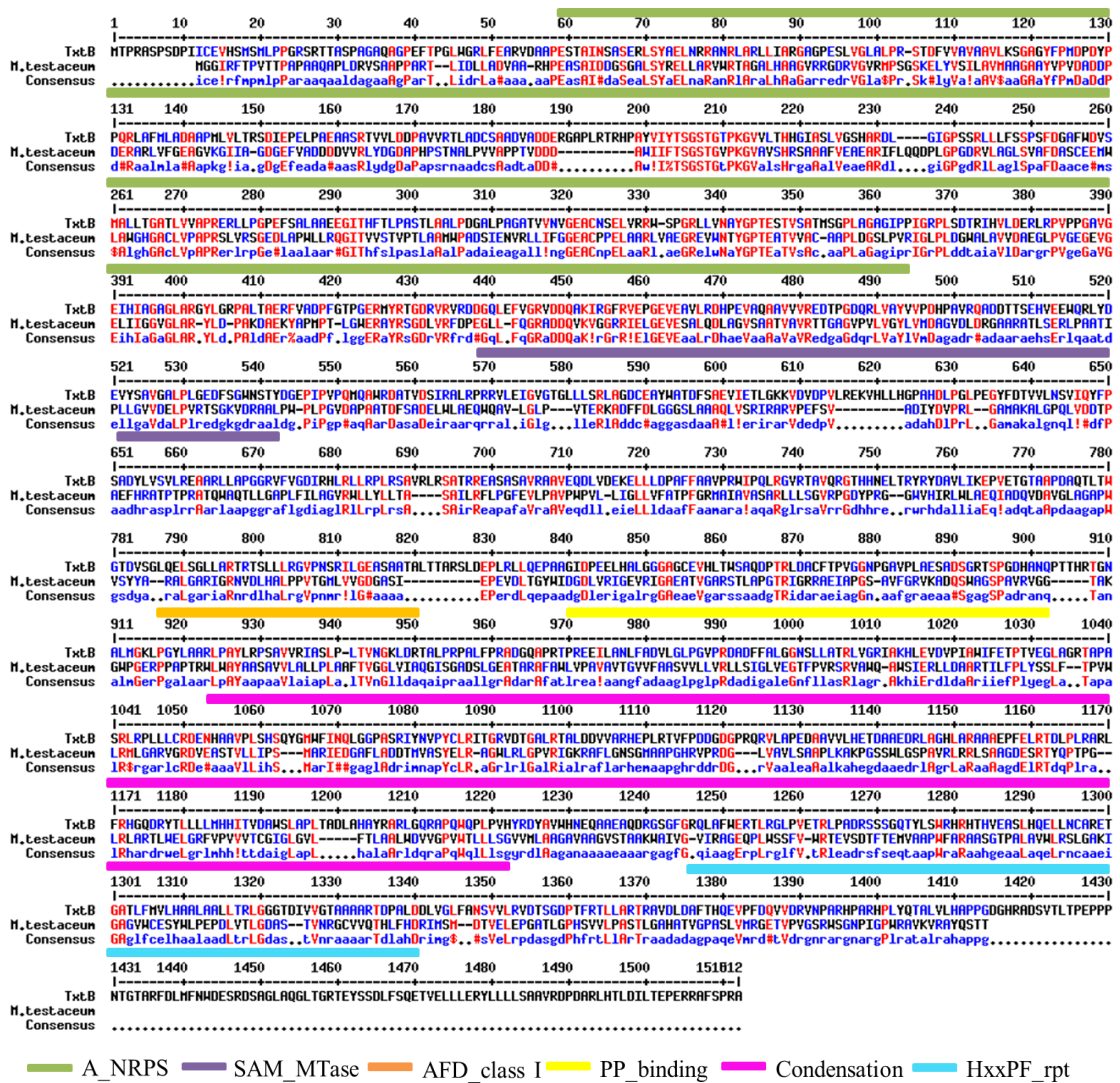


Figure 44: Alignment of the TxtB sequence with that of an NRPS module of *M. testaceum* StLB037 (Identity: 38%, E-value: 2E-50). Highly conserved regions are highlighted in red. Less conserved domains are highlighted in blue. The domains are designated according to their known functions in the TxtA sequence and are indicated by colour, with the adenylation domain of NRPS (A_NRPS) (green), the S-adenosylmethionase-dependent methyltransferase domain (SAM_MTase) (purple), adenylylating domain (AFD_class I) (orange), phosphopantetheine attachment site (PP_binding) (yellow), a condensation domain (pink) and HxxPF-repeated (HxxPF_rpt) (light blue) domains identified.

Appendix VII BLAST Search for DasR within the *Microbacterium testaceum* StLB037 Genome.

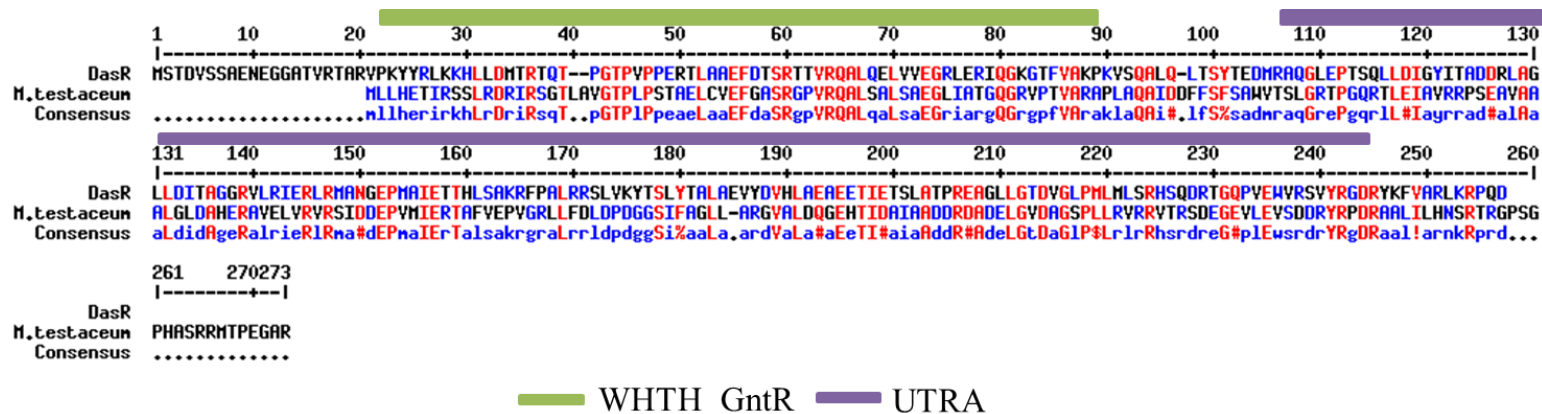


Figure 45: Alignment of the DasR sequence with that of a transcriptional regulator of *M. testaceum* StLB037 (Identity: 30%, E-value: 2E-14). Highly conserved regions are highlighted in red. Less conserved domains are highlighted in blue. The domains are designated according to their known functions in the DasR sequence and are indicated by colour. The winged-helix-turn-helix DNA-binding domain (WTHH_GntR) and UbiC transcription regulator-associated domain (UTRA) are labelled with green and purple, respectively.

Appendix VII BLAST Search of Surfactin Biosynthetic Clusters within the *Microbacterium testaceum* StLB037 Genome

VIIA Alignment of surfactin synthetase srfAA and NRPS modules from *Microbacterium testaceum* StLB037

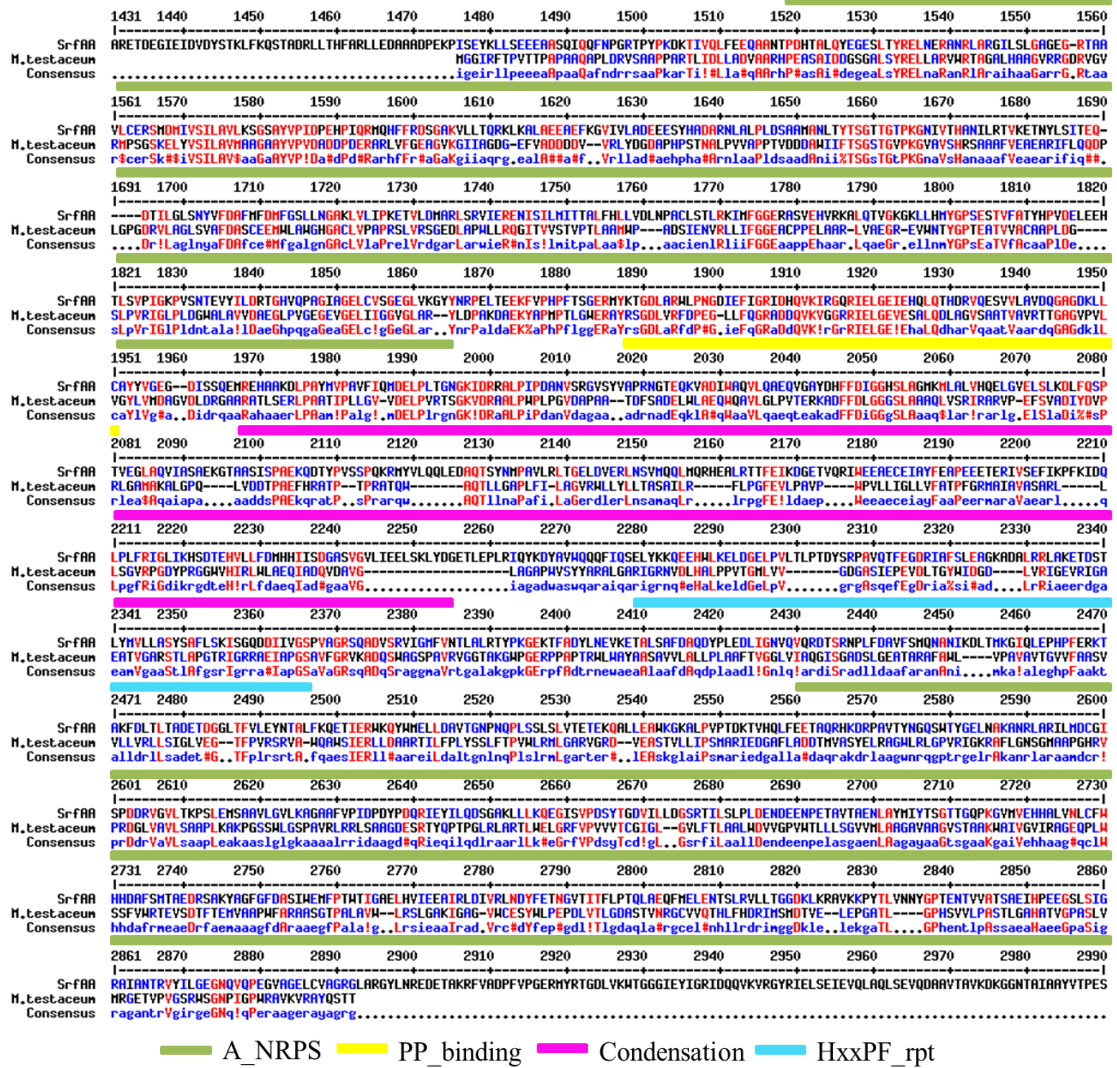


Figure 46: Alignment of the SrfAA sequence with that of an NRPS module of *M. testaceum* StLB037 (Identity: 31%, E-value: 4E-62). Highly conserved regions are highlighted in red. Less conserved domains are highlighted in blue. The domains are designated according to their known functions in the SrfAA sequence and are indicated by colour, with the adenylation domain of NRPS (A_NRPS) (green), the phosphopantetheine attachment site (PP_binding) (yellow), condensation (pink) and HxxPF-repeated (HxxPF_rpt) (light blue) domains identified.

VIIB Alignment of surfactin synthetase srfAB and NRPS modules from *Microbacterium testaceum* StLB037

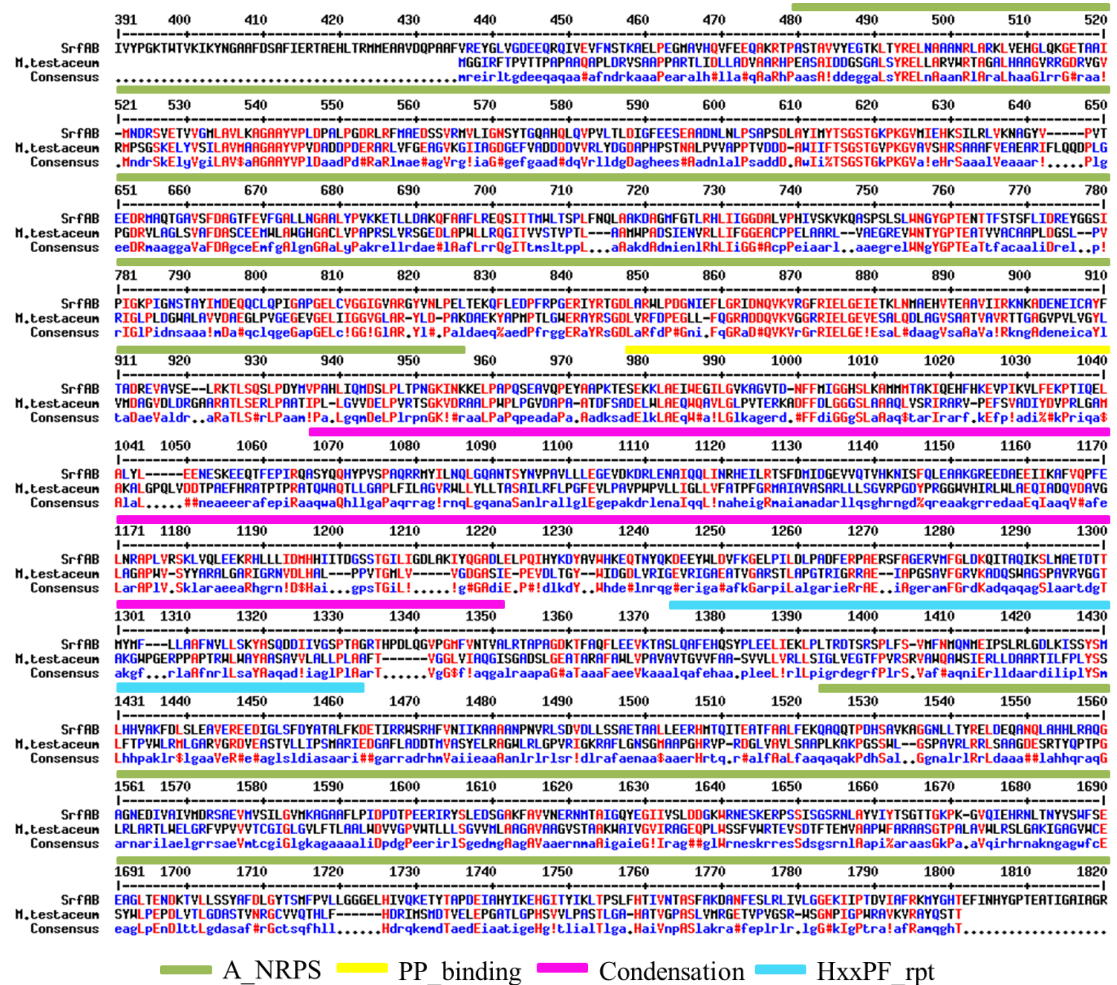


Figure 47: Alignment of the SrfAB sequence with that of an NRPS module of *M. testaceum* StLB037 (Identity: 33%, E-value: 2E-63). Highly conserved regions are highlighted in red. Less conserved domains are highlighted in blue. The domains are designated according to their known functions in the SrfAA sequence and are indicated by colour, with the adenylation domain of NRPS (A_NRPS) (green), the phosphopantetheine attachment site (PP_binding) (yellow), condensation (pink) and HxxPF-repeated (HxxPF_rpt) (light blue) domains identified.

VIIC Alignment of surfactin synthetase srfAC and NRPS modules from *Microbacterium testaceum* StLB037

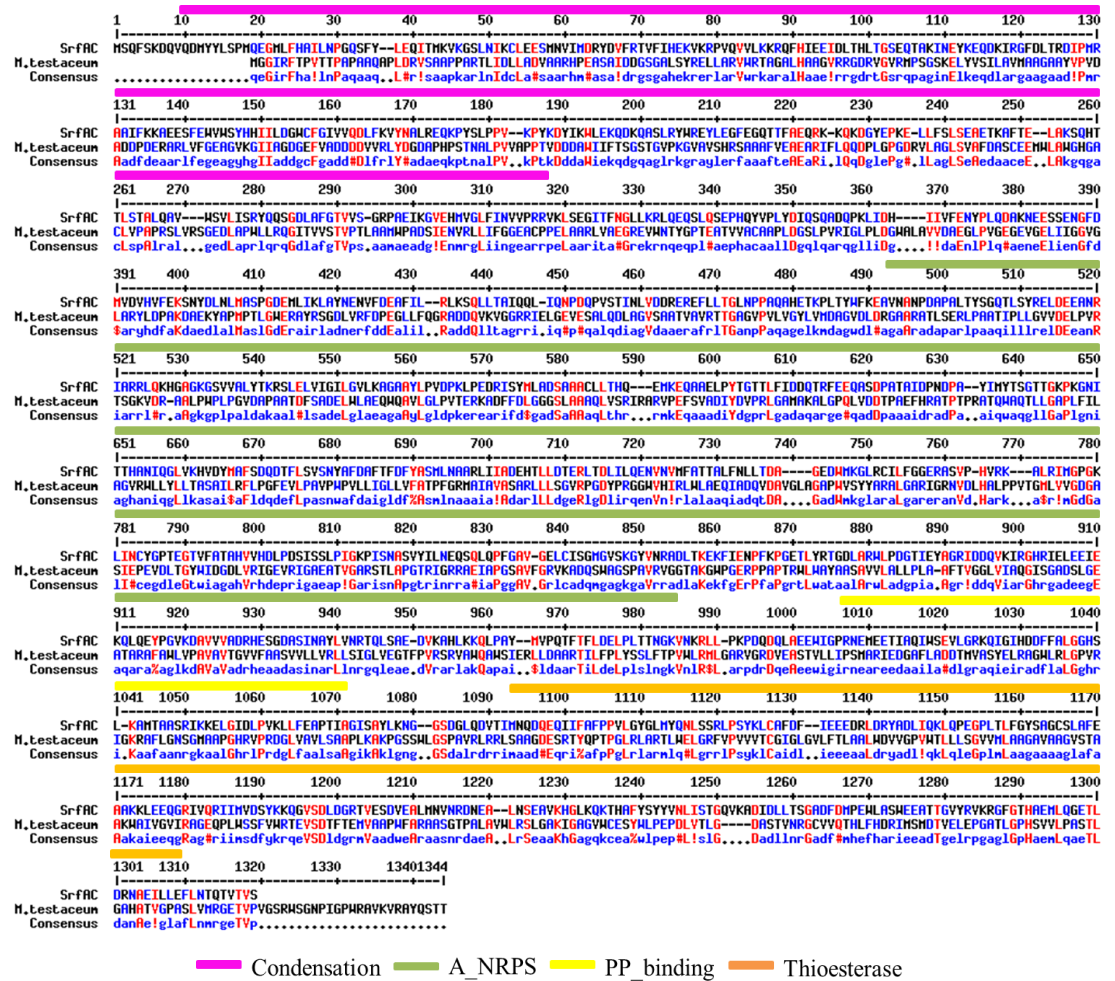


Figure 48: Alignment of the SrfAB sequence with that of an NRPS module of *M. testaceum* StLB037 (Identity: 33%, E-value: 2E-63). Highly conserved regions are highlighted in red. Less conserved domains are highlighted in blue. The domains are designated according to their known functions in the SrfAA sequence and are indicated by colour, with the condensation domain (pink), adenylation domain of NRPS (A_NRPS) (green), phosphopantetheine attachment site (PP_binding) (yellow), and thioesterase (orange) domains identified.

Appendix VIII Posters and Publications from This Thesis

METABOLOMICS AS A TOOL IN THE IDENTIFICATION AND PRODUCTION OF NEW MARINE-DERIVED ANTIBIOTICS FROM SPONGES AND ENDOSYMBIOTIC BACTERIA

Christina Viegelmann¹, Cheung Hoe Leong¹, Dominick Perrocco¹, Jennifer Parker¹, Carol Clements¹, Usama Ramadan Abelmohe², Ute Hentschel², Lekha Menon³, Jonathan Kennedy³, Alan Dobson³ and RuAngelie Edrada-Ebel¹

¹Strathclyde Institute of Pharmacy and Biomedical Sciences, University of Strathclyde, The John Arbuthnot Building, 161 Cathedral Street, Glasgow G4 0RE, Scotland, ruangelie.edrada-ebel@strath.ac.uk

²Julius-von-Sachs Institute for Biological Sciences, University of Wuerzburg, Germany

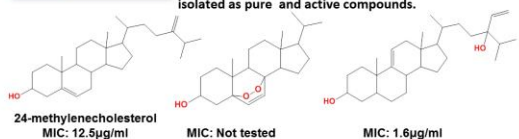
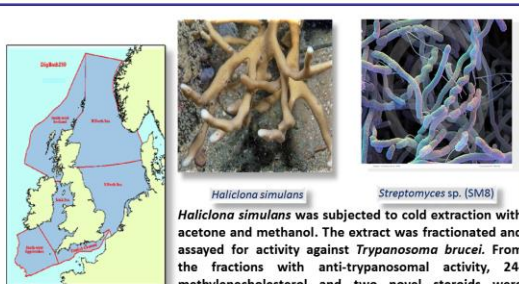
³Environmental Research Institute, University College Cork, Ireland

ABSTRACT

Metabolomic methods can be utilised to screen diverse biological systems for potentially novel and sustainable sources of antibiotics and pharmacologically-active drugs. Marine sponges and their endosymbionts have proven to be abundant in bioactive compounds. HR-LC/MS and NMR were used in the identification of compounds isolated from a bacteria and its host sponge, as well as in the dereplication and metabolic profiling of other sponge-associated bacteria.

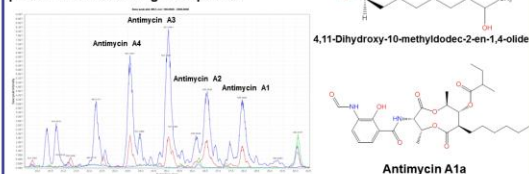
24-methylenecholesterol and two novel steroids, both significantly active against *Trypanosoma brucei*, were isolated from the Irish Sea sponge *Haliclona simulans*. Extracts from *Streptomyces* sp. isolated from *H. simulans* demonstrate anti-bacterial and anti-fungal activities. HR-LC/MS assisted in identifying antimycins as the anti-fungal compounds. NMR and HR-LC/MS were applied to the dereplication of extracts from bacteria from Mediterranean sponges. EG4 was selected and its cultivation optimised from small scale to larger scale production with the aid of metabolomic methods to identify and trace biomarkers.

Metabolomics has become a powerful tool in systems biology which allows us to gain insights into the potential of natural marine isolates for synthesis of significant quantities of promising new agents, and allows us to manipulate the environment within fermentation systems in a rational manner to select a desired metabolome.



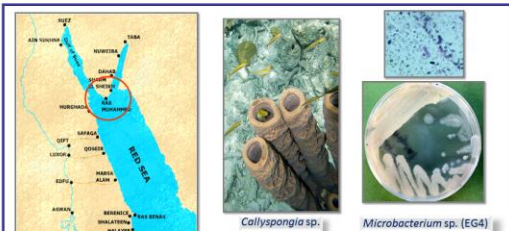
SM8, a *Streptomyces* sp. isolated from *H. simulans*, produces anti-bacterial and anti-fungal compounds. The antibacterial compounds were found by NMR to be predominantly hydroxylated saturated fatty acids. A fraction containing two isomeric butenolides was isolated and showed quorum signalling activity in a TLC overlay assay using a strain of *Chromobacterium violaceum*.

High-resolution LCMS identified anti-fungal antimycins, the presence of which was confirmed by knockout studies of the antimycin gene cluster. The mutants did not contain the Antimycin A isomers but still retained anti-fungal activity, albeit much reduced, indicating that SM8 produces other anti-fungal compounds.

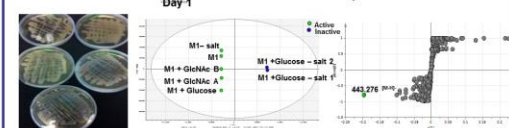
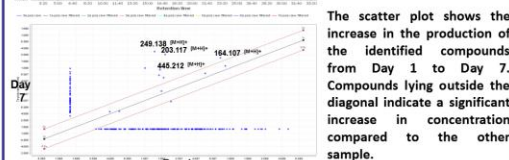
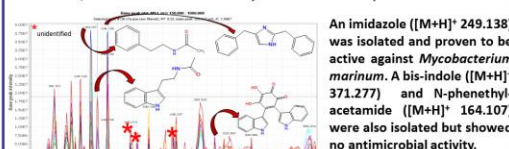


Conclusion

Metabolomics is an efficient tool in detecting differences, as well as similarities, in the chemical profiles of samples. It can be used to determine the quantity of unknown compounds in a sample, and also to identify the known metabolites present. It is also useful in comparing different extraction and culture methods as it gives a picture of the metabolome and the variations produced by each method. The identification of biomarkers aids further in the optimisation of the fermentation conditions.



EG4 (*Microbacterium* sp.) was selected for further work following dereplication of seven sponge-associated bacteria using HR-LCMS and NMR. Extracts from EG4 cultured in M1 broth show anti-trypanosomal and antimycobacterial activity. Metabolic profiling of EG4 over the course of seven days using NMR and HR-LCMS indicated when the production of new metabolites began. A biomarker was identified in the extracts of days six and seven, both of which had anti-mycobacterial activity.



EG4 was cultured on variations of M1 agar media to determine changes in metabolite production. OPLS-DA was performed to identify the compounds that contribute to the anti-trypanosomal activity. A compound with an m/z of 443.276 [M+H]⁺ and a retention time of 18.03 min was strongly correlated with activity and was unidentified by the database.

Communication

Isolation and Identification of Antitrypanosomal and Antimycobacterial Active Steroids from the Sponge *Haliclona simulans*

Christina Viegelmann ^{1*}, Jennifer Parker ¹, Thengtheng Ooi ¹, Carol Clements ¹, Gráinne Abbott ¹, Louise Young ¹, Jonathan Kennedy ², Alan D. W. Dobson ² and RuAngelie Edrada-Ebel ^{1*}

¹ Strathclyde Institute of Pharmacy and Biomedical Sciences, University of Strathclyde, The John Arbuthnott Building, 161 Cathedral Street, Glasgow, Scotland G4 0RE, UK; E-Mails: jennifer.parker.100@strath.ac.uk (J.P.); thengthengooi@hotmail.com (T.O.); c.j.clements@strath.ac.uk (C.C.); grainne.abbott@strath.ac.uk (G.A.); louise.c.young@strath.ac.uk (L.Y.)

² Marine Biotechnology Centre, Environmental Research Institute, University College Cork, Lee Road, Cork, Ireland; E-Mails: jonathan.kennedy@ucc.ie (J.K.); A.Dobson@ucc.ie (A.D.W.D.)

* Authors to whom correspondence should be addressed;

E-Mails: christina.viegelmann@strath.ac.uk (C.V.); ruangelie.edrada-ebel@strath.ac.uk (R.E.-E.); Tel.: +44-141-548-3728 (C.V.); Fax: +44-141-552-2562 (C.V.); Tel.: +44-141-548-5968 (R.E.-E.); Fax: +44-141-552-2562 (R.E.-E.).

Received: 30 January 2014; in revised form: 25 April 2014 / Accepted: 28 April 2014 /

Published: 16 May 2014

Abstract: The marine sponge *Haliclona simulans* collected from the Irish Sea yielded two new steroids: 24-vinyl-cholest-9-ene-3 β ,24-diol and 20-methyl-pregn-6-en-3 β -ol,5 α ,8 α -epidioxy, along with the widely distributed 24-methylenecholesterol. One of the steroids possesses an unusually short hydrocarbon side chain. The structures were elucidated using nuclear magnetic resonance spectroscopy and confirmed using electron impact- and high resolution electrospray-mass spectrometry. All three steroids possess antitrypanosomal and anti-mycobacterial activity. All the steroids were found to possess low cytotoxicity against Hs27 which was above their detected antitrypanosomal potent concentrations.

Keywords: *Haliclona simulans*; marine sponges; steroids; antitrypanosomal; anti-mycobacterial

1. Introduction

Since the discovery of penicillin and its widespread use during World War II, many people have become complacent about infectious diseases, believing that with antibiotics, death due to infection has become a thing of the past. However, in 2004, infectious and parasitic diseases ranked as the second leading cause of death in the world, after cardiovascular diseases, with respiratory infections considered as the fourth and fifth most common cause of death in women and men respectively, worldwide [1].

Trypanosomiasis is a vector-transmitted disease caused by parasitic protozoa called trypanosomes. Both American trypanosomiasis (Chagas disease) and human African trypanosomiasis (sleeping sickness) are included in the list of the World Health Organization's neglected tropical diseases [2]. Chagas disease, caused by *Trypanosoma cruzi*, infects an estimated 7–8 million people worldwide, although infection predominantly occurs in Latin America and spreads to other countries due to travel by infected persons. Sleeping sickness affects an estimated 20,000 people a year. Approximately 98% of reported cases are the chronic form of sleeping sickness caused by infection with *T. brucei gambiense* whereas the acute form, due to infection with *T. b. rhodesiense*, accounts for 2% of reported cases [2]. Currently, only a few medicines are registered for trypanosomiasis and many of them have serious adverse effects [3,4]. In addition, both Chagas disease and sleeping sickness are expensive to treat. As such, one of the targets of the WHO is to provide cheaper, more effective, and less toxic medicines for the management and elimination of these diseases [2].

Tuberculosis (TB) is a disease caused by *Mycobacterium tuberculosis*, a Gram-positive, acid-fast bacillus. The most common form of tuberculosis is pulmonary; however, extrapulmonary TB can also occur. TB, if left untreated, is an often-fatal disease with up to 70% of HIV negative patients dying within 10 years. The mortality rate is higher for HIV positive patients with untreated TB as the average survival rate becomes less than 6 months [5]. Although treatment is available, TB remains the second leading cause of death from infectious disease in the world, after HIV [6]. Despite the consistent decrease in incidence and mortality of TB cases globally since 2006 and probability that the Millennium Development Goal of 2015 will be achieved, the global burden of TB is still high. Approximately 8.7 million new cases of TB and 1.4 million deaths due to TB were reported in 2011 [6]. In addition, there is insufficient data to determine the global trend of multidrug-resistant TB (MDR-TB), largely due to lack of testing for resistance in many countries. However, in 2011 the estimated number of MDR-TB cases was 310,000. At least one case of extensively drug-resistant TB (XDR-TB) has been reported in 84 countries [6].

It has been approximately half a century since the first-line TB drugs were first used. New medicines are necessary in order to combat MDR-TB and XDR-TB, shorten the current treatment regimens, treat latent TB in patients that are infected with the bacteria but have not developed the disease, and to improve the prognosis of patients with both TB and HIV. Eleven prospective TB drugs are undergoing clinical trials. Research is also underway on TB vaccines, with 12 in clinical trials [6]. While this is encouraging, it is still important to continue the search for lead compounds with different mechanisms of action.

Sterols have shown promise as new antitrypanosomal and anti-mycobacterial compounds. Recent research has shown that steroids may be used to treat trypanosomiasis by inhibiting the

glucose-6-phosphate dehydrogenase (G6PD) enzyme in trypanosomes [7,8] which is the enzyme involved in the first committed step of the pentose-phosphate pathway. This prevents the formation of NADPH, increasing the susceptibility of the trypanosomes to oxidative stress [8]. The sterol biosynthetic pathway of trypanosomes has also come into focus. 24-Sterol methyltransferase (24-SMT) and sterol 14 α -demethylase (CYP51) are two examples of enzymes that serve as targets for new antitrypanosomal drugs [9–11]. The genus *Mycobacterium* has also been reported to possess a sterol biosynthetic pathway that is homologous to that of the yeast, *Saccharomyces cerevisiae* [12]. Sterol 14 α -demethylase is also a target in *M. tuberculosis* [13]. Sterols could therefore prove to be interesting lead compounds for the treatment of *Mycobacterium* sp. infections.

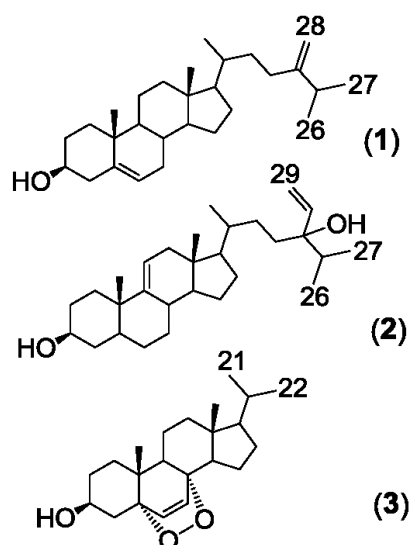
Sponges (Phylum Porifera) are primitive metazoic organisms that are among the oldest multicellular animals in the world [14]. Despite their simple morphology, marine sponges are well-known for being abundant sources of novel compounds, particularly steroids with a diverse range of conventional and unconventional side chains and nuclei [15–17]. Interest in sponge metabolites began in the 1950s when Bergmann and Feeney first reported the isolation of two sponge nucleosides, spongouridine and spongothymidine [18–20]. The knowledge gained from this discovery eventually led to the development of several FDA- and EMEA-approved drugs: cytarabine arabinoside (Ara-C), an anti-leukemic agent, adenine arabinoside (Vidarabine or Ara-A), an antiviral agent, and even azidothymidine (AZT) which is used in the treatment of HIV [21].

The sponge *Haliclona simulans* belongs to the family *Chalinidae* of the order *Haplosclerida* and the class *Demospongiae* [22]. The genus *Haliclona* has already given rise to many interesting metabolites, with as many as 190 compounds of various chemical classes and functions having been reported [23]. *Haliclona simulans*, by virtue of its genus, which has already produced a large quantity of active metabolites, therefore appears to be a very promising source of lead compounds. This paper describes the isolation and identification of three antitrypanosomal and anti-mycobacterial steroids from the Irish Sea sponge *Haliclona simulans*.

2. Results and Discussion

Three steroids (Figure 1) were isolated from *Haliclona simulans* following HP20 chromatography and flash chromatography. One steroid was identified as 24-methylenecholesterol (**1**) whereas the other two were unidentified based on a literature search. These steroids were found to be active against *Trypanosoma brucei brucei* and *Mycobacterium marinum*.

24-Methylenecholesterol (**1**) was the major non-polar compound present in the sponge. It was first isolated from the sponge *Chalina arbuscula* Verill [24] and has since been isolated from a variety of marine sources, including other *Haliclona* sponges [17]. 24-Methylenecholesterol has been reported as a precursor to many other sponge sterols [25]. The ¹H and ¹³C NMR data (Tables 1 and 2) of the 24-methylenecholesterol isolated in this study closely matched those reported in the literature [26]. The orientation of the 3-hydroxyl group was determined using ROESY and by analysis of the coupling constants. The large *J* value of H-3 (10.98 Hz) indicated axial-axial correlations. H-3 was therefore assigned an α -orientation whereas OH-3 was designated a β -orientation. The steroid was derivatised using MSTFA to facilitate ionization using GCMS. EI-GCMS showed a peak with *m/z* 470.4 [M]⁺ which corresponded to a TMS derivatised 24-methylenecholesterol.

Figure 1. Structures of steroids isolated from *H. simulans*.**Table 1.** ^1H (400 MHz) NMR chemical shifts (CDCl_3) of the steroids isolated from *H. simulans*.

Position	1	2	3
1	1.81 (d, 5.1)	1.82 (d, 11.5)	1.68, 1.94 (d, 4.6)
2	1.50	1.45 (d, 12.9)	1.52, 1.83
3	3.52 (td, 5.3, 11.0)	3.51 (tt, 4.7, 10.6)	3.96 (tt, 5.1, 11.1)
4	2.27 (m)	2.24 (m)	1.90 (s), 2.12 (d, 4.8)
6	5.34 (d, 5.7)	0.90 (d, 4.0)	6.23 (d, 8.5)
7	1.95		6.49 (d, 8.5)
9			1.50 (m)
11		5.32 (d, 5.0)	1.20, 1.49
12		1.14, 1.94	1.21, 1.97
14		1.06	1.57, (d, 3.6)
15			0.99
16			1.24 (s)
17			1.20
18	0.67 (t, 3.1)	0.66 (s)	0.80 (s)
19	0.99 (s)	0.98 (s)	0.87 (s)
20		1.41 (d, 3.9)	1.98 (m)
21	0.93 (d, 6.7)	0.93 (d, 6.3)	0.98 (d, 7.0)
22		1.85	1.02 (d, 7.0)
23		1.11, 1.99	
25		1.99	
26	1.02 (d, 2.3)	0.98	
27	1.02 (d, 2.3)	0.87	
28	4.64 (s), 4.70 (s)	5.72 (m)	
29		5.12 (d, 17.9) 5.25 (d, 11.4)	

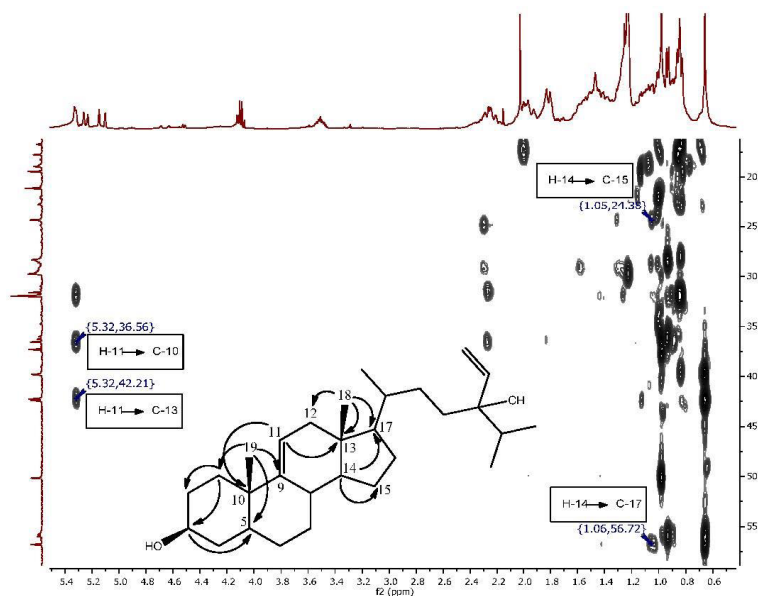
Table 2. ^{13}C (100 MHz) NMR chemical shifts (CDCl_3) of the steroids isolated from *H. simulans*.

Position	1	2	3
1	37.3 (CH_2)	37.3 (CH_2)	34.8 (CH_2)
2	31.7 (CH_2)	31.6 (CH_2)	30.2 (CH_2)
3	71.9 (CH)	71.9 (CH)	66.6 (CH)
4	42.3 (CH_2)	42.3 (CH_2)	37.0 (CH_2)
5	140.8 (C)	50.2 (CH)	82.2 (C)
6	121.8 (CH)	34.8 (CH_2)	135.50 (CH)
7	31.0 (CH_2)	22.0 (CH_2)	130.8 (CH)
8	32.0 (CH)	21.1 (CH)	79.5 (C)
9	50.2 (CH)	140.8 (C)	51.1 (CH)
10	36.6 (C)	36.6 (C)	36.0 (C)
11	21.2 (CH_2)	121.8 (CH)	23.5 (CH_2)
12	39.8 (CH_2)	39.8 (CH_2)	39.5 (CH_2)
13	42.4 (C)	42.4 (C)	44.8 (C)
14	56.8 (CH)	56.0 (CH)	51.7 (CH)
15	24.4 (CH_2)	24.4 (CH_2)	20.7 (CH_2)
16	28.3 (CH_2)	29.8 (CH_2)	29.8 (CH_2)
17	56.1 (CH)	56.8 (CH)	56.2 (CH)
18	11.9 (CH_3)	11.9 (CH_3)	12.7 (CH_3)
19	19.5 (CH_3)	19.5 (CH_3)	18.3 (CH_3)
20	35.9 (CH_2)	36.3 (CH)	33.9 (CH)
21	18.8 (CH_2)	19.0 (CH_3)	22.1 (CH_3)
22	23.9 (CH_2)	28.3 (CH_2)	28.4 (CH_2)
23	34.8 (CH_2)	28.5 (CH_2)	28.1 (CH_3)
24	157.0 (C)	89.2 (C)	
25	33.9 (CH)	32.0 (CH)	
26	22.1 (CH_3)	17.8 (CH_3)	
27	28.1 (CH_3)	16.7 (CH_3)	
28	106.0 (CH_2)	137.2 (CH)	
29		116.3 (CH_2)	

The second isolated steroid (**2**) is a derivative of saringosterol, which was first isolated from a brown algae [27]. The difference lies in the position of the double bond of the steroid nucleus. In saringosterol it is found in the $\Delta^{5(6)}$ position, whereas in this derivative from *H. simulans* it is found in the $\Delta^{9(11)}$ position. The ^1H and ^{13}C NMR data (Tables 1 and 2, Supplementary Figures S1 and S3–S5) of the saringosterol derivative were comparable to the values found in the literature [28]. The olefinic system of the steroid nucleus was elucidated using the COSY (Supplementary Figures S2 and S8) and HMBC spectra as shown in Figure 2, Supplementary Figures S6, S8, and S9. The broad doublet at δ_{H} 5.32 assigned to H-11 showed the coupling of the olefinic hydrogen with one of the two protons at H-12 (δ_{H} 1.94). The HMBC confirmed the position of C-12 as it is one of the three carbons correlating with the methyl group on C-13. Crosspeaks were observed from CH_3 -18 (δ_{H} 0.66) to C-12 (δ_{C} 39.8), C-13 (δ_{C} 42.4) and C-17 (δ_{C} 56.8). HMBC correlations of H-14 (δ_{H} 1.06) with C-15 (δ_{C} 24.4), and of H-14 to C-17 were also visible. The doublet for H-11 at δ_{H} 5.32 correlated with C-10 (δ_{C} 36.6) and C-13 (δ_{C} 42.4) (Supplementary Figure S7). The β -orientation of 3-OH was once again determined

using the ROESY spectrum and the J values (tt, 4.7, 10.6 Hz) of the H-3 peak at 3.51 ppm. High resolution ESI-MS analysis of compound **2** showed an ion peak at m/z 429.37303 $[M + H]^+$ which corresponded to the molecular formula of $C_{29}H_{49}O_2$ (Supplementary Figure S11). Sterol **2** was elucidated as 24-vinyl-cholest-9-ene-3 β ,24-diol (Figure 1 and Supplementary Figure S10).

Figure 2. Expansion of the HMBC spectrum highlighting the correlations which indicate the change in the position of the double bond in Compound **2**.



Another new sterol (**3**) was also isolated (Figure 1, Supplementary Figures S12, S14–S16; Tables 1 and 2). It eluted later from the generic flash silica column than the previous two sterols as it is more polar. This sterol possessed a 5 α ,8 α -epidioxy nucleus with a shortened side chain. The two doublets at δ_H 6.23 and 6.49 (H-6 and H-7, respectively) were shown on the COSY (Supplementary Figure S13) to form an isolated spin system. The HMBC spectrum confirmed that H-6 and H-7 correlated with oxygenated carbons at δ_C 82.2 and 79.5 (C-5 and C-8 respectively). The orientation of the 5,8-epidioxy peroxide group was confirmed by comparing the chemical shifts and coupling patterns of H-6 and H-7 (Supplementary Figure S12) to the values found in literature. A 5 α ,8 α -epidioxy group results in chemical shifts of 6.5 and 6.3 ppm for H-6 and H-7 whereas a 5 β ,8 β -epidioxy group would result in chemical shifts of 5.9 and 5.6 respectively [29].

The chemical shifts of the methyl groups on C-20 were assigned based on the COSY (Supplementary Figure S13) and J -resolved spectra (Figure 3, Supplementary Figures S18 and S19). The J -resolved spectra showed that the peaks at δ_H 0.98 (H-21) and δ_H 1.02 (H-22) were doublets; therefore, both methyl groups must be attached to C-20. The COSY spectrum showed that both CH_3 -21 and CH_3 -22 correlated with a peak at δ_H 1.98, which was assigned to H-20. CH_3 -21 and CH_3 -22 were also correlating on the HMBC with C-17 as shown in Figure 4, Supplementary Figures S17 and S20. Sterol **3** gave a retention time of 23.67 min on a C_{18} -HPLC column and exhibited an ion peak at m/z of

347.2580 [M + H]⁺ by high resolution ESI-MS with a molecular formula of C₂₂H₃₅O₃ (Supplementary Figure S22). The structure of sterol **3** was elucidated as 20-methyl-pregn-6-en-3 β -ol, 5 α ,8 α -epidioxy (Supplementary Figure S21).

Figure 3. *J*-resolved spectrum showing the splitting of H-21 (δ_H 0.98) and H-22 (δ_H 1.02).

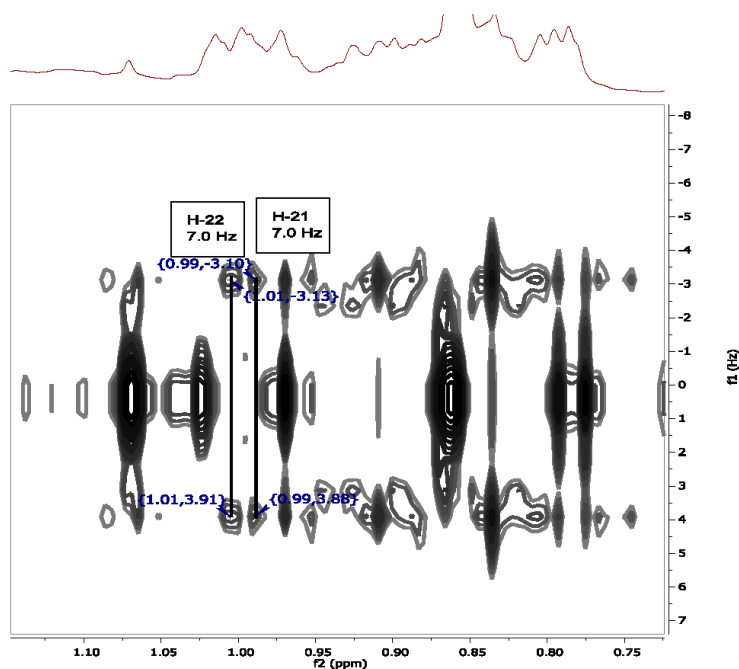
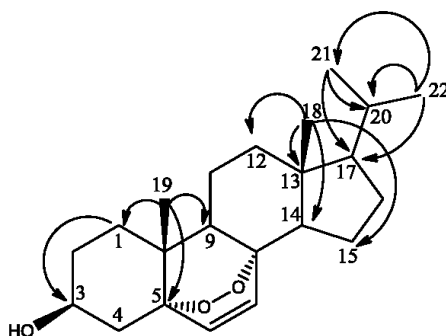


Figure 4. HMBC correlations (H to C) of methyl groups in sterol **3**.



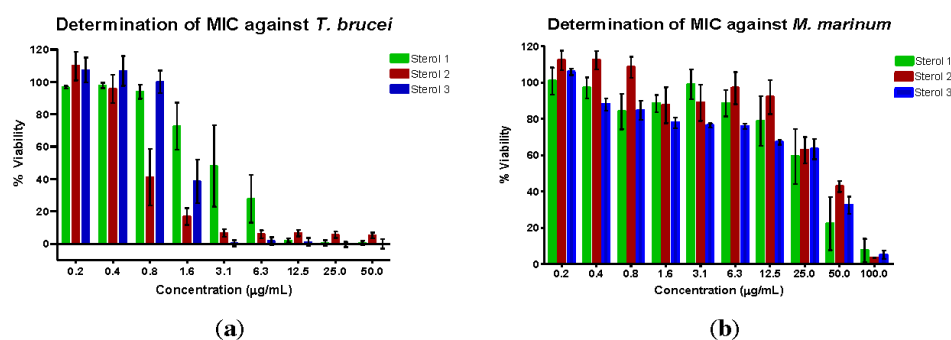
The inhibitory activities of the three sterols against *Trypanosoma brucei brucei* and *Mycobacterium marinum* are shown in Table 3 and Figure 5. Suramin, the positive control for the *T. brucei* assay, is the treatment of choice for stage 1 sleeping sickness [3]. The positive control for the *M. marinum* assay was gentamicin, an aminoglycoside antibiotic. Sterol **1**, 24-methylenecholesterol, was the most potent against *M. marinum* but the least active against *T. b. brucei*. The MIC against *M. marinum* was less than that of 24-methylenecholesterol isolated from the sponge *Svenzea zeai* against *M. tuberculosis* (MIC:

120.1 µg/mL or 251.26 µM) [30]. Sterol **2**, the saringosterol derivative, was the most active against *T. b. brucei*. Saringosterol has been reported to have an IC₅₀ of 7.8 ± 1.2 µM against *T. b. brucei* [31]. The shift in double bond position from Δ⁵⁽⁶⁾ to Δ⁹⁽¹¹⁾ in the new congener seems to improve the antitrypanosomal activity of saringosterol. Steroids with the Δ⁹⁽¹¹⁾ double bond have previously been isolated from marine invertebrates such as starfish [32–35] and sea cucumbers [36,37], as well as from another sponge, *Haliclona rubens* (renamed as *Amphimedon compressa*) [38]. The activity of saringosterol against *M. tuberculosis* has also been previously reported (MIC: 0.25 µg/mL or 0.58 µM) [39]. The change in the position of the double bond may therefore have had a detrimental effect on the anti-mycobacterial activity of the steroid. Saringosterol is often isolated as a mixture of 24*R/S* epimers [31,39] although the 24*R* epimer has been found to be more active than the 24*S* epimer against *M. tuberculosis* [39]. The optical rotation of sterol **2** in this study was determined to be −4.5, indicating that it is likely a mixture of epimers which may plausibly explain the loss of activity in the isolated congener. In addition, the test microorganisms that were used were different, although *M. marinum* is often used as the model organism for *M. tuberculosis*.

Table 3. Antimicrobial activities and cytotoxicity on Hs27 cells of *H. simulans* sterols.

Sterol	MIC Average ± Std Dev (n = 4)		Cytotoxicity on HS27 Cells
	<i>T. b. brucei</i> (µM)	<i>M. marinum</i> (µM)	IC ₅₀ (µM) ± Std Dev (n = 3)
1	21.56 ± 11.80	156.90 ± 54.35	58 ± 3.53
2	4.58 ± 1.80	233.44 ± 0	>100 ± 4.03
3	9.01 ± 0	288.81 ± 0	100 ± 2.95
Suramin	0.11 ± 0		
Gentamycin		13.48 ± 0	

Figure 5. Determination of the minimum inhibitory concentration value (MIC) of the sterols against (a) *T. b. brucei* and (b) *M. marinum*. The assay was performed using various concentrations of the sterols in µg/mL. The mean values were then converted to µM.



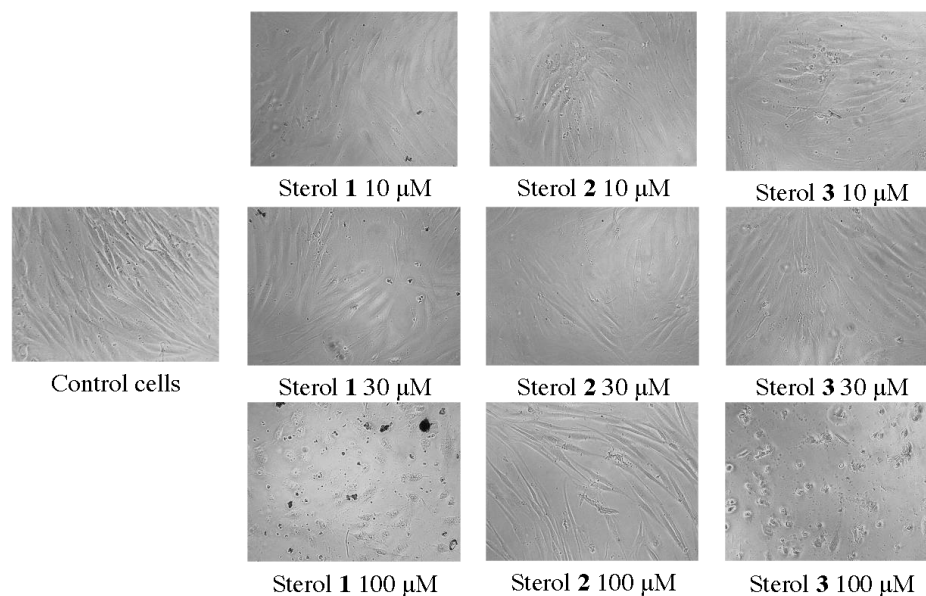
Sterol **3** was the next most active against *T. b. brucei*. The 5α,8α-epidioxy sterol could be an artefact, a result of oxidation of a Δ^{5,7}-sterol, as has been observed in *Dysidea* sp. [40]. However, 5α,8α-epidioxy sterols have previously been isolated from the sponge *Luffariella* cf. *variabilis* and these sterols are believed to be natural products and not artifacts as the isolation was performed rapidly and no precursors were found [29]. In addition, some fungi produce these epidioxy sterols, such as ergosterol

peroxide [41], and so it cannot be ruled out that **3** is a natural product of *H. simulans* or even of an endosymbiont. The peroxide functional group may contribute to the antitrypanosomal activity. 24-hydroperoxy-24-vinylcholesterol, a peroxide derivative of saringosterol, was reported to have an IC_{50} of 3.2 μ M against *T. b. brucei* as opposed to that of saringosterol which was 7.8 μ M [31]. Ergosterol peroxide, a fungal metabolite, has also been known to have antitrypanosomal activity, although the assay was performed against *T. cruzi* [42]. It is also active against *M. tuberculosis* (MIC 3.5 μ M) and indeed was the most active of the nine sterols that were assayed in the study [43]. Another endoperoxide-containing natural product well-known for its anti-protozoal activity is artemisinin. Short side chain sterols are uncommon but have previously been isolated from marine invertebrates, including from tunicates, gorgonians and sponges [44,45]. These sterols may be *in vivo* oxidative products from sterols with unsaturated side chains and not degradation products obtained during laboratory work-up. A sterol bearing the same side chain as in **3** has been isolated from the gorgonian *Murecia californica* and the sponge *Damiriana hawaiiiana* [45].

Previous studies have drawn some conclusions regarding the structure-activity relationships of sterols and their antitrypanosomal and anti-mycobacterium activity. Hydroxylated side chains, such as the one proposed for sterol **2**, result in an increase in antitrypanosomal activity [31]. The peroxide functional group on sterol **3** may also contribute to activity, as 24-hydroperoxy-24-vinylcholesterol, a peroxide derivative of saringosterol, had an IC_{50} of 3.2 μ M against *T. b. brucei* whereas saringosterol had an IC_{50} of 7.8 μ M against the same microorganism [31]. Another functional group of sterols that contributes to bioactivity is the 3 β -hydroxy group, which is required for the inhibition of 24-sterol methyltransferase of *Leishmania major* by azasterols [46] as well as for the binding of sterols to plant yeast SMT [47]. As previously mentioned, 24-SMT is also a target for antitrypanosomal drugs. Although the mechanism of action of the sterols in this study is unknown, it is possible that they act by inhibiting 24-SMT and thereby disrupting the sterol biosynthetic pathway in *T. b. brucei*. The 3-hydroxy group, as well as a 14 α -methyl group, is also essential for the binding of sterols to sterol 14 α -demethylase in *M. tuberculosis* [13]. Although the three sterols isolated from *H. simulans* all contain the 3 β -hydroxy moiety, none possess the 14 α -methyl group required to bind to this enzyme. It is possible that they act upon another enzyme in the pathway or by a different mechanism altogether. The steroid nucleus itself also affects the anti-mycobacterium activity of the compound, as it has been found that a 5(6 \rightarrow 7)abeo-steroidal nucleus leads to an increase in the potency of the compound [30]. The effect of the presence of the double bond at $\Delta^{9(11)}$ on the antimicrobial activity of sterols has not been studied; however, $\Delta^{9(11)}$ sterols have found applications as lead compounds for anti-inflammatory drugs as they possess fewer side effects than the conventional corticosteroids [48]. It would therefore be of interest to determine the advantages of $\Delta^{9(11)}$ sterols as antimicrobial agents.

All sterols at concentration ranges of 0.1 to 100 μ M were subjected to cell cytotoxicity assay on normal fibroblasts derived from human foreskin (Hs27 cells). The most antitrypanosomal active saringosterol congener (**2**) showed no cytotoxicity and no difference with the control in terms of changes in cell morphology of Hs27 (Figure 6). Sterols **1** and **3** exhibited cytotoxicity at 58 and 100 μ M, respectively as shown in Table 3. At 100 μ M concentration of sterols **1** and **3**, the Hs27 shrunk 10 \times to irregularly shaped cells (see Figure 6). The cytotoxicity of sterols **1** and **3** is still above their dosage threshold as potential antitrypanosomal drugs.

Figure 6. Change in morphology of normal fibroblasts Hs27 observed under the microscope in the cell cytotoxicity assay of *H. simulans* sterols.



3. Experimental Section

3.1. Acquisition of Sponge Sample

The sponge, *Haliclona simulans*, was collected from Kilkieran Bay, Galway, Ireland by the Environmental Research Institute, University College Cork. It was freeze-dried, sealed under vacuum and sent to the Strathclyde Institute of Pharmacy and Biomedical Sciences, University of Strathclyde where it was stored at -20°C until the extraction of its metabolites.

3.2. Extraction and Isolation of Sponge Metabolites

The freeze-dried sponge (dry weight: 107.20 g) was finely ground using an analytical mill. The powder was macerated in acetone at room temperature with constant stirring for three hours. This was repeated three times, after which the extraction procedure was performed with methanol. The acetone and methanol extracts were combined and subjected to Diaion[®] HP20 (Mitsubishi Chemical Corporation, Tokyo, Japan) chromatography. The compounds were eluted using a stepwise gradient of 100% water to 100% methanol in 10% increments. The column was washed with 50:50 acetone methanol and 100% methanol. These non-polar wash fractions were pooled and further fractionated using the Reveleris[®] Flash Forward system (Grace Davison Discovery Sciences, Columbia, MD, USA). The sample was loaded onto a generic silica 24 g/32 mL (20 × 130 mm) column and eluted in a three-step gradient (5 min: 100% hexane, 45 min: 100% hexane to 100% ethyl acetate, 10 min: 100% ethyl acetate) at a flow rate of 10 mL/min. The sterols eluted at approximately 26–30 min (**1**), 31–32 min (**2**) and 35–36 min (**3**) with following yield 334.8 mg = 0.31%, 11.5 mg = 0.011%, 6.7 mg = 0.006%, respectively.

24-Methylenecholesterol (**1**). White, needle-like crystals; $[\alpha]_D^{20} -23$ (*c* 0.1, CHCl₃); *R*_f: 0.52 (TLC silica, 95:5 CH₂Cl₂); EIMS: *m/z* 470.4 [M + CH₃Si]⁺ (derivatised steroid), calculated for C₃₁H₅₄O_{Si}, 470.3938.

24-Vinyl-cholest-9-ene-3β,24-diol (**2**). Very fine crystals; $[\alpha]_D^{20} -4.5$ (*c* 0.1, CHCl₃); *R*_f: 0.42 (TLC silica, 95:5 CH₂Cl₂); HRESIMS *m/z* 429.3731 [M + H]⁺, calculated for C₂₉H₄₉O₂, 429.3727.

20-Methyl-pregn-6-en-3β-ol, 5α,8α-eipidioxy (**3**). Small crystals; $[\alpha]_D^{20} +5$ (*c* 0.1, CHCl₃); *R*_f: 0.36 (TLC silica, 95:5 CH₂Cl₂:MeOH); HRESIMS *m/z* 347.2580 [M + H]⁺, calculated for C₂₂H₃₅O₃, 347.2581.

3.3. Analysis of Sterols

NMR spectra were taken using a Jeol-LA400 FT-NMR spectrometer system (JEOL Ltd., Tokyo, Japan) with an AS400 magnet (Oxford Instruments, Inghilterra, UK) at 400 MHz for ¹H and 100 MHz for ¹³C, using a Pulse Field Gradient “Autotune” 40TH5AT/FG broadband high sensitivity probe (JEOL Ltd., Tokyo, Japan) to accept 5 mm tubes. LC-HRFTMS analysis was performed on a Dionex UltiMate-3000 (DIONEX, Sunnyvale, CA, USA) coupled to a ThermoScientific Exactive Orbitrap system (Thermo Fisher Scientific (Bremen) GmbH, Bremen, Germany). The column used was an ACE 5 C18 75 × 3.0 mm column from Hichrom Ltd., Reading, UK. Compounds were eluted with a flow rate of 300 μL/min using water (A) and acetonitrile (B), both of which contained 0.1% formic acid, by a gradient starting with 10% B and increasing to 100% B in 30 min. The mobile phase was maintained at 100% B for 5 min after which the column was equilibrated with 10% B. Sterol **2** eluted at 37.60 min and sterol **3** eluted at 23.67 min. The optical rotations of the compounds were measured using a Perkin-Elmer 341 polarimeter (Perkin-Elmer, Waltham, MA, USA). The derivatisation of 24-methylenecholesterol was carried out by dissolving 1 mg of the steroid in 500 μL of acetonitrile. This was dried at 50 °C after which 200 μL of MSTFA (Sigma-Aldrich, St. Louis, MO, USA) was added and the sample heated at 80 °C for 30 min. The sample was then submitted for EI-GCMS using a Thermo Finnigan Polaris Q (Thermo Fisher Scientific (Bremen) GmbH, Bremen, Germany) with Trace GC. The column used was an Agilent DB5-ms UI (ID: 0.25 mm, length: 30 m, df: 0.25 μm, Agilent, Santa Clara, CA, USA).

3.4. Antitrypanosomal Assay

The sterols were prepared in stock solutions of 10 mg/mL in DMSO. Four microliters of these stock solutions were pipetted into one column of the transparent flat-bottomed 96-well plates after which 196 μL of HMI-9 was added, resulting in a concentration of 200 μg/mL. One-to-one serial dilutions with HMI-9 were carried out in the other columns of the plate. One hundred microliters of trypanosome suspension (containing *Trypanosoma brucei* S427 blood stream form at 3 × 10⁴ trypanosomes/mL) were added so that the final concentration of the compounds ranged from 100 μg/mL to 0.17 μg/mL. DMSO was included as a negative control at a concentration of 1% to 0.002% and suramin (Calbiochem-Novabiochem Co., La Jolla, CA, USA) was included as a positive control at a concentration range of 1 to 0.008 μM. The plate was incubated at 37 °C, 5% CO₂ with a humidified atmosphere for 48 h, after which 20 μL of Alamar blue was added. The plate was incubated under the

same conditions for another 24 h and the fluorescence read using the Wallac Victor microplate reader (Perkin Elmer, Cambridge, UK) with excitation at 530 nm and emission at 590 nm. The results were calculated as percentages of control values and the minimum inhibitory concentration values (MICs) were determined.

3.5. Anti-*Mycobacterium* Assay

Mycobacterium marinum ATCC.BAA535 from a thawed stock cryoculture was streaked onto Columbia (5% horse blood) agar slopes and incubated at 31 °C for 5 days. A loopful of the culture was then transferred into 10 mL of sterile 0.9% NaCl containing glass beads. The suspension was mixed and allowed to settle. Aliquots of the supernatant were added to a tube containing sterile 0.9% NaCl until the turbidity matched that of a 0.5 McFarland standard. A few drops of sterile 0.02% Tween 80 were added to homogenize the suspension. This was then shaken and the inoculum diluted 1 in 10 with cation-adjusted Mueller Hinton Broth (MHB) for use in the assay. The steroids were prepared in 10 mg/mL DMSO stock solutions and were diluted ten times to 1 mg/mL using cation-adjusted MHB. The final concentrations of the test solutions in the 96-well plate ranged from 100 to 0.17 µg/mL. DMSO was included as a negative control at a concentration range of 1% to 0.002% and gentamycin was included as a positive control at a concentration range of 100 to 0.78 µg/mL. One hundred microliters of the bacterial suspension was added to the wells. The plates were sealed and incubated at 31 °C for 5 days before the addition of 10 µL of Alamar blue. The plates were re-sealed and incubated at the same temperature for 24 h after which fluorescence was determined using the Wallac Victor microplate reader (excitation 530 nm, emission 590 nm). The results were calculated as percentages of control values and the minimum inhibitory concentration values (MICs) were determined.

3.6. Cell Cytotoxicity Assay

Normal fibroblasts derived from human foreskin (Hs27 cells) were obtained from ECACC (Sigma-Aldrich, Dorset, UK). They were cultured in DMEM media supplemented with 10% (v/v) foetal bovine serum, 2 mM glutamine and 50 µg/mL penicillin/streptomycin (all Invitrogen, Paisley, UK) solution in a humidified incubator at 37 °C in the presence of 5% CO₂. Cells were routinely passaged at 90%–95% confluence.

Subsequently, cells were seeded at a concentration of 7500 cells/well in black 96 flat-bottomed plates and allowed to adhere overnight. After that time, Sterols **1**, **2** and **3** were added to the cells in the concentration range of 0.1 to 100 µM (in half log units) and incubated for a further 48 h.

Viability was determined using a CellTiter-Glo[®] (Promega, Southampton, UK) kit according to the manufacturer's instructions. The resulting luminescence was measured using a Wallac Victor 2 (Perkin Elmer, Cambridge, UK). Results were expressed as "percentage of control" where the control is the luminescence value of cells in the absence of compound. All results were confirmed microscopically.

4. Conclusions

Sponges are recognized as possessing a diverse range of steroids that have both conventional and unconventional side chains and nuclei. This was confirmed by the diversity of nuclei and

side chains isolated from *H. simulans*. Two novel sterols, 24-vinyl-cholest-9-ene-3 β ,24-diol and 20-methyl-pregn-6-en-3 β -ol, 5 α ,8 α -epidioxy were among the three obtained. The former sterol possessed a $\Delta^{9(11)}$ double bond that distinguished it from the known compound saringosterol, whereas the latter contained an endoperoxide moiety and an uncommonly short side chain. Both sterols were more active against *T. brucei* than the known sterol 24-methylenecholesterol, but they were less active against *M. marinum*. Nevertheless, they serve as useful lead compounds in the search for new drugs and add weight to the theory that a large number of novel compounds remain to be discovered from marine sponges. The $\Delta^{9(11)}$ double bond may be beneficial to the design of a compound that is more efficacious and safer than conventional therapy as shown by their inactivity in the cytotoxicity assay. It is worth mentioning that the endoperoxide moiety may play a role in the efficacy of the drug at which its potency threshold is above its level of cytotoxicity as an antitrypanosomal drug. Such types of compounds are needed in the development of drugs with less toxic side effects.

Acknowledgments

C.V. would like to acknowledge the scholarship funded by the Scottish Overseas Research Students Award Scheme (SORSAS). This research was supported in part by the Beaufort Marine Biodiscovery Research award funded by the Irish Government under the National Development Plan (2007–2013).

Author Contributions

CV. Designed and optimised the bioassay-guided isolation work, structure elucidation, and wrote the manuscript; JP. Chromatographical purification work; TO. Initial extraction and fractionation work; CC. Microbial assay; GA LY. Cytotoxicity assay on Hs27; JK ADWD. provided the sponge samples, conceived and designed the project; REE. Structure elucidation work, supervised, designed, and coordinated the bioassay-guided isolation work as well as main editor of the manuscript.

Conflicts of Interest

The authors declare no conflict of interest.

References

1. WHO. *The Global Burden of Disease 2004 Update*; World Health Organization: Geneva, Switzerland, 2008.
2. WHO. *Sustaining the Drive to Overcome the Global Impact of Neglected Tropical Diseases: Second Who Report on Neglected Tropical Diseases*; World Health Organization: Geneva, Switzerland, 2013.
3. Legros, D.; Ollivier, G.; Gastellu-Etchegorry, M.; Paquet, C.; Burri, C.; Jannin, J.; Büscher, P. Treatment of human *African trypanosomiasis*—Present situation and needs for research and development. *Lancet Infect. Dis.* **2002**, *2*, 437–440.
4. Bern, C.; Montgomery, S.P.; Herwaldt, B.L.; Rassi, A.; Marin-Neto, J.A.; Dantas, R.O.; Maguire, J.H.; Acquatella, H.; Morillo, C.; Kirchoff, L.V.; *et al.* Evaluation and treatment of chagas disease in the united states: A systematic review. *JAMA* **2007**, *298*, 2171–2181.

5. Tiemersma, E.; van der Werf, M.; Borgdorff, M.; Williams, B.; Nagelkerke, N. Natural history of tuberculosis: Duration and fatality of untreated pulmonary tuberculosis in HIV negative patients: A systematic review. *PLoS One* **2011**, *6*, e17601.
6. WHO. *Global Tuberculosis Report 2012*; World Health Organization: Geneva, Switzerland, 2012.
7. Cordeiro, A.T.; Thiemann, O.H.; Michels, P.A. Inhibition of *Trypanosoma brucei* glucose-6-phosphate dehydrogenase by human steroids and their effects on the viability of cultured parasites. *Bioorg. Med. Chem.* **2009**, *17*, 2483–2489.
8. Gupta, S.; Cordeiro, A.T.; Michels, P.A. Glucose-6-phosphate dehydrogenase is the target for the trypanocidal action of human steroids. *Mol. Biochem. Parasitol.* **2011**, *176*, 112–115.
9. Magaraci, F.; Jimenez, C.J.; Rodrigues, C.; Rodrigues, J.C.; Braga, M.V.; Yardley, V.; de Luca-Fradley, K.; Croft, S.L.; de Souza, W.; Ruiz-Perez, L.M.; *et al.* Azasterols as inhibitors of sterol 24-methyltransferase in *Leishmania* species and *Trypanosoma cruzi*. *J. Med. Chem.* **2003**, *46*, 4714–4727.
10. Gros, L.; Castillo-Acosta, V.M.; Jiménez Jiménez, C.; Sealey-Cardona, M.; Vargas, S.; Manuel Estévez, A.; Yardley, V.; Rattray, L.; Croft, S.L.; Ruiz-Perez, L.M.; *et al.* New azasterols against *Trypanosoma brucei*: Role of 24-sterol methyltransferase in inhibitor action. *Antimicrob. Agents Chemother.* **2006**, *50*, 2595–2601.
11. Lepesheva, G.I.; Ott, R.D.; Hargrove, T.Y.; Kleshchenko, Y.Y.; Schuster, I.; Nes, W.D.; Hill, G.C.; Villalta, F.; Waterman, M.R. Sterol 14 α -demethylase as a potential target for antitrypanosomal therapy: Enzyme inhibition and parasite cell growth. *Chem. Biol.* **2007**, *14*, 1283–1293.
12. Lamb, D.; Kelly, D.; Manning, N.; Kelly, S. A sterol biosynthetic pathway in *Mycobacterium*. *FEBS Lett.* **1998**, *437*, 142–144.
13. Bellamine, A.; Mangla, A.; Dennis, A.; Nes, W.; Waterman, M. Structural requirements for substrate recognition of *Mycobacterium tuberculosis* 14 α -demethylase: Implications for sterol biosynthesis. *J. Lipid Res.* **2001**, *42*, 128–136.
14. Taylor, M.; Radax, R.; Steger, D.; Wagner, M. Sponge-associated microorganisms: Evolution, ecology, and biotechnological potential. *Microbiol. Mol. Biol. Rev.* **2007**, *71*, 295–347.
15. Blunt, J.W.; Copp, B.R.; Keyzers, R.A.; Munro, M.H.; Prinsep, M.R. Marine natural products. *Nat. Prod. Microbiol. Rep.* **2013**, *30*, 237–323.
16. Blunt, J.W.; Copp, B.R.; Munro, M.H.; Northcote, P.T.; Prinsep, M.R. Marine natural products. *Nat. Prod. Rep.* **2004**, *21*, 1–49.
17. Sheikh, Y.; Djerassi, C. Steroids from sponges. *Tetrahedron* **1974**, *30*, 4095–4103.
18. Bergmann, W.; Feeney, R. The isolation of a new thymine pentoside from sponges. *J. Am. Chem. Soc.* **1950**, *72*, 2809–2810.
19. Bergmann, W.; Feeney, R. Contributions to the study of marine products. 32. The nucleosides of sponges. 1. *J. Org. Chem.* **1951**, *16*, 981–987.
20. Bergmann, W.; Burke, D. Contributions to the study of marine products. 39. The nucleosides of sponges. 3. Spongothymidine and spongouridine. *J. Org. Chem.* **1955**, *20*, 1501–1507.
21. Newman, D.; Cragg, G. Marine natural products and related compounds in clinical and advanced preclinical trials. *J. Nat. Prod.* **2004**, *67*, 1216–1238.

22. Kennedy, J.; Baker, P.; Piper, C.; Cotter, P.; Walsh, M.; Mooij, M.; Bourke, M.; Rea, M.; O'Connor, P.; Ross, R.; *et al.* Isolation and analysis of bacteria with antimicrobial activities from the marine sponge *Haliclona simulans* collected from Irish waters. *Mar. Biotechnol.* **2009**, *11*, 384–396.
23. Yu, S.; Deng, Z.; Proksch, P.; Lin, W. Oculatol, oculatolide, and a-nor sterols from the sponge *Haliclona oculata*. *J. Nat. Prod.* **2006**, *69*, 1330–1334.
24. Bergmann, W.; Schedl, H.; Low, E. Contributions to the study of marine products. 19. Chalinasterol. *J. Org. Chem.* **1945**, *10*, 587–593.
25. Giner, J. Biosynthesis of marine sterol side chains. *Chem. Rev.* **1993**, *93*, 1735–1752.
26. Bazin, M.A.; Loiseau, P.M.; Bories, C.; Letourneux, Y.; Rault, S.; El Kihel, L. Synthesis of oxysterols and nitrogenous sterols with antileishmanial and trypanocidal activities. *Eur. J. Med. Chem.* **2006**, *41*, 1109–1116.
27. Ikekawa, N.; Tsuda, K.; Morisaki, N. Saringosterol: A new sterol from brown algae. *Chem. Ind.* **1966**, *85*, 1179–1180.
28. Ayyad, S.E.; Sowellim, S.Z.; El-Hosini, M.S.; Abo-Atia, A. The structural determination of a new steroidal metabolite from the brown alga *Sargassum asperifolium*. *Z für Naturforschung. C J. Biosci.* **2003**, *58C*, 333–336.
29. Gauvin, A.; Smadja, J.; Aknin, M.; Faure, R.; Gaydou, E. Isolation of bioactive 5 α ,8 α -epidioxy sterols from the marine sponge *Luffariella cf. variabilis*. *Can. J. Chem.* **2000**, *78*, 986–992.
30. Wei, X.; Rodríguez, A.D.; Wang, Y.; Franzblau, S.G. Synthesis and *in vitro* biological evaluation of ring B abeo-sterols as novel inhibitors of Mycobacterium tuberculosis. *Bioorg. Med. Chem. Lett.* **2008**, *18*, 5448–5450.
31. Hoet, S.; Pieters, L.; Muccioli, G.G.; Habib-Jiwan, J.L.; Opperdoes, F.R.; Quetin-Leclercq, J. Antitrypanosomal activity of triterpenoids and sterols from the leaves of *Strychnos spinosa* and related compounds. *J. Nat. Prod.* **2007**, *70*, 1360–1363.
32. Kitagawa, I.; Kobayashi, M.; Sugawara, T.; Yosioka, I. Thornasterol a and b, two genuine sapogenols from the starfish *Acanthaster planci*. *Tetrahedron Lett.* **1975**, *16*, 967–970.
33. Kitagawa, I.; Kobayashi, M.; Sugawara, T. Saponin and sapogenol. 25. Steroidal saponins from the starfish *Acanthaster planci* L. (crown of thorns). 1. Structures of two genuine sapogenols, thornasterol a and thornasterol b, and their sulfates. *Chem. Pharm. Bull.* **1978**, *26*, 1852–1863.
34. ApSimon, J.; Buccini, J.; Badriper, S. Marine organic chemistry. 1. Isolation of 3 β ,6 α -dihydroxy-5 α -pregn-9(11)-en-20-one from saponins of starfish *Asterias forbesi*. A rapid method for extracting starfish saponins. *Can. J. Chem.* **1973**, *51*, 850–855.
35. ApSimon, J.; Badripersaud, S.; Buccini, J.; Eenkhoorn, J. Marine organic chemistry. 4. Isolation of (20r)-5 α -pregn-9(11)-ene-3 β ,6 α ,20-triol from the saponins of the starfish, *Asterias forbesi* and *Asterias vulgaris*, and its synthesis. *Can. J. Chem.* **1980**, *58*, 2703–2708.
36. Goad, L.; Garneau, F.; Simard, J.; ApSimon, J.; Girard, M. Isolation of delta-9(11)-sterols from the sea cucumber *Psolus fabricii*. Implications for holothurin biosynthesis. *Tetrahedron Lett.* **1985**, *26*, 3513–3516.

37. Cordeiro, M.; Djerassi, C. Biosynthetic studies of marine lipids. 25. Biosynthesis of delta-9(11)-sterols and delta-7-sterols and saponins in sea cucumbers. *J. Org. Chem.* **1990**, *55*, 2806–2813.
38. Ballantine, J.; Williams, K.; Burke, B. Marine sterols. 4. C₂₁ sterols from marine sources. Identification of pregnane derivatives in extracts of sponge *Haliclona rubens*. *Tetrahedron Lett.* **1977**, *18*, 1547–1550.
39. Wachter, G.; Franzblau, S.; Montenegro, G.; Hoffmann, J.; Maiese, W.; Timmermann, B. Inhibition of *Mycobacterium tuberculosis* growth by saringosterol from *Lessonia nigrescens*. *J. Nat. Prod.* **2001**, *64*, 1463–1464.
40. Elenkov, I.; Milkova, T.; Andreev, S.; Popov, S. Sterol composition and biosynthesis in the black sea sponge *Dysidea fragilis*. *Comp. Biochem. Physiol. B* **1994**, *107*, 547–551.
41. Pinheiro, A.; Dethoup, T.; Bessa, J.; Silva, A.; Kijjoo, A. A new bicyclic sesquiterpene from the marine sponge associated fungus *Emericellopsis minima*. *Phytochem. Lett.* **2012**, *5*, 68–70.
42. Ramos-Ligonio, A.; López-Monteón, A.; Trigos, A. Trypanocidal activity of ergosterol peroxide from pleurotus ostreatus. *Phytother. Res.* **2012**, *26*, 938–943.
43. Truong, N.B.; Pham, C.V.; Doan, H.T.; Nguyen, H.V.; Nguyen, C.M.; Nguyen, H.T.; Zhang, H.J.; Fong, H.H.; Franzblau, S.G.; Soejarto, D.D.; *et al.* Antituberculosis cycloartane triterpenoids from *Radermachera boniana*. *J. Nat. Prod.* **2011**, *74*, 1318–1322.
44. Palermo, J.; Brasco, M.; Hughes, E.; Seldes, A.; Balzaretto, V.; Cabezas, E. Short side chain sterols from the tunicate *Polizoa opuntia*. *Steroids* **1996**, *61*, 2–6.
45. Carlson, R.; Popov, S.; Massey, I.; Delseth, C.; Ayanoglu, E.; Varkony, T.; Djerassi, C. Minor and trace sterols in marine invertebrates. 6. Occurrence and possible origins of sterols possessing unusually short hydrocarbon side chains. *Bioorg. Chem.* **1978**, *7*, 453–479.
46. Lorente, S.O.; Rodrigues, J.C.; Jiménez Jiménez, C.; Joyce-Menekse, M.; Rodrigues, C.; Croft, S.L.; Yardley, V.; de Luca-Fradley, K.; Ruiz-Pérez, L.M.; Urbina, J.; *et al.* Novel azasterols as potential agents for treatment of leishmaniasis and trypanosomiasis. *Antimicrob. Agents Chemother.* **2004**, *48*, 2937–2950.
47. Song, Z.; Nes, W.D. Sterol biosynthesis inhibitors: Potential for transition state analogs and mechanism-based inactivators targeted at sterol methyltransferase. *Lipids* **2007**, *42*, 15–33.
48. Reeves, E.K.; Hoffman, E.P.; Nagaraju, K.; Damsker, J.M.; McCall, J.M. Vbp15: Preclinical characterization of a novel anti-inflammatory delta 9,11 steroid. *Bioorg. Med. Chem.* **2013**, *21*, 2241–2249.

© 2014 by the authors; licensee MDPI, Basel, Switzerland. This article is an open access article distributed under the terms and conditions of the Creative Commons Attribution license (<http://creativecommons.org/licenses/by/3.0/>).